



HAL
open science

Mechanical and molecular signals underlying tendon cell differentiation

Ludovic Gaut

► **To cite this version:**

Ludovic Gaut. Mechanical and molecular signals underlying tendon cell differentiation. Development Biology. Sorbonne Université, 2018. English. NNT : 2018SORUS301 . tel-02865870

HAL Id: tel-02865870

<https://theses.hal.science/tel-02865870>

Submitted on 12 Jun 2020

HAL is a multi-disciplinary open access archive for the deposit and dissemination of scientific research documents, whether they are published or not. The documents may come from teaching and research institutions in France or abroad, or from public or private research centers.

L'archive ouverte pluridisciplinaire **HAL**, est destinée au dépôt et à la diffusion de documents scientifiques de niveau recherche, publiés ou non, émanant des établissements d'enseignement et de recherche français ou étrangers, des laboratoires publics ou privés.



**PHD THESIS
FROM SORBONNE UNIVERSITÉ**

**Specialty : Developmental Biology
Doctoral School n°515: Complexité du Vivant**

presented by

Ludovic Gaut

to obtain the academic degree of :

PHILOSOPHÆ DOCTOR FROM SORBONNE UNIVERSITÉ

PhD thesis subject :

**Mechanical and molecular signals underlying tendon cell
differentiation**

Publicly presented and defended on the 12th of October, 2018

in front of a PhD committee composed by :

Dr	Céline Colnot	Reviewer
Dr	Ronen Schweitzer	Reviewer
Dr	Athanassia Sotiropoulos	Examiner
Pr	Christophe Egles	Examiner
Pr	Isabelle Petropoulos	Sorbonne Université representative
Dr	Delphine Duprez	PhD director
Dr	Mathias Mericskay	PhD director

There they stood, ranged along the hillsides, met
To view the last of me, a living frame
For one more picture! In a sheet of flame
I saw them and I knew them all. And yet
Dauntless the slug-horn to my lips I set,
And blew. 'Childe Roland to the Dark Tower came.'
Robert Browning (1855)
Childe Roland to the Dark Tower came (34)

Contents

Acknowledgments	xiii
Résumé	xvii
Abstract	xix
Abbreviations	xxi
Nomenclature	xxiii
I Introduction	1
I.1 Overview of the musculoskeletal system	2
I.1.1 Skeletal muscle	2
I.1.2 Specialized connective tissues : bone and cartilage	4
I.1.3 Tendon : a dense regular connective tissue	5
a) Tendon structure in vertebrates	5
b) Tendon and muscle interface : the myotendinous junction	8
c) Tendon to bone attachment : the enthesis	8
I.2 Muscle, bone and cartilage development	9
I.2.1 Muscle development	9
I.2.2 Cartilage and bone development	12
I.3 Tendon development	15
I.3.1 Tendon markers to study tendon development in vertebrates	15
a) Scleraxis	15
b) Tenomodulin	16
c) Mohawk	17
d) Early Growth Response 1	18
I.3.2 Embryological origins of tendons	19
a) Multiple origins	19
b) Cranofacial tendons	20
c) Axial tendons	21
d) Limb tendons	21
e) Development of tendon interfaces	23
I.3.3 Signaling pathways	26
a) Tendon cell specification	26
b) Tendon cell differentiation	28

I.4	Achieving tenogenic differentiation in cell cultures through biochemical treatments	29
I.4.1	Starting with a model: mesenchymal stem cells, adipose-derived cells and tendon stem/ progenitor cells	29
a)	Mesenchymal stem cells	29
b)	Adipose-derived mesenchymal stem cells	30
c)	Tendon stem / progenitor cells	31
I.4.2	Biochemical cues driving tenogenic differentiation	32
I.5	Mechanobiology and development	35
I.5.1	Mechanical forces in development	38
a)	Intrinsic mechanical cues and early development	38
b)	Extrinsic mechanical cues: extracellular matrix and external factors in morphogenetic control	41
I.5.2	Mechanical signal transduction at molecular level	43
a)	Mechanosensing: how cells detect forces	44
b)	Mechanotransduction and gene expression	48
I.6	Tendon mechanobiology	53
I.6.1	Mechanical properties of tendons and response to mechanical loading	53
I.6.2	Mechanobiology of tendon development	55
I.6.3	Tendon cell behavior in regard with its physical environment	58
a)	Importance of the environment: 2D vs 3D	58
b)	Stretching the cells as a way to direct tendon differentiation	60
II	Aims and objectives	65
III	Muscle contractions are required to maintain tendon development and mechanosensitive gene expression in tendons of chicken fetuses	67
III.1	Context	67
III.2	Results	67
III.2.1	Immobilization of chicken fetuses is deleterious for limb tendon formation	67
III.2.2	Immobilization of chicken fetuses increases cartilage gene expression, while decreasing muscle gene expression in limbs	73
III.2.3	Mechanosensitive genes are affected by limb paralysis	76
III.2.4	The mechanosensitive factor SRF is not expressed in limb tendons of chicken fetuses	80
III.2.5	Residual tenogenic-like niches persist in paralyzed limbs	82
III.2.6	Restored muscle contractions after 24H of immobilization is paired with recovery of tendon gene expression	84
III.2.7	Restored muscle contractions after 48H of immobilization enables a partial recovery of tendon formation based on <i>SCX</i> expression	87
III.3	Discussion	90
III.3.1	Paralysis differentially affect lineage markers in limbs	90
III.3.2	Defective muscle splitting in immobilized chicken fetuses	91
III.3.3	Remaining tenogenic niches in limbs of paralyzed chicken fetuses and recovery of muscle contractions	91
III.3.4	YAP and <i>EGR1</i> expression is correlated to mechanical signals in the limb	92
III.3.5	SRF does not appear to be involved in limb tendon development of chicken fetuses	92
III.4	Conclusion	92

IV	Effect of mechanical constraints and TGFβ2 on the tendon differentiation potential of mouse mesenchymal stem cells	95
IV.1	Abstract	95
IV.2	Introduction	95
IV.3	Results	97
IV.3.1	The initial cell number did not change the expression of tendon genes in C3H10T1/2 cells, 16H after plating.	98
IV.3.2	Substrate effects on the expression of cell lineage and differentiation markers in C3H10T1/2 cells cultured for 16H	100
IV.3.3	Effect of confluence on the differentiation potential of C3H10T1/2 cells cultured on plastic substrate	102
IV.3.4	Effect of confluence on the differentiation potential of C3H10T1/2 cells cultured on silicon substrate overtime	105
IV.3.5	Inverse correlation between active TGF β signalling pathway and <i>Tnmd</i> expression in C3H10T1/2 cells in 2D cell cultures and 3D-engineered tendons	107
IV.4	Discussion	111
IV.4.1	Comparison of the tendon differentiation potential for C3H10T1/2 cells cultured on plastic and silicon substrates in confluence conditions	111
IV.4.2	TGF β 2 is a negative regulator of <i>Tnmd</i> expression in C3H10T1/2 cells in 2D and 3D culture systems	112
IV.5	Conclusion	112
V	Role of mechanical constraints, EGR1 and YAP in a 3-dimensional culture system of C3H10T1/2 cells mimicking tendon formation	115
V.1	Context	115
V.2	Results	115
V.2.1	<i>Egr1</i> overexpression prevents the decrease of tendon gene expression in fibrin-based 3D-constructs after tension release	115
V.2.2	Collagen 3D-constructs made of C3H10T1/2 cells harbor a tendon-like structure	117
V.2.3	Modifications of mechanical parameters in the collagen 3D-constructs affect cell organization	119
V.2.4	Mechanical state affects the expression of tendon genes and other lineage genes in collagen 3D-constructs	124
V.2.5	YAP and EGR1 mechanosensitive pathways in collagen 3D-constructs	125
V.2.6	Proportions of cells with YAP ⁺ and/or Scx ⁺ nuclei depend on collagen 3D-construct mechanical state	130
V.2.7	Verteporfin-induced YAP knock-down impairs tendon gene expression in collagen 3D-constructs	132
V.2.8	Mechanical stimulation of Verteporfin-treated collagen 3D-constructs does not rescue the downregulation of tendon gene expression	137
V.2.9	Chemical modulation of mechanotransduction pathways in collagen 3D-constructs made of C3H10T1/2 cells	137
V.3	Discussion	139
V.3.1	Tendon and cartilage gene expression in fibrin and collagen 3D-constructs favors collagen over fibrin constructs as model to study tendon cell differentiation	140
V.3.2	Variation in the internal structure in 3D constructs is representative of their mechanical state	141
V.3.3	<i>Scx</i> expression is modulated by mechanical cues	141
V.3.4	EGR1 and YAP act downstream of mechanical cues	142
V.3.5	YAP is involved in the regulation of tendon phenotype	142

V.3.6	Possible relationship between YAP and EGR1	143
V.4	Conclusion	143
VI	Discussion and Perspectives	145
VI.1	The tendon phenotype is sensitive to mechanical signals both in <i>in vivo</i> and <i>in vitro</i> models	145
VI.2	How mechanical signals are sensed and interpreted by tendon cells	146
VI.2.1	YAP acts as an intracellular relay of mechanical signals to regulate tendon gene expression	146
VI.2.2	Possible interactions between YAP and EGR1 in tendon cells	147
VI.2.3	How are mechanical signals sensed by cells achieving tenogenic differentiation?	148
VI.3	Tnmd expression to assess tendon cell differentiation	149
VI.3.1	Consistent dichotomy in <i>Scx</i> and <i>Tnmd</i> expression independently of the model	149
VI.3.2	Link between <i>Egr1</i> and <i>Tnmd</i> expression	150
VI.4	Validity of cellular model	150
VI.4.1	MSC: what the acronym is all about	150
VI.4.2	Naive cells or tendon cells?	151
VII	Conclusion	153
VIII	Material & Methods	155
IX	References	161
X	Annexes	187
X.1	EGR1 Regulates Transcription Downstream of Mechanical Signals during Tendon Formation and Healing	188
X.2	The Osteogenic and Tenogenic Differentiation Potential of C3H10T1/2 (Mesenchymal Stem Cell Model) Cultured on PCL/PLA Electrospun Scaffolds in the Absence of Specific Differentiation Medium	205
X.3	Tendon development and diseases	225
X.4	Signaux moléculaires et mécaniques intervenant dans la différenciation des cellules tendineuses	245
X.5	Curriculum Vitae	249

List of Figures

I.1	Histological organization of skeletal muscles.	2
I.2	The neuromuscular junction.	3
I.3	Anatomy of a long bone.	5
I.4	Tendon architecture.	7
I.5	Structure of the myotendinous junction.	8
I.6	Simplified representation of muscle cell differentiation and the myogenic regulatory factors.	10
I.7	Origin of skeletal muscles of the trunk and limbs.	11
I.8	Embryonic and fetal myogenesis.	12
I.9	Embryonic origins of bone and cartilage.	13
I.10	Schematic representation of endochondral bone formation.	14
I.11	Representation of Scx expression in developmental, postnatal and adult tendons.	16
I.12	Embryonic origins of tendons.	20
I.13	Muscle-dependency for head, limb and axial tendon development.	23
I.14	Formation of the myotendinous junction.	24
I.15	The developing eminence and enthesis.	26
I.16	The differentiation potential of mesenchymal stem cells.	30
I.17	Summary of the biochemical cues inducing tenogenesis <i>in vitro</i>	35
I.18	Number of publications per year related to the PubMed search “Mechanobiology” between 1920 and 2017	36
I.19	The three major types of protein filaments forming the cytoskeleton.	39
I.20	Epithelial tissue closure.	41
I.21	Extrinsic mechanical cues applied on the cells.	43
I.22	Integrins and adhesion points.	45
I.23	Cell-cell junction at the cadherin complex.	47
I.24	The two principal pathways regulating SRF activity.	49
I.25	Yap activity is influenced by the Hippo signaling pathway and mechanical cues.	51
I.26	Mechanical stimuli influencing YAP activity and subcellular localization.	53
I.27	Generic changes observed in tendon structure upon strain.	54
I.28	Tissue elasticity scale.	59
I.29	Examples of 3D culture systems.	60
III.1	DMB-induced paralysis between E7 and E9 affects <i>SCX</i> expression in limbs of chicken fetuses	68
III.2	Wholemout hybridization to <i>SCX</i> in limbs of chicken fetuses from control or paralyzed groups.	69

III.3	<i>In situ</i> hybridization to limb transverse sections with <i>SCX</i> , <i>TNMD</i> and <i>COL1A1</i> of 24H DMB limbs.	71
III.4	<i>In situ</i> hybridization to limb transverse sections with <i>SCX</i> and <i>TNMD</i> probes of 48H DMB limbs.	72
III.5	<i>In situ</i> hybridization to limb transverse sections with <i>SCX</i> and <i>COL1A1</i> probes of 48H DMB limbs.	73
III.6	Cartilage gene expression is modified in paralyzed limbs.	74
III.7	Muscle gene expression is impaired in paralyzed limbs for 24H and 48H.	76
III.8	Rigid paralysis impairs <i>EGR1</i> gene expression in tendons.	77
III.9	YAP signaling is impaired by rigid paralysis in limbs of paralyzed chicken fetuses.	78
III.11	<i>SRF</i> is not expressed in limb tendons of chicken fetuses.	81
III.12	Persistence of COLXII staining, a tendon-ECM marker, in E7+48H DMB limbs.	82
III.13	Reintroduction of muscle contractions after 24H of rigid paralysis induces a recovery of <i>SCX</i> expression.	85
III.14	Reintroduction of muscle contractions for 24H is sufficient to recover <i>SCX</i> expression in limbs paralyzed for 24H.	86
III.15	48H reintroduction of muscle contractions after 48H of paralysis.	88
III.16	48H reintroduction of muscle contractions after 48H of paralysis allows for a partial reformation of tendon structures and <i>SCX</i> expression.	89
IV.1	The initial cell number at the plating time does not change tendon gene expression, 16H after plating.	99
IV.2	The nature of the substrate does not modify the initial expression profile of tendon genes in C3H10T1/2 cells 16H after plating.	101
IV.3	Effect of cell confluence overtime on tendon gene expression in C3H10T1/2 cells cultured on plastic substrate	103
IV.4	Effect of cell confluence overtime on tendon gene expression in C3H10T1/2 cells cultured on silicone substrate	107
IV.5	Correlation between TGF β 2 activity and <i>Scx</i> and <i>Tnmd</i> expression and dual effect of TGF β 2 on <i>Tnmd</i> and <i>Scx</i> expression in C3H10T1/2 cells cultured in 2D or 3D-engineered tendon.	109
IV.6	Comparison of cell expansion effect on gene expression between the plastic and substrate culture conditions.	111
V.1	(Previous page) <i>Egr1</i> overexpression prevents the downregulation of tendon-associated gene expression in tension released engineered tendons.	117
V.2	Width of collagen 3D-constructs reduces overtime.	118
V.3	Evolution of gene expression overtime in fibrin and collagen 3D-constructs.	119
V.4	Schematic representation of the different mechanical states applied to collagen 3D-constructs	120
V.5	Cell organization in collagen 3D-constructs.	120
V.6	Nucleus and cell orientations in collagen 3D-constructs in different mechanical states.	122
V.7	Alterations of mechanical states do not affect cell proliferation in collagen 3D-constructs.	123

V.8	Alteration of mechanical states induces changes in tendon gene expression in collagen 3D-constructs.	124
V.9	Mechanosensitive gene expression in collagen 3D-constructs in de-tensioned and stretched conditions.	126
V.10	Tension release in collagen 3D-constructs induces a decrease in the proportion of cells with EGR1 ⁺ nuclei.	127
V.11	YAP activity in collagen 3D-constructs is linked to mechanical signals.	128
V.12	YAP/SCX double staining in collagen 3D-constructs.	130
V.13	Proportions of cells with YAP ⁺ and/or SCX ⁺ nuclei in collagen 3D-constructs.	131
V.14	VTPF-treatment induces changes in gene expression in 2D-cultured C3H10T1/2 cells.	133
V.15	24H VTPF-treatment in collagen 3D-constructs impairs the expres-sion of mechanosensitive genes but not the number of YAP ⁺ nuclei. .	134
V.16	VTPF-induced YAP knock-down impairs tendon phenotype in colla-gen 3D-constructs.	135
V.17	YAP knock-down in collagen 3D construct induces a decrease in the proportion of SCX ⁺ nuclei in cells already exhibiting YAP ⁺ nuclei. .	136
V.18	Stretch does not rescue gene expression in collagen 3D-constructs with VTPF-induced YAP knock-down.	137
V.19	LPA treatment of collagen 3D-constructs made of C3H10T1/2 cells. .	138
V.20	CCG-1423 treatment of collagen 3D-constructs made of C3H10T1/2 cells.	139
VI.1	Link between mechanical signals, YAP activity and tendon gene ex-pression.	146
VI.2	Hypothetical model of tendon gene expression regulation by mechan-ical signals through YAP activity.	147
VI.3	Egr1 mechanosensitive expression is also regulated by another mechan-otransduction pathway.	148
VI.4	Evolution of <i>Scx</i> and <i>Tnmd</i> gene expression overtime in fibrin-based 3D-construct made of mouse tail tenocytes.	152

List of Tables

I.1	Introduction to terms and concepts in mechanobiology.	37
I.2	Mechanical properties of various tendons.	55
I.3	Examples of genetic and chemical manipulations enabling the study of the mechanoregulation of musculoskeletal formation and home- ostasis.	57
I.4	Stretch protocols modulating tendon-genes expression <i>in vitro</i>	61
VIII.1	RT-qPCR primers	159

Acknowledgments

I have taken efforts in this project these last 4 years, but this would not have been possible without the help, guidance and advices from many people to whom I would like to express my gratitude hereafter. As French is my maternal language and not all these persons are English-speakers, I will do so both in English and French, when appropriate.

To Delphine Duprez and Mathias Mericskay, my two supervisors. I am deeply thankful to both of you for accepting me in this project. You both trusted me and were always opened to discuss the project regularly between the three of us, offering me numerous advices to develop it.

To Delphine, for your guidance, your fruitful advices, your never-ending time when it came to your patient proofreading, or to answer my numerous questions, doubts and burst of optimism: thank you so much. You offered me a good working and scientific environment and several opportunities to present my work, in the lab, in France and abroad. All of those are part of the scientific wealth that I will cherish in the future.

To Mathias, for always offering me your advices and critical thinking on my experiments and results. I really benefited from your point of view and particularly during the lab meetings in B2A. You made me part of your team although I was not always physically with you and even from Châtenay you were ready to discuss and comment my project. Thank you very much, Mathias.

Je remercie la Fondation pour la Recherche Médicale, qui a financé ma 4^{ème} année de thèse et qui m'as permis de mener ce projet à bien.

To the members of my jury, who accepted to read my thesis, review it, and for their participation the day of my defense, I would like to express my gratitude. To Dr. Céline Colnot, Pr. Christophe Egles, Pr. Isabelle Petropoulos, to Dr. Athanassia Sortiropoulos and finally to Dr. Ronen Schweitzer who accepted to be part of this jury and to come from Portland, USA, I am really grateful.

I would also like to extend my gratitude to the members my thesis committee, Pr. Onnik Agbulut, Dr. Sigolène Meilhac and Dr. Athanassia Sotiropoulos. You accepted to meet during my thesis to look at the development of this project and to give me your advices that were really helpful during that time.

À Estelle Hirsinger et Tommaso Lucchesi, qui avez accepté de relire cette thèse en plus de Delphine et Mathias. Pour vos relectures attentives et vos critiques constructives sur le présent manuscrit, je vous remercie sincèrement.

À tous les membres de l'équipe Duprez, passés et présents, je tiens à vous remercier de façon générale. Merci pour votre accueil, votre soutien technique, scientifique et moral dont j'ai énormément bénéficié et sans lesquels je ne serai pas venu à bout de ces 4 années. Mes excuses, sincères, pour vous avoir fait subir autant de fausses notes lors de mes reprises incessantes de Céline Dion, Garou, Shakira, ou lors de mes longues sessions de sifflotement !

Beatriz – I sincerely enjoyed getting to know you, Señorita de la emoji Poopy face!

Cédrine - Pour avoir répondu à mes questions incessantes sur tous les aspects des marquages par immunofluorescence, la microscopie, mais aussi pour tes rires et ta bonne humeur, je te remercie sincèrement, ma copine du labo.

Cécile M. – A tes gâteaux et ce merveilleux batteur à œufs !

Claire - Merci Claire pour tes conseils toujours aussi constructifs et bienveillants à mon égard. Merci aussi de m'avoir appris à implanter et stimuler les embryons de poulet, c'est une expérience qui a été aussi difficile que passionnante pour moi et pour laquelle je regrette de n'avoir pas été plus loin.

Emmanuelle – Ne nous mentons pas, tu es déjà la meilleure dresseuse ! Un grand merci à toi pour tous ces rires, mais aussi pour tes conseils et ton aide avec mes expériences. Je n'ai jamais oublié cette discussion qu'on a eu avant que j'aie donné ma première présentation à un congrès et qui m'a servi à de nombreuses reprises depuis. Pour tout ça, merci Emmanuelle.

Estelle – Estelle, merci à toi pour tous ces échanges sincères, amicaux et scientifiques qui sont autant de bons moments passés au labo ces dernières années. Et merci pour l'intérêt et l'aide que tu m'as apporté pendant cette thèse.

Hélène Rouard - Hélène, j'ai beaucoup apprécié le temps que nous avons passé ensemble au labo. Merci aussi à toi pour tes conseils scientifiques et professionnels qui m'ont aidé à mûrir mon projet d'après-thèse.

Isabelle – Pour ces discussions sur les modèles 3D, mais aussi ces conseils de lecture et ces desserts, merci à toi !

Joana – Quel plaisir de t'avoir rencontrée, Kiki-Joana. Merci à toi d'avoir guidé mes premiers pas à notre paillasse, avec beaucoup de patience et de pédagogie. Et merci pour ton amitié et ton énergie, qui ont toujours une place spéciale pour moi.

Kwang-Pyo - Naneun uli moim-eul jeulgyeossda! Annyeong Kwang-Pyo!

Marianne – Ma dernière voisine de paillasse. Et quelle voisine ! Il y a de belles rencontres à faire tout au long de la thèse. Merci Mamie pour tous nos rires et ces superbes moments passés ensemble et au grand plaisir d'en passer encore de nombreux comme ceux-ci !

Marie-Ange - A toi, ma géniale colocataire de bureau. Il y aurait tellement de choses à dire, tant tu as vécu ces 4 années au plus près de mes explosions de joie, de rire, de tristesse et de doute, aussi. Ton soutien et ton attention toute particulière à mon égard, sur le plan technique, moral ou amical ont fait office de fil d'Ariane pour me retrouver dans ce dédale doctoral ! A ta fleur qui par sa chute nous aura ouvert tant de rires et de complicité, à tous ces petits-déjeuners pépèresques, à nos nombreux échanges : je les garderai précieusement en mémoire et je t'en remercie du fond du cœur.

Marvin - I will never forget your kindness...and the Stroopwafles !

Mickael – Merci Mickael pour tes conseils et ton aide qui m'ont été précieux et m'ont bien fait réfléchir à mon projet. Et au-delà de ça, merci à toi Papy thésard d'avoir été si bienveillant, amical, musicalement et cinématographiquement cultivé. Kiki-Micky, merci !

Nicolas – Nous ne nous sommes vus que brièvement, mais il est sûr que tu auras marqué mon début de thèse. Sache que je chasse toujours les envahisseurs!

Pau – If I can say I was lucky during so many aspects of my PhD, it is because of occasions like the time we spent together in the lab. Thank you for being such a great, enthusiast, smart and motivated co-worker and friend.

Sonya - Que j'ai aimé nos rires, nos discussions, sérieuses ou non, nos repas à la cantine

(et terminer tes desserts au goûter), et tous ces autres moments qu'il serait trop long de citer mais qui foisonnent dans mon esprit alors que j'écris ces lignes. Plus qu'une voisine de bureau, une co-thésarde de labo, j'ai trouvé une amie sincère, de ces amis à qui je sais pouvoir dire « A très bientôt !! », quelque soit le côté de l'Atlantique où nous nous trouverons. Alors, ma Kiki-Soso, je te dis à très bientôt pour d'autres bonnes tranches de rire et de vie !

À l'équipe de Zhenlin Li, mon « autre équipe » de Biological Adaptation and Aging (B2A) : Zhenlin, Denise Paulin, Dario, Ara, Jocelyne, Jacqueline, Zhigang, Jeff, Lei, Robin, Cynthia, Marie-Thérèse et Alexandra. Je vous remercie pour votre accueil toujours aussi chaleureux, que ce soit pour un lab meeting ou un pot. Jeff, merci à toi que j'ai rencontré lors de mon premier entretien de M2 à Cochin et qui depuis as toujours été cette présence bienveillante dans mon environnement.

Aux personnes du 6^{ème} étage, parmi lesquelles j'ai évolué ces dernières années. Votre accueil et votre esprit de groupe ont grandement participé à mon bien-être quotidien ! À Thierry, Pierre, Pierre-Yves, Laurence, Cécile D., Charles, Grégoire, Keirthhana, merci à vous tous !

À Hanane - Nous sommes arrivés en même temps mais excuse-moi de partir avant toi. Merci pour ta chaleur et tes rires, ta bonne humeur, ta gentillesse. Tu es une personne formidable !

À Rodolphe – Merci pour ta gentillesse, ta bonne humeur et tes jeux de mots sans égal, tous tes rires et tes sourires.

À Sophie – Cette thèse serait bien fade sans tes illustrations, aussi belles qu'instructives. Tes marques d'attention m'ont toujours touché, qu'il s'agisse d'un sourire depuis l'autre bout du couloir ou d'une bonne discussion. Pour tout cela, merci Sophie !

À Viviane – Tu prends soin de tous les étudiants, « tes enfants » et tu t'assures qu'on ait toujours de quoi bien travailler et de quoi prendre un bon goûter. Pour toutes tes attentions, tes mots et tes sourires de ces dernières années, je te remercie du fond du cœur.

Mes remerciements vont aussi à Teresa Ferraro et Vlad Costache qui m'ont aidé à analyser les orientations des noyaux et des cellules de mes constructions 3D.

Je remercie également toutes les autres personnes du Laboratoire de Biologie du Développement que je n'ai pas citées mais qui ont participé au bon déroulement de cette thèse, que ce soit par de bons échanges scientifiques ou leur bonne humeur !

I was motivated enough to follow the adventure of the PhD and to dedicate myself to it these last years. For that I want to thank amazing people who led me to it and who taught me things that I still carry with me today. I am deeply grateful to Pr. James G. Martin, Nobuaki Hirota, PhD, Shannon McKinney-Freeman, PhD, Per Holmfeldt, PhD, Christophe Houbroun, Philippe Daubas, PhD and Pascal Maire, PhD.

À Yves Bergeret, dont la parole ne m'a jamais quittée depuis de nombreuses années maintenant. Tu m'as appris à observer, à écouter et à toujours m'émerveiller. Yves, merci pour tous ces échanges, si stimulants et passionnants. Si vivants.

À tous mes amis, je suis sûr qu'ils se reconnaîtront, je vous remercie du fond du cœur pour ce soutien extraordinaire. À Agathe, Alexandre, Amandine et Sébastien P., Anaïs, Anna et Thomas D., Annaelle et Ben, Charles-Henry, Charlotte et François B., Chloway et Thibeault, Christelle, Christophe, Daniel, David, Djihad et Marine, Emeric, Flore et Quentin, Floriane L., Floriane S., Guivrus, Haser, Jeanne, Jessica et Romain, Julien, Laure, Letty, Leyre et

Tommaso, Lisa et Xavier, Lydie, Maël et Elizabeth, Manon, Marie L. et Pierrick B. (Et Cham & Sem !), Marie et Maxime S., Marine D., Maud, Mélissandre, Morgane M., Morgane C. et Nicolas L., Nga et Kouroch, Nicolas T., Patrick T., Perrine, Rachael, Ségolène et Mathias, Simon C., Tamara et Jun, Thomas F., Victoire. La liste est non-exhaustive et chacun d'entre vous mériterait des pages entières dans ces remerciements, tant votre amitié, votre affection, votre soutien m'ont été indispensables lors de ces dernières années.

À Véronique, Patrick, Laure et Kevin. J'ai une chance extraordinaire de pouvoir vous appeler ma famille. Pour vous être toujours intéressés à ce que j'ai fait ces dernières années, mais surtout pour votre soutien précieux et essentiel, je vous remercie. A Véronique et Patrick : vous êtes des beaux-parents formidables et c'est bien peu de le dire. Ces dernières années lorsqu'il m'a semblé être perdu en pleine nuit dans une mer agitée, vous avez brillé comme un phare et m'avez ramené à bon port, je vous remercie tous les deux du fond du cœur.

À mon père, Jean-Pierre. Ça y est Papa, j'ai fini l'école. J'ai du mal à trouver les mots qui exprimeraient toute la gratitude que j'ai pour toi, non pas seulement pour ces années de thèse, mais pour ton aide et tes encouragements incessants depuis que j'ai franchi le seuil d'une salle de classe. Merci Papa.

To my wonderful wife, Margaux. Tu as toujours été là pour moi, à chaque seconde, une force essentielle dans toute cette aventure et bien plus encore. T'aimer et être aimé de toi, c'est respirer la vie.

Résumé

Les tendons représentent une forme unique de tissu conjonctif au sein du système musculo-squelettique. Ils sont composés d'une matrice dense de fibrilles de collagène de type I, organisées de façon à supporter les forces générées par les contractions musculaires et transmises à l'os. Bien que le collagène de type I soit le principal composant structural et fonctionnel des tendons, il est aussi exprimé dans de nombreux autres tissus. Ainsi, il ne peut servir seul de marqueur de la différenciation tendineuse et il doit être analysé en parallèle d'autres marqueurs de tendon. À ce jour, les meilleurs marqueurs tendineux sont Scleraxis (*Scx*), un facteur de transcription bHLH et Tenomodulin (*Tnmd*), une protéine transmembranaire. Le développement, l'homéostasie et la réparation du tendon reposent sur des combinaisons de paramètres moléculaires et aussi mécaniques, régulant la production et l'assemblage des fibres de collagène (Gaut et Duprez, 2016).

Notre objectif est de comprendre quelles sont les voies de mécanotransduction sous-jacentes à la différenciation tendineuse et quels sont en ce sens les rôles de deux (co-)facteurs de transcription : EGR1 (Early Growth Response 1) et YAP (Yes-Associated Protein). EGR1, le facteur de transcription à doigts de zinc, est encodé par un gène mécanosensitif et est impliqué dans la régulation de la transcription des gènes *Col1a1* et *Col1a2* au cours du développement et de la réparation des tendons (Guerquin et al., 2013). YAP est un co-facteur de transcription activé par les signaux mécaniques arrivant à la cellule (Dupont et al., 2011). Au cours de ce projet et en utilisant des approches *in vivo* et *in vitro*, nous avons testé l'hypothèse selon laquelle YAP et EGR1 joueraient le rôle de relais intracellulaire des forces mécaniques pour réguler la différenciation tendineuse.

Nous avons montré que l'expression du gène de tendon *SCX* était réduite dans les tendons de membres de fœtus de poulet immobilisés à partir de E7 entre 5H et 48H. Le gène mécanosensitif *EGR1* et la protéine YAP ont aussi montré une réduction de leur expression dans des conditions d'immobilisation. De plus, nous avons montré par marquage en immunofluorescence que la protéine YAP était exprimée dans les noyaux des cellules de tendon contrôles, mais pas dans les tendons des membres paralysés. Ceci renforce l'hypothèse selon laquelle YAP agit dans les tendons au cours de leur développement. Malgré une réduction de l'expression des marqueurs de tendon en contexte d'immobilisation, nous avons montré que des noyaux étaient toujours présents après immobilisation dans des zones de type tendineuses définies par un marquage du COLXII. De plus, la reprise des contractions musculaires après 24H ou 48H d'immobilisation a conduit à une récupération de l'expression des gènes de ten-

don comparable à celle des fœtus n'ayant jamais été immobilisés. Ceci montre que la perte d'expression de gène de tendon en contexte d'immobilisation est réversible.

La mécanobiologie du tendon a été étudiée grâce à des constructions cellulaires en 3-dimensions (3D) à base de gel de fibrine ou de collagène et composées de cellules souches mésenchymateuses reproduisant la formation des tendons. Une perte de tension de ces constructions 3D a induit une chute de l'expression de *Egr1* et des gènes de tendon. Une surexpression de *Egr1* dans les constructions 3D en gel de fibrine a permis d'éviter la chute d'expression des gènes de tendon en condition de perte de tension (Gaut et al., 2016). Dans les constructions 3D en gel de collagène, les cellules et leurs noyaux ont montré un alignement le long de l'axe principal de la construction 3D dans les constructions contrôles et étirées. Cependant, cet alignement est complètement perdu dans les constructions 3D sans tension, témoignant d'un changement d'organisation interne de ces constructions 3D en rapport avec leur état mécanique. L'activité de YAP a diminué dans les constructions 3D sans tension et a augmenté lorsque ces constructions ont été étirées, comme en témoignent les changements d'expression des gènes cibles de YAP et de la proportion de cellules avec des noyaux YAP⁺. L'activité de YAP a aussi été corrélée avec l'expression de *Scx* ainsi que la proportion de cellules avec des noyaux SCX⁺. Une inactivation chimique de l'activité de YAP par traitement à la vertéporfin (VTPF) a aussi permis d'établir un lien entre la chute de l'activité de YAP et une diminution de la proportion de cellules avec des noyaux SCX⁺, sans affecter celle des cellules avec des noyaux YAP⁺. De plus, nous avons montré que dans les constructions cellulaires en 3D, une proportion significative des noyaux était YAP⁺ et SCX⁺. Nous avons aussi montré que les changements dans la proportion de noyaux SCX⁺ induits par différentes conditions mécaniques ou par la VTPF se produisaient dans des cellules exhibant déjà des noyaux YAP⁺. Ce dernier résultat suggérerait que YAP serait en partie impliqué dans le contrôle de SCX. De plus, l'expression d'aucun des gènes de tendon n'a été restaurée lorsque des constructions 3D traitées à la VTPF ont été étirées. Ceci renforce l'hypothèse selon laquelle YAP agirait comme relai intracellulaire des signaux mécaniques pour réguler l'expression des gènes de tendon.

Ensemble, les résultats de ce projet montrent l'importance de YAP et EGR1 en aval des signaux mécaniques pour réguler la différenciation des cellules tendineuses.

Abstract

Tendons are unique forms of connective tissue of the musculoskeletal system. They are composed of a dense extracellular matrix of type I collagen fibrils that are hierarchically organized to withstand tensile forces transmitted from muscle to bone. Even though type I collagen is the main tendon structural and functional component, it is also expressed in many tissues and organs. To date the bHLH transcription factor Scleraxis (Scx) and the transmembrane protein Tenomodulin (Tnmd) are the best-known tendon markers. Tendon development, homeostasis and repair rely on specific combinations of mechanical parameters and molecular factors that regulate the production and assembly of collagen fibers (Gaut and Duprez, 2016). Our objective is to decipher the mechanotransduction pathways underlying tendon cell differentiation, notably through the activity of two transcription (co-)factors, EGR1 (Early Growth Response 1) and YAP (Yes-Associated Protein). The zinc finger transcription factor EGR1 is a mechanosensitive gene involved in *Col1a1* and *Col1a2* transcription during tendon development and repair (Guerquin et al., 2013). YAP is a co-factor of transcription activated upon a mechanical input in the cell (Dupont et al., 2011). During this project, we tested the hypothesis that YAP and EGR1 act as intracellular relays of mechanical forces during tendon cell differentiation using *in vivo* and *in vitro* approaches.

We showed that the expression of the tendon gene *SCX* was downregulated at the transcript levels in limb tendons of chicken fetuses immobilized from 5Hh to 48H at E7. The mechanosensitive gene *EGR1* and YAP activity also displayed decreased expression in immobilization conditions. Besides, we showed by immunofluorescent staining that the YAP protein is expressed in the nucleus of tendon cells of chicken fetuses, but not in tendons of paralyzed limbs. This strengthens the hypothesis that YAP is acting during *in vivo* tendon development. Despite the molecular downregulation of tendon markers after immobilization, nuclei were still observed in tendons, defined by COLXII immunostaining. Moreover, restored muscle contraction after 24H or 48H of immobilization led to a recovery of tendon gene expression comparable to that of fetuses that were never immobilized. This showed that the loss of tendon gene expression was reversible.

Tendon mechanobiology was studied *in vitro* in fibrin-based or collagen-based 3-dimensional (3D) constructs made of mesenchymal stem cells and mimicking tendon formation. Tension release in fibrin and collagen 3D-constructs induced a drop of the expression of *Egr1* and tendon genes. Forced-expression of *Egr1* was able to prevent the downregulation of tendon

gene expression in de-tensioned fibrin 3D-constructs (Gaut et al., 2016). Cell and nucleus orientations have been studied in collagen 3D-constructs and showed an alignment of both cell and nucleus along the construct long axis, under static and dynamic tension. However, this alignment was completely disrupted in the de-tensioned constructs, attesting for a change in their organization depending on the mechanical conditions.

YAP activity was decreased in de-tensioned collagen 3D-constructs and was upregulated in constructs on which a dynamic stretch was applied, as shown by changes in Yap target gene expression and in YAP⁺ nuclei proportion. The YAP activity was also paired with the expression of the tendon gene *Scx* as well as with the number of Scx⁺ nuclei in the 3D constructs. Chemical knock-down of YAP activity was also paired with a decrease in the proportion of Scx⁺ nuclei, but not in the one of YAP⁺ nuclei.

Besides, we showed that in collagen 3D-constructs, a significant part of the nuclei was positive for both YAP and Scx. We also showed that the variation previously observed in the proportion of Scx⁺ nuclei in different mechanical conditions, or under VTPF-treatment, happened in a population of cells already exhibiting YAP⁺ nuclei. This last result would suggest that YAP is at least partly involved in the control of Scx in the cells. Furthermore, none of the tendon genes had their expression restored when a dynamic stretch was applied in VTPF-treated tendon constructs. This strengthens the hypothesis that YAP acts as an intracellular relay of mechanical cues regulating tendon gene expression.

All together, these results highlight the importance of EGR1 and YAP downstream of mechanical forces during tendon cell differentiation.

Abbreviations

2D – 2-Dimensional	Cyr61/CYR61 – Cystein Rich Angiogenic Inducer 61
3D – 3-Dimensional	Dcn - Decorin
Acan/ACAN - Aggrecan	Dlx5/DLX5 – Distal-less homeobox 5
ACh – Acetylcholin	DMB – Decamethonium bromide
AChR – Acetylcholin receptor	E – Young’s Modulus
Acta2/ACTA2 – Actin, alpha 2, smooth muscle, aorta	E (+Number) – Embryonic day
ADSC – Adipose-derived Stem Cell	ECM – Extracellular matrix
AER – Apical Ectodermal Ridge	Egr/EGR (1, 2) – Early Growth Response
AMOT - Angiomotin	Etv4/ETV4 – Ets variant 4
Aqp1/AQP1 – Aquaporin 1	FACITs - Fibril-Associated Collagens with Interrupted Triple helices
BAT – Bioartificial Tendon	FAK – Focal Adhesion Kinase
Bglap/BGLAP – Bone gamma carboxyglutamate protein	FDP – Flexor Digitorum Profundus
BMP – Bone Morphogenetic Protein	FDS – Flexor Digitorum Superficialis
BMSC – Bone Marrow Stem Cell	FGF – Fibroblast Growth Factor
Cebpb – CCAAT/enhancer binding protein beta	FLNA – Filamin A
cMM – chicken MicroMass	FLP – Finger-like processes
Col1a1/COL1A1 – Type I collagen, chain α 1	Fmod - Fibromodulin
Col1a2/COL1A2 – Type I collagen, chain α 2	FN - Fibronectin
Col2a1/COL2A1 – Type II collagen, chain α 1	GDF (5, 6, 7, 8) – Growth Differentiation Factor
Col3a1 – Type III collagen, chain α 1	GFP – Green Fluorescent Protein
Col5a1 – Type V collagen, chain α 1	Hh - Hedgehog
Col12a1 – Type XII collagen, chain α 1	HSS – Hank’s saline solution
Col14a1/COL14A1 – Type XIV collagen, chain α 1	Ihh – Indian Hedgehog
COLXII – Type XII collagen	Inhba/INHBA – Inhibin beta A subunit
COLXIV – Type XIV collagen	ISB – Intersegmental Boundary
Ctgf/CTGF – Connective Tissue Growth Factor	K - stiffness
	Lama2 – Laminin, alpha 2
	Lats (1, 2) – Large tumor suppressor kinase
	LPA – Lysophosphatidic acid

MAPK – Mitogen-activated kinase protein	Runx2/RUNX2 – Runt related transcription factor 2
Mdg – Muscular dysgenesis	Scx/SCX - Scleraxis
MEK – MAP kinase-ERK kinase	SLRP – Small Leucine Rich Repeat
Mkx/MKX - Mohawk	Sox/SOX (5, 6, 9) – SRY-related HMG-box
MRF – Myogenic Regulatory Factor	Sp – Splotch
Mrf4 – Myogenic regulatory factor 4	Spd – Splotch delayed
MRTF – Myocardin-Related Transcription Factor	SRF – Serum Response Factor
MSC – Mesenchymal Stem Cell	TAZ - Tafazzin
Mst (1, 2) – Macrophage stimulating	Tbx1 – T-box 1
MTJ – Myotendinous junction	TCF – Ternary Complex Factor
Myf5/MYF5 – Myogenic factor 5	TEAD – TEA Domain protein
MyoD – Myogenic differentiation	TGF β – Transforming Growth Factor β
Myog - Myogenin	Thbs/Tsp (2,4) - Thrombospondin
NCC – Neural Crest Cell	TnC – Tenascin C
NMJ - Neuromuscular Junction	Tnmd/TNMD – Tenomodulin
Osx - Osterix	TPC – Tendon Progenitor Cell
Pax/PAX (1,3,7) – Paired box	TR – Tension Release
Pparg – Peroxisome proliferator activated receptor gamma	TRP – Transient Receptor Potential
PTHrP – Parathyroid hormone-related protein	TSPC – Tendon Stem and Progenitor Cell
PZ – Progress Zone	Vcl/VCL - Vinculin
RhoA – Ras homolog family member A	VTPF - Verteporfin
Rn18S – 18S ribosomal RNA	Wnt – Wingless-related integration site
Rplp0 – Ribosomal protein, large, P0	YAP – Yes-Associated Protein
	ZP – Zona Pellucida

Nomenclature

The current established gene nomenclature is as follows:

- for mouse, in italic, the first letter is upper case, the rest is lower case
- for chicken and human, in italic, full name is in upper case
- for zebrafish, in italic, full name is in lower case

Gene expression is systematically displayed in “*italic*”.

Proteins are indicated in upper case.

I. Introduction

“The man in black fled across the desert and the gunslinger followed”

The Gunslinger – Stephen King

This scene of pursuit is how we enter the quest of Roland of Gilead, in the famous Stephen King’s novel “The Gunslinger” from its saga “The Dark Tower”. Besides laying the groundwork for the whole series in one sentence, King also sets the reader directly into the action by depicting one of the most common things in the animal kingdom: two bodies in motion in an act of flight and pursuit. In the body, form, movements, stability and balance are supported by the musculoskeletal system, which is composed by muscles, bones, cartilage, tendons, ligaments and other connective tissues. These tissues are all arranged to work together in order to achieve these functions and their particular organization is set up since developmental life. Among these tissues, the tendons link muscles to bones to transmit forces generated by muscle contractions to the bones, resulting in a movement. During my PhD project, I tried to understand how this tissue was impacted by its mechanical environment, either by muscle-generated forces or by a lack of tension, at the developmental, cellular and molecular levels. In that aim, I used the chick fetus as an *in vivo* developmental model and a murine cell line of mesenchymal stem cell cultured in 2-dimension (2D) or 3-dimension (3D) to mimick tendon cell differentiation.

In this introduction, I wish to present the tendon in relation to its musculoskeletal counterparts in order to better understand how they shape its role in this system. I will first give an overview of muscle, bone and cartilage tissues before giving a description of tendon structure and its interface with these tissues.

I will then explain how these tissues develop, with a particular interest on what is currently known about tendon development, at the embryological, cellular and molecular levels.

The understanding of tendon cell differentiation is also studied outside of its *in vivo* paradigm, in cell culture systems. As such, I would like to describe what are the main biological sources used as a “starting point” and the biochemical and molecular cues driving the specification of a naive cell into the tenogenic lineage.

Then, as the title of this PhD thesis indicates, the chemical and molecular factors are not the only parameters to take into account in Biology. Thus, I will explain how the mechanical parameters generally affects developmental and cellular systems and what are the main molecular actors integrating them in the cells. I will give a specific description of one of these factors as it was studied during my PhD project, the Yes-Associated protein (YAP). Finally, I will give an overview as how tendons and tendon cells are studied in the context of the mechanobiology. This will be done both for understanding the development of this tissue as for inducing tendon cell differentiation.

I.1 Overview of the musculoskeletal system

I.1.1 Skeletal muscle

Skeletal muscles constitute, with cardiac muscles, a form of striated muscles representing 40% of the human body weight and the most abundant type of tissue in the vertebrate body . (Yin et al., 2013). The best-known feature of the skeletal muscle is to contract and cause movement through its interaction with the other components of the musculoskeletal system, but it also has a role in general metabolism (Trovato et al., 2016). Histologically, each skeletal muscle includes various tissues: the muscle fibers, blood vessels, nerves and connective tissues. These connective tissues compartmentalize the skeletal muscle. Each muscle is thus wrapped into a sheath of dense irregular connective tissue termed the epimysium, maintaining its structural integrity. Inside each skeletal muscle, the muscle fibers are bundled together into fascicles by an intermediate layer of connective tissue called the perimysium. Finally, inside each fascicle, a thin layer of collagen and reticular fibers, called the endomysium isolates the muscle fibers (Figure I.1) (Trovato et al., 2016). This connective tissue has numerous roles with regard to the skeletal muscle development, homeostasis and regeneration (Nassari et al., 2017; Trovato et al., 2016; Webster et al., 2016). The muscle fibers enwrapped by the endomysium are differentiated and multinucleated contractile cells called the myofibers.

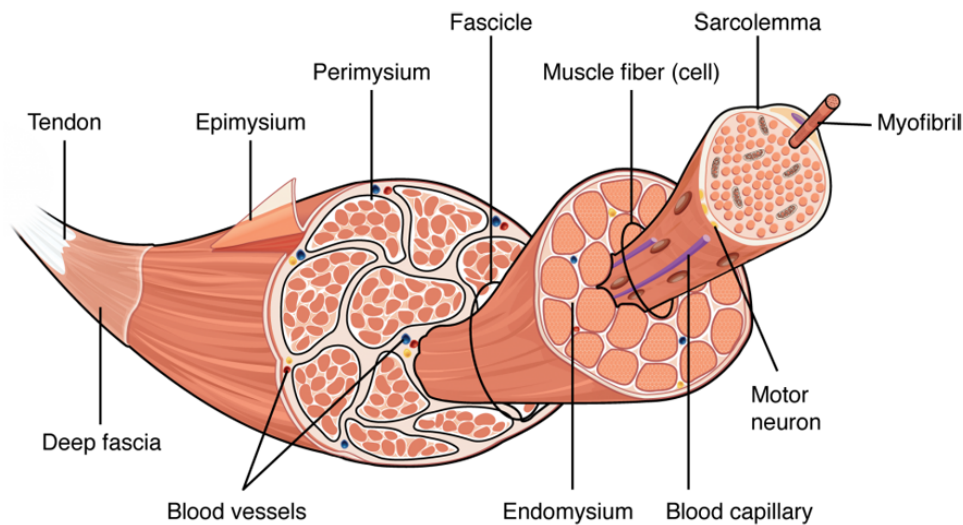


Fig. I.1 **Histological organization of skeletal muscles.** The skeletal muscles are linked to tendons at both ends and surrounded by the epimysium, a dense sheath of connective tissue. They are then hierarchically compartmentalized into fascicles by the perimysium and into muscle fibers by the endomysium. The endomysium will delimit the immediate environment of the muscle fibers, with blood capillaries, junction of motor neurons or extracellular fluids. Adapted from the Open Textbook “Anatomy and Physiology - Chapter 10: Muscle Tissue” from the Oregon State University.

A single myofiber originates from the fusion of a large number of muscle progenitors and are thus multinucleated. Their sarcoplasm, containing all the cytoplasmic organelles, consists mainly of myofibrils that are all aligned to the longitudinal axis of the fiber and push the nuclei at its periphery. All these myofibrils are specifically arranged to allow contraction of the myofiber (Trovato et al., 2016).

Voluntary control of muscle contractions by the central nervous system is dependent of the effective innervation of the skeletal muscles and of the efficiency of the neuromuscular junction (NMJ) (Figure I.2). The NMJ is a chemical synapse formed by the motoneuron on one side and the muscle fiber on the other side. Upon the arrival of action potentials, the nerve terminal will release acetylcholine (ACh) that will then activate their ACh receptors (AChR) located on the near muscle fiber. The activation of the AChR will trigger the depolarization of the muscle fiber through an entry of Na^+ ions, driving an action potential to an invagination of the muscle fiber called the T-tubule. This phenomenon will initiate subsequently Ca^{2+} release from the sarcoplasmic reticulum that will act on the myosins and their associated molecules to initiate muscle contraction (Figure I.2) (Darabid et al., 2014; Purves et al., 2004). Ultimately, the pre- and post-synaptic parts of this system become tuned with one another, the level of pre-synaptic transmitter released being adapted to the capacity of the post-synaptic activation.

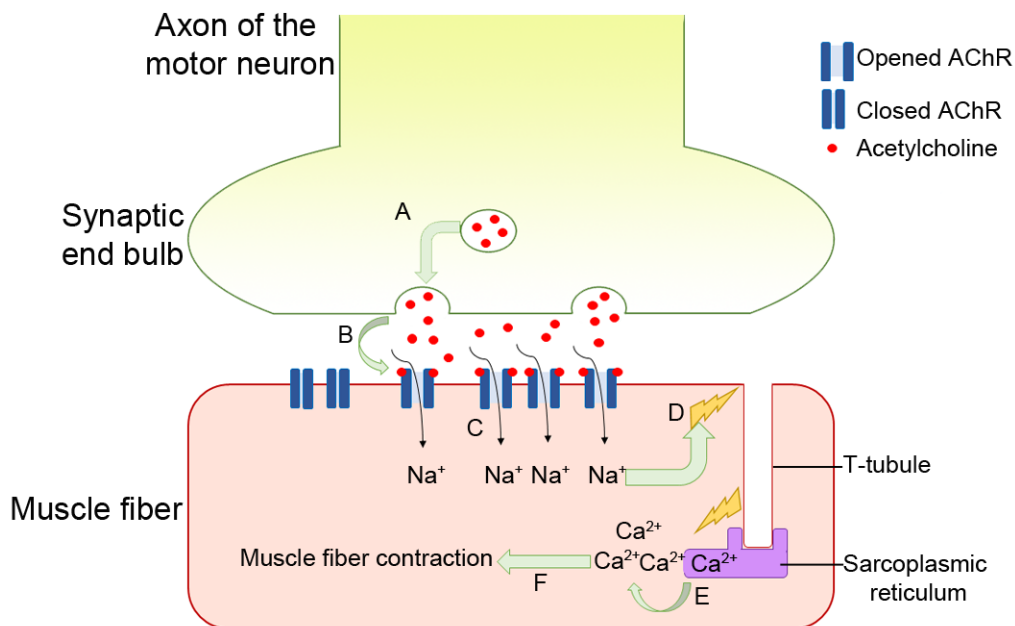


Fig. I.2 **The neuromuscular junction.** (A) Acetylcholine (ACh) vesicles in the moto neuron will be released in the synaptic cleft. (B) ACh molecules (red dots) will bind their receptors (AChR), resulting in their opening. (C) Upon opening of these receptors Na^+ will enter the muscle fiber. (D) This will create a membrane depolarization and an action potential (yellow strike). (E) The action potential will be transmitted all along the T-tubule to the sarcoplasmic reticulum, releasing Ca^{2+} ions in the muscle fiber. (F) Ca^{2+} will act on the myosins and their associated molecules, resulting in the muscle fiber contraction. Self-made illustration

Interestingly, it is possible to chemically act on this complex to induce a paralysis of the muscle fibers. The decamethonium bromide (DMB) is such an agent, among others, that is used to induce rigid paralysis of organisms. DMB is an AChR agonist, that will bind to these receptors but that will not be degraded and thus will continuously activate them. This technique is of particular interest when it comes to study the effects of muscles contractions, as it allows to block them (Esteves de Lima et al., 2016; Hall and Herring, 1990; Nowlan et al., 2010).

1.1.2 Specialized connective tissues : bone and cartilage

The skeleton is a complex organ consisting in more than 200 distinct skeletal elements, all with different shapes, sizes and locations. The bones are linked to the tendons and will receive the force generated by muscle contraction in order to allow movement. Bones are divided with regard to their morphological appearance into flat and long bones. Flat bones include skull, scapula and mandible while long bones compose the appendicular skeleton, i.e. humerus, tibia and femur. The long bones possess an architecture enabling them to bear weight and accomplish their metabolic and protective functions (Winding et al., 1999). They can be divided into three compartments: two wide extremities termed the epiphyses, separated from the long cylindrical diaphysis by a developmental zone called the metaphysis. The epiphyses are also separated from the metaphyses by the growth plate, a cartilaginous area responsible for the longitudinal growth of the long bone (Figure I.3). The periphery of the diaphysis is made of a compact layer of calcified matrix called the cortical bone and its function is mainly mechanical and protective. In the metaphysis, before the growth plate, the interior part of the bone is filled with a thin and calcified trabecular network termed the trabecular bone, which is highly metabolic and confers a high mechanical strength (Winding et al., 1999).

Long bones also contain two different tissues (cartilage and bone) as well as three different cell types: the chondrocytes for the cartilage and the osteoblasts and osteoclasts for the bones (Karsenty et al., 2009). The osteoblasts and osteoclasts will be involved in the process of bone remodeling. The osteoblasts form new bone while the osteoclasts will be responsible for its resorption, both of them continuously renewing the bone. The bone extracellular matrix (ECM) contains types I collagen and has the particularity of being mineralized by hydroxyapatite crystals, conferring to the bone its high resistance (Karsenty et al., 2009; Murshed, 2018).

The cartilage ECM is produced by the chondrocytes and is characterized by its elasticity and resistance, which is due to its composition in fibrillar collagen II, with type XI and IX collagens (Assis-Ribas et al., 2018; Karsenty et al., 2009). Besides, this ECM is also rich in proteoglycans such as Aggrecan (Lauing et al., 2014).

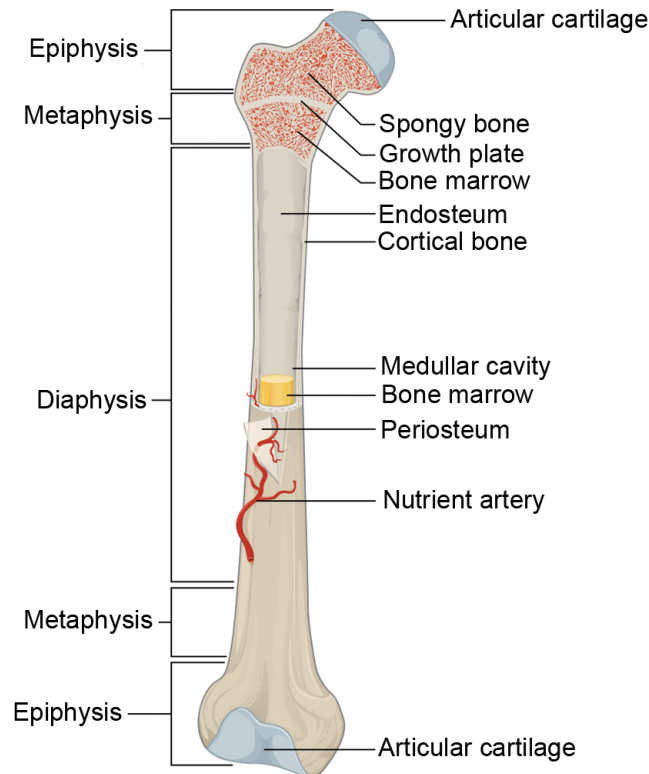


Fig. I.3 **Anatomy of a long bone.** Adapted from the Open Textbook “Anatomy and Physiology - Chapter 06: Bone Tissue and the Skeletal system” Oregon State University.

I.1.3 Tendon : a dense regular connective tissue

a) Tendon structure in vertebrates

Tendons can be defined as a dense regular connective tissue connecting muscle and bone and transmitting the force generated by the contraction of the first to the second, enabling posture or motion (Figure I.4A). The ligaments are similar to tendons, except that they link bones in order to stabilize joints.

Tendons are highly organized hypocellular connective tissues that are made of collagen, up to 70-80% of their dry weight (Mienaltowski and Birk, 2014). They also display a hierarchical fibrillar arrangement of type I collagen fibers that are all parallel to the bone-muscle axis (Figure I.4B) (Nourissat et al., 2015). The triple-helical molecules of type I collagen are assembled into fibrils that will themselves form fibers and fascicles that form the tendon unit (Figure I.4B) (Screen et al., 2015). Parallel collagen fascicles are separated by the endotenon, a loose connective tissue that also contains fibroblasts as well as blood vessels and nerves (Benjamin and Ralphs, 2000). The whole tendon is surrounded by the epitenon and then by a synovial sheath, the paratenon, composed of collagen fibers organized in a perpendicular direction to those of tendon (Benjamin and Ralphs, 2000; Screen et al., 2015). The collagen fibrils are the main structural and functional component of the tendon as they

are responsible for the transmission of the force generated by muscle contractions. Collagen molecules are synthesized by tendon fibroblasts or tenocytes, which display an elongated shape lying between the collagen fibers and forming a 3-dimensional network of cells linked by gap junctions (Figure I.4B) (Benjamin and Ralphs, 2000; McNeilly et al., 1996).

While making up to 95% of all the collagens in the tendon, type I collagen is not the only one involved in its composition and function, as other collagens include type III, V, VI, XII and XIV (Mienaltowski and Birk, 2014). Types III, V and VI collagens belong to the Fibril-Forming class of collagens, involved in regulation of fibril assembly. Types XII and XIV belong to the class of Fibril-associated Collagen with Interrupted Triple helix (FACIT), which closely interact with fibril-forming collagens to affect the surface properties of fibrils and fibril packing (Mienaltowski and Birk, 2014). Altogether, these other types of collagen provide to the tendon ECM a cohesion necessary to accomplish its function correctly. Besides, there is also an important role played in the tendon function by the non-collagenous matrix that is interspersed between all the collagens. These molecules are primarily glycoproteins : proteoglycans, collagen oligomeric matrix proteins, lubricin, tenomodulin (Tnmd) and tenascin-C (TnC) (Thorpe et al., 2013). Among these proteoglycans, a small amount of versican and aggrecan can be found in tendons, this last one being also strongly expressed in cartilage, but the majority of the proteoglycans are the small leucine-rich proteoglycans (SLRPs) such as decorin (Dcn), biglycan, fibromodulin (Fmod) and lumican (Lauing et al., 2014; Rees et al., 2000; Thorpe et al., 2013). The role of these molecules is still not completely well understood, yet some differences in matrix composition have been observed between compressive and tensile regions in the tendon. For example, they are more abundant in regions experiencing compressive loads. An explanation for this phenomenon being that the high concentration of these proteins, such as aggrecan, allows an increase in water content and thus a better resistance to compressive loads (Thorpe et al., 2013; Yoon and Halper, 2005).

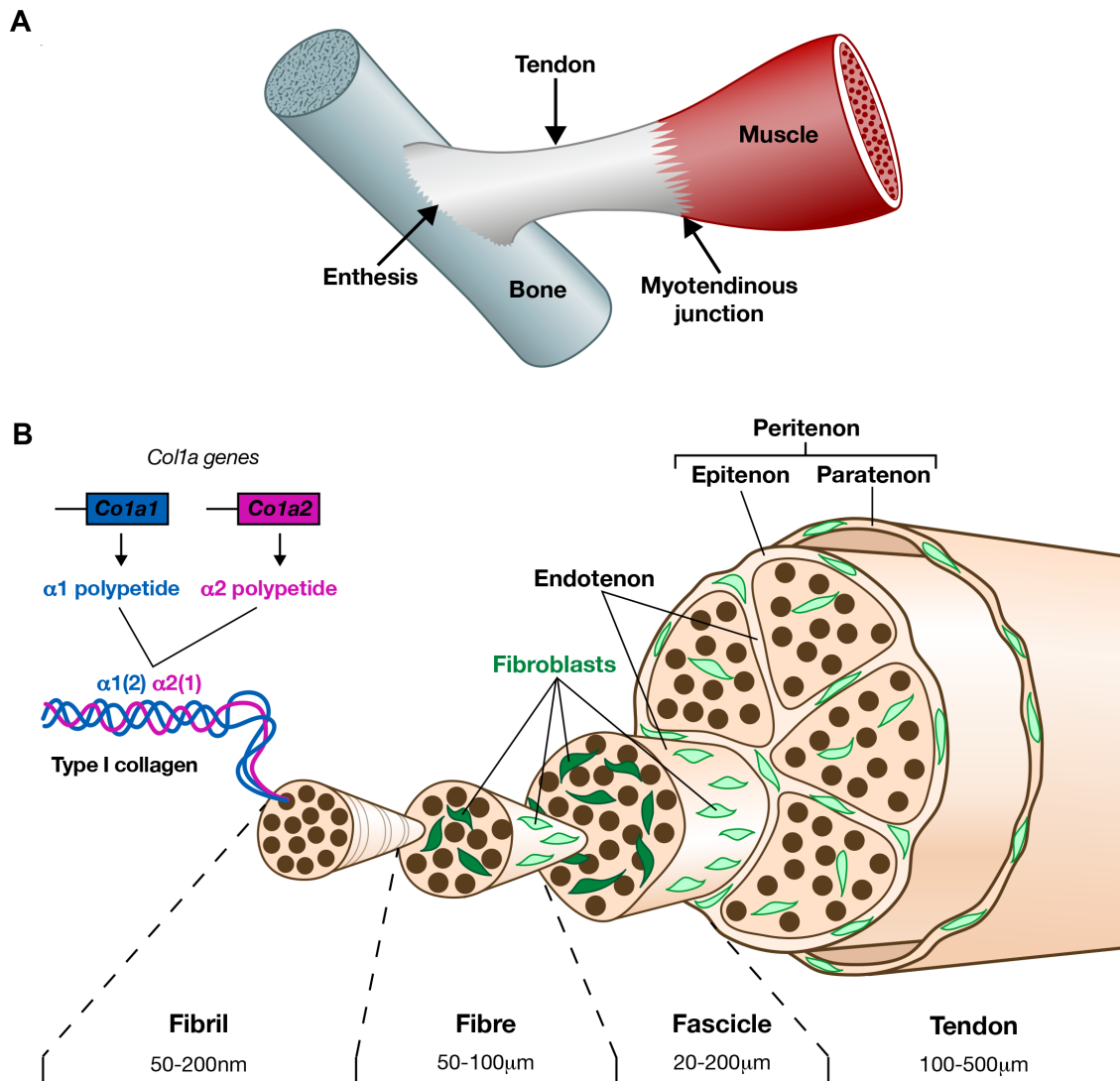


Fig. I.4 **Tendon architecture.** (A) Tendon links muscle to bone and is fixed to bone by the enthesis and to muscle by the myotendinous junction. (B) Type I collagen, the functional and structural component of tendon, is depicted at different scales. *Col1a1* and *Col1a2* code respectively for collagen $\alpha 1(I)$ and $\alpha 2(I)$ polypeptides. Type I collagen triple-helical molecules containing two $\alpha 1(I)$ and one $\alpha 2(I)$ chains assemble into fibrils that combine to form fibres. Tendon fibroblasts reside between collagen fibres. Fibres are surrounded by a connective tissue, the endotenon, which also contains fibroblasts. Fibres combine to form fascicles. Tendons are ensheathed by an outer layer of connective tissue, the epitenon, which is surrounded by another layer of connective tissue, the paratenon. The epitenon and paratenon compose the peritenon. Adapted from Nourissat et al., 2015

b) Tendon and muscle interface : the myotendinous junction

The myotendinous junction (MTJ) is the region where the tendon is attached to the muscle. The attachment between tendon and muscle consists of interdigitations of the plasma membranes of both tendon and muscle cells, named finger-like processes (FLPs), which dramatically increase the interface area between both cell types (Tidball and Lin, 1989). The FLPs consist in interdigitation of sarcolemma where the actin filaments extending from the last Z line in the muscle fiber are indirectly connected to extracellular components through subsarcolemmal proteins (Figure I.5) (Charvet et al., 2012). This allows an efficient function of these FLPs in transmitting muscle contraction forces to the tendon. At a molecular level, collagen fibrils produced by tendon cells bind to laminin or integrins present at the level of sarcolemma and produced by muscle cells (Bökel and Brown, 2002).

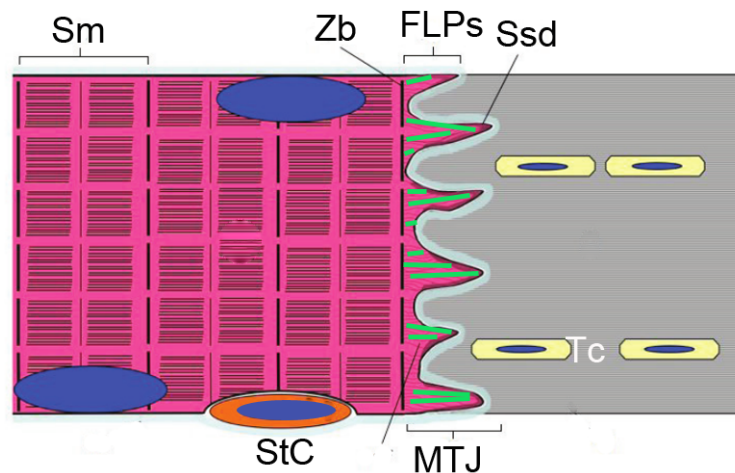


Fig. I.5 **Structure of the myotendinous junction.** Schematic representation of adult myotendinous junction (MTJ). Muscle is colored in pink and tendon in grey. The collagen fibers, produced by tenocytes (Tc), are anchored perpendicularly to the sarcolemma of the finger-like processes (FLPs). The sub-sarcolemmal densities (Ssd) present at the tips of FLPs correspond to the muscle side of the MTJ. These Ssd result from the massive recruitment of protein linkage-complexes that connect actin filaments (actF, green arrays) from the last Z-band (Zb) to the tendinous extracellular matrix. Sm: Sarcomer; StC: Satellite cell. Adapted from Charvet et al., 2012

c) Tendon to bone attachment : the enthesis

The region where tendon attaches to bone is known as the osteotendinous junction, or the enthesis. The region of the bone where the tendon will attach forms an eminence providing a stable anchoring. Depending on the attachment sites, fibrous and fibrocartilaginous entheses have been described (Benjamin et al., 2002). This fibrocartilage presents physical properties in between those of cartilage and tendons. The complexity of this structure lays in the establishment of a proper transition of a bone-like and stiff ECM to a less rigid, more cartilage-like ECM closer to the tendon in order to minimize stress concentrations and allow for load transfer (Subramanian and Schilling, 2015; Zelzer et al., 2014). In addition, the

development of this structure obeys to a gradation in both mineral concentration and collagen fiber orientation (Genin et al., 2009; Schwartz et al., 2012; Thomopoulos et al., 2003, 2006). The maturation of this interface continues after birth and the mice display a mineral gradient at this interface a week after birth (Schwartz et al., 2012).

Histologically, the fibrocartilaginous enthesis is characterized by different cellular zones, proceeding from tendon to bone: tenocytes, uncalcified fibrocartilage cells, calcified fibrocartilage cells and osteocytes (Benjamin and Ralphs, 2000). This cellular arrangement yields a direct connection between soft tissue (tendon) and hard tissue (bone). The part of the bones where the tendons will attach are termed “bone eminence”, according to their form. They consist in a protuberance, a broad elevation of the bone, a tubercle, being a small eminence, or a tubercle, a sharp and pointed eminence (Zelzer et al., 2014). All of these bone eminences provide a stable anchoring for tendons and an efficient point for muscle force transfer and dissipation of stress at the interface.

1.2 Muscle, bone and cartilage development

1.2.1 Muscle development

Skeletal muscle formation involves successive and overlapping waves of embryonic, fetal, perinatal and adult myogenesis. While the establishment of the basic muscle pattern takes place during embryonic myogenesis, fetal myogenesis will be notably critical for muscle growth (Biressi et al., 2007; Hutcheson et al., 2009; Kassam-duchossoy et al., 2005), while perinatal and adult myogenesis allow for growth and repair of damaged muscles.

At the molecular level, the formation of skeletal muscle is controlled by a family of transcription factors called the Myogenic Regulatory Factors (MRF) (Figure I.6) (Buckingham and Rigby, 2014; Moncaut et al., 2013). This family comprises MYOD, MYF5, MRF4 and Myogenin (MYOG) and all four belong to the basic helix-loop-helix superfamily of proteins. While MYOD, MYF5 and MRF4 are all three required as myogenic determination factors, without which no muscle can be formed, MYOG, MYOD and MRF4 are considered as differentiation factors. Two other transcription factors, PAX3 and PAX7, are critical during myogenesis as they define the pool of muscle stem cell in all the successive waves of myogenesis (Gros et al., 2005; Kassam-duchossoy et al., 2005). PAX3 and PAX7 both belong to the Pax family of paired domain transcription factors. While they have expression pattern when it comes to embryonic and fetal myogenesis, they are both upstream regulators of the MRFs and thus of the myogenesis (Buckingham and Rigby, 2014).

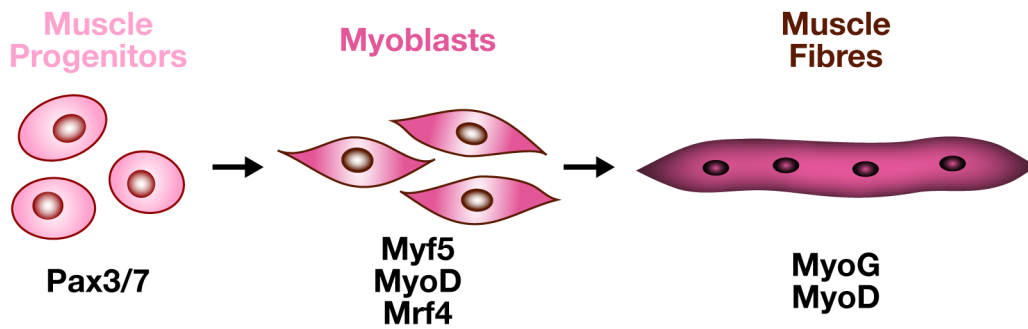


Fig. I.6 **Simplified representation of muscle cell differentiation and the myogenic regulatory factors.** Illustration showing the specification of Muscle progenitors (light pink) into Myoblasts (pink) and their subsequent differentiation into Muscle fibres (dark pink). Below each type of muscle cell is indicated the MRFs expressed at that stage. From Nassari et al., 2017

Myogenesis is established in different regions of the organism during development. While all skeletal muscles derive from the mesoderm, in amniotes, there are clear differences between cranial and trunk myogenesis (Buckingham and Mayeuf, 2012; Sambasivan et al., 2011). For clarity purposes, we will here only focus on the trunk and limb myogenesis.

In the trunk, the paraxial mesoderm will divide into somites, epithelial balls expressing *Pax3* and whose ventral part give rise to the sclerotome (Figure I.7A). The dorsal part of the somite, called the dermomyotome, retain an epithelial identity and give rise to dorsal dermis and all the skeletal muscles of trunk and limbs (Buckingham and Rigby, 2014; Christ and Ordahl, 1995). The formation of the myotome from the dermomyotome starts at embryonic day 8 (E8) in mice and E2.5 in chicken embryo (Endo, 2015). Cells expressing *Pax3* will delaminate from different areas of the dermomyotome and will start expressing MYF5 and MYOD (Figure I.7A). They will move under the dermomyotome to form the primary myotome, composed of elongated and mononucleated myocytes (Gros et al., 2004). These cells will extend from the rostral and caudal ends of each myotomal segment in the trunk. Another set of cells will migrate from the hypaxial dermomyotome to a further location in limbs (Figure I.7B). These cells will start to express *MyoD* and *Myf5* and will be determined as myoblasts and will give rise to the skeletal muscles. By E10.5 in mouse embryos and E4 in chicken embryos, the dermomyotome loses its epithelial structure and a subset of *Pax3*⁺/*Pax7*⁺ cells enters the myotome. These cells either differentiate upon activation of MYF5 and MYOD or will provide a reserve population for further growth during development (Buckingham and Mayeuf, 2012; Endo, 2015).

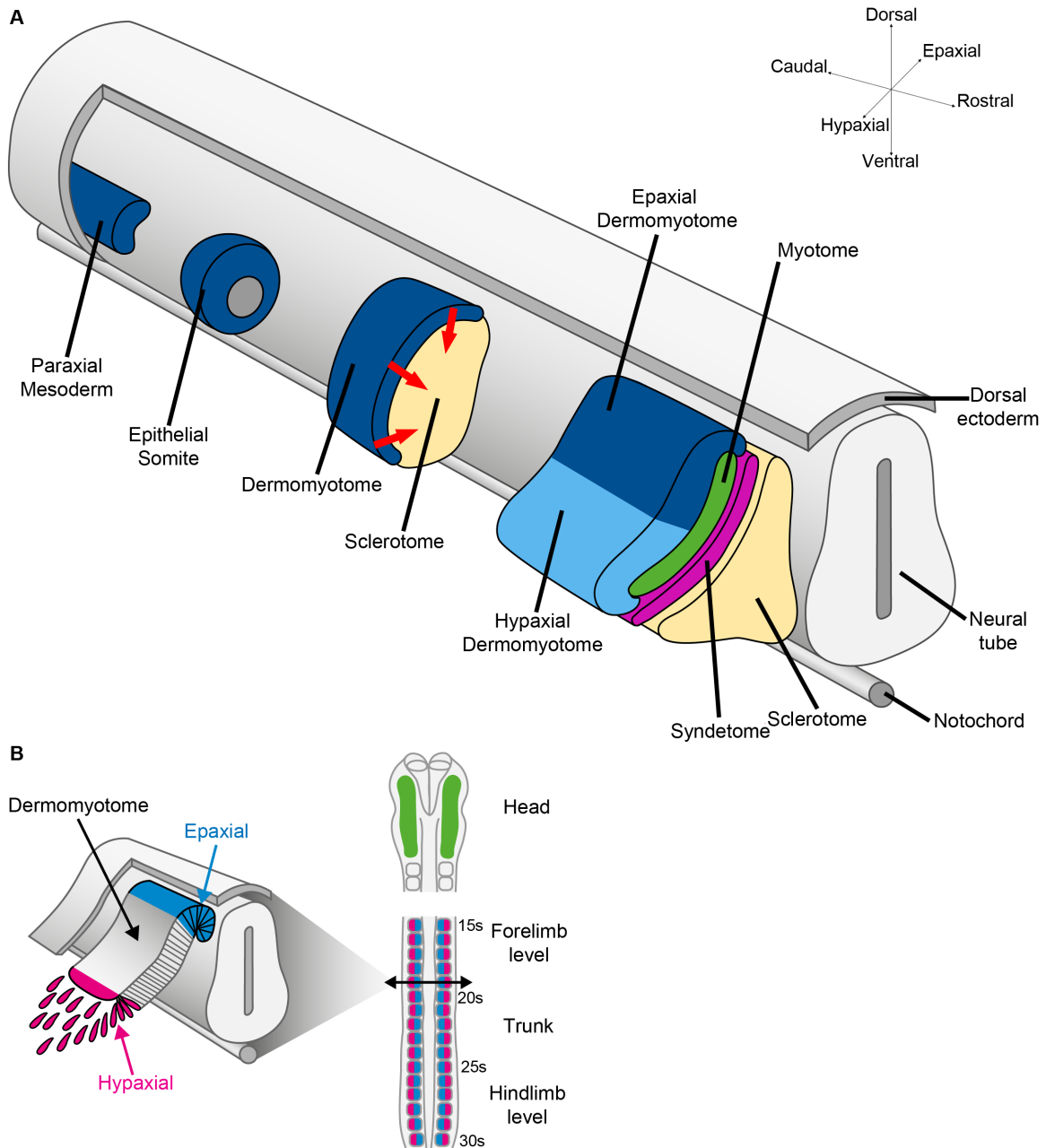


Fig. I.7 **Origin of skeletal muscles of the trunk and limbs.** (A) Somites are formed by the segmentation of paraxial mesoderm. Initially they have an epithelial structure and then their ventral part undergoes an epithelial-mesenchymal transition giving rise to the $Pax1^+$ sclerotome (light yellow). The epithelium is maintained in the dorsal part of the somite, as the dermomyotome (dark blue), where all cells express $Pax3$. The first skeletal muscle, the myotome (in green), is progressively established by delamination of $PAX3^+$ progenitor cells (Red arrows), which have activated $MYF5/MRF4$. Myotome (green) and Sclerotome (light yellow) give rise to the Scx^+ Syndetome (pink), containing tendon progenitors. The Myotome subsequently grows to give rise to all trunk muscles. Illustration from Sophie Gournet. (B) At the level of the limb buds, $PAX3^+$ progenitors, present in the hypaxial lip of the dermomyotome (pink), delaminate and migrate to the limbs (pink cells) where they form skeletal muscles. This process occurs from E9 to E11.5. (E, Embryonic day of mouse development). From Nassari et al., 2017.

Once all the muscle primordia are set, secondary myogenesis or fetal myogenesis takes place (Figure I.8). This phase is characterized by muscle growth and the establishment of sensory innervation but also neuromuscular junction, including excitation-contraction coupling (Buckingham and Mayeuf, 2012; Harris, 1981; Kelly and Zacks, 1969). Around the same time, there will be a wave of proliferation of progenitors molecularly distinct from primary embryonic progenitors. These progenitors were already present at embryonic stages and were shown to co-express *Pax3* and *Pax7* (Gros et al., 2005; Kassam-duchossoy et al., 2005; Relaix et al., 2005). They are thought to be the source of all the cells of the myogenic lineage. Fetal myoblasts fuse either with each other or with embryonic muscle fibers and form thinner secondary muscle fibers around the primary muscle fibers (Biressi et al., 2007; Buckingham and Mayeuf, 2012).

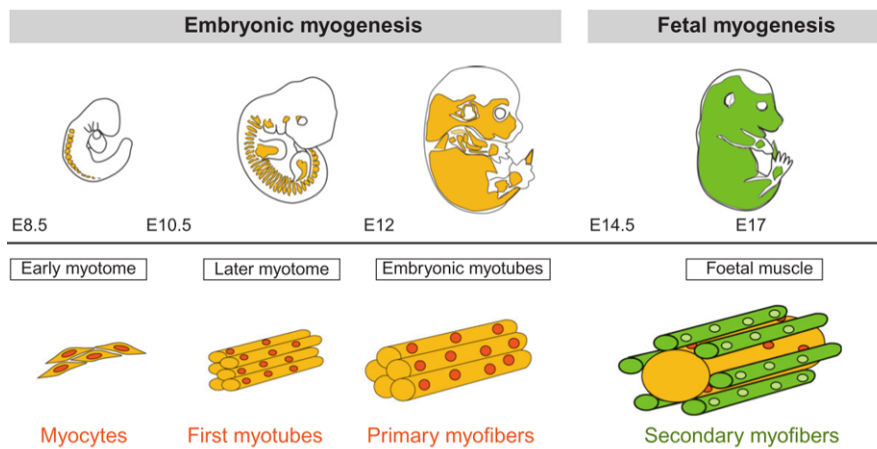


Fig. I.8 **Embryonic and fetal myogenesis.** Myocytes, first myotubes and primary myofibers produced during embryonic myogenesis are colored in yellow. Secondary myofibers produced during Fetal myogenesis are colored in green. *E*, Embryonic day of mouse development. Adapted from Buckingham et al., 2012

I.2.2 Cartilage and bone development

Mammalian skeleton presents distinct origins during embryonic life (Figure I.9). While the craniofacial skeleton originates from Neural Crest Cells (NCCs) and prechordal mesodermal cells, bone and cartilage elements of the trunk and the limbs originate from the paraxial mesoderm (somites) and the lateral plate mesoderm respectively (Berendsen and Olsen, 2015). We will here only focus on the skeletogenesis of the axial and appendicular skeleton.

Skeletogenesis begins with the growth of a limb bud in which mesenchymal cells aggregate and form condensations of a higher cellular density, without an increase in cellular proliferation, and with the shape of the future bones (Berendsen and Olsen, 2015; DeLise et al., 2000; Hall and Miyake, 1992). By E10.5, most mesenchymal condensations have formed and a template of the skeleton exists. The mesenchymal cells in these structures express an ECM made of type I collagen (Karsenty et al., 2009). This aspect of skeletal development is

commonly referred as “skeletal patterning” and will be critical to lay down the proper field for subsequent cartilage and bone development.

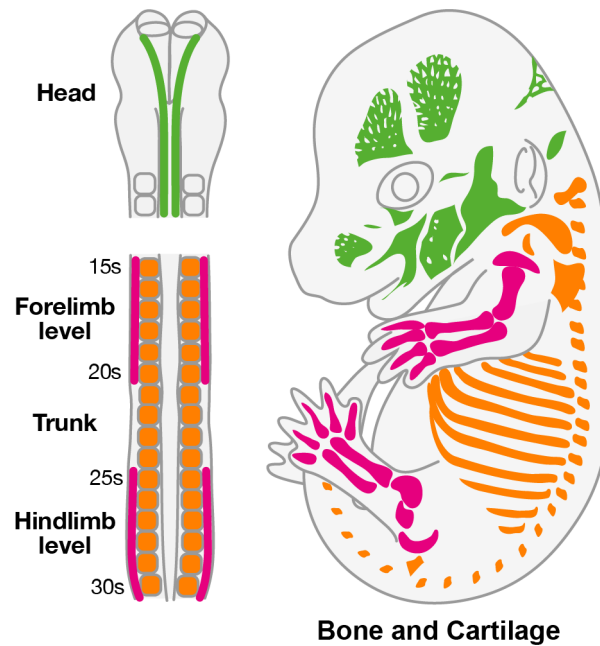


Fig. I.9 **Embryonic origins of bone and cartilage.** Bone and Cartilage tissues are depicted in E14.5 embryos. The color code corresponds to their embryological origins, which differ depending on their location in the body. Bone and Cartilage of the head mainly derive from neural crest cells (green) but also paraxial mesoderm, while in the trunk they arise from the somites (orange) and those from the limbs arise from the lateral plate mesoderm (pink).E, Embryonic day of mouse development. Adapted from Nassari et al., 2017

Following condensation, the mesenchymal cells differentiate either into chondrocytes or osteoblasts, giving rise respectively to cartilage or bone. Osteogenesis, namely the process of ossification, can occur through two different mechanisms: intramembraneous or endochondral ossification. Intramembraneous ossification consists in a direct transition of undifferentiated mesenchymal cells of the condensations into osteoblasts. The other mechanism, endochondral ossification, occurs sequentially, following the establishment of chondrocytes, the cartilage cells (Figure I.10). We will here only focus on endochondral ossification that we will describe in its chronological order, showing the link between cartilage and bone development.

Chondrocytes are the first skeleton-specific cells to appear from the undifferentiated mesenchymal cells of the center of the condensations. They have multiple roles: allowing bone formation, participating in longitudinal bone growth and forming joints. Chondrocytes are round cells that stop producing the type I collagen ECM of the mesenchymal condensations, to replace it with type II collagen and the proteoglycan aggrecan (Karsenty et al., 2009; Lauing et al., 2014). Cells in the periphery of the condensation do not differentiate into chondrocyte and continue to produce a type I collagen ECM, to form a structure called the perichondrium. At E13.5, chondrocytes in the center of the condensations will elongate and

become prehypertrophic chondrocytes and will eventually exit the cell cycle to become hypertrophic chondrocytes. These hypertrophic chondrocytes are genetically and morphologically distinct from non-hypertrophic chondrocytes and produce a type X collagen ECM instead of type II collagen. At the same time, cells of the perichondrium start to express *Runx2*, a master gene for osteoblast differentiation (Ducy et al., 1997). This cortical structure is the precursor of the bone collar.

A vascular invasion coming from the bone collar will allow for blood vessels to bring cells of the osteoblast lineage in the cartilage anlagen that are responsible for mineralization. Meanwhile, hypertrophic chondrocytes will enter apoptosis and die. Becoming osteoblasts, the cells brought by the blood vessels will produce type I collagen ECM on top of the type X collagen ECM that was produced by the now-dead hypertrophic chondrocytes. The orchestrations of this serie of events requires the activity of Indian Hedgehog (IHH) signaling in cartilage (Colnot et al., 2005). This process occurs first in the center of the longitudinal bones and goes on centrifugally. The chondrocytes, both proliferating and hypertrophic, are now arranged into columns and are adjacent to the ossification front. They continue to proliferate and to produce their ECM as the ossification process will progressively consume most of it. Together all these chondrocytes form a structure called the growth plate, that is responsible for the longitudinal growth of the skeleton, when followed by the sequence of the ossification events (reviewed in Karsenty et al., 2009).

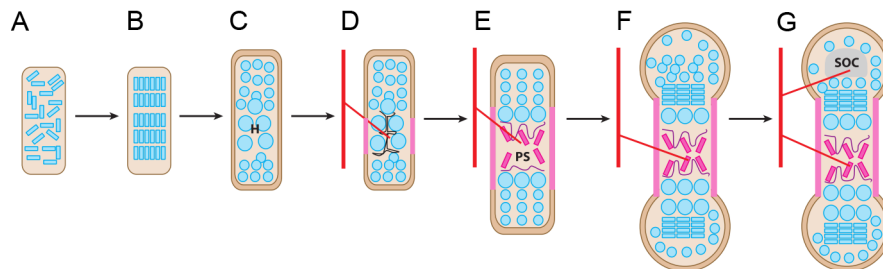


Fig. I.10 **Schematic representation of endochondral bone formation.** (A) Condensations of Mesenchymal cells (blue) at the location of the future bone. (B) Mesenchymal cells differentiate into Chondrocytes and start to proliferate. (C) Hypertrophic chondrocyte differentiation (H). (D) Perichondrial cells differentiate in osteoblasts, forming bone collar (pink). Hypertrophic chondrocyte apoptosis favors matrix mineralization and blood vessel invasion (red). (E) Osteoblasts accompany vascular invasion, forming the primary spongiosa (PS). (F) Chondrocytes continue to proliferate, lengthening the bone. Osteoblasts of primary spongiosa form trabecular bone, while at the bone collar osteoblasts form cortical bone. (G) The secondary ossification center (SOC) forms through cycles of chondrocyte hypertrophy, vascular invasion and osteoblast activity. Adapted from Karsenty et al., 2009

At the molecular level, mechanisms leading to cartilage and bone formation are well understood. Regarding the chondrogenic lineage, the SOX (SRY-related HMG-box) family of transcription factors have been shown to be key players. Indeed, Sox9 is required for

specification and differentiation of the cartilage cells. Sox9 controls the expression of *Sox5* and *Sox6* and the three of them are involved in *Col2a1* and *Acan* gene expression (Lefebvre et al., 2001; Nassari et al., 2017). Concerning the osteogenic lineage, the known master regulator is the Runt-related transcription factor 2 (*Runx2*) (Ducy et al., 1997; Komori et al., 1997). This gene is involved in osteogenic specification, but not differentiation as this role is devoted to the zinc finger containing transcription factor Osterix (*Osx*) (Nakashima et al., 2002; Takarada et al., 2013).

I.3 Tendon development

I.3.1 Tendon markers to study tendon development in vertebrates

a) Scleraxis

The main structural and functional tendon component, type I collagen, is expressed in many tissues and organs. Consequently, tendon development cannot be studied just by following type I collagen expression. To date, the only early tendon marker in vertebrates is the bHLH transcription factor Scleraxis (SCX) (reviewed in Huang et al., 2015a; Schweitzer et al., 2001). SCX has been shown to regulate positively *Col1a1* transcription in mouse tendons and *in vitro* in human mesenchymal stem cells (Alberton et al., 2012; Léjard et al., 2007; Murchison et al., 2007). However, SCX is not the unique transcription factor driving *Col1a1* transcription in tendons, since in *Scx*-deficient mice *Col1a1* transcription is diminished but not abolished in developing tendons (Murchison et al., 2007). *Scx/SCX* is recognized to be a powerful marker for tendons during chick, mouse and zebrafish development (Brent et al., 2003; Chen and Galloway, 2014; Schweitzer et al., 2001). It is also expressed in post-natal tendons but is restricted to epitenon from 4 months postnatally (Figure I.11) (Mendias et al., 2012; Pryce et al., 2007). At early stages, *Scx* is expressed in tendon presumptive regions at the level of branchial arches, somites and limbs (Brent et al., 2003; Grenier et al., 2009; Schweitzer et al., 2001). It also labels tendon progenitor cells and the *Scx*⁺ cell population gives rise to tendons (Blitz et al., 2013; Sugimoto et al., 2013). All together these data clearly show how important is *Scx* as a tendon marker in a broad range of species and stages of life. However, *Scx* is not a master regulatory gene of the tendon lineage as the MRFs are for the skeletal muscle lineage, since tendons retain their capacity to attach muscle to bone in *Scx* mutant mice, which are viable and mobile (Murchison et al., 2007; Yoshimoto et al., 2017). It is possible that SCX needs one or several partners to fulfill the function of master gene for tenogenesis. Nonetheless, in the absence of SCX activity, force-transmitting tendons (limb and tail tendons) and intermuscular tendons are severely disrupted, while anchoring tendons (back tendons) are moderately affected (Murchison et al., 2007; Yoshimoto et al., 2017). The first tendon defects are observed from E13.5 in mouse limbs and the expression of differentiation markers *Col14a1* and *Tnmd* is completely lost in tendons from E16.5 in *Scx* mutant mice (Murchison et al., 2007). Overall, loss of *Scx* causes loss of tenogenic differentiation markers such as *Tnmd* and defective maturation of tendons, ligaments and other dense connective tissues (Murchison et al., 2007; Yoshimoto et al., 2017). In summary

Scx is the unique early tendon marker that provides a powerful tool to study early stages of tendon development.

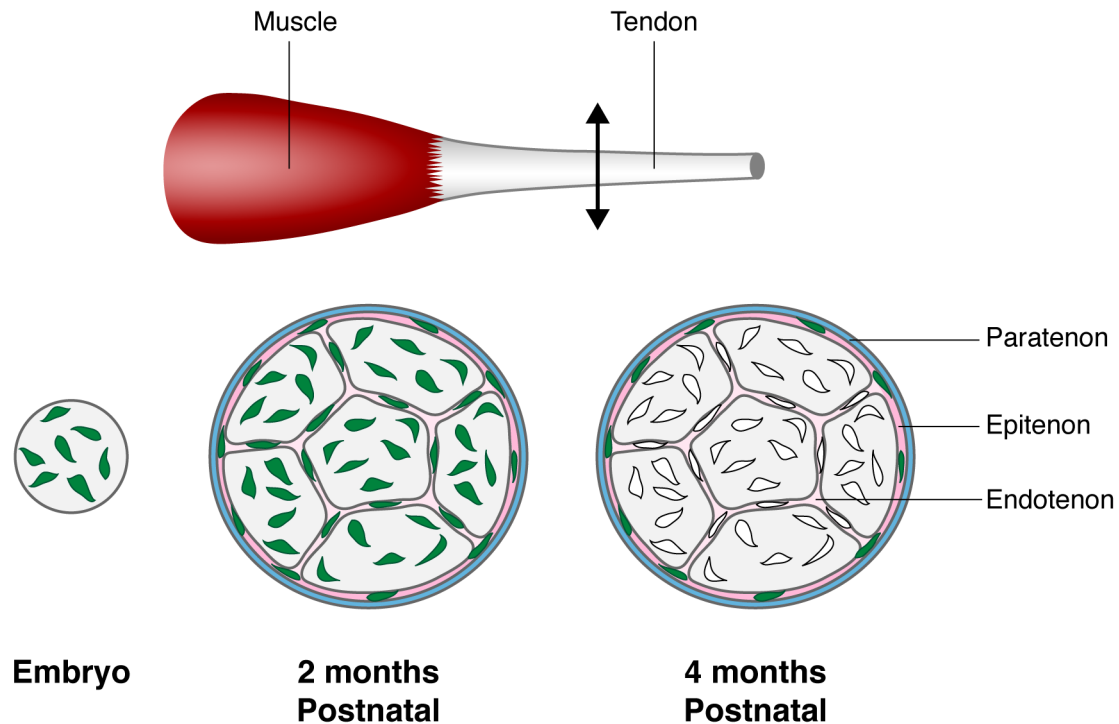


Fig. I.11 **Representation of *Scx* expression in developmental, postnatal and adult tendons.** *Scx*⁺ cells are schematized in green. During development, *Scx* expression is expressed in all tendon cells. During tendon maturation at postnatal stages, is expressed in the tendon proper, endotenon and external sheaths including epitenon and paratenon, but is restricted to the epitenon by the fourth postnatal month. From Gaut and Duprez, 2016.

b) Tenomodulin

Tenomodulin (*Tnmd*) is a gene highly expressed in tendons, involved in their maturation and necessary for tendon stem and progenitor cells (reviewed in Dex et al., 2016). *Tnmd* is a 7-exon gene located on the X chromosome and encoding a type II transmembrane glycoprotein with a highly conserved cleavable C-terminal cystein-rich domain (Brandau et al., 2001; Shukunami et al., 2001). *Tnmd* is considered a highly specific marker of differentiated tenocytes, but its expression can also be found in other dense connective tissues such as ligaments, muscle sheet epimysium, as well as in skin and tendon-like structures of the heart, eyes and other tissues (reviewed in Dex et al., 2016; Huang et al., 2015a; Jelinsky et al., 2010; Sugimoto et al., 2013).

Tnmd mutant mice display an altered structure of collagen fibrils (shift toward large diameters) in tendons at postnatal stages (Docheva et al., 2005). Also, *Tnmd*-deficient mice display reduced self-renewal and increased senescence properties of tendon progenitors (Alberton et al., 2015). In the opposite way, overexpression of *Tnmd* in a murine cell line of mouse embryonic fibroblasts, the C3H10T1/2 cells, enhanced their proliferation, as well as

their morphology (Jiang et al., 2016). TNMD was revealed to be an important factor in the functional performance of tendons (Dex et al., 2017). Mice lacking *Tnmd* were shown to have significantly inferior running performances and their tendons exhibited disturbed structural and biomechanical properties of type I collagen fibers (Dex et al., 2017). Interestingly, activations of the *Tnmd* promoter and *TNMD* mRNA levels of human Tendon Stem/Progenitor Cells (TSPCs) were observed upon a 5% axial cyclic strain of these cells (Dex et al., 2017). These data also establish *Tnmd* as a mechanosensitive gene.

Finally, the transcription factor SCX has been known to be a transcriptional activator of *Tnmd*, as it contains binding sequences for SCX in its 5' flanking region and its expression is lost *in vivo* in the absence of *Scx* (Murchison et al., 2007; Shukunami et al., 2006, 2018; Yoshimoto et al., 2017). Conversely, it was also shown *in vitro* that human mesenchymal stem cells overexpressing *SCX* presented a remarkable upregulation of *Tnmd* expression (Alberton et al., 2012). All together these data show how important *Tnmd* is as a marker of tendon cell differentiation but also as a fundamental actor in tendon functionality and tendon cell adaptation to its physical environment.

c) Mohawk

The role of the transcription factor Mohawk (Mkx) in tendon differentiation was highlighted several years after the identification of *Scx*. The *Mkx* gene codes for a three-amino-acid loop superclass of atypical homeodomain transcription factor, that is expressed in several tissues but notably at E13.5 in mouse limb and tail tendons (Anderson et al., 2006; Huang et al., 2015a; Liu et al., 2010). Also, *Mkx* is expressed in early somites, in progenitor cell populations of skeletal muscle, tendon, cartilage and bone (Anderson et al., 2006). *Mkx*^{-/-} mutant mice exhibit smaller tendons than wild-type mice and display defects in postnatal growth of tendon collagen fibrils and outer annulus fibrosus collagen fibrils diameter (Ito et al., 2010; Kimura et al., 2011; Liu et al., 2010; Nakamichi et al., 2016). The first tendon defects in *Mkx*^{-/-} mice are observed at E16.5 fetal stages (Ito et al., 2010). In addition to the reduction of *Colla1* gene expression, *Mkx*^{-/-} mice display significant reduction in *Tnmd*, *Fmod* and *Dcn* gene expression in neonatal tendons (Liu et al., 2010).

Mkx overexpression in cells activated the transcription of multiple tendon and ligament genes, among them *Scx*, *Colla1*, as well as in human bone marrow derived mesenchymal stem cells (reviewed in Liu et al., 2015a; Nakamichi et al., 2016; Otabe et al., 2015; Suzuki et al., 2016). Also, *Mkx* overexpression in C3H10T1/2 cells also upregulated the expression of genes coding for components of the protenogenic TGFβ2/ SMAD2/3 signaling pathway, such as *Smad2* and *Smad3* (Nakamichi et al., 2016). This could account for the promoted signal response of this pathway in this model of mesenchymal stem cells. Besides, MKX directly activates the expression of the *TGFβ2* gene by binding to its promoter (Liu et al., 2015a). MKX has been shown to inhibit muscle differentiation in mouse cell cultures and to impair muscle development in zebrafish embryos by directly repressing *MyoD* transcription (Anderson et al., 2009, 2012; Chuang et al., 2014). However, *Mkx* mutant mice do not display any

obvious skeletal muscle defects (Kimura et al., 2011). Besides, *Mkx* deficiency accelerated chondrogenic and osteogenic differentiation, while its overexpression had the opposite effect, consistent with a role in repressing other lineages and promoting the tendon lineage (Liu et al., 2015a; Suzuki et al., 2016).

Scx and *Mkx* expression in developing tendons appears to be normal in *Mkx*^{-/-} and *Scx*^{-/-} mutant mice, respectively, suggesting that *Scx* and *Mkx* act in different genetic cascades during tendon development (Kimura et al., 2011; Liu et al., 2010). Added to the other data about MKX, this shows its importance in regard of the other main transcription factors acting on tendon differentiation.

d) Early Growth Response 1

Early Growth Response 1 (EGR1) is a zinc finger transcription factor belonging to the EGR family of genes. The *Egr1* gene was discovered as being rapidly and transiently activated in mouse 3T3 cells and expressed in many organs and tissues such as the brain and the thymus (Christy et al., 1988). *Egr1* is also known to be a target of the Serum Response Factor (SRF), notably through the mitogen-activated protein kinase-ERK kinase (MEK) signaling (Bahrami and Drabløs, 2016; Esnault et al., 2014; Gineitis and Treisman, 2001). EGR1 shares a three-zinc-finger sequence in the DNA binding domain with the other members of the EGR family, however among those members only EGR1/*Egr1* and EGR2/*Egr2* are expressed in chick and mouse tendons during development (Léjard et al., 2011; Veyrac et al., 2014). Phosphorylation of EGR1 by the casein kinase II was shown to inhibit its transcriptional activity *in vitro* (Jain et al., 1996). It has to be noted that *EGR1* expression domain is close to muscle attachments (Léjard et al., 2011; Orgeur et al., 2018).

During fetal development, EGR1 is sufficient for the expression of *Scx*, *Tnmd* and tendon-associated collagen genes (*Cola1*, *Col5a1*, *Col12a1* and *Col14a1*) (Léjard et al., 2011). Also, *Egr1*^{-/-} mice display defects in collagen fibril organization in tendons at fetal and post-natal stages (Guerquin et al., 2013; Léjard et al., 2011). Tendons of these mutant mice also show a mechanical weakness and a deficiency in their capacity to heal following injury (Guerquin et al., 2013). In addition, *Egr1*^{-/-} mice also displayed significant reductions in the expression of tendon-associated collagens genes (*Col3a1*, *Col5a1*, *Col12a1* and *Col14a1*) and tendon-associated molecules genes (*Tnmd*, *Fmod* and *Dcn*) in fetal limbs and adult tendons (Guerquin et al., 2013; Léjard et al., 2011). Also, *Scx* expression is downregulated, while *Mkx* is not modified in *Egr1*-deficient tendons, strengthening a possible relation with *Scx* but not with *Mkx* (Guerquin et al., 2013; Léjard et al., 2011). Conversely, it was shown that *Egr1* overexpression in C3H10T1/2 cells increased the expression of *Scx* and several other tendon-associated genes, but not that of *Mkx* (Guerquin et al., 2013). In addition, EGR1 overexpression in a chicken micromass (cMM) explant model showed an increase of *TNMD* expression (Orgeur et al., 2018). Besides, *Egr1*-overexpressing C3H10T1/2 cells also lost their capacity to differentiate into bone and fat lineages, strengthening a role of EGR1 in tendon differentiation (Guerquin et al., 2013).

Several studies have pointed out the capacity for EGR1 to be activated by mechanical signals, both at the gene expression and transcription factor activity levels (Joshi et al., 2012; Ogata, 2008; Schwachtgen et al., 1998; Wu et al., 2010). Besides, *Egr1* expression, as well as other tendon genes, was reduced in adult tendons with limited movements (Gaut et al., 2016). Its expression was upregulated in healing tendons of adult mice, but not in *Egr1*^{-/-} mice or when the tendons healed with a reduced load condition (Gaut et al., 2016; Guerquin et al., 2013). These data show that EGR1 is not only involved in tendon development and repair but is responding to mechanical stimulations of tendons *in vivo*.

In *Drosophila*, the transcription factor stripe, homolog of the EGR family in vertebrates, is the key gene for tendon development (Becker et al., 1997; Frommer et al., 1996; Volk and VijayRaghavan, 1994). The stripe gene produces two isoforms stripeA and stripeB. StripeB has been shown to be involved in tendon progenitor induction, while stripeA is involved at a later muscle-dependent stage of tendon differentiation (Becker et al., 1997; Frommer et al., 1996; Volohonsky et al., 2007).

1.3.2 Embryological origins of tendons

a) Multiple origins

Tendons can be organized into three main groups according to their position in the body: head, trunk and limb tendons (Figure I.12). Even if functionally similar, tendons of the different parts of the whole organism have distinct embryological origins, which have been studied mainly using the quail and chick chimera system (Dupin and Le Douarin, 2014). Using this technique, it has been shown that vertebrate tendons originate from mesoderm or NCCs. The craniofacial tendons originate from NCCs, in mouse, chick and zebrafish (Chen and Galloway, 2014; Crane and Trainor, 2006; Grenier et al., 2009). Axial tendons derive from a somitic compartment, named the syndetome, while the limb tendons originates from the limb lateral plates (Brent et al., 2003; Kieny and Chevallier, 1979). Independently of their anatomical location, tendons share the same embryological origins with skeletal tissues such as cartilage and bone and have origins distinct from those of skeletal muscles. However, it should be noted that in the head, tendon progenitors migrate into muscle-containing regions, whereas in limbs, muscle progenitors undergo a migration step toward the limb lateral-plate containing skeleton and tendon progenitors.

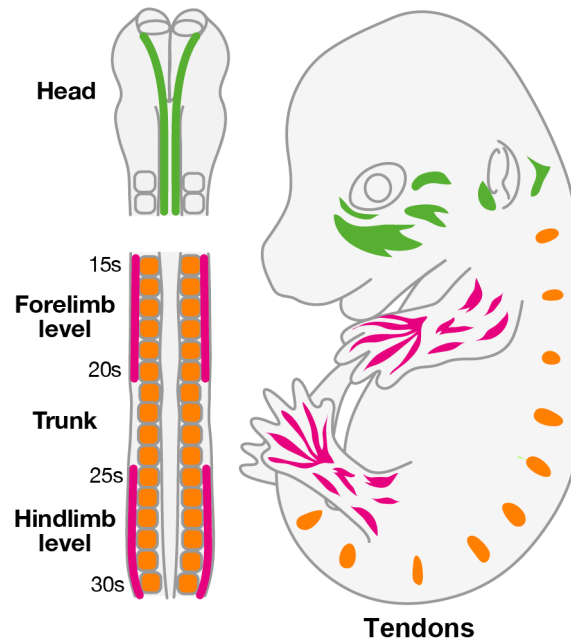


Fig. I.12 **Embryonic origins of tendons.** Tendons are depicted in E14.5 embryos. The color code corresponds to their embryological origins, which differ depending on their anatomical location. Tendons of the head derive from neural crest cells (green), while in the trunk they arise from the somites (orange) and those from the limbs arise from the lateral plate mesoderm (pink). E, Embryonic day of mouse development. Adapted from Nassari et al., 2017

b) Cranofacial tendons

The NCCs are a pluripotent cells population derived from the lateral ridges of the neural plate during embryogenesis. The NCCs will migrate into the branchial arches of the embryo, the more rostral of them being involved in the formation of the musculoskeletal structures of the jaws (Chai et al., 2000). The branchial arches are formed by a pharyngeal endoderm and a surface ectoderm both surrounding two cell populations: the NCCs and the cranial mesoderm cells. The NCCs were originally thought to be co-distributed with the paraxial mesoderm cells in the branchial arch but with a distinct segregation, by just surrounding it (Trainor and Tam, 1995). It has then been shown that NCCs are actually extensively mixed with the myogenic precursors of the mesoderm during branchial arch development (Grenier et al., 2009). The NCCs then proliferate around the myogenic core and later within the arch muscles, this latter proliferation being correlated with an appearance of tendon progenitor expressing Scleraxis (Grenier et al., 2009). Despite this intermingling between the mesodermal cells and the NCCs both populations initiate their respective differentiation independently. However, in the absence of one, the other cannot achieve its differentiation. It is the case for example in the *Tbx1*^{-/-} mice where the myogenic fate is severely impaired in the head. In these mice *Scx* expression is normally established in the absence of differentiated muscles in the first branchial arch of E12.5 but is lost at E15.5 (Grenier et al., 2009). Interestingly, *Mkx* also seems to play a role in this interplay since it has been shown in the

zebrafish to be necessary for the maintenance of the NCC pool –and then the establishment of the tendon lineage- and the repression of the myogenic differentiation of the mesodermal cells (Chuang et al., 2010, 2014). The *Mkx*^{-/-} mice are viable but present defects in tendon differentiation, including those of the head, confirming in part its role in craniofacial tendon formation (Kimura et al., 2011). In zebrafish, *sox9a-sox9b*-deficient zebrafish embryos display abnormal craniofacial tendons based on *scxa* and *tnmd* expression, suggesting that cartilage is necessary for the proper organization of craniofacial tendon cells (Chen and Galloway, 2014). However, it is difficult to dissociate tendon and cartilage defects.

c) Axial tendons

The skeletal muscles and the bones of the vertebrate body are all derived from the somites (Ordahl and Douarin, 1992). The ventral part of the somite will give rise to the sclerotome from which will originate all the axial bones. A group of PAX3⁺ cells from the dermomyotome will delaminate and migrate underneath the dermomyotome to form the myotome (Figure I.7). This last compartment will be composed of the precursors of the future axial muscle (Brent and Tabin, 2002). Another compartment form from the interaction between the Myotome and the sclerotome and giving rise to all the connective tissues of the axial musculoskeletal system: the syndetome (Figure I.7) (Brent et al., 2003). The syndetome is marked by the expression of the bHLH transcription factor *Scx* and is derived from a dorso-lateral domain of the early sclerotome. The FGF signaling pathway produced by the central postmitotic cells of the adjacent myotome will be responsible, through the activation of its effectors *Etv4*, for inducing *Scx* expression in cells of the sclerotome in which the expression of the sclerotomal marker *Pax1* will be consequently lost in chicken embryo (Brent and Tabin, 2004; Brent et al., 2003). Even if there are two distinct populations of mesenchymal cells, one expressing *Scx* in the syndetome and the other *Pax1* in the sclerotome, there is no morphological distinction between them. However the tendon and cartilage fates of these mesenchymal cells are mutually exclusive and overexpression of *PAX1* (known to promote cartilage formation) in sclerotome inhibits *SCX* expression in chick somites (Brent et al., 2003, 2005). Also, the expression of *Tnmd* will follow that of *Scx* in the syndetome all along the craniocaudal axis, marking the differentiated tenocytes (Shukunami et al., 2006).

d) Limb tendons

Tendon cells originate from the lateral plate mesoderm and tendon progenitors are mixed with the PAX3⁺ myoblasts in the developing limb (Chevallier et al., 1977; Christ et al., 1979; Schweitzer et al., 2001). These mixed populations form two pre-muscle masses surrounding a prechondrogenic core region (Schramm and Solursh, 1990).

In a first step, the early expression of *Scx* in the tendon progenitor population in limb is induced by signals from the near ectoderm (Schweitzer et al., 2001). Interestingly, the formation of tendon primordia expressing *Scx* is autonomous regarding muscle formation. Tendon primordia can form in muscleless limbs resulting either from surgical alterations or genetic alterations in *Pax3* or *Myf5/MyoD* mutant mice (Bonnin et al., 2005; Brent et al.,

2005; Kardon, 1998; Kieny and Chevallier, 1979).

In a second step, the expression of *Scx* will develop from proximal to distal regions of the forming limb. In the mouse, after the induction of *Scx* in tendon progenitors and until E12.5 spatial rearrangements will occur between muscle, cartilage and tendon primordia. The tendon primordia will be organized and individualized in loose cellular aggregations between the nascent muscles and cartilages (Edom-Vovard and Duprez, 2004; Kardon, 1998; Schweitzer et al., 2001, 2010).

For the third step of limb development, the tendon primordia will be completely distinct from the other tissues in formation in both mouse and chick (Kardon, 1998; Schweitzer et al., 2010). By E12.5 in the mouse and E7.5 in the avian model, the tendons progenitors will be more aggregated and condensed and form structurally distinct tendons that will attach the muscle to the cartilage (Edom-Vovard and Duprez, 2004; Schweitzer et al., 2010). This third phase of tendon development is completely muscle-dependent (Figure I.13). Indeed, the absence of muscle eventually prevents further tendon development and leads to a loss of *Scx* expression in limb but also head tendons, in mouse, chick and zebrafish embryos (Bonnin et al., 2005; Chen and Galloway, 2014; Grenier et al., 2009; Schweitzer et al., 2001). This demonstrates that muscles are not required for the initiation but are necessary for the maintenance of *Scx* expression in both limb and craniofacial tendons (Figure I.13).

Developing tendons in the distal limbs, in the future digits, will also derive from lateral plate mesoderm cells starting to express *Scx* (Schweitzer et al., 2001). However, the formation of distal tendons will also benefit from the induction of the Apical Ectodermal Ridge (AER) at the apex of the early limb bud. The distal region of the limb bud under the AER contains mesodermal progenitors and is termed the “progress zone” (PZ). During digit formation PZ progenitors will group to form radial chondrogenic aggregates, constituting the future phalanges of the developing digit. The interdigital regions will undergo massive cell death, delimiting the forming digits (Lorda-diez et al., 2014). The first tendon blastemas will appear after the formation of the chondrogenic aggregates and they have been described to benefit from signals from both the forming cartilage and the adjacent ectoderm for their own development (D’Souza and Patel, 1999; Hurle et al., 1990; Mérimo et al., 1998; Schweitzer et al., 2001; Yamamoto-Shiraishi and Kuroiwa, 2013). Tendons can develop autonomously from muscles in the digits but the differentiating tendons need to be attached to the muscles to be maintained (Brand et al., 1985; Huang et al., 2013; Kardon, 1998; Kieny and Chevallier, 1979). Besides, the tendon progenitors of this area show the same requirement in *Scx* expression than for the other tendons of the organism. The *Scx*^{-/-} mutant mice will exhibit an absence of flexor activity due to a loss of the flexor digitorum profundus (FDP) and flexor digitorum superficialis (FDS) tendons (Murchison et al., 2007). This phenotype is due to a failure in differentiation and condensation of tendon progenitors (Murchison et al., 2007).

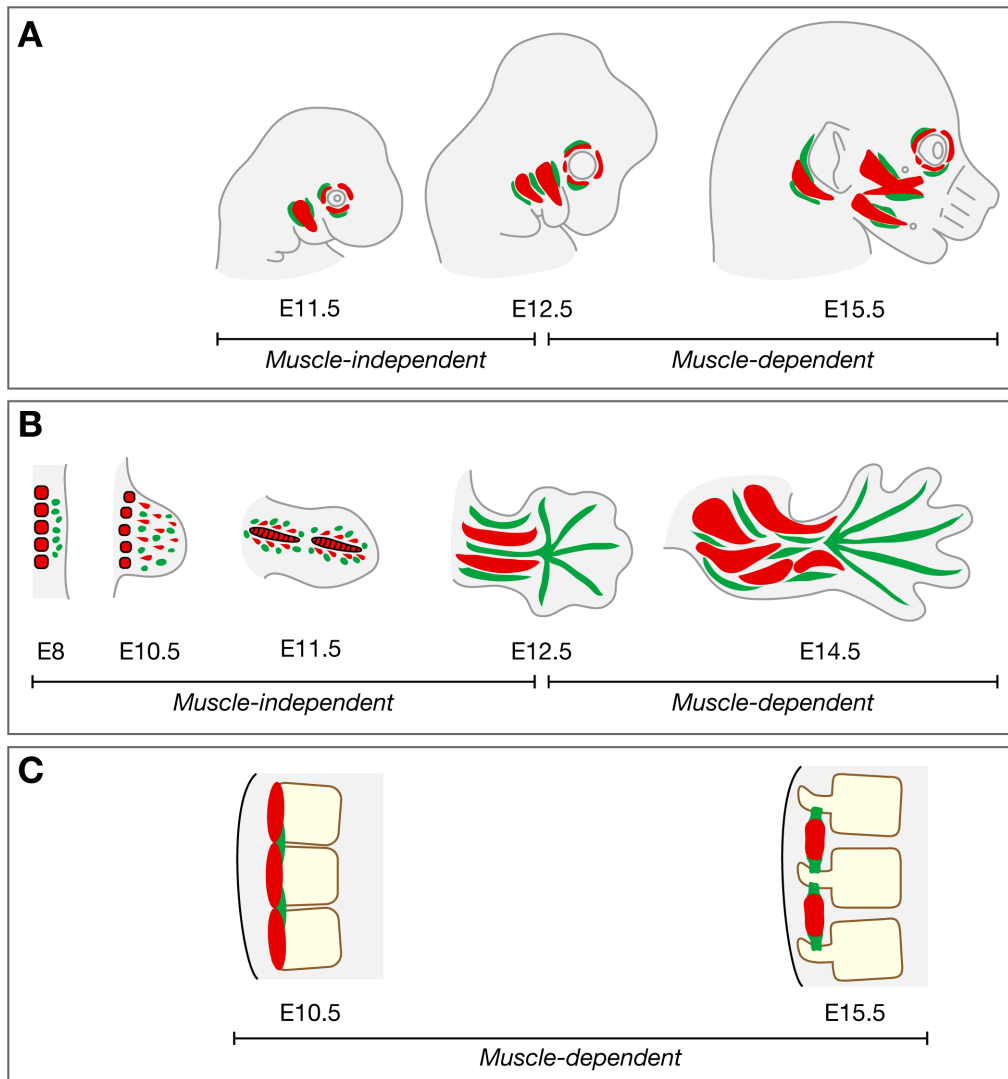


Fig. I.13 **Muscle-dependency for head, limb and axial tendon development.** Muscle and tendon are schematized in red and green, respectively. In the head (A) and limbs (B), tendons initiate their development independently of muscle, but further tendon development requires the presence of muscle. In contrast, the initiation of axial tendon development requires the presence of muscle (C). From Gaut and Duprez, 2016

e) Development of tendon interfaces

Development of the myotendinous junction

To date, the development of the MTJ has been best studied in the zebrafish model. During initial establishment of the MTJ, ECM from both muscle and tendon cells might play important roles. During embryogenesis the muscles first attach to intersegmental boundaries (ISBs) before the appearance of tendon progenitor cells (TPCs) (reviewed in Subramanian and Schilling, 2015). They bound to these regions where the ECM is similar to that of tendons during a first tendon-independent phase. Myoblasts will then synthesize a “pre-

tendon” ECM that will accumulate without tendon cells and which includes Fibronectin (FN), laminin-alpha 2 (Lama2) and thrombospondin 4 (Thbs4 / Tsp4) (Figure I.14) (reviewed in Subramanian and Schilling, 2015). In zebrafish, *tsp4* was shown to be required to maintain muscle attachment at the ISB (Subramanian and Schilling, 2014). This molecule might be a crucial actor in the establishment of MTJs as it is also expressed in mammalian myoblasts and play an important role in the formation of the *Drosophila* MTJ (Subramanian and Schilling, 2015; Subramanian et al., 2007). In a second tendon-dependent phase, an ECM will be produced by the now-present TPCs on site, particularly rich in collagens I, XII and XIV. These mature TPCs, which also benefited from the presence TGF β 2 in the ECM, will then also extend processes and attach to the muscle cells through the FLPs (reviewed in Charvet et al., 2012; Subramanian and Schilling, 2015).

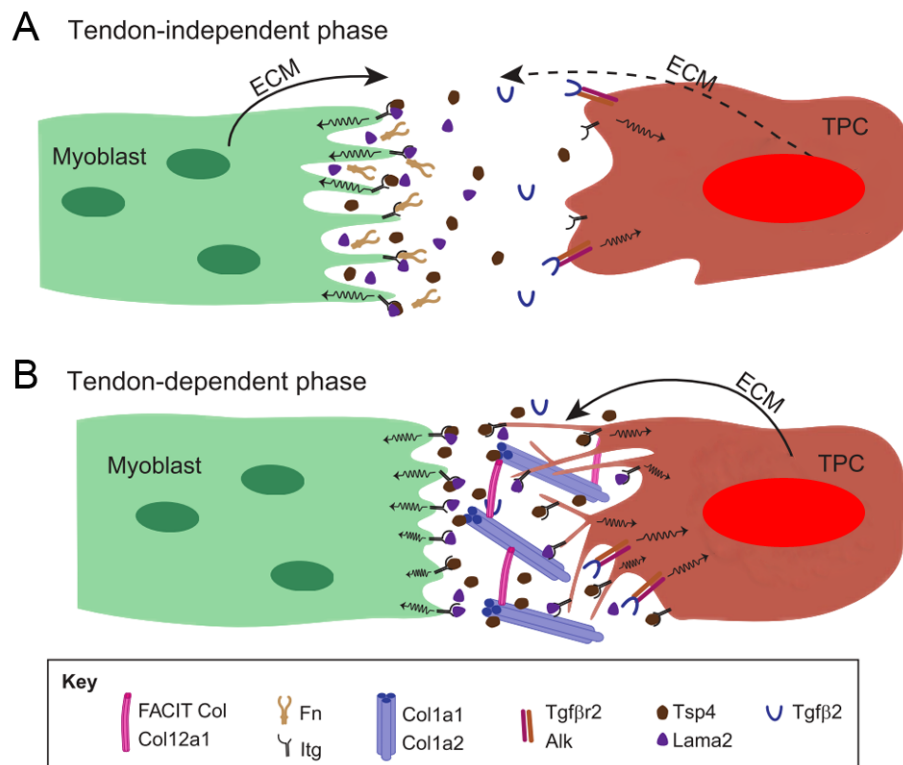


Fig. I.14 **Formation of the myotendinous junction.** (A) In the initial tendon-independent phase in vertebrates, myoblasts (green cells) synthesize a ‘pre-tendon’ ECM including *Tsp4* and *Lama2*. This ECM accumulates in the absence of TPCs (brown cells). (B) A later tendon-dependent phase relies on the production of ECM, particularly *Col1a1*, *Col1a2*, *Col12a1* and *Col14a1*, by more mature TPCs, which extend processes into the ECM to then form the finger-like processes. Adapted from Subramanian et al., 2015

Development of the enthesis

The development of this structure at the cellular level remains quite unclear. The appearance of bone eminences takes place after the differentiation of chondroprogenitors from which they are clearly distinct (Blitz et al., 2013; Zelzer et al., 2014). However, the existence of a specific pool of "eminence progenitors" responsible for the tendon-to-bone junction has been confirmed (Blitz et al., 2013; Sugimoto et al., 2013). These cells express both SCX and SOX9 ($Scx^+/Sox9^+$), two main transcription factors respectively involved in tendon and cartilage differentiation. They will give rise to the differentiated cells composing the cartilaginous bone eminence, but also to tenocytes in the closest part to the bone of the tendon (Blitz et al., 2013; Sugimoto et al., 2013). These double-positive cells progressively disappear as the expression of both *Sox9* and *Scx* become mutually exclusive and by E13.5 the $Scx^+/Sox9^+$ cells are not present anymore (Blitz et al., 2013).

The specification of the eminence progenitors is influenced by TGF β signaling, establishing the cartilaginous side of tendon attachment (Figure I.15) (Blitz et al., 2013; Zelzer et al., 2014). Then the bone ridge formation also requires the action of Scleraxis, that will stimulate the expression of *Bmp4* and the subsequent protein secreted will be interpreted by near chondrocytes as the initiation signal (Blitz et al., 2009). The *Scx/Bmp4* axis will then control the differentiation of eminence progenitor cells into eminence-forming cells (Figure I.15) (Blitz et al., 2009, 2013). The mineralization of the tendon-bone attachment unit requires the action of the IHH/PTHrP signaling : IHH will stimulate the synthesis of PTHrP, which will in turn downregulate the expression of *Ihh*, providing a fine control chondrocytes proliferation (Zelzer et al., 2014). Besides, PTHrP is also present at the site of tendon-to-bone attachment, as well as *Ihh*, (Blitz et al., 2009; Chen et al., 2006, 2007b). PTHrP will play a role in modeling cortical bone surfaces at these sites and in fibrochondrogenic differentiation, confirming its crucial role for the mineralization and the formation of the tendon-to-bone attachment (Han et al., 2014; Wang et al., 2013). This role is also reinforced by the fact that the defect of cortical bone modeling was induced by a conditional deletion of the *PTHrP* gene in *Scx*-expressing cells (Wang et al., 2013).

Concerning IHH, this molecule is also present at this junction site (Blitz et al., 2009; Liu et al., 2012) and is required for the normal differentiation of the fibrocartilaginous insertion site and the expression of its markers (Liu et al., 2013). Besides, it has been shown that the enthesis fibrocartilage cells all originate from a population of hedgehog-responsive cells modulated by the mechanical environment (Schwartz et al., 2015). This result is concordant with other studies concerning the variation of *PTHrP* expression regarding its mechanical environment (Chen et al., 2007b; Han et al., 2014; Wang et al., 2013).

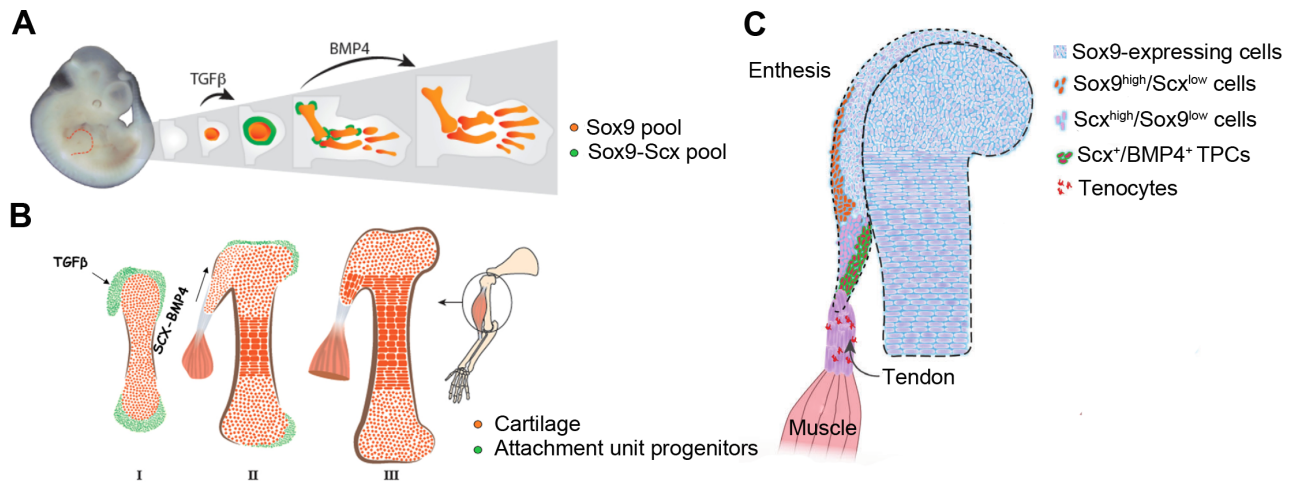


Fig. I.15 **The developing eminence and enthesis.** (A, B) A modular model for bone eminence development as presented in Blitz et al., 2013. The formation of bone eminences is illustrated in the context of limb development (A) and of musculoskeletal development (B). Two distinct pools of progenitor cells form the cartilaginous template of the long bone in a modular fashion. The first pool of Sox9⁺ progenitors forms the cartilaginous anlage. Then a second pool of Sox9⁺/Scx⁺ progenitors forms the module of the bone eminence. TGFβ signaling controls the specification of eminence progenitors, whereas SCX-BMP4 signaling mediates their differentiation. (C) The enthesis is delimited by the small-dotted line. In wild-type embryos, different subsets of Scx-expressing cells are found in the enthesis, from tendon to bone: Scx⁺/BMP4⁺ (green and red cells), Scx^{high}/Sox9^{low} (purple and blue cells) and Sox9^{high}/Scx^{low} (orange and blue cells). Adapted from Subramanian et al., 2015

I.3.3 Signaling pathways

a) Tendon cell specification

In addition to intrinsic regulators of tenogenesis, the Transforming Growth Factor β (TGFβ) and Fibroblast Growth Factor (FGF) signaling pathways have been shown to be involved in tendon development in mouse and chick embryos (Brent and Tabin, 2004; Brent et al., 2003, 2005; Edom-Vovard et al., 2002; Pryce et al., 2009). Bioinformatics analysis of a transcriptome of tendon cells also highlighted that these two were the main pathways displaying significant regulation during mouse limb development (Havis et al., 2014).

TGFβ ligand is a potent inducer of *Scx/SCX* expression in embryonic mouse and chick limbs, tendon progenitors and mesenchymal stem cells. The genes coding for TGFβ2 and TGFβ3 are expressed in early chick and mouse limbs to fulfill a role in *Scx/SCX* induction (Havis et al., 2014; Lorda-Diez et al., 2010; Pryce et al., 2009). In mice, TGFβ2 is sufficient to increase *Scx* expression in E10.5 limbs, tendon progenitors and mesenchymal stem cells (Havis et al., 2014; Maeda et al., 2011; Pryce et al., 2009). A similar result can be observed in chick limbs grafted with TGFβ2 beads (Havis et al., 2016). Moreover, the canonical TGFβ intracellular pathway, SMAD2/3, has been shown to be required for *Scx* expression in E10.5

mouse limbs during the muscle-independent phase of limb tendon formation, as well as in the chick between E3 and E4 (Havis et al., 2014, 2016). Also at E16.5, tendons of *Smad3*^{-/-} mice exhibited a disturbed architecture as well as a reduction in *Col1a1* and *TnC* expression (Berthet et al., 2013). This same study also showed that SMAD3 was able to physically interact with SCX and MKX (Berthet et al., 2013).

Blocking classical TGF β intracellular pathway using chemical inhibitors also decreases *scx* expression in zebrafish embryos (Chen and Galloway, 2014). However, *Scx* expression appears to be normal in E11.5 limbs of *Tgfb2*^{-/-}; *TGFB3*^{-/-} double mutant mouse embryos, suggesting that other TGF β ligands might be responsible for the initiation of *Scx* expression in mouse limbs (Pryce et al., 2009). Another TGF β ligand, myostatin (GDF-8), is a putative candidate to be involved in tendon development, since tendons are small, brittle and hypocellular in *Mstn*^{-/-} mice (Mendias et al., 2008). Moreover, myostatin treatment of primary culture of mouse tendon fibroblasts increases cell proliferation, in addition to increasing *Scx* and *Tnmd* expression (Mendias et al., 2008). BMP ligands that signal via the intracellular Smad1/5/8 pathway have the opposite effect from TGF β and restricts *Scx* expression, while inhibition of BMP signaling using the antagonist Noggin increases *SCX* expression in early chick limbs (Schweitzer et al., 2001). Myostatin is a potent negative regulator of muscle growth, while BMP positively regulates muscle progenitors during embryonic development (Manceau et al., 2008; Wang et al., 2010). The antagonist roles of TGF β and BMP signaling pathways in tendon cell specification is consistent with their antagonist role in the regulation of fetal muscle progenitors.

The FGF pathway has been shown to be required and sufficient for the initiation of SCX expression in somites during chicken axial tendon development. An ectopic source of FGF induces ectopic expression of *SCX/Scx* in chick and mouse somites and chick limbs, while inhibition of FGF signaling prevents *SCX* expression (Brent et al., 2003, 2005; Edom-Vovard et al., 2002). Two members of the ERK/MAPK pathway, *ETV4* (effector) and *SPROUTY2* (modulator) are both expressed in tendon progenitor regions in chick syndetome and FGF has been shown to act on somitic tendon progenitors via the ERK/MAPK intracellular pathway (Brent and Tabin, 2004; Smith et al., 2005). Besides, implantation of FGF4-beads in developing chick limbs resulted in an increase of *EGR1* and *SCX* genes expression, showing again the positive effect of the FGF pathway on tendon development in chick (Havis et al., 2016; L ejard et al., 2011). The FGF pathway also seems to respond to mechanical signals during chick limb development in order to induce *SCX* expression in developing tendons (Havis et al., 2016). However in mouse limbs, the ERK/MAPK signaling pathway appears to have a different effect, since a downregulation of ERK/MAPK was sufficient to increase *Scx* expression in mouse limb explants and in mouse mesenchymal stem cells (Havis et al., 2014). Consistent with this result, FGF inhibited *Scx* expression in mouse mesenchymal stem cells (Havis et al., 2014).

b) Tendon cell differentiation

In addition to being involved at early stages of tendon induction, the TGF β and FGF extracellular signals have been shown to be involved in tendon differentiation during the muscle-dependent phase of limb tendon formation (Edom-Vovard et al., 2002; Havis et al., 2014, 2016; Pryce et al., 2009). In the absence of TGF β 2 and TGF β 3 function, there is a complete loss of *Scx* expression in head, axial and limb tendons and subsequently tendons are lost (Pryce et al., 2009). TGF β gain-of-function experiments in E12.5 mouse limbs lead to an upregulation of *Scx* and *Tnmd* expression (Havis et al., 2014; Pryce et al., 2009). TGF β gain-of-function experiments in a high-density cell culture system of HH25 chick hindlimbs (micromass) also lead to an up regulation of *SCX* and *TNMD* expression via the SMAD2/3 intracellular pathway (Lorda-Diez et al., 2009). TGF β -interacting factor (Tgif1) has been shown to promote the fibrogenic effect of TGF β 2/SMAD2/3 intracellular pathway in chicken micromass cultures (Lorda-Diez et al., 2009). It has to be noted that the addition of TGF β ligands in 2D cell culture systems activates *Scx*, but drastically inhibits *Tnmd* expression (Brown et al., 2014; Guerquin et al., 2013; Liu et al., 2015a). This indicates that TGF β ligands cannot induce complete tenogenesis in 2D stem cell cultures, in contrast to *ex vivo* experiments, where TGF β activates *Tnmd* in addition to increasing *Scx* expression in mouse limb explants (Havis et al., 2014). FGF has been shown to increase the number of SCX⁺ cells at the expense of muscle cells in chick limbs during fetal development (Edom-Vovard et al., 2001, 2002). The expression of the ERK effector *ETV4/Etv4* and modulator *SPRY2/Spry2* is observed in both muscle and tendon and is increased at the muscle-tendon interface in chick and mouse limbs (Eloy-Trinquet et al., 2009). However, despite similar expression in fetal chick and mouse tendons of FGF signaling components, FGF appears to have a distinct effect in mouse fetal tendon development compared to that in chick. FGF has been shown to downregulate *Scx* and *Tnmd* expression in mouse tendon cells isolated from E13 mouse embryos at the limb or axial levels (Brown et al., 2014). FGF appears to be crucial for *SCX* induction and maintenance in chick but not in mouse embryos.

Other signaling pathways might also be involved in tendon cell specification or differentiation. The WNT pathway is significantly regulated in mouse tendon cells during limb development, according to bioinformatics analysis of a tendon transcriptome (Havis et al., 2014). Moreover, *Wnt3a* has been shown to positively regulate *Six2*, another putative tenogenic transcription factor, in autopod tendons of developing chick limbs (Liu et al., 2015b; Yamamoto-Shiraishi and Kuroiwa, 2013). In another study, WNT3a was able to induce a re-specification of chondrogenic progenitors toward soft connective tissues progenitors (ten Berge et al., 2008). In the same way, the WNT pathway positively regulated *TNMD* expression in equine mesenchymal stem cells (Miyabara et al., 2014). Also, a genome-wide study identified *WNT4* as a downstream target of *EGR1* in a cMM explant model overexpressing *EGR1* (Orgeur et al., 2018). However, the WNT/ β -catenin signaling pathway was also shown to be a potent repressor of tenogenic gene expression. Activation of Wnt/ β -catenin signaling in rat tendon-derived cells suppressed the expression of *Scx*, *Tnmd* and *Mkx*

(Kishimoto et al., 2017). The activation of this pathway also antagonized the upregulation of *Scx* by the TGF β /SMAD2/3 signaling pathway (Kishimoto et al., 2017).

1.4 Achieving tenogenic differentiation in cell cultures through biochemical treatments

1.4.1 Starting with a model: mesenchymal stem cells, adipose-derived cells and tendon stem/ progenitor cells

Directing tendon cell differentiation is of crucial importance both for fundamental and applied research to understand tendon development and tendon tissue engineering. However, there is still a lack of specific protocol for tenogenic differentiation coupled with a great diversity of cell types used to achieve tenogenesis *in vitro*. Indeed, Mesenchymal Stem Cells (MSCs), Bone Marrow Stromal Cells (BMSCs), Tendon Stem/Progenitors Cells (TSPCs) or other cellular models can be used to that aim (Bi et al., 2007; Bianco, 2014; Docheva et al., 2015; Shearn et al., 2011). In this way, it seems necessary to define the major types of cells used, those aforementioned, before going any further in the effects of the chemical treatments that could be applied to them. Only then will we be able to take a closer look at the current strategies employed to direct tenogenic differentiation through biochemical cues.

a) Mesenchymal stem cells

The idea of bone marrow-derived fibroblasts involved in wound healing was first envisioned in the nineteenth century (Conheim, 1867). BMSCs were first isolated from bone marrow when their osteogenic potential was proven upon its transplantation in a diffusion chamber allowing for diffusion of nutrients while barring cell migration in and out of the chamber (Friedenstein et al., 1966, 1968). The “Mesenchymal” stem cell concept first originated from this discovery of an osteogenic potential in bone marrow, residing in fibroblast-like adherent cells. This concept was also extended as MSCs were thought to give rise to a broad spectrum of mesenchymal lineages specified through different pathways, notably including osteocytes, chondrocytes and adipocytes (Figure I.16) (Caplan, 1991; Pittenger et al., 1999; Prockop, 1997; Wachtler, 1981). *in vivo*, these cells are thought to be the pericytes, located on the abluminal side of the blood vessels (Bianco, 2014; Caplan and Correa, 2011). The pericytes would give rise to MSCs in long-term culture, with a multilineage differentiation potential at the clonogenic level. Also and independently of their origin in the organism, the pericytes display a large panel of markers known to be MSCs markers, such as CD44, CD105 or CD146, (Crisan et al., 2008). However, they were also shown to retain the expression of the markers displayed in their tissue of origin (Crisan et al., 2008). Keeping a trace of their origin, combined with the important number of extraction protocols could be a major point in the apparent diversity of MSCs (Caplan and Correa, 2011; Sharma et al., 2014). Thus, MSCs can be harvested from a wide variety of tissues, even if they might retain

some of these tissues characteristics. This particularity alone is already a great advantage for research, but they were also shown to possess trophic, paracrine, anti-inflammatory and immunomodulatory functions (Murphy et al., 2013; Sharma et al., 2014). C3H10T1/2 cells are a multipotent murine cell line with a fibroblast-like morphology harboring MSCs characteristics as they are able to differentiate into chondrocytes, osteocytes and adipocytes when cultured under appropriate differentiation culture media (Guerquin et al., 2013; Ji et al., 2010; Kim and Jang, 2017; Lee et al., 2017). However, these immortalized cells are not strictly adult multipotent stem cells as they were first isolated from mouse embryos (Reznikoff et al., 1973). They constitute a fair example of the versatility expected from such a model of MSCs. All the possibilities offered by the MSCs establish them as a powerful biological material, but this concept is also challenged precisely because of this incredible versatility (Bianco, 2014).

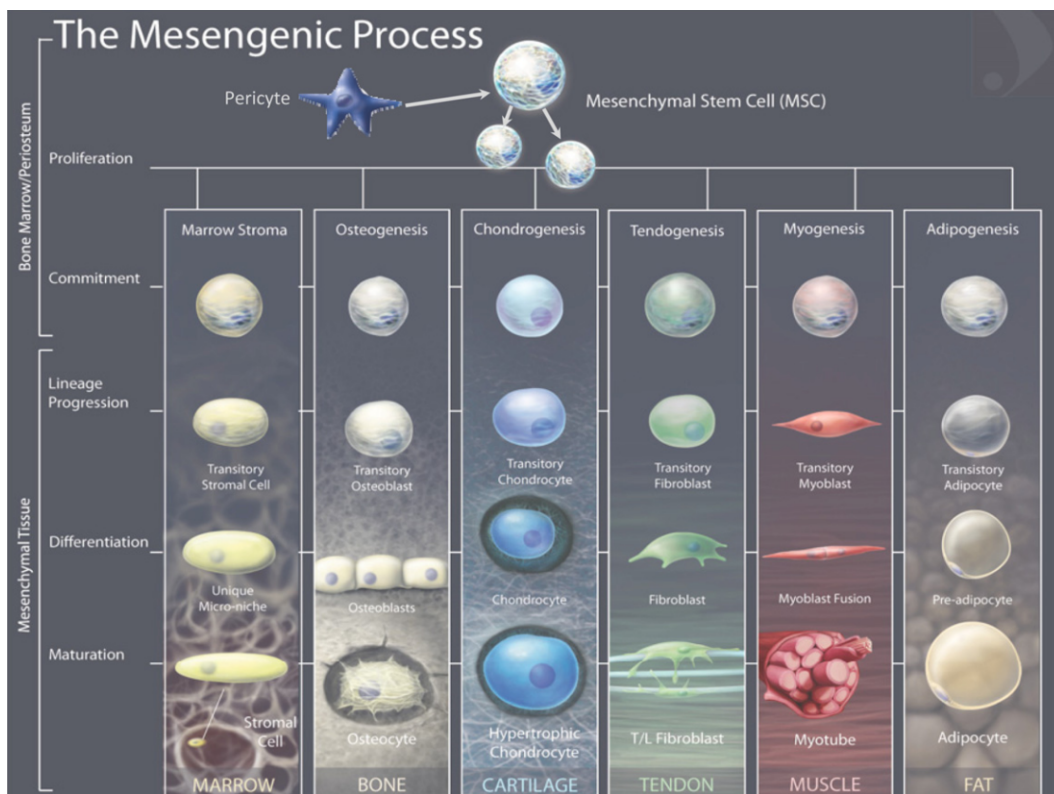


Fig. I.16 **The differentiation potential of mesenchymal stem cells.** Schematic representation of the differentiation potential of MSCs, as envisioned by Caplan and colleagues. Here we can see that the MSCs come from the pericytes and can give rise to several lineages, notably tendon cells (in green). Adapted from Caplan et al., 2011

b) Adipose-derived mesenchymal stem cells

Other cell types are also used such as MSCs derived from adipose tissue (ADSCs) and are attractive notably due to their easy isolation in addition to the properties aforementioned such as multidifferentiation. However, compared to BMSCs these cells are less prone to

osteogenic and chondrogenic differentiation, while they are really efficient when it comes to adipogenesis (Docheva et al., 2015). These cells are also able to express tenogenic markers, proliferate faster in cell culture and to respond to biochemical and topographical cues in order to differentiate into tendon cells (Docheva et al., 2015; Kryger et al., 2007; Madhurakkat Perikamana et al., 2018; Park et al., 2010).

Altogether, these studies show that ADSCs might be established as a good source to model tendon cell differentiation as they are able to achieve multidifferentiation, but less toward osteogenesis, while being relatively easy to harvest.

c) Tendon stem / progenitor cells

Another major source to study the tendon cell differentiation in culture would be the Tendon Stem/Progenitor Cells (TSPCs). We decided to group under this acronym the tendon-derived stem cells, tendon progenitor cells and generally all the naïve cells derived from tendons, with characteristics and properties of stem or progenitor cells of this tissue, namely self-renewal and tenogenic differentiation.

A definitive TSPC population was first identified *in vivo* in mouse and human tendons by Bi et al. in 2007 (Bi et al., 2007). In this paper, they generated and cultured single-cell suspensions from wild-type C57BL/6 mouse patellar tendon or human hamstring tendon. These cells were first quiescent and then formed adherent colonies. These TSPCs were molecularly distinct from BMSCs, notably through higher expression of *Scx*, *TNMD*, *Runx2/RUNX2* and *Sox9/SOX9*. TSPCs also displayed multidifferentiation potential toward osteogenesis, chondrogenesis and adipogenesis. Besides, they showed self-renewing capacities and formed tendon-like tissues upon subcutaneous transplantation in nude mice (Bi et al., 2007). This unique pool of progenitors reside within a unique niche, mainly controlled by *Fmod* and biglycan and playing a role in the tenogenic efficiency of TSPCs (Bi et al., 2007). In double mutants for these molecules, TSPCs responded more effectively to BMP signaling and favored the osteogenic lineage (Bi et al., 2007). It appears that the environment of these cells is also critical for correct maintenance and differentiation.

Other studies demonstrated the existence of TSPCs in human tendons, or even generated tendon cell lines (Kohler et al., 2013; Salingcarnboriboon et al., 2003; Tempfer et al., 2009). One of them showed that perivascular cells from tendon capillaries were indeed such progenitors, which would be concordant with the Pericyte-MSCs hypothesis mentioned above, although tendons are really poorly vascularized (Crisan et al., 2008; Tempfer et al., 2009).

Another study showed the existence of TSPCs in tendon proper and peritenon, both population harboring stem cell, fibroblast and perivascular markers (Mienaltowski et al., 2013). Besides, cells harvested from tendon proper showed higher tenogenic -differentiation- properties than those of the peritenon (Mienaltowski et al., 2013, 2014).

These inherent tenogenic properties, the expression of early and late tenogenic markers, make of the TSPCs a really relevant model, even if some challenges are still going on regarding the standardization of their extraction, characterization and final differentiation in culture (Docheva et al., 2015; Yan et al., 2018).

1.4.2 Biochemical cues driving tenogenic differentiation

Directing tendon cell differentiation *in vitro* is of crucial importance for the understanding of the molecular processes involved, the cellular changes the cells are going through, but also to better explain what is happening *in vivo* both during development and healing process. We will here see how biochemical treatments are used for that aim, *in vitro*.

TGF β signaling pathway

The TGF β signaling is known *in vivo* to participate in tendon development to induce *Scx* expression (Havis et al., 2014, 2016). Regarding *in vitro* tenogenic differentiation, TGF β also plays important role. TGF β 2 is able to induce *Scx* and *Col1a1* expression in cultures of C3H10T1/2 cells, adult MSCs and embryonic TSPCs with TGF β 2-supplemented medium (Brown et al., 2014, 2015; Havis et al., 2014; Pryce et al., 2009). Interestingly, this treatment also downregulated the expression of the cartilage gene *Sox9/SOX9* in C3H10T1/2 cells and cMM culture, indicating that TGF β signaling would really favor the tenogenic differentiation (Havis et al., 2014; Lorda-Diez et al., 2009). Similar effects can be found for type I collagen production in MEFs isolated from SCX-GFP cells and cultured in 3D constructs in fibrin gel, which have been treated with TGF β 2 (Chien et al., 2017). This indicates that TGF β effects go from the activation of gene expression to matrix production.

Also, TGF β 1 had similar effects in BMSCs, but it also enhanced the expression of *Tnmd* and *Egr1*, especially when used in combination with Connective Tissue Growth Factor (CTGF) (Yin et al., 2016). This last study showed that initial treatment with TGF β 1 was able to initiate tendon-associated gene expression, while its combination with CTGF allowed its maintenance during several days of culture. TGF β 3 was also shown to play a role in *in vitro* models of tenogenic differentiation. In 3D-engineered tendon constructs of fibrin gel, it is required for the proper formation of the constructs and the expression of *TNC* and *COL1A1*, but never for *SCX* (Barsby et al., 2014). However, in cell cultures of human ADSCs, TGF β 3 treatment in combination with a proper ECM scaffold upregulated *SCX* and *TNC* expression (Yang et al., 2017b). It was also able to upregulate tendon gene expression and collagen I content in rabbit BMSCs and C3H10T1/2 cultures (Bottagisio et al., 2017; Havis et al., 2014).

TGF β signaling could be effective for tenogenic differentiation through its intracellular SMAD2/3 pathway. It was shown by co-immunoprecipitation in C3H10T1/2 cells that SMAD3 physically interacts with SCX and MKX (Berthet et al., 2013). Besides, a treatment of tendon fibroblasts with Myostatin (GDF-8, member of the TGF β superfamily) induced the activation of the SMAD2/3 signaling pathway, as well as *Scx*, *Tnmd* and *Col1a2* expression (Mendias et al., 2008). Finally, the beneficial effect of TGF β 2 treatment in C3H10T1/2 cells and cMM culture was abrogated when they were co-treated with an inhibitor of the SMAD2/3 pathway, confirming once more the role of this intracellular pathway (Havis et al., 2014; Lorda-Diez et al., 2009).

Interestingly, the effects of the TGF β signaling are also very effective regarding tenogenic initiation in other cell types. Indeed, in C2C12 cells, a murine myoblast cell line, treated with

Myostatin showed an increase in *Scx* and *Tnmd* expression in a time- and dose-dependent manner (Uemura et al., 2017). Also, its effects were abrogated when a siRNA knockdown of *Smad3* was operated in these cells, confirming once more the role of the SMAD2/3 pathway (Uemura et al., 2017).

Connective tissue growth factor

Ctgf belongs to the CCN (*Cyr61/Ctgf/Nov*) gene family and is also known as *Ccn2*. It was discovered and named as such because of its mitogenic activity in connective tissue (Bradham et al., 1991). CTGF and the proteins of this family belong to the matricellular proteins, which are proteins present in the ECM but that regulate cell function rather than ECM structure (Murphy-Ullrich and Sage, 2014). CTGF is considered a positive regulator of adhesion, migration, survival and apoptosis (Malik et al., 2015). The CCN proteins act either by interacting with cell surface receptors or ligands. This last mode of action could explain the interaction observed (and described previously) that CTGF in combination with TGF β 1 was able to upregulate and maintain tendon-associated gene expression (Yin et al., 2016).

Alone, CTGF has been demonstrated to induce the differentiation of human BMSCs into fibroblasts with an increase in synthesis of type I collagen and tenascin-c. This came along a reduced capacity for these cells to differentiate into osteocytes, chondrocytes and adipocytes (Lee et al., 2006, 2010). However, it is suggested that CTGF could have a biphasic role, promoting either fibroblastic or osteoblastic differentiation depending on its environment and its combinatorial effect with other molecules (Zhang et al., 2018). In rat TSPCs cultures and in combination with ascorbic acid, it also enhanced tendon-associated genes expression while downregulating that of chondrogenic and osteogenic markers (Lui et al., 2016; Ni et al., 2013). In cultures of mice TSPCs, cells treated at confluence with CTGF in combination with ascorbic acid were able to form cell sheet which, once hooked between two anchors, produced models of 3D-engineered tendons (Wang et al., 2018a).

When overexpressed in rat TSPCs, *Ctgf* promoted the tenogenic differentiation and the expression of related genes *Scx*, *Tnmd*, *ColI* and *TnC* and its knockdown had the opposite effect (Liu et al., 2015c). Its effect was shown to promote the tenogenic differentiation induced by the BMP12 treatment of these cells (Liu et al., 2015c).

Bone morphogenetic proteins

The Bone Morphogenetic Proteins (BMPs) and their subfamily of Growth Differentiation Factors (GDFs) play important roles in skeletal tissue development, notably BMP12, 13 and 14 (respectively GDF-7, -6 and -5) (Wolfman et al., 1997). *In vitro*, these factors also play on tenogenic differentiation as we will next see. GDF-5 was demonstrated to lead to an increase of tenogenic (*Scx*, *Tnmd*, *TnC*) and ECM (*Col1a1*, *Dcn*, *Acan*) markers, ECM synthesis and proliferation in ADSCs cultured or not on biomaterials (James et al., 2011; Park et al., 2010; Shen et al., 2013). In human MSCs or BMSCs in 2D or 3D cultures, GDF5 also induced an

upregulation of tendon genes expression, as well as collagen expression and an elevated ratio of type I to type III collagen, a marker of tendon cells (Govoni et al., 2017; Tan et al., 2012).

Regarding other GDF members, GDF-6 treatment has similar effects. It upregulates *Thbs4* in C3H10T1/2 cultures and *Scx* expression, as well as *Tnmd*/TNMD both at the levels of gene and protein expression (Berasi et al., 2011; Zhang et al., 2018). GDF-7 (BMP12) also induces tenogenic differentiation, as it was previously shown when used in combination with CTGF for example (Liu et al., 2015c). Treatments of GDF-7 in ADSCs cultures induced the expression of tendon genes such as *Scx*, *Tnmd*, notably via the SMAD1/5/8 pathway and more potently than GDF-5 in the same conditions (Shen et al., 2013). All together, these studies clearly show that the trio GDF-5, -6, -7 have a particular role in inducing tenogenic differentiation.

Fibroblasts growth factors

FGFs are crucial *in vivo* during chicken limb tendon development (Gaut and Duprez, 2016; Havis et al., 2014, 2016). In human BMSCs, FGF-2 (also known as bFGF) enhanced matrix production through tenogenic-ECM genes expression (COL I, COL III, FN) in late stages (Hankemeier et al., 2005). Also, FGF-2 upregulated *Scx* expression in cultures of C3H10T1/2 cells, but also in C2C12 myoblasts and primary muscle-derived stem cells (Ker et al., 2011). However not all the FGF ligands have the same effect, since FGF-4 was shown to inhibit *Scx* and *Tnmd* expression on mouse TSPCs and C3H10T1/2 cultures (Brown et al., 2014; Havis et al., 2014). Conversely, FGF inhibition by PD18 treatment -an inhibitor of the ERK MAPK signaling pathway- activated the expression of *Scx* and *Col1a1* (Havis et al., 2014). Interestingly, FGF-4 has the opposite effect on tendon gene expression in chick limb explant culture and show a species-specific role notably between chick and mouse (Havis et al., 2016).

Together, these studies show how powerful are growth factors to drive tendon cells differentiation *in vitro* (Figure I.17). The biochemical cues are potent by themselves but should also be used in combination with mechanical cues to see how their effects can be improved (Zhang et al., 2018). Although these treatments are not able to completely achieve a terminal differentiation, as well as others that have not been presented here, they show promising results in regard to clinical application and understanding of the molecular pathways involved in tenogenesis (Docheva et al., 2015; Zhang et al., 2018).

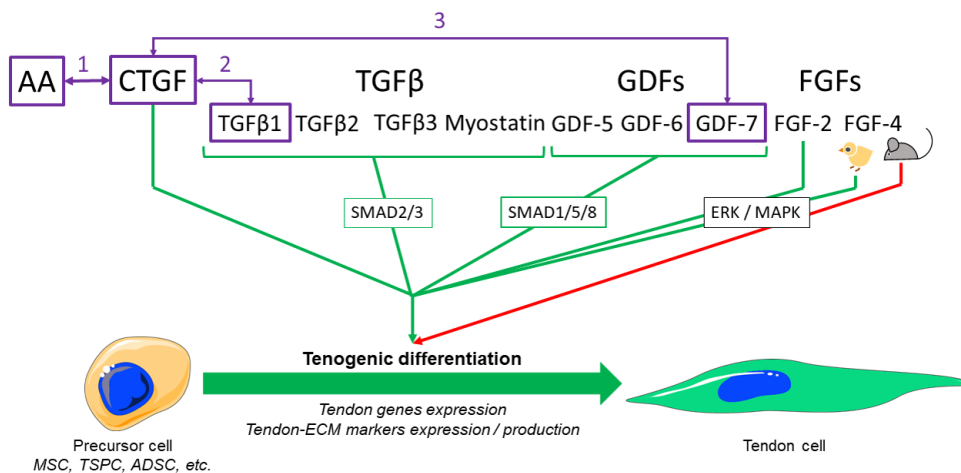


Fig. I.17 **Summary of the biochemical cues inducing tenogenesis *in vitro*.** Schematic representation of the biochemical cues inducing *in vitro* tendon cell differentiation, tendon marker expression or tendon-ECM production. The purple arrows and lines indicates the combinatory treatments in which CTGF has been used, with (1) Acid Ascorbic (AA), (2) TGF β 1 and (3) GDF-7. Green brackets and arrows indicate a positive effect of these molecules on tenogenesis in cell cultures. The red arrow indicates a negative effect on *in vitro* tenogenesis. FGF-4 is beneficial or not depending on the species (chick or mouse). Inside the green or black squares are indicated the intracellular pathways activated by their respective biochemical treatments. Self-made illustration.

I.5 Mechanobiology and development

In the previous chapters, we reviewed how the components of the musculoskeletal system, particularly tendons, developed during embryogenesis and fetal life. We also presented what were the biochemical signals and the intracellular molecular factors known to date to regulate these processes, both in *in vivo* and *in vitro* contexts. Thus, we showed how important these biochemical signals could be in modulating tenogenesis.

However, this presentation is far from being complete in that it does not include the involvement of the physical forces in all these biological processes. Mechanobiology focuses on how physical forces and changes in the mechanical properties of cells and tissues will be involved in cell differentiation, development, but also physiology and disease.

This field has drawn a lot of interest since the beginning of the XXth century and particularly since the second half of this same century (Figure I.18). The idea of coordination between different branches of science was already mentioned at the beginning of the XXth century. It concerned notably the need for physiologists and biologists to make a better use of mathematics and physics to describe living matter (D'Arcy, 1945; Forbes, 1920). D'Arcy already started to describe the form and shapes of living matter from a mathematical point of view and to consider forces such as surface tension acting on cells in his book "On Growth

and Forms” in 1917 (and in revised editions of 1942, 1945) (D’Arcy, 1945). To date, with the evolution of technology and science, we are better able to understand how these physical forces shape the living matter and how they are interpreted and dealt with at the molecular level by the cells.

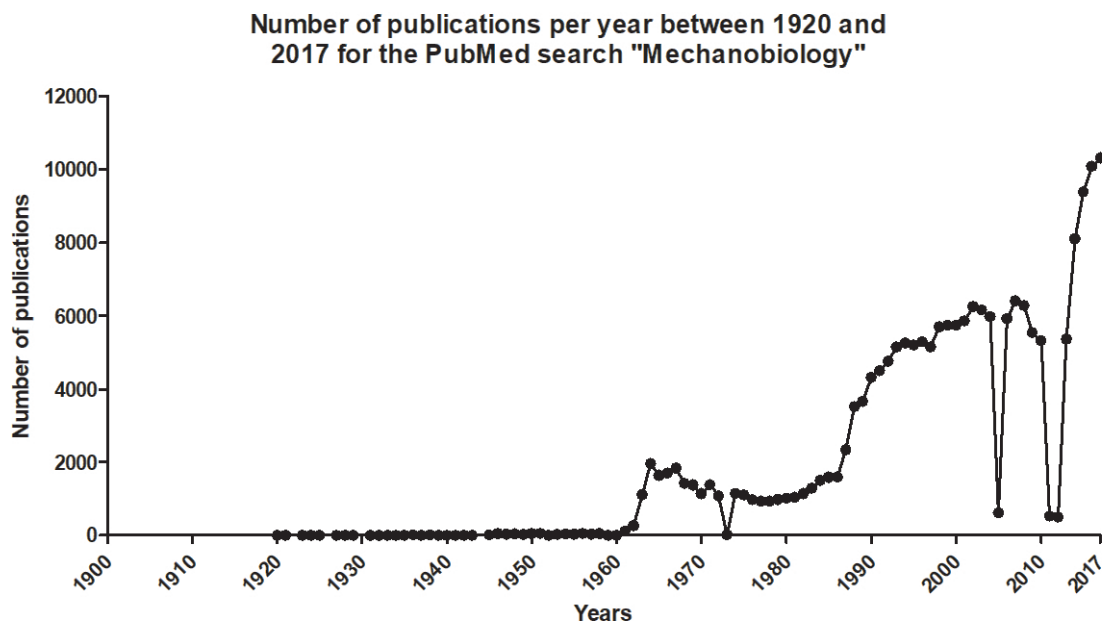


Fig. I.18 *Number of publications per year related to the PubMed search “Mechanobiology” between 1920 and 2017*

In this chapter, we will go through an overview of how the mechanical signals step in developmental mechanisms. Also, we will see that the ECM is deeply involved in this paradigm by conveying the forces from the environment to the cells in the tissues, to act during morphogenesis. Then, we will pay attention to the means used by the cells to sense these mechanical signals and to transduce them in intracellular molecular events, all the way down to their nuclei and the regulation of their genomes. Finally, we will take some time to introduce the Yes-Associated Protein (YAP), as one of the intracellular molecular effectors of mechanical signals. Various physical and mechanical concepts and terms might be used in the following chapters, as mechanobiology can be studied from physical, engineering and biological point of views. Also, please refer to the following table for a brief description of the terms used.

Terms	Definition
Stress	Measure of force intensity, given as “force per area” and expressed in newton per square meter (N/m^2), also called pascal (Pa). As a reference, $1\text{nN}/\mu\text{m}^2 = 1\text{kPa}$
Strain	Normalized measure of deformation, indicating changes in lengths or angles within a material under applied stresses. The strain is dimensionless; however, it can be expressed as a percent of change (%)
Stiffness	The stiffness (k) of a body is a measure of the resistance offered by an elastic body to deformation. For an elastic body with a single degree of freedom (e.g. stretching or compressing of a rod), the stiffness is defined as $k=F/\delta$ where F is the force applied to the body and δ the displacement produced by the force (the change in length, for example)
Material stiffness	Measure of resistance to deformation: how stress changes in response to strain. An ideal material with an infinite material stiffness is said to be rigid and presents a infinite Young’s modulus (see below).
Strength	Measure of resistance to material damage or failure reflecting the maximal values of stress that can be tolerated before failure.
Elastic	Mechanical behavior that does not dissipate energy. An elastic material returns to its original geometry when unloaded. The elasticity is defined as the Young Modulus (see below).
Young’s Modulus (E)	The Young’s modulus (E) also known as the elastic modulus, is a measure of the stiffness of a solid material. It defines the relationship between stress and strain in a material. As mentioned above, an elastic material will deform when a load is applied to it and returns to its original shape after the load is removed. In the range where the ratio between load and deformation remains constant, the stress–strain curve is linear. Not many materials are linear and elastic beyond a small amount of deformation (typically 1-5% strain). As explained above, a stiff material needs more force to deform compared to a soft material and an infinite force would be needed to deform a perfectly rigid material, implying that it would have an infinite E. E is the ratio of stress (units of pressure) to strain (dimensionless) and so is expressed in units of pressure, therefore in Pa. The practical units used are megapascals (MPa or N/mm^2) or gigapascals (GPa or kN/mm^2).

Table I.1: **Introduction to terms and concepts in mechanobiology.** Sources: Humphrey et al., 2014; Vining et al., 2017; Wikipedia page on Young’s modulus

1.5.1 Mechanical forces in development

a) Intrinsic mechanical cues and early development

The growth, differentiation and morphogenesis during development are dependent on the interaction between biochemical cues and intrinsic and extrinsic mechanical forces, driving cell assembly and growth into higher-order structures. This starts from the very earliest step of fertilization. The penetration of the extracellular zona pellucida (ZP) by the sperm to go through the oocyte membrane will trigger a cortical reaction that will harden the ZP by crosslinking its molecular filaments to block the entry of other sperm (Boccaccio et al., 2012). The presence of these cells-generated forces was first demonstrated by macro-scale dissection of embryos of *Rana temporaria* (Beloussov et al., 1975). In this study, embryos have been dissected and shape alterations of different parts of the embryo were analyzed. A part of the deformations observed could be inhibited either by temperature or by cytochalasin B treatment -an inhibitor of actin filament formation-, which led to the conclusion that these processes resulted from active work of intracellular contractile systems. These internal forces are generated by non-muscle myosin II in actomyosin complexes. Together, they form a contractile cytoskeletal network spanning from the nucleus to the cell cortex. Myosin II and the contractile actomyosin network are required for elastic properties of the cells and for junction remodeling during planar cell intercalation during axis elongation in the *Drosophila* embryo (Bertet et al., 2004; Fernandez-Gonzalez et al., 2009; Kumar et al., 2006; Rauzi et al., 2008). The mechanical strain resulting from morphogenetic movements will continue to act during embryogenesis, activating several molecular pathways and in all species. In *Drosophila*, studies demonstrated the mechanical induction of the expression of Twist, mesoendodermal transcription factor, in response to convergence-extension cell movements and mediated by the β -catenin pathway (Desprat et al., 2008; Farge, 2003). Also, the specification of early mesoderm was shown to be a conserved mechanism in Bilateria. A common mechanosensitive pathway mediated by the phosphorylation of β -catenin is involved in early mesoderm specification at gastrulation both in zebrafish and *Drosophila* (Brunet et al., 2013).

Similar mechanosensitive mechanisms were also demonstrated in the shoot apex of the plant *Arabidopsis thaliana*. Its morphogenesis is dependent on the microtubule cytoskeleton, its own coordinated patterns of arrays being regulated by mechanical stress (Hamant et al., 2008). These studies show how important, diverse and conserved are the mechanical cues during development.

That sort of cell-generated events are also observed as soon as the first steps of mouse embryogenesis, where cell contractility drives compaction in the embryo (Maître et al., 2015, 2016). At the 8-cell stage, this compaction involves the development of cell-cell contacts, the cell-medium interface and relies on the actomyosin cortex, giving rise to cellular contractions (Maître et al., 2015). The difference of contractility between each blastomere will impact their localization into inner or outer positions, which will have a direct influence on their lineage specification (Maître et al., 2016).

Inside these cells, the cytoskeleton is a crucial element influencing their shape, internal components, reaction to their environment, coordinated movements and indirectly such phenomenon as symmetric vs asymmetric divisions. As such, a brief description of this apparatus should be given to clarify its structure and role inside the cells, in order to provide a better understanding of the events exposed in this chapter.

The cytoskeleton consists in an adaptable web of filaments spread all over the cell, with a highly dynamic structure. Cytoskeletal structures can change or persist according to the cell needs. However, the individual molecular components making up these structures are in a constant state of flux. It is composed by intermediate filaments, microtubules and actin filaments (Figure I.19).

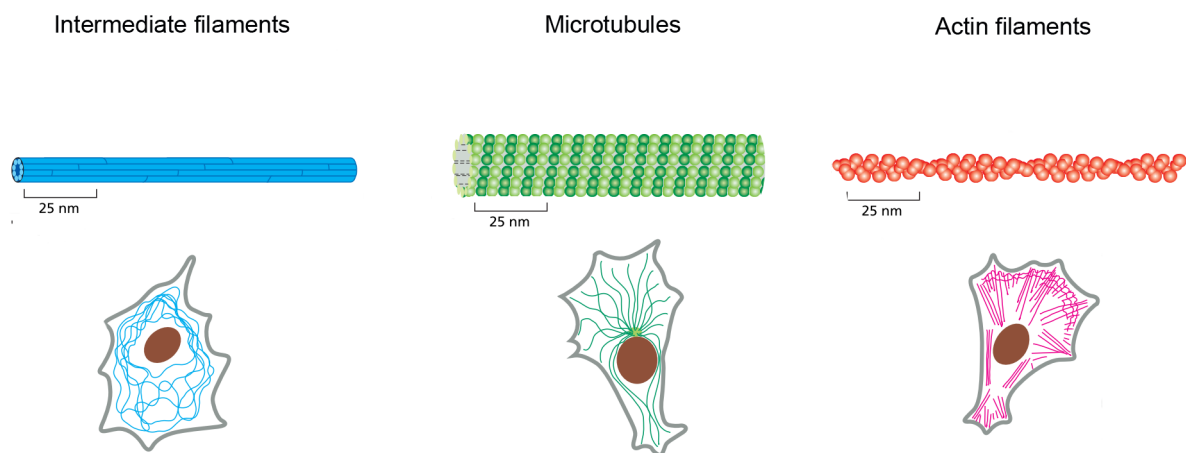


Fig. I.19 The three major types of protein filaments forming the cytoskeleton. Intermediate filaments (blue) extend across the cytoplasm and around the nucleus (brown), giving mechanical strength. Microtubules (green) are long and straight and all have one end attached to the centrosome. Actin filaments (red) are dispersed throughout the cell and mostly concentrated below the plasma membrane. Adapted from Alberts and Johnson, *Molecular Biology of the Cell*, 5th ed., 2007

Intermediate filaments

Intermediate filaments provide mechanical strength to the cell, they are rope-like filaments with a 10 nm diameter. They support the nuclear envelope and are spread all over the cytoplasm and often linked to the plasma membrane at intercellular junctions by desmosomes. They are particularly present in the cytoplasm of cells subjected to mechanical stress and play an important role in providing mechanical strength (Alberts and Johnson, 2007). Interestingly, the nuclear lamins are related to these filaments, they form a meshwork underlying the inner nuclear membrane, thus providing anchorage for chromosomes and nuclear pores.

Microtubules

The microtubules possess a crucial role in the organization of eukaryotic cells. They are long and relatively rigid tubes of 25 nm diameter. Their walls are composed of parallel filaments of polymerized tubulin, the basic unit of tubulin being itself a dimer of α and β subunits. They are structurally strong but constantly dynamic: they expand and contract in length and can sometimes completely depolymerize. They originate from a structure called the centrosome and spread in a star-like cytoplasmic array from that point in interphase cell. Microtubules can also form permanent structures on the surface of the cell called cilia. Cilia are efficient motility machines that beat quite synchronously in a whip-like motion. Another type of cilia is the primary cilium, which is found on the surface of many different cell types, including fibroblasts, bone cells and chondrocytes (Alberts and Johnson, 2007). The interesting point is that they concentrate many signaling proteins, notably mechanosensitive calcium channels that open when the fluid flow bends the primary cilia (Corrigan et al., 2018).

Actin filaments

Finally, the third major component of the cytoskeleton are the actin filaments, which are required for the determination of the shape of the cell's surface as well as for locomotion. They are helical polymer of the globular G-actin that associate to form strong and flexible structures. The F-actin filament consist of two parallel protofilaments twisting around each other in a helix (Alberts and Johnson, 2007). Actin filaments are dispersed throughout the cells where they have various functions, but they are highly concentrated in the cortex, beneath the plasma membrane where they form a meshwork involved in regulating cell shape and movements. Subcortical actin fibers have also been shown to exert some influence on mitotic spindle positioning, relaying the effects of external forces in that process (Fink et al., 2011). These filaments however are very unstable and display a highly dynamic behavior. Under their G- or F-actin forms, they can be associated with other proteins, such as MAL, a co-factor of transcription acting with SRF, or F-actin capping/severing proteins, thus making their state of polymerization important for other types of signaling (Aragona et al., 2013; Posern and Treisman, 2006).

In the context of the blastocyst, the changes in forces and mechanical properties of the ECM applied to the cells complete the intrinsic forces generated by the cells and contribute to the change in gene expression driving different cell fates. This can go through the adaptation of the cytoskeletal elements modulating molecular factors sensible to the cell mechanical state, such as YAP (Mammoto et al., 2013). Contractile forces induced by the cytoskeleton were also shown to be involved in *Drosophila* development. Here, they are required for closure of the dorsal epidermal opening at the end of the gastrulation (Kiehart et al., 2000). This is rendered possible by actin cables in the dorsal epidermis migrating cells, but also by the underlying amnioserosal cells pulling the above cells by apical constriction-driven forces (Figure I.20).

Generally speaking, all these studies and the tremendous number of others that were not presented here all show how mechanical forces generated by the cells thanks to their cytoskeleton play key roles during multiple, or all, developmental processes.

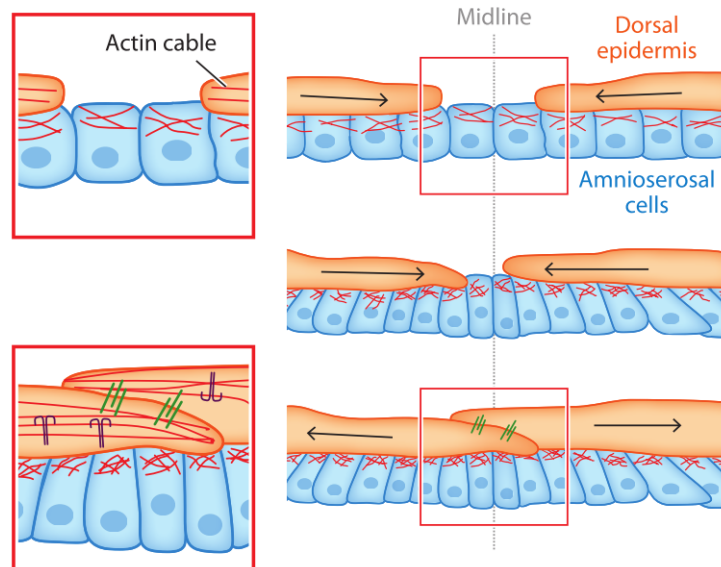


Fig. I.20 **Epithelial tissue closure.** Epithelial tissue closure as described in Kiehart et al., 2000. Migrating cells at the edge of the epidermis extend their filopodia to interact with each other through cell-cell junctions (in green). The underlying amnioserosal cells pull the cells above by using apical constriction-driven forces rendered possible by the modulation of they actin filaments at their apical side. Adapted from Mammoto et al., 2013.

b) Extrinsic mechanical cues: extracellular matrix and external factors in morphogenetic control

We previously reviewed the effects of intrinsic forces generated by the cells during contractions and morphogenetic movements. The cells are able to change their own fate through these mechanical cues they exert on each other and within themselves. During development, progenitor cells will differentiate and produce the ECM to which they will adhere. Morphogenetic movements also involve constant remodeling of the ECM, which connects cells within tissues and act as a 3D elastic scaffold. By doing so, the ECM will distribute forces among its cells, altering their own traction forces and even modifying their shapes (Mammoto et al., 2013). It was demonstrated *in vivo* in early mouse embryos that mechanical strains developed by the external environment was able to regulate the distal visceral endoderm formation and its intrinsic transcriptional program (Hiramatsu et al., 2013). This is only an example of the broad range of functions that is affected by forces conveyed by the ECM, including growth, apoptosis, cell migration, specification and differentiation, etc.

The composition of the ECM is continuously modulated by the cells attached, which in turn can affect the morphogenetic movements. Adherent cells and their traction forces

can remodel the ECM and its collagen fibers, creating or strengthening bundles between cells *in vitro* (Kim et al., 2017). This is also the case *in vivo* for FN modulation in matrix by cell-cell and cell-ECM adhesions. In *Xenopus laevis*, changes in cadherin adhesion and cell-cell junction impact tissue cohesivity and its response to the tension applied, resulting in deficient FN assembly (Dzamba et al., 2009). On the opposite, FN is required in the ECM to affect cells during developmental processes, such as the establishment of the asymmetric gene expression pattern in mouse embryos (Pulina et al., 2011). Also, the ECM's stiffness is able to induce lineage specification, as it was demonstrated with naïve MSCs cultured on substrates of different stiffness mimicking either -from soft to rigid- brain, muscle and bone. When cultured on these matrices, cells were specified to the lineage mimicked. Namely, cells on soft ECM gels differentiated into a neuronal-like lineage, those on stiff gels into osteoblasts and in myoblasts for MSCs cultured on ECM of intermediate stiffness (Engler et al., 2006). Thus, the cell-ECM interactions are of crucial importance for cell fate and development in general. Integrins are important actors of this interaction between cells and their ECM, especially in the context of mechanical forces transduction (Sun et al., 2016). These transmembrane proteins allow binding to the ECM components through their external parts, such as laminin or FN and transduce the mechanical or biochemical signals to the intracellular molecular components on which they are (in)directly linked, notably the F-actin fibers (Alberts and Johnson, 2007). There are many types of integrins, each with a specific activity, that also each have different ligand-binding specificities depending on the cell type in which they are expressed. Thus, they constitute a major tool for the cells to bind and respond to the tremendous diversity of ECM types encountered and a single mechanical cue could then have different impacts depending on these environments (Alberts and Johnson, 2007; Gasiorowski et al., 2013; Sun et al., 2016).

The loads, tensile forces or the strain then imposed by the ECM will promote the assembly of the cytoskeleton into actin stress fibers or focal adhesions, activating several signaling pathways of molecular factors, such as YAP or SRF (Aragona et al., 2013; Humphrey et al., 2014; Posern and Treisman, 2006; Yang et al., 2000). This is a typical mechanism through which cells can adapt and respond on the molecular level to the mechanical signals coming from their environment.

The cues coming from the ECM represent a vast catalog of biomechanical signals for the adherent cells. However, they are not the only external mechanical signals the cells are subjected to. Shear forces generated by the flow of the fluids surrounding the cells are also sensed and trigger several responses (Figure I.21A). For example, fluid shear stress is able to activate the transcription of *EGR1* gene in human endothelial and epithelial cell culture systems (Schwachtgen et al., 1998). Blood flow is also required during heart valve morphogenesis in zebrafish embryos and are required for both the proper migration and mechanotransduction response of endocardial cells (Boselli et al., 2017; Goddard et al., 2017). Also this kind of stress is able to bend the primary cilia on the cells, thus enabling the activation of several of

the signaling proteins concentrated there, or the opening of mechanosensitive Ca^{2+} channels (Alberts and Johnson, 2007).

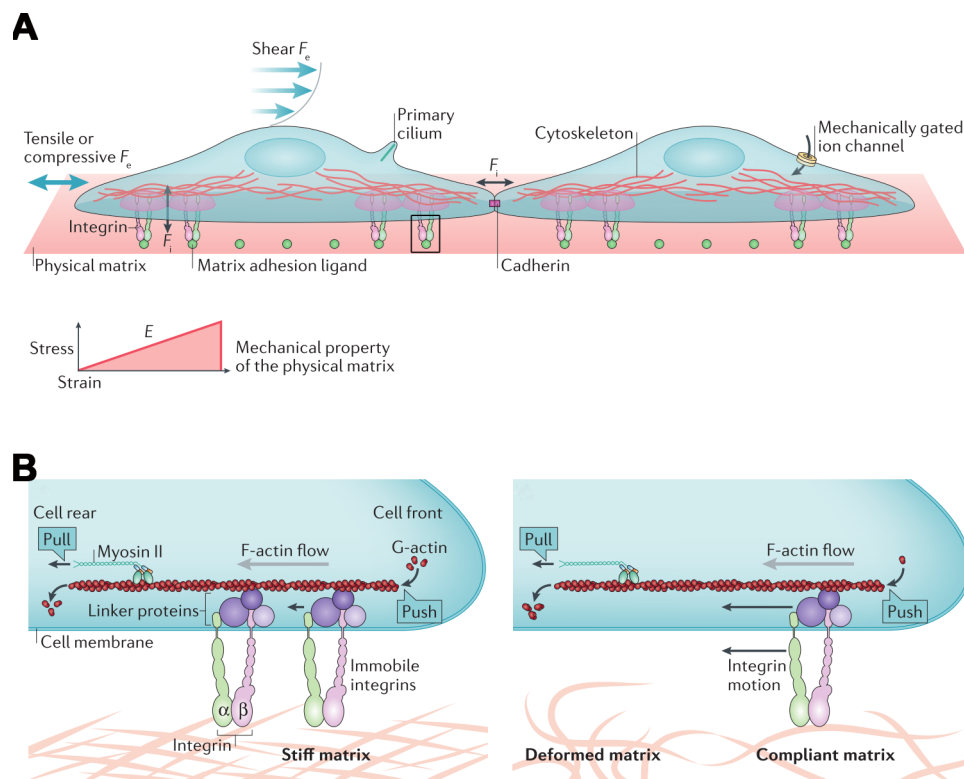


Fig. I.21 **Extrinsic mechanical cues applied on the cells.** (A) Brief summary of the mechanical cues to which cells can be subjected. Extrinsic forces (F_e) are applied by tension or compression of the cells, shear stress, mechanically gated ion channels, deformation of the primary cilium or by the ECM. Intrinsic forces (F_i) are also depicted here through the cell-cell junctions. Picture adapted from Vining et al., 2017. (B) Focus on the area delimited by the black square in (A). Schematic of the adhesion of the cells on stiff (left panel) or soft (right panel) substrates through integrin-binding. In all cases integrins are coupled to F-actin filaments via linker proteins (violet discs). These proteins and the integrins will move accordingly to the forces generated by actin polymerization and/or Myosin II contractions. On stiff substrates the integrins remain immobile and resist these forces, on soft substrates they follow the forces and move backward, altering cellular responses. Picture adapted from Humphrey et al., 2014.

1.5.2 Mechanical signal transduction at molecular level

Mechanical forces exerted by the cell through cell-cell junction and contraction, or on the cells through cell-ECM adhesions are critical for morphogenesis and developmental processes. The process by which the cells sense changes in physical force balance is termed “mechanosensing” and is realized through multiple ways as we will see in this part. Then the intracellular process by which the mechanical signals detected by mechanosensing are transduced into changes in biochemistry and gene expression is termed “mechanotransduction”.

a) **Mechanosensing: how cells detect forces**

Integrin-mediated adhesions are stabilized under force and they constitute a way for the cell to detect and respond to the biophysical properties of the external environment. They truly are a bridge between the ECM and the F-actin cytoskeleton (Figure I.21B). Integrins are the principal receptors in animal cells for binding the majority of ECM proteins. They are very various, but all share common features. An integrin molecule is made up by two glycoproteins subunits, α and β , that are noncovalently associated. They are transmembrane subunits with short intracellular C-domain and large N-terminal extracellular domains (Alberts and Johnson, 2007). The C-terminal portion is responsible for the binding of a complex of proteins linking the integrin to the cytoskeleton, such as focal adhesion kinase (FAK), talin, vinculin (VCL), paxillin, kindlin and others (Figure I.22A). The N-terminal part binds ECM structural proteins such as laminins or FN, or other ligands (Figure I.22A). Integrins are subjected to allosteric regulation, meaning that as an integrin binds or detaches to its ligand, it will undergoes conformational changes that will have a similar impact to its binding properties at the other end of the molecule, enabling signal propagation in both ways (Alberts and Johnson, 2007; Sun et al., 2016). Upon ligand binding, different proteins will be recruited to the site of the short intracellular C-terminal end of the integrin, composing an adhesion structure. This structure changes over time in size and composition and is influenced by both chemical and mechanical properties of the ECM substrate (Schiller and Fässler, 2013). This adhesion-mediated rigidity sensing induces the reorganization of cell-matrix adhesions. Thus, for example in a migrating cell, nascent adhesion will first form on its leading edge, that are able to transmit pushing forces from the actin cytoskeleton polymerization (Figure I.22B). Then, as most nascent adhesion will be quickly disassembled, some of them will grow in size along F-actin bundles into focal adhesions. In these focal adhesion, where the traction force is the most important, the link between integrins and F-actin, via linker proteins, is reinforced (Figure I.22B). The maturation into large focal adhesion requires myosin II -mediated cell contractility (Schiller and Fässler, 2013). In the end, focal adhesion will disassemble for the majority and some of the integrins will be translocated into central fibrillar adhesion points, with relaxed actin bundle (Figure I.22B) (Sun et al., 2016). Thus, on stiff substrates, adhesion maturation accelerates and consequently decreases on soft substrate (Figure I.21B).

The mechanical loads will trigger conformational changes into the focal adhesions. Talin for example, undergoes stress-dependent unfolding, thus exposing a cryptic binding site for VCL. This will in turn trigger a clustering of other integrins, enhancing the transduction of the mechanical signal on the focal adhesion site (del Rio et al., 2016). This phenomenon is not specific to talin and VCL and also happens between other proteins at these sites, such as the actin-binding protein filamin A (FLNA), that reveals a cryptic binding site for integrins when it is mechanically deformed by the actin cytoskeleton (Ehrlicher et al., 2011).

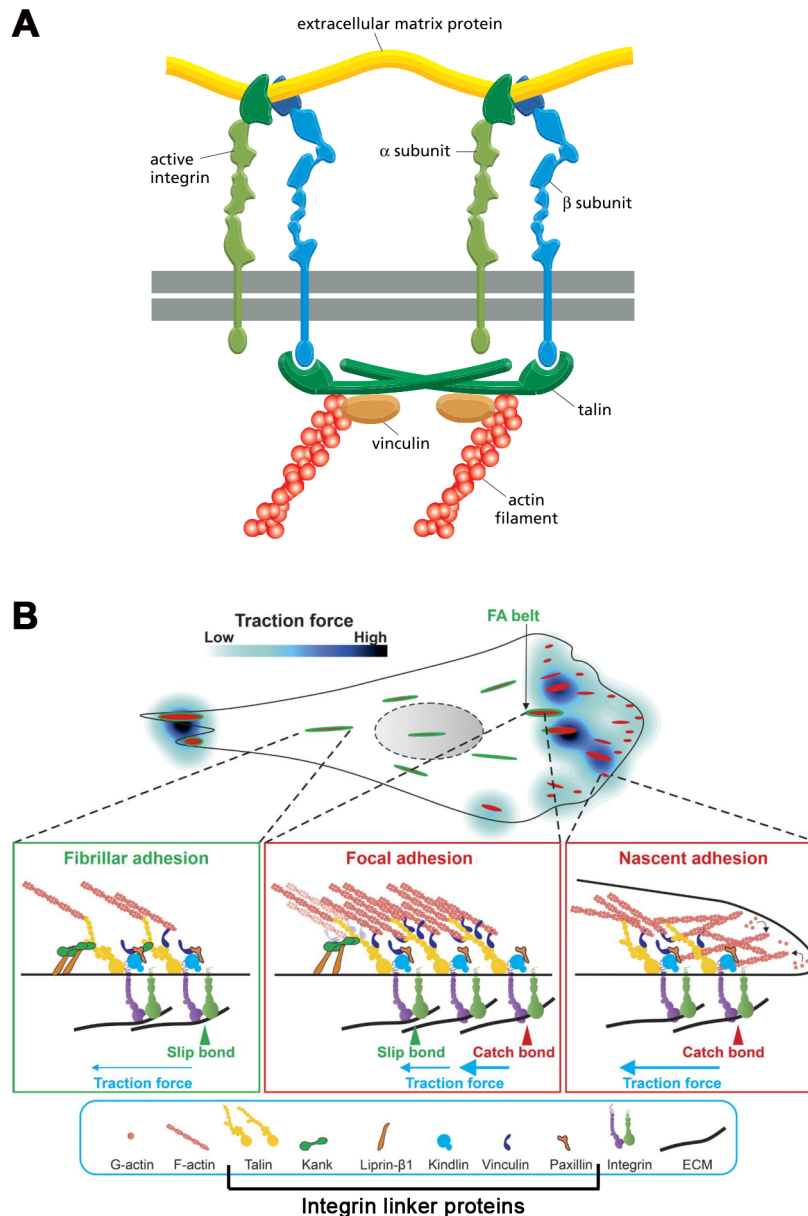


Fig. I.22 **Integrins and adhesion points.** (A) Schematic representation of the integrins with their adhesion complex. The α subunit (light green) and the β subunit (blue) are in an active state and bind the ECM protein (yellow). They both span the plasma membrane and the β subunit is linked the actin cytoskeleton (red) by linker proteins, as talin (dark green) and vinculin (brown) that are here represented. Picture from Alberts et al., 2007 (B) Formation of adhesion points in a motile cell. At the leading edge (on the right), nascent adhesion will first assemble by mobilization of actin filaments and the formation of catch bond between active integrins (green and violet) and ECM proteins (black), these bonds are force-stabilized and durable. Some nascent adhesion will grow into focal adhesion where the traction force is highest, with a higher mobilization of actin cytoskeleton and greater force transmission between ECM and actin cytoskeleton. Starting from the fibrillar adhesion (FA) belt, F-actin will less strongly bind talin, resulting in a progressive demobilization of the actin cytoskeleton concomitant to a reduction in the traction force. This will give rise to smaller fibrillar adhesion, mainly forming slip bond, whose lifetimes are shortened by application of forces, leading to loosened interactions. Adapted from Sun et al., 2016.

Traction forces are also exerted on cell-cell adhesions and are mainly transmitted along the cells in tissues through cadherin-based intercellular junctions (Mammoto et al., 2013). These adhesions work, in a way similar to the integrins, as force transmitters and mechanosensors able to induce several cell behaviors. Cadherins form a superfamily of transmembrane proteins mainly requiring Ca^{2+} to achieve their extracellular binding and keep adjacent cells together. Cadherins bind on their extracellular part by homophilic binding, meaning with cadherins of the same -or close- subtype and on their intracellular part they are indirectly anchored to the cytoskeleton (Alberts and Johnson, 2007). This anchorage is mediated by several proteins, among which the catenins are the main components. In general, β -catenin is involved with p120- or α -catenin and intracellular anchor proteins to link the cadherin to the cytoskeleton (Figure I.23A).

When activated, cadherin adhesions promote the local assembly and new branching of F-actin filaments, more efficient in producing contractility and recruitment of non-muscle myosin II (Figure I.23B). These recruitments and polymerization will also activate several signaling pathways such as RHOA (Charras and Yap, 2018). In a similar way to its role in focal adhesion, myosin II will increase intercellular tension that will induce conformational changes at the cadherin-catenin complex. It was already demonstrated that under such a force, α -catenin at this complex will expose a cryptic binding site recruiting VCL to cell-cell contacts (Figure I.23C) (Charras and Yap, 2018; Yonemura et al., 2010). Also, forces applied to E-cadherin complex activated the AMP-activated protein kinase signaling, as well as favoring the recruitment and phosphorylation of VCL (Bays et al., 2014, 2017). These studies offer a good view on how the cell-cell junction complexes enable each cell to sense the force spread among all of them and a way to respond to this force.

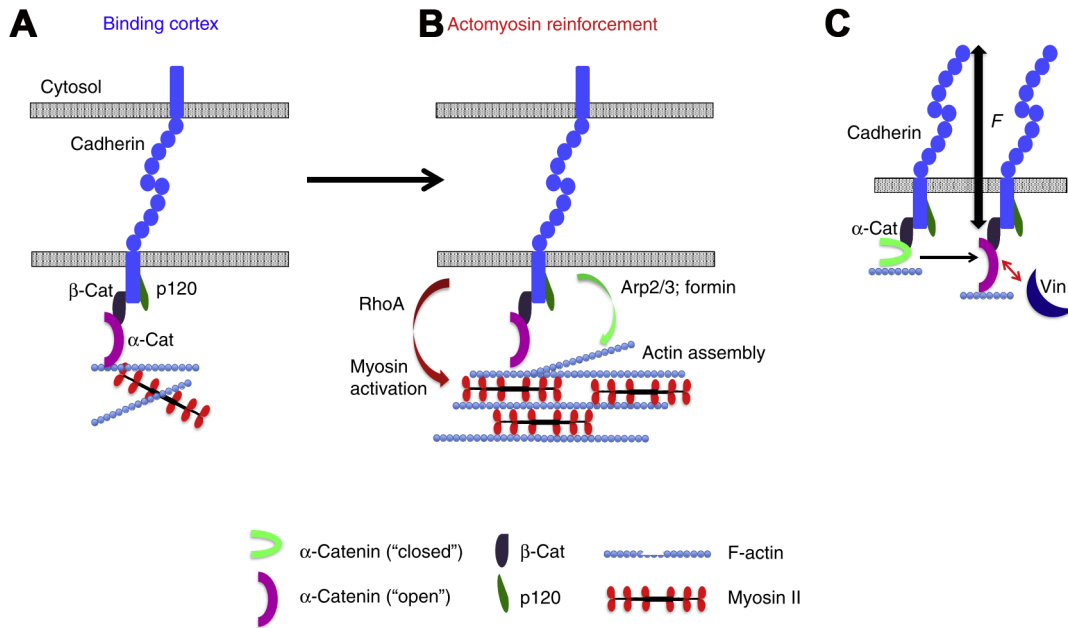


Fig. I.23 **Cell-cell junction at the cadherin complex.** (A) Structure of the cadherin complex, with cadherin, α -, β - and p120-catenin, F-actin filaments and Myosin II. (B) Prolonged cadherin adhesion will reinforce the cadherin complex and promote the recruitment of Myosin II and polymerization/new branching of F-actin notably through Arp2/3 and formin. (C) Conformation change of α -catenin upon application of force promotes recruitment of vinculin to the complex. Adapted from Charras *et al.*, 2018.

By itself, the cytoskeleton is also able to sense alterations in cell shape and to reorganize itself to better adapt. This is notably the case when cells are subjected to cyclic loading, they will actively remodel and reorient their cytoskeleton (Dhein *et al.*, 2014; Liu *et al.*, 2014). Also, RHO GTPase activity is a consequence of cell shape distortion. When cells are round and the actin cytoskeleton is disrupted and RHOA is activated through a cascade of molecular events and inversely in the opposite case (Mammoto *et al.*, 2013). Through RHO GTPases and actin cytoskeleton remodeling, several molecular factors involved in mechanotransduction will then relay the information to the cell nucleus and enable the cell to respond, which is notably the case for SRF and YAP (Dupont *et al.*, 2011; Posern and Treisman, 2006).

The primary cilium is another way for the cell to sense its mechanical environment and especially fluid shear stress. This structure concentrate many signaling proteins and is able to bend under sufficient force produced by shear stress. Thus, the primary cilium acts as a single sensory cellular extension. It was demonstrated that it had a pro-osteogenic mechanosensory role, notably in MSCs stimulated by oscillatory fluid flow (Hoey *et al.*, 2012; Stavenschi *et al.*, 2017). It was also shown that primary cilium could work with the TRPV4 ion channel (Corrigan *et al.*, 2018). This receptor belongs to the family of Transient Receptor Potential (TRP) and its subfamily V, from which it is the 4th member. These ion channels display diverse stimulatory mechanisms including mechanical activation (Nilius and Owsianik, 2011). The bending of the primary cilium induced by shear stress is able to open TRPV4 localized

on it, enabling the entry in the cell of Ca^{2+} ions and subsequent osteogenic gene expression (Corrigan et al., 2018).

All the mechanisms presented above are crucial for the cell to properly sense the mechanical signals. However, numerous other receptors and strategies of mechanosensing exist and have not been presented here, notably regarding the mechanically activated ion channels (Murthy et al., 2017). Subsequently to these first modifications elicited in the cells, various biochemical signaling pathways and other molecular factors will be triggered, all the way to gene expression, to achieve a proper response of the cell.

b) Mechanotransduction and gene expression

After the detection of mechanical signals, cells will have to transduce this information into an intracellular biochemical signal. The transition of a mechanical signal into a biochemical information is termed mechanotransduction. There are already numerous mechanosensing processes adopted by the cells and the possibilities are multiplied intracellularly. We will here focus only on SRF, EGR1 and YAP, since they will be of particular interest in the context of this thesis and to give a good view of some of mechanotransduction strategies.

b).1 Serum Response Factor SRF is a transcription factor that is involved in the control of many cytoskeletal, muscle specific genes and “immediate-early” genes (Esnault et al., 2014; Posern and Treisman, 2006). SRF recruits two families of coactivators, the myocardin-related transcription factors (MRTFs) and the ternary complex factors (TCFs) in order to achieve proper gene transcription. It does so regarding the biochemical context and the signaling pathway triggered to elicit a specific response in the cell. To properly activate its context-dependent transcriptional program, SRF form a complex with one of its coactivators, TCF or MRTF-A (also known as MAL or MKL1) (Figure I.24). However, SRF can activate common targets of these two coactivator families (Esnault et al., 2014). While TCF activity is controlled by RAS-ERK signaling, MRTF-A activity is controlled by RHO GTPases and actin polymerization (Miralles et al., 2003; Posern and Treisman, 2006). As we saw before, this second family of signal involving RHO GTPases and actin polymerization is typically involved in the mechanosensing process of the cells. This makes of SRF an ideal mechanosensitive transcription factor able to achieve a proper mechanotransduction. In turn, SRF-MRTF-A mediated transcription regulates the expression of actin- and cytoskeleton-regulatory proteins, transcription and cell growth (Esnault et al., 2014). Besides, MRTF-A-mediated transcriptional activity was linked to cell geometry (Jain et al., 2013).

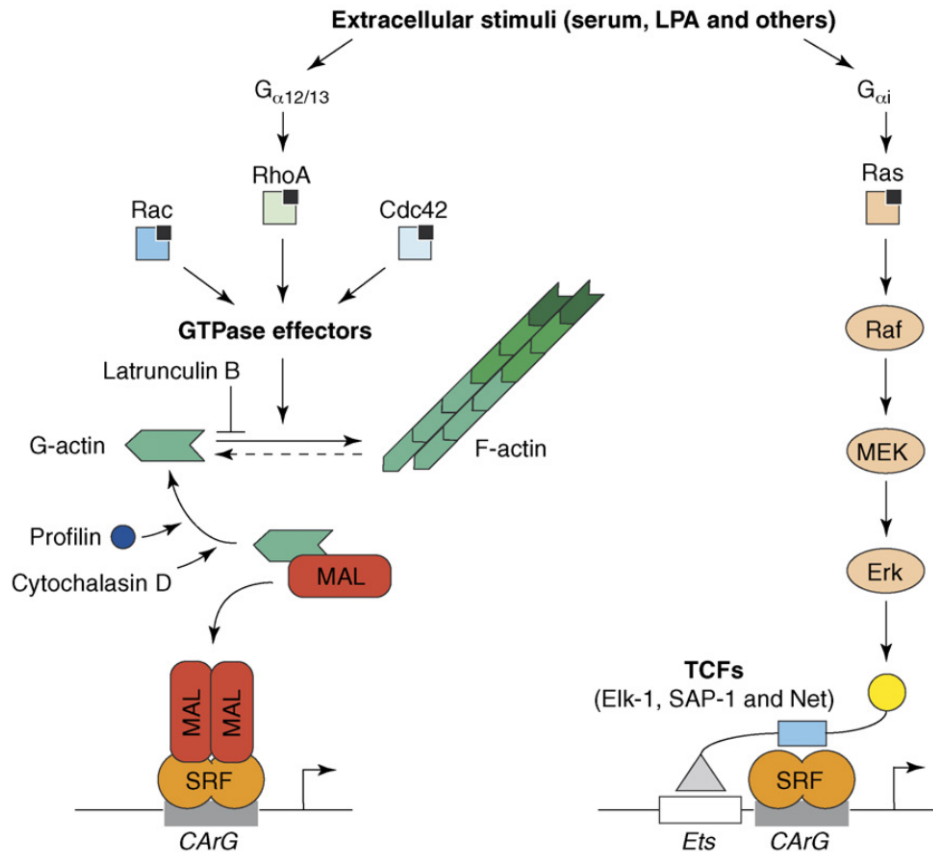


Fig. I.24 **The two principal pathways regulating SRF activity.** (On the left) Mechanical stimuli -among others- activate the Rho-family of GTPases (squares with black dots for GTP), that will promote the polymerization of F-actin filaments from G-actin subunits. By doing so, the G-actin subunits will free the coactivator MAL (MRTF-A) that will be able to bind SRF to activate their transcriptional program. (On the right) External stimuli will activate the MAP kinase pathway through Ras, Raf, MEK and ERK. This last one will phosphorylate TCFs (such as Alk-1, SAP-1 and Net) that will then be able to bind its own DNA recognition site and SRF in what is called the “grappling hook” model. Picture from Posern and Treisman, 2006.

b).2 EGR1 as a mechanosensitive transcription factor As previously explained, *EGR1* belong to a group of genes able to respond very quickly to a broad range of regulatory signals and known as immediate-early genes (Bahrami and Drabløs, 2016). Interestingly, *Egr1* is also a target gene of SRF, but through the SRF-TCF activation and independent of MRTF-A activity (Bahrami and Drabløs, 2016; Esnault et al., 2014). However, it does not prevent it from being transcribed in response to fluid shear stress and through MAPK signaling (Ogata, 2008; Schwachtgen et al., 1998). Mechanosensitivity to fluid flows of *Egr1* transcription was also shown *in vitro* in cultures of osteoblasts (Hamamura et al., 2008) Also, *Egr1* expression was reduced in adult tendons with limited movements, showing that at least its transcription results from a mechanosensitive process (Gaut et al., 2016). Besides, *in vitro*

in 3-dimensional (3D) cell cultures of MEFs, the transcription of *Egr1* is dependent of the static tension in these constructs (Gaut et al., 2016). However, if *Egr1* expression is forced in de-tensioned constructs, the tendon gene expression is restored, showing that EGR1 act downstream of the mechanical signals in the cell to control tendon gene expression (Gaut et al., 2016). In compressed 3D cultures of primary chondrocytes, *Egr1* expression was once again upregulated.

EGR1 activity is also linked to focal adhesion dynamics and caveola biogenesis, since under a mechanical stress pCAV1 will phosphorylate EGR1, thus preventing it from inhibiting the transcription of the *Cav1* and *Cavin-1* genes (Joshi et al., 2012). Also, after a stretch in C2C12 cells, EGR1 activates the transcription of the *Sirt1* gene, leading to regulation of the Reactive Oxygen Species levels in the cells.

All the studies presented above show how fast is the transcription of *Egr1* in response to mechanical signals and also confirm its role downstream of mechanical signals in the regulation of transcription of several genes. However, to this day there is not a well-defined *modus operandi* of EGR1 in response to mechanical signals, as it can be activated by stretch, focal adhesions and fluid shear stress. Nonetheless, it constitutes a really good example of versatility in regard to the mechanosensitive context.

b).3 The Yes-Associated Protein as a molecular effector of mechanical signals in cells

YAP and the Hippo pathway The YAP was first discovered to be an effector of the Hippo pathway that was described in *Drosophila melanogaster* to suppress cell proliferation, tumor growth and to regulate organ size (Zhao et al., 2011). Hippo is a Serine/Threonine kinase whose mammalian homologs are called MST1/2. When MST1/2 are phosphorylated, they are activated and phosphorylate the LATS1/2 kinases (mammalian homolog of Wts in *Drosophila*). Once phosphorylated, LATS1/2 will themselves phosphorylate YAP/TAZ (both being mammalian homologs of Yki in *Drosophila*) (Huang et al., 2005). However, the phosphorylation of YAP by the Hippo signaling pathway will lead to its sequestration in the cytosol by the 14-3-3 protein, which will prevent it for activating its transcriptional program (Figure I.25).

Upstream of the Hippo pathway, it is known that MST1/2 can be activated by binding to Ras association domain family proteins (Zhao et al., 2011). However, the other mechanisms leading to their activation are poorly understood. Multiple proteins in the Hippo pathway interact through WW domains that bind to proline-rich motifs. This is notably the case between MST1/2 and its auxiliary SAV1 or with LATS1/2 that binds the WW domain of YAP/TAZ (Wackerhage et al., 2014). Also, LATS1/2 have been shown to be negatively regulated by G-protein coupled receptors (GPCR) signaling, thus enhancing YAP activity in the cells (Yu et al., 2012). YAP/TAZ and angiomin (AMOT) proteins were also shown to interact, which promotes the YAP/TAZ localization to tight junctions and its inhibition through phosphorylation (Zhao et al., 2011).

YAP is a transcriptional co-activator that is unable by itself to bind DNA. In order to exert its trans-activator function, it must interact with transcription factors such as those of the TEAD family (Stein et al., 2015; Zanconato et al., 2015). TEAD transcription factors recognize and bind MCAT elements (CATTCC) in promoters or enhancers of genes to regulate their transcription. Direct targets of YAP/TEAD complex have been identified, like *Ctgf*, *Cyr61*, Inhibin beta-A (*Inhba*). Interestingly, YAP-TEAD share a lot of common target genes with SRF-MRTF-A and both pathways can be dependent on each other for activating some of these genes (Esnault et al., 2014; Foster et al., 2018).

Increased YAP activity is observed in cancers and *Yap1* overexpression in the liver increases its size and leads to tumor formation. A similar phenotype is observed in mutant mice which are deficient for *Mst1/2* (Zhao et al., 2011). In stem and progenitor cell models, YAP is beneficial for stem cell proliferation and in certain cases an inhibitor of differentiation. Concordant with that role, YAP was also found to be required in several regeneration processes (Zhu et al., 2014).

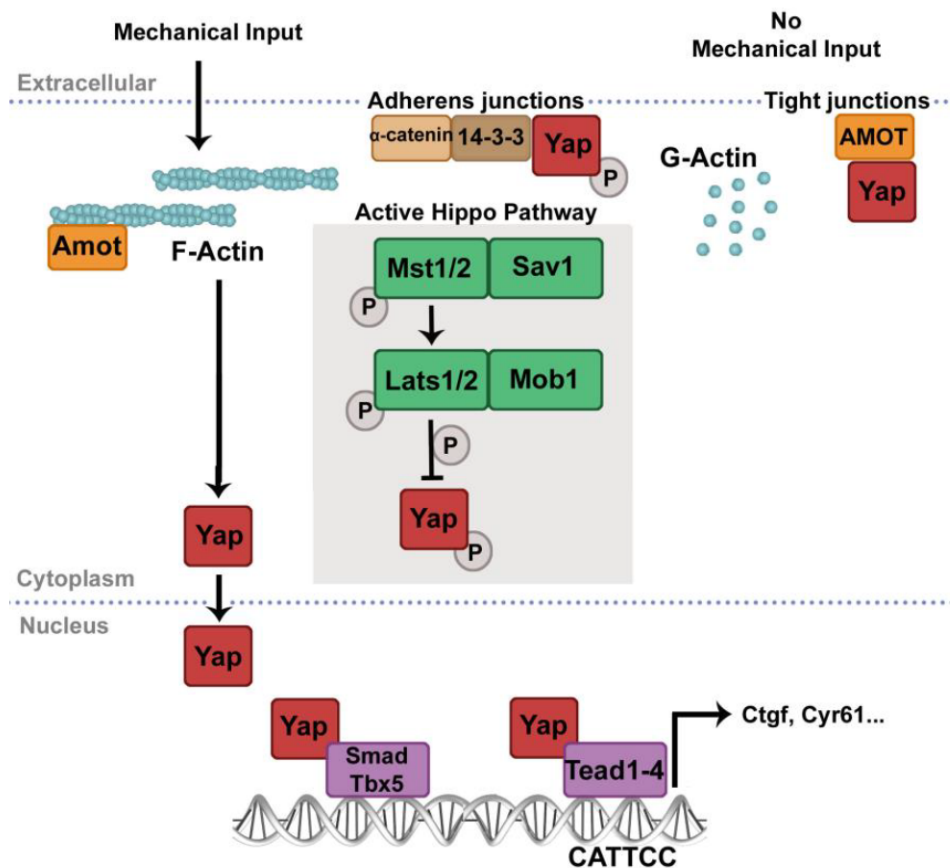


Fig. I.25 *Yap activity is influenced by the Hippo signaling pathway and mechanical cues. Illustration from Sophie Gournet*

YAP as a mechanotransducer In this chapter, we saw that cells perceive their microenvironment through mechanical cues and that they are able to respond to it through mechanotransduction systems. Apart from its roles in cell proliferation, organ size control and as a target of the Hippo pathway, YAP is also known to be a major actor in mechanotransduction processes in multiple type of cells (Panciera et al., 2017). In cells, YAP (as well as TAZ) was shown to be a nuclear relay of mechanical signals exerted by ECM rigidity and cell shape (Dupont et al., 2011). This mechanotransduction process is independent of the Hippo pathway and requires RHO GTPase activity and tension of the actomyosin cytoskeleton. On small areas or soft substrates, YAP will be inactive, while it will be the opposite on large area, stiff substrates, low cell density or other mechanical stimulations (Panciera et al., 2017) (Figure I.26). Also, mechanical regulation of YAP subsequent to changes in physical and architectural features happening in multicellular sheets are able to affect cell behavior. This is notably going through the polymerization of the actin cytoskeleton, as F-actin-capping and -severing proteins act as YAP inhibitors (Aragona et al., 2013). Besides, as F-actin competes with YAP for the binding of YAP-inhibitor protein AMOT, the polymerization of F-actin cytoskeleton will free YAP from this interaction, enabling it to pursue its activity (Figure I.25) (Mana-Capelli et al., 2014). The mechanosensing focal adhesion complexes have also been involved in YAP and TAZ regulation, establishing again their role as effector of the mechanical signals (Panciera et al., 2017).

Regarding its role in stem cell mechanobiology, it was shown that YAP was strongly involved in MSCs differentiation regulation by multiple mechanical signals. YAP promotes the osteogenic fate in MSCs on stiff substrates and also on soft substrates when Yap1 is overexpressed (Panciera et al., 2017). Generally speaking, YAP will be activated along an increase in substrate stiffness and in cells cultured *in vitro* in 3D gels it will be the relay of the particular mechanical signals of this environment, to promote stiff substrate (Panciera et al., 2017). However, some studies suggest that YAP would be an inhibitor of chondrocyte differentiation, even if this lineage is favored on stiff substrates (Yang et al., 2017a; Zhong et al., 2013). While no study clearly establish a link between YAP activity and tenogenic differentiation, a transcriptome analysis, notably of YAP/TAZ target genes, in chick fibroblasts embedded in different 3D gels established that collagen gels might desensitize this type of mechanotransduction pathway (Yeung et al., 2015).

Altogether, these studies establish YAP as a potent relay of the mechanical cues to induce gene expression allowing the cell to offer a proper response to its physical environment.

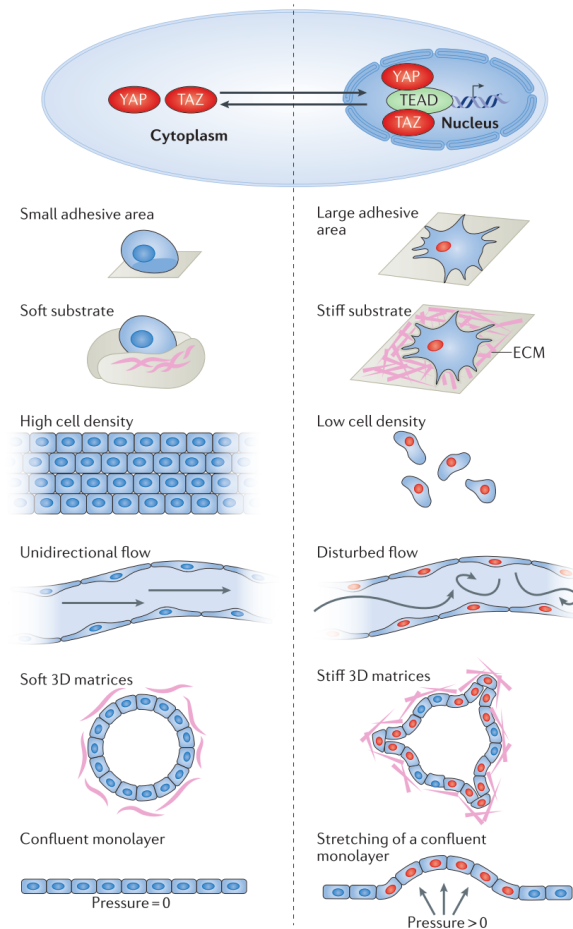


Fig. I.26 *Mechanical stimuli influencing YAP activity and subcellular localization.* From Panciera et al., 2017

I.6 Tendon mechanobiology

I.6.1 Mechanical properties of tendons and response to mechanical loading

The study of tendon mechanical behavior allows for a better understanding of the mechanical loads applied on tendon cells. Tendons adapt to the load generated by muscle contractions to transmit forces to bone but also to improve locomotion efficiency by acting like springs. Tendons display a hierarchical fibrillar arrangement of type I collagen fibers that are the fundamental force-transmitting elements of the tendon. The parallel orientation of these fibers along the muscle-to-bone axis promotes very high tensile strength in that direction and account for tendon's viscoelastic response (Khayyeri et al., 2015) (Figure I.4). When observed under the microscope, longitudinal sections of tendons present a periodic striation, termed "crimp". This crimp results from the spatial arrangement of collagen fibrils in tendon fascicle sheaths (endotenon, epitenon and paratenon) and is thought to be a shock-absorber and to play a role in elastic recoil (Wang, 2006).

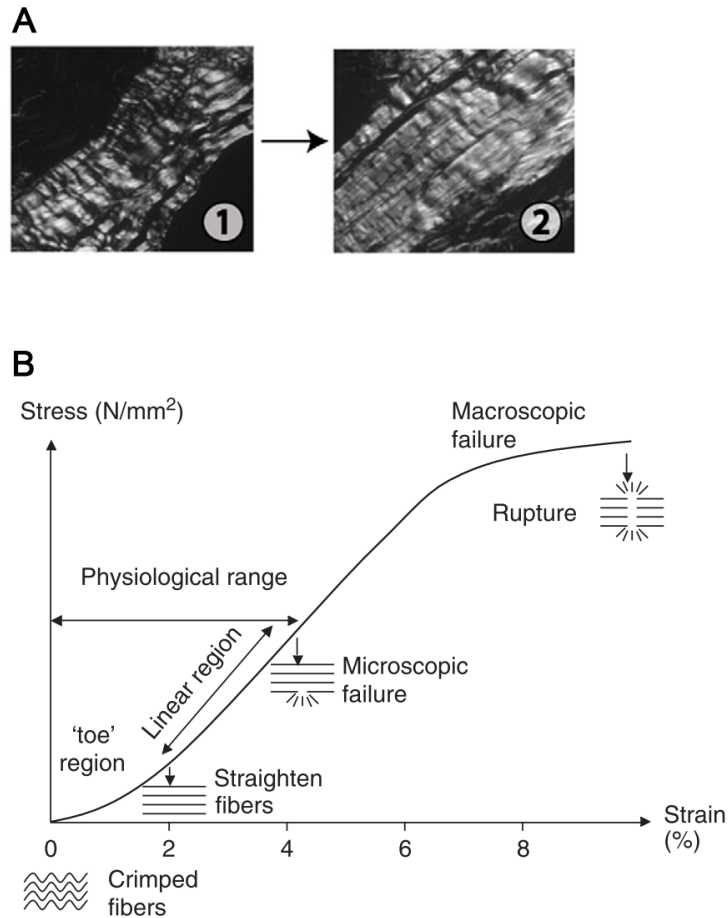


Fig. I.27 **Generic changes observed in tendon structure upon strain.** (A) Tendon with the crimp pattern (1) and uncrimped tendon (2). Image from Connizzo *et al.*, 2013. (B) Typical Stress-Strain curve of tendons. Stress values are tendon- and species-dependent, as indicated in Table 2. Image from Wang *et al.*, 2006.

The collagen fibers arrangement defines a structure that is seen as a “crimp-pattern” under longitudinal sections of tendons and often seen in the non-linear regions of the tendon strain-stress curve (Figure I.27). Upon mechanical stretch, the fibers rearrange consequently, contributing to the mechanical behavior of the tendon. This can be visualized in the stress-strain curve depicting typical changes occurring in tendons upon mechanical loads (Figure I.27). The stress-strain curve has an initial “toe region”, up to 2% strain, representing the crimp-pattern stretching-out. The crimp-pattern is lost in the linear region, between 2% and 4% strain and the slope in this region defines the Young’s modulus of the tendon. In this range of strain, the uncrimped collagen fibrils extend but also slide past one another. Above 4% and up to 8% of strain, microscopic damages to fibrils occur, which become major between 8% and 10% of strain and lead to tendon rupture at further stretches (Figure I.27) (Wang, 2006). However, the failure can happen at higher strain values, between 10% and 18% in tendons from young donors or 14% in avian flexor tendons (Table I.2) (Butler *et al.*, 1978; Devkota and Weinhold, 2003).

Species	Tissue	E (MPa)	UTS (MPa)	US (%)
Chicken	Flexor digitorum profundus tendon	600 - 1200	120	14
Human	Patellar tendon	504 - 680	54 - 65	12 - 15
Human	Gracilis tendon	590 - 1734	111 - 112	7 - 19.4
Human	Semitendinous tendon	540 - 1081	89 - 124	8 - 23
Human	Achilles tendon	819	79 +/- 22	9
Mouse	1-month-old tail tendon	473.87 - 748.33	17.57 - 48.40	6.30 - 8.33
Mouse	2-month-old tail tendon	1137	86.2	17.3
Mouse	8-month-old tail tendon	855.25 - 1112.17	56.03 - 87.60	10.19 - 11.41

Table I.2: **Mechanical properties of various tendons.** E: Young’s Modulus; UTS: Ultimate Tensile Strain; US: Ultimate Strain (Guerquin et al., 2013; Jung et al., 2009; Liu et al., 2009)

Other collagen types are found in tendons that strengthen ECM structure and reduce stress concentrations (Wang, 2006). Also, Achilles tendons from *Dcn*- and *biglycan*-null mouse models were found to have altered mechanical and structural properties (Gordon et al., 2015). Tendon cells produce the ECM components enabling tendon to sustain mechanical load, which, in turn also influence tenocytes production of these components (Kjær, 2004; Shwartz et al., 2013).

Apart from ECM content, ECM structure plays an important role in the capacity of tendons to withstand mechanical loads. Tendon mechanical properties seem to be also improved by ECM collagen cross-linking. Inhibition of this cross-linking by the alteration of the lysyl oxidase impairs tendon elastic modulus during chick development (Marturano et al., 2013). Cell-ECM interactions and their adaptations to the loads imposed to tendons *in vivo* also play a role in overall tendon structure and functions *in vivo*. For example, *Thmd*-null mice displayed a significantly inferior endurance-running performance and inadequate type I collagen fiber thickness and elasticity (Dex et al., 2017). Besides in rat Achilles tendons, loading was shown to regulate the expression of several genes, among which genes coding for the ECM (Eliasson et al., 2012, 2013). Furthermore, loading of tendons are also required for an efficient healing process, inducing the expression of several tendon-ECM and -transcription factor genes, such as *Egr1* (Andersson et al., 2012; Eliasson et al., 2008, 2009, 2012, 2013; Gaut et al., 2016). In addition, mechanical forces were demonstrated to positively regulate *Scx* in tendon cells through the SMAD2/3 intracellular pathway in adult mouse Achilles tendon (Maeda et al., 2011). Importantly, the downregulation of *Scx* in tendon cell induced by the loss of tensile loading is reversible as recovering of the movements in mice restore its expression and other tendon markers (Maeda et al., 2011). All of these results truly show that *in vivo* the mechanical state of the tendon is crucial for tendon genes expression.

1.6.2 Mechanobiology of tendon development

During embryogenesis, the musculoskeletal system develops in a coordinated manner. We saw how the signaling pathways and different transcription factors were involved in the

regulation of specification and differentiation for each component. However, this system also functions as development proceeds, as muscles will exert a mechanical load on their neighbors (Hamburger et al., 1965).

Genetic and chemical manipulations on animal models have contributed in the understanding of how mechanical forces regulate the development of the musculoskeletal system (Table I.3). The mouse and chick models have their own interests but both present a great advantage in that their musculoskeletal structures and development are similar to those of humans. Chick development occurring externally within an egg, which it is of great interest for a direct mechanical perturbation or measurements during developmental stages. Immobilization can be easily induced by the application of pharmaceutical agents altering the neuromuscular junction (Table I.3). For example, DMB is an agonist of the AChR that strongly binds and activates the post-synaptic AChR, causing prolonged paralysis (Macharia et al., 2004). Treatments enabling hypermotility also exist and have some effects on skeletal development. For example reserpine induces hypermotility or paralysis in a dose-dependent manner (Ruano-Gil et al., 1985). Mouse is a widely spread model organism and even if the application of neuromuscular blocking agents is impaired by the internal mammalian gestation, it benefits from an extended set of genetic tools. For example, in *Spotch* (*Sp*) or *Spotch-delayed* (*Spd*) mutant models, migration of muscle progenitors is impaired and the developing limbs are therefore muscleless. Also, mutations targeting MRFs such as *Myod* and *Myf5*, or the *mdg* model for muscular dysgenesis impair muscle differentiation or muscle contractions and present a similar effect on musculoskeletal development (Table I.3).

Regarding the mechanical regulation of tendon development, it is important to remember that the first phase of tendon development is muscle independent, except for axial tendons (Figure I.13) (Gaut and Duprez, 2016; Kardon, 1998). However, tendon maintenance and elongation during development are likely due to mechanical loads, as the presence of an adjacent contracting muscle is required during development (Kardon, 1998; Schweitzer et al., 2001). This phenomenon is also seen during translocation of the FDS muscles during development. These muscles will relocate to their final position in the arm, while being attached to their tendons that will elongate accordingly following muscles movements and contractions (Huang et al., 2013). The process attests for the capacity of tendons to withstand mechanical load and evolve and adapt according to them during development of the musculoskeletal system. It was shown that in *Spd* and *mdg* mutant embryos, with muscleless limbs or non-tractile muscles respectively (Table I.3), autopod tendons were formed but not properly elongated (Huang et al., 2015a). However, as tendons were not dramatically smaller in *mdg* as they could be in *Spd* mutants, it suggests that muscle activity is necessary to provide an additional independent signal to regulate tendon size. Autopod tendons from *Spd* embryos were significantly smaller than in wild-type embryos. Apart from regulating tendon size, muscle contractions were also shown in this same study to impact tendon patterning and fusion in the zeugopod, establishing the requirement of muscle contractions for a proper tendon development *in vivo* (Huang et al., 2015a). Similarly during chicken limb

development, muscle contraction are required to maintain *SCX*, *TNMD* and other tendon-associated genes, especially in the zeugopod (Havis et al., 2016). Besides, the same study also showed that the maintenance of tendon-genes subsequent to muscle contraction was going through the independent activation of the TGF β and FGF pathways. This is concordant with what seems to happen in adult tendons, where it was also demonstrated that mechanical forces were converted into TGF β -mediated signals to maintain *Scx* expression (Maeda et al., 2011). However, other molecular actors could be activated in the mechanotransduction process leading to tendon cell maintenance during development. For example, in adult tendons, both *Egr1* and *Mkx* gene expression is increased in presence of mechanical load and physical treadmill exercises (Gaut et al., 2016; Kayama et al., 2016).

Genetic manipulation	Chemical manipulation	Phenotype or Effect	Reference
/	Decamethonium bromide	Rigid paralysis	Drachman and Sokoloff, 1966; Hall and Herring, 1990
/	Botulinum toxin	Flaccid paralysis	Drachman and Sokoloff, 1966
/	Pancuronium bromide	Flaccid paralysis	Esteves de Lima et al., 2016
/	Reserpine	Hypermotility	Ruano-Gil et al., 1985
/	4-aminopyridine	Hypermotility	Pollard et al., 2016
<i>Splotch</i> and <i>Splotch delayed</i> mutants	/	Lack of limb muscle	Bober et al., 1994; Vogan et al., 1993
(1) <i>Myod1</i> ^{-/-} ; <i>Myf5</i> ^{-/-} and (2) <i>Myod1</i> ^{-/-} ; <i>Myf5</i> ^{-/+}	/	(1) Lack of muscle formation and (2) reduced muscles	Rudnicki et al., 1993
mdg/mdg	/	Noncontractile muscles	Pai, 1965
Sox9 flox/flox; Prx1-Cre	/	Skeletal-less limbs	Akiyama et al., 2002; Huang et al., 2015b

Table I.3: **Examples of genetic and chemical manipulations enabling the study of the mechanoregulation of musculoskeletal formation and homeostasis.**

Regarding its interactions with its adjacent muscle, the tendon also has to adapt in that end. The first stage of MTJ development is independent of mechanical loads, as seen previously. As we saw, *tsp4* is crucial in zebrafish model, for the proper attachment of muscles to tendons in the MTJ (Subramanian and Schilling, 2014). This might reflect the importance of the ECM at that point of force-transmission. This is notably seen as alteration in the expression of ECM genes all disrupt the MTJ and its function, as it is the case with *col22a1* and *tsp4* (Charvet et al., 2013; Subramanian and Schilling, 2014, 2015).

Another potential regulator of tendon growth is also the skeleton itself and its growth, notably through the tendon-to-bone attachment. Indeed, apart from its role in linking ten-

don and bone, the enthesis is also mechanically important and gradually attenuates stresses from bone to tendon, as explained previously (Subramanian and Schilling, 2015; Zelzer et al., 2014). Most importantly, the second phase of formation of the enthesis is known to be sensitive to mechanical signals. Yet, the precise signals involved and the precise adaptation of the tendon part is not known (Blitz et al., 2009; Felsenthal and Zelzer, 2017). However, some clues indicate that the Hedgehog (Hh) signaling could be involved in this process, as it is already known to be involved in mineralized fibrocartilage formation as well as being mechanoresponsive (Jahan et al., 2014; Schwartz et al., 2015). For reasons similar to those involving the Hh signaling pathway, PTHrP is also a potential actor. Indeed, its specific ablation in *Scx*⁺ cells impairs fibrous enthesis formation and PTHrP expression is mechanically regulated (Chen et al., 2007b; Wang et al., 2013).

Together, these studies show numerous examples of the impact of mechanical forces in tendon development and how tendons adapt in consequence to those signals *in vivo*.

1.6.3 Tendon cell behavior in regard with its physical environment

a) Importance of the environment: 2D vs 3D

The ability to properly model and control tendon cell differentiation *in vitro* would be a key factor in both fundamental and applied research. We already took a look at the diversity of biochemical cues involved in this process. In this chapter and the previous one, we also saw that mechanical cues were crucial in developmental processes and notably for tendon formation. As such, modulating mechanical signals in cell cultures would have some effects regarding tendon cell differentiation.

As seen before, cell behavior is regulated by the extracellular matrix mechanics, as the cells sense the stiffness of their microenvironment. This also impacts cell differentiation potential, as soft substrates drive naive cells to neurogenesis and stiff ones to osteogenesis (Engler et al., 2006). Since this study, it was demonstrated that naive cells could be directed toward a lot of different lineages just by modulating the stiffness of the material they adhered to (Figure I.28) (Discher et al., 2009; Smith et al., 2018). Manipulations of ECM stiffness also proved to influence cell behavior, notably their migration ability (Rehfeldt et al., 2012). Besides, several methods allow for production of specific materials varying in their stiffness and composition and allowing for a proper control of a simple 2-dimensional (2D) cell culture system. It was shown that cells are specified to tendon lineage in presence of an increased matrix stiffness, with aligned fibers or fibers of a higher diameter (Baudequin et al., 2017; Islam et al., 2017). However, no precise range of elasticity inducing tendon cell differentiation has been defined as it was for other lineages (Figure I.28) (Discher et al., 2009; Islam et al., 2017).

Although numerous studies keep uncovering the tendon cell response to various mechanical stimuli, over simplification of tendon cell culture in 2D models is still an obstacle in that way. As for other tissues, tendon cells are to be considered in their 3-dimensional

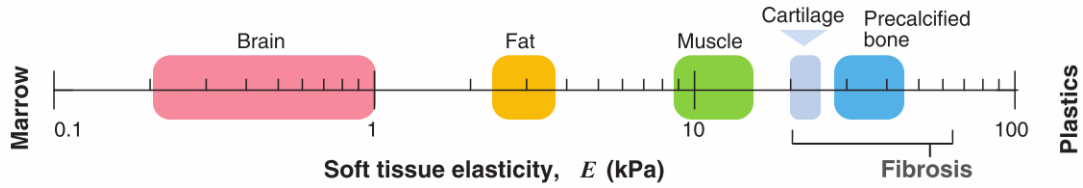


Fig. I.28 **Tissue elasticity scale.** Picture from Discher et al., 2009

(3D) environment, but in that case this parameter is even more crucial that it concerns a mechanoresponsive tissue. The 3D cell culture system will allow a better simulation of what is happening to the cells *in vivo*, regarding the way the mechanical cues are applied and how cells behave and interact with their ECM in this regard. The 3D *in vitro* models typically contain cells homogeneously embedded within a 3D material. Depending on the technique used, these constructs can be placed in a bioreactor for *in vitro* loading of the samples (Figure I.29).

Hydrogels are generally preferred to porous or fibrous scaffolds, as they homogeneously transfer strains to the cells (Wang et al., 2018b). Tendon cells cultured within hydrogels showed a histological organization similar to the one of *in vivo* tendon, with longitudinally aligned tenocytes and an epitendon-like layer (Garvin et al., 2003; Wang et al., 2018a). Also, the effects of the 3D model might vary depending on its composition, not only regarding the mechanical properties of its structure but also the chemical compounds retained in it and supplied to the cells. Indeed, administration of TGF β 2 in 3D tendon constructs induced a tenogenic phenotype depending on their timing of formation (Chien et al., 2017). The cells also seem to be “better served by themselves”, as chicken tendon fibroblasts were shown to exhibit a behavior and gene expression closer to what it is *in vivo* when embedded in fibrin-gel allowing them to synthesize their own collagen matrix (Yeung et al., 2015). This study showed that compared to their 2D counterparts, cells in 3D fibrin gels showed numerous genes differentially regulated. Among those upregulated genes could be found those coding for the ECM, biological adhesion and skeletal system development. In collagen-gels, the difference was less striking and the authors suggested that this gel impaired the mechanosensing ability of the cultured cells. Another study confirmed that TSPCs seeded in fibrin constructs exhibited improved tenogenic gene expression patterns compared to their collagen-based counterparts (Breidenbach et al., 2015). However, in that same study they also showed that collagen constructs showed improved tenogenic expression in the presence of mechanical stimulation, attesting again for differences of ECM properties *in vitro*. Nonetheless, these studies among others highlight the need for a cell-culture system as close to what the cells experience *in vivo*. In that way, the 3D cell culture systems seem to fit this requirement.

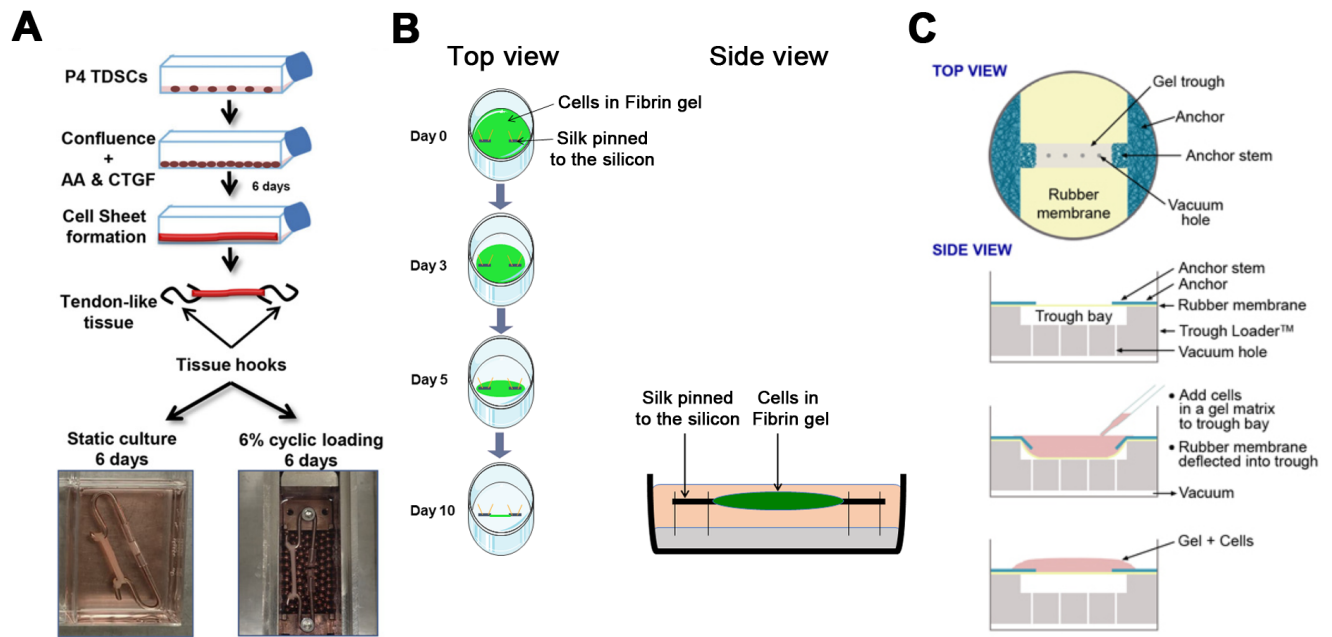


Fig. I.29 **Examples of 3D culture systems.** (A) TSPCs at passage 4 (P4) are grown to confluence and then cultured with CTGF and Ascorbic Acid (AA) for 6 days to promote cell sheet formation through ECM production. The resulting ECM sheet is then wrapped and anchored around tissue hooks to form a 3D construct (bottom left panel) that can be stretched if loaded on a proper device (bottom right panel). Adapted from Wang et al., *The FASEB Journal*, 2018. (B) 3D-engineered tendons made of fibrin gels. Cells are embedded in fibrin and thrombin gel (green gel) and seeded in a cell culture well filled with silicon (grey in the bottom right panel) and where two silk anchors were pinned on both sides. Upon 10 days of culture in culture medium supplemented with AA (orange in bottom right panel), the gel rolls up on itself and around the anchors to finally be suspended between them, forming the *in vitro* 3D-engineered tendon. Protocol used by Guerquin et al., 2013 (C) Formation of bioartificial tendons (BATs) in the FlexCell bioreactor (FlexCell Inc.). Cells are embedded in a collagen gel loaded in a special cell culture plate whose silicon bottom is stretched by vacuum to form an elongated mold between two anchor stems. After polymerization, vacuum is released and medium supplemented in AA is added and the BAT is forming between the two anchors. Image adapted from FlexCell Inc. and depicting the protocol used in Garvin et al., 2003.

b) Stretching the cells as a way to direct tendon differentiation

A great diversity of mechanobiological models has been used in the study of tendon mechanobiology to direct tendon cell differentiation. As we saw in the previous part, the environment in which the cells are seeded is of a great interest in terms of fidelity to the *in vivo* situation. This is true for the ECM all around the cell in 2D or 3D models, but also for the loads that are applied to them. The stretching models add in physiological relevance as they allow for a better understanding of the relationship between cells and their mechanical environment. Other loadings are applied *in vivo* to the cells, notably minor shear force and compression,

generated by the collagen structure, but will not be taken into account here, as we decided to focus on the stretch, the main component of mechanical stress. Tendon cells mainly receive uniaxial stretch, between 4% and 6% strain in a physiological context (Wang et al., 2018b). Stretching above this threshold is not physiologically relevant anymore but could be of interest in the case of traumatism or overuse models. In 2D *in vitro* loading models, the mechanical strain is applied to a flexible substrate on which grows a monolayer of cells. This substrate is either directly stretched by pulling on it or by a vacuum-generated force, as it is the case in the FlexCell system (FlexCell Inc.). The advantage of this model is the homogeneity of the strain between the substrate and the cells and the easiness of studying the response upon several loading protocols. However, as previously seen, it does not take into account the interactions occurring between cells and ECM during mechanical loads. In this model, the cells can be stretched in uniaxial or biaxial way. Uniaxial loading, also known as longitudinal loading, means that the strain will happen on one axis only. In biaxial loading, the strain will be applied on two axes and the cells will be stretched on their whole circumference. In 3D models, cells are embedded in hydrogels suspended between two anchor points. When confined in a specifically designed bioreactor, these models will be uniaxially stretched.

In order to better understand tendon cell response to its mechanical environment, numerous tendon cell cultures and loading protocols have been studied. A part of these studies presenting variations in tendon gene or protein expression is summarized in Table I.4. We can focus on the studies showing an increase in *Scx* expression to better appreciate the effects of different environments and loading protocols for tendon cells. Cell cultures expressing *Scx* are subjected to either uniaxial or biaxial stretches, in a range of strain between 0.1 and 10%. This range is wider than the 4-6% strain range previously established for physiological relevance (Wang et al., 2018b). However, a direct comparison of uniaxial and biaxial stretches showed that uniaxial stretch was more beneficial for tendon gene expression (Wang et al., 2018a). Among the studies presenting an increase in *Scx* expression, the frequency used to stimulate the cells can be narrowed down to a range of 0.1-0.5Hz, independently of 2D or 3D environments. There is, however, a huge diversity in the duration of the protocols used, between few hours of stimulation to several days or weeks. Yet, even if the protocols are really different, all of those inducing an increase in *Scx* expression include rest periods for the cells, during which they are not at all stimulated, again independently of their 2D or 3D environments. Altogether, these studies and those on which we did not focus here show a great diversity of loading protocols. They show how essential it is to establish a good mechanobiological model for tendon cell differentiation, taking into account the direction and strength of the loads as well as the environment in which they are applied.

Table I.4 is displayed below

Table I.4: **Stretch protocols modulating tendon-genes expression *in vitro*.** FX: FlexCell; CSD: Custom Stretch Device; TSPCs: Tendon Stem/Progenitor Cells; Uniaxial: Cells are stretched in a single axis; Biaxial: Cells are stretched on 2 axes; 2D: 2-dimensional cell culture system; 3D: 3-dimensional cell culture system (Bioartificial tendon). Entries are indexed in alphabetical order of the references used.

Reference	Machine	Cells	Direction	Strain (%)	Frequency (Hz)	Protocol	2D or 3D	Treatment	Gene expression		Protein	
									Up	Down	Up	Down
(Asparuhova et al., 2011)	FX	NIH3T3	Biaxial	10,0%	0,3	1, 3 or 6h	2D		Tenascin			
(Breidenbach et al., 2015)	CSD	Mouse ScxGFP+ TSPCs	Uniaxial	2,4%	1	3000 cycles / day Rest period: stretch at 0,12Hz	3D		Normal tendon gene expression compared to <i>in vivo</i> TSPCs			
(Brown et al., 2014)	FX	Mouse ScxGFP+ TSPCs from Limbs or trunk at E16 or E17	Uniaxial	1,0%	0,5	2h/day 3 days	2D		Scx			
									Scx			
								TGFβ2	Scx	Tnmd		
								FGF4		Tnmd, TGFβ2		
						TGFβ2+FGF4		Scx	Tnmd			
(Brown et al., 2015)	FX	Mouse BMSCs or TSPCs	Uniaxial	1,0%	0,5	1h/day for 3 days	2D		Scx, Col1a1	Tnmd		
										Scx, TGFβ2, Tnmd, Col1a1		
								TGFβ2+FGF4	Scx	Tnmd		
(Chen et al., 2007a)	FX	Porcine tenocytes	Biaxial	5,0%	0,5	24h	2D	Triamcinolon acetetonide	Col1a1, Decorin			
(Chen et al., 2015)	CSD	Human Tenocytes	Uniaxial	4 or 8 or 12%	1		2D			Collagen I		
(Garvin et al., 2003)	FX	Avian Tenocytes	Uniaxial	1,0%	1	1h/day for 3 days	3D		Col XII, Prolyl hydroxylase			
(Han et al., 2014)	FX	Ghizou's miniature pig fibrochondrocytes	Biaxial	4,0%	1	3h	2D		Col II	Coll X		
						12h		Col1a1, PTHrP		Collagen I, PTHrP		
						3h			Coll X			
						12h		Col1a1, PTHrP		PTHrP		
						6h			Coll X			
12h		Col1a1, Coll X										

Reference	Machine	Cells	Direction	Strain (%)	Frequency (Hz)	Protocol	2D or 3D	Treatment	Gene expression		Protein	
									Up	Down	Up	Down
(Huisman et al., 2014)	FX	Human Tenocytes	Biaxial	3 to 5%	0,1	100 cycles + 10 rest between each 1000 cycles + 10s between each	2D		Scx Col1a1		Pro-collagen I	
									Scx Col1a1			
(Jiang et al., 2012)	CSD	Human Tenocytes	Uniaxial	4,0%	0,5	8h	2D				Collagen I	
				8,0% 4% or 8%							Col1a1	Col1a1
(Kayama et al., 2016)	FX	Rat TSPCs	Biaxial	2,0%	0,25	6h	2D		Mkx, Tnmd, Col1a1, Col1a2			
(Kuo and Tuan, 2008)	FX	Human MSCs	Uniaxial	1,0%	1	30nm/day from 1 to 7 days	3D		Col1a1, Col III, Elastin, B-cat, Frizzled 5	Scleraxis, MMP13, Wnt4, Wnt5a, MMP1, MMP2, MMP3		
(Lee et al., 2004)	FX	Porcine Ligament cells	Biaxial	5,0%	0,5	24h	2D	Estrogen		Col1a1, Collagen 3, Biglycan		
(Liu et al., 2017)	FX	Mouse MSCs, BMSCs, Fibroblasts	Biaxial	10,0%	0,1	16h/day for 24h or 10 days	2D		Scx, Tnmd, Col1a1, Col3a1		Scx, Tnmd, Col1a1, Col3a1	
(Lohberger et al., 2014)	FX	Human Intraoral MSCs	Uniaxial	10,0%	0,5	continuous for 7 to 14 days	2D		Col1a1			
(Qi et al., 2011)	FX	Human Tenocytes	Uniaxial	3,5%	1	1h/day up to 5 days	3D	IL1-beta	Col1a1, Biglycan, Fibronectin, TGFB1, COX2, MMP27, ADAMTS5			
									Cox2, ADAMTS5			

Reference	Machine	Cells	Direction	Strain (%)	Frequency (Hz)	Protocol	2D or 3D	Treatment	Gene expression		Protein	
									Up	Down	Up	Down
(Scott et al., 2011)	FX	C3H10T1/2	Uniaxial	5,0%	0,1	2h/ day for 2 to 3 weeks	3D		Scx			
				10,0%					Scx Col1a1			
				10,0%					Scx Col1a1			
				10,0%					Scx			
(Tsuji et al., 2006)	FX	Human Tenocytes	Biaxial	20,0%	0,5	up to 36h	2D				Tenascin C	
(Wang et al., 2018a)	FX	Mouse TSPCs	Uniaxial	6,0%	0,25	8h / day for 6 days	2D		Uni- vs Bi-axial : Scx, Mlx, Col1a1, ALP	Uni- vs Bi-axial : Sox9, Col2a1, CEBP/B, Pparg		
			Biaxial	6,0%					Versus Static : Scx, Mlx, Tnmd, Col1a1	Versus Static : Runx2, ALP, Sox9, Col2a1, CEBP/B		
	CSD		Uniaxial	6,0%	0,25	8h / day for 6 days	3D	CTGF + AA	Versus no- LY294002: Runx2, Sox9	Versus no- LY294002: Scx, Mlx, Col1a1, Col2a1, Pparg		
				6,0%					CTGF + AA + LY294002 (inhibitor of PI3K/Akt)			
(Zhang and Wang, 2013)	CSD	Mouse TSPCs	Uniaxial	4,0%	0,5	12h	2D		Col1a2, Tnmd			
				8,0%					Col1a2, Tnmd, LPL, Sox9, Runx2			
				4% or 8%					Col1a2, Tnmd			
(Zhang and Wang, 2015)	CSD	Mouse TSPCs	Uniaxial	4% or 8%	0,5	2h/day for 3 days	2D		Col1a1, Tnmd, Nanog, Sox9, Runx2, LPL			

II. Aims and objectives

Tendon development is controlled by a wide variety of cellular and molecular signals that act together to form a tissue whose primary function involves mechanical signals transmission (reviewed in Gaut and Duprez, 2016; Huang et al., 2015). The importance of mechanical signals in numerous processes is largely recognized and their role in early embryonic tendon development has already been pinpointed (Havis et al., 2016). However, the effects of mechanical signals on fetal stages of tendon development and the mechanotransduction pathways during tendon differentiation have to be further elucidated.

During my PhD project, I have tried to understand and hierarchize the relationships between mechanical signals, transcription (co-)factors and signaling pathways in the context of fetal tendon development and tendon cell differentiation.

This project tackled the following aspects of tendon development:

Aim 1 – Role of mechanical signals during tendon development in chicken fetuses

- Analyze tendon gene expression in the absence of muscle contractions
- Assess tendon cell behavior in the presence or absence of mechanical signals
- Compare the effects of mechanical signals on the development of tendon and other tissues in the limb

Aim 2 – Define a mechanical environment favoring tendon gene expression and differentiation *in vitro*

- Characterize the fate of naive cells in 2D and 3D culture systems with their mechanical environment
- Define tendon gene behavior depending on mechanical state

Aim 3 – Characterization of the mechanosensitive transcription (co-)factors YAP, EGR1 and SRF as intracellular relays of mechanical signals involved in the control of tendon development *in vivo* and tendon cell differentiation *in vitro*

- Potential role of YAP, EGR1 and SRF in the regulation of tendon development
- Role of mechanotransduction pathways involving YAP and EGR1 in tendon cell differentiation *in vitro*

To address the questions raised above, I used *in vivo* and *in vitro* models. I took advantage of paralyzed chicken fetus as an *in vivo* model to study the effect on tendon development. I also used C3H10T1/2 cells in 2D- and 3D-cultures to assess *in vitro* the relationship between mechanical signals and tendon cell differentiation. The results of these experiments are presented below in three distinct but interconnected parts. At the end of each part, I will discuss the results I obtained in my experiments and I will compare them to the current scientific knowledge. After exposing all of my results, I will discuss them in regard of each other in order to highlight a putative model and to open other perspectives. The results are presented as such:

1. Muscle contractions are required to maintain tendon identity and mechanosensitive gene expression in tendons of chicken fetuses.
2. Effect of mechanical constraints and TGF β 2 on the tendon differentiation potential of mouse mesenchymal stem cells.
3. Role of mechanical constraints, EGR1 and YAP in a 3-dimensional culture system of C3H10T1/2 cells mimicking tendon formation.

III. Muscle contractions are required to maintain tendon development and mechanosensitive gene expression in tendons of chicken fetuses

III.1 Context

Genetic and chemical manipulations on animal models have contributed to the understanding of how mechanical forces regulate development, notably for the musculoskeletal system (reviewed in Nowlan et al., 2010). Because chicken development occurs externally within an egg, it is easy to introduce mechanical perturbations in chicken embryos and fetuses. The blockade of muscle contractions can be induced with the administration of pharmaceutical agents altering the neuromuscular function, such as DMB. DMB is an agonist of the AChR that acts as a depolarizing agent, causing rigid paralysis of muscles (Macharia et al., 2004). Muscle contractions are required to maintain tendon gene expression during embryonic development (Havis et al., 2016). In the context of my PhD project we hypothesized that mechanical cues generated by muscle contractions are also important for tendon formation during fetal stages of chicken development. DMB administration during fetal development has been shown to perturb limb muscle formation in chicken fetuses (Esteves de Lima et al., 2016). However, the consequences of DMB-induced rigid paralysis for tendon development during chicken fetal development have not been studied so far.

III.2 Results

III.2.1 Immobilization of chicken fetuses is deleterious for limb tendon formation

Mechanobiology of tendons and other components of the musculoskeletal system was studied *in vivo* during chicken fetal development between E7 and E9. We analyzed limb development of chicken fetuses immobilized at E7 for 5H, 12H, 24H or 48H compared to naturally and rhythmically moving fetuses harvested at the same time points (Figure III.1A). Rigid paralysis was induced by treatment of DMB while control fetuses were treated with Hank's saline solution. Hank's and DMB solutions were changed at E8 to ensure their efficiency. Analysis of gene expression by RT-qPCR on whole limbs revealed a decrease in *SCX* expression at 5H, 12H, 24H and 48H in paralyzed limbs compared to control limbs (Figure III.1B). However, *TNMD* and *COL1A2*, two downstream markers of tendon cell differentiation showed no variation at these times of treatment (Figure III.1B).

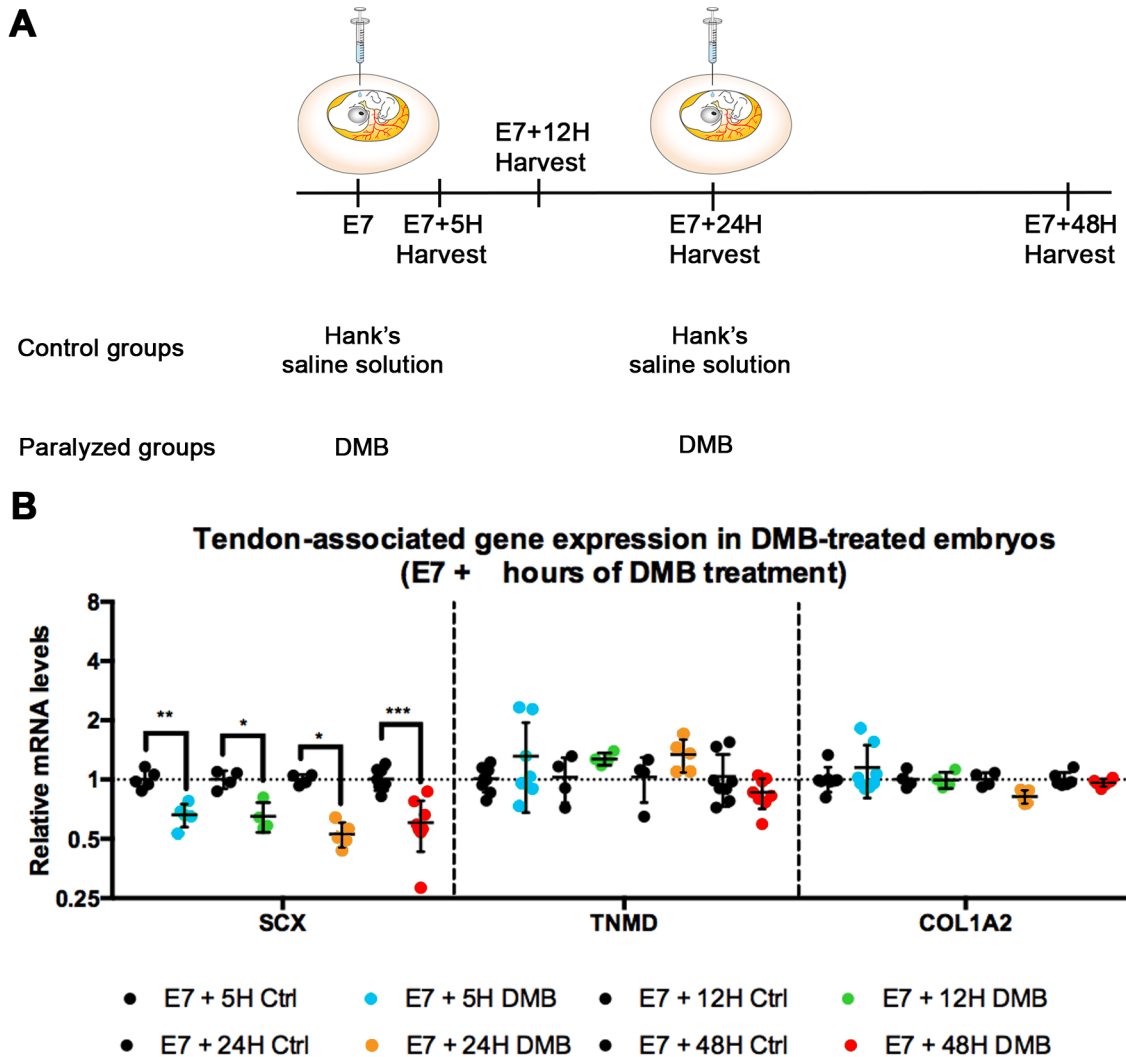


Fig. III.1 *DMB-induced paralysis between E7 and E9 affects SCX expression in limbs of chicken fetuses* (A) Schematic representation of the experimental procedure to induce paralysis. All fetuses were treated at E7 and E8 with either Hank's saline solution (control group) or DMB (paralyzed group). Limbs of both groups were harvested at 5H, 12H, 24H and 48H following treatment application (B) Analysis of tendon mRNA levels by RT-qPCR of control groups (in black) versus DMB-treated groups at 5H (blue), 12H (green), 24H (orange) and 48H (red) between E7 and E9. Each dot represents an independent biological sample. Samples were analyzed with the non-parametric Mann-Whitney test and stars indicate significant *p*-values under 0.05.

Since this gene expression analysis by RT-qPCR is based on mRNA samples extracted from whole limbs of paralyzed and control chicken fetuses, it does not provide the information on variation of gene expression in one given tissue. Thus, we performed *in situ* hybridization to wholemounds and tissue sections to assess tendon gene expression in the absence of muscle contractions.

In limbs that were paralyzed for 24H or 48H, we observed a global decrease of *SCX* expression as compared to stage-matched control limbs by *in situ* hybridization to whole-

mounts (Figure III.2). The wholemount *in situ* hybridization analysis is consistent with the RT-qPCR analysis and both experiments show that *SCX* expression is downregulated in paralyzed limbs.

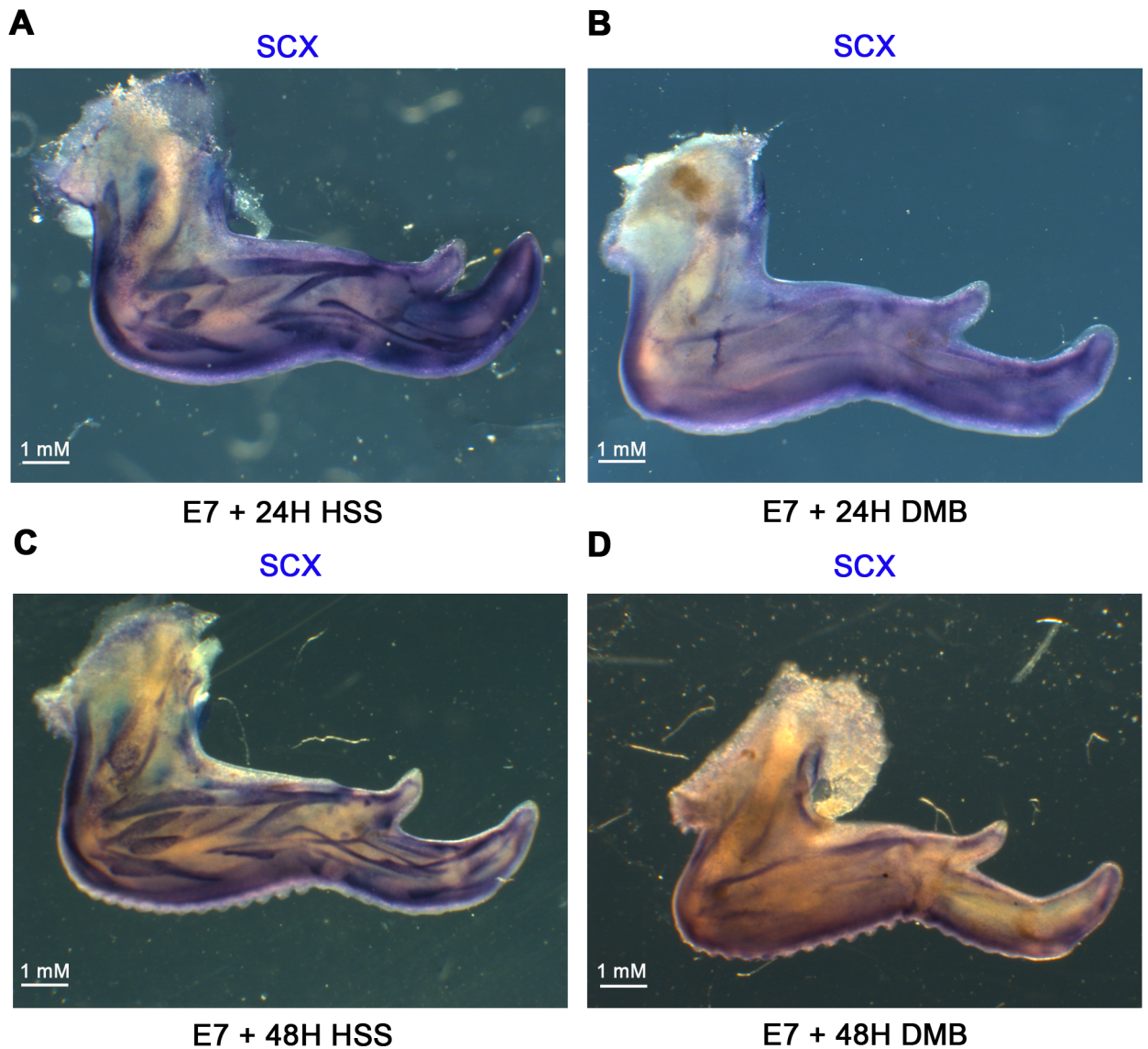


Fig. III.2 **Wholemount hybridization to *SCX* in limbs of chicken fetuses from control or paralyzed groups.** *SCX* staining appears in blue in limbs of E8 chicken fetuses in control (A) and paralyzed (B) groups and of E9 control (C) and paralyzed (D) groups. Abbreviations: HSS: Hank's Saline Solution, used for treatment of the controls; DMB: Decamethonium bromide.

A decrease of *SCX* expression was also observed in paralyzed limbs for 24H with *in situ* hybridization to transverse limb sections, compared to *SCX* expression in the control group (Figure III.3A). However, no obvious decrease was observed for *TNMD* and *COL1A1* expression in 24H-paralyzed limbs (Figure III.3B, C), which is consistent with RT-qPCR analysis (Figure III.1B).

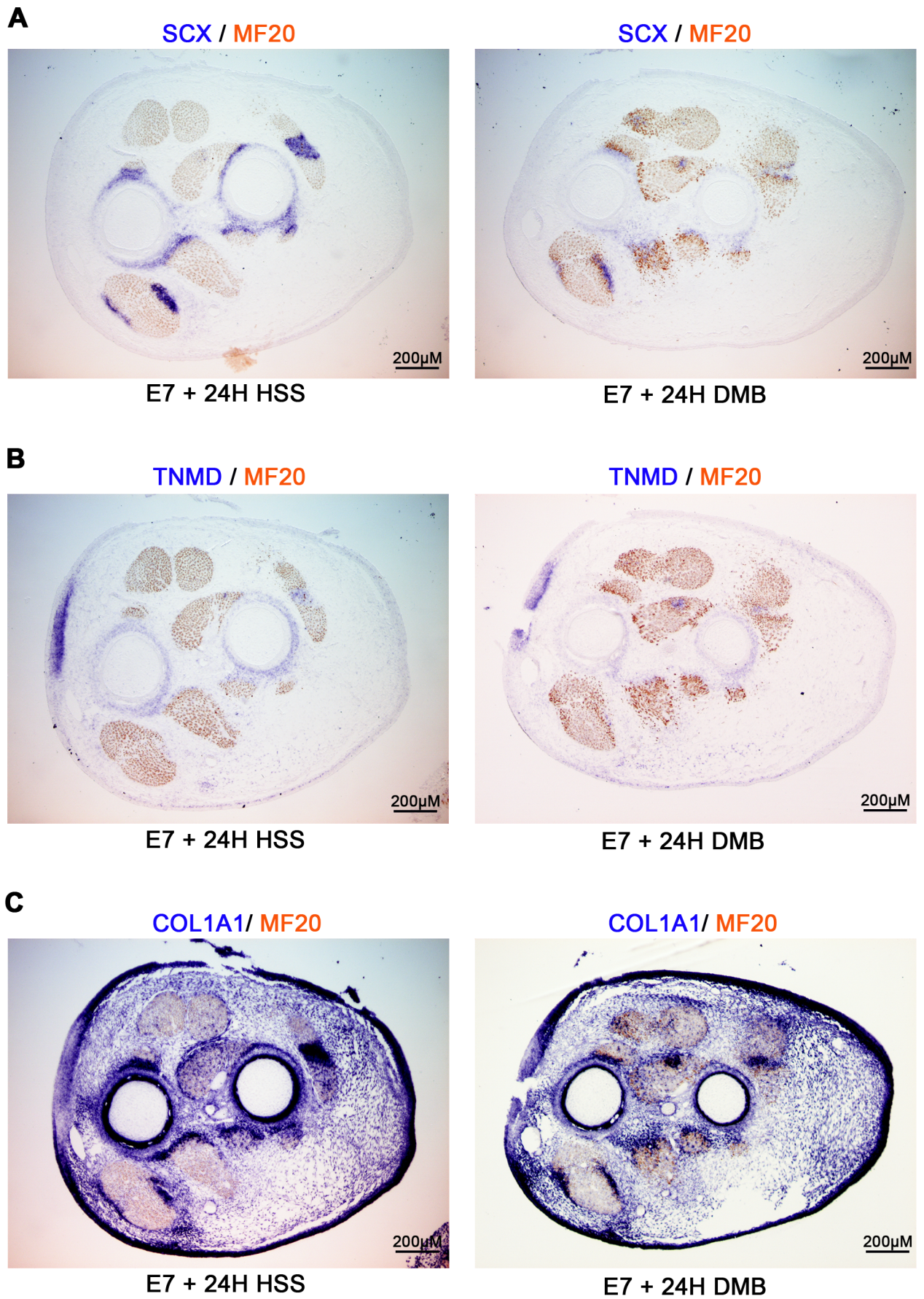


Fig. III.3 (Caption next page.)

Fig. III.3 (Previous page) ***In situ hybridization to limb transverse sections with SCX, TNMD and COL1A1 of 24H DMB limbs.*** *In situ hybridization with (A) SCX, (B) TNMD and (C) COL1A1 (blue) probes to transverse sections of E8 control limbs at E7 + 24H HSS (left panels) and E8 paralyzed limbs at E7 + 24H DMB (right panels). In all sections, immunohistochemistry was performed after in situ hybridization with MF20 antibody to label muscles. Abbreviations: HSS: Hank's Saline Solution, used for treatment of the controls; DMB: Decamethonium bromide.*

At 48H of paralysis, we observed a pronounced decrease of *SCX*, *TNMD* and *COL1A2* expression in DMB-treated limbs compared to control limbs, by *in situ* hybridization (Figures III.4, III.5); although discrete remaining signals could be observed for *SCX* and *COL1A2* in ventral tendons (Figures III.4A, III.5A, B, arrows). The absence of obvious decrease of mRNA levels of *COL1A1* and *TNMD* by RT-q-PCR in paralyzed limbs (Figures III.1B) can be explained by the other sites of *COL1A1* and *TNMD* expression. Indeed, *COL1A1* is also expressed in bone and dermis (Karsenty and Park, 1995), while *TNMD* is also expressed in muscle sheet epimysium, skin and adipose tissue (Oshima et al., 2003; Sato et al., 2014; Senol-cosar et al., 2016). As already observed (Esteves de Lima et al., 2016), the muscle splitting, normally occurring between E6 and E8 (Shellswell, 1977; Tozer et al., 2007), was affected as muscles were not well individualized in paralyzed limbs (Figures III.4, III.5).

Altogether these results show that the *SCX* tendon gene expression is impaired by rigid paralysis induced by DMB-treatment during fetal development. Regarding the expression of *TNMD* and *COL1A1*, there was an obvious change in their expression only at 48H of DMB treatment, but not at 24H.

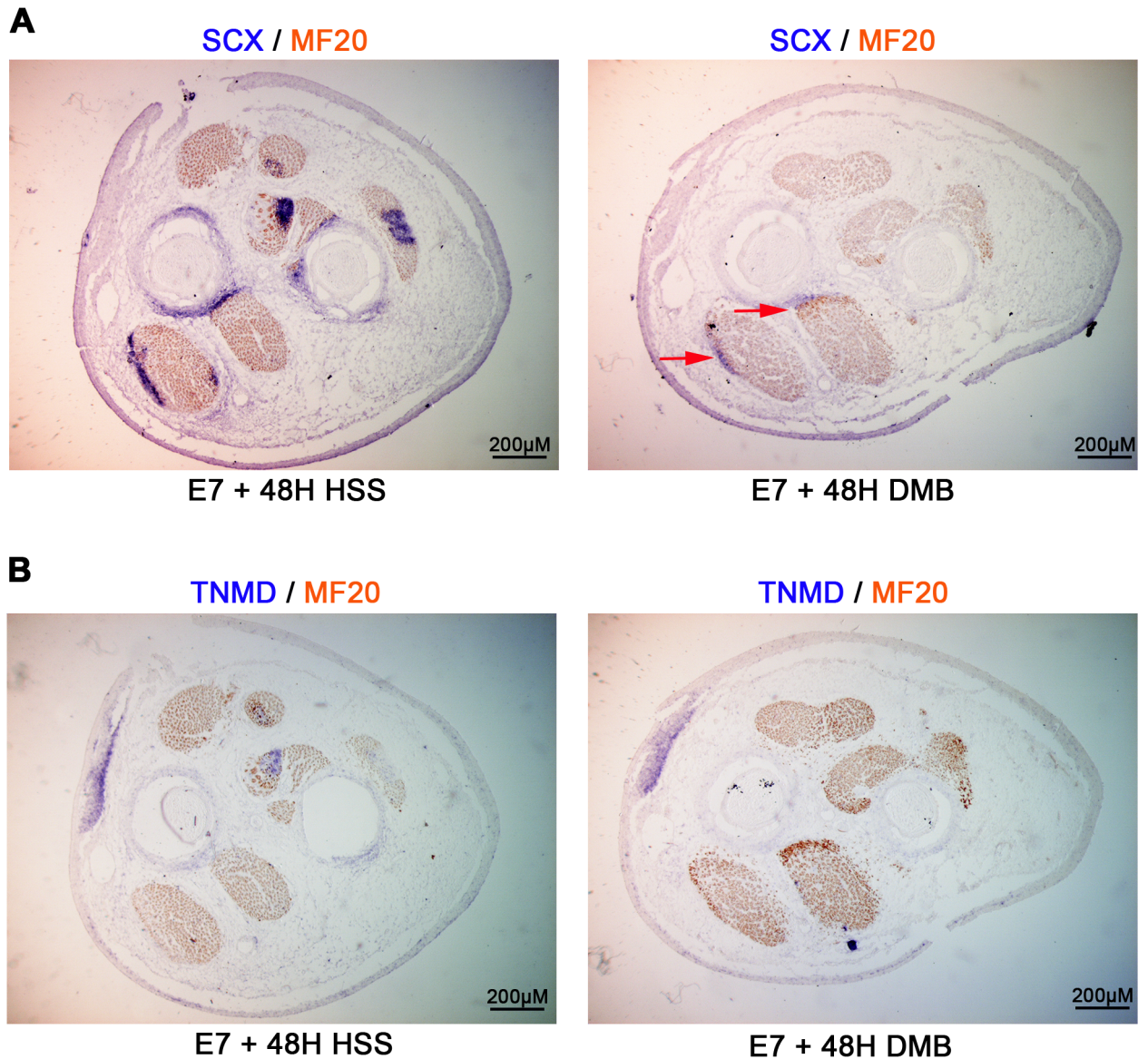


Fig. III.4 *In situ* hybridization to limb transverse sections with *SCX* and *TNMD* probes of 48H DMB limbs. *In situ* hybridization with (A) *SCX* and (B) *TNMD* probes (blue) to transverse limb of E9 control limbs at E7 + 48H HSS (left panels) and E9 paralyzed limbs E7 + 48H DMB (right panels). In all sections, immunohistochemistry was performed after *in situ* hybridization with MF20 antibody to label muscles. Red arrows indicate remaining signals in ventral tendons of paralyzed limbs. Abbreviations: HSS: Hank's Saline Solution, used for treatment of the controls; DMB: Decamethonium bromide.

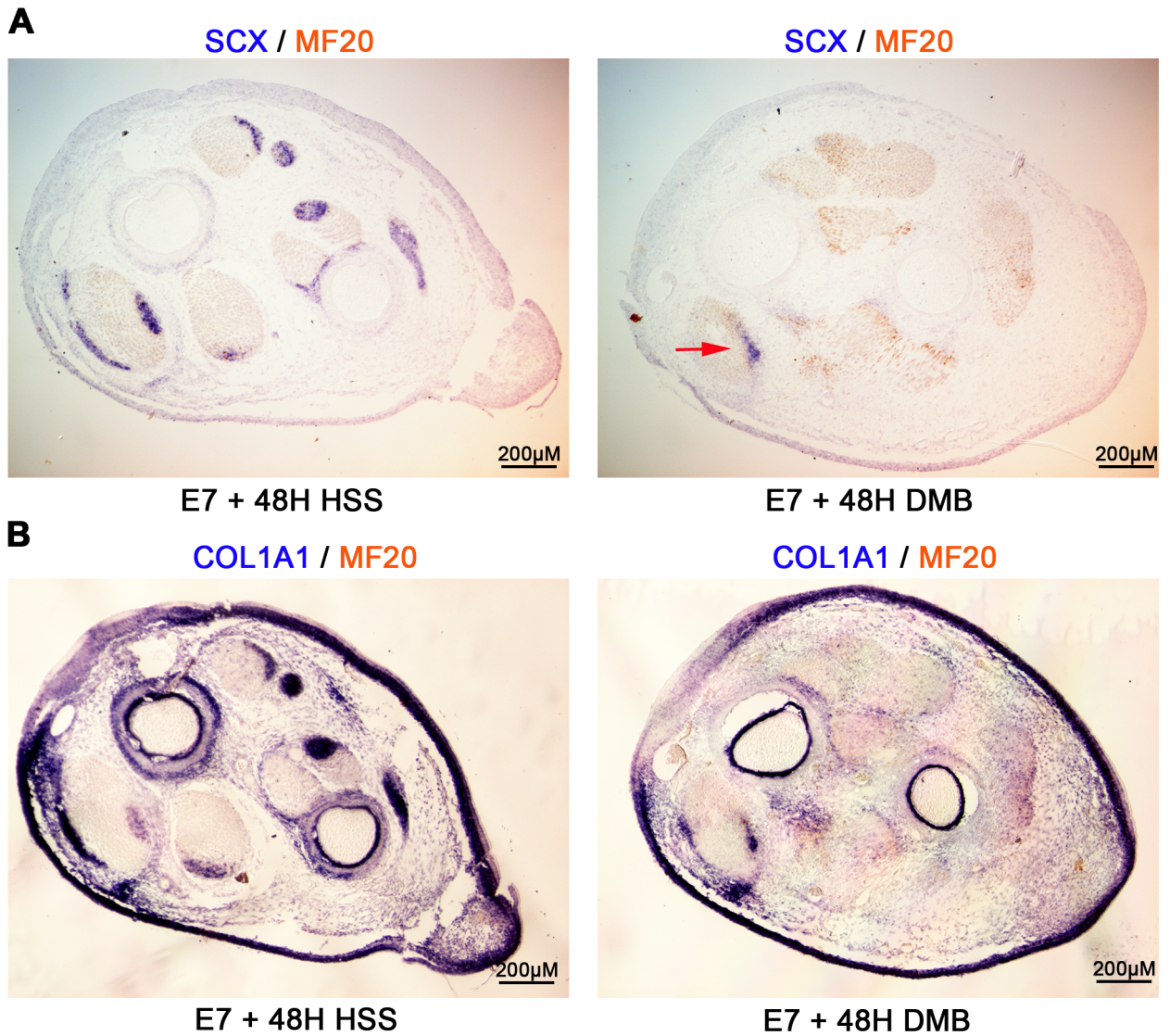


Fig. III.5 *In situ* hybridization to limb transverse sections with *SCX* and *COL1A1* probes of 48H DMB limbs. *In situ* hybridization with (A) *SCX* and (B) *COL1A1* probes (blue) to transverse limb of E9 control limbs at E7 + 48H HSS (left panels) and E9 paralyzed limbs at E7 + 48H DMB (right panels). In all sections, immunohistochemistry was performed after *in situ* hybridization with MF20 antibody to label muscles. Red arrows indicate remaining signals in ventral tendons of paralyzed limbs. Abbreviations: HSS: Hank's Saline Solution, used for treatment of the controls; DMB: Decamethonium bromide.

III.2.2 Immobilization of chicken fetuses increases cartilage gene expression, while decreasing muscle gene expression in limbs

We also analyzed cartilage gene expression by RT-qPCR (Figure III.6A) and *in situ* hybridization (Figure III.6B-D) in immobilized chicken fetuses. We observed an overall increase in cartilage gene expression upon DMB treatment. Cartilage gene expression varied depending on the time of DMB treatment, *SOX9* and *ACAN*, as cartilage specification and

differentiation markers respectively, showed an increased expression in paralyzed limbs at E7+5H and +48H, as well as *COL2A1* at E7+48H. These results have been confirmed at E7+48H of rigid paralysis by *in situ* hybridization on wholemounts and sections (Figure III.6B, C). *ACAN* was increased in limbs of immobilized fetuses, notably in the autopod (Figure III.6B arrows) and in the elbow (Figure III.6C). We also observed an increase in pSMAD1/5/8 signal in cartilage elements of paralyzed limbs, indicating an increase of BMP activity in cartilage elements of DMB-treated fetuses (Figure III.6D).

Regarding muscle gene expression, we studied the expression of *PAX7* and *MYF5*, an upstream regulator of myogenesis and a myogenic determination factor, respectively. We observed a decrease in *PAX7* and *MYF5* expression by RT-qPCR in whole limbs of the E7+24H and +48H of DMB treatment (Figure III.7), similarly to what was previously shown by Esteves de Lima and colleagues (Esteves de Lima et al., 2016). Interestingly, in these experiments, the first decrease in muscle gene expression was observed at 24H (Figure III.7), while the decrease of *SCX* expression was observed as soon as 5H of paralysis (Figure III.1B).

Fig. III.6 (Figure next page) **Cartilage gene expression is modified in paralyzed limbs.** (A) Relative mRNA levels of cartilage genes in control limbs (black) and DMB-treated limbs (in green) between E7 and E9. Each dot represents a biological independent sample. Samples were analyzed with the non-parametric Mann-Whitney test and stars indicate significant p-values (under 0.05). (B) Wholemount hybridization of *ACAN* (blue) in E7+48H HSS limbs (left panel) and E7+48H DMB limbs (right panel). Red arrows indicate regions with noticeable differences in *ACAN* expression between control and DMB-treated groups. (C) *in situ* hybridization of *ACAN* (blue) to transverse sections of control limbs at E7 + 48H HSS (left panel) and paralyzed limbs at E7+48H DMB (right panel) at the level of the arm. MF20 antibody labels muscles. (D) Immunofluorescent staining to transverse limb sections of E7+48H HSS (left panel) and E7+48H DMB (right panel) limbs, with pSMAD1/5/8 (green), MF20 (red) and DAPI (blue). Abbreviations: HSS: Hank's Saline Solution, used for treatment of the controls; DMB: Decamethonium bromide.

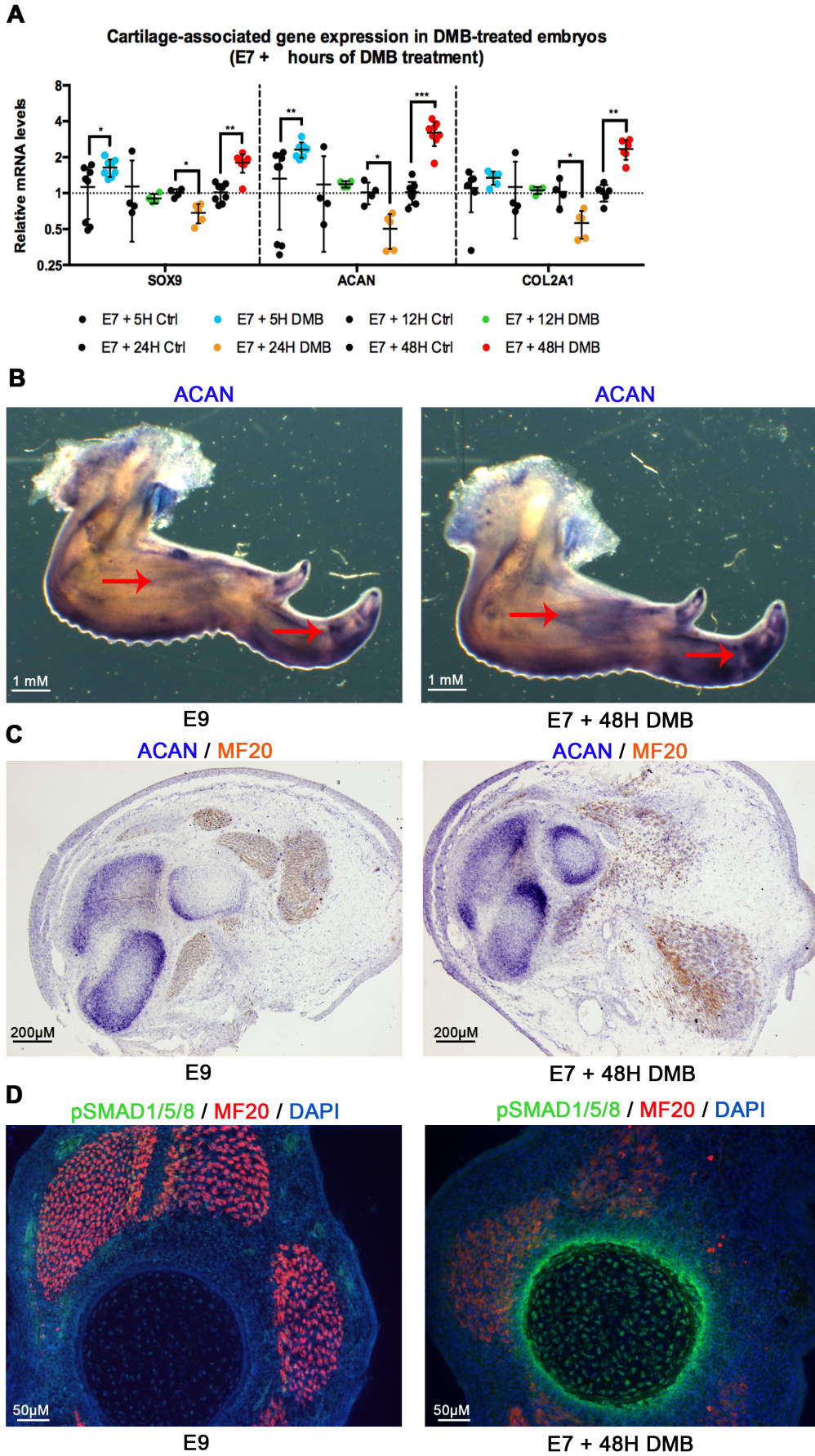


Fig. III.6 (Caption previous page)

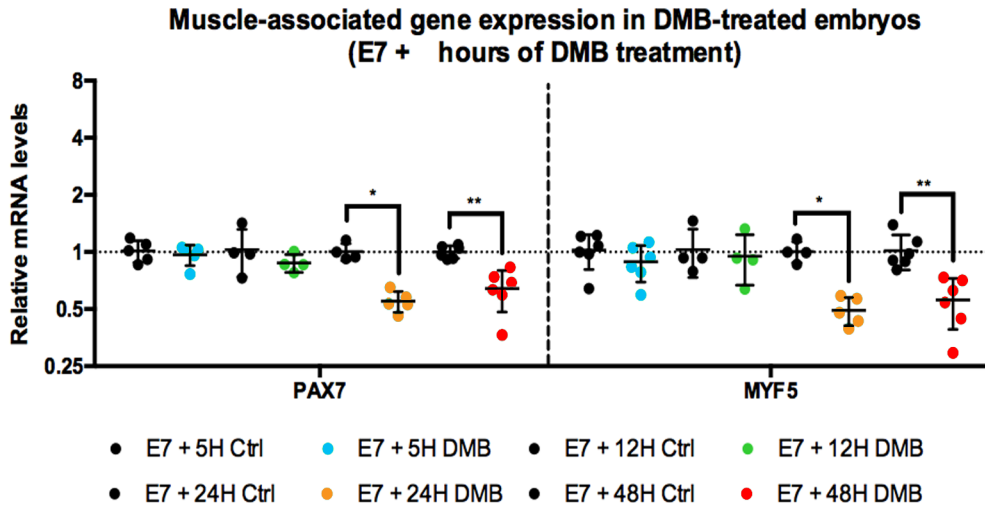


Fig. III.7 *Muscle gene expression is impaired in paralyzed limbs for 24H and 48H.* Relative mRNA levels of muscle genes by RT-qPCR in control limbs (black) and in DMB-treated limbs at 5H (blue), 12H (green), 24H (orange) and 48H (red) between E7 and E9. Each dot represents an independent biological sample. Samples were analyzed with the non-parametric Mann-Whitney test and stars indicate significant *p*-values (under 0.05).

III.2.3 Mechanosensitive genes are affected by limb paralysis

We also studied the expression of mechanosensitive factors in limbs. *EGR1* is known *in vivo* to be involved in tendon development and homeostasis (Guerquin et al., 2013; Léjard et al., 2011), as well as being regulated by mechanical signals (Gaut et al., 2016). Analysis of gene expression by RT-qPCR and *in situ* hybridization on whole limbs revealed that *EGR1* expression was downregulated in paralyzed limbs in tendons, near the myotendinous junction, after 12H, 24H and 48H of DMB treatment (Figure III.8A, B).

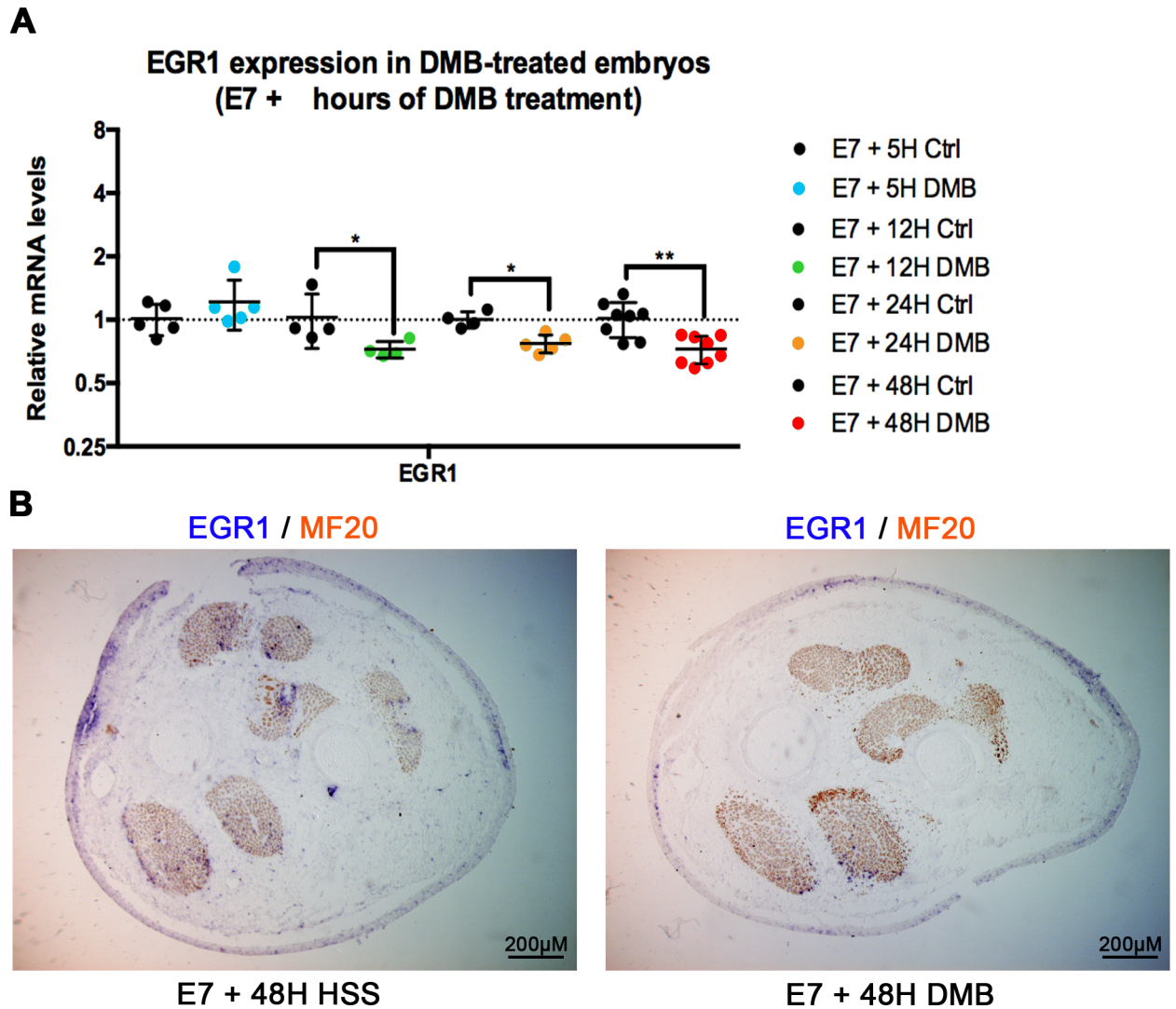


Fig. III.8 **Rigid paralysis impairs *EGR1* gene expression in tendons.** (A) *EGR1* gene expression in whole limbs of control (in black) and in DMB-treated at 5H (blue), 12H (green), 24H (orange) and 48H (red) between E7 and E9. Each dot represents an independent sample. Samples were analyzed with the non-parametric Mann-Whitney test, and stars indicate significant *p*-values under 0.05. (B) *in situ* hybridization to transverse section with *EGR1* probe (blue) of control (left panel) and E7+48H DMB limbs (right panel). MF20 stains for muscles. Abbreviations: HSS: Hank's Saline Solution, used for treatment of the controls; DMB: Decamethonium bromide.

YAP is known to be activated upon mechanical signals (Dupont et al., 2011; Panciera et al., 2017). We tested YAP activity in tendons of immobilized chicken fetuses by analyzing the expression of transcriptional readout of YAP activity. The YAP target gene *INHBA* is expressed in tendons (Orgeur et al., 2018). It appears that the YAP target gene *INHBA* showed a downregulated expression in paralyzed limbs at 24H and 48H, while *YAP1* mRNA levels were not affected (Figure III.9).

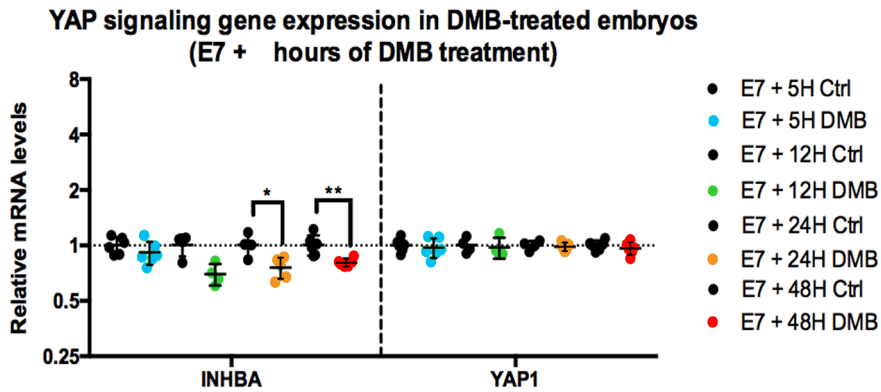


Fig. III.9 *YAP signaling is impaired by rigid paralysis in limbs of paralyzed chicken fetuses.* (A) *YAP1* and *YAP* target gene *INHBA* expression in whole limbs of control (in black) and in DMB-treated groups at 5H (blue), 12H (green), 24H (orange) and 48H (red) between E7 and E9. Each dot represents an independent sample. Samples were analyzed with the non-parametric Mann-Whitney test, and stars indicate significant p-values under 0.05.

In order to visualize a change in YAP activity in tendons, we analyzed YAP protein on limb sections. The YAP protein is expressed in tendons in E9 control limbs, tendons being visualized with *SCX* expression on adjacent sections (Figure III.10A). YAP signals were also detected in nucleus of tendon cells (Figure III.10B). YAP is known to be translocated into cell nucleus upon activation (Panciera et al., 2017), indicating that it is probably active in control limb tendons of E9 chicken fetuses. In paralyzed limbs, YAP expression is lost in tendons as *SCX* expression (Figure III.10C). We conclude that YAP activity is downregulated in limb tendons in immobilized fetuses.

Fig. III.10 (Figure next page) *YAP is expressed in tendons and is impaired by rigid paralysis.* (A) Upper panel: *in situ* hybridization of *SCX* (in blue) in E9 control limb, MF20 stains for muscles. Lower panel: Immunofluorescent staining on adjacent sections for YAP (in green). MF20 (in red) and DAPI staining (in blue) in E9 control limbs. (B) Zoom in the area delineated by the yellow square in the lower panel of (A). Upper panel is a merge of immunofluorescent staining on adjacent sections for YAP (in green), MF20 (in red) and DAPI staining (in blue), middle panel is the channel for YAP signal, lower panel is the channel for DAPI signal. Yellow arrowheads point at YAP- nuclei in corresponding panels and yellow arrows at YAP+ nuclei. (C) Left panel: *in situ* hybridization of *SCX* (in blue) in E7+48H DMB limb, MF20 stains for muscles. Right panel: Immunofluorescent staining on adjacent sections for YAP (in green), MF20 (in red) and DAPI staining (in blue) in E7+48H DMB limb. Abbreviations: HSS: Hank's Saline Solution, used for treatment of the controls; DMB: Decamethonium bromide.

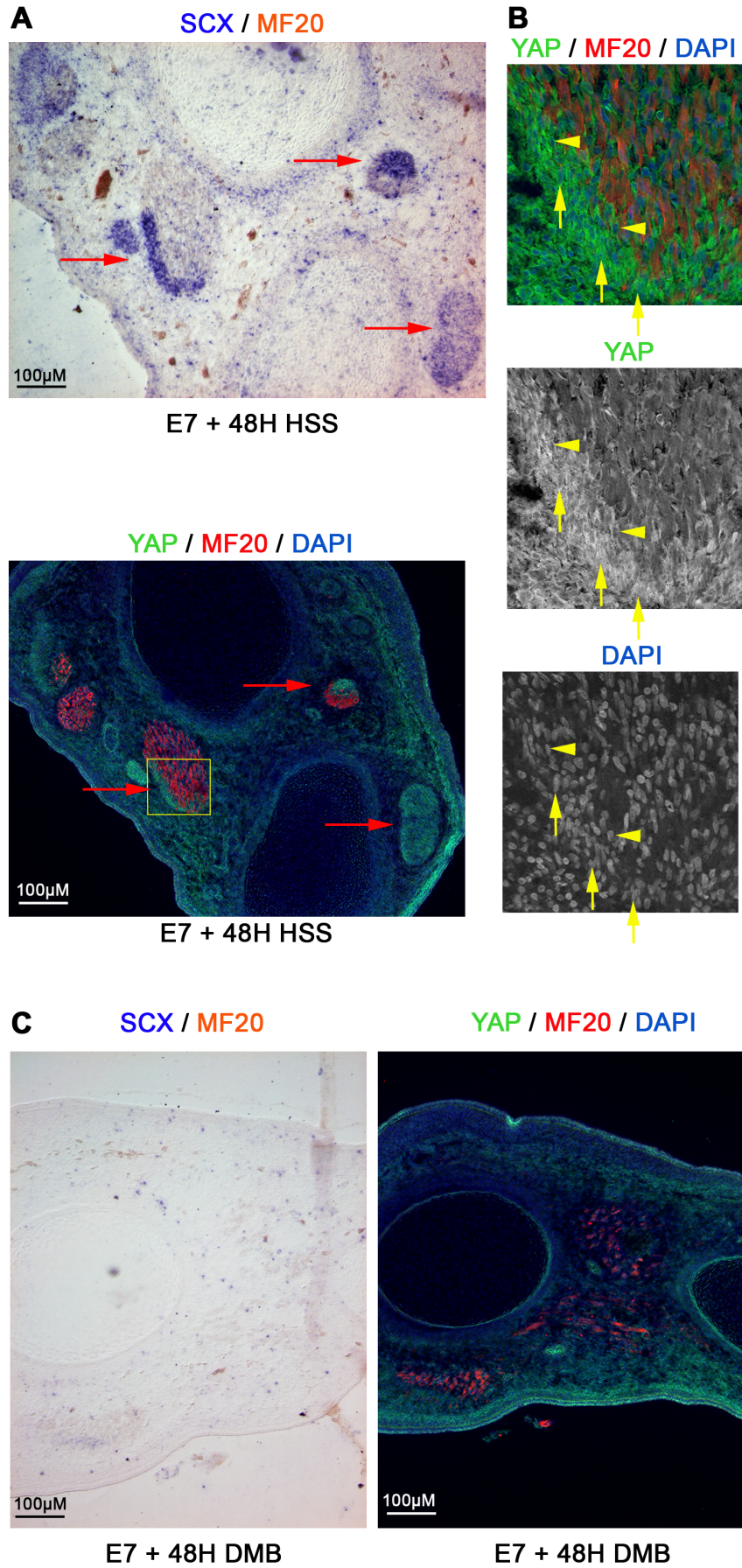


Fig. III.10 (Previous page)
79

III.2.4 The mechanosensitive factor SRF is not expressed in limb tendons of chicken fetuses

SRF-MRTFA is another mechanosensitive pathway, linked to *EGR1* and YAP pathways (Esnault et al., 2014; Foster et al., 2018). *ACTA2* and *VCL* genes are recognized target genes of SRF-MRTFA and code for Smooth Muscle Actin and a component of focal adhesion, respectively (Esnault et al., 2014; Posern and Treisman, 2006). We studied the activity of the SRF-MRTFA signaling pathway using *ACTA2* and *VCL* gene expression as readout of SRF-MRTFA activity in limbs of paralyzed chicken fetuses. The relative mRNA levels of *ACTA2* and *VCL* did not show any variations in paralyzed versus control limbs of chicken fetuses (Figure III.11A). The relative mRNA levels of the components of the SRF-MRTFA pathway, MRTFA and SRF did not display any change in paralyzed and control limbs (Figure III.11A).

SRF has been described to display an ubiquitous expression and is involved in many tissues (Posern and Treisman, 2006). We looked at the endogenous expression of *SRF* in chicken limbs of E9 chicken fetuses. *In situ* hybridization experiments to limb sections showed *SRF* expression in muscles but not in tendons visualized by *SCX* expression in E9 chicken limbs (Figure III.11B). These results show that the mechanosensitive factor *SRF* is not expressed in tendons of E9 chicken fetuses. However, consistent with the mechanosensitivity of the SRF-MRTFA pathway, *SRF* expression was decreased in limb muscles of chicken fetuses treated for 48H with DMB, but we did not observe any *SRF* expression related to tendon locations (Figure III.11B). Variations of *SRF* expression in 48H-DMB-treated limbs was observed only with *in situ* hybridization, while it was not with RT-qPCR analysis (Figure III.11A, B). This could be due to the expression of *SRF* in several other tissues (Posern and Treisman, 2006), notably in dermis (Figure III.11B).

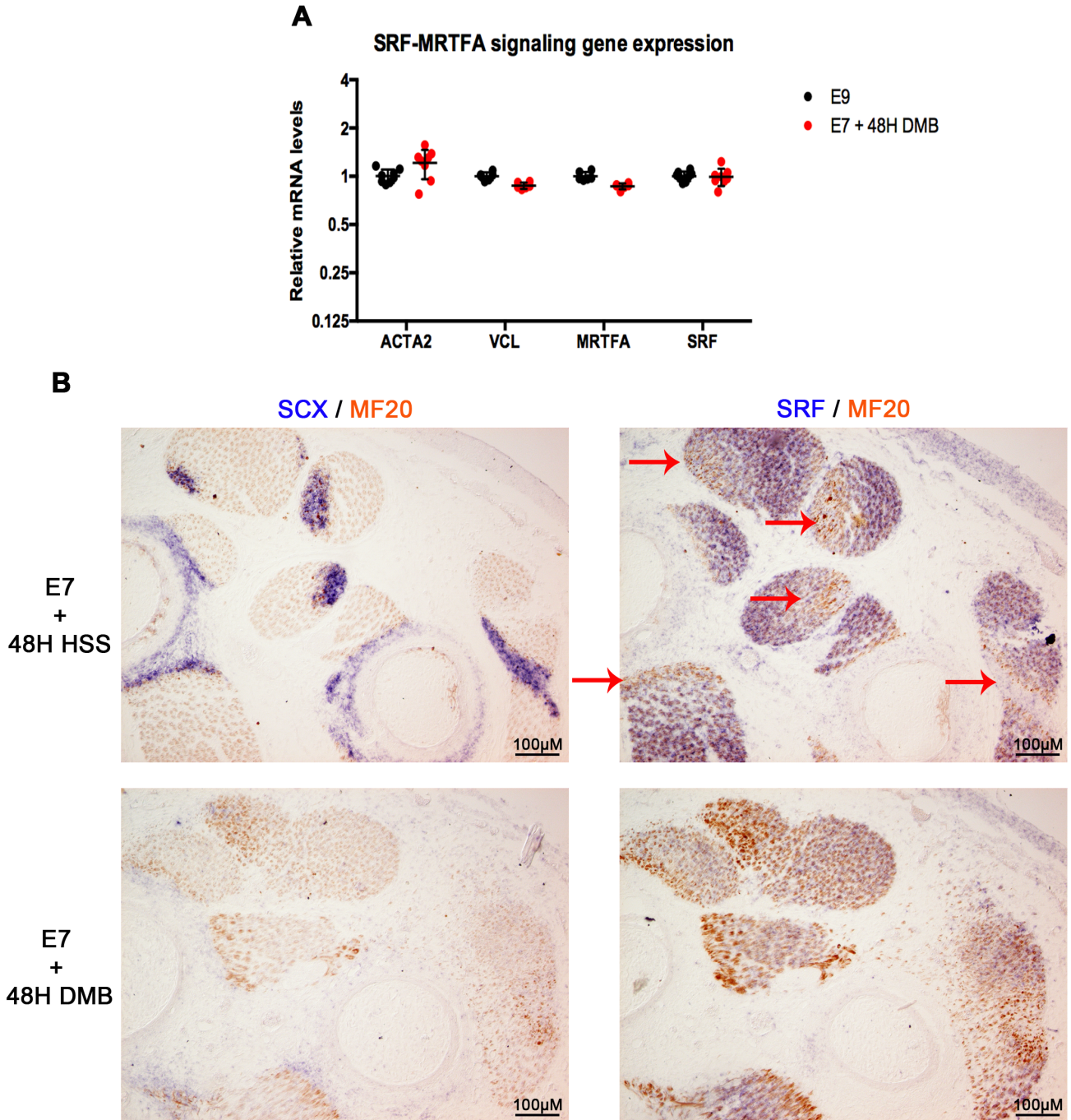


Fig. III.11 ***SRF is not expressed in limb tendons of chicken fetuses.*** (A) Relative mRNA levels of components of SRF-MRTFA signaling pathway in whole limbs of control (black) and in DMB-treated (red) groups between E7 and E9 by RT-q-PCR. Each dot represents an independent sample. Samples were analyzed with the non-parametric Mann-Whitney test and stars indicate significant p-values under 0.05. (B) *In situ* hybridization to transverse limb sections with SCX probe of control (upper left panel) and E7+48H DMB limbs (lower left panel). *In situ* hybridization to transverse limb sections with SRF probe of control (upper right panel) and E7+48H DMB limbs (lower right panel). MF20 antibody labels myosins in muscles. Red arrows indicate sites of SCX expression, where SRF is not expressed. Abbreviations: HSS: Hank's Saline Solution, used for treatment of the controls; DMB: Decamethonium bromide.

III.2.5 Residual tenogenic-like niches persist in paralyzed limbs

The rigid paralysis induced by DMB treatment led to a downregulation of tendon gene expression as well as mechanosensitive genes in tendons. However, the loss of tendon marker in paralyzed limbs does not allow us to discriminate between the persistence of cells that would not express any tendon genes or the disappearance of tendon cells. To test this, we compared the expression of the tendon marker *SCX* (*in situ* hybridization) with that of COLXII (immunohistochemistry), a marker of tendon ECM, in control and paralyzed limbs (Figure III.12). The tendon-ECM marker COLXII was observed at the *SCX*-expressing sites in control limbs of E9 fetuses (Figure III.12A). We also observed persistence of COLXII staining in tendon-like areas exhibiting a residual expression of *SCX* in limbs that were paralyzed for 48H (Figure III.12B, red square). These COLXII-staining areas presented a tendon-like structure, at the extremity of the muscle, as defined by MF20 staining, and close to an adjacent bone (Figure III.12B, C). These structures also contain cells, assessed by DAPI staining in the COLXII⁺ area, as defined by the yellow outline (Figure III.12C). These results show that cells are still present in tendon-like structures labeled with COLXII in paralyzed limbs.

Fig. III.12 (Figure next page) **Persistence of COLXII staining, a tendon-ECM marker, in E7+48H DMB limbs.** (A) Left panel: *in situ* hybridization to limb transverse sections of E9 control limbs with *SCX* probe (blue) and immunohistochemistry with MF20 (light brown) antibody. Right panel: Immunohistochemistry with COLXII (green) and MF20 (red) antibodies with DAPI (blue) labeling nuclei of adjacent transverse sections of E9 control limbs. (B) Left panel: *in situ* hybridization to transverse sections of E7+48H DMB limbs with *SCX* probe (blue) and with MF20 antibody. Right panel: Immunohistochemistry with COLXII (in green) and MF20 (in red) antibodies with DAPI (blue) of adjacent transverse sections of E7+48H DMB limbs. In both panels, the red squares indicate the tendon-like areas with no *SCX* expression but with a persistence of COLXII. (C) Zoom on the areas defined by the red squares in (B). Left panel is and immunohistochemistry with COLXII (in green) and MF20 (in red) antibodies and DAPI (in blue). Right panel: DAPI staining channel is singled in black and white. In both panels, the yellow outlines define the areas of COLXII expression, where nuclei (DAPI) can be observed. Abbreviations: HSS: Hank's Saline Solution, used for treatment of the controls; DMB: Decamethonium bromide.

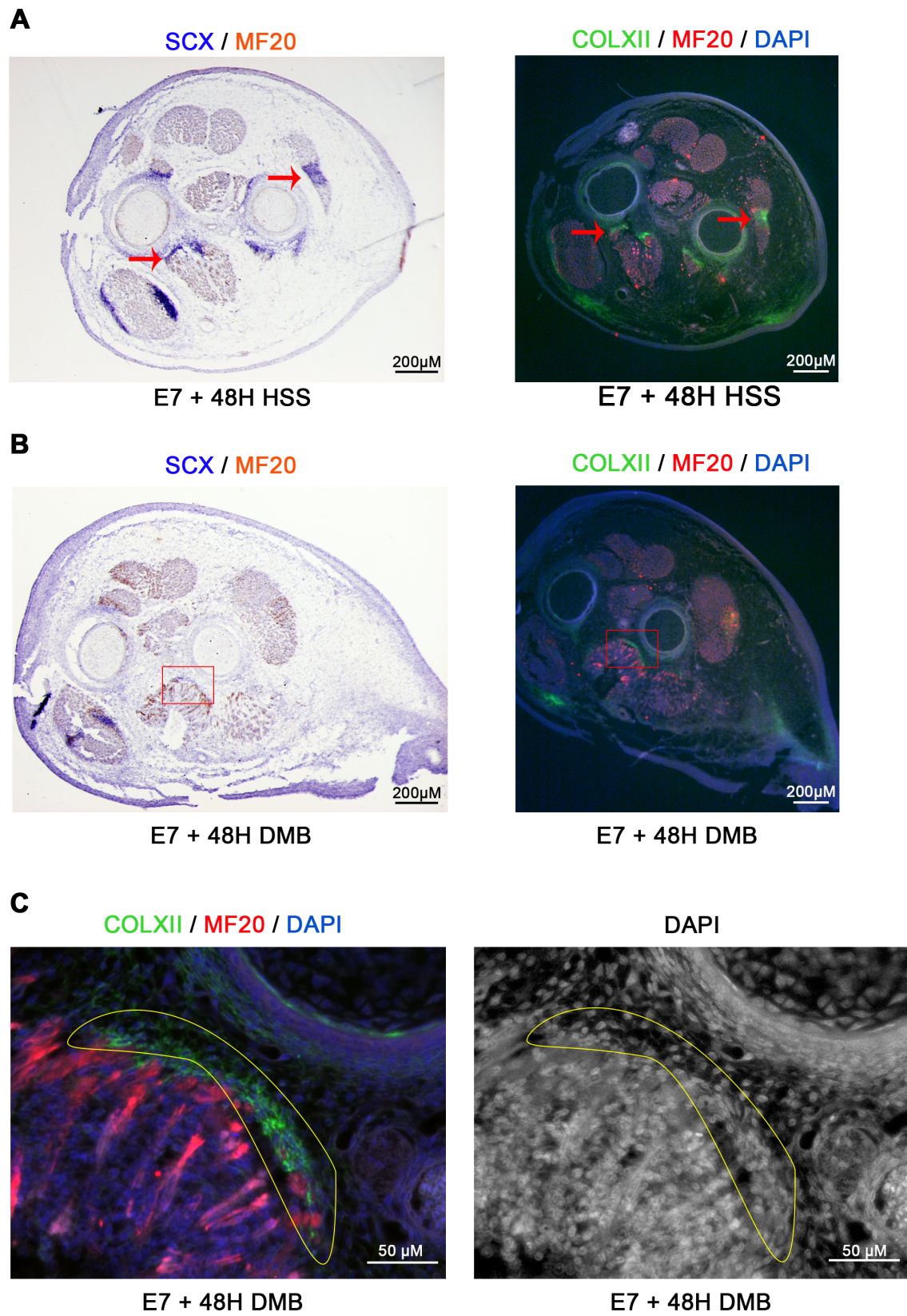


Fig. III.12 (Previous page)

III.2.6 Restored muscle contractions after 24H of immobilization is paired with recovery of tendon gene expression

Since we observed persistent staining of COLXII in paralyzed limbs with DMB treatment for 48H (Figure III.12), we assessed the potential of the remaining cells to re-express tendon genes after paralysis. To that aim, we restored muscle contraction after 24H of immobilization and analyze the expression of the *SCX* tendon gene. The experimental design is the following, we compared 3 groups of chicken fetuses at E9 with different regimes of muscle contractions (Figure III.13A).

The first group is the control group of E9 chicken fetuses that were never treated by DMB. The second group is the group of E7+48H DMB treated fetuses, for which we observed a drastic decrease in tendon gene expression (Figures III.1B, III.2C, D, III.4). The third group is the “24H recovery group”, we blocked muscle contractions during the first 24H starting at E7, then washed the DMB at E8, allowing for the recovery of muscle contractions between E8 and E9 and the subsequent rhythmic movements of the fetus (Figure III.13A). We had observed that E7+24H of DMB treatment induced a downregulation of *SCX* expression, as observed by RT-qPCR and *in situ* hybridization to whole mount and tissue sections (Figures III.1B, III.2A, B and III.3A). Analysis of gene expression by RT-qPCR of whole limbs show that the “24H Recovery” displayed a rescue of *SCX* expression similar to the E9 control group (Figure III.13B). No changes of mRNA levels were observed for *TNMD* and *COL1A2* genes between the 3 groups, consistent with the absence of changes in the expression of both genes after 24H DMB treatment (Figures III.1, III.3). Lastly, for the *EGR1* and YAP mechanosensitive pathways, *EGR1* and *INHBA* displayed a significant downregulation of mRNA levels in limbs after 24H of DMB treatment (Figures III.8A, III.9). Restored muscle contractions for 24H induced a recovery of *EGR1* and *INHBA* expression (Figure III.13C, D). Consistently with the absence of modification of *YAP1* mRNA levels after 24H and 48H DMB treatments (Figure III.9), there were no change for *YAP1* expression among the 3 groups (Figure III.13D).

We concluded that the restored muscle contractions after 24H of immobilization (for 24H) led to a significant recovery of the expression of the tendon gene *SCX* and to a tendency of recovery for the mechanosensitive genes, *EGR1* and *INHBA*, in limbs.

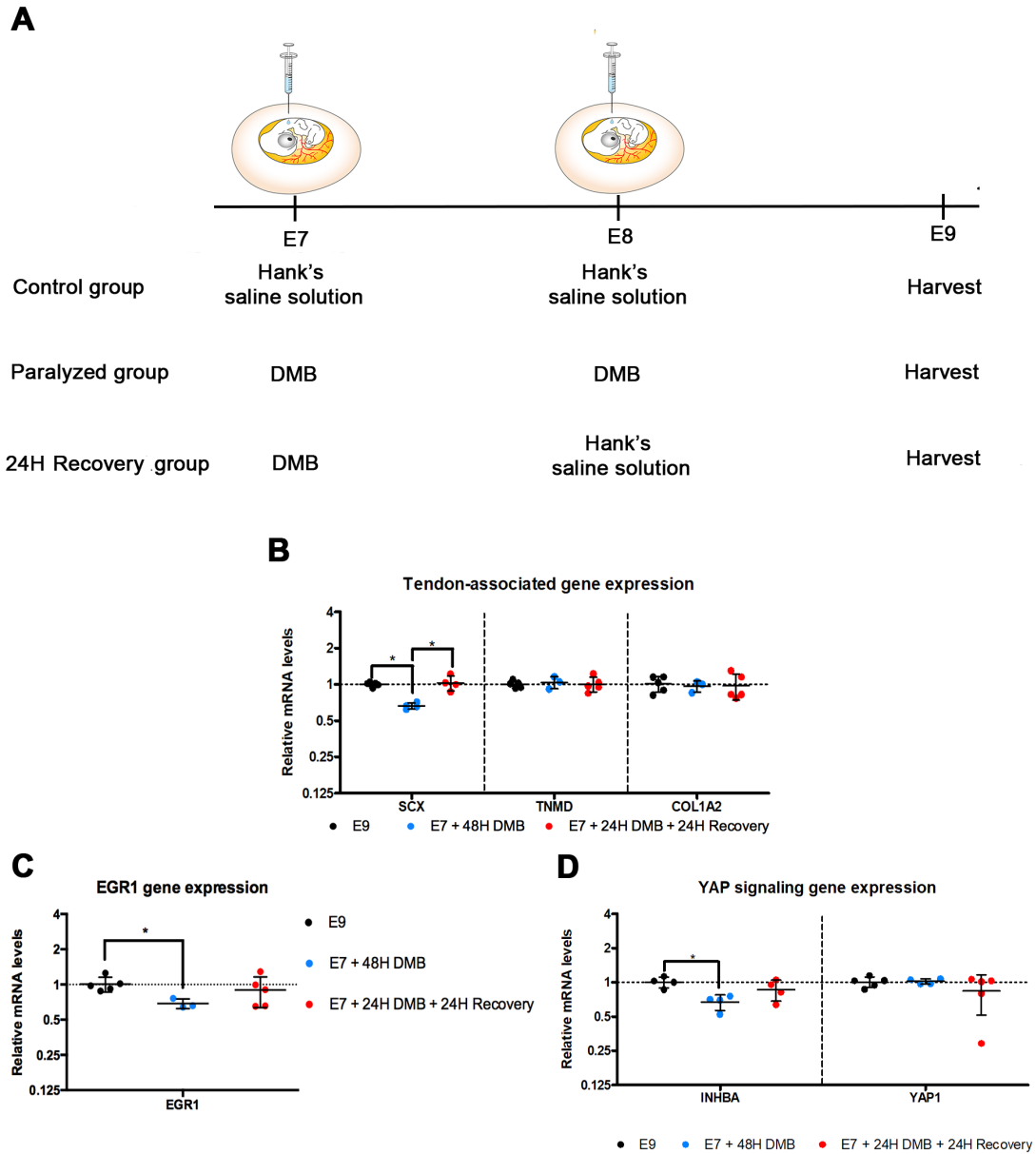


Fig. III.13 **Reintroduction of muscle contractions after 24H of rigid paralysis induces a recovery of SCX expression.** (A) Schematic representation of the experimental design to modulate muscle contractions in the 3 groups. All the chicken fetuses were treated at E7 with either Hank's saline solution (Control group), DMB for 48H (paralyzed group) or DMB for 24H and Hank's saline solution for 24H (recovery group), in order to allow recovery of muscle contractions between E8 and E9. Limbs of the three groups were harvested at E9. (B-D) Analysis of gene expression by RT-qPCR for tendon genes (B), the mechanosensitive gene *EGR1* (C) and YAP signaling genes (D). Each dot represents an independent sample. Samples were analyzed with the non-parametric Mann-Whitney test and stars indicate significant *p*-values under 0.05.

The recovery of *SCX* mRNA levels in 24H DMB limbs after 24H of restored muscle contractions (Figure III.13B) was confirmed by *in situ* hybridization experiments (Figure III.14). *In situ* hybridization with *SCX* probe to limb transverse sections of the control (III.14A) or the recovery (III.14B) groups showed similar *SCX* expression in tendons (III.14A, B). In addition, muscles were shaped similarly in both control and recovery groups (III.14A, B), unlike the disrupted muscle organization in 24H DMB limbs (Figure III.3) and 48H DMB limbs (Figure III.4).

Altogether, these results show that a 24H-period of reintroduction of movements is able to reinitiate *SCX* expression in E8 limbs that were paralyzed for 24H.

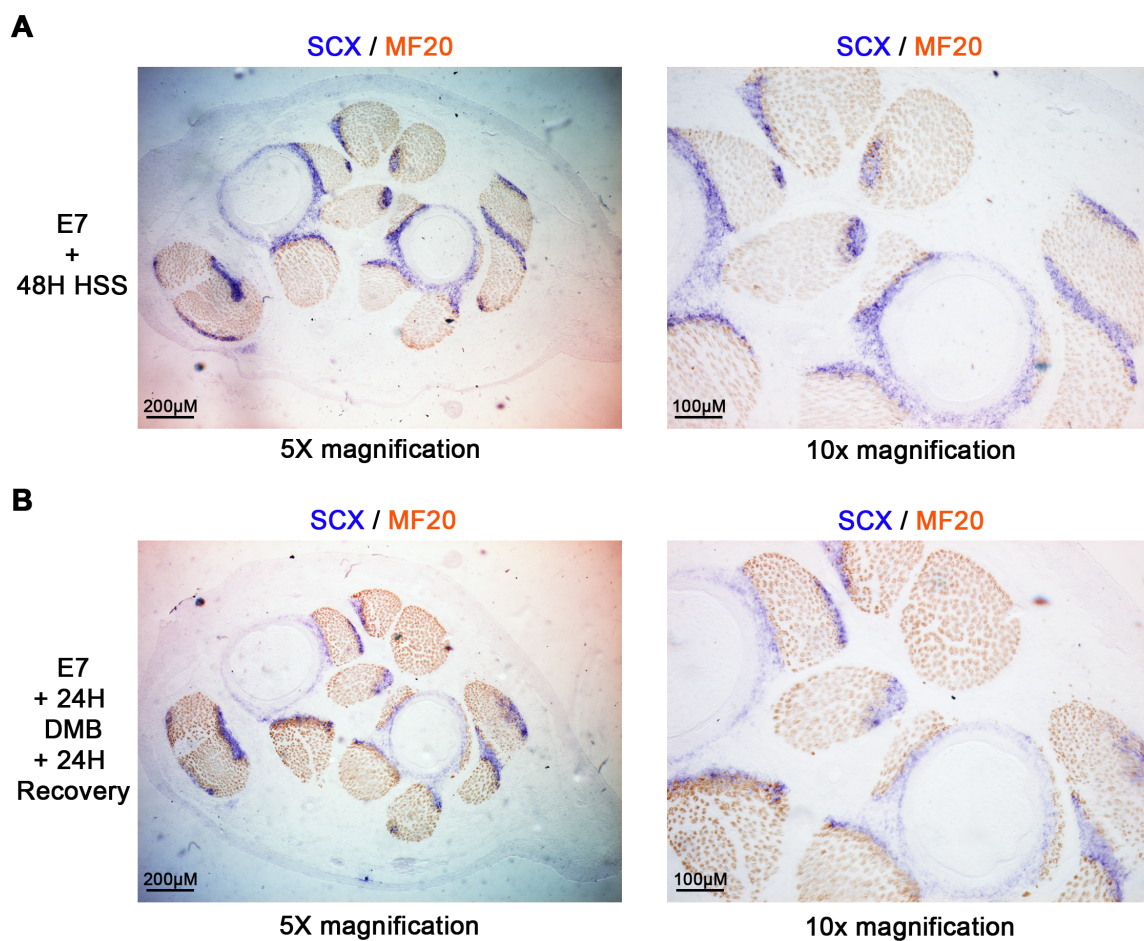


Fig. III.14 **Reintroduction of muscle contractions for 24H is sufficient to recover *SCX* expression in limbs paralyzed for 24H.** *in situ* hybridization to transverse sections of E9 (A) and 24H recovery (B) limbs with *SCX* probe (blue) followed by an immunohistochemistry with MF20 antibody for muscles. (A, B) left panels are pictures of limbs taken at 5x magnification, while the right panels are 10x magnification of the dorsal regions of the same limbs. Abbreviations: HSS: Hank's Saline Solution, used for treatment of the controls; DMB: Decamethonium bromide.

III.2.7 Restored muscle contractions after 48H of immobilization enables a partial recovery of tendon formation based on *SCX* expression

As a 24H-period of muscle contraction after 24H of paralysis from E7 was sufficient to recover normal *SCX* expression at E9, we extended the recovery experiment to 48H of paralysis followed by 48H of recovery. We previously observed a drastic loss of tendon gene expression in paralyzed limbs for 48H in E7+48H DMB-treated chicken fetuses (Figure III.4, III.5 and III.12).

In this 48H recovery experiments, we compared two groups of chicken fetuses: the first one was administered Hank's saline solution at E7 and E8, then nothing until the harvesting time at E11; the second group was administered DMB at E7 and E8 (48H treatment), then nothing until E11 in order to allow for movement recovery during 48H and was named "48H Recovery" (Figure III.15A). Analysis of mRNA levels of tendon genes by RT-qPCR in the 48H Recovery group revealed a recovery for *SCX*, which harbored a 0.70-fold expression compared to control (Figure III.15B). *SCX* expression in the 48H Recovery group is close to the 0.60-fold *SCX* expression in limbs of 48H DMB-treated chicken fetuses (Figure III.1B) but is not significantly decreased when compared to E11 control limbs (Figure III.15B). No changes were observed for *TNMD* and *COL1A2* mRNA levels between the two groups (Figure III.15B); consistent with the absence of decrease in the *TNMD* and *COL1A2* mRNA levels in E7+48H DMB-treated chicken fetuses (Figure III.1B).

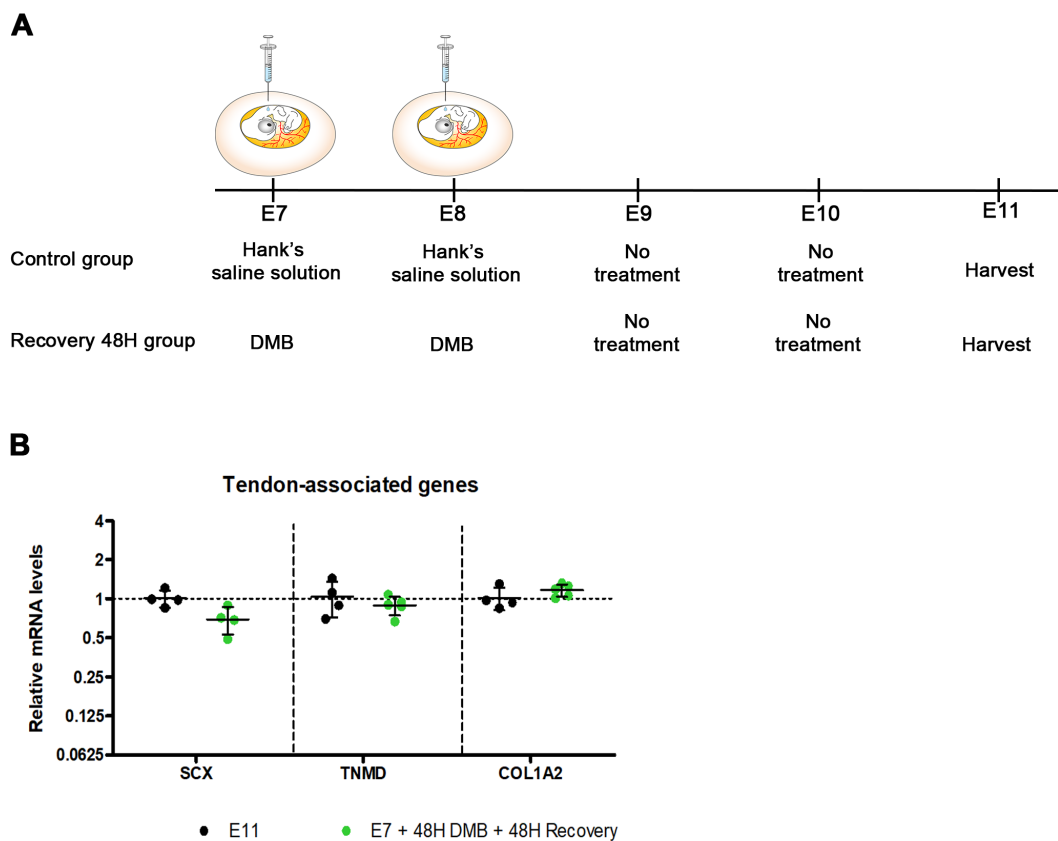


Fig. III.15 (Caption next page.)

Fig. III.15 **48H reintroduction of muscle contractions after 48H of paralysis.** (A) Schematic representation of the experimental procedure for the 48H recovery experiment. The control group was administered Hank's saline solution at E7 and E8, then nothing until the harvesting time at E11; the "48H recovery" group was administered DMB at E7 and E8 (for 48H), then nothing until E11 in order to allow movement recovery after 48H of paralysis. (B) Analysis of mRNA levels of tendon genes by RT-qPCR in the control group (black) versus the 48H recovery group (green) at each time point. Each dot represents an independent biological sample. Samples were analyzed with the non-parametric Mann-Whitney test but did not show any significant difference.

Histological analysis by *in situ* hybridization with *SCX* probe to limb sections allowed us to observe a partially restored tendon structures that expressed *SCX* as compared to the control group (Figure III.16B). The drastic diminution of *SCX* expression in E7 + 48H DMB group compared to control E9 limbs is shown as reference (Figure III.16A). Although the recovery is not complete, muscles visualized with MF20, in the 48H recovery group, clearly adopted a shape resembling those of control muscles (Figure III.16B). While the recovery of muscles and tendons subsequent to the 48H recovery of muscle contractions seems incomplete, it has to be taken into account that at E9, after 48H of paralysis, both muscles and tendons almost completely failed to form properly (Figure III.16A).

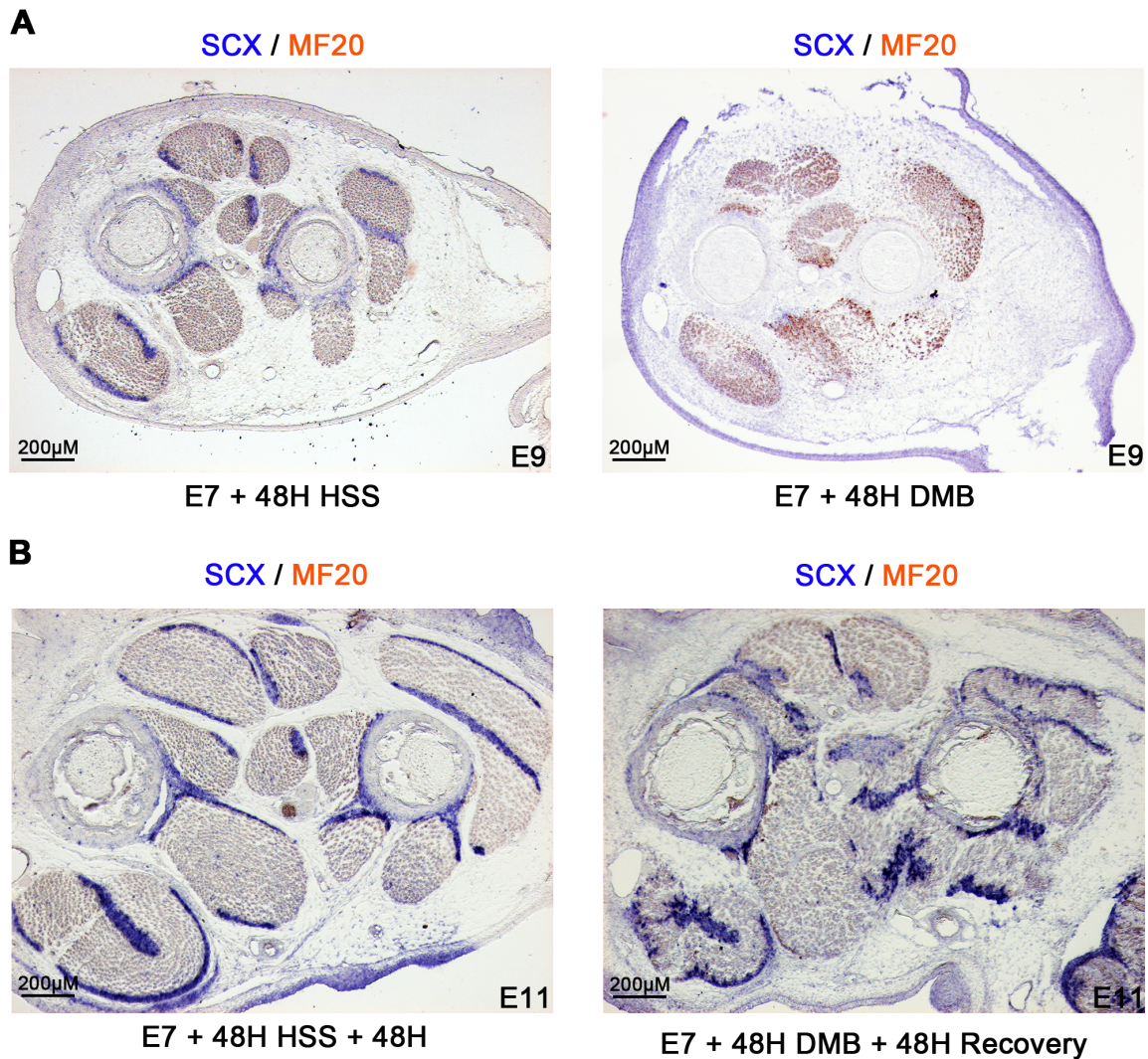


Fig. III.16 **48H reintroduction of muscle contractions after 48H of paralysis allows for a partial reformation of tendon structures and SCX expression.** (A) *In situ* hybridization to transverse sections of control E9 (left panel) and E7+48H DMB (right panel) limbs. (B) *In situ* hybridization to transverse sections of control E11 (left panel) and E7+48H DMB + 48H recovery (right panel) limbs. *In situ* hybridization with SCX probe (blue) followed by an immunohistochemistry with MF20 antibody for muscles. Abbreviations: HSS: Hank's Saline Solution, used for treatment of the controls; DMB: Decamethonium bromide.

III.3 Discussion

In this first part, we show that immobilization of chicken fetuses at E7 leads to a drastic downregulation of tendon marker expression and tendon structure disappearance in two days. We found that, similarly to tendon markers, *EGR1* and YAP expression in tendons was also lost in limbs immobilized for 48H. Interestingly, we observed that nuclei were present in tendon regions, which have lost tendon gene expression. Restored muscle contractions after 24H and 48H of paralysis led to recovery of *SCX* mRNA levels and to a partial-to-complete recovery of tendon structures and muscle splitting. Altogether, these results show that muscle contractions are required for tendon maintenance in limbs during chicken fetal development and that the phenotype induced by paralysis of chicken fetuses is reversible.

III.3.1 Paralysis differentially affect lineage markers in limbs

Regarding the effect of paralysis by DMB treatment, we showed that the decrease in *SCX* expression occurred as soon as 5H of paralysis, while 24H of paralysis was required for a decrease of *PAX7* and *MYF5* expression (Figure III.1B and III.7).

Regarding cartilage, we observed an overall increase in cartilage gene expression in 48H DMB-treated limbs (Figure III.6A) which mirrors the downregulation of tendon genes expression observed in the same condition (Figure III.1B). The increase of cartilage gene expression is consistent with the increase of BMP activity (Figure III.6D), which is known to promote cartilage differentiation (Karsenty et al., 2009). Together, these results highlight an opposition between tendon and cartilage fates, which is concordant in the context of enthesis development *in vivo*. During the formation of the enthesis, *SCX*⁺/*SOX9*⁺ enthesis-forming cells will differentiate either in *SCX*⁺ or *SOX9*⁺ cells, with *SCX* and *SOX9* expression becoming mutually exclusive (Blitz et al., 2013).

We observed that cartilage gene expression was decreased in 24H DMB-treated limbs, which is not consistent with the overall increase of cartilage gene expression that we observed at other time points (Figure III.6A). However, we know from the study of Esteves de Lima and colleagues that DMB-induced limb paralysis is responsible for a decrease of Notch signaling pathway activity (Esteves de Lima et al., 2016). Furthermore, a study by Kohn and colleagues established a Notch-dependent *SOX9* expression *in vivo* (Kohn et al., 2015). Thus, one possibility in our model of paralyzed chicken fetuses is that at 24H of DMB-treatment, the downregulation of Notch signaling would be responsible for the decrease in cartilage gene expression. Since prolonged Notch signaling suppresses *SOX9* transcription (Kohn et al., 2015), the downregulation of Notch signaling at 48H of DMB-treatment could then explain the increase of cartilage gene expression at that time point.

In paralyzed fetuses, we observed an overall increase of cartilage gene expression (Figure 6). However, another study performed in immobilized zebrafishes and *Spd* mutant mice showed that mechanical loads generated by muscle contractions were required for skeletal development (Shwartz et al., 2012). The difference that we observed might be due to our timing of development or is possibly specific to the chicken model.

III.3.2 Defective muscle splitting in immobilized chicken fetuses

Muscle masses undergo a splitting process between E6 and E8 during chicken limb development (Tozer et al., 2007). Since we applied DMB-treatment from E7, we induced rigid paralysis during this specific period of muscle patterning in chicken wing forearm. Interestingly, we observed misshaped muscles in limbs with 24H or 48H of DMB-treatment. The same defect in muscle shape was also observed in the study of Esteves de Lima and colleagues, using the same model at similar times of development (Esteves de Lima et al., 2016). Our observation of misshaped muscles in limbs of immobilized chicken fetuses is concordant with the study of Kardon (Kardon, 1998). Our results showed a mispatterning of muscle concomitant with a defect in tendon maintenance due to the lack of muscle contractions and Kardon showed that proper muscle patterning requires the presence of tendons (Kardon, 1998).

It could be so that the loss of tendons in paralyzed chicken fetuses drove the defect in muscle splitting that we observed. This idea is supported by the effects of restored muscle contractions. In the 48H Recovery group, we observed reappearance of tendon structures, marked by *SCX* expression, concomitant with a restoration of muscle shape. Yet, the muscle patterning observed in the 48H Recovery group was not completely similar to that of control fetuses.

III.3.3 Remaining tenogenic niches in limbs of paralyzed chicken fetuses and recovery of muscle contractions

Interestingly, even with the gradual loss of tendon markers along the 48H period of paralysis, we were still able to detect the tendon-ECM component COLXII (Figure III.12). This collagen belongs to the family of Fibril-Associated Collagens with Interrupted Triple helices (FACITs) (reviewed in Mienaltowski and Birk, 2014). The COLXII staining allowed us to visualize remaining tenogenic niches in paralyzed limbs. This result indicates that tendon cells are still present in paralyzed limbs induced by DMB treatment. Yet, this assumption has not been clearly assessed by analysis of putative apoptotic phenomenon induced by paralysis. Nonetheless, the fact that we were able to restore *SCX* gene expression in limbs that were previously paralyzed would be in favor of the hypothesis that cells are not dying in the absence of mechanical cues. We favor the idea that naïve cells express tendon genes upon mechanical cues. Yet, as we could see in the 24H and 48H recovery groups, the recovery of tendon structures and the profiles of tendon gene expression were similar but not identical to those of the control group. These results attest for the link between tendon development and mechanical cues during fetal stages.

However, recovery experiments made in our team showed that a 48H period of recovery following 48H of DMB treatment initiated at E5.5 was not sufficient to recover tendon gene expression (data not shown). These results indicate that tendon recovery is not possible at earlier developmental stages.

III.3.4 YAP and *EGR1* expression is correlated to mechanical signals in the limb

We were also interested in the behavior of mechanosensitive factors such as *EGR1* and YAP. As expected, *EGR1* expression varied similarly to that of the other tendon genes regarding the mechanical cues (Figure 8). YAP also displayed a similar pattern of expression. Interestingly, YAP seems to be strongly expressed in tendon (Figure III.9). We did not perform any YAP functional study in fetal tendons. Nonetheless, we hypothesize that YAP acts as a mediator of the mechanical cues in order to favor tendon development. Yet, gene expression analysis by RT-qPCR for *EGR1* and YAP target gene *INHBA* showed a decrease in their expression after that of *SCX*. However, we did not assess their expression by *in situ* hybridization on sections of limbs treated at earlier time points. Thus, it could be so that we did not observe a decrease in *EGR1* and *INHBA* expression before that of *SCX* expression because *EGR1* and *INHBA* are also expressed in other tissues. Indeed, *INHBA* is also expressed in bone and cartilage (Kim and Lee, 2014; Melas et al., 2014), while *EGR1* is also expressed in vascular smooth muscle cells and skeletal muscle (Lee et al., 2013; Pardo and Boriek, 2012). Another possibility would be to verify the absence of YAP in tendon nuclei of limbs treated with DMB at earlier time points. The molecular factors relaying mechanical cues might indeed be *EGR1* and YAP, but several experiments are needed to confirm this hypothesis.

III.3.5 SRF does not appear to be involved in limb tendon development of chicken fetuses

We did not observe any expression of the mechanosensitive factor *SRF* in limb tendons of E9 chicken fetuses (Figure III.11B), which would indicate that SRF would not be involved in the development of limb tendons. However, SRF is involved in a wide variety of cellular processes (Esnault et al., 2014). Also, SRF and YAP share common target genes, and these pathways exhibit mutual dependence in cancer associated fibroblast (Esnault et al., 2014; Foster et al., 2018). MRTFA was shown in certain contexts to associate with TAZ, another target of the Hippo pathway similar to YAP (Speight et al., 2016). SRF acting through the actin/MRTFs is also known to be a key mechanotransduction pathway in muscle (Collard et al., 2014). Thus, its role in mechanotransduction events regulating tendon gene expression would be consistent with what is already known in other tissues. Besides, SRF-MRTFA was shown to regulate mechanosensitive *TnC* expression (Asparuhova et al., 2011). Our data alone do not allow us to rule out the possibility that SRF might be involved at earlier or latter stages of tendon formation, or in adult tendon homeostasis.

III.4 Conclusion

Together, our results show that mechanical loads generated by muscle contractions are required for tendon maintenance in chicken fetuses, mainly based in *SCX* gene expression. Mechanical signals enable tendon gene expression and allow for a recovery of *SCX* gene expression and tendon formation after paralysis. Also, we show that YAP is expressed in limb

tendons of chicken fetuses and that its expression is dependent of the same mechanical loads controlling tendon gene expression.

IV. Effect of mechanical constraints and TGF β 2 on the tendon differentiation potential of mouse mesenchymal stem cells

This part of the results has been written for a paper soon to be submitted

IV.1 Abstract

Mesenchymal stem cells present the ability to self-renew and differentiate into multiple lineages in cultures under different cues ranging from chemical treatment to physical constraints. The optimum culture conditions that favour tendon cell differentiation are not known. We analysed the tendon differentiation potential of a murine cell line of mesenchymal stem cells upon different culture conditions. C3H10T1/2 cells were cultured at confluence on two different substrates, plastic and silicone, which display different stiffness on the rigidity scale. We observed that upon confluence C3H10T1/2 cells cultured on silicone substrate were more prone to tendon differentiation based on the expression of the tendon markers *Scx* and *Tnmd* as compared to cells cultured on plastic substrate. Interestingly, the expression profile of the tendon differentiation gene *Tnmd* was inversely correlated with that of *Smad7*, a transcriptional readout for the TGF β /SMAD2/3 signalling pathway in C3H10T1/2 cells upon confluence. Consistently, C3H10T1/2 cells treated with TGF β 2, to chemically activate this signalling pathway, displayed a decrease of *Tnmd*, while displaying an increase of *Scx* expression, both in 2D cultures and 3D-engineered tendons. All together, our results provide us with a better understanding of the effects of mechanical constraints induced by confluence and substrate rigidity on the tendon differentiation potential of mesenchymal stem cells. We also identified TGF β 2 as a negative regulator of tendon differentiation based on *Tnmd* expression in C3H10T1/2 2D and 3D cell cultures. Our results confirm the importance of both mechanical and molecular parameters for tenogenic differentiation of mesenchymal stem cells culture.

IV.2 Introduction

Stem cells are multipotent cells that can be induced by various molecular or mechanical cues to differentiate in tissue-functional lineages. Mesenchymal stem cells (MSCs) are stromal cells that were first isolated from bone marrow as a non-hematopoietic population with stem cell properties (Friedenstein et al., 1966). MSCs present the ability to self-renew and differentiate

into multiple lineages when cultured in appropriate conditions (Pittenger et al., 1999). MSCs are most studied for their multidifferentiation potential, comprising bone, cartilage and fat lineages, as well as their immunomodulatory capacities (reviewed in Caplan and Correa, 2011; DiMarino et al., 2013). Based on specific lineage markers and identified master genes, established protocols are now recognized to drive specific differentiation towards osteocytes, chondrocytes and adipocytes. Although studies highlight tendon cell differentiation upon molecular and mechanical cues from MSCs (reviewed in Nourissat et al., 2015; Wang et al., 2018; Zhang et al., 2018), tendon lineage is less studied as compared to other tissue-specific lineages. In addition, there is no master gene known to initiate the tenogenic program in cell cultures as there are for cartilage (*Sox9*), bone (*Runx2*) and muscle (*MyoD*) programs (reviewed in Buckingham and Mayeuf, 2012; Karsenty et al., 2009). Moreover, there is no established protocol with external inducers to differentiate MSCs to tendon phenotype. Another limitation is the limited number of specific tendon markers. The main structural and functional component of tendon, the type I collagen is not specific to tendon and is expressed in many other connective tissues (reviewed in Gaut and Duprez, 2016). Type I collagen one of the most abundant protein in the body relies on two collagen genes, *Col1a1* and *Col1a2*. One of the main challenges in tendon differentiation relies in the understanding of the intrinsic and extrinsic regulators of type I collagen production and spatial organisation by the tenocytes.

To date, the bHLH transcription factor Scleraxis (*Scx*) is the best and specific marker for tendon and ligaments (Schweitzer et al., 2001, 2010). Although being a powerful tendon marker, the exact function of *Scx* in tendon development, homeostasis and repair is not fully understood (Murchison et al., 2007; reviewed in Schweitzer et al., 2010, Huang et al., 2015). The type II transmembrane protein Tenomodulin, encoded by the *Tnmd* gene, is recognized to be a tendon differentiation marker with potential roles in tenocyte proliferation and differentiation, in addition to type I collagen fibril adaptation to mechanical loads (Alberston et al., 2015; Dex et al., 2017; Docheva et al., 2005, reviewed in Dex et al., 2016). Scleraxis is required for *Tnmd* expression in tendons (Murchison et al., 2007; Yoshimoto et al., 2017) by direct binding on *Tnmd* promoter (Shukunami et al., 2018). Other putative tendon markers have been identified via transcriptomic analysis during mouse development (Havis et al., 2014).

The main extracellular signal known to promote tendon development is the TGF β ligand and the associated SMAD2/3 intracellular signalling pathway (Havis et al., 2014, 2016; Maeda et al., 2011; Pryce et al., 2009). TGF β ligands are recognized to have a tenogenic effect based on the increase of *Scx* transcription in cell cultures (Guerquin et al., 2013; Havis et al., 2014, 2016; Lorda-Diez et al., 2009; Pryce et al., 2009). The increase of *Scx* expression upon TGF β 2 exposure is abolished in the presence of TGF β inhibitors, which block TGF β transduction at the level of the receptors or at the level of the SMAD2/3 intracellular pathways in C3H10T1/2 cells (Guerquin et al., 2013; Havis et al., 2014).

In addition to chemical signals, physical/mechanical signals are important parameters to

consider when studying tendon cell differentiation. Because tendons transmit forces from muscle to bone in the musculoskeletal system, tendon cells are continuously subjected to variations in their mechanical environment (reviewed in Schiele et al., 2013). Physical parameters have been shown to be important for developmental processes and during adult life (Mammoto et al., 2013). It is recognized that substrate stiffness controls many cellular processes such as cell fate, migration, proliferation and differentiation in culture systems of stem cells or progenitor cells (reviewed in Bellas and Chen, 2014; Smith et al., 2018). MSCs are particularly responsive to matrix stiffness in term of lineage commitment, ranging from neurogenic phenotype for soft substrates to osteogenic when cultured on rigid substrates (Engler et al., 2006). Based on the seminal work of the Discher laboratory, it is established that MSC differentiation towards osteogenic, chondrogenic, myogenic or adipogenic lineages can be oriented by different substrate stiffness that proportionally scale with the tissue stiffness. The universal scale of micro-stiffness for tissues and substrates is established to be 100 kPa for bone, 20 kPa for cartilage, 10 kPa for muscle and 1 kPa for fat (reviewed in Discher et al., 2009; Smith et al., 2018). Mechanotransduction pathways have been identified in stem cells and translate mechanical signals into molecular signals all the way down to the nucleus (Ning Wang, 2017). The forces sensed by the cell have proven to be critical for cell differentiation potential. The forces transmitted through cell contacts upon confluence is another parameter that mechanically constrains cells in culture dishes and influence cell differentiation (Abo-Aziza and Zaki, 2016; Ren et al., 2015).

The optimum culture conditions that drive tendon cell differentiation from mesenchymal stem cells have not been yet identified. In the present study, we analyzed the tendon differentiation potential of C3H10T1/2 cells with different mechanical constraints induced by confluence and two different substrates, plastic and silicon, which both display distinct rigidity. We also analyzed the effect of the confluence on the activity of the TGF β 2/SMAD2/3 pathway and the role of this signalling pathway in tendon cell differentiation.

IV.3 Results

In order to investigate the tendon differentiation potential, we used the multipotent murine cell line, the C3H10T1/2 cells (Reznikoff et al., 1973). C3H10T1/2 cells are known to differentiate into chondrocytes, osteocytes and adipocytes when cultured under appropriate differentiation culture media (Guerquin et al., 2013; Ji et al., 2010; Kim and Jang, 2017; Lee et al., 2017). These cells have the ability to display a tendon phenotype under inductive molecular cues, such as the transcription factors EGR1 and MKX (Guerquin et al., 2013; Otabe et al., 2015). The ability to differentiate into different cell lineages related to the musculoskeletal system makes of the C3H10T1/2 cells an ideal tool to study tendon commitment and differentiation under different mechanical constraints such as confluence and substrate stiffness.

To assess tendon differentiation, we used the *Scx* and *Tnmd* markers in addition to *Col1a1*. We also used one of the tendon genes identified in transcriptomic analysis of mouse

tendon cells (Havis et al., 2014), the aquaporin1 (*Aqp1*) gene coding for a water channel protein. Regarding the other lineages, we used well-established differentiation markers. For the cartilage we used the *Sox9* gene coding for the *Sox9* transcription factor, which is required for cartilage formation and cartilage cell differentiation (Akiyama et al., 2002; Takimoto et al., 2012). The chondroitin sulphated proteoglycan aggrecan, encoded by the *Acan* gene, is known to be highly upregulated during chondrocyte differentiation and to be essential for cartilage structure and function (Lauing et al., 2014). To assess the bone differentiation potential, we used the master gene for osteogenesis, *Runx2* (Runt-related transcription factor 2) (Ducy et al., 1999; Komori et al., 1997) and the *Dlx5* (distal-less homeobox 5) gene known to play a key role in skeletal development (Robledo et al., 2002) and recently shown to be a master regulator of osteogenic differentiation in mesenchymal stem cells (Heo et al., 2017). The *Bglap* gene encodes the most abundant non-collagenous bone matrix protein (also known as Osteocalcin) and is used as a late differentiation marker for osteogenesis (Boskey et al., 1985; Tsao et al., 2017). To assess adipocyte differentiation, we used the expression of two early and late adipogenic regulators, *Cebpb* and *Pparg*, respectively (Cristancho and Lazar, 2011). We assessed muscle differentiation with the expression of the myogenic differentiation factor Myogenin (*Myog*) (Buckingham, 2017).

IV.3.1 The initial cell number did not change the expression of tendon genes in C3H10T1/2 cells, 16H after plating.

We first tested whether the initial cell number interfered with the expression of tendon genes. Different cell numbers (0.5×10^5 , 10^5 and 2×10^5 cells) were seeded in 10 cm culture plates (plastic substrate) and left for 16H in culture. After 16H of culture, C3H10T1/2 cell density was illustrated for the initial plating of 0.5×10^5 cells (Figure IV.1A), 10^5 cells (Figure IV.1B) and 2×10^5 cells (Figure IV.1C). The relative mRNA levels of tendon-associated genes were assessed for the 3 different plating conditions (Figure IV.1D). The relative mRNA levels for each gene were normalized to those observed in the plating condition with 10^5 cells. The expression of tendon genes, *Scx*, *Tnmd*, *Col1a1* and *Aqp1* did not display any obvious change in different cell density conditions (Figure IV.1D). This shows that the initial cell number at seeding time does not have any major influence on the expression of tendon genes after 16H of culture. We also compared the expression levels of tendon genes at the 10^5 cells density condition, 16H after plating. The expression levels of each tendon gene were reported to the *Rplp0* gene (19.5 of Ct for 250ng of mRNAs) (Figure IV.1E). *Col1a1* gene displayed very high levels of expression compared to those of *Scx*, *Tnmd* and *Aqp1* in C3H10T1/2 cells cultured on plastic substrate (Figure IV.1E). For a preparation of 250 ng mRNAs, we found that the *Col1a1* gene (17.6Ct) displayed 9 cycles less than *Scx* (26.5Ct) and 10 less than *Tnmd* (27.6Ct). Even with consideration for the fact that Ct are also dependent of GC composition of amplified fragments and oligonucleotides primers, these data led us to conclusions about the expression of tendon genes 16H after plating. We conclude that *Col1a1* display a massive expression as compared to *Scx* and *Tnmd* genes in C3H10T1/2 cells 16H after plating.

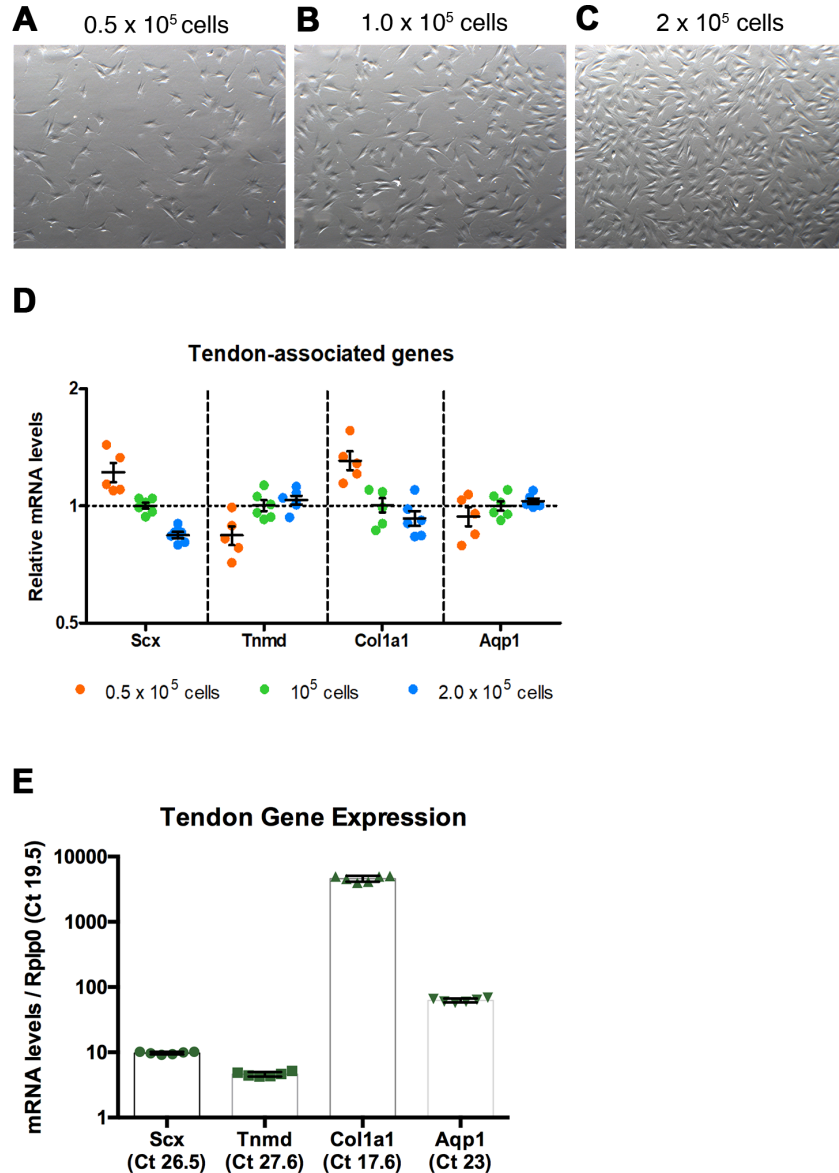


Fig. IV.1 **The initial cell number at the plating time does not change tendon gene expression, 16H after plating.** (A-C) Photographs of cell density 16H after plating 0.5 10^5 (A), 10^5 (B) and 2×10^5 (C) C3H10T1/2 cells on plastic culture plates. (D) RT-q-PCR analyses of the expression levels of tendon markers, *Scx*, *Tnmd*, *Col1a1* and *Aqp1*, in C3H10T1/2 cells 16H after initial plating of 0.5×10^5 , 10^5 and 2×10^5 cells. The relative mRNA levels were calculated using the $2^{-\Delta\Delta Ct}$ method using the 10^5 plating condition as control. For each gene, the mRNA levels of the 10^5 plating condition were normalized to 1 (green spots). Graph shows means \pm standard deviations of six biological samples. The p-values calculated with the Mann-Whitney test did not show any significant variation between different conditions. (E) RT-q-PCR analyses of the expression levels of tendon markers, *Scx*, *Tnmd*, *Col1a1* and *Aqp1*, in C3H10T1/2 cells 16H after initial plating of 10^5 cells. mRNA levels were reported to the *Rplp0* gene ($2^{-\Delta\Delta Ct} \times 1000$). Graph shows means \pm standard deviations of six biological samples. The means of the initial Cts (obtained from 250 ng of mRNAs) are indicated in brackets for each gene.

IV.3.2 Substrate effects on the expression of cell lineage and differentiation markers in C3H10T1/2 cells cultured for 16H

We compared the expression levels of tendon genes with those of other cell lineages at the 10^5 cells density condition. The same number (10^5) of C3H10T1/2 cells was plated on classic culture plates (plastic substrate). This type of plastic substrate displays a Young modulus of GPa order of magnitude and is considered extremely rigid. Cells were harvested 16H after (Figure IV.2A, B). Tendon genes displayed the same expression profile than that shown in Figure 1E. For a 500ng RNA preparation, we generally found around one cycle less than with 250ng preparation as a gage of reproducibility. Tendon genes displayed higher levels of expression as compared to other differentiation markers for other lineages such as *Bglap* (bone), *Acan* (cartilage), *Myog* (muscle) and *Pparg* (fat) (Figure IV.2B). *Acan* and *Pparg* displayed cycles above 31/32 cycles indicating an absence of expression of these genes in C3H10T1/2 cells in this culture condition. We next analysed whether the substrate affected tendon gene expression. The same number (10^5) of C3H10T1/2 cells was plated on Uniflex Flexcell plates (silicone substrate coated with type I collagen), which displayed a stiffness estimated to 5MPa by the company. The silicone plates displayed a lower stiffness than that of plastic plates. Cells were harvested 16H after (Figure IV.2C, D). The expression pattern of lineage markers in C3H10T1/2 cells cultured in silicone substrate was very similar to that observed with plastic substrate (Figure IV.2B compared to Figure IV.2D). Here again, the tendon genes (*Scx*, *Tnmd*, *Col1a1* and *Aqp1*) displayed higher expression levels than those of differentiation markers for the other lineages (Figure IV.2D). These results were not obtained with the same reference gene (*Rn18S* for cells seeded on plastic and *Rplp0* for cells cultured on silicon substrate), but their similarity tends to confirm that C3H10T1/2 cells cultured for 16H on either substrate behaved in a similar manner for gene expression. This quantification of mRNA levels showed that tendon genes were expressed at higher levels than the other differentiation markers in C3H10T1/2 cells cultured for 16H on plastic or silicone substrates after initial plating at 10^5 cells.

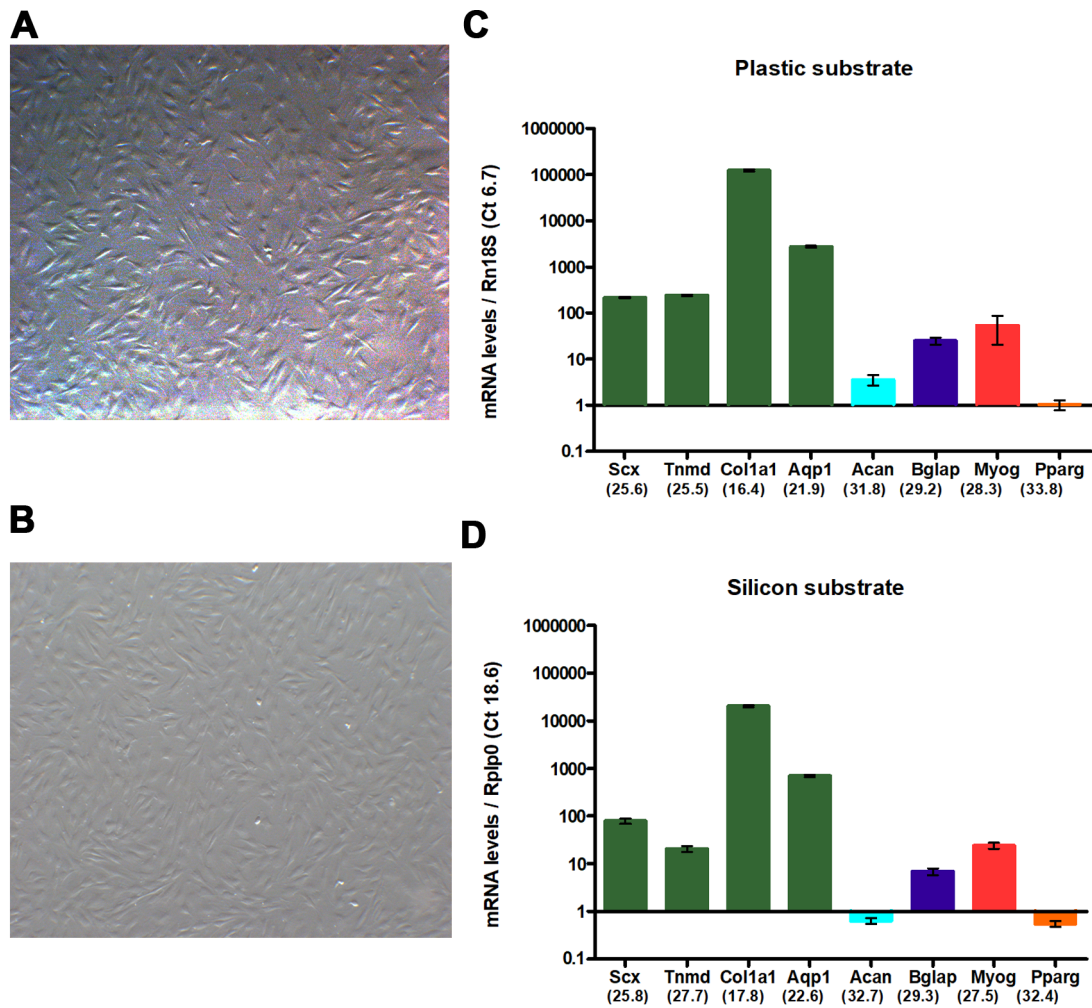


Fig. IV.2 **The nature of the substrate does not modify the initial expression profile of tendon genes in C3H10T1/2 cells 16H after plating.** (A, C) Photographs of C3H10T1/2 cells, 16H after plating at 10^5 density condition on plastic culture plates. (A) and on Uniflex culture plates (FlexCell Int) made of silicon coated with type I collagen (C). (B, D) RT-q-PCR analyses of the expression levels of tendon gene markers, *Scx*, *Tnmd*, *Col1a1*, *Aqp1*, *Acan* (cartilage), *Bglap* (bone), *Myog* (muscle) and *Pparg* (fat), in C3H10T1/2 cells 16H after initial plating at 10^5 density condition on plastic (B) and silicone (D) substrates. (B) The relative mRNA levels were reported to the 18S gene ($2^{-\Delta\Delta Ct} \times 1000$) for the plastic substrate. Graph shows means \pm standard deviations of four biological samples. The means of the initial Cts (obtained from 500 ng of mRNAs) are indicated in brackets for each gene. (D) The relative mRNA levels were reported to the *Rplp0* gene ($2^{-\Delta\Delta Ct} \times 10000$) for the silicone substrate. Graph shows means \pm standard deviations of six biological samples. The means of the initial Cts (obtained from 500 ng of mRNAs) are indicated in brackets for each gene.

IV.3.3 Effect of confluence on the differentiation potential of C3H10T1/2 cells cultured on plastic substrate

In order to investigate the effect of confluence on the tendon differentiation potential of C3H10T1/2 cells cultured on plastic substrate, 10^5 cells were plated on classic culture plates and left for 16H to define the T=0. C3H10T1/2 cells were let to grow from this time (T0) for up to 14 days with no passage. C3H10T1/2 cells were harvested at 24H, 7 days, 10 days and 14 days of culture (Figure IV.3A). The cell density of C3H10T1/2 cells at each harvesting time point was illustrated in Figure IV.3A. After confluence was reached at 24H, C3H10T1/2 cells adopted a non-oriented and rather anarchic/random arrangement (Figure IV.3A).

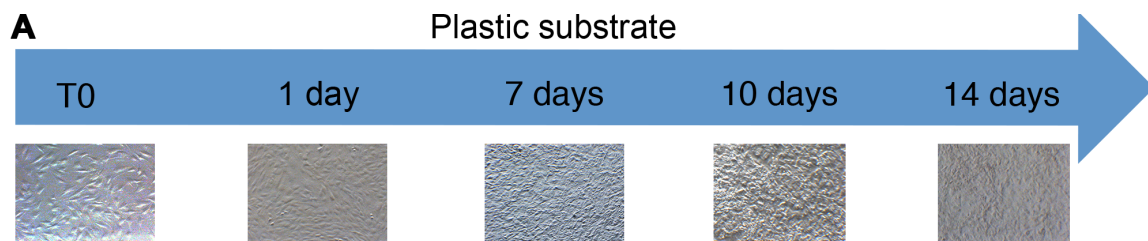
Lineage-specific gene expression analysis was conducted at different time points in order to assess the differentiation behaviour of C3H10T1/2 cells cultured on plastic substrate overtime. The global expression pattern of the tendon-associated genes indicated a general decrease of expression, although being different between each tendon gene (Figure IV.3B). *Scx* expression displayed a drastic and continuous downregulation from 24H to 14 days. *Col1a1* and *Aqp1* genes displayed a decrease of expression at the beginning of the culture until 7 days and then reached a plateau (Figure IV.3B). In contrast, the tendon differentiation marker *Tnmd* displayed a 2-fold increase during the first 24H to reach a plateau and then decreased from 7 days of culture (Figure IV.3B). This result indicated that tendon genes displayed a tendency to decrease overtime in C3H10T1/2 cells cultured on plastic substrate.

We also analyzed the expression of differentiation markers for the components of the musculoskeletal system, ranging from high to soft intrinsic tissue stiffness: bone, cartilage, muscle and fat. The differentiation markers for the other cell lineages did not display the same expression profile as compared to tendon genes in C3H10T1/2 cells cultured on plastic substrate overtime. The early bone markers (*Dlx5* and *Runx2*) did not displayed any major changes of expression overtime (Figure IV.3D). However, the bone differentiation marker *Bglap* displayed a 26-fold increase at 7 days to reach a 41-fold increase at 10 days (Figure IV.3D). It has to be noticed that the bone markers were not expressed at early time point (Ct above 33 cycles Figure IV.2). The expression of the specification and differentiation markers for cartilage, *Sox9* and *Acan* was not changed overtime, except for a 4-fold drop of *Acan* expression at 10 days (Figure IV.3C). The expression of the muscle differentiation marker *Myog* did not change much overtime although displaying a 2-fold increase at 10 days (Figure IV.3E). Lastly, the expression of the early fat marker *Cebpb* did not change overtime, while that of the late differentiation fat marker *Pparg* displayed an impressive 148-fold increase after 14 days of culture (Figure IV.3F). However, as bone markers, it has to be noticed that *Pparg* gene was not expressed in C3H10T1/2 cells at T=0 (Ct above 33 cycles, Figure IV.3B). These results showed that confluence did not affect the expression of the cartilage and muscle markers. However, it drastically increased the expression of bone and fat differentiation markers, in C3H10T1/2 cells cultured on plastic substrate overtime. This result is

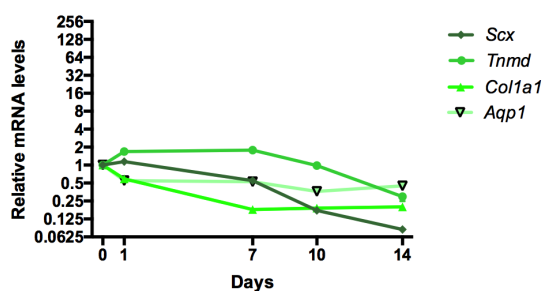
intriguing since bone and fat tissues are located at both ends on the intrinsic tissue stiffness scale high for bone and soft for fat and their differentiations are generally mutually exclusive.

We conclude that cell confluence has a global negative effect on tendon lineage, while promoting bone and fat differentiation in C3H10T1/2 cells cultured on plastic substrate over 14 days of culture.

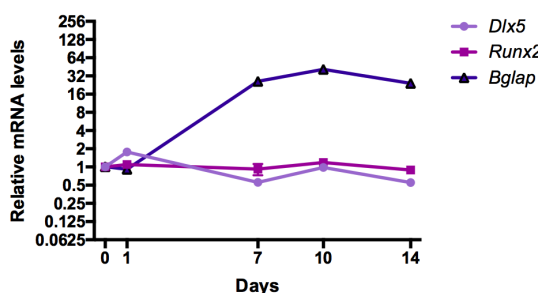
Fig. IV.3 (Figure next page) **Effect of cell confluence overtime on tendon gene expression in C3H10T1/2 cells cultured on plastic substrate** (A) Photographs of C3H10T1/2 cells cultured on plastic culture plates at different time points. 10^5 C3H10T1/2 cells were plated on plastic culture plates and left for 16H to define the T=0 time point. Cells were then fixed at 24H, 7 days, 10 days and 14 days for RT-q-PCR analyses. (B) RT-q-PCR analyses of the expression levels of tendon markers, *Scx*, *Tnmd*, *Col1a1* and *Aqp1* genes. The relative mRNA levels were calculated using the $2^{-\Delta\Delta C_t}$ method using the T=0 condition as controls. For each gene, the mRNA levels of the T=0 condition were normalized to 1. Graph shows means +/- standard deviations of four biological samples for T=0, 1 day/24H, 7 days and 14 days and of five biological samples for 10 days. The expression of tendon genes displayed a tendency to decrease overtime on plastic substrate. (C-F) RT-q-PCR analyses of the expression levels for other cell lineage markers: bone-associated genes, *Dlx5*, *Runx2* and *Bglap* (C); cartilage-associated genes, *Sox9*, *Acan* (D); the muscle-associated gene, *Myog* (E); and the fat-associated gene *Cebpb*, *Pparg*, (F), in C3H10T1/2 cells cultured on plastic culture plates at different time points. The relative mRNA levels were calculated using the $2^{-\Delta\Delta C_t}$ method using the T=0 condition as controls. For each gene, the mRNA levels of the T=0 condition were normalized to 1. Graph shows means +/- standard deviations of four biological samples for T=0, T=1day/24H, 7 days and 14 days and of five biological samples for 10 days. (C-D) The scales of the y-axes have been standardized to facilitate comparison of gene expression profile overtime. The standard deviations are so tiny that they are not visible on the graphs. The p-values were calculated using the Mann-Whitney test.



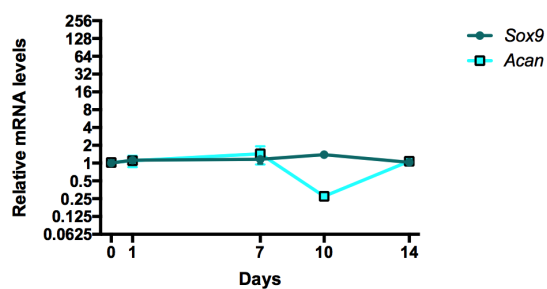
B Tendon-associated genes



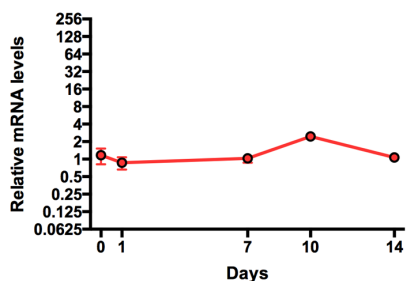
C Bone-associated genes



D Cartilage-associated genes



E Muscle-associated gene - *Myog*



F Fat-associated genes

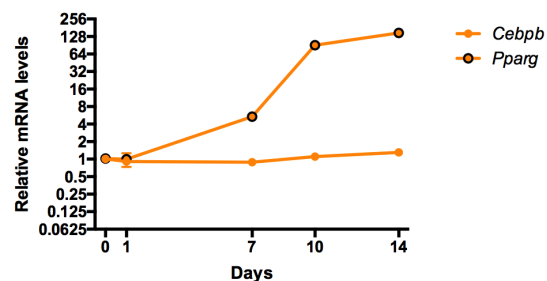


Fig. IV.3 (Previous page)

IV.3.4 Effect of confluence on the differentiation potential of C3H10T1/2 cells cultured on silicon substrate overtime

We investigated the effect of confluence on the differentiation potential of C3H10T1/2 cells cultured on silicon substrate. The silicon substrate is 200-fold less rigid (5 MPa) compared to plastic substrate (1GPa) but is still considered as rigid on the tissue scale (Discher et al., 2009). Similarly to cultures on plastic substrate, 10^5 cells were plated on the Uniflex Flexcell plates (made of silicon coated with type I collagen) and left for 16H, which defined the T=0. Cells were then cultured for 24H, 48H, 4 days, 7 days and 11 days with no passage (Figure IV.4A). C3H10T1/2 cells cultured on silicon substrate reached confluence at 48H. At 4 days, cells seemed to exhibit an alignment becoming robust after 7 days of culture showing that C3H10T1/2 cells would probably arrange in a less random manner in silicon than on plastic substrates. However, we had to stop the experiment at 11 days of culture, since cells started to detach from that time point. Lineage-specific gene expression analysis of C3H10T1/2 cells cultured on silicon substrate showed that the expression of the tendon genes, *Scx*, *Col1a1* and *Aqp1* remained unchanged overtime (Figure IV.4B). However, the mRNA levels of the differentiation tendon gene *Tnmd* started to increase at 48H, to reach a plateau with a 3-4 fold increase between 4 and 7 days (Figure IV.4B). This showed that the confluence had a transient beneficial effect on *Tnmd* expression in C3H10T1/2 cells culture on silicone substrate, while not affecting that of *Scx*. As for plastic substrate, the bone marker *Bglap* displayed a massive increase in C3H10T1/2 cells cultured on silicone substrate overtime (16-fold increase) with a peak of 35-fold increase at 7 days of culture (Figure IV.4C). The expression of the representative markers of differentiation for cartilage (*Acan*), muscle (*Myog*) and fat (*Pparg*) displayed a slow increase to reach 4-fold at 11 days of culture (Figure IV.4D-F). We conclude that confluence has a positive effect on the tendon differentiation potential of C3H10T1/2 cells cultured on silicone substrate overtime. Confluence on silicon substrate also has a positive effect on bone differentiation.

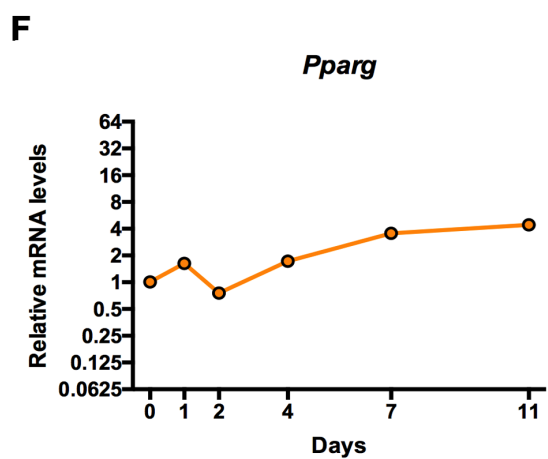
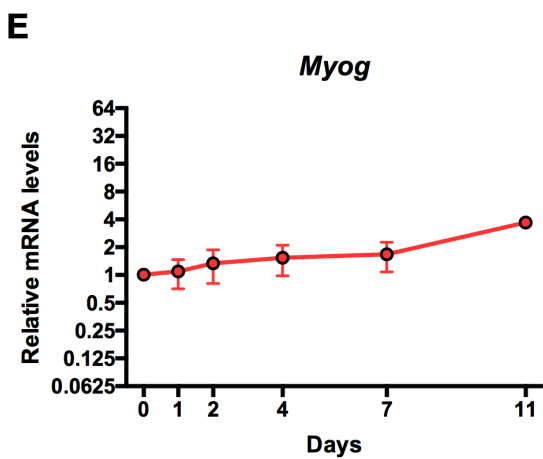
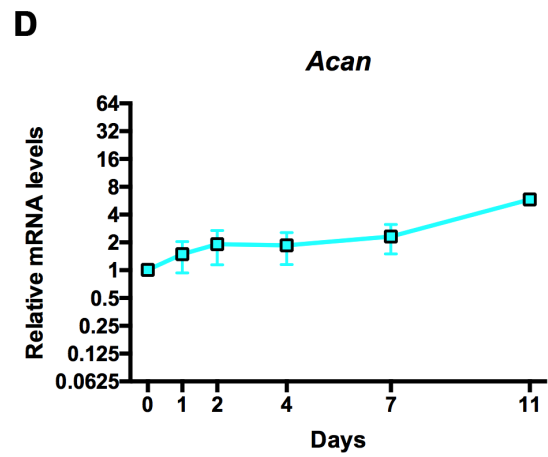
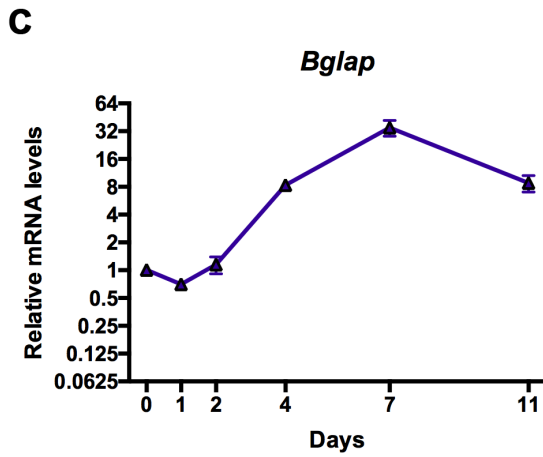
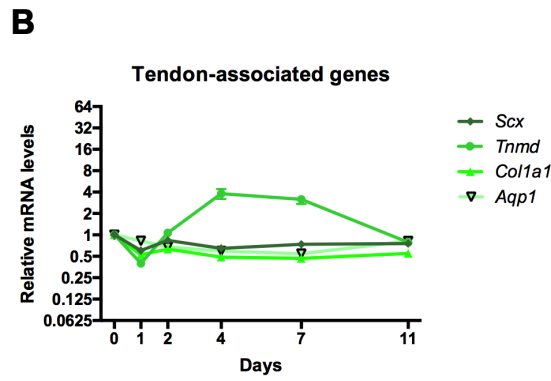
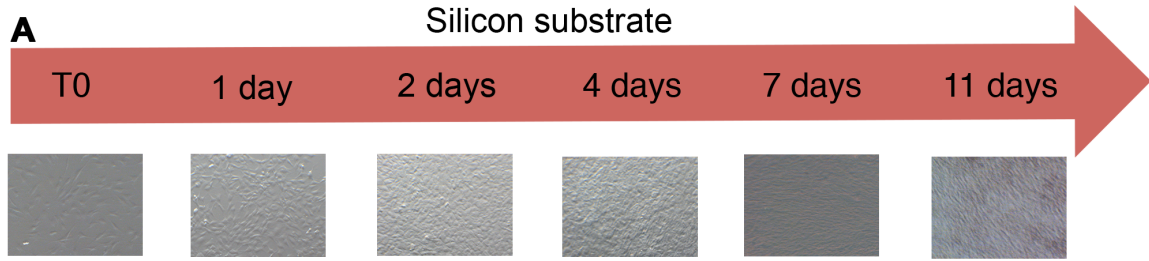


Fig. IV.4 (Caption next page)
106

Fig. IV.4 (Figure previous page) **Effect of cell confluence overtime on tendon gene expression in C3H10T1/2 cells cultured on silicone substrate** (A) Illustration of C3H10T1/2 cells cultured on silicone substrate at different time points. 10^5 C3H10T1/2 cells were plated on Uniflex Flexcell plates (made of silicone and coated with type I collagen) and left for 16H to define the T=0 time point. Cells were then fixed at 24H, 48H, 4 days, 7 days and 11 days for RT-q-PCR analyses. (B) RT-q-PCR analyses of the expression levels of tendon gene markers, *Scx*, *Tnmd*, *Col1a1* and *Aqp1*. The relative mRNA levels were calculated using the $2^{-\Delta\Delta C_t}$ method using the T=0 condition as controls. For each gene, the mRNA levels of the T=0 condition were normalized to 1. Graph shows means +/- standard deviations of five biological samples for T=0 and of six biological samples for 1day/24H, 2days/48H, 4 days, 7 days and 11 days. The expression of tendon genes did not show any obvious changes overtime, except for *Tnmd* gene, which increased at 4 and 7 days. (C-F) RT-q-PCR analyses of the expression levels of the bone-associated gene *Bglap*, (C); cartilage-associated gene *Acan* (D); muscle-associated gene *Myog* (E) and fat-associated gene *Pparg* (F), in C3H10T1/2 cells cultured on silicone substrate at different time points. The relative mRNA levels were calculated using the $2^{-\Delta\Delta C_t}$ method. For each gene, the mRNA levels of the T=0 condition were normalized to 1. (C-D) The scales of the y-axes have been standardized to facilitate comparison of gene expression profile overtime. The p-values were calculated using the Mann-Whitney test.

IV.3.5 Inverse correlation between active TGF β signalling pathway and *Tnmd* expression in C3H10T1/2 cells in 2D cell cultures and 3D-engineered tendons

The canonical TGF β 2/SMAD2/3 pathway is recognized to have a protenogenic effect in cell cultures based on *Scx* expression (Guerquin et al., 2013; Havis et al., 2014, 2016; Lorda-Diez et al., 2009; Pryce et al., 2009). There are not many recognized transcriptional readout of TGF β 2 activity, but *Smad7* is a negative-feedback regulator that is considered to be a general SMAD2/3 transcriptional target gene (Massagué, 2012). We assessed the activity of TGF β 2/SMAD2/3 signalling pathway with *Smad7* expression in C3H10T1/2 cells cultured with plastic and silicon substrates overtime. The initial cycle number for *Smad7* gene with both substrates (Ct=23.9 for plastic and Ct = 24.7 for silicone) indicated that *Smad7* gene was expressed in C3H10T1/2 cells, 16H after plating in both substrate culture conditions. This suggested that TGF β 2/SMAD2/3 signalling pathway was active in C3H10T1/2 cells. The expression profile of *Smad7* displayed a similar shape (decrease and slight re-increase) in cells cultured on both substrate conditions overtime. *Smad7* expression reaching its lowest mRNA levels around (0.125-fold) at 7 days of culture for plastic (Figure IV.5A) and around (0.25-fold) at 4 days for silicone (Figure IV.5B). This result indicated that the activity of TGF β 2/SMAD2/3 signalling pathway was decreased overtime in C3H10T1/2 cells upon confluence.

The expression profiles of *Scx*, *Tnmd* and *Col1a1* genes shown in Figures IV.3B, IV.4B was added on Figure IV.5A, B to compare tendon gene expression profiles with that of *Smad7* overtime. We observed that *Smad7* expression profile displayed a mirror image to that of *Tnmd* in cells cultured on plastic or silicon substrates (Figure IV.5A, B), while *Smad7* expression followed that of *Scx* and *Col1a1* in C3H10T1/2 cells cultured in both substrate culture conditions (Figure IV.5A, B). We also analysed the expression of *Tgfb2* gene coding for the TGF β 2 ligand and observed that *Tgfb2* expression did not follow that of *Smad7*, but rather followed that of *Tnmd* expression in C3H10T1/2 cells in plastic or silicone culture conditions (Figure IV.5A, B). These results showed that *Tnmd* expression was upregulated when the activity of TGF β 2/SMAD2/3 signalling was decreased. The fact that the activity of TGF β 2/SMAD2/3 signalling pathway followed that of *Scx* expression in C3H10T1/2 cells under confluence whatever the culture substrates was consistent with the recognized positive regulation of *Scx* expression by the TGF β 2/SMAD2/3 signalling pathway in C3H10T1/2 cultures (Guerquin et al., 2013; Havis et al., 2014, 2016).

The opposite direction of *Tnmd* and *Smad7* expression profiles in C3H10T1/2 cells under confluence (Figures IV.5A, B) suggested that active TGF β 2/SMAD2/3 signalling pathway downregulated *Tnmd* expression. In order to test this, we analysed the TGF β 2 effect on *Tnmd* expression in C3H10T1/2 cells (Figure IV.5C). C3H10T1/2 cells were treated with TGF β 2 ligand for 24H and then grew for an additional 24H without any TGF β 2 supplementation in culture medium. TGF β 2 treatment drastically decreased (down to 0.06-fold) *Tnmd* mRNA levels, while increasing those of *Scx* up to 9-fold in C3H10T1/2 cells compared to no treatment (Figure IV.5C, D). These results showed that TGF β 2 abolished *Tnmd* expression in C3H10T1/2 cells. Other tendon markers such as *Col1a1*, *Aqp1* and *Thbs2* did not display any significant variations upon TGF β 2 exposure, indicating a specific and differential effect on this signalling pathway on *Scx* and *Tnmd* expression in C3H10T1/2 cells.

In order to test if the negative effect of TGF β 2 on *Tnmd* expression was inherent to the 2D culture system, we also applied TGF β 2 in C3H10T1/2 cells cultured in 3D fibrin gel (Guerquin et al., 2013). TGF β 2 was added in the culture medium of tendon constructs for 24H and compared to non-treated constructs harvested at the same time. No apparent differences could be observed in the general morphology of the TGF β 2-treated constructs when compared to controls (Figure IV.5F). Consistent with the results obtained in 2D cultures (Figure IV.5C-E), we found an increase in the expression of *Scx* and *Col1a1* (2.6-fold and 1.5-fold, respectively) and a concomitant 0.26-fold decrease in *Tnmd* expression in TGF β 2-treated tendon constructs compared to control tendon constructs (Figure IV.5G). This shows that TGF β 2 has a similar negative effect on *Tnmd* expression, while having a positive effect on *Scx* expression in C3H10T1/2 cells cultured in 2D and 3D culture conditions. However, in contrast to the 2D conditions, the relative expression levels of *Aqp1* and *Thbs2* genes (0.55-fold and 0.68-fold, respectively) were decreased in TGF β 2-treated compared to control tendon constructs (Figure IV.5G).

We conclude that the activity of TGF β 2/SMAD2/3 signalling pathway follows *Scx* expression and anti-mirror that of *Tnmd* in C3H10T1/2 cells in plastic and silicon substrates upon confluence overtime. Moreover, TGF β 2 is a negative regulator of *Tnmd* expression in C3H10T1/2 cells in 2D and 3D culture systems.

Fig. IV.5 (Figure next page) **Correlation between TGF β 2 activity and *Scx* and *Tnmd* expression and dual effect of TGF β 2 on *Tnmd* and *Scx* expression in C3H10T1/2 cells cultured in 2D or 3D-engineered tendon.** (A,B) RT-q-PCR analyses of the expression levels of *Smad7* and TGF β 22 genes in C3H10T1/2 cells cultured at different time upon plastic (A) or silicone substrates (B). The relative mRNA levels were calculated using the $2^{-\Delta\Delta C_t}$ method. For each gene, the mRNA levels of the T0 conditions were normalized to 1. (A) Graph shows means +/- standard deviations of four biological samples for T=0, 1 day/24H, 7 days and 14 days and of five biological samples for 10 days. (B) Graph shows means +/- standard deviations of five biological samples for T=0 and of six biological samples for 1day/24H, 2days/48H, 4 days, 7 days and 11 days. The expression profiles of *Scx* and *Tnmd* genes have been plotted again on panels A and B to facilitate comparison between tendon gene and *Smad7* gene. (C-E) RT-q-PCR analyses of the expression levels of tendon gene expression in C3H10T1/2 cells cultured in control or TGF β 2 supplemented media. The relative mRNA levels were calculated using the $2^{-\Delta\Delta C_t}$ method. For each gene, the mRNA levels of control conditions were normalized to 1. Upon TGF β 2 exposure, the relative mRNA levels of *Tnmd* displayed a drastic decrease (C), while those of *Scx* was significantly increased (D) compared to control conditions. The expression levels of *Col1a1*, *Aqp1* and *Thbs2* genes did not changed in the presence of TGF β 2 as compared to control. (F-G) 3D-engineered tendon constructs in control or TGF β 2 supplemented media. Images showing no significant variations in the morphology of the treated constructs (below) compared to the control (above). (G) Graph shows mean +/- standard deviation of RT-qPCR analysis of the expression of tendon-associated genes in constructs treated or not with TGF β 2. The relative mRNA levels were calculated using the $2^{-\Delta\Delta C_t}$ method. TGF β 2 treatment had a similar effect than observed in 2D cultures for *Scx* and *Tnmd* expression (C-D and G). This time, *Col1a1* was slightly upregulated and *Aqp1* and *Thbs2* slightly downregulated. For each gene, the mRNA levels of control conditions were normalized to 1. The p-values were calculated using the Mann-Whitney test.

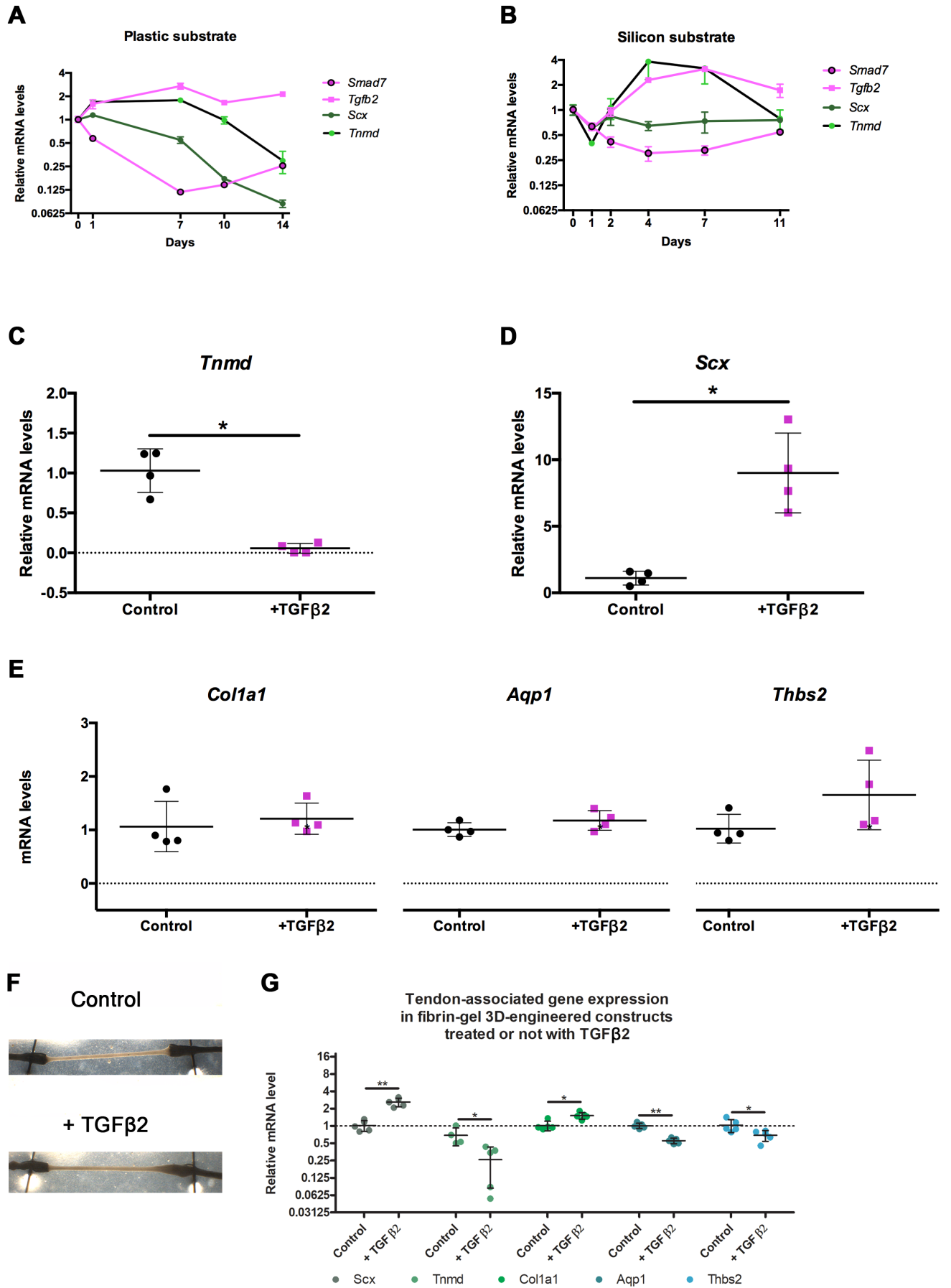


Fig. IV.5 (Previous page)

IV.4 Discussion

IV.4.1 Comparison of the tendon differentiation potential for C3H10T1/2 cells cultured on plastic and silicon substrates in confluence conditions

We found that silicone substrate was more prone to favour tendon differentiation compared to plastic substrate of C3H10T1/2 cells upon confluence and overtime (Figures IV.3,IV.4,IV.6). Although the range/scale of substrate stiffness promoting the tendon phenotype in cultured stem cells has not been established yet, it has been proposed to be close to the scale of rigid substrates promoting bone differentiation. This assumption is based on the tissue elasticity of tendons (1GPa for Achilles tendons) and ligaments (100 MPa) that is close to that of bone 10 GPa (Maganaris and Paul, 1999). The design of our study allowed us to compare the effect on tendon gene expression of two substrates with a 200-fold difference in stiffness on the rigid scale. The extreme rigidity of plastic substrate (of GPa magnitude) decreases the expression of *Scx*, while a relatively less rigid substrate (5 MPa) does not modify *Scx* expression in C3H10T1/2 cells under confluence overtime (Figure IV.6). The silicone substrate favours the expression of the tendon differentiation marker, *Tnmd* (Figure IV.6). Based on *Scx* and *Tnmd* expression, we conclude that a substrate of 5 MPa rigidity favours the tendon phenotype in C3H10T1/2 cells overtime.

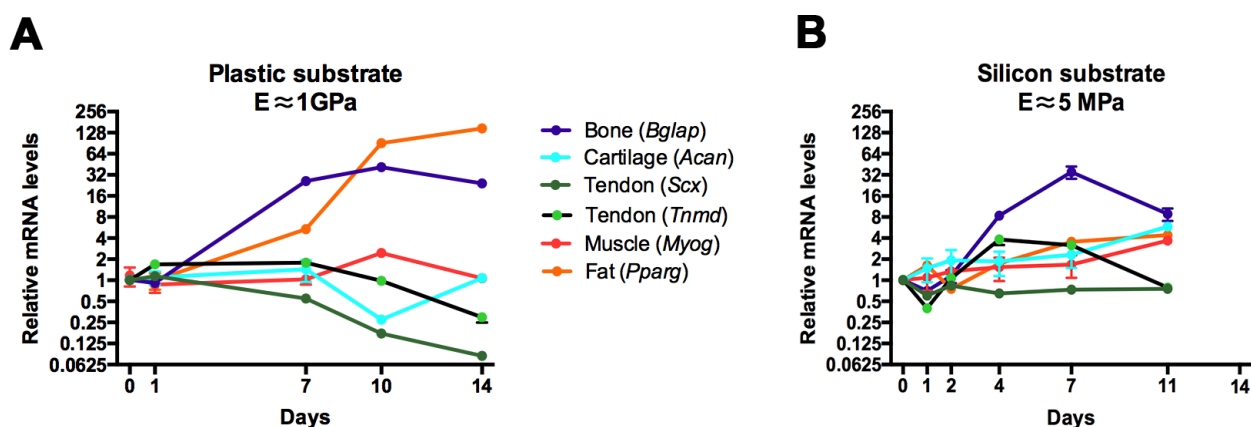


Fig. IV.6 *Comparison of cell expansion effect on gene expression between the plastic and substrate culture conditions.* Relative mRNA levels of selected lineage markers shown in Figures IV.3 and IV.4 in C3H10T1/2 cells cultured on plastic substrate (A) and silicone substrate (B) overtime. Graphs were shown at the same scale for the Y-axis (relative mRNA levels) to facilitate visual comparison of gene expression between both substrate culture conditions. Plastic substrate has an estimated E of 1 GPa, while Silicone substrate has an $E= 5$ MPa.

Although the stiffness values of both substrates display a 200-fold difference between plastic (GPa magnitude) and silicone (5 MPa), these two substrates are still in the rigid scale favourable for bone differentiation (Discher et al., 2009). Consistently, the C3H10T1/2 mesenchymal stem cells cultured on these two substrates (plastic and silicone) display a significant and drastic increase in the expression of the bone differentiation marker (*Bglap*)

overtime. Because there is no addition of bone differentiation medium in the culture conditions, we believe that confluence favours bone differentiation of C3H10T1/2 cells cultured on these two rigid substrates. The dramatic increase in the expression of the differentiation fat marker *Pparg* in plastic substrate (high stiffness) is counter-intuitive with the range of soft stiffness known to promote fat differentiation (Discher et al., 2009). We interpret the ability of C3H10T1/2 cells to differentiate towards the fat lineage under a stiff substrate with the fact that C3H10T1/2 cells makes multilayers upon confluence. One obvious hypothesis is that cells expressing *Pparg* at 14 days of culture could be those not in contact with the plastic substrate, but with a soft environment created by cells the superficial multilayers.

IV.4.2 TGF β 2 is a negative regulator of *Tnmd* expression in C3H10T1/2 cells in 2D and 3D culture systems

Our work identifies a striking inverse correlation between *Tnmd* expression and TGF β activity (assessed with *Smad7* expression) in C3H10T1/2 cells cultured on both plastic and silicone substrates overtime. Consistently, TGF β 2 drastically decreases *Tnmd* expression, while promoting that of *Scx* in C3H10T1/2 cells cultured in 2D and 3D cell culture systems. The opposite behaviour of *Scx* and *Tnmd* expression upon TGF β 2 application in cell cultures could reflect different steps of tenogenesis. *Scx* would reflect a more progenitor step than *Tnmd*. During development, *Scx* is expressed before *Tnmd* and *Scx* is required and sufficient for *Tnmd* expression in developing tendons (Murchison et al., 2007; Shukunami et al., 2006). Moreover, *Scx* has recently been shown to directly regulate *Tnmd* transcription in C3H10T1/2 cells and in primary tendon cells (Shukunami et al., 2018). The absence of *Tnmd* activation following *Scx* increase upon TGF β 2 application indicates that TGF β 2 prevents achieved tendon differentiation in C3H10T1/2 cells in 2D and 3D culture conditions. It has to be noted that TGF β 2 activates the expression of both *Scx* and *Tnmd* genes in chick and mouse limb explants (Havis et al., 2014, 2016), in high density cultures of chick limb cells (Lorda-Diez et al., 2009) or in 3D culture systems of human tendon cells (Bayer et al., 2014). We cannot exclude that the negative regulation of TGF β 2 on *Tnmd* expression is cell-type specific.

However, another possibility would be that confluence plays a dominant role in this system by preventing cells to achieve tenogenic differentiation even in presence of a tenogenic agent like TGF β 2. We showed that cell confluence on plastic substrate prevented an increase in *Tnmd* expression in C3H10T1/2 cells, so this effect could potentially override that of TGF β 2.

IV.5 Conclusion

This study shows that culture conditions such as confluence and substrate affect the differentiation potential of a murine cell line of mesenchymal stem cells, C3H10T1/2 cells. We identify a substrate of 5 MPa stiffness that favours tendon differentiation in addition to bone differentiation upon confluence. We also identify TGF β 2 as a negative regulator of *Tnmd*

expression in C3H10T1/2 cells in 2D and 3D culture systems. The identification of the optimum conditions that induce tendon cell differentiation in a dish is of particular interest in order to optimize tendon cell culture protocols that can be used as grafting for tendon repair.

V. Role of mechanical constraints, EGR1 and YAP in a 3-dimensional culture system of C3H10T1/2 cells mimicking tendon formation

V.1 Context

Numerous studies use 2D-cell-culture systems to understand tendon cell differentiation induced either by biochemical or mechanical cues (reviewed in Wang et al., 2018a; Zhang et al., 2018). However, 3D-culture systems, in which cells are embedded in hydrogels, offer an environment closer to those experienced by tendon cells *in vivo* than in 2D-cell-culture systems. Hydrogels allow for a homogeneous transmission of the strains to the cells and thus facilitate the control of experimental conditions.

In this study, we took advantage of fibrin- and collagen-based 3D-cell-culture systems mimicking native tendons to better understand the relationship between mechanical signals and tendon cell differentiation. Since tendon is a tissue with a role in the transmission of mechanical signals from muscle to bone, we were interested in putative intracellular molecular relays of the mechanical cues, such as YAP and EGR1. We hypothesize that YAP and EGR1 act as intracellular relays of mechanical signals in order to direct tendon cell differentiation.

V.2 Results

V.2.1 *Egr1* overexpression prevents the decrease of tendon gene expression in fibrin-based 3D-constructs after tension release

Fibrin-based 3D cell cultures recapitulate tendon formation based on tenogenic marker expression and tendon-like collagen fibrillogenesis (Bayer et al., 2010; Breidenbach et al., 2015; Kapacee et al., 2008, 2010; Yeung et al., 2015). This *in vitro* engineered tendon system involves tension (Bayer et al., 2010; Kapacee et al., 2010). Forced expression of *Egr1* in fibrin-based 3D C3H10T1/2 cell cultures increases *Scx*, *Col1a1* and *Col1a2* expression levels compared to control fibrin-based 3D C3H10T1/2 cell cultures (Guerquin et al., 2013). We now show that the expression of the tendon differentiation marker *Tnmd* was also increased in the presence of *Egr1* in 3D constructs (Figure V.1A). The *Tgfb2* mRNA levels were also increased in *Egr1*-producing 3D constructs compared to 3D constructs (Figure V.1A). The tension release of the 3D constructs induces the appearance of immature collagen fibrils with no preferred orientation in engineered chick tendons (Kapacee et al., 2008) and loss of *Tnmd* expression in engineered human tendons (Bayer et al., 2014). The tension was released by

cutting one edge of the engineered mouse tendons made of C3H10T1/2 cells (Figure V.1B). Tension release led to a decrease in the expression of *Egr1* and tendon genes including *Scx*, *Tnmd*, *Col1a1* and *Col1a2* (Figure V.1B). The expression of *Tgfb2* was also decreased in tension-released engineered tendons (Figure V.1B). Tension release in *Egr1*-producing 3D-constructs did not trigger any significant changes in tendon gene expression compared to *Egr1*-producing 3D constructs under tension (Figure V.1C). This shows that constitutive *Egr1* overexpression is able to activate tendon gene expression independently of tension in engineered tendons. We conclude that *Egr1* expression is sensitive to tension in fibrin-based engineered mouse tendons and *Egr1*-forced expression prevents the downregulation of tendon gene expression in the absence of mechanical input. These results are included in a paper (Gaut et al., 2016) that is provided in the annexe part of this manuscript.

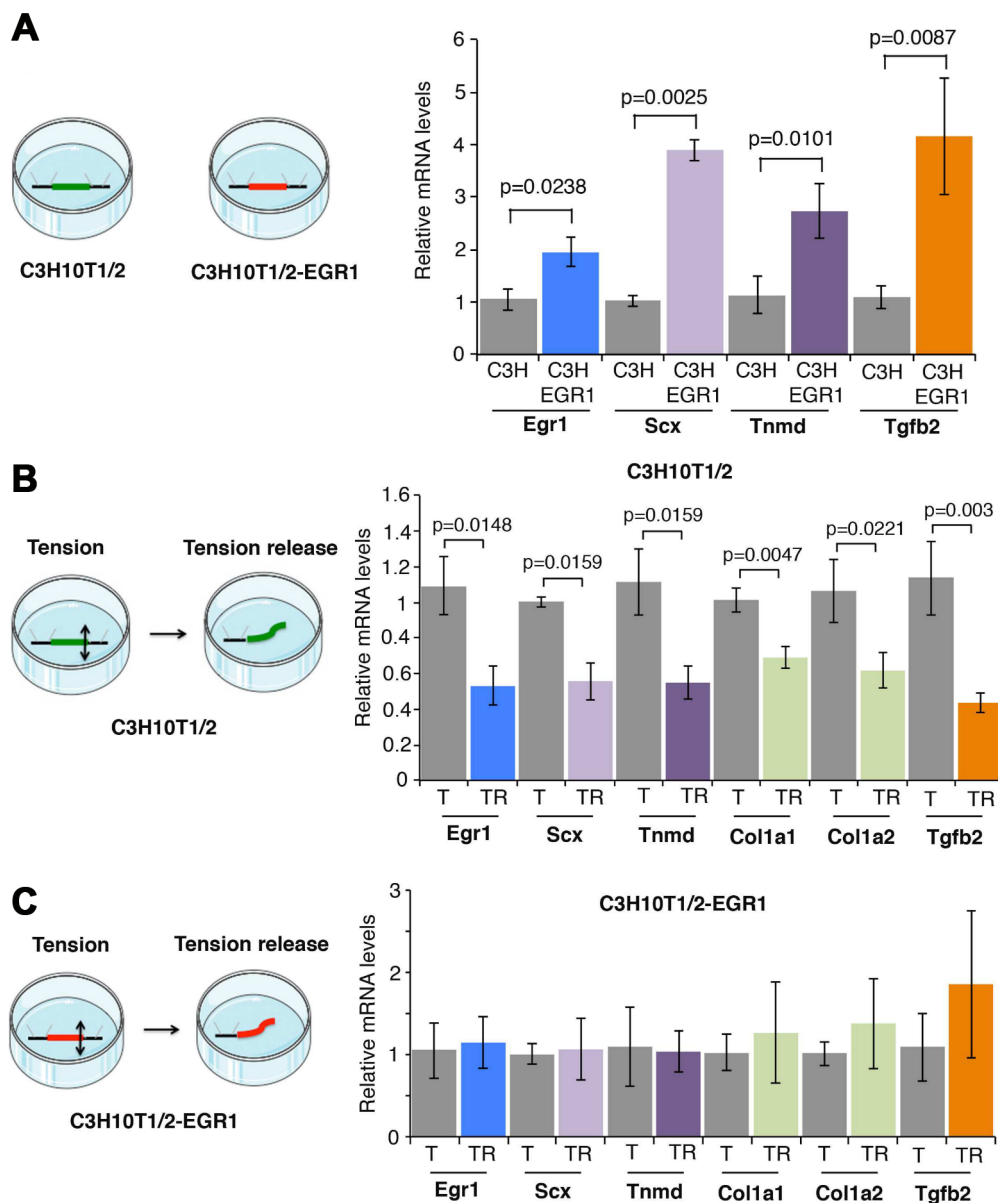


Fig. V.1 Caption next page

Fig. V.1 ***Egr1* overexpression prevents the downregulation of tendon-associated gene expression in tension released engineered tendons.** (A) Two weeks-old fibrin gel constructs made of mouse C3H10T1/2 cells or C3H10T1/2-*Egr1* cells were analyzed for tendon gene expression by RT-q-PCR analyses. The mRNA levels of C3H10T1/2 constructs were normalized to 1. Errors bars represent standard errors of the mean of 5 C3HT101/2 constructs and 7 C3H10T1/2-*Egr1* constructs. The p values were calculated using the Mann-Whitney test. The mRNA levels of *Egr1*, *Scx*, *Tnmd* and *Tgfb2* genes were increased in C3H10T1/2-*Egr1* constructs compared to those of C3H10T1/2 constructs. (B) Tension was released in C3H10T1/2 constructs by sectioning one end of the construct. Transcript levels were analyzed by RT-q-PCR analyses in tension-released C3H10T1/2 constructs and compared to C3H10T1/2 constructs. The mRNA levels of C3H10T1/2 constructs were normalized to 1. Errors bars represent standard errors of the mean of 7 C3H10T1/2 constructs and 7 tension-released C3H10T1/2 constructs. The p-values were calculated using the Mann-Whitney test. We observed a decrease in the transcript levels of *Egr1*, *Scx*, *Tnmd*, *Col1a1*, *Col1a2* and *Tgfb2* genes in tension-released C3H10T1/2 constructs (TR) compared to tensioned C3H10T1/2 constructs (T). (C) The mRNA levels of tendon genes were analyzed in tension-released C3H10T1/2-*Egr1* constructs and compared with tensioned C3H10T1/2-*Egr1* constructs by RT-q-PCR analyses. The mRNA levels of C3H10T1/2-*Egr1* constructs were normalized to 1. Errors bars represent standard errors of the mean of 7 C3HT101/2-*Egr1* constructs and 5 tension-released C3H10T1/2-*Egr1* constructs. The p values were calculated using the Mann-Whitney test. There was no significant change in tendon gene expression in tension-released C3H10T1/2-*Egr1* constructs (TR) compared to tensioned C3H10T1/2-*Egr1* constructs (T). T, Tension, TR, Tension release.

V.2.2 Collagen 3D-constructs made of C3H10T1/2 cells harbor a tendon-like structure

The collagen 3D-constructs made of C3H10T1/2 cells consists in cells homogeneously embedded in a type I collagen-gel tube anchored at both extremities. Compared to their fibrin counterpart, collagen 3D-constructs are made with the FlexCell FX-T5000 bioreactor, which allows for both high reproducibility and mechanical stretch of these constructs.

We first studied the evolution of collagen 3D-constructs between the initial time of the collagen-gel polymerization, termed T0, and up to 14 days of culture (Figure V.2A). We observed a decrease overtime of the width of the collagen 3D-constructs (Figure V.2B), as it has been reported in previous studies (Garvin et al., 2003).

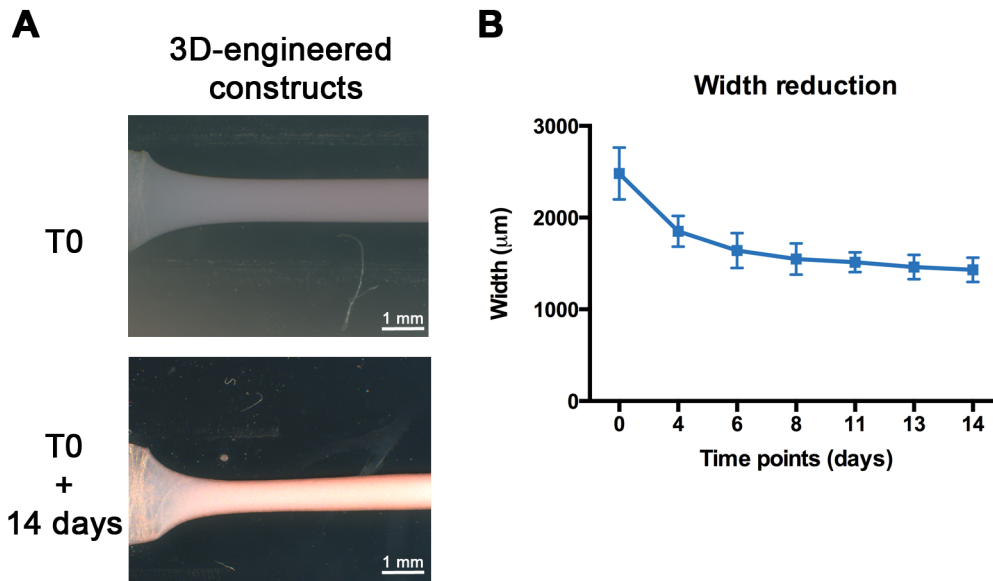


Fig. V.2 **Width of collagen 3D-constructs reduces overtime.** (A) Pictures of collagen 3D-constructs at one of their anchor points, at the initial time of culture T0 (upper panel) or at 14 days of culture (lower panel). (B) Reduction of the Collagen 3D-constructs width over 14 days of culture. Mean and standard deviation are indicated by dots and were calculated from 6 independent samples.

To compare with the collagen 3D-constructs, we analyzed the evolution of gene expression in fibrin 3D-constructs between 3 and 21 days of culture (Figure V.3A). While *Scx* did not present obvious variations between 3 and 21 days of culture, *Col1a1* expression was upregulated at 2-fold until 21 days (Figure V.3A). *Tnmd* expression was strongly downregulated to 0.125-fold decrease. In addition, we observed an important increase of *Col2a1* expression overtime, a cartilage marker, in the fibrin 3D-constructs (Figure V.3A). The increase in *Col2a1* expression in fibrin 3D-constructs shows that cells in this type of construct express cartilage markers over tendon markers, which is not the case in collagen 3D-constructs (Figure V.3B, C). We analyzed the evolution of gene expression in collagen 3D-constructs between T0 and 14 days of culture (Figure V.3B-D). Compared to T0, both *Scx* and *Col1a1* expression showed an increase overtime, reaching 8-fold and 2-fold peaks, respectively, at 14 days (Figure V.3B). *Tnmd* expression was overall decreased along the time of culture, reaching a lowest level at 5 days of culture (0.25-fold) and then slightly increased up to 0.5-fold at 14 days (Figure V.3B). Concerning the cartilage genes, we observed a decrease of *Sox9* and *Col2a1* expression, decrease especially marked for the differentiation cartilage gene, *Col2a1* (Figure V.3C). First decreased between T0 and 5 days, *Acan* expression was then upregulated up to a 4-fold increase (Figure V.3C). Finally, we also showed that the mechanosensitive genes all varied in 3D cell culture, with a decrease in the first 24H of culture for *Egr1* and *Cyr61*, but all showing a trend to increase overtime until 14 days (Figure V.3D). Together, these results place the collagen-based model over the fibrin-based model as the collagen-based 3D-constructs favor the expression of tendon gene over that of cartilage gene.

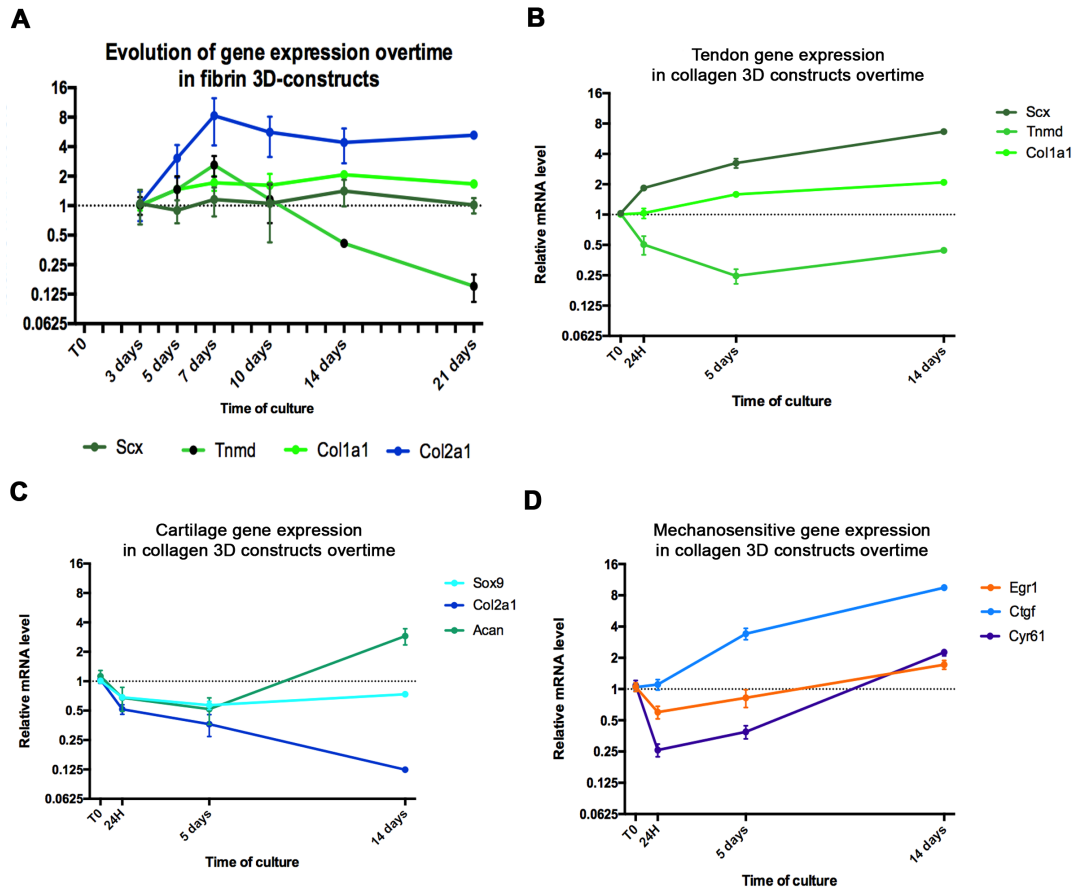


Fig. V.3 **Evolution of gene expression overtime in fibrin and collagen 3D-constructs.** (A) Evolution of gene expression overtime in fibrin 3D-constructs. Experiment performed in the laboratory by Isabelle Cacciapuoti. (B-D) Analysis in collagen 3D-constructs of tendon (B), cartilage (C) and mechanosensitive (D) gene expression by RT-qPCR over 14 days of culture. Dots and bars represent mean and standard deviation, respectively, calculated from 2-4 independent samples (A) and from 6 independent samples (B-D). For each gene, results from each timepoint were normalized to gene expression at 3 days (A) and T0 (B-D).

V.2.3 Modifications of mechanical parameters in the collagen 3D-constructs affect cell organization

In order to assess the effects of the mechanical signals on tendon cell differentiation in the collagen 3D-constructs, we induced changes in the mechanical state of the constructs between T0 and 24H of culture (Figure V.4). Tension release was induced by cutting one anchor point of the collagen 3D-constructs at T0 (Figure V.4). Consequences were analyzed during 24H in de-tensioned condition at 24H of culture. To establish the stretched condition, collagen 3D-constructs were submitted at T0 to a loading protocol of 1% strain at 1Hz and during 1h and were then allowed to rest for the following 23h before being harvested at 24H of culture (Figure V.4). Both of these conditions were then compared to control collagen 3D-constructs that were neither de-tensioned nor mechanically stimulate and harvested at 24H of culture.

We first analyzed cell organization of collagen 3D-constructs subjected to different me-

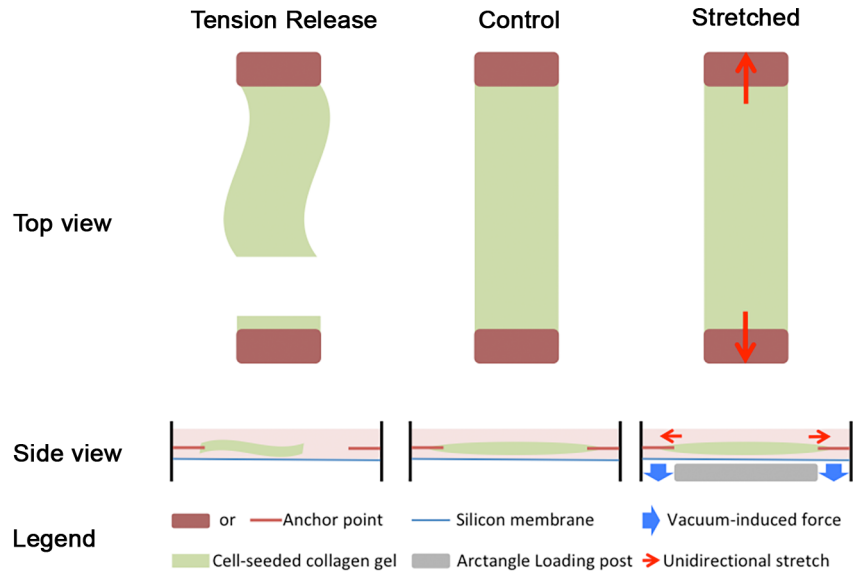


Fig. V.4 **Schematic representation of the different mechanical states applied to collagen 3D-constructs**

chanical states on longitudinal sections (Figure V.5A). Phalloidin and DAPI staining, highlighting actin stress fibers and nuclei, respectively, allowed us to observe how cells were organized inside the collagen 3D-constructs in each condition (Figure V.5B-D). At first sight, the signals obtained for Phalloidin staining are different in de-tensioned constructs when compared to control and stretched conditions.

Fig. V.5 (Next page) **Cell organization in collagen 3D-constructs.**(A) Schematic representation of a collagen 3D-constructs. (B-D) Phalloidin (in green, for actin stress fibers) and DAPI (in blue, for cell nucleus) staining of longitudinal section of control (B), tension release (C) and stretched (D) collagen 3D-constructs. All the sections (B-D) are oriented as presented in (A).

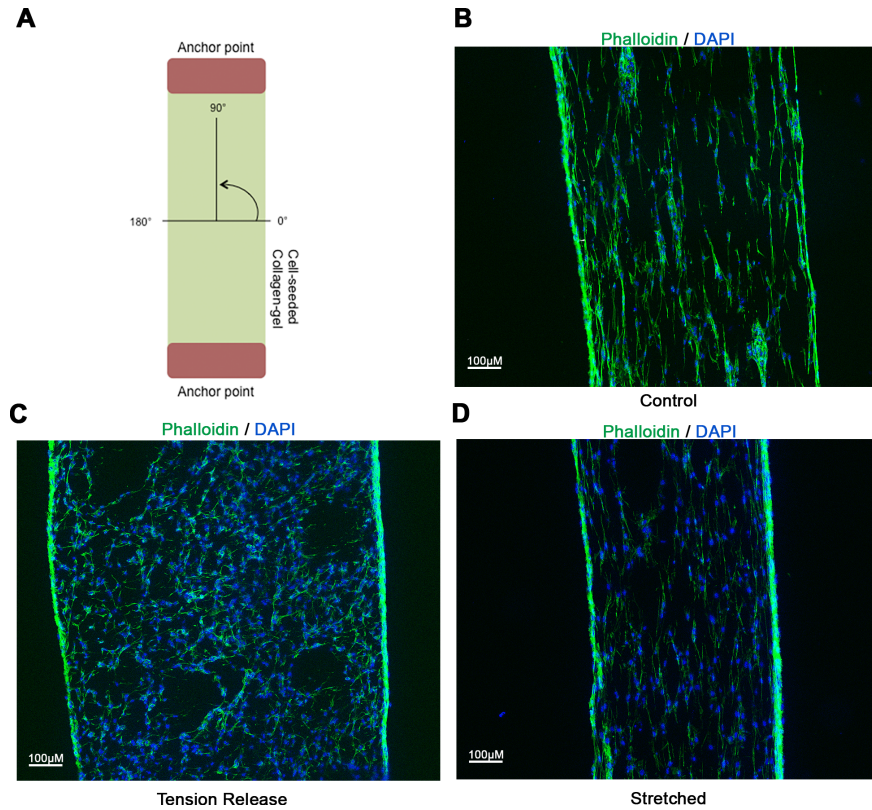


Fig. V.5 *Caption previous page*

We next performed computer-based analysis of these stainings. We showed that the distribution of the ellipse-shaped nucleus orientations, visualized with DAPI, indicated a preferential orientation at 90° along the axis defined by the two anchor points (Figure V.5A), for both control and stretched conditions (Figure V.6A). This indicated that nuclei were aligned along the axis of the collagen 3D-constructs. In contrast, the nuclei in the tension release condition did not display any preferential organization, but rather showed a random organization (Figure V.6A). Regarding the Phalloidin staining, we were able to draw the same conclusions than those for nucleus orientations. We found a similar alignment of cell shapes in control and stretched conditions, while cells in tension release 3D-constructs were randomly organized (Figure V.6B). Interestingly, in control and stretched conditions, cells and nuclei were aligned along the axis of the *in vitro* tendon, as tendon cells *in vivo* (aligned along the axis of native tendons), which strengthens the use of this model to study tendon cell differentiation.

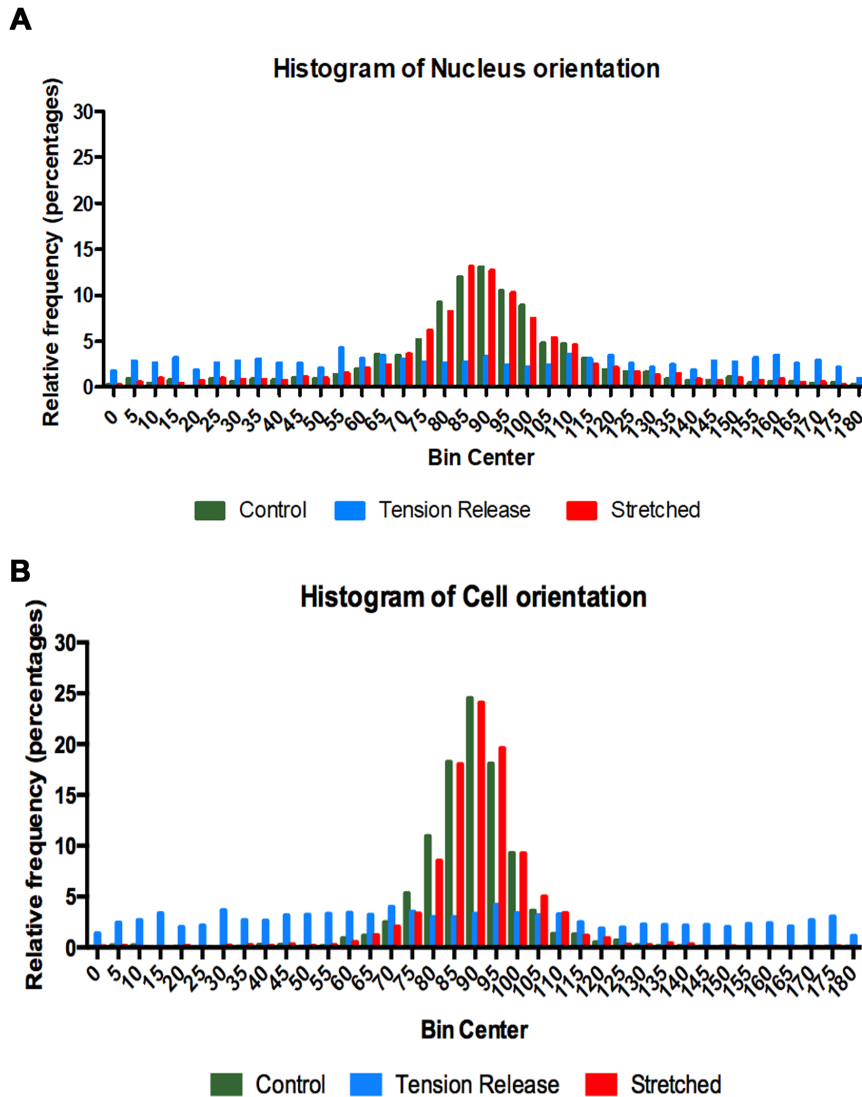


Fig. V.6 *Nucleus and cell orientations in collagen 3D-constructs in different mechanical states.* Histograms showing the distribution of nucleus (A) and cell (B) orientation angles in longitudinal sections of collagen 3D-constructs from Control (in green), Tension Release (in blue) and Stretched (in red) conditions. For each condition, population are composed by data obtained from 5 samples for Control and Tension Release condition and 4 samples for the Stretched condition.

We also assessed the proliferation status of the cells in collagen 3D-constructs upon different mechanical conditions by Ki67 staining (Figure V.7A-C). Ki67 is a proliferation marker that labels all cell cycle phases except the G0 phase (Scholzen and Gerdes, 2000). In the control condition, 14% of the cells exhibit Ki67⁺ nuclei in transverse sections of the collagen 3D-constructs (data not shown). The de-tensioned and stretched conditions exhibited 85.39% and 96.83%, respectively, when normalized to the control condition (Figure V.7D). We thus did not detect any differences in the number of Ki67⁺ nuclei between the three conditions, indicating that the lack of tension or the stretch condition was not affecting cell proliferation in this model (Figure V.7D). Obviously, Ki67⁺ nuclei proportions were assessed at 24H of culture and variations in these proportions at latter time points cannot be excluded.

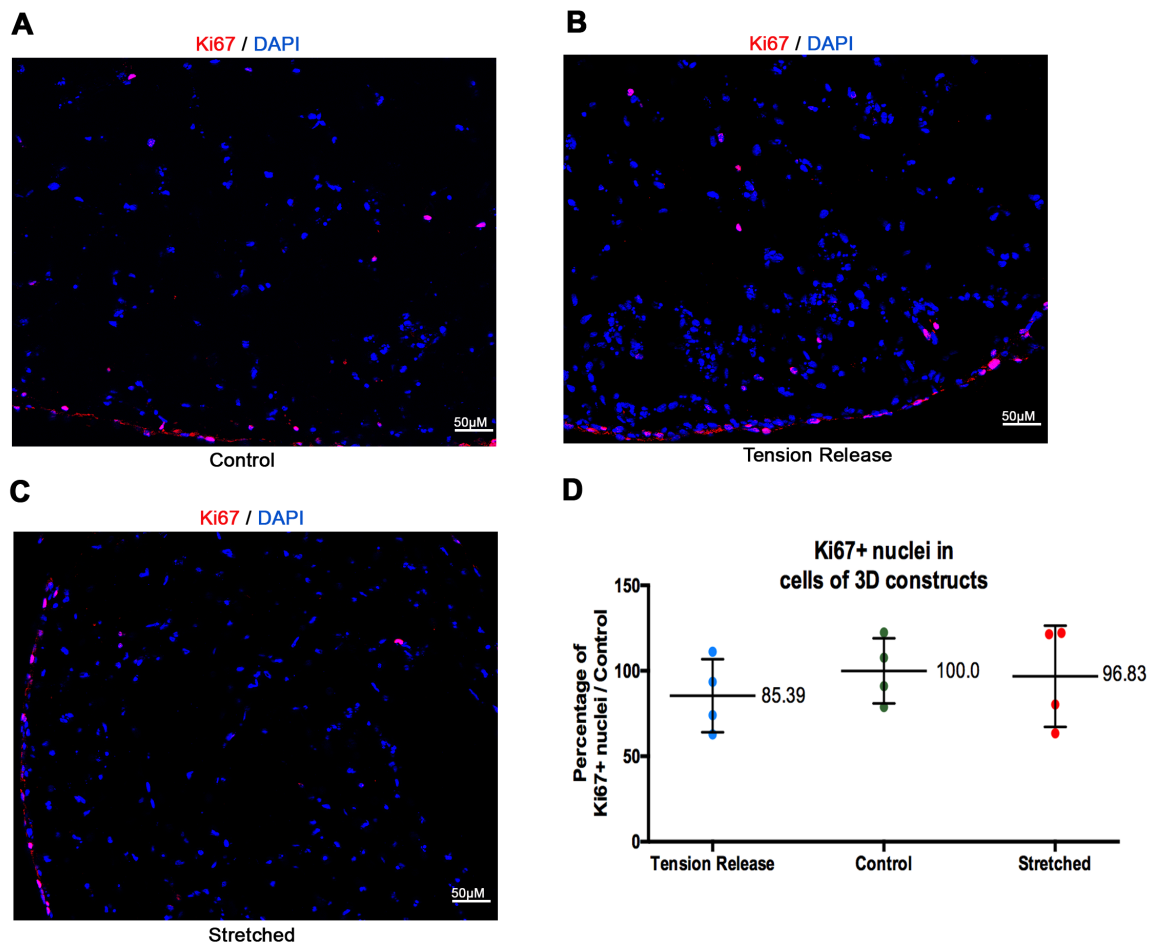


Fig. V.7 *Alterations of mechanical states do not affect cell proliferation in collagen 3D-constructs.* Ki67 (in red) and DAPI (in blue) staining in transverse sections of collagen 3D-constructs from Control (A), Tension Release (B) and Stretched (C) conditions. (D) Proportion of cells with Ki67⁺ nuclei in collagen 3D-constructs from Control (in green), Tension Release (in blue) or Stretched (in red) conditions. In the control condition, the 100% proportion indicated is normalized to the absolute proportion of Ki67⁺ nuclei in the control condition, which corresponds to 14% of the nuclei. Each dot represents an independent sample. Results were normalized to the control conditions. Samples were analyzed with the non-parametric Mann-Whitney test but showed no statistical differences.

V.2.4 Mechanical state affects the expression of tendon genes and other lineage genes in collagen 3D-constructs

We assessed tendon gene expression in collagen 3D-constructs in de-tensioned and stretched conditions compared to control condition. In this experiment, *Scx* expression was obtained with an initial mRNA quantity of 200ng, and 27.4Ct in control 3D-constructs (data not shown). De-tensioned collagen 3D-constructs displayed a decrease in *Tnmd* and *Col1a1* expression, but not *Scx* (Figure V.8A). This results differs from the de-tensioned fibrin 3D-constructs, since we observed a decrease of *Scx* expression compared to the control condition (Figure V.1B, Gaut et al., 2016).

Stretched collagen 3D-constructs displayed an increase in *Scx* expression (Figure V.8B). *Tnmd* expression was decreased in stretched condition, but the decrease was lower than that observed in the tension released condition (Figure V.8B). These results show that tendon gene expression is linked to mechanical signals in collagen 3D-constructs.

In order to highlight a link between SCX and mechanical signals imposed on collagen 3D-constructs, we performed SCX immunostaining on transverse sections of collagen 3D-constructs in each condition (Figure V.8C-E). As SCX is a transcription factor, we assumed that the proportion of SCX⁺ nuclei would reflect SCX activity in collagen 3D-constructs cells. Counting SCX⁺ showed that the proportion of SCX⁺ nuclei was slightly but significantly decreased in de-tensioned constructs and slightly increased in stretched condition compared to controls (Figure V.8F). Thus, we concluded that SCX protein expression was linked to the mechanical signals received by collagen 3D-constructs.

Fig. V.8 (Next page) **Alteration of mechanical states induces changes in tendon gene expression in collagen 3D-constructs.** (A, B) Analysis of tendon gene expression between Control and Tension Release collagen 3D-constructs (A) or between Control and Stretched collagen 3D-constructs (B). Each dot represents an independent sample. (C-E) SCX (in red) and DAPI (in blue) staining in transverse sections of collagen 3D-constructs from Control (C), Tension Release (D) and Stretched (E) conditions. (F) Proportion of cells with SCX⁺ nuclei in collagen 3D-constructs from Control (in green), Tension Release (in blue) or Stretched (in red) conditions. In the control condition, the 100% proportion indicated is normalized to the absolute proportion of SCX⁺ nuclei in the control condition, which corresponds to 70,2% of the nuclei. Each dot represents an independent sample. Results were normalized to the control condition. (A, B, F) Samples were analyzed with the non-parametric Mann-Whitney test and stars indicate significant *p*-values under 0.05.

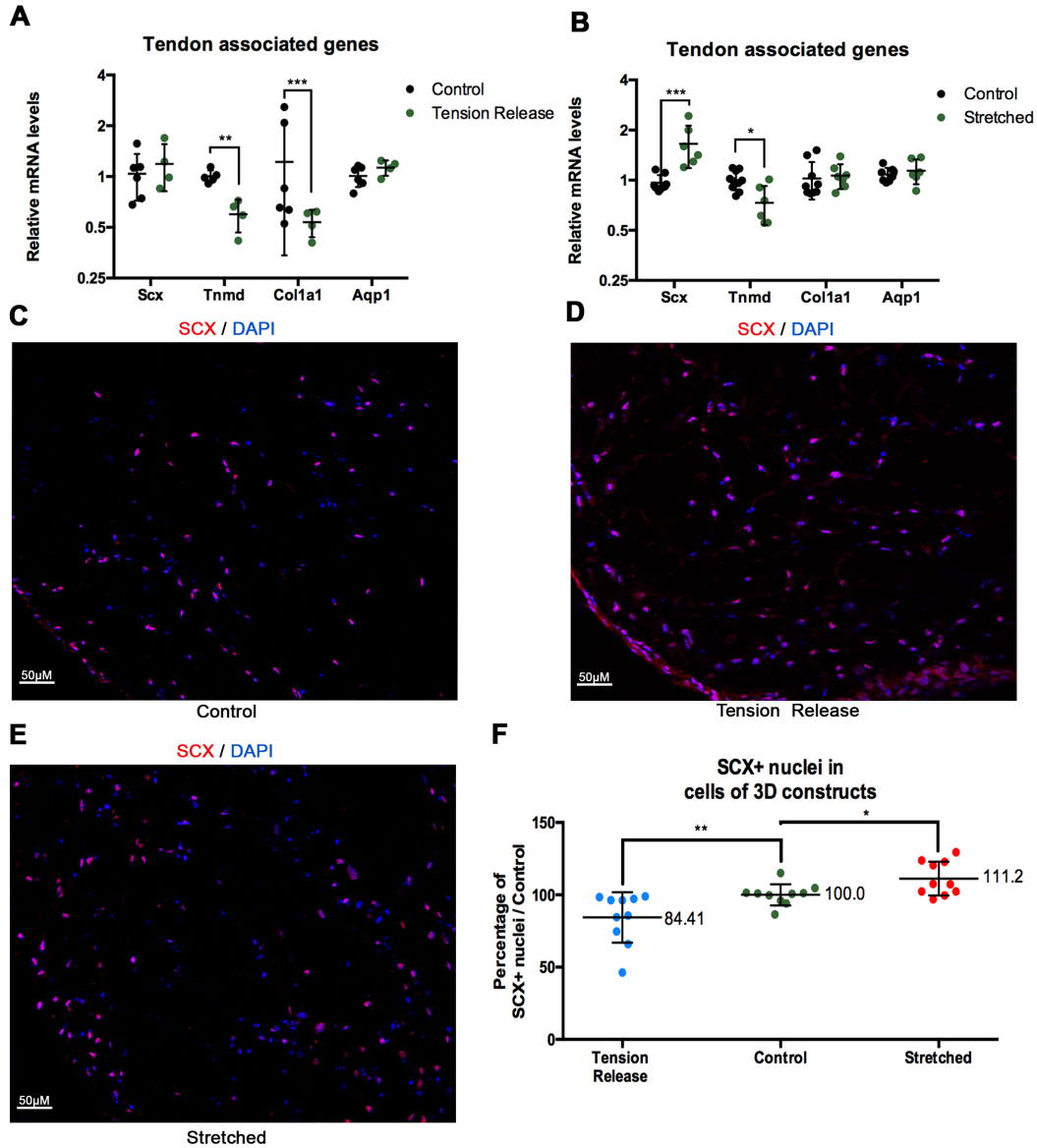


Fig. V.8 Caption previous page

V.2.5 YAP and EGR1 mechanosensitive pathways in collagen 3D-constructs

EGR1 and YAP are known to be responsive to mechanical signals and to be involved in mechanotransduction events in a lot of biological systems (Gaut et al., 2016; Panciera et al., 2017). In order to assess the behavior of EGR1 and YAP in collagen 3D-constructs under different mechanical states, we first looked at the expression of *Egr1* and two YAP transcriptional target genes, *Cyr61* and *Ctgf*. *Egr1* expression was significantly decreased by 0.5-fold in de-tensioned collagen 3D-constructs (Figure V.9A) but not increased in mechanically stimulated collagen 3D-constructs (Figure V.9B). Both YAP target genes *Cyr61* and *Ctgf* displayed a decrease of expression in de-tensioned condition (Figure V.9A) and an increase in stretched 3D-constructs (Figure V.9B).

We next performed EGR1 and YAP immunostainings to transverse sections of collagen

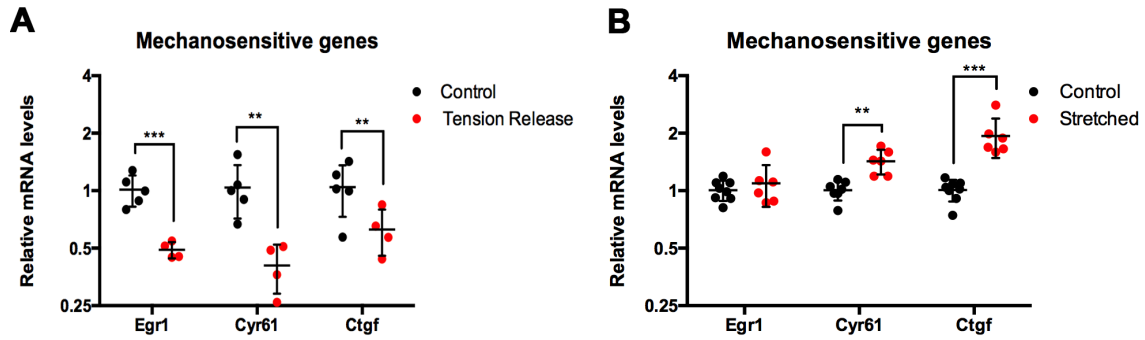


Fig. V.9 *Mechanosensitive gene expression in collagen 3D-constructs in de-tensioned and stretched conditions.* (A, B) Analysis of tendon gene expression between Control and Tension Release collagen 3D-constructs (A) or between Control and Stretched collagen 3D-constructs (B). Each dot represents an independent sample. Samples were analyzed with the non-parametric Mann-Whitney test and stars indicate significant p -values under 0.05.

3D-constructs transverse sections (Figures V.10, V.11). As EGR1 is a transcription factor and is thus active in cell nucleus, we assumed that the proportion of cells in collagen 3D-constructs with EGR1⁺ nuclei would mirror EGR1 activity. EGR1 immunostaining showed that 23.5% of cells (data not represented) harbored EGR1⁺ nuclei in control collagen 3D-constructs (Figure V.10A-C). The percentage of EGR1⁺ nuclei significantly decreased in de-tensioned constructs compared to the controls, but did not change in stretched 3D-constructs (Figure V.10D). This result is consistent with the changes in transcript levels obtained by RT-qPCR (Figure V.9A, B).

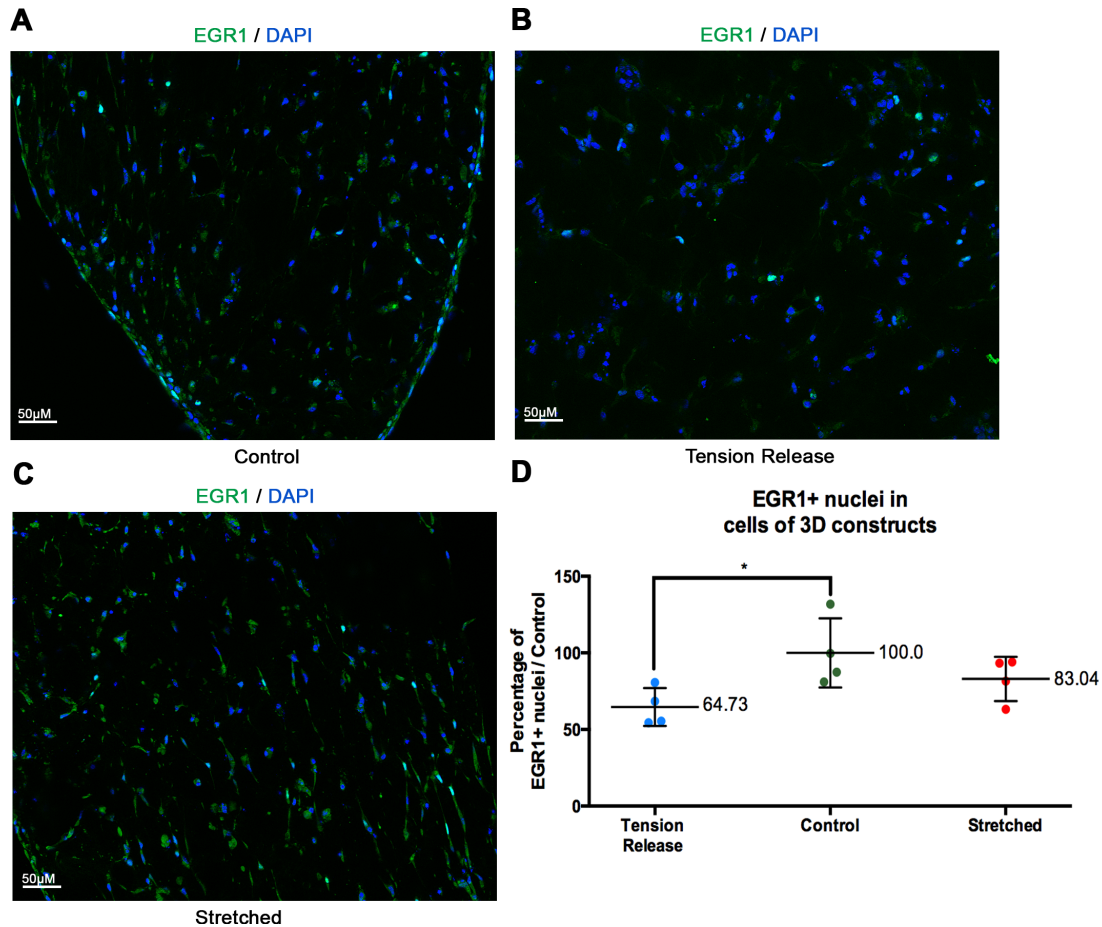


Fig. V.10 **Tension release in collagen 3D-constructs induces a decrease in the proportion of cells with EGR1⁺ nuclei.** EGR1 (in green) and DAPI (in blue) staining in transverse sections of Collagen 3D-constructs from Control (A), Tension Release (B) and Stretched (C) conditions. (D) Proportion of cells with EGR1⁺ nuclei in Collagen 3D-constructs from Control (in green), Tension Release (in blue) or Stretched (in red) conditions. In the control condition, the 100% proportion indicated is normalized to the absolute proportion of EGR1⁺ nuclei in the control condition, which corresponds to 23.5% of the nuclei. Each dot represents an independent sample. Results were normalized to the control condition. Samples were analyzed with the non-parametric Mann-Whitney test and stars indicate significant p-values under 0.05.

The co-factor YAP is known to be translocated in the nucleus where it regulates transcription with DNA binding proteins (reviewed in Panciera et al., 2017). We realized immunostaining for YAP in order to count the proportion of cells with YAP⁺ nucleus (Figure V.11A-C). Counting revealed a significant decrease in YAP⁺ nuclei in de-tensioned collagen 3D-constructs (Figure V.11E), which is fully consistent with the decrease of mRNA levels of *Cyr61* and *Ctgf* (YAP target genes) observed in the same de-tensioned condition (Figure V.9A). However, we did not observe any increase in the proportion of YAP⁺ nuclei proportion in stretched constructs (Figure V.11E), despite an increase of YAP target genes expression observed in the same condition (Figure V.9B). To assess a potential increase in YAP activity in cells, we analyzed the intensity of YAP in each nucleus. We analyzed and compared the

distribution of nuclei from each intensity scores to highlight differences between control and stretched collagen 3D-constructs (Figure V.11E). We observed a high proportion of nuclei with very low YAP intensity in control constructs, up to 30% of the total population. In the stretched constructs, we observed a shift from low YAP intensity scores to middle-intensity scores, which could reflect a high YAP activity (Figure V.11E).

Fig. V.11 (Next page) **YAP activity in collagen 3D-constructs is linked to mechanical signals.** YAP (in green) and DAPI (in blue) staining in transverse sections of collagen 3D-constructs from Control (A), Tension Release (B) and Stretched (C) conditions. (D) Proportion of cells with YAP⁺ nuclei in collagen 3D-constructs from Control (in green), Tension Release (in blue) or Stretched (in red) conditions. In the control condition, the 100% proportion indicated is normalized to the absolute proportion of YAP⁺ nuclei in the control condition, which corresponds to 70,6% of the nuclei. Each dot represents an independent sample. Results were normalized to the control condition. Samples were analyzed with the non-parametric Mann-Whitney test and stars indicate significant p-values under 0.05. (E) Distribution of the intensity of YAP signals in nuclei of Collagen 3D-constructs for control (in green) and stretched (in red) constructs.

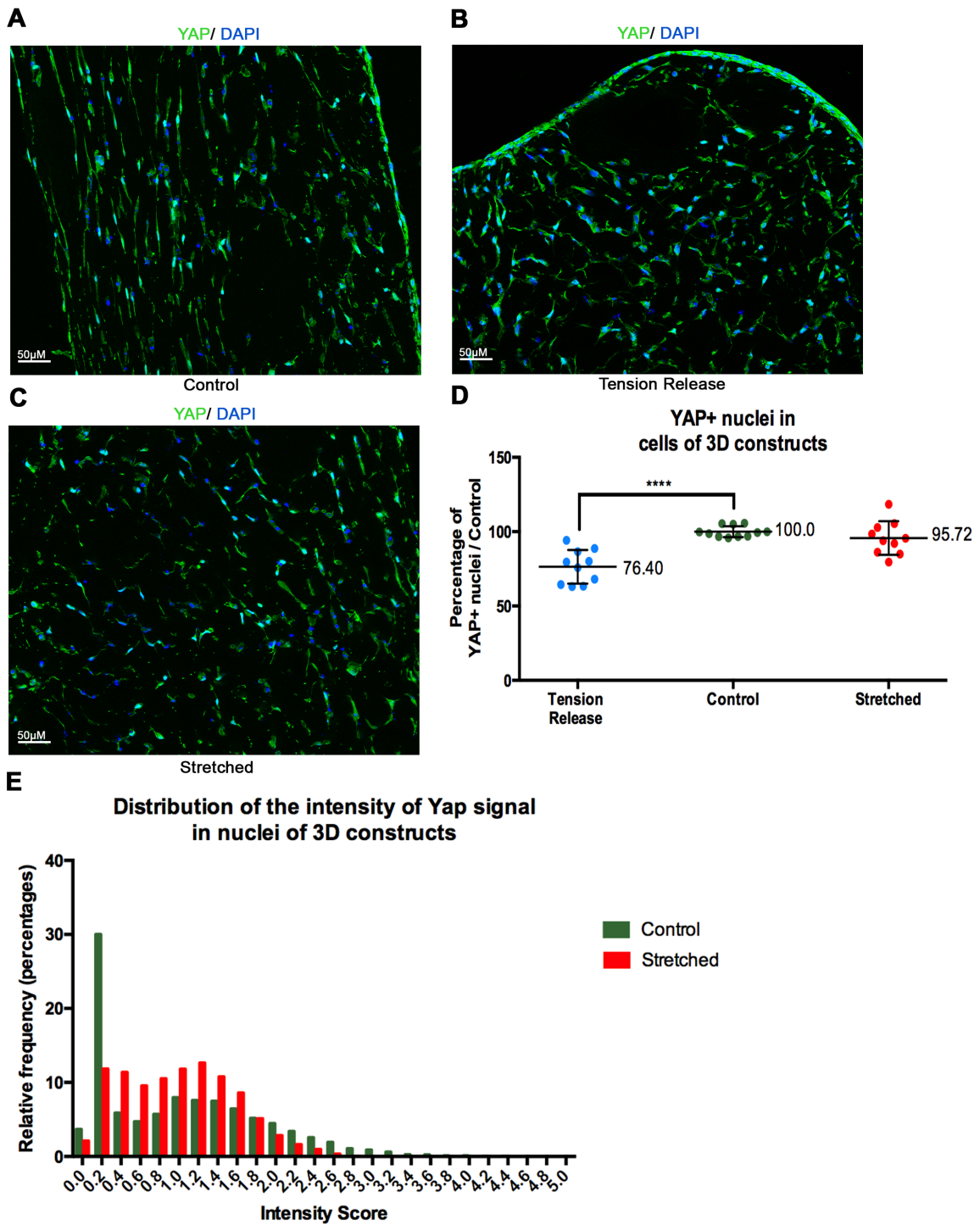


Fig. V.11 *Caption previous page*

V.2.6 Proportions of cells with YAP⁺ and/or Scx⁺ nuclei depend on collagen 3D-construct mechanical state

As we previously saw, *Scx* gene expression and the proportion of cells with SCX⁺ nuclei are dependent on the mechanical state of collagen 3D-constructs (Figure V.8). Similarly, YAP activity is correlated with levels of mechanical signals (Figure V.9 and V.11). In order to highlight a potential link between YAP activity and SCX, we performed double immunostaining for YAP and SCX along with DAPI staining, in regard with the mechanical state of the collagen 3D-constructs (Figure V.12).

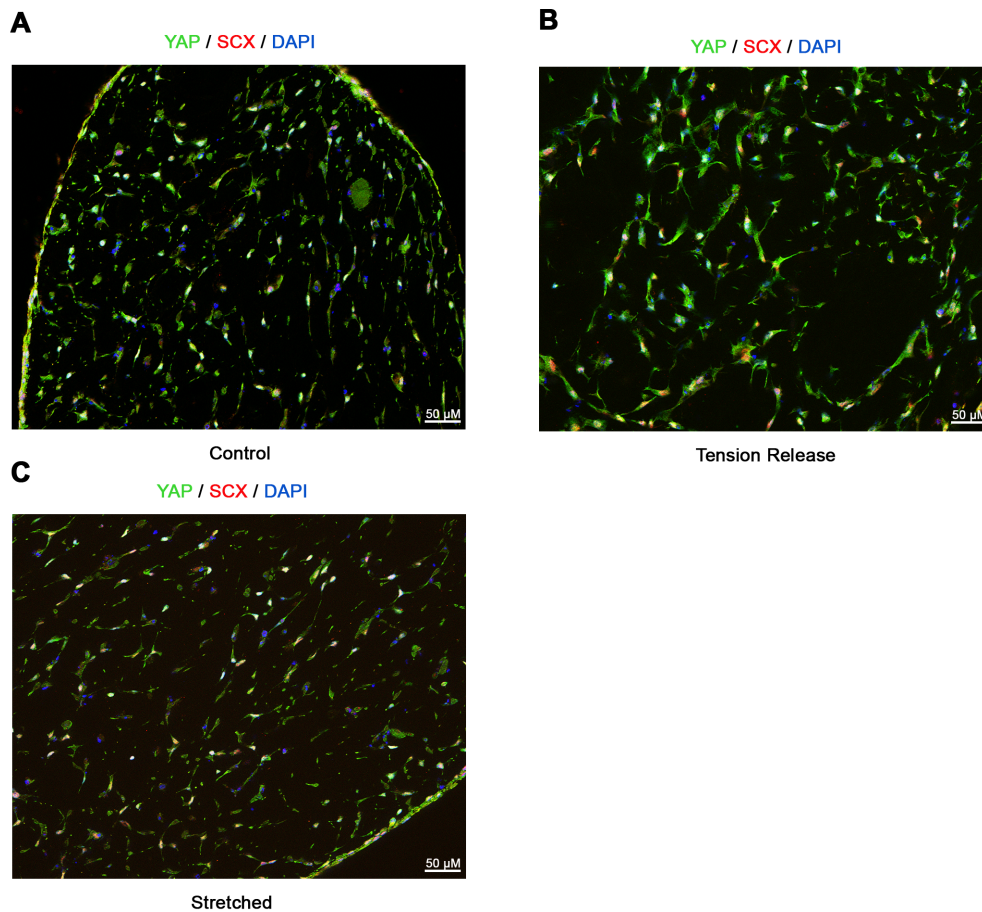


Fig. V.12 ***YAP/SCX double staining in collagen 3D-constructs.*** YAP (green) and SCX (red) immunostainings and DAPI (blue) staining in transverse sections of collagen 3D-constructs in control (A), tension release (B) and stretched (C) conditions.

Double YAP/SCX immunostaining allowed us to analyze changes in cell populations in collagen 3D-constructs depending on their mechanical state. We defined four cell populations, YAP⁺-only nuclei, SCX⁺-only nuclei, double YAP⁺/SCX⁺ nuclei or YAP⁻/SCX⁻ nuclei. When compared to the controls, the de-tensioned constructs exhibited a significant decrease in Scx⁺/YAP⁺ nuclei, along with an increase of SCX⁻/YAP⁻ nuclei (Figure V.13). As expected, we saw a significant decrease in the total number of YAP⁺ nuclei and of SCX⁺ nuclei (as also indicated in Figure V.11) in de-tensioned constructs compared to controls.

We also observed an increase of cells with SCX⁺/YAP⁻ nuclei that could be cells that have “turned off” YAP signaling but not SCX expression yet. Conversely, in stretched collagen 3D-constructs we observed a significant increase in the total number of SCX⁺/YAP⁺ nuclei and a concomitant decrease in SCX⁻/YAP⁺ (Figure V.13). This last result would indicate an increase in the proportion of SCX⁺ nuclei in a population already exhibiting YAP⁺ nuclei.

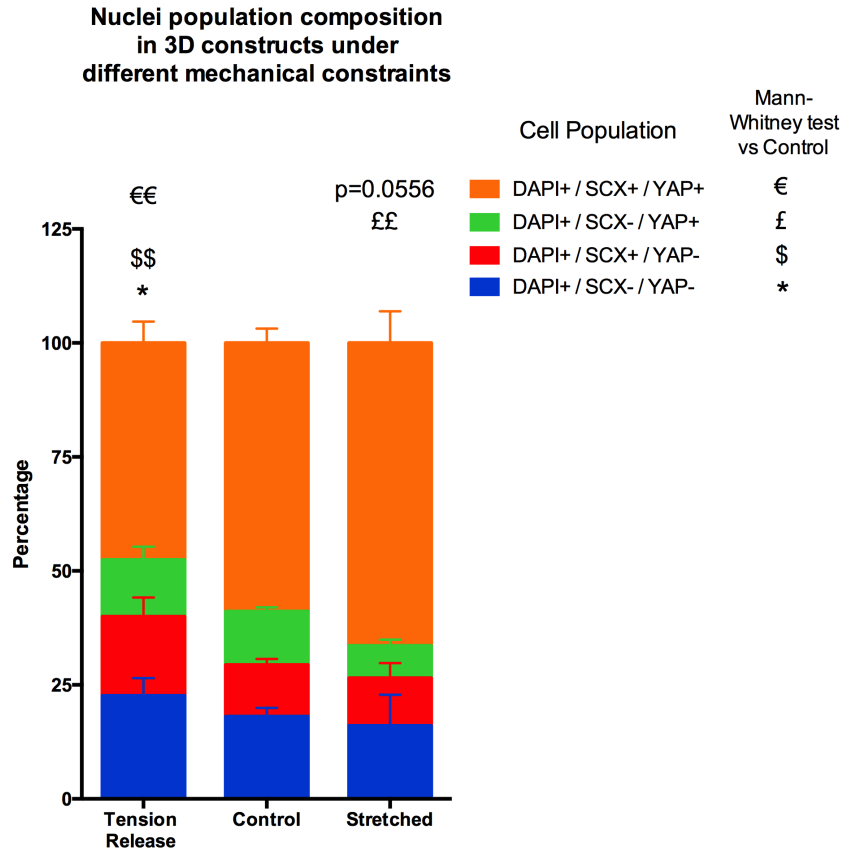


Fig. V.13 **Proportions of cells with YAP⁺ and/or SCX⁺ nuclei in collagen 3D-constructs.** Analysis of YAP and SCX double immunostaining allowed us to define different cell populations depending on YAP and SCX signals in collagen 3D-constructs for each mechanical condition. Samples were analyzed and compared to the control condition by the non-parametric Mann-Whitney test. Significant p-values under 0.05 were indicated for each group compared to its counterpart in the control condition by * (DAPI⁺/SCX⁻/YAP⁻, in blue), \$ (DAPI⁺/SCX⁺/YAP⁻, in red), £ (DAPI⁺/SCX⁻/YAP⁺, in green) and E (DAPI⁺/SCX⁺/YAP⁺, in orange).

V.2.7 Verteporfin-induced YAP knock-down impairs tendon gene expression in collagen 3D-constructs

In order to assess the putative role of YAP in tendon gene expression regulation, we induced a chemical knock-down of YAP in collagen 3D-constructs. This was performed using verteporfin (VTPF) a chemical inhibitor of the liaison of YAP and its associated transcription factors, inhibiting YAP transcriptional program (Chen et al., 2015). We first tested the effects of 24H treatment of different concentration of VTPF on 2D cultures of C3H10T1/2 cells in order to select the most efficient VTPF concentrations. Based on the expression of YAP target genes *Cyr61* and *Ctgf*, we observed that VTPF-treatment induced a loss of *Cyr61* expression at 2.5 μ M and *Ctgf* expression at 5.0 μ M (Figure V.14A). Both *Cyr61* and *Ctgf* genes displayed a marked decrease of expression at 10.0 μ M of VTPF, and more pronounced than that observed with the 5.0 μ M VTPF concentration (Figure V.14A). These results led us to the conclusion that the 10.0 μ M concentration of VTPF is the more efficient to induce a knock-down of YAP.

Regarding tendon gene expression, VTPF treatment did not change *Scx* expression independently of VTPF concentration. However, the decrease of *Tnmd* and *Col1a1* expression was proportional to the VTPF concentration (Figure V.14B). These data show a regulation of tendon gene expression by YAP activity in 2D cell cultures.

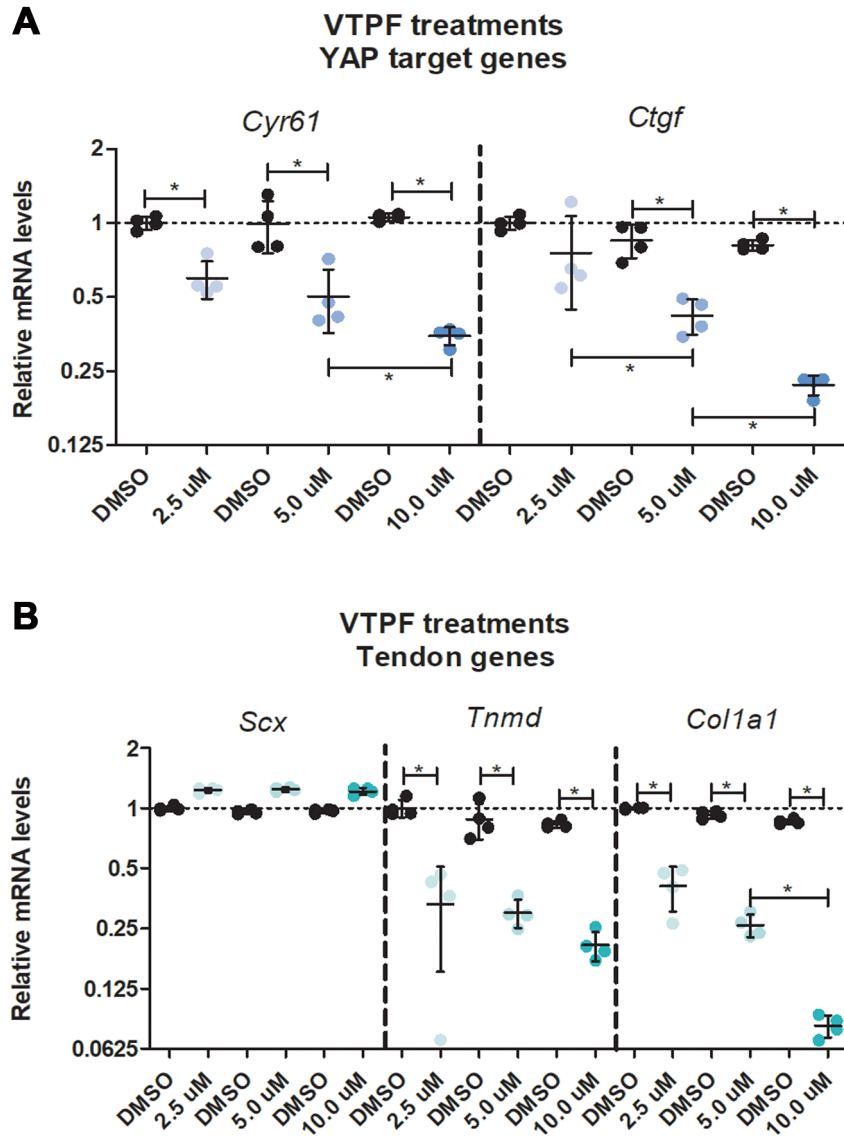


Fig. V.14 **VTPF-treatment induces changes in gene expression in 2D-cultured C3H10T1/2 cells.** Analysis of YAP target (A) and tendon (B) gene expression between Control and VTPF-treated cells. Each dot represents an independent sample. Samples were analyzed with the non-parametric Mann-Whitney test and stars indicate significant *p*-values under 0.05.

Based on the efficiency of the 10.0 μ M of VTPF concentration was to induce a loss of function of YAP in 2D cultures of C3H10T1/2 cells, we used the same concentration for collagen 3D-constructs. At T0, we treated collagen 3D-constructs with 10.0 μ M VTPF for 24H before harvesting them and comparing them with DMSO-treated collagen 3D-constructs. YAP target genes *Cyr61* and *Ctgf* showed a decrease of expression in VTPF-treated 3D-constructs (Figure V.15A), without any change in the proportion of cells with YAP⁺ nuclei (Figure V.15B). This is consistent with the fact that VTPF does not prevent nuclear translocation of YAP. Interestingly, we also observed that in a context of YAP loss-of-function, *Egr1* exhibited a decreased expression of mRNA levels (Figure V.15A).

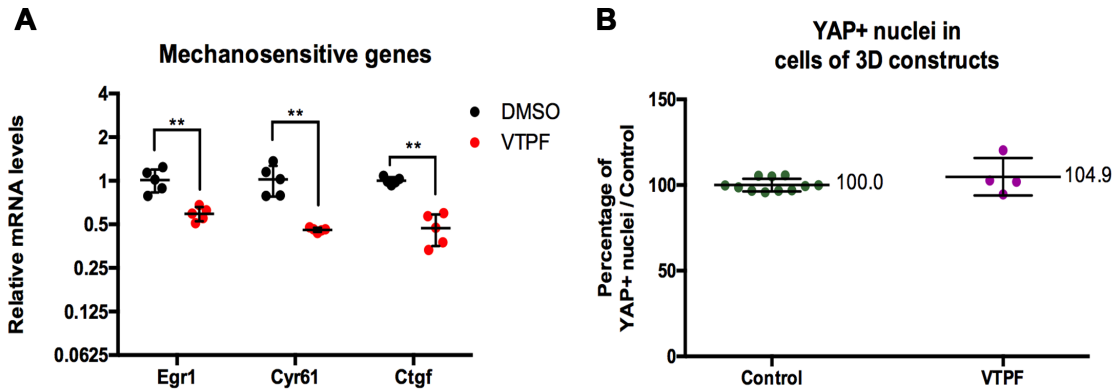


Fig. V.15 **24H VTPF-treatment in collagen 3D-constructs impairs the expression of mechanosensitive genes but not the number of YAP⁺ nuclei.** (A) Analysis of mechanosensitive gene expression between Control and VTPF-treated collagen 3D-constructs. (B) Proportion of cells with YAP⁺ nuclei in Collagen 3D-constructs from Control (in green) and VTPF (in purple) conditions. In the control condition, the 100% proportion indicated is normalized to the absolute proportion of YAP⁺ nuclei in the control condition, which corresponds to 70,6% of the nuclei. Each dot represents an independent sample. Samples were analyzed with the non-parametric Mann-Whitney test and stars indicate significant p-values under 0.05.

We performed Phalloidin and DAPI staining in VTPF-treated collagen 3D-constructs for 24H (Figure V.16A) and did not observe any change in cell organization compared with control 3D-constructs (Figure V.5B). Regarding tendon phenotype, we observed a decrease of gene expression for all tendon genes, namely *Scx*, *Tnmd*, *Col1a1* and *Aqp1* in VTPF-treated collagen 3D-constructs (Figure V.16B). In addition, we observed a pronounced decrease in the proportion of cells with SCX⁺ nuclei compared to control collagen 3D-constructs (Figure V.16C). Together, these results establish a link between YAP knock-down tendon gene expression.

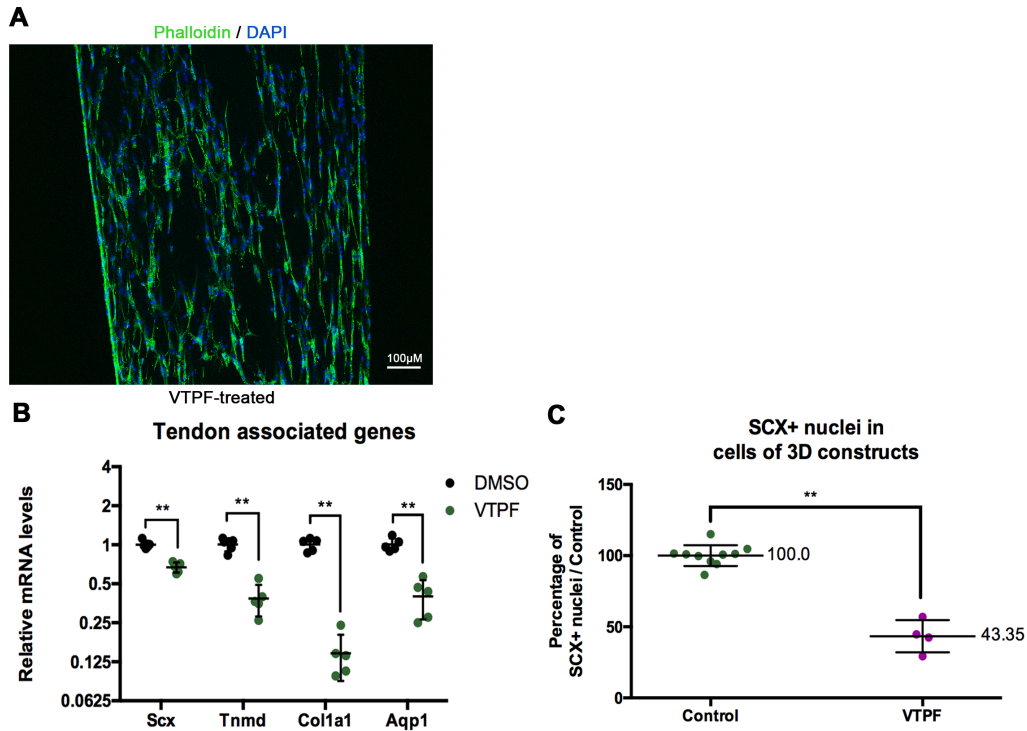


Fig. V.16 **VTPF-induced YAP knock-down impairs tendon phenotype in collagen 3D-constructs.** (A) Phalloidin (in green, for actin stress fibers) and DAPI (in blue, for cell nucleus) staining of longitudinal section of VTPF-treated collagen 3D-constructs. (B) Analysis of tendon gene expression between Control and VTPF-treated Collagen 3D-constructs. (C) Proportion of cells with SCX⁺ nuclei in collagen 3D-constructs from Control (in green) and VTPF (in purple) conditions. In the control condition, the 100% proportion indicated is normalized to the absolute proportion of SCX⁺ nuclei in the control condition, which corresponds to 70,2% of the nuclei. Each dot represents an independent sample. Samples were analyzed with the non-parametric Mann-Whitney test and stars indicate significant p-values under 0.05.

In order to better understand the relationship between YAP and SCX, we analyzed YAP/SCX double immunostaining in control and VTPF-treated collagen 3D-constructs (Figure V.17A, B). In VTPF-treated collagen 3D-constructs, we observed a marked decrease in the proportion of SCX⁺/YAP⁺ nuclei and a concomitant increase in the proportion of SCX⁻/YAP⁺ nuclei (Figure V.17C). This result indicates that the loss of SCX⁺ nuclei mainly occurs in a cell population already exhibiting YAP⁺ nuclei and in which YAP is not active. Thus it strengthens the hypothesis of a regulation of SCX by YAP.

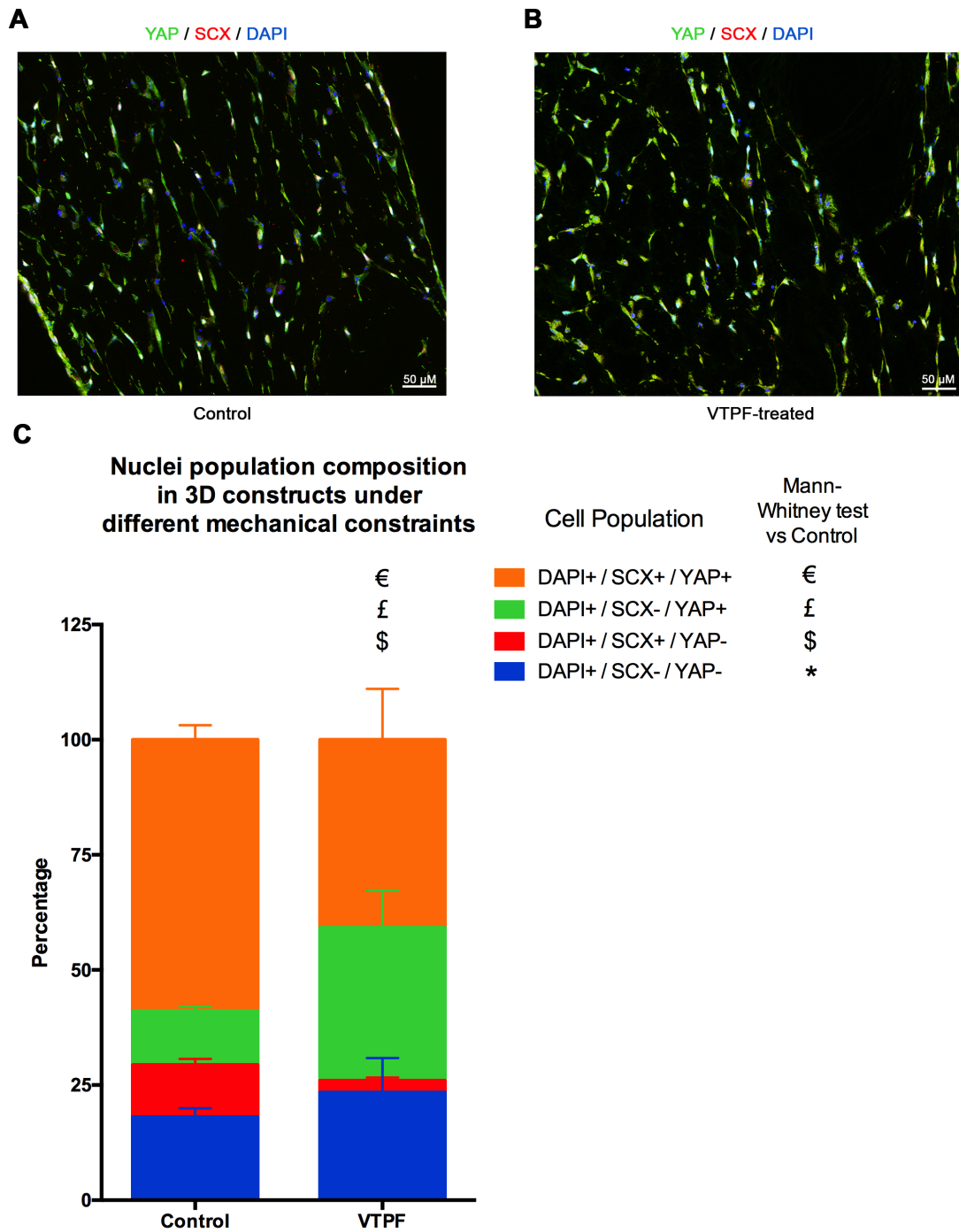


Fig. V.17 *YAP knock-down in collagen 3D construct induces a decrease in the proportion of SCX⁺ nuclei in cells already exhibiting YAP⁺ nuclei.* (A, B) YAP (in green), SCX (in red) and DAPI (in blue) staining in transverse sections of collagen 3D-constructs from Control (A) and VTPF (B) conditions. (C) Analysis of YAP and SCX double immunostaining allowed to defined different cell populations depending on YAP and SCX signals for each collagen 3D-construct condition. Samples were analyzed and compared to the control condition by the non-parametric Mann-Whitney test. Significant p-values under 0.05 were indicated for each group compared to its counterpart in the control condition by * (DAPI⁺/SCX⁻/YAP⁻, in blue), \$ (DAPI⁺/SCX⁺/YAP⁻, in red), £ (DAPI⁺/SCX⁻/YAP⁺, in green) and € (DAPI⁺/SCX⁺/YAP⁺, in orange).

V.2.8 Mechanical stimulation of Verteporfin-treated collagen 3D-constructs does not rescue the downregulation of tendon gene expression

YAP activity is regulated in collagen 3D-constructs by mechanical signals (Figure V.9, V.11) and YAP could be involved in the regulation of tendon gene expression and the proportion of SCX⁺ nuclei (Figures V.16, V.17). We also showed that mechanical signals controlled the expression of tendon genes at the mRNA level and the number of SCX⁺ cells (Figure V.8). In order to define if YAP acts as an intracellular relay of mechanical signals to regulate tendon gene expression, we decided to stretch collagen 3D constructs in a context of YAP loss-of-function induced by VTPF treatment. According to our hypothesis, mechanical stimulation of collagen 3D constructs would not be able to induce tendon gene expression since YAP is not active. Indeed, we observed that compared to control collagen 3D-constructs that were neither stretched nor treated with VTPF, the VTPF + Stretch collagen 3D-constructs exhibited a decrease in tendon gene expression (Figure V.18A). This indicated that YAP could be an intracellular relay downstream of mechanical signals that enables tendon gene expression. It has to be noted that *Egr1* expression showed no difference between control or VTPF+Stretch collagen 3D-constructs (Figure V.18B), indicating that *Egr1* expression was rescued by mechanical signals in VTPF-treated 3D-constructs through an unknown intracellular pathway.

Together, these results confirm that YAP serves as an intracellular relay of mechanical signals in collagen 3D-constructs to enable tendon gene expression. Yet, other mechanotransduction pathways could be involved as suggested by the recovery of *Egr1* expression.

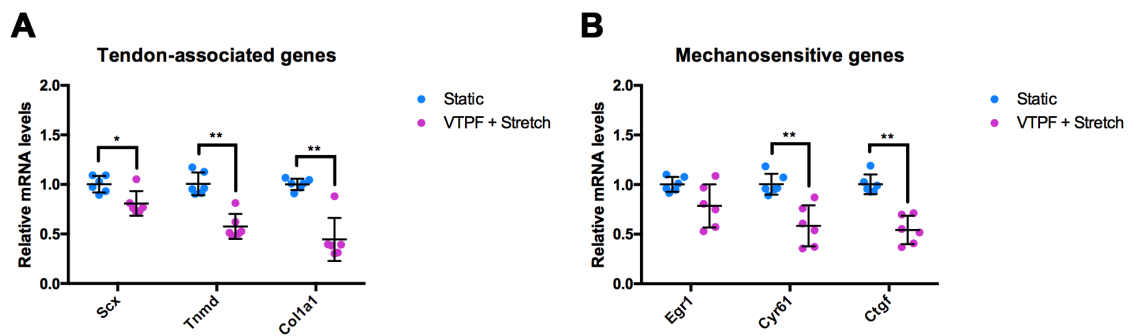


Fig. V.18 **Stretch does not rescue gene expression in collagen 3D-constructs with VTPF-induced YAP knock-down.** Analysis of tendon (A) and mechanosensitive (B) gene expression between control and stretched VTPF-treated collagen 3D-constructs. Each dot represents an independent sample. Samples were analyzed with the non-parametric Mann-Whitney test and stars indicate significant p-values under 0.05.

V.2.9 Chemical modulation of mechanotransduction pathways in collagen 3D-constructs made of C3H10T1/2 cells

In order to further assess the role of YAP in tendon gene expression regulation, we took advantage of the property of lysophosphatidic acid (LPA) to enhance YAP activity by in-

hibiting the Hippo pathway through the action of the G-protein-coupled receptors G12/13 (Yu et al., 2012). We treated collagen 3D constructs made of C3H10T1/2 cells with LPA between T0 and 24H and compared them to controls treated with DMSO. LPA treatment did not enhanced YAP activity in our collagen 3D-constructs, as no change was observed in *Cyr61* expression upon treatment (Figure V.19A), indicating a probable failure in LPA treatment. Concomitantly, no changes were detected in tendon gene expression upon LPA treatment of 3D constructs (Figure V.19B).

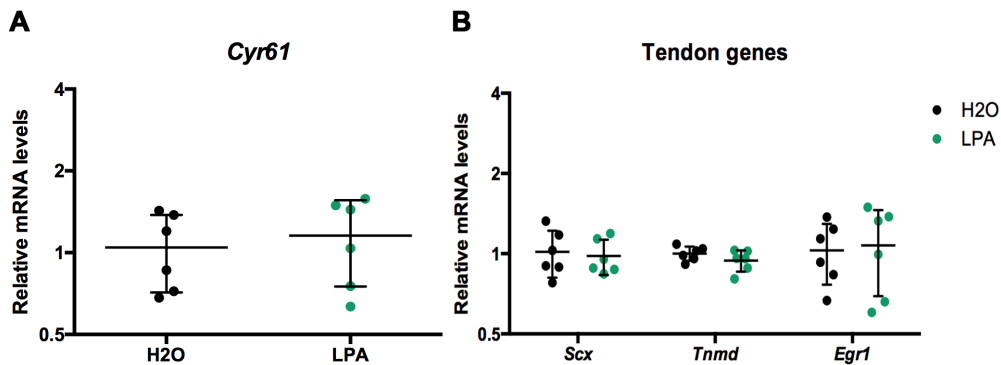


Fig. V.19 **LPA treatment of collagen 3D-constructs made of C3H10T1/2 cells.** Analysis of *Cyr61* (A) and tendon (B) gene expression between control and LPA-treated collagen 3D-constructs. Each dot represents an independent sample. Samples were analyzed with the non-parametric Mann-Whitney test and stars indicate significant *p*-values under 0.05.

In order to assess or rule out the action of another putative mechanotransduction pathway in the regulation of tendon gene expression, we tested the possibility that the SRF-MRTF-A complex could be involved in this process (Esnault et al., 2014; Posern and Treisman, 2006). We took advantage of the property of the small molecule CCG-1423 to inhibit SRF-MRTF-A-dependent transcription (Watanabe et al., 2015). We treated collagen 3D-constructs with CCG-1423 between T0 and 24H and compared them to control 3D-constructs treated with H₂O. CCG-1423 did not have any effect on 3D-constructs when compared to controls, as assessed by the similar mRNA level of *Acta2*, a SRF-MRTF-A target gene (Esnault et al., 2014; Figure V.20A). This result indicates a probable failure of the CCG-1423 treatment in collagen 3D-constructs. Concomitantly we did not observe any effect of CCG-1423 treatment on tendon gene expression (Figure V.20B).

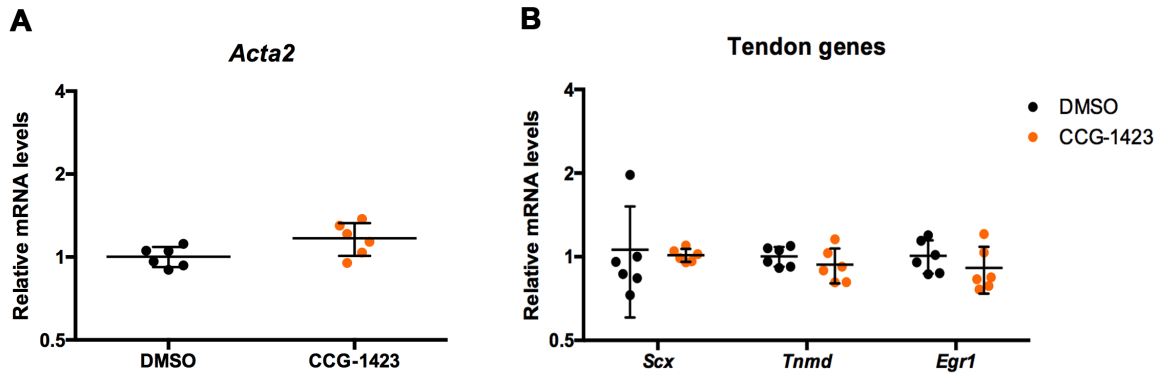


Fig. V.20 *CCG-1423 treatment of collagen 3D-constructs made of C3H10T1/2 cells.* Analysis of *Acta2* (A) and tendon (B) gene expression between control and CCG-1423-treated collagen 3D-constructs. Each dot represents an independent sample. Samples were analyzed with the non-parametric Mann-Whitney test and stars indicate significant *p*-values under 0.05.

V.3 Discussion

In this part, we analyzed the behavior of C3H10T1/2 cells in fibrin or collagen 3D-constructs mimicking native tendons and subjected to different mechanical conditions. We first used a fibrin-gel method that allows the formation of engineered tendons (Guerquin et al., 2013; Kapacee et al., 2010). We showed that EGR1 was a mechanotransduction transcription factor whose overexpression was able to bypass the lack of mechanical signals in de-tensioned 3D fibrin-gel constructs (Gaut et al., 2016). However, the fibrin-gel 3D-culture system did not allow the application of additional mechanical parameters. Consequently, we turned to a 3D-culture system made of collagen-gel that could be subjected to different mechanical conditions using the FlexCell FX-T5000 system. In collagen 3D-constructs, we observed that cells displayed different spatial organizations upon different mechanical constraints. Cells were aligned along the axis of control and stretched 3D-constructs, while they displayed a random organization in de-tensioned collagen 3D-constructs. Among these conditions, we did not observe any change in cell proliferation. We also linked mechanical states to tendon gene expression. We also correlated YAP activity in cells with the mechanical state of the 3D-construct. We showed that YAP loss-of-function by chemical inhibition with Verteporfin (VTPF) impaired the expression of tendon genes. Finally, mechanical stimulation did not rescue the downregulation of tendon gene expression observed in 3D-constructs treated with VTPF. This establishes YAP as an intracellular relay of mechanical signals to regulate tendon gene expression. Altogether, our results establish a link between mechanical signals, YAP and EGR1 activities and tendon gene expression in 3D-culture systems made of C3H10T1/2 cells.

V.3.1 Tendon and cartilage gene expression in fibrin and collagen 3D-constructs favors collagen over fibrin constructs as model to study tendon cell differentiation

In collagen 3D-constructs between T0 and 14 days of culture, we observed a constant increase in *Scx* and *Col1a1* genes expression (Figure V.3B). However, we could also observe a decrease in *Tnmd* expression during the first five days of culture, before a subsequent increase after the fifth day (Figure V.3B). However, at the final day of culture, *Tnmd* expression was still decreased at around 0.5-fold compared to its initial expression at T0. Yet, in fibrin-based 3D-constructs, *Tnmd* expression constantly decreased overtime, up to 21 days of culture (Figure V.3A). These differences between fibrin- and collagen-based 3D-constructs show that tendon gene expression seems to be favored in collagen versus fibrin gel. It has to be noted that *Tnmd* was markedly decrease overtime in both fibrin and collagen 3D-constructs, which mean that C3H10T1/2 cells never fully achieved tenogenic differentiation in these models.

Interestingly, our conclusion here is in opposition to a study comparing fibrin- and collagen-based 3D-constructs made of chicken tendon cells (Yeung et al., 2015). In this study, they showed that cells in fibrin 3D-constructs synthesized their own ECM and consequently reproduced more accurately tendon cells behavior. They also showed that mechanotransduction pathways such as YAP/TAZ, were desensitized from 2D to collagen gels. In addition, fibers in fibrin-based constructs were aligned, while in collagen-based constructs they were randomly organized. They hypothesized that chicken tendon cells in collagen 3D-constructs are so adherent to randomly-organized collagen fibers that they cannot adapt to mechanical constraints. Yet, we showed that in control and stretched collagen 3D-constructs, cells were aligned along the long axis of the constructs defined by the two anchor points. The cellular alignment observed in our collagen 3D-constructs could explain the differences between our study and that of Yeung and colleagues (Yeung et al., 2015).

There is a marked decrease in the expression of the cartilage marker, *Col2a1* in collagen 3D-constructs, while there is an important increase in the expression of *Col2a1* expression in fibrin 3D-constructs overtime. This result indicates that fibrin-gel constructs favor cartilage differentiation, while collagen-gel would inhibit cartilage differentiation of C3H10T1/2 cells.

Also, we observed a steady increase of *Acan* after the fifth day of culture in collagen constructs (Figure V.3C). Although *Acan* is described as a cartilage differentiation marker (Lauing et al., 2014), it is also known to be expressed at fibrocartilaginous sites such as the enthesis and in the tendon ECM (reviewed in Thorpe et al., 2013). *Acan* could also be a possible marker of tenogenic differentiation. This explanation would fit with the evolution of *Acan* pattern of expression that resembles more to that of tendon genes (*Scx* and *Col1a1*) than that of cartilage genes (*Sox9* and *Col2a1*). The marked increase of *Col2a1* expression and the relative light increase of *Scx* in fibrin 3D-constructs could mark a preferential specification toward cartilage lineage, that would favor collagen 3D-construct as a model to study

tendon cell differentiation.

V.3.2 Variation in the internal structure in 3D constructs is representative of their mechanical state

We focused on the effects of the mechanical signals between T0 and 24H of culture in collagen 3D-constructs. We first showed that collagen 3D-constructs mechanical state elicited changes in their internal structure. Control and stretched collagen 3D-constructs had aligned cells and nuclei along the axis of the construct, as compared to the random organization in tensionless collagen 3D-constructs (Figure V.5). Differences were striking between control and tensionless collagen 3D-constructs, but no obvious difference was observed between controls and stretched constructs. I would have expected to observe higher proportions of cells and nuclei parallel to the axis of the constructs (90°) in stretched constructs compared to controls. However, it was not the case and this would mean that the structure of the collagen 3D-constructs cannot be further changed by the loading protocol, or that the loading protocol was not efficient enough in that way. The proportion of proliferating cells (Ki67⁺ nuclei) does not show any significant difference in stretched and tensionless conditions compared to control conditions (Figure V.7). However, it has to be noticed that only 14% of cells exhibiting Ki67⁺ nuclei. We based our analysis on a 24H-period following T0 and we cannot exclude further changes in cell proliferation at later stages in 3D-constructs. Since our analysis is on a 24H-period, we can conclude that the observed changes of cell orientation and gene expression are not due to difference in cell proliferation.

V.3.3 *Scx* expression is modulated by mechanical cues

Regarding tendon gene expression, *Scx* appears to be regulated by mechanical cues in 3D-constructs. *Scx* expression was upregulated upon stretched conditions compared to control collagen 3D-constructs. We also observed an increase in the proportion of SCX⁺ nuclei in stretched conditions compared to control collagen 3D-constructs, indication of an increase of SCX activity. The *Scx* upregulation is consistent with previous studies using different loading protocols (Scott et al., 2011; Wang et al., 2018b). However, *Scx* expression was not downregulated in absence of tension in collagen 3D-constructs, as observed in fibrin 3D-constructs (Gaut et al., 2016). However, the proportion of cells with SCX⁺ nuclei was decreased in absence of tension in collagen 3D-constructs, indicating a possible decrease in SCX activity, or a post-transcriptional regulation of *Scx* to rapidly adapt to load changes. The difference between collagen and fibrin constructs could be due to the short culture time (24H) with collagen 3D-constructs versus longer period in fibrin-gel constructs, due to the difference of production between these models (Gaut et al., 2016). Another explanation could be the difference of ECM in each model, collagen and fibrin gels could elicit different cell responses, as it was already shown for chick tendon fibroblasts in 3D constructs (Yeung et al., 2015).

V.3.4 EGR1 and YAP act downstream of mechanical cues

For the YAP and EGR1 mechanosensitive factors, we showed that they were regulated by mechanical signals in collagen and fibrin 3D-constructs. EGR1 is already known to be involved in tendon development and tendon cell (Guerquin et al., 2013; L ejard et al., 2011). *Egr1* expression and activity are dependent on mechanical states of the 3D-constructs, and *Egr1* overexpression was able to bypass the lack of mechanical signals in 3D fibrin-gel constructs (Figures V.9, V.10,V.11). However, the mechanical stimulation of collagen 3D-constructs does not induce an increase in *Egr1* expression (Figure V.9B) or an increase in the proportion of EGR1⁺ nuclei (Figure V.10D). This could mean that we did not find a loading protocol able to elicit such changes or that EGR1 is responsive only to an absence of mechanical signals and that its activity cannot adapt above a certain upper threshold of mechanical signals.

YAP activity changed accordingly to the mechanical state of collagen 3D-constructs (Figures V.9 and V.11), which is concordant with what is known for other models in literature (reviewed in Panciera et al., 2017). Yet, if changes for YAP activity were striking in tension release conditions, they were more difficult to see in stretched collagen 3D-constructs as YAP target genes *Cyr61* and *Ctgf* showed increased expression but we could not detect an increase in YAP⁺ nuclei (Figures V.9 and V.11). However, when we looked at the intensity of YAP signal in nuclei, we could observe a difference between control and stretched conditions (Figure V.11E). This difference consists in an increase of the nuclei exhibiting higher YAP signal, suggesting that the number of YAP⁺ nuclei is not the only parameter to be taken into account but also the intensity of YAP signal.

V.3.5 YAP is involved in the regulation of tendon phenotype

We showed that YAP was regulated by mechanical signals in collagen 3D-constructs. In order to link YAP with tendon cell differentiation, we used VTPF treatment that inhibits the binding between YAP and TEAD transcription factor, thus resulting in a chemical induction of YAP loss-of-function (Chen et al., 2015). VTPF activity was confirmed by the decrease in the expression of *Cyr61* and *Ctgf*, two transcriptional readout of YAP activity. Moreover, there was no change in the proportion of YAP⁺ nuclei in VTPF treated collagen 3D-constructs (Figure V.15). This is consistent with the fact that VTPF does not impair YAP nuclear translocation but the YAP binding to TEAD transcription factor. In VTPF-treated collagen 3D-constructs, we observed a decrease in tendon and cartilage gene expression, as well as a decrease in the proportion of cells with SCX⁺ nuclei (Figure V.16). This would indicate that YAP is effectively involved in the regulation of tendon gene expression. Yet these results do not allow to determine if this regulation is direct or indirect. However, in 2D cultures of C3H10T1/2 cells treated with VTPF, *Tnmd* and *Col1a1* expression shows a decrease dependent on the VTPF dose, hence hinting at a putative direct regulation (Figure V.14B). A way to answer this question would be to perform chromatin immunoprecipitation (ChIP) with YAP antibody and transactivation tests to verify the binding and activity of TEAD transcription factors on regulating sequences of tendon genes.

Nevertheless, the counting of double YAP/SCX nuclei in collagen 3D-constructs in different conditions could offer us highlights. We observed that in the total cell population with YAP⁺ nuclei, the proportion of cells with SCX⁺/YAP⁺ nuclei changed accordingly to mechanical states of the collagen 3D-constructs (Figure V.13). Moreover, in VTPF-treated collagen 3D-constructs, in which YAP was inactive, we observed a striking decrease in the proportion of cells with SCX⁺/YAP⁺ nuclei, while the total amount of cells with YAP⁺ nuclei remained unchanged, indicating that the loss of SCX signal in nuclei occurred in only in cells exhibiting YAP⁺ nuclei. These results strongly favor the hypothesis in which YAP would be upstream of *Scx* expression and SCX activity in a molecular cascade initiated by mechanical signals. The fact that we could not rescue tendon gene expression by enhancing the mechanical signals in a YAP⁻ deficient context further confirms this model (Figure V.18). Altogether, our results establish YAP as an intracellular relay of mechanical signals regulating tendon gene expression.

V.3.6 Possible relationship between YAP and EGR1

Regarding the relationship between YAP and EGR1, we showed with the VTPF-treatment that *Egr1* expression was reduced in the absence of YAP function, which would be in favor of YAP regulating *Egr1* expression. However, the stretching of collagen 3D-constructs treated with VTPF showed a rescued *Egr1* expression back to the control levels (Figure V.18), this indicates that another intracellular pathway than YAP regulates *Egr1* transcription in this context. SRF is known to be an activator of *Egr1* expression (Esnault et al., 2014; Posern and Treisman, 2006). However, this regulation is achieved through the ERK/MEK pathway and the SRF-TCF complex, rather than the known mechanosensitive pathway involving the actin cytoskeleton polymerization and leading to the activity of the SRF-MRTF-A complex. Thus, the mechanosensitive regulation of *Egr1* still remains unclear and further experiments are required in that way. Since *Egr1* expression is known to be sensitive to fluid shear stress (Schwachtgen et al., 1998), maybe one putative mechanosensing element regulating of *Egr1* expression would be the primary cilium, which is sensitive to that kind of mechanical signal (Corrigan et al., 2018).

V.4 Conclusion

In this study, we analyzed the behavior of C3H10T1/2 cells in fibrin and collagen 3D-constructs, mimicking native tendons. The collagen 3D-culture system was subjected to different mechanical conditions. We observed that cells were organized depending on mechanical states of collagen 3D-constructs. We also linked mechanical states to tendon gene expression and the activity of two mechanosensitive factors EGR1 and YAP. We also showed that a pool of cells exhibiting YAP⁺ nuclei is responsible for the positive regulation of SCX activity regarding mechanical cues. Finally, mechanical stimulation of collagen 3D-constructs treated with VTPF was not sufficient to rescue tendon gene expression, except for *Egr1* expression, establishing YAP as an intracellular relay of mechanical signals to regulate tendon

gene expression. EGR1 was also shown to rescue tendon gene expression in tensionless fibrin constructs, establishing it as another mechanotransduction factor regulating tendon gene expression. Taken together, our results establish a link between mechanical signals, YAP activity and tendon gene expression in cells of collagen 3D-constructs.

VI. Discussion and Perspectives

VI.1 The tendon phenotype is sensitive to mechanical signals both in *in vivo* and *in vitro* models

In chicken fetuses, mechanical signals are required for the tendon maintenance of tendon gene expression. We showed that the expression of two key tendon markers, *SCX* and *TNMD*, requires muscle contractions in chicken fetuses, as it was also observed in chicken embryos earlier during development (Havis et al., 2016). However, these results have to be compared with the observations made by Huang and colleagues (Huang et al., 2013, 2015b). They used *mdg* mutant mice lacking excitation-contraction coupling in muscles and *Spd* mutant mice, two models comparable to the DMB-treated chicken fetuses. Tendon patterning was similar in *mdg* mutant mice and wild-type mice and tendons were formed in *Spd* embryos, although they were shorter (Huang et al., 2013, 2015b). They suggested that muscle contractions mainly played a key role in tendon growth.

Yet, we also showed that tendon gene expression is related to the mechanical state of C3H10T1/2 cells in different 3D culture systems. A parallel can be established between the immobilized chicken fetus model and the de-tensioned fibrin- and collagen-based 3D-constructs, in which we observed a decrease in the expression of tendon genes. Yet, control 3D-constructs do not benefit from repetitive stretches as *in vivo* tendons experience thanks to muscle contractions. As such, the *in vitro* model that would be the most representative of *in vivo* tendons would be the stretched collagen-based 3D-constructs, that is both subjected to a static tension between its two anchor points and to a mechanical stimulation similar to what is occurring in *in vivo* tendons. In the stretched condition, we did observe an increase in *Scx* expression and of SCX⁺ nuclei.

As we previously saw in the introduction, there is a large catalog of loading protocols that can be applied to 3D-constructs. In our stretching experiments of collagen 3D-constructs, we observed an increase of *Scx* expression and a slight but significant increase in the proportion of Scx⁺ nuclei, indicating of a switch towards the tendon fate of C3H10T1/2 mesenchymal stem cells. We also monitored changes in cell and nucleus organization upon mechanical stimulation and we did not observe any change in nucleus orientation compared to controls. One obvious explanation is that the nucleus orientation along the axis of the 3D-constructs had reach it maximum in this 3D culture system. Alternatively, we cannot exclude the fact that we might not have found the most efficient loading protocol. Indeed, we did not test any other stretching parameters such as percentage of elongation, frequency of stimulation

or protocol duration.

VI.2 How mechanical signals are sensed and interpreted by tendon cells

VI.2.1 YAP acts as an intracellular relay of mechanical signals to regulate tendon gene expression

The results we obtained argue in favor of a regulation of tendon gene expression by the transcription co-factor YAP, probably via its binding to the TEAD transcription factors. In chicken fetuses, we established a correlation between YAP and tendon gene expression in limb tendons. We also showed that the expression of YAP and tendon genes was sensitive to mechanical signals produced by muscle contractions. However, these results do not prove that tendon gene expression is directly regulated by YAP signaling pathway. We were able to link the mechanical state of 3D-constructs to YAP and tendon gene expression. We obtained similar results in de-tensioned 3D-construct model and in the immobilized chicken fetus model, *i.e.* a decrease in YAP target genes and tendon gene expression in de-tensioned conditions. Besides, we further confirmed the link between YAP and mechanical cues in this model thanks to the ability of the collagen 3D-constructs to be stretched, which showed an increase in YAP activity (Figure VI.1).

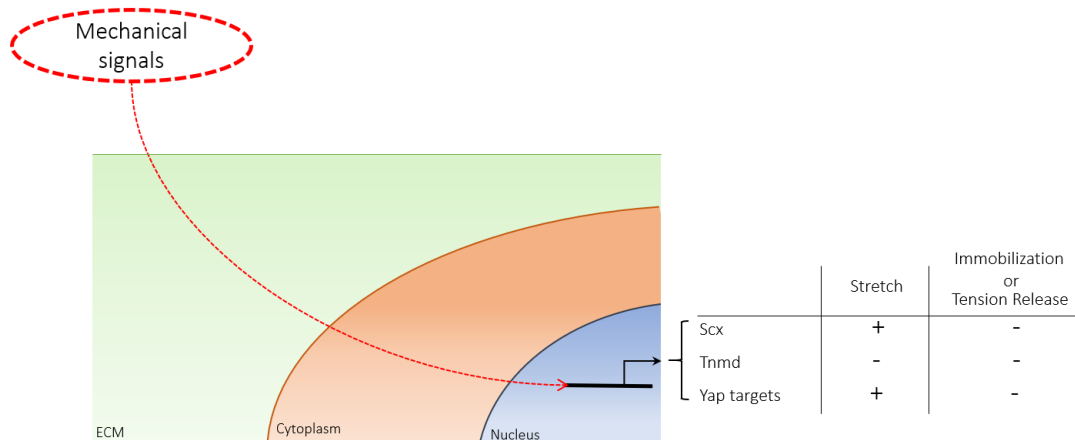


Fig. VI.1 **Link between mechanical signals, YAP activity and tendon gene expression.** Table on the right summarizes the positive (+) or negative (-) output of gene expression regarding the mechanical signals in collagen 3D-constructs (“Stretch” and “Tension Release”) and limb tendons of immobilized chicken fetus (“Immobilization”). Self-made illustration.

Interestingly, VTPF-treatment gave more insights, as we could confirm that chemical inactivation of YAP activity significantly affected tendon gene expression, as well as *Egr1* expression. Counting cells with double YAP⁺/Scx⁺ nuclei in VTPF-treated 3D-constructs also showed that YAP would be upstream of Scx in a molecular cascade since the variation in the proportion of Scx⁺ nuclei occurred in cells exhibiting YAP⁺ nuclei. In addition,

mechanical signals could not rescue the downregulation of tendon gene observed by VTPF treatment, indicating that YAP could be a major intracellular relay of mechanical signals regulating tendon gene expression (Figure VI.2). However, a direct regulation of YAP to tendon gene expression have to be confirmed by ChIP experiments to evaluate the fixation of TEAD transcription factor on genomic sequences regulating tendon genes.

Finally, other studies have identify a crosstalk or interference between YAP and TGF β 2/Smad2/3 signaling pathways (Grannas et al., 2015; Speight et al., 2016; Szeto et al., 2016) which could then further strengthen a role for YAP in tendon gene expression regulation.

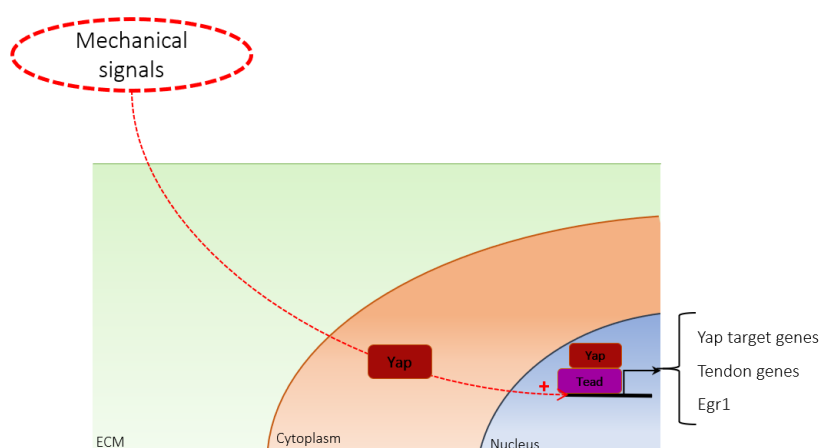


Fig. VI.2 **Hypothetical model of tendon gene expression regulation by mechanical signals through YAP activity.** Red cross indicates the positive effect of mechanical signals on tendon gene expression through YAP-TEAD (red and purple squares) activity. Self-made illustration.

VI.2.2 Possible interactions between YAP and EGR1 in tendon cells

In contrast to tendon genes, stretching VTPF-treated 3D-constructs did rescue *Egr1* expression (Figure VI.3), which argues in favor of another molecular mechanosensitive pathway involved in the regulation of *Egr1*. Yet, it does not entirely rule out YAP as a regulator of *Egr1* gene expression, especially since another study found out that siRNA-induced knock-down of YAP decreased EGR1 protein expression in endothelial cells (Yi et al., 2016). However, the interaction between YAP and EGR1 might be considered at another level than that of the regulation of *Egr1* transcription by YAP. Indeed, YAP and EGR1 have been shown to form a complex in order to activate the transcription of their target genes, in endothelial cells and irradiated carcinoma cells (Yi et al., 2016; Zagurovskaya et al., 2009).

Other signaling pathways were shown to be activated by mechanical cues during tendon cell differentiation, such as PI3K/AKT pathway (Wang et al., 2018), and could be involved in the regulation of *Egr1* expression in that context.

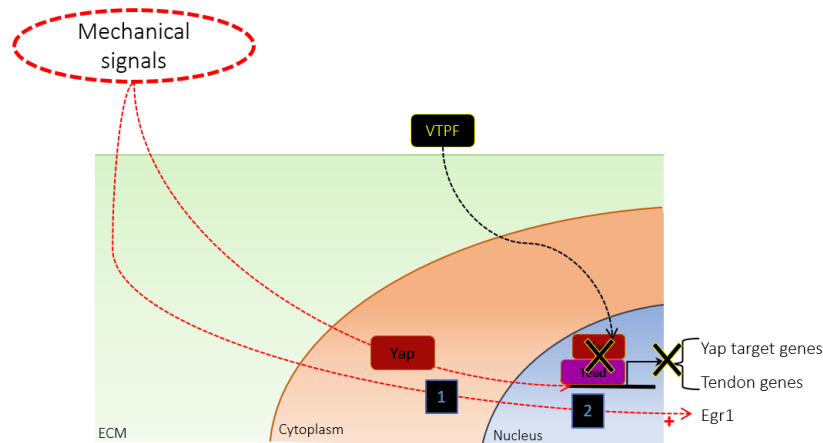


Fig. VI.3 *Egr1* mechanosensitive expression is also regulated by another mechanotransduction pathway. Stretching of collagen 3D-construct does not rescue YAP targets and tendon genes expression but does rescue that of *Egr1*. Blackbox 1 indicates the unknown mechanosensing elements relaying mechanical cues in the cell all the way down to unknown mechanosensitive transcription factors regulating *Egr1* expression and represented as Blackbox 2. Self-made illustration.

VI.2.3 How are mechanical signals sensed by cells achieving tenogenic differentiation?

Our results identified YAP and EGR1 mechanotransduction pathways as intracellular relays of the mechanical signals in order to regulate tendon gene expression. However, we did not identify how the tension is converted from the cell membrane to YAP- and EGR1-mediated transcriptional response in the nucleus.

It is possible that the actin cytoskeleton itself would be directly involved in mechanosensing processes. Cytoskeleton directly sensing mechanical cues through its reorganization would allow cells to sense topographical cues. Indeed, it has already been proposed that in the case of biomaterials, fiber alignment sensed by the cells would be a major cue driving tenogenic differentiation (Kishore et al., 2012). However, this idea is fairly discussed as fiber alignment was also shown to be insufficient by itself to promote tenogenic differentiation (Baudequin et al., 2017; Madhurakkat Perikamana et al., 2018). Yet, aligned fibers were also shown to act synergistically with the deposition of PDGF, which would not discard the importance of this topographical parameter in driving tenogenesis (Madhurakkat Perikamana et al., 2018). Also, in the study from Baudequin and colleagues, it was shown that while the fiber alignment was not a parameter involved in tendon gene expression, the fiber size would be important in tendon gene expression (Baudequin et al., 2017). If fiber size is important, it would not rule out the possibility that the mechanosensing responsible for tenogenic differentiation is partly directly achieved by the cytoskeleton. This possibility is strengthened by the fact that YAP activity has been linked to actin cytoskeleton dynamics (Pancier et al., 2017).

In the introduction of this thesis, we also saw that other cellular components played crucial roles in mechanosensing, such as the primary cilia. Primary cilia of tenocytes are

aligned to tendon native ECM (Donnelly et al., 2010). Besides, defects in primary cilia, such as those caused by hypoxic conditions, affect tendon cell mechanoresponsiveness, confirming their role as mechanosensory apparatus in tendon cells (Lavagnino et al., 2016). EGR1 could be a mechanosensitive factor benefiting from primary cilia mechanosensing activity, since EGR1 mechanosensitivity has been linked to fluid shear stress that can be typically sensed by primary cilia (Hamamura et al., 2008; Ogata, 2008; Schwachtgen et al., 1998).

Many other cellular mechanosensory components are known, some of them in the context of tendon cells, such as connexins 32 and 43 that transmit Ca^{2+} waves in response to mechanical loads (reviewed in Wall et al., 2016). However, the work I did during my thesis did not allow to further explore this aspect of tendon cell behavior. It would then be very interesting to understand how tendon cells sense mechanical cues before the activation of mechanotransduction pathways such as those involving YAP and EGR1.

VI.3 *Tnmd* expression to assess tendon cell differentiation

VI.3.1 Consistent dichotomy in *Scx* and *Tnmd* expression independently of the model

Along all our experiments, we frequently observed a differential behavior of *Scx/SCX* and *Tnmd/TNMD* expression in different experimental contexts. when *Scx* expression was up-regulated, *Tnmd* was not modified or was downregulated and *vice versa*. In C3H10T1/2 cells grown on plastic substrate we observed a first decrease of *Scx* expression, while *Tnmd* exhibited a bell-shaped expression and started to decrease long after that of *Scx*. When C3H10T1/2 cells are grown on silicon substrate, *Tnmd* expression is the only tendon gene to be upregulated, while *Scx* expression does not vary overtime. Also, when treated with TGF β 2, C3H10T1/2 cells displayed a significant increase in *Scx* expression and a concomitant decrease of *Tnmd* expression, in both 2D- or 3D-culture systems. Finally, *Tnmd* expression was decreased in de-tensioned and stretched collagen 3D-constructs while that of *Scx* was not modified. The explanation for the dichotomy between *Scx/SCX* and *Tnmd/TNMD* expression is not clear. However SCX has been shown to be an upstream regulator of *Tnmd/TNMD* expression (Murchison et al., 2007; Shukunami et al., 2006), which is consistent with the role for *Scx* as a marker of tendon progenitors and for *Tnmd* in tenogenic differentiation. A recent study recently reported that SCX acts as a direct transcriptional activator of *Tnmd* expression in mouse tenocytes and C3H10T1/2 cells *in vitro* (Shukunami et al., 2018). However, in the same study they also observed a concomitant increase of *Scx* and decrease of *Tnmd* in rat tenocytes cultured overtime, (Shukunami et al., 2018). *Scx* expression would be related to a specification process toward tendon lineage, followed by a subsequent phase of tenogenic differentiation marked by *Tnmd* expression. This is consistent with the coordinated *SCX* and *TNMD* expression profiles in in DMB-treated fetuses.

VI.3.2 Link between *Egr1* and *Tnmd* expression

In our results, we also observed a link between *Egr1* and *Tnmd* expression. *Egr1* overexpression induces *Tnmd* expression in fibrin-based 3D-constructs or in cMM cultures (Guerquin et al., 2013; Orgeur et al., 2018). De-tensioned fibrin-based 3D-constructs lead to a concomitant decrease of *Egr1* and *Tnmd* (Gaut et al., 2016). *Egr1* forced-expression in de-tensioned fibrin-based 3D-constructs prevents *Tnmd* downregulation. In VTPF-treated collagen 3D-constructs, both *Egr1* and *Tnmd* expression are downregulated. Also, in immobilized chicken fetuses, *EGR1* expression is downregulated at earlier time points than *TNMD*. In adult mice, *Egr1* overexpression in normal or injured Achilles tendons of immobilized mice is able to rescue tendon gene expression, including *Tnmd* (Gaut et al., 2016). Similarly, *Egr1*^{-/-} mice display a decrease in *Tnmd* expression (Guerquin et al., 2013). These results indicate that EGR1 could regulate *Tnmd* expression. Altogether, these results are in favor of a regulation of *Tnmd*/*TNMD* by the transcription factor EGR1 but a direct regulation needs to be confirmed through ChIP experiments

VI.4 Validity of cellular model

VI.4.1 MSC: what the acronym is all about

As stated in the introduction of this manuscript, the “Mesenchymal” stem cell concept first originated from the discovery of an osteogenic potential in bone marrow, residing in fibroblast-like adherent cells (Friedenstein et al., 1966). MSCs were also thought to give rise to a broad spectrum of mesenchymal lineages and *in vivo* would correspond to the pericytes (Bianco, 2014; Caplan, 1991; Crisan et al., 2008). Thus, MSCs can potentially be harvested from a large set of tissues. On top of that, they were also shown to possess trophic, paracrine, anti-inflammatory and immunomodulatory functions (Murphy et al., 2013; Sharma et al., 2014).

However, this definition of MSCs is challenged because they are defined by *in vitro* characteristics established by consensus. The “Multiple Significations-Code” that lies behind the MSC acronym attests for this broad range of characteristics. Mesenchymal Stem Cells, Multipotent Stromal Cells, Mesenchymal Stromal Cells and Medicinal Signaling Cells are examples of the large set of characteristics adopted for MSCs (Bianco, 2014; Caplan and Correa, 2011). All these properties seemed to have generated another stem cell population, really different from the BMSCs that were first isolated *in vivo* (Friedenstein et al., 1966). Besides, the MSCs are found in a large palette of tissues, most of them not having stromal cells, as it is the case for some connective tissues. Also, it is really surprising to see that one of their biggest interest lies in their immunomodulatory properties, which seem to be far from a stem cell identity (Bianco, 2014; Caplan and Correa, 2011).

While all the possibilities offered by the MSCs make a really powerful biological material, we also have to be careful with this concept and the results we draw from it. As such, Bianco et al. proposed the term of Cultures of Connective Tissue cells, which should be more adequate with the properties observed previously (Bianco, 2014). In that way, maybe

we should think of the C3H10T1/2 cells (cells we used in our experiments), as a cell line of Mouse Embryonic Fibroblasts (MEFs) rather than to strictly assimilate them to MSCs. This simple change of term would be correct regarding their origin, while not impairing their multidifferentiation and MSC-like properties. Besides, it does not invalidate our model in the way that we are assessing the potential of a naïve cell to achieve tenogenic differentiation and tendon gene expression.

VI.4.2 Naive cells or tendon cells?

In the introduction, I presented different cellular models used for the study of tendon cell differentiation induced either by biochemical or mechanical cues. Among them are stem cell models, such as ADSCs or MSCs, primary cell cultures or cell lines, but also TSPCs that are directly harvested from tendons (Bi et al., 2007).

The use of stem cell models or TSPCs does not allow the study of tendon cell differentiation in the same conditions. With stem cells, we start from naive cells with the idea to reach a tenogenic phenotype. With TSPCs, we already are in a cell population exhibiting tendon cell specification markers, such as *Scx* expression that is already often used for their isolation. Thus, we already are in a tenogenic context that would certainly allow for a better characterization of the cues driving final tenogenic differentiation.

Experiments realized in our laboratory by Isabelle Cacciapuoti indicate that the tendon gene expression profiles are different in fibrin-based 3D-constructs made of mouse tail tenocytes (Figure VI.4) versus those made of C310T1/2 cells (Figure V.3A). We observed that *Tnmd* expression displayed a striking increase overtime in fibrin-based 3D-constructs made of mouse tail tenocytes. The increase of *Tnmd* was more important compared to that observed in fibrin-based 3D-constructs made of C3H10T1/2 cells in 2D- or 3D-cultures, overtime.

**Evolution of tendon gene expression in
fibrin-based 3D-constructs made of
mouse tail tenocytes**

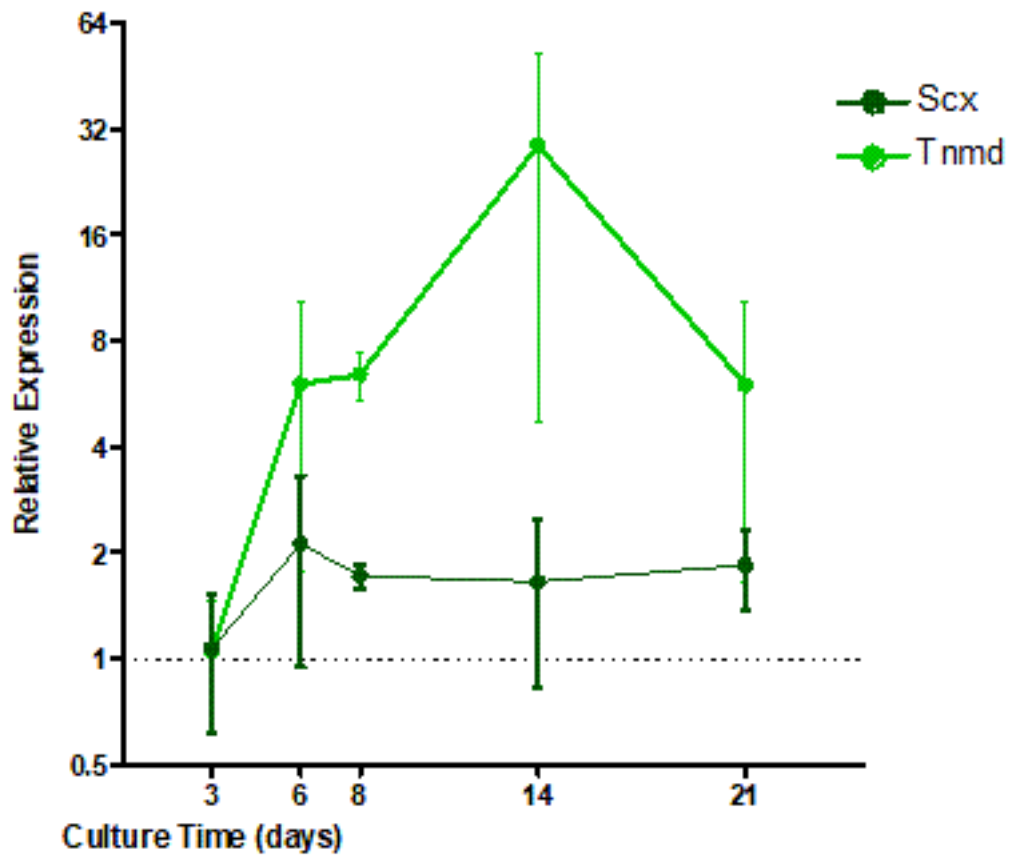


Fig. VI.4 *Evolution of Scx and Tnmd gene expression overtime in fibrin-based 3D-construct made of mouse tail tenocytes.* Dots and bars represent mean and standard deviation, respectively, calculated from 2-3 independent samples. Experiment performed in the laboratory by Isabelle Cacciapuoti.

VII. Conclusion

Altogether, the results I presented in this manuscript show that mechanical signals are involved in the control of tendon gene expression and tendon cell differentiation. This phenomenon seems to be conserved between *in vivo* and *in vitro* models, in chicken fetuses and in 2D-culture or 3D-construct made of C3H10T1/2 cells. EGR1 and YAP are already known to be involved in tendon differentiation and in response to mechanical stress, respectively. However, these results are the first to establish EGR1 and YAP as intracellular relays of mechanical signals to regulate the tendon phenotype.

VIII. Material & Methods

Experiments on chicken fetuses

Chicken eggs

Fertilized chicken eggs strain JA57 were obtained from commercial sources (Morizeau, Dangers) and incubated at 37.5°C. Chicken embryos and fetuses were staged according to days in ovo.

Drug administration in ovo

The stock solution for decamethonium bromide (DMB) (Sigma, D1260) was prepared at 10% in Hank solution (Sigma H9269). A DMB working solution was freshly prepared before each experiment at 0.5% in Hank's saline solution with Penicillin-Streptomycin at 1% (Gibco, 15140). The control solution was prepared using Hank's saline solution with 1% of Penicillin-Streptomycin. 100µL of the working solution for DMB or Hank's saline solution was administrated in ovo at E7 and renewed every 24H when necessary at each of the time points required (Figure 1A).

C3H10T1/2 cell cultures

The multipotent mouse mesenchymal stem cells, C3H10T1/2 cells (Reznikoff et al., 1973) were cultured on plastic culture plates or Uniflex Flexcell plates (silicone substrate coated with type I collagen, FlexCell Int.) in Dulbeccos Modified Eagles Medium (DMEM, Invitrogen) supplemented with 10% fetal bovine serum (FBS, Sigma) 1% penicillin-streptomycin (Sigma) 1% glutamin (Sigma) and incubated at 37°C in humidified atmosphere with 5% of CO₂. C3H10T1/2 cells cultured on plastic substrate were cultured in 6-wells TPP Tissue Culture Plates (Merck).

To study the effect of initial cell number on tendon gene expression, 0.5×10^5 , 10^5 and 2×10^5 C3H10T1/2 cells were seeded in 10 cm culture plates (plastic substrate) and left for 16H in culture and analyzed for tendon gene expression by RT-qPCR. In all cases, the culture medium was changed every 48H. For the study of the effects of the initial cell number, 6 samples (N=6) were analyzed in each condition of cell density. 250 ng of RNA were extracted from each sample before proceeding with the RT-qPCR. The *Rplp0* gene was used as the reference gene.

Regarding the analysis of the differentiation potential of C3H10T1/2 cells seeded on plastic substrate, 10^5 cells were seeded in 10 cm culture plates (plastic substrate) and left

for 16 H in culture. This defined the T=0 (N=4) and then cells were cultured for another 24H (N=4), 7 days (N=4), 10 days (N=5) and 14 days (N=4). 500 ng of RNA were extracted from each sample before proceeding with the RT-qPCR. Regarding the analysis of the differentiation potential of C3H10T1/2 cells seeded on silicon substrate coated with type I collagen, 10^5 C3H10T1/2 cells were seeded in 6 cm Uniflex Flexcell plates and left for 16 H in culture. This defined the T=0 (N=5) and then cells were cultured for another 24H (N=6), 48 H (n=6), 7 days (N=6), 11 days (N=6). 500 ng of RNA were extracted from each sample before proceeding with the RT-qPCR.

3D-engineered tendons

Fibrin-based 3D-constructs

Mouse Embryonic Fibroblasts, C3H10T1/2 cells were used to establish fibrin-based 3D tendon constructs. Tendon-like structures made of mouse C3H10T1/2 cells were performed as previously described (Kapacee et al., 2008, Guerquin et al., 2013). Briefly, for each construct, 400 μ l of cell suspension (7.5×10^5 cells) were mixed with 20 mg/ml fibrinogen (Sigma, St Louis, MO, USA) and 200 U/ml thrombin (Sigma, St Louis, MO, USA). The fibrin gels containing cells were seeded in already prepared SYLGARD-covered wells (DowChemical, Midland, MI, USA), in which two 8 mm- sutures (Ethican, Sommerville, NJ, USA) were pinned 10 mm apart. Culture medium containing 200 μ M of L-ascorbic acid 2-phosphate was added to the wells and gels were scored every day for a proper contraction into a linear construct. After 7 days, the C3H10T1/2 cells formed continuous tendon-like constructs between the 2 anchors. Each tendon construct was considered as a biological sample. The mRNA levels of each construct were analyzed by q-RT-PCR.

Collagen-based 3D-constructs

Collagen-based 3D-constructs made of C3H10T1/2 stem cells were produced to apply diverse mechanical conditions to the cells in a 3D environment. Cultured cells were detached from the culture plates using 4mL of 0.25% Trypsin during 5-10min. Subsequently, detached cells were resuspended in culture medium and counted with a hemocytometer. Each collagen 3D-construct is made of 6.010^5 cells. Cells were resuspended in a solution made of 20% of DMEM, 10% fetal bovine serum and 70% Type I collagen from Purecol EZ (Sigma- Aldrich, Oakville, Canada). When required, the pH level of the collagen solution was adjusted with 0.1M NaOH solution to reach 7.0 pH prior to the seeding of the constructs. Tendon-like constructs were produced using a FlexCell Culture system FX-5000T (FlexCell International, Hillsborough NC) in which a four-place base is assembled with Through loader 100 mold (FlexCell International, Hillsborough NC). It consists in a cylinder containing a longitudinal mold with vertical holes by which vacuum is applied along the elastic silicon membrane of the TissueTrain plates (FlexCell International, Hillsborough NC). Vacuum induces the silicon elastic surface of TissueTrain plate to acquire the shape of the mold where 150 μ l of cell-collagen mixture containing 600.000 cells were deposited between the two nylon-anchor

stems of each well, into according to manufacturer's instructions. No culture medium was added to the wells and the loading station was left under vacuum for 2H in a humidified incubator at 37°C and 5% of CO₂ to let the collagen gel polymerize and bond to the anchor stems. Afterwards, vacuum is released and the collagen gel constructs assumed a linear cylindrical structure assembled to both anchor stems withstanding a static uniaxial load. Then, each well was covered with 3mL of culture medium containing DMEM and 200 µM of L-ascorbic acid 2-phosphate.

Before applying any change in mechanical load, engineered tendons containing C3H10T1/2 cells were left 48H after production to completely polymerize and bond the anchor stems under static load, considering this time point as initial or T₀. Control, stretched and de-tensioned constructs were all harvested and compared 24H after T₀. We used 6 independent control samples for RT-qPCR analysis (N=6) and between 4 and 10 for image analysis on immunostained sections (N=4 and N=10).

Regarding the stretched collagen 3D-constructs, they were uniaxially stretched installing Arcangle Loading posts (FlexCell International, Hillsborough NC) beneath TissueTrain plates in a gasketed baseplate through vacuum. FlexCell FX-5000T system provides a control unit to define single variables such as strain, frequency and duration in cyclic loading regimens that we used as follow:

- Frequency was defined at 1Hz to minimize the risk of detaching from the anchor stems
- Strain was specified at 1% of elongation
- Duration was set 1H per day, followed by a 23H-rest period.

We used 6 independent stretched samples for RT-qPCR analysis (N=6) and between 4 and 10 for image analysis on immunostained sections (N=4 and N=10).

Regarding the de-tensioned collagen 3D-constructs, static tension was released by cutting one end of each construct thus detaching from the corresponding anchor stem. De-tensioned collagen-3D constructs were let to grow during 24H before harvesting. We used 6 independent de-tensioned samples for RT-qPCR analysis (N=6) and between 4 and 10 for image analysis on immunostained sections (N=4 and N=10).

Chemical treatments applied on C3H10T1/2 cell cultures

TGFβ₂ treatment

Regarding the TGFβ₂ treatment of 2D cultures, 10⁵ C3H10T1/2 cells were plated on classic cultures plates (plastic) and grown for 40H. Then, human recombinant TGFβ₂ (RD System) was applied at 20 ng/ml to C3H10T1/2 cells for 24H. Cells were grown for another 24H without TGFβ₂supplementation in the medium. Control cells were treated with Bovin

Serum Albumin and HCl (BSA-HCl) in the same volume than that applied for TGF β 2 treatment. TGF β 2-treated and non-treated C3H10T1/2 cells were then fixed and processed for q-PCR assays to analyze gene expression. In each condition, 4 biological samples (N=4) were used. For 3D tendon constructs were treated for 24H with TGF β 2 (the controls were treated with BSA-HCl) at the 7th day of culture, when they form continuous tendon-like constructs between the 2 silk anchors. In each condition, 5 biological samples (N=5) were used.

VTFP treatment

Cell cultures were treated with VTPF (Sigma- Aldrich, Oakville, Canada) molecule to chemically induce a knock-down of YAP activity. Regarding VTPF treatment of 2D cultures, 10⁵ C3H10T1/2 cells were plated on classic cultures plates (plastic) and grown for 16H. Then, cultures were treated with 2.5 μ M, 5.0 μ M or 10 μ M VTPF diluted in DMSO for 24H and control C3H10T1/2 cultures were treated with the same volume of DMSO. We used 5 independent VTPF and control-DMSO samples for RT-qPCR analysis (N=4).

At T0, collagen 3D-constructs were treated with 10 μ M VTPF diluted in DMSO for 24H and control collagen 3D-constructs were treated with the same volume of DMSO. We used 5 independent VTPF and control-DMSO samples for RT-qPCR analysis (N=5) and 4 independent samples for image analysis on immunostained sections (N=4).

RNA isolation, Reverse transcription and quantitative real time PCR

Total RNA was isolated using the RNeasy mini kit (Qiagen) with 15 min of DNase I (Qiagen) treatment according to the manufacturer's protocol. For RT-qPCR analyses, depending on the experiment between 200 ng and 1000 ng RNA was Reverse-Transcribed using the High Capacity Retrotranscription kit (Applied Biosystems). Quantitative PCR was performed using SYBR Green PCR Master Mix (Applied Biosystems) using primers listed in Table 1. We used as housekeeping genes, the *Rn18S* (other named 18S), *Rplp0* (other named 36b4) and RPS17 genes, depending on the experiment. The relative mRNA levels were calculated using the $2^{-\Delta\Delta Ct}$ method (Livak and Schmittgen, 2001). The ΔCt values were obtained by calculating the differences: $Ct_{\text{gene of interest}} - Ct_{\text{housekeeping gene}}$ in each sample. $\Delta\Delta Ct$ values were obtained by calculating the differences between ΔCt (Experimental condition) and the average of $\Delta Ct_{\text{control}}$ values. The *Rn18S*, *Rplp0* and Rps17 genes did not show any variation in the different experimental conditions.

Regarding our experiments quantifying gene expression levels, the *Rplp0* gene is detected around a Ct (threshold cycle) of 19.5 for 250 ng of RNA and around an 18 Ct of 18.5 Ct for 500 ng of RNA. This result is consistent with the log2-linear plot of the PCR signal. A decrease of one cycle corresponds to a fold-2 increase of RNA (Livak and Schmittgen, 2001). The *Rn18S* gene was detected around 7.5 Ct for 500 ng of RNA. For the analysis of the relative mRNA levels of cells cultured in classic culture plates (plastic substrate) or

Uniflex Flexcell plates (silicone substrate) over time, the values of the T0 time points were considered as controls and were normalized to 1. For the relative mRNA level analysis in TGFβ2-treated cells, the cells in the absence of TGFβ2 supplementation were considered as controls and were normalized to 1. For the absolute quantification of gene expression, 16H after plating 10⁵ cells, we used 2^{-ΔCt} × 10³ against the *Rplp0* house keeping gene from 250 ng of RNA (plastic substrate); 2^{-ΔCt} × 10³ against the *Rn18S* house keeping gene from 500 ng of RNA (plastic substrate) and 2^{-ΔCt} × 10⁴ against the *Rplp0* house keeping gene from 500 ng of RNA (silicone substrate).

Gene	Forward primer	Reverse primer	Species	Accession no.
<i>Acan</i>	5-CGCTGCAGTGATCTCAGAAGAAGT-3	5-TCACGCTCAGTGAGTTGTCATGGT-3	Mus musculus	NM_001361500.1
<i>ACAN</i>	5-CGCTGCAGTGATCTCAGAAGAAGT-3	5-TCACGCTCAGTGAGTTGTCATGGT-3	Gallus gallus	NM_204955.2
<i>Acta2</i>	5-ACCCACCCAGAGTGGAGAAG-3	5-TACAGAGCCAGAGCCATTG-3	Mus musculus	NM_007392.3
<i>ACTA2</i>	5-TGCTCCAAGAGCAGTTTTCC-3	5-CCCATAACCAACCATCACACC-3	Gallus gallus	XM_015288391.2
<i>Aqp1</i>	5-CAATTCACCTGGCCGAATGACCT-3	5-TACCAGCTGCAGAGTGCCAATGAT-3	Mus musculus	NM_007472.2
<i>Bglap</i>	5-GCCTTCATGTCCAAGCAGA-3	5-GCGCCGAGCTCTGTCTACTA-3	Mus musculus	NM_007541.2
<i>Cebpb</i>	5-CGCCTTTAGACCCATGGAAAG-3	5-AGGCAGTCGGGCTCGTAGTAG-3	Mus musculus	NM_009883
<i>Col1a1</i>	5-TGGAGAGAGCATGACCGATG-3	5-GAGCCCTCGCTTCCGTA-3	Mus musculus	NM_007742
<i>Col1a2</i>	5-CCAGCGAAGAAGCTCATAAC-3	5-GGACACCCCTTCTACGTTGT-3	Mus musculus	NM_007743.3
<i>COL1A2</i>	5-GCAGTAACTTCATACCTAGCAACAAGC-3	5-TGCAGATCCCTCACATG-3	Gallus gallus	NM_204426.1
<i>Col2a1</i>	5-GGGCAACAGCAGGTTTACA-3	5-TGTTTCGTGCAGCCATCCT-3	Mus musculus	NM_001113515.2
<i>COL2A1</i>	5-AGATTACTGGATTGACCCGAACC-3	5-ACTTTGTATGGCGTCCAAGGT-3	Gallus gallus	NM_204426.1
<i>Ctgf</i>	5-GTGTGCACTGCCAAGATGG-3	5-TGCTTTGGAAGGACTCACCG-3	Mus musculus	NM_010217.2
<i>Cyr61</i>	5-TCTGTGAAGTGCCTCCTTGT-3	5-CTGGTTCTGGGATTCTTG-3	Mus musculus	NM_010516.2
<i>Dlx5</i>	5-CGTCTCAGGAATCGCCAACT-3	5-AGTCAGAATCGGTGGCCG-3	Mus musculus	NM_198854
<i>Egr1</i>	5-CAGCGCCTCAATCCTCAAG-3	5-GCGATGTCAGAAAAGGACTCTGT-3	Gallus gallus	NM_007913.5
<i>EGR1</i>	5-CGGCAGACACTTTTCTGAG-3	5-CTGGTTTCTGGCATGGTTTTCT-3	Gallus gallus	NM_204136.2
<i>INHBA</i>	5-TTGTGGAGCAAACCTCAGAA-3	5-CTGATAATTCGCTGCCTTCC-3	Gallus gallus	NM_205396.1
<i>MRTFA</i>	5-GAATTGCACTTTGCTCACGA-3	5-TCAGCCAGATCCAAGGCTAT-3	Gallus gallus	XM_416243.6
<i>MYF5</i>	5-ACCAGAGACTCCCCAAGTG-3	5-TCGATGTACCTGATGGCGTT-3	Gallus gallus	NM_001030363.1
<i>Myog</i>	5-CACTGGAGTTCGGTCCCAAC -3	5-TGGGCGTCTGTAGGGTCA-3	Mus musculus	NM_031189.2
<i>PAX7</i>	5-AGAAGAAGGCCAAGCACAGCATAG-3'	5-ATTCGACATCGGAGCCTTCATCCA-3'	Gallus gallus	NM_205065.1
<i>Pparg</i>	5-TCGCTGATGCACTGCCTATG-3	5-GAGAGGTCCACAGAGCTGATT-3	Mus musculus	NM_011146
<i>Rn18S</i>	5-GGCGACGACCCATTCCG-3	5-ACCCGTGGTCAACATGGTA-3	Mus musculus	NR_003278.3
<i>RPS17</i>	5-TGCCTGAGCGGAGGAGCAAACA-3	5-ACCTGGTTCCTGCACAGGGCTT-3	Gallus gallus	NM_204217.1
<i>Rplp0</i>	5-ACCTCCTTCTTCCAGCTTT-3	5-CTCCACCTTGTCTCCAGTC-3	Mus musculus	NM_007475.5
<i>Runx2</i>	5-GGTCCCCGGGAACCAA-3	5-GGCGATCAGAGAACAACTAGGTTT-3	Mus musculus	NM_001145920
<i>Scx</i>	5-CCTTCTGCCTCAGCAACCAG-3	5-GGTCAAAGTGGGGCTCTCCGTGACT-3	Mus musculus	NM_198885.3
<i>SCX</i>	5-CACCAACAGCGTCAACACC-3	5-CGTCTGCATCTTGACAGC-3	Gallus gallus	NM_204253.1
<i>Smad7</i>	5-CAGCACTGCCAAGCATGGT-3	5-ACCGAAACGCTGATCCAAAG-3	Mus musculus	NM_001042660.1
<i>Sox9</i>	5- AGTACCCGCATCTGCACAAC-3	5-CCTCCACGAAGGGTCTCTTCT-3	Mus musculus	NM_011448.4
<i>SOX9</i>	5-AGACGCTGGCAAGCTGT-3	5-AGGGACGCTTCTCGCTCTC-3	Gallus gallus	NM_204281.1
<i>Srf</i>	5-CACCTACCAGGTGTCGAAT-3	5-GCTGTCTGGATTGTGAGGT-3	Mus musculus	NM_020493.2
<i>SRF</i>	5-CCGACCTTCACTGTACCAA-3	5-CCGTCTGGATGGTGGATGTT-3	Gallus gallus	NM_001252141.1
<i>Tgfb2</i>	5-GAATAAAAGCGAAGAGCTCGAGG-3	5-GAGGTGCCATCAATACCTGCA-3	Mus musculus	NM_009367
<i>Thbs2</i>	5-AGGTGCATCTCGAGAGTCACTTCA-3	5-CTGCAAAACAGAGATGGACATTCTGC-3	Mus musculus	NM_011581.3
<i>Tnmd</i>	5-AACACTTCTGGCCGAGGTAT-3	5-AGTGTGCTCCATGTCTATAGGTTT-3	Mus musculus	NM_022322.2
<i>TNMD</i>	5-ACTACAGAGGCCAAGATCCCTG-3	5-GCTCAAAGTAGGTGGTGGTGATT-3	Gallus gallus	NM_206985.2
<i>Vcl</i>	5-TGGCACATCTGACCTACTGC-3	5-TTCCACTACCTCTGCCACTG-3	Mus musculus	NM_009502.5
<i>VCL</i>	5-GCTGGCTGAGAGATCCAAAC-3	5-CTGCCTTATTGCTTGTCTACC-3	Gallus gallus	NM_205441.2
<i>Yap1</i>	5-AGGAGAGACTGCGTTGAAA-3	5-CGCAGAGCTAATCTCTGACA-3	Mus musculus	NM_001171147.1
<i>YAP1</i>	5-ATGGAGAAGGAAAGGCTGAG-3	5-GGAGATGATACGGGATTTTGGAG-3	Gallus gallus	NM_205243.1

Table VIII.1: RT-qPCR primers

In situ hybridization and immunostaining

For in situ hybridization, on paraffin-embedded tissue sections, limbs of chicken fetuses were fixed overnight at 4°C in 60% ethanol, 30% formaldehyde at 37% and 10% acetic acid and further processed as previously described (Orgeur et al., 2018). For whole-mount in situ hybridization, chick embryos were fixed overnight at 4°C with 4% formaldehyde in 1X PBS and processed as previously described (Orgeur et al., 2018). The following digoxigenin-labeled mRNA probes were used: chicken SCX (Bonnin et al., 2005), chicken COL1A1 (produced

from EST clones from ARK Genomics), chicken TNMD (Havis et al., 2016), chicken EGR1 (Léjard et al., 2011), chicken SOX9 and chicken ACAN (produced from EST clones from ARK Genomics). For limbs of chicken fetuses, experimental and control limbs were positioned in the same orientation for transverse sectioning to allow comparison.

For immunostaining on sections, samples were fixed in a 4% paraformaldehyde solution in PBS supplemented with 4% sucrose and 0.1 mM CaCl₂, rinsed in PBS, embedded in a 15% sucrose solution, frozen in chilled isopentane before cryostat sectioning at 16µm. Sections were collected on Superfrost/Plus slides (CML, France) and processed for immunostaining. For immunostaining, the following primary antibodies were used: EGR1 (1:200, Protein-Tech), Ki67 (1:100, Invitrogen), P-Smad1/5/8 (1:200, Cell Signalling), SCX (1:500, Abcam), TNMD (1:500, Abcam), YAP (1:100, Santa Cruz). Immunolabelings were performed using secondary antibodies conjugated to Alexa Fluor 488 and 555 (1:200, Invitrogen). Nuclei were stained using DAPI (1:1000, Sigma). Actin fibers were stained using Phalloidin 488 (1:100, Life Technologies). Stained tissue sections were observed with Zeiss Apotome using the ZEN software (Zeiss Microscopy).

Image analysis

All image analyses were carried out using the ImageJ software.

Statistical analysis

Results are shown as means +/- standard deviation (SD). The exact number of independent biological samples (4 to 6) is reported for each experiment. RT-q-PCR data were analyzed with the non-parametric Mann-Whitney test with GraphPad Prism V6. The asterisks in histograms indicate p values that was considered significant, *<0.05, **<0.01, ***<0.001, ****<0.0001.

IX. References

Abo-Aziza, F.A.-A.M., and Zaki, A.E.-K.A. (2016). The Impact of Confluence on BMMSC Proliferation and Osteogenic Differentiation. *Int. J. Hematol. Stem Cell Res.* 0.

Akiyama, H., Chaboissier, M.C., Martin, J.F., Schedl, A., and De Crombrughe, B. (2002). The transcription factor Sox9 has essential roles in successive steps of the chondrocyte differentiation pathway and is required for expression of Sox5 and Sox6. *Genes Dev.* 16, 2813–2828.

Alberton, P., Popov, C., Prägert, M., Kohler, J., Shukunami, C., Schieker, M., and Docheva, D. (2012). Conversion of Human Bone Marrow-Derived Mesenchymal Stem Cells into Tendon Progenitor Cells by Ectopic Expression of Scleraxis. *Stem Cells Dev.* 21, 846–858.

Alberton, P., Dex, S., Popov, C., Shukunami, C., Schieker, M., and Docheva, D. (2015). Loss of Tenomodulin Results in Reduced Self-Renewal and Augmented Senescence of Tendon Stem/Progenitor Cells. *Stem Cells Dev.* 24, 597–609.

Alberts, B., and Johnson, A. (2007). *Molecular Biology of the Cell* (Garland Sciences - Taylor and Francis Group).

Anderson, D.M., Arredondo, J., Hahn, K., Valente, G., Martin, J.F., Wilson-Rawls, J., and Rawls, A. (2006). Mohawk is a novel homeobox gene expressed in the developing mouse embryo. *Dev. Dyn.* 235, 792–801.

Anderson, D.M., Beres, B.J., Wilson-Rawls, J., and Rawls, A. (2009). The homeobox gene Mohawk represses transcription by recruiting the Sin3A/HDAC co-repressor complex. *Dev. Dyn.* 238, 572–580.

Anderson, D.M., George, R., Noyes, M.B., Rowton, M., Liu, W., Jiang, R., Wolfe, S. a., Wilson-Rawls, J., and Rawls, A. (2012). Characterization of the DNA-binding properties of the Mohawk homeobox transcription factor. *J. Biol. Chem.* 287, 35351–35359.

Andersson, T., Eliasson, P., Hammerman, M., Sandberg, O., and Aspenberg, P. (2012). Low-level mechanical stimulation is sufficient to improve tendon healing in rats. *J. Appl. Physiol.* 113, 1398–1402.

Aragona, M., Panciera, T., Manfrin, A., Giulitti, S., Michielin, F., Elvassore, N., Dupont, S., and Piccolo, S. (2013). A mechanical checkpoint controls multicellular growth through YAP/TAZ regulation by actin-processing factors. *Cell* 154, 1047–1059.

Asparuhova, M.B., Ferralli, J., Chiquet, M., and Chiquet-Ehrismann, R. (2011). The transcriptional regulator megakaryoblastic leukemia-1 mediates serum response factor-independent activation of tenascin-C transcription by mechanical stress. *FASEB J.* 25, 3477–3488.

Assis-Ribas, T., Forni, M.F., Winnischofer, S.M.B., Sogayar, M.C., and Trombetta-Lima,

M. (2018). Extracellular Matrix dynamics during Mesenchymal Stem Cells Differentiation. *Dev. Biol.*

Bahrani, S., and Drabløs, F. (2016). Gene regulation in the immediate-early response process. *Adv. Biol. Regul.* 62, 37–49.

Barsby, T., Bavin, E.P., and Guest, D.J. (2014). Three-Dimensional Culture and Transforming Growth Factor Beta3 Synergistically Promote Tenogenic Differentiation of Equine Embryo-Derived Stem Cells. *Tissue Eng. Part A* 20, 2604–2613.

Baudequin, T., Gaut, L., Mueller, M., Huepkes, A., Glasmacher, B., Duprez, D., Bedoui, F., and Legallais, C. (2017). The Osteogenic and Tenogenic Differentiation Potential of C3H10T1/2 (Mesenchymal Stem Cell Model) Cultured on PCL / PLA Electrospun Scaffolds in the Absence of Specific Differentiation Medium. *Materials (Basel)*. 2, 1–19.

Bayer, M.L., Yeung, C.Y.C., Kadler, K.E., Qvortrup, K., Baar, K., Svensson, R.B., Peter Magnusson, S., Krogsgaard, M., Koch, M., and Kjaer, M. (2010). The initiation of embryonic-like collagen fibrillogenesis by adult human tendon fibroblasts when cultured under tension. *Biomaterials* 31, 4889–4897.

Bayer, M.L., Schjerling, P., Herchenhan, A., Zeltz, C., Heinemeier, K.M., Christensen, L., Krogsgaard, M., Gullberg, D., and Kjaer, M. (2014). Release of tensile strain on engineered human tendon tissue disturbs cell adhesions, changes matrix architecture, and induces an inflammatory phenotype. *PLoS One* 9.

Bays, J.L., Peng, X., Tolbert, C.E., Guilluy, C., Angell, A.E., Pan, Y., Superfine, R., BurrIDGE, K., and DeMali, K.A. (2014). Vinculin phosphorylation differentially regulates mechanotransduction at cell-cell and cell-matrix adhesions. *J. Cell Biol.* 205, 251–263.

Bays, J.L., Campbell, H.K., Heidema, C., Sebbagh, M., and Demali, K.A. (2017). Linking E-cadherin mechanotransduction to cell metabolism through force-mediated activation of AMPK. *Nat. Cell Biol.* 19, 724–731. Becker, S., Pasca, G., Strumpf, D., Min, L., and Volk, T. (1997). Reciprocal signaling between *Drosophila* epidermal muscle attachment cells and their corresponding muscles. *Development* 124, 2615–2622.

Bellas, E., and Chen, C.S. (2014). Forms , forces , and stem cell fate. *Curr. Opin. Cell Biol.* 31, 92–97. Belousov, L. V., Dorfman, J.G., and Cherdantzev, V.G. (1975). Mechanical stresses and morphological patterns in amphibian embryos. *J. Embryol. Exp. Morphol.* 34, 559–574.

Benjamin, M., and Ralphs, J.R. (2000). The Cell and Developmental Tendons and Ligaments. *Int. Rev. Cytol.* Benjamin, M., Kumai, T., Milz, S., Boszczyk, B.M., Boszczyk, A.A., and Ralphs, J.R. (2002). The skeletal attachment of tendons — tendon ‘ entheses ’ *Comp. Biochem. Physiol.* 133, 931–945.

Berasi, S.P., Varadarajan, U., Archambault, J., Cain, M., Souza, T.A., Abouzeid, A., Li, J., Brown, C.T., Dorner, A.J., J. Seeherman, H., et al. (2011). Divergent activities of osteogenic BMP2, and tenogenic BMP12 and BMP13 independent of receptor binding affinities. *Growth Factors* 29, 128–139.

Berendsen, A.D., and Olsen, B.R. (2015). Bone development. *Bone* 80, 14–18.

ten Berge, D., Brugmann, S. a, Helms, J. a, and Nusse, R. (2008). Wnt and FGF

signals interact to coordinate growth with cell fate specification during limb development. *Development* 135, 3247–3257.

Bertet, C., Sulak, L., and Lecuit, T. (2004). Myosin-dependent junction remodeling controls planar cell intercalation and axis elongation. *Nature* 429, 667–671.

Berthet, E., Chen, C., Butcher, K., Schneider, R. a, Alliston, T., and Amirtharajah, M. (2013). Smad3 binds Scleraxis and Mohawk and regulates tendon matrix organization. *J. Orthop. Res.* 31, 1475–1483.

Bi, Y., Ehreichiou, D., Kilts, T.M., Inkson, C. a, Embree, M.C., Sonoyama, W., Li, L., Leet, A.I., Seo, B.-M., Zhang, L., et al. (2007). Identification of tendon stem/progenitor cells and the role of the extracellular matrix in their niche. *Nat. Med.* 13, 1219–1227.

Bianco, P. (2014). “Mesenchymal” Stem Cells. *Annu. Rev. Cell Dev. Biol.* 30, 677–704.

Biressi, S., Molinaro, M., and Cossu, G. (2007). Cellular heterogeneity during vertebrate skeletal muscle development. *Dev. Biol.* 308, 281–293.

Blitz, E., Viukov, S., Sharir, A., Shwartz, Y., Galloway, J.L., Pryce, B. a, Johnson, R.L., Tabin, C.J., Schweitzer, R., and Zelzer, E. (2009). Bone ridge patterning during musculoskeletal assembly is mediated through SCX regulation of Bmp4 at the tendon-skeleton junction. *Dev. Cell* 17, 861–873.

Blitz, E., Sharir, A., Akiyama, H., and Zelzer, E. (2013). Tendon-bone attachment unit is formed modularly by a distinct pool of Scx- and Sox9-positive progenitors. *Development* 140, 2680–2690.

Bober, E., Franz, T., Arnold, H., Gruss, P., and Tremblay, P. (1994). Pax-3 is required for the development of limb muscles: a possible role for the migration of dermomyotomal muscle progenitor cells. *Development* 120, 603–612.

Boccaccio, A., Frassanito, M.C., Lamberti, L., Brunelli, R., Maulucci, G., Monaci, M., Papi, M., Pappalettere, C., Parasassi, T., Sylla, L., et al. (2012). Nanoscale characterization of the biomechanical hardening of bovine zona pellucida. *J. R. Soc. Interface* 9, 2871–2882.

Bökel, C., and Brown, N.H. (2002). Integrins in development: Moving on, responding to, and sticking to the extracellular matrix. *Dev. Cell* 3, 311–321.

Bonnin, M.-A., Laclef, C., Blaise, R., Eloy-Trinquet, S., Relaix, F., Maire, P., and Duprez, D. (2005). Six1 is not involved in limb tendon development, but is expressed in limb connective tissue under Shh regulation. *Mech. Dev.* 122, 573–585.

Boselli, F., Steed, E., Freund, J.B., and Vermot, J. (2017). Anisotropic shear stress patterns predict the orientation of convergent tissue movements in the embryonic heart. *Development* 144, 4322–4327. Boskey, A.L., Wians, F.H., and Hauschka, P. V. (1985). The effect of osteocalcin on In vitro lipid-induced hydroxyapatite formation and seeded hydroxyapatite growth. *Calcif. Tissue Int.* 37, 57–62.

Bottagisio, M., Lopa, S., Granata, V., Talò, G., Bazzocchi, C., Moretti, M., and Barbara Lovati, A. (2017). Different combinations of growth factors for the tenogenic differentiation of bone marrow mesenchymal stem cells in monolayer culture and in fibrin-based three-dimensional constructs. *Differentiation* 95, 44–53.

Bradham, D.M., Igarashi, A., Potter, R.L., and Grotendorst, G.R. (1991). Connective

tissue growth factor: a cysteine-rich mitogen secreted by human vascular endothelial cells is related to the SRC-induced immediate early gene product CEF-10. *J. Cell Biol.* 114, 1285–1294.

Brand, B., Christ, B., and Jacob, H.J. (1985). An experimental analysis of the developmental capacities of distal parts of avian leg buds. *Am. J. Anat.* 173, 321–340.

Brandau, O., Meindl, A., and Fa, R. (2001). A Novel Gene, *tendin*, Is Strongly Expressed in Tendons and Ligaments and Shows High Homology With. *Dev. Dyn.* 80, 72–80.

Breidenbach, A.P., Dymont, N. a., Lu, Y., Rao, M., Shearn, J.T., Rowe, D.W., Kadler, K.E., and Butler, D.L. (2015). Fibrin Gels Exhibit Improved Biological, Structural, and Mechanical Properties Compared with Collagen Gels in Cell-Based Tendon Tissue-Engineered Constructs. *Tissue Eng. Part A* 21, 438–450.

Brent, A.E., and Tabin, C.J. (2002). Developmental regulation of somite derivatives: muscle, cartilage and tendon. *Curr. Opin. Genet. Dev.* 548–557.

Brent, A.E., and Tabin, C.J. (2004). FGF acts directly on the somitic tendon progenitors through the Ets transcription factors *Pea3* and *Erm* to regulate *scleraxis* expression. *Development* 131, 3885–3896.

Brent, A.E., Schweitzer, R., and Tabin, C.J. (2003). A Somitic Compartment of Tendon Progenitors. *Cell* 113, 235–248.

Brent, A.E., Braun, T., and Tabin, C.J. (2005). Genetic analysis of interactions between the somitic muscle, cartilage and tendon cell lineages during mouse development. *Development* 132, 515–528.

Brown, J.P., Finley, V.G., and Kuo, C.K. (2014). Embryonic mechanical and soluble cues regulate tendon progenitor cell gene expression as a function of developmental stage and anatomical origin. *J. Biomech.* 47, 214–222.

Brown, J.P., Galassi, T. V, Stoppato, M., Schiele, N.R., and Kuo, C.K. (2015). Comparative analysis of mesenchymal stem cell and embryonic tendon progenitor cell response to embryonic tendon biochemical and mechanical factors. *Stem Cell Res. Ther.* 6, 1–8.

Brunet, T., Bouclet, A., Ahmadi, P., Mitrossilis, D., Driquez, B., Brunet, A.-C., Henry, L., Serman, F., Béalle, G., Ménager, C., et al. (2013). Evolutionary conservation of early mesoderm specification by mechanotransduction in Bilateria. *Nat. Commun.* 4, 1–15.

Buckingham, M. (2017). Gene regulatory networks and cell lineages that underlie the formation of skeletal muscle. *Proc. Natl. Acad. Sci.* 114, 5830–5837.

Buckingham, M., and Mayeuf, A. (2012). *Skeletal muscle development* (Elsevier Inc.).

Buckingham, M., and Rigby, P.W.J. (2014). Gene regulatory networks and transcriptional mechanisms that control myogenesis. *Dev. Cell* 28, 225–238.

Butler, D.L., Grood, E.S., and Noyes, F.R. (1978). Biomechanics of Ligaments and Tendons. *Exerc. Sport Sci. Rev.* 6, 125–182.

Caplan, A. (1991). Mesenchymal stem cells. *J. Orthop. Res.* 9, 641–650.

Caplan, A.I., and Correa, D. (2011). The MSC: An injury drugstore. *Cell Stem Cell* 9, 11–15.

Chai, Y., Jiang, X., Ito, Y., Bringas, P., Han, J., Rowitch, D.H., Soriano, P., McMahon, A.P., and Sucov, H.M. (2000). Fate of the mammalian cranial neural crest during tooth and mandibular morphogenesis. *Development* 127, 1671–1679. Charras, G., and Yap, A.S. (2018). Tensile Forces and Mechanotransduction at Cell – Cell Junctions. *Curr. Biol.* 28, 445–457.

Charvet, B., Ruggiero, F., and Le Guellec, D. (2012). The development of the myotendinous junction. A review. *Muscles. Ligaments Tendons J.* 2, 53–63.

Charvet, B., Guiraud, A., Malbouyres, M., Zwolanek, D., Guillon, E., Bretaud, S., Monnot, C., Schulze, J., Bader, H.L., Allard, B., et al. (2013). Knockdown of *col22a1* gene in zebrafish induces a muscular dystrophy by disruption of the myotendinous junction. *Development* 140, 4602–4613.

Chen, J.W., and Galloway, J.L. (2014). The development of zebrafish tendon and ligament progenitors. *Development* 141, 2035–2045.

Chen, C.-H., Marymont, J. V, Huang, M.-H., Geyer, M., Luo, Z.-P., and Liu, X. (2007a). Mechanical strain promotes fibroblast gene expression in presence of corticosteroid. *Connect. Tissue Res.* 48, 65–69.

Chen, W.-S., Cao, Z., Krishnan, C., and Panjwani, N. (2015a). Verteporfin without light stimulation inhibits YAP activation in trabecular meshwork cells: Implications for glaucoma treatment. *Biochem. Biophys. Res. Commun.* 466, 221–225.

Chen, W., Deng, Y., Zhang, J., and Tang, K. (2015b). Uniaxial repetitive mechanical overloading induces influx of extracellular calcium and cytoskeleton disruption in human tenocytes. *Cell Tissue Res.* 359, 577–587.

Chen, X., Macica, C.M., Dreyer, B.E., Hammond, V.E., Hens, J.R., Philbrick, W.M., and Broadus, A.E. (2006). Initial characterization of PTH-related protein gene-driven lacZ expression in the mouse. *J. Bone Miner. Res.* 21, 113–123.

Chen, X., Macica, C., Nasiri, A., Judex, S., and Broadus, A.E. (2007b). Mechanical regulation of PTHrP expression in entheses. *Bone* 41, 752–759.

Chevallier, B.A., Kieny, M., and Mauger, A. (1977). Limb-somite relationship: origin of the limb musculature. *J. Embryol. Exp. Morph.* 41, 245–258.

Chien, C., Pryce, B., Tufa, S.F., Keene, D.R., and Huang, A.H. (2017). Optimizing a 3D model system for molecular manipulation of tenogenesis. *Connect. Tissue Res.* 1–14.

Christ, B., and Ordahl, C.P. (1995). Early stages of chick somite development. *Anat. Embryol. (Berl)*. 191, 381–396.

Christ, B., Jacob, H.J., and Jacob, M. (1979). Differentiating abilities of avian somatopleural mesoderm. *Experientia* 569, 1376–1378.

Christy, B.A., Lau, L.F., and Nathans, D. (1988). A gene activated in mouse 3T3 cells by serum growth factors encodes a protein with “zinc finger” sequences. *Proc. Natl. Acad. Sci. U. S. A.* 85, 7857–7861.

Chuang, H.-N., Cheng, H.-Y., Hsiao, K.-M., Lin, C.-W., Lin, M.-L., and Pan, H. (2010). The zebrafish homeobox gene *irx11* is required for brain and pharyngeal arch morphogenesis. *Dev. Dyn.* 239, 639–650.

Chuang, H.-N., Hsiao, K.-M., Chang, H.-Y., Wu, C.-C., and Pan, H. (2014). The home-

obox transcription factor *Irx11* negatively regulates *MyoD* expression and myoblast differentiation. *FEBS J.* 281, 2990–3003.

Collard, L., Herledan, G., Pincini, A., Guerci, A., Randrianarison-Huetz, V., and Sotiropoulos, A. (2014). Nuclear actin and myocardin-related transcription factors control disuse muscle atrophy through regulation of *Srf* activity. *J. Cell Sci.* 127, 5157–5163.

Colnot, C., de la Fuente, L., Huang, S., Hu, D., Chuangyong, L., St-Jacques, B., and Helms, J.A. (2005). Indian hedgehog synchronizes skeletal angiogenesis and perichondrial maturation with cartilage development. *Development* 132, 1057–1067.

Conheim, J. (1867). Ueber Entzündung und Eiterung. *Arch. Für Pathol. Anat. Und Physiol. Und Für Klin. Med.* 40.

Corrigan, M.A., Johnson, G.P., Stavenschi, E., Riffault, M., Labour, M.N., and Hoey, D.A. (2018). TRPV4-mediates oscillatory fluid shear mechanotransduction in mesenchymal stem cells in part via the primary cilium. *Sci. Rep.* 8, 1–13.

Crane, J.F., and Trainor, P. a (2006). Neural crest stem and progenitor cells. *Annu. Rev. Cell Dev. Biol.* 22, 267–286.

Crisan, M., Yap, S., Casteilla, L., Chen, C.W., Corselli, M., Park, T.S., Andriolo, G., Sun, B., Zheng, B., Zhang, L., et al. (2008). A Perivascular Origin for Mesenchymal Stem Cells in Multiple Human Organs. *Cell Stem Cell* 3, 301–313.

Cristancho, A.G., and Lazar, M.A. (2011). Forming functional fat: a growing understanding of adipocyte differentiation. *Nat. Rev. Mol. Cell Biol.* 12, 722–734.

D’Arcy, W.T. (1945). *On Growth and Form* (University Press of Cambridge & The Macmillan Company of New York). D’Souza, D., and Patel, K. (1999). Involvement of long- and short-range signalling during early tendon development. *Anat. Embryol. (Berl.)* 200, 367–375.

Darabid, H., Perez-Gonzalez, A.P., and Robitaille, R. (2014). Neuromuscular synaptogenesis: Coordinating partners with multiple functions. *Nat. Rev. Neurosci.* 15, 703–718.

DeLise, A.M., Fischer, L., and Tuan, R.S. (2000). Cellular interactions and signaling in cartilage development. *Osteoarthr. Cartil.* 8, 309–334.

Desprat, N., Supatto, W., Pouille, P.A., Beaurepaire, E., and Farge, E. (2008). Tissue Deformation Modulates Twist Expression to Determine Anterior Midgut Differentiation in *Drosophila* Embryos. *Dev. Cell* 15, 470–477. Devkota, A.C., and Weinhold, P.S. (2003). Mechanical response of tendon subsequent to ramp loading to varying strain limits. *Clin. Biomech.* 18, 969–974.

Dex, S., Lin, D., Shukunami, C., and Docheva, D. (2016). Tenogenic modulating insider factor: Systematic assessment on the functions of tenomodulin gene. *Gene*.

Dex, S., Alberton, P., Willkomm, L., Söllradl, T., Bago, S., Milz, S., Shakibaei, M., Ignatius, A., Bloch, W., Clausen-Schaumann, H., et al. (2017). Tenomodulin is Required for Tendon Endurance Running and Collagen I Fibril Adaptation to Mechanical Load. *EBioMedicine* 20, 240–254.

Dhein, S., Schreiber, A., Steinbach, S., Apel, D., Salameh, A., Schlegel, F., Kostelka, M., Dohmen, P.M., and Mohr, F.W. (2014). Mechanical control of cell biology. Effects of cyclic

mechanical stretch on cardiomyocyte cellular organization. *Prog. Biophys. Mol. Biol.* 1–10.

DiMarino, A.M., Caplan, A.I., and Bonfield, T.L. (2013). Mesenchymal stem cells in tissue repair. *Front. Immunol.* 4, 1–9.

Discher, D.E., Mooney, D.J., and Zandstra, P.W. (2009). Growth factors, matrices, and forces combine and control stem cells. *Science* (80-.). 324, 1673–1677.

Docheva, D., Hunziker, E.B., Fa, R., and Brandau, O. (2005). Tenomodulin Is Necessary for Tenocyte Proliferation and Tendon Maturation. *Mol. Cell. Biol.* 25, 699–705.

Docheva, D., Müller, S. a., Majewski, M., and Evans, C.H. (2015). Biologics for tendon repair. *Adv. Drug Deliv. Rev.* 84, 222–239.

Donnelly, E., Ascenzi, M.G., and Farnum, C. (2010). Primary cilia are highly oriented with respect to collagen direction and long axis of extensor tendon. *J. Orthop. Res.* 28, 77–82.

Drachman, D.B., and Sokoloff, L. (1966). The role of movement in embryonic joint development. *Dev. Biol.* 14, 401–420.

Ducy, P., Zhang, R., Geoffroy, V., Ridall, A.L., and Karsenty, G. (1997). *Osf2/Cbfa1*: A transcriptional activator of osteoblast differentiation. *Cell* 89, 747–754.

Ducy, P., Starbuck, M., Priemal, M., Shen, J., and Karsenty, G. (1999). A *Cbfa1*-dependent genetic pathway control bone formation beyond embryonic development. *Genes Dev.* 13, 1025–1036.

Dupin, E., and Le Douarin, N. (2014). The neural crest, a multifaceted structure of the vertebrates. *Birth Defects Res. C. Embryo Today.*

Dupont, S., Morsut, L., Aragona, M., Enzo, E., Giulitti, S., Cordenonsi, M., Zanconato, F., Le Digabel, J., Forcato, M., Bicciato, S., et al. (2011). Role of YAP/TAZ in mechanotransduction. *Nature* 474, 179–183.

Dzamba, B.J., Jakab, K.R., Marsden, M., Schwartz, M.A., and DeSimone, D.W. (2009). Cadherin Adhesion, Tissue Tension, and Noncanonical Wnt Signaling Regulate Fibronectin Matrix Organization. *Dev. Cell* 16, 421–432.

Edom-Vovard, F., and Duprez, D. (2004). Signals regulating tendon formation during chick embryonic development. *Dev. Dyn.* 229, 449–457.

Edom-Vovard, F., Bonnin, M.A., and Duprez, D. (2001). *Fgf8* transcripts are located in tendons during embryonic chick limb development. *Mech. Dev.* 108, 203–206.

Edom-Vovard, F., Schuler, B., Bonnin, M.-A., Teillet, M.-A., and Duprez, D. (2002). *Fgf4* Positively Regulates scleraxis and Tenascin Expression in Chick Limb Tendons. *Dev. Biol.* 247, 351–366.

Ehrlicher, A.J., Nakamura, F., Hartwig, J.H., Weitz, D.A., and Stossel, T.P. (2011). Mechanical strain in actin networks regulates FilGAP and integrin binding to filamin A. *Nature* 478, 260–263.

Eliasson, P., Fahlgren, A., and Aspenberg, P. (2008). Mechanical load and BMP signaling during tendon repair: a role for follistatin? *Clin. Orthop. Relat. Res.* 466, 1592–1597.

Eliasson, P., Andersson, T., and Aspenberg, P. (2009). Rat Achilles tendon healing: mechanical loading and gene expression. *J. Appl. Physiol.* 107, 399–407.

- Eliasson, P., Andersson, T., and Aspenberg, P. (2012). Influence of a single loading episode on gene expression in healing rat Achilles tendons. *J. Appl. Physiol.* 112, 279–288.
- Eliasson, P., Andersson, T., Hammerman, M., and Aspenberg, P. (2013). Primary gene response to mechanical loading in healing rat Achilles tendons. *J. Appl. Physiol.* 114, 1519–1526.
- Eloy-Trinquet, S., Wang, H., Edom-Vovard, F., and Duprez, D. (2009). Fgf signaling components are associated with muscles and tendons during limb development. *Dev. Dyn.* 238, 1195–1206.
- Endo, T. (2015). Molecular mechanisms of skeletal muscle development, regeneration, and osteogenic conversion. *Bone* 80, 2–13.
- Engler, A.J., Sen, S., Sweeney, H.L., and Discher, D.E. (2006). Matrix Elasticity Directs Stem Cell Lineage Specification. *Cell* 126, 677–689.
- Esnault, C., Stewart, A., Gualdrini, F., East, P., Horswell, S., Matthews, N., and Treisman, R. (2014). Rho-actin signaling to the MRTF coactivators dominates the immediate transcriptional response to serum in fibroblasts. *Genes Dev.* 28, 943–958.
- Esteves de Lima, J., Bonnin, M.-A., Birchmeier, C., and Duprez, D. (2016). Muscle contraction is required to maintain the pool of muscle progenitors via YAP and NOTCH during fetal myogenesis. *Elife* 513–516.
- Evelyn, C.R., Wade, S.M., Wang, Q., Wu, M., Iniguez-Lluhi, J.A., Merajver, S.D., and Neubig, R.R. (2007). CCG-1423: a small-molecule inhibitor of RhoA transcriptional signaling. *Mol. Cancer Ther.* 6, 2249–2260.
- Farge, E. (2003). Mechanical induction of Twist in the Drosophila foregut/stomodaeal primordium. *Curr. Biol.* 13, 1365–1377.
- Felsenthal, N., and Zelzer, E. (2017). Mechanical regulation of musculoskeletal system development. *Development* 144, 4271–4283.
- Fernandez-Gonzalez, R., Simoes, S. de M., Röper, J.C., Eaton, S., and Zallen, J.A. (2009). Myosin II Dynamics Are Regulated by Tension in Intercalating Cells. *Dev. Cell* 17, 736–743.
- Fink, J., Carpi, N., Betz, T., Bétard, A., Chebah, M., Azioune, A., Bornens, M., Sykes, C., Fetler, L., Cuvelier, D., et al. (2011). External forces control mitotic spindle positioning. *Nat. Cell Biol.* 13, 771–778. Forbes, A. (1920). Biophysics. *Science* (80-). 52, 331–332.
- Foster, C.T., Gualdrini, F., and Treisman, R. (2018). Mutual dependence of the MRTF – SRF and YAP – TEAD pathways in cancer-associated fibroblasts is indirect and mediated by cytoskeletal dynamics. *Genes Dev.* 31, 2361–2375.
- Friedenstein, A.J., Piatetzky-Shapiro, I.I., and Petrakova, K. V (1966). Osteogenesis in transplants of bone marrow cells. *J. Embryol. Exp. Morph.* 16, 381–390.
- Friedenstein, A.J., Petrakova, K. V, Kurolesova, A.I., and Frolova, G.P. (1968). Heterotopic Transplants of Bone Marrow - Analysis of Precursor Cells for Osteogenic and Hematopoietic Tissues. *Transplantation* 6, 230–247. Frommer, G., Vorbrüggen, G., Pasca, G., Jäckle, H., and Volk, T. (1996). Epidermal egr-like zinc finger protein of Drosophila participates in myotube guidance. *EMBO J.* 15, 1642–1649.

- Garvin, J., Qi, J., Maloney, M., and Banes, A.J. (2003). Novel system for engineering bioartificial tendons and application of mechanical load. *Tissue Eng.* 9, 967–979.
- Gasiorowski, J.Z., Murphy, C.J., and Nealey, P.F. (2013). Biophysical Cues and Cell Behavior: The Big Impact of Little Things. *Annu. Rev. Biomed. Eng.* 15, 155–176.
- Gaut, L., and Duprez, D. (2016). Tendon development and diseases. *Wiley Interdiscip. Rev. Dev. Biol.* 5, 5–23.
- Gaut, L., Robert, N., Delalande, A., Bonnin, M.-A., Pichon, C., and Duprez, D. (2016). EGR1 Regulates Transcription Downstream of Mechanical Signals during Tendon Formation and Healing. *PLoS One* 11, e0166237.
- Genin, G.M., Kent, A., Birman, V., Wopenka, B., Pasteris, J.D., Marquez, P.J., and Thomopoulos, S. (2009). Functional grading of mineral and collagen in the attachment of tendon to bone. *Biophys. J.* 97, 976–985.
- Gineitis, D., and Treisman, R. (2001). Differential Usage of Signal Transduction Pathways Defines Two Types of Serum Response Factor Target Gene. *J. Biol. Chem.* 276, 24531–24539.
- Goddard, L.M., Duchemin, A.L., Ramalingan, H., Wu, B., Chen, M., Bamezai, S., Yang, J., Li, L., Morley, M.P., Wang, T., et al. (2017). Hemodynamic Forces Sculpt Developing Heart Valves through a KLF2-WNT9B Paracrine Signaling Axis. *Dev. Cell* 43, 274–289.e5.
- Gordon, J.A., Freedman, B.R., Zuskov, A., Iozzo, R. V., Birk, D.E., and Soslowky, L.J. (2015). Achilles tendons from decorin- and biglycan-null mouse models have inferior mechanical and structural properties predicted by an image-based empirical damage model. *J. Biomech.* 48, 2110–2115.
- Govoni, M., Berardi, A.C., Muscari, C., Campardelli, R., Bonafè, F., Guarnieri, C., Reverchon, E., Giordano, E., Maffulli, N., and Della Porta, G. (2017). An Engineered Multiphase Three-Dimensional Microenvironment to Ensure the Controlled Delivery of Cyclic Strain and Human Growth Differentiation Factor 5 for the Tenogenic Commitment of Human Bone Marrow Mesenchymal Stem Cells. *Tissue Eng. Part A* 23, 811–822.
- Grannas, K., Arngården, L., Lönn, P., Mazurkiewicz, M., Blokzijl, A., Zieba, A., and Söderberg, O. (2015). Crosstalk between Hippo and TGF β : Subcellular Localization of YAP/TAZ/Smad Complexes. *J. Mol. Biol.* 427, 3407–3415.
- Grenier, J., Teillet, M.-A., Grifone, R., Kelly, R.G., and Duprez, D. (2009). Relationship between neural crest cells and cranial mesoderm during head muscle development. *PLoS One* 4, e4381.
- Gros, J., Scaal, M., and Marcelle, C. (2004). A two-Step mechanism for myotome formation in chick. *Dev. Cell* 6, 875–882.
- Gros, J., Manceau, M., Thomé, V., and Marcelle, C. (2005). A common somitic origin for embryonic muscle progenitors and satellite cells. *Nature* 435, 954–958.
- Guerquin, M., Charvet, B., Nourissat, G., Havis, E., Ronsin, O., Bonnin, M., Ruggiu, M., Olivera-martinez, I., Robert, N., Lu, Y., et al. (2013). Transcription factor EGR1 directs tendon differentiation and promotes tendon repair. *J. Clin. Invest.* 123, 3564–3576.
- Hall, B.K., and Herring, S.W. (1990). Paralysis and growth of the musculoskeletal system

in the embryonic chick. *J. Morphol.* 206, 45–56.

Hall, B.K., and Miyake, T. (1992). The membranous skeleton: the role of cell condensations in vertebrate skeletogenesis. *Anat. Embryol. (Berl)*. 186, 107–124.

Hamamura, K., Weng, Y., Zhao, J., Yokota, H., and Xie, D. (2008). PEG attachment to osteoblasts enhances mechanosensitivity. *Biomed. Mater.* 3, 25017.

Hamant, O., Heisler, M.G., Jönsson, H., Krupinski, P., Uyttewaal, M., Bokov, P., Corson, F., Sahlin, P., Boudaoud, A., Meyerowitz, E.M., et al. (2008). Developmental patterning by mechanical signals in *Arabidopsis*. *Science* (80-.). 322, 1650–1655.

Hamburger, V., Balaban, M., Oppenheim, R., and Wenger, E. (1965). Periodic Motility of Normal and Spinal Chick Embryos Between 8 and 17 Days of Incubation. *J. Exp. Zool.* 159, 1–14.

Han, X., Guo, L., Wang, F., Zhu, Q., and Yang, L. (2014). Contribution of PTHrP to mechanical strain-induced fibrochondrogenic differentiation in entheses of Achilles tendon of miniature pigs. *J. Biomech.* 47, 2406–2414.

Hankemeier, S., Keus, M., Zeichen, J., Jagodzinski, M., Barkhausen, T., Bosch, U., Krettek, C., and Van Griensven, M. (2005). Modulation of proliferation and differentiation of human bone marrow stromal cells by fibroblast growth factor 2: potential implications for tissue engineering of tendons and ligaments. *Tissue Eng.* 11, 41–49.

Harris, A.J. (1981). Embryonic Growth and Innervation of Rat Skeletal Muscles I: Neural Regulation of Muscle Fibre Numbers. 293, 257–277.

Havis, E., Bonnin, M.-A., Olivera-Martinez, I., Nazaret, N., Ruggiu, M., Weibel, J., Durand, C., Guerquin, M.-J., Bonod-Bidaud, C., Ruggiero, F., et al. (2014). Transcriptomic analysis of mouse limb tendon cells during development. *Development* 141, 3683–3696.

Havis, E., Bonnin, M., de Lima, J., Charvet, B., Milet, C., and Duprez, D. (2016). TGF β and FGF promote tendon progenitor fate and act downstream of muscle contraction to regulate tendon differentiation during chick limb development. *Development* 3839–3851.

Heo, J., Lee, S., and Kim, H. (2017). Distal-less homeobox 5 is a master regulator of the osteogenesis of human mesenchymal stem cells. *Int. J. Mol. Med.* 1486–1494.

Hiramatsu, R., Matsuoka, T., Kimura-Yoshida, C., Han, S.W., Mochida, K., Adachi, T., Takayama, S., and Matsuo, I. (2013). External mechanical cues trigger the establishment of the anterior-posterior axis in early mouse embryos. *Dev. Cell* 27, 131–144.

Hoey, D.A., Tormey, S., Ramcharan, S., O'Brien, F.J., and Jacobs, C.R. (2012). Primary cilia-mediated mechanotransduction in human mesenchymal stem cells. *Stem Cells* 30, 2561–2570.

Huang, a. H., Riordan, T.J., Pryce, B., Weibel, J.L., Watson, S.S., Long, F., Lefebvre, V., Harfe, B.D., Stadler, H.S., Akiyama, H., et al. (2015a). Musculoskeletal integration at the wrist underlies modular development of limb tendons. *Development* 2431–2441.

Huang, A.H., Riordan, T.J., Wang, L., Eyal, S., Zelzer, E., Brigande, J. V, and Schweitzer, R. (2013). Repositioning forelimb superficialis muscles: tendon attachment and muscle activity enable active relocation of functional myofibers. *Dev. Cell* 26, 544–551.

Huang, A.H., Lu, H.H., and Schweitzer, R. (2015b). Molecular regulation of tendon cell

fate during development. *J. Orthop. Res.* 33, 800–812.

Huang, J., Wu, S., Barrera, J., Matthews, K., and Pan, D. (2005). The Hippo signaling pathway coordinately regulates cell proliferation and apoptosis by inactivating Yorkie, the *Drosophila* homolog of YAP. *Cell* 122, 421–434.

Huisman, E., Lu, A., McCormack, R.G., and Scott, A. (2014). Enhanced collagen type I synthesis by human tenocytes subjected to periodic in vitro mechanical stimulation. *BMC Musculoskelet. Disord.* 15, 386. Humphrey, J.D., Dufresne, E.R., and Schwartz, M.A. (2014). Mechanotransduction and extracellular matrix homeostasis. *Nat. Publ. Gr.* 1–11.

Hurle, J.M., Ros, M. a., Gañan, Y., Macias, D., Critchlow, M., and Hinchliffe, J.R. (1990). Experimental analysis of the role of ECM in the patterning of the distal tendons of the developing limb bud. *Cell Differ. Dev.* 30, 97–108.

Hutcheson, D.A., Zhao, J., Merrell, A., Haldar, M., and Kardon, G. (2009). Embryonic and fetal limb myogenic cells are derived from developmentally distinct progenitors and have different requirements for β -catenin. *Genes Dev.* 23, 997–1013.

Islam, A., Mbimba, T., Younesi, M., and Akkus, O. (2017). Effects of substrate stiffness on the tenoinduction of human mesenchymal stem cells. *Acta Biomater.* 58, 244–253.

Ito, Y., Toriuchi, N., Yoshitaka, T., Ueno-Kudoh, H., Sato, T., Yokoyama, S., Nishida, K., Akimoto, T., Takahashi, M., Miyaki, S., et al. (2010). The Mohawk homeobox gene is a critical regulator of tendon differentiation. *Proc. Natl. Acad. Sci. U. S. A.* 107, 10538–10542.

Jahan, E., Matsumoto, A., Rafiq, A.M., Hashimoto, R., Inoue, T., Udagawa, J., Sekine, J., and Otani, H. (2014). Fetal jaw movement affects *Ihh* signaling in mandibular condylar cartilage development: The possible role of *Ihh* as mechanotransduction mediator. *Arch. Oral Biol.* 59, 1108–1118.

Jain, N., Mahendran, R., Philp, R., Guy, G.R., Tan, Y.H., and Cao, X. (1996). Casein kinase II associates with *Egr-1* and acts as a negative modulator of its DNA binding and transcription activities in NIH 3T3 cells. *J. Biol. Chem.* 271, 13530–13536.

Jain, N., Iyer, K.V., Kumar, A., and Shivashankar, G. V (2013). Cell geometric constraints induce modular gene-expression patterns via redistribution of HDAC3 regulated by actomyosin contractility. *Proc. Natl. Acad. Sci.* 110, 11349–11354.

James, R., Kumbar, S.G., Laurencin, C.T., Balian, G., and Chhabra, A.B. (2011). Tendon tissue engineering: Adipose-derived stem cell and GDF-5 mediated regeneration using electrospun matrix systems. *Biomed. Mater.* 6. Jelinsky, S.A., Archambault, J., Li, L., and Seeherman, H. (2010). Tendon-Selective Genes Identified from Rat and Human Musculoskeletal Tissues. *J. Orthop. Res.* 289–297.

Ji, Y., Ji, J., Sun, F., Zeng, Y., He, X., Zhao, J., Yu, Y., Yu, S., and Wu, W. (2010). Quantitative proteomics analysis of chondrogenic differentiation of C3H10T1/2 mesenchymal stem cells by iTRAQ labeling coupled with on-line two-dimensional LC/MS/MS. *Mol. Cell. Proteomics* 9, 550–564.

Jiang, C., Shao, L., Wang, Q., and Dong, Y. (2012). Repetitive mechanical stretching modulates transforming growth factor- β induced collagen synthesis and apoptosis in human

patellar tendon fibroblasts. *Biochem. Cell Biol.* 90, 667–674.

Jiang, Y., Shi, Y., He, J., Zhang, Z., Zhou, G., Zhang, W., Cao, Y., and Liu, W. (2016). Enhanced tenogenic differentiation and tendon-like tissue formation by tenomodulin overexpression in murine mesenchymal stem cells. *J. Tissue Eng. Regen. Med.* 4, 524–531.

Joshi, B., Bastiani, M., Strugnell, S.S., Boscher, C., Parton, R.G., and Nabi, I.R. (2012). Phosphocaveolin-1 is a mechanotransducer that induces caveola biogenesis via Egr1 transcriptional regulation. *J. Cell Biol.* 199, 425–435.

Jung, H.-J., Fisher, M.B., and Woo, S.L.-Y. (2009). Role of biomechanics in the understanding of normal, injured, and healing ligaments and tendons. *BMC Sports Sci. Med. Rehabil.* 1, 9.

Kapacee, Z., Richardson, S.H., Lu, Y., Starborg, T., Holmes, D.F., Baar, K., and Kadler, K.E. (2008). Tension is required for fibroblast formation. *Matrix Biol.* 27, 371–375.

Kapacee, Z., Yeung, C.Y.C., Lu, Y., Crabtree, D., Holmes, D.F., and Kadler, K.E. (2010). Synthesis of embryonic tendon-like tissue by human marrow stromal/mesenchymal stem cells requires a three-dimensional environment and transforming growth factor β 3. *Matrix Biol.* 29, 668–677.

Kardon, G. (1998). Muscle and tendon morphogenesis in the avian hind limb. *Development* 4032, 4019–4032. Karsenty, G., and Park, R. (1995). Regulation of Type I Collagen Genes Expression. *Intern. Rev. Immunol.* 12, 177–185.

Karsenty, G.G., Kronenberg, H.M., and Settembre, C. (2009). Genetic control of bone formation. *Annu. Rev. Cell Dev. Biol.* 25, 629–648.

Kassar-duchossoy, L., Giaccone, E., Gayraud-morel, B., Jory, A., Gomès, D., and Tajbakhsh, S. (2005). Pax3 / Pax7 mark a novel population of primitive myogenic cells during development. *Development* 133, 1426–1431.

Kayama, T., Mori, M., Ito, Y., Matsushima, T., Nakamichi, R., Suzuki, H., and Ichinose, S. (2016). Gtf2ird1-Dependent Mohawk Expression Regulates Mechanosensing. *Mol. Cell Biol.* 36, 1297–1309.

Kelly, A.M., and Zacks, S.I. (1969). The fine structure of motor endplate morphogenesis. *J. Cell Biol.* 42, 154–169.

Ker, E.D.F., Chu, B., Phillippi, J.A., Gharaibeh, B., Huard, J., Weiss, L.E., and Campbell, P.G. (2011). Engineering spatial control of multiple differentiation fates within a stem cell population. *Biomaterials* 32, 3413–3422.

Khayyeri, H., Gustafsson, A., Heuwerkerk, A., Matikainen, M.K., Julkunen, P., Eliasson, P., Aspenberg, P., and Isaksson, H. (2015). A fibre-reinforced poroviscoelastic model accurately describes the biomechanical behaviour of the rat Achilles tendon. *PLoS One* 10, e0126869.

Kiehart, D.P., Galbraith, C.G., Edwards, K.A., Rickoll, W.L., and Montague, R.A. (2000). Multiple forces contribute to cell sheet morphogenesis for dorsal closure in *Drosophila*. *J. Cell Biol.* 149, 471–490. Kieny, M., and Chevallier, A. (1979). Autonomy of tendon development in the embryonic chick wing. *J. Embryol. Exp. Morph.* 49, 153–165.

Kim, H.S., and Lee, N.K. (2014). Gene Expression Profiling in Osteoclast Precursors by Insulin Using Microarray Analysis. *Mol. Cells* 37, 827–832.

Kim, K.-M., and Jang, W.-G. (2017). Zaluzanin C (ZC) induces osteoblast differentiation through regulating of osteogenic genes expressions in early stage of differentiation. *Bioorg. Med. Chem. Lett.* 27, 4789–4793. Kim, J., Feng, J., Jones, C.A.R., Mao, X., Sander, L.M., Levine, H., and Sun, B. (2017). Stress-induced plasticity of dynamic collagen networks. *Nat. Commun.* 8.

Kimura, W., Machii, M., Xue, X., Sultana, N., Hikosaka, K., Sharkar, M.T.K., Uezato, T., Matsuda, M., Koseki, H., and Miura, N. (2011). *Irx11* mutant mice show reduced tendon differentiation and no patterning defects in musculoskeletal system development. *Genesis* 49, 2–9.

Kishimoto, Y., Ohkawara, B., Sakai, T., Ito, M., Masuda, A., Ishiguro, N., Shukunami, C., Docheva, D., and Ohno, K. (2017). Wnt/ β -catenin signaling suppresses expressions of *Scx*, *Mxk*, and *Tnmd* in tendon-derived cells. *PLoS One* 12, 1–17.

Kishore, V., Bullock, W., Sun, X., Van Dyke, W.S., and Akkus, O. (2012). Tenogenic differentiation of human MSCs induced by the topography of electrochemically aligned collagen threads. *Biomaterials* 33, 2137–2144. Kjær, M. (2004). Role of Extracellular Matrix in Adaptation of Tendon and Skeletal Muscle to Mechanical Loading. *Physiol Rev* 84, 649–698.

Kohler, J., Popov, C., Klotz, B., Alberton, P., Prall, W.C., Haasters, F., Müller-Deubert, S., Ebert, R., Klein-Hitpass, L., Jakob, F., et al. (2013). Uncovering the cellular and molecular changes in tendon stem/progenitor cells attributed to tendon aging and degeneration. *Aging Cell* 12, 988–999.

Kohn, A., Rutkowski, T.P., Liu, Z., Mirando, A.J., Zuscik, M.J., Keefe, R.J.O., and Hilton, M.J. (2015). Notch signaling controls chondrocyte hypertrophy via indirect regulation of *Sox9*. *Bone Res.*

Komori, T., Yagi, H., Nomura, S., Yamaguchi, A., Sasaki, K., Deguchi, K., Shimizu, Y., Bronson, R., Gao, Y.-H., Inada, M., et al. (1997). Targeted Disruption of *Cbfa1* Results in a Complete Lack of Bone Formation owing to Maturation Arrest of Osteoblasts. *Cell* 89, 755–764.

Kryger, G.S., Chong, a K., Costa, M., Pham, H., Bates, S.J., and Chang, J. (2007). A comparison of tenocytes and mesenchymal stem cells for use in flexor tendon tissue engineering. *J Hand Surg Am* 32, 597–605.

Kumar, S., Maxwell, I.Z., Heisterkamp, A., Polte, T.R., Lele, T.P., Salanga, M., Mazur, E., and Ingber, D.E. (2006). Viscoelastic retraction of single living stress fibers and its impact on cell shape, cytoskeletal organization, and extracellular matrix mechanics. *Biophys. J.* 90, 3762–3773.

Kuo, C.K., and Tuan, R.S. (2008). Mechanoactive tenogenic differentiation of human mesenchymal stem cells. *Tissue Eng. Part A* 14, 1615–1627.

Lauring, K.L., Cortes, M., Domowicz, M.S., Henry, J.G., Baria, A.T., and Schwartz, N.B. (2014). Aggrecan is required for growth plate cytoarchitecture and differentiation. *Dev. Biol.* 396, 224–236. Lavagnino, M., Oslapas, A.N., Gardner, K.L., and Arnoczky, S.P.

(2016). Hypoxia inhibits primary cilia formation and reduces cell-mediated contraction in stress-deprived rat tail tendon fascicles. *Muscles. Ligaments Tendons J.* 6, 193–197.

Lee, C.H., Moioli, E.K., and Mao, J.J. (2006). Fibroblastic differentiation of human mesenchymal stem cells using connective tissue growth factor. *Conf Proc IEEE Eng Med Biol Soc* 1, 775–778. Lee, C.H., Shah, B., Moioli, E.K., and Mao, J.J. (2010). CTGF directs fibroblast differentiation from human mesenchymal stem/stromal cells and defines connective tissue healing in a rodent injury model. *J. Clin. Invest.* 120, 3340–3349.

Lee, C.Y., Liu, X., Smith, C.L., Zhang, X., Hsu, H.C., Wang, D.Y., and Luo, Z.P. (2004). The combined regulation of estrogen and cyclic tension on fibroblast biosynthesis derived from anterior cruciate ligament. *Matrix Biol.* 23, 323–329.

Lee, H., Lee, Y.J., Choi, H., Seok, J.W., Yoon, B.K., Kim, D., Han, J.Y., Lee, Y., Kim, H.J., and Kim, J. (2017). SCARA5 plays a critical role in the commitment of mesenchymal stem cells to adipogenesis. *Sci. Rep.* 7, 1–13.

Lee, J., Wong, M., Smith, Q., and Baker, A.B. (2013). A novel system for studying mechanical strain waveform-dependent responses in vascular smooth muscle cells. *Lab Chip* 13, 4573–4582.

Lefebvre, V., Behringer, R.R., and De Crombrughe, B. (2001). L-Sox5, Sox6 and SOx9 control essential steps of the chondrocyte differentiation pathway. *Osteoarthr. Cartil.* 9, 69–75.

Léjard, V., Brideau, G., Blais, F., Salingcarnboriboon, R., Wagner, G., Roehrl, M.H. a, Noda, M., Duprez, D., Houillier, P., and Rossert, J. (2007). Scleraxis and NFATc regulate the expression of the pro- α 1(I) collagen gene in tendon fibroblasts. *J. Biol. Chem.* 282, 17665–17675.

Léjard, V., Blais, F., Guerquin, M.-J., Bonnet, A., Bonnin, M.-A., Havis, E., Malbouyres, M., Bidaud, C.B., Maro, G., Gilardi-Hebenstreit, P., et al. (2011). EGR1 and EGR2 involvement in vertebrate tendon differentiation. *J. Biol. Chem.* 286, 5855–5867.

Liu, C.-F., Aschbacher-Smith, L., Barthelery, N.J., Dymont, N., Butler, D., and Wylie, C. (2012). Spatial and Temporal Expression of Molecular Markers and Cell Signals During Normal Development of the Mouse Patellar Tendon. *Tissue Eng. Part A* 18, 598–608.

Liu, C., Baek, S., Kim, J., Vasko, E., Pyne, R., and Chan, C. (2014). Effect of static pre-stretch induced surface anisotropy on orientation of mesenchymal stem cells. *Cell. Mol. Bioeng.* 7, 106–121.

Liu, C.F., Breidenbach, A., Aschbacher-Smith, L., Butler, D., and Wylie, C. (2013). A Role for Hedgehog Signaling in the Differentiation of the Insertion Site of the Patellar Tendon in the Mouse. *PLoS One* 8.

Liu, H., Zhang, C., Zhu, S., Lu, P., Zhu, T., Gong, X., Zhang, Z., Hu, J., Yin, Z., Heng, B.C., et al. (2015a). Mohawk Promotes the Tenogenesis of Mesenchymal Stem Cells Through Activation of the TGF β Signaling Pathway. *Stem Cells* 443–455.

Liu, H., Xu, J., Liu, C., Lan, Y., Wylie, C., Jiang, R., Biology, D., Children, C., Surgery, P., Children, C., et al. (2015b). Whole Transcriptome Expression Profiling of Mouse Limb Tendon Development by Using RNA-Seq. *J. Orthop. Res.* 840–848.

- Liu, J., Chou, S.M., and Goh, K.L. (2009). Age Effects on the Tensile and Stress Relaxation Properties Of Mouse Tail Tendons. *IFMBE Proc.* 23, 1631–1635.
- Liu, J., Tao, X., Chen, L., Han, W., Zhou, Y., and Tang, K. (2015c). CTGF Positively Regulates BMP12 Induced Tenogenic Differentiation of Tendon Stem Cells and Signaling. *Cell. Physiol. Biochem.* 1831–1845.
- Liu, W., Watson, S.S., Lan, Y., Keene, D.R., Ovitt, C.E., Liu, H., Schweitzer, R., and Jiang, R. (2010). The atypical homeodomain transcription factor Mohawk controls tendon morphogenesis. *Mol. Cell. Biol.* 30, 4797–4807.
- Liu, W., Yin, L., Yan, X., Cui, J., Liu, W., Rao, Y., Sun, M., Wei, Q., and Chen, F. (2017). Directing the Differentiation of Parthenogenetic Stem Cells into Tenocytes for Tissue Engineered Tendon Regeneration. *Stem Cells Transl. Med.* 6, 106–116.
- Livak, K.J., and Schmittgen, T.D. (2001). Analysis of relative gene expression data using real-time quantitative PCR and the $2^{(-\Delta\Delta CT)}$ method. *Methods* 25, 402–408.
- Lohberger, B., Kaltenecker, H., Stuenkel, N., Payer, M., Rinner, B., and Leithner, A. (2014). Effect of cyclic mechanical stimulation on the expression of osteogenesis genes in human intraoral mesenchymal stromal and progenitor cells. *Biomed Res. Int.* 2014, 189516.
- Lorda-Diez, C.I., Montero, J. a, Martinez-Cue, C., Garcia-Porrero, J. a, and Hurle, J.M. (2009). Transforming growth factors beta coordinate cartilage and tendon differentiation in the developing limb mesenchyme. *J. Biol. Chem.* 284, 29988–29996.
- Lorda-Diez, C.I., Montero, J. a, Garcia-Porrero, J. a, and Hurle, J.M. (2010). Tgfbeta2 and 3 are coexpressed with their extracellular regulator Ltbp1 in the early limb bud and modulate mesodermal outgrowth and BMP signaling in chicken embryos. *BMC Dev. Biol.* 10, 69.
- Lorda-Diez, C.I., Montero, J.A., Garcia-porrero, J.A., and Hurle, J.M. (2014). Divergent Differentiation of Skeletal Progenitors into Cartilage and Tendon: Lessons from the Embryonic Limb. *ACS Chem. Biol.* 9, 72–79.
- Lui, P.P.Y., Wong, O.T., and Lee, Y.W. (2016). Transplantation of tendon-derived stem cells pre-treated with connective tissue growth factor and ascorbic acid in vitro promoted better tendon repair in a patellar tendon window injury rat model. *Cytotherapy* 18, 99–112.
- Macharia, R., Patel, K., Otto, W.R., McKinnel, I.W., and Christ, B. (2004). Decamethonium bromide-mediated inhibition of embryonic muscle development. *Anat Embryol* 208, 75–85.
- Madhurakkat Perikamana, S.K., Lee, J., Ahmad, T., Kim, E.M., Byun, H., Lee, S., and Shin, H. (2018). Harnessing biochemical and structural cues for tenogenic differentiation of adipose derived stem cells (ADSCs) and development of an in vitro tissue interface mimicking tendon-bone insertion graft. *Biomaterials* 165, 79–93.
- Maeda, T., Sakabe, T., Sunaga, A., Sakai, K., Rivera, A.L., Keene, D.R., Sasaki, T., Stavnezer, E., Iannotti, J., Schweitzer, R., et al. (2011). Conversion of Mechanical Force into TGF- β -Mediated Biochemical Signals. *Curr. Biol.* 21, 933–941.
- Maganaris, C.N., and Paul, J.P. (1999). In vivo human tendon mechanical properties. *J Physiol* 521 Pt 1, 307–313.

Maître, J.-L., Niwayama, R., Turlier, H., Nédélec, F., and Hiragi, T. (2015). Pulsatile cell-autonomous contractility drives compaction in the mouse embryo. *Nat. Cell Biol.* 17, 849–855.

Maître, J.L., Turlier, H., Illukkumbura, R., Eismann, B., Niwayama, R., Nédélec, F., and Hiragi, T. (2016). Asymmetric division of contractile domains couples cell positioning and fate specification. *Nature* 536, 344–348.

Malik, A.R., Liszewska, E., and Jaworski, J. (2015). Matricellular proteins of the Cyr61/CTGF/NOV (CCN) family and the nervous system. *Front. Cell. Neurosci.* 9, 1–13.

Mammoto, T., Mammoto, A., and Ingber, D.E. (2013). Mechanobiology and developmental control. *Annu. Rev. Cell Dev. Biol.* 29, 27–61.

Mana-Capelli, S., Paramasivam, M., Dutta, S., and McCollum, D. (2014). Angiomotins link F-actin architecture to Hippo pathway signaling. *Mol. Biol. Cell* 25, 1676–1685.

Manceau, M., Gros, J., Savage, K., Thomé, V., McPherron, A., Paterson, B., and Marcelle, C. (2008). Myostatin promotes the terminal differentiation of embryonic muscle progenitors. *Genes Dev.* 22, 668–681.

Marturano, J.E., Arena, J.D., Schiller, Z. a, Georgakoudi, I., and Kuo, C.K. (2013). Characterization of mechanical and biochemical properties of developing embryonic tendon. *Proc. Natl. Acad. Sci. U. S. A.* 110, 6370–6375.

Massagué, J. (2012). TGF β signalling in context. *Nat. Rev. Mol. Cell Biol.* 13, 616–630.

McNeilly, C.M., Banes, A.J., M., B., and Ralphs, J.R. (1996). Tendon cells in vivo form a three dimensional network of cell processes linked by gap junctions. *J. Anat.* 190, 477–478.

Melas, I.N., Chairakaki, A.D., Chatzopoulou, E.I., Messinis, D.E., Katopodi, T., Pliaka, V., Samara, S., Mitsos, A., Dailiana, Z., Kollia, P., et al. (2014). Modeling of signaling pathways in chondrocytes based on phosphoproteomic and cytokine release data. *Osteoarthr. Cartil.* 22, 509–518.

Mendias, C.L., Bakhurin, K.I., and Faulkner, J. a (2008). Tendons of myostatin-deficient mice are small, brittle, and hypocellular. *Proc. Natl. Acad. Sci. U. S. A.* 105, 388–393.

Mendias, C.L., Gumucio, J.P., Bakhurin, K.I., Lynch, E.B., and Brooks, S. V. (2012). Physiological loading of tendons induces scleraxis expression in epitenon fibroblasts. *J. Orthop. Res.* 30, 606–612.

Mérino, R., Ganan, Y., Macias, D., Economides, A.N., Sampath, K.T., and Hurle, J.M. (1998). Morphogenesis of Digits in the Avian Limb Is Controlled by FGFs , TGF-betas , and Noggin through BMP Signaling. *Dev. Biol.* 45, 35–45.

Mienaltowski, M.J., and Birk, D.E. (2014). Structure, Physiology, and Biochemistry of Collagens. *Adv. Exp. Med. Biol.* 5–29.

Mienaltowski, M.J., Adams, S.M., and Birk, D.E. (2013). Regional Differences in Stem Cell/Progenitor Cell Populations from the Mouse Achilles Tendon. *Tissue Eng. Part A* 19, 199–210.

Mienaltowski, M.J., Adams, S.M., and Birk, D.E. (2014). Tendon proper- and peritenon-derived progenitor cells have unique tenogenic properties. *Stem Cell Res. Ther.* 5, 86.

- Miralles, F., Posern, G., Zaromytidou, A.I., and Treisman, R. (2003). Actin dynamics control SRF activity by regulation of its coactivator MAL. *Cell* 113, 329–342.
- Miyabara, S., Yuda, Y., Kasashima, Y., Kuwano, A., and Arai, K. (2014). Regulation of Tenomodulin Expression Via Wnt/ β -catenin Signaling in Equine Bone Marrow-derived Mesenchymal Stem Cells. *J. Equine Sci. / Japanese Soc. Equine Sci.* 25, 7–13.
- Moncaut, N., Rigby, P.W.J., and Carvajal, J.J. (2013). Dial M(RF) for myogenesis. *FEBS J.* 280, 3980–3990.
- Murchison, N.D., Price, B. a, Conner, D. a, Keene, D.R., Olson, E.N., Tabin, C.J., and Schweitzer, R. (2007). Regulation of tendon differentiation by scleraxis distinguishes force-transmitting tendons from muscle-anchoring tendons. *Development* 134, 2697–2708.
- Murphy-Ullrich, J.E., and Sage, E.H. (2014). Revisiting the matricellular concept. *Matrix Biol.* 37, 1–14.
- Murphy, M.B., Moncivais, K., and Caplan, A.I. (2013). Mesenchymal stem cells: environmentally responsive therapeutics for regenerative medicine. 45, e54-16.
- Murshed, M. (2018). Mechanism of Bone Mineralization. *Cold Spring Harb. Perspect. Med.* 1–12.
- Murthy, S.E., Dubin, A.E., and Patapoutian, A. (2017). Piezos thrive under pressure: Mechanically activated ion channels in health and disease. *Nat. Rev. Mol. Cell Biol.* 18, 771–783.
- Nakamichi, R., Ito, Y., Inui, M., Onizuka, N., Kayama, T., Kataoka, K., Suzuki, H., Mori, M., Inagawa, M., Ichinose, S., et al. (2016). Mohawk promotes the maintenance and regeneration of the outer annulus fibrosus of intervertebral discs. *Nat. Commun.* 7, 1–14.
- Nakashima, K., Zhou, X., and Al., G.K. et (2002). The novel zinc fingercontaining transcription factor Osterix is required for osteoblast 12 BioMed Research International differentiation and bone formation. *Cell* 108, 17–29.
- Nassari, S., Duprez, D., and Fournier-thibault, C. (2017). Non-myogenic Contribution to Muscle Development and Homeostasis: The Role of Connective Tissues Different Types of Connective Tissues. *Front. Cell Dev. Biol.* 5, 1–17.
- Ni, M., Rui, Y.F., Tan, Q., Liu, Y., Xu, L.L., Chan, K.M., Wang, Y., and Li, G. (2013). Engineered scaffold-free tendon tissue produced by tendon-derived stem cells. *Biomaterials* 34, 2024–2037.
- Nilius, B., and Owsianik, G. (2011). The transient receptor potential family of ion channels. *Genome Biol* 12, 218.
- Ning Wang (2017). Review of cellular mechanotransduction. *J. Phys. D Appl. Phys.* 50.
- Nourissat, G., Berenbaum, F., and Duprez, D. (2015). Tendon injury: from biology to tendon repair. *Nat. Rev. Rheumatol.* 1–11.
- Nowlan, N.C., Sharpe, J., Roddy, K.A., Prendergast, P.J., and Murphy, P. (2010). Mechanobiology of embryonic skeletal development: Insights from animal models. *Birth Defects Res. Part C - Embryo Today Rev.* 90, 203–213.
- Ogata, T. (2008). Egr-1 mRNA induction by medium flow involves mRNA stabilization and is enhanced by the p38 inhibitor SB203580 in osteoblast-like cells. *Acta Physiol.* 194, 177–188.

Ordahl, C.P., and Douarin, N.M.L.E. (1992). Two myogenic lineages within the developing somite. *Development* 353, 339–353.

Orgeur, M., Martens, M., Leonte, G., Nassari, S., Bonnin, M.-A., Börno, S.T., Timmermann, B., Hecht, J., Duprez, D., and Stricker, S. (2018a). Genome-wide strategies identify downstream target genes of connective tissue-associated transcription factors. *Development* dev.161208.

Orgeur, M., Martens, M., Börno, S.T., Timmermann, B., Duprez, D., and Stricker, S. (2018b). A dual transcript-discovery approach to improve the delimitation of gene features from RNA-seq data in the chicken model. *Biol. Open* 7, bio028498.

Oshima, Y., Shukunami, C., Honda, J., Nishida, K., Tashiro, F., Miyazaki, J.I., Hiraki, Y., and Tano, Y. (2003). Expression and localization of tenomodulin, a transmembrane type chondromodulin-I-related angiogenesis inhibitor, in mouse eyes. *Investig. Ophthalmol. Vis. Sci.* 44, 1814–1823.

Otabe, K., Nakahara, H., Hasegawa, A., Matsukawa, T., Ayabe, F., Onizuka, N., Inui, M., Takada, S., Ito, Y., Sekiya, I., et al. (2015). Transcription Factor Mohawk Controls Tenogenic Differentiation of Bone Marrow Mesenchymal Stem Cells In Vitro and In Vivo. *J. Orthop. Res.* 1–8.

Pai, A.C. (1965). Developmental Muscular Genetics Dysgenesis of a Lethal Mutation , in the Mouse I. Genetic Analysis and Gross Morphology. *Dev. Biol.* 11, 82–92.

Panciera, T., Azzolin, L., Cordenonsi, M., and Piccolo, S. (2017). Mechanobiology of YAP and TAZ in physiology and disease. *Nat. Rev. Mol. Cell Biol.* 18, 758–770.

Pardo, P.S., and Boriek, A.M. (2012). An autoregulatory loop reverts the mechanosensitive Sirt1 induction by EGR1 in skeletal muscle cells. *Aging (Albany. NY).* 4, 456–461.

Park, A., Hogan, M. V., Kesturu, G.S., James, R., Balian, G., and Chhabra, A.B. (2010). Adipose-Derived Mesenchymal Stem Cells Treated with Growth Differentiation Factor-5 Express Tendon-Specific Markers. *Tissue Eng. Part A* 16, 2941–2951.

Pittenger, M.F., Mackay, A.M., Beck, S.C., Jaiswal, R.K., Douglas, R., Mosca, J.D., Moorman, M.A., Simonetti, D.W., Craig, S., and Marshak, D.R. (1999). Multilineage Potential of Adult Human Mesenchymal Stem Cells. *Science (80-)*. 284, 143–147.

Pollard, A.S., Boyd, S., McGonnell, I.M., and Pitsillides, A.A. (2016). The role of embryo movement in the development of the furcula A. *J. Anat.*

Posern, G., and Treisman, R. (2006). Actin' together: serum response factor, its cofactors and the link to signal transduction. *Trends Cell Biol.* 16, 588–596.

Prockop, D.J. (1997). Marrow Stromal Cells as Stem Cells for Nonhematopoietic Tissues. *Science (80-)*. 276, 71–74.

Pryce, B.A., Brent, A.E., Murchison, N.D., Tabin, C.J., and Schweitzer, R. (2007). Generation of transgenic tendon reporters, ScxGFP and ScxAP, using regulatory elements of the scleraxis gene. *Dev. Dyn.* 236, 1677–1682. Pryce, B.A., Watson, S.S., Murchison, N.D., Staverosky, J. a, Dünker, N., and Schweitzer, R. (2009) Recruitment and maintenance of tendon progenitors by TGFbeta signaling are essential for tendon formation. *Development* 136, 1351–1361.

Pulina, M. V., Hou, S.Y., Mittal, A., Julich, D., Whittaker, C.A., Holley, S.A., Hynes, R.O., and Astrof, S. (2011). Essential roles of fibronectin in the development of the left-right embryonic body plan. *Dev. Biol.* 354, 208–220.

Purves, D., Augustine, G.J., Fitzpatrick, D., Hall, W.C., Lamantia, A.-S., Mcnamara, J.O., and Willians, S.M. (2004). *Neuroscience*.

Qi, J., Chi, L., Bynum, D., and Banes, A.J. (2011). Gap junctions in IL-1 β -mediated cell survival response to strain. *J. Appl. Physiol.* 110, 1425–1431.

Rauzi, M., Verant, P., Lecuit, T., and Lenne, P.F. (2008). Nature and anisotropy of cortical forces orienting *Drosophila* tissue morphogenesis. *Nat. Cell Biol.* 10, 1401–1410.

Rees, S.G., Flannery, C.R., Little, C.B., Hughes, C.E., Caterson, B., and Dent, C.M. (2000). Catabolism of aggrecan, decorin and biglycan in tendon. *Biochem. J.* 188, 181–188.

Rehfeldt, F., Brown, A.E.X., Raab, M., Cai, S., Zajac, A.L., Zemel, A., and Discher, D.E. (2012). Hyaluronic acid matrices show matrix stiffness in 2D and 3D dictates cytoskeletal order and myosin-II phosphorylation within stem cells. *Integr. Biol.* 4, 422.

Relaix, F., Rocancourt, D., Mansouri, A., and Buckingham, M. (2005). A Pax3/Pax7-dependent population of skeletal muscle progenitor cells. *Nature* 435, 948–953.

Ren, J., Wang, H., Tran, K., Civini, S., Jin, P., Castiello, L., Feng, J.I., Kuznetsov, S.A., Robey, P.G., Sabatino, M., et al. (2015). Human bone marrow stromal cell confluence: effects on cell characteristics and methods of assessment. *J. Cytotherapy* 17, 897–911.

Reznikoff, C. a, Brankow, D.W., and Heidelberger, C. (1973). Establishment and Characterization of a Cloned Line of C3H Mouse Embryo Cells Sensitive to Postconfluence Inhibition of Division Establishment and Characterization of a Cloned Line of C3H Mouse Embryo Cells Sensitive to Postconfluence Inhibition of. *Cancer Res.* 3231–3238.

del Rio, A., Perez-Jimenez, R., Liu, R., Roca-Cusachs, P., Fernandez, J.M., and Sheetz, M.P. (2016). Stretching Single Talin Rod molecules activates vinculin binding. *Science* (80-). 323, 638–641.

Robledo, R.F., Rajan, L., Li, X., Lufkin, T., Dll, D.D., and Dll, D. (2002). The *Dlx5* and *Dlx6* homeobox genes are essential for craniofacial, axial, and appendicular skeletal development. *Genes Dev.* 5, 1089–1101. Ruano-Gil, D., Nardi-Villardaga, J., and Teixidor-Johé, A. (1985). Embryonal hypermotility and articular development. *Acta Anat. (Basel)*. 192, 90–92.

Rudnicki, M.A., Schnegelsberg, P.N.J., Stead, R.H., Braun, T., Arnold, H., and Jaenisch, R. (1993). MyoD or Myf-5 Is Required for the Formation of Skeletal Muscle. *Cell* 75, 1351–1359.

Salincarnboriboon, R., Yoshitake, H., Tsuji, K., Obinata, M., Amagasa, T., Nifuji, A., and Noda, M. (2003). Establishment of tendon-derived cell lines exhibiting pluripotent mesenchymal stem cell-like property. *Exp. Cell Res.* 287, 289–300.

Sambasivan, R., Kuratani, S., and Tajbakhsh, S. (2011). An eye on the head: the development and evolution of craniofacial muscles. *Development* 138, 2401–2415.

Sato, I., Miwa, Y., Hara, S., Fukuyama, Y., and Sunohara, M. (2014). Tenomodulin regulated the compartments of embryonic and early postnatal mouse masseter muscle. *Ann.*

Anat. 196, 410–415.

Schiele, N.R., Marturano, J.E., and Kuo, C.K. (2013). Mechanical factors in embryonic tendon development: Potential cues for stem cell tenogenesis. *Curr. Opin. Biotechnol.* 24, 834–840.

Schiller, H.B., and Fässler, R. (2013). Mechanosensitivity and compositional dynamics of cell-matrix adhesions. *EMBO Rep.* 14, 509–519.

Scholzen, T., and Gerdes, J. (2000). The Ki-67 Protein: From the Known and. *J. Cell. Physiol.* 322, 311–322. Schramm, C., and Solursh, M. (1990). Anatomy and Embryology The formation of premuscle masses during chick wing bud development. *Anat. Embryol. (Berl.)* 235–247.

Schwachtgen, J.L., Houston, P., Campbell, C., Sukhatme, V., and Braddock, M. (1998). Fluid shear stress activation of egr-1 transcription in cultured human endothelial and epithelial cells is mediated via the extracellular signal-related kinase 1/2 mitogen-activated protein kinase pathway. *J. Clin. Invest.* 101, 2540–2549.

Schwartz, A.G., Pasteris, J.D., Genin, G.M., Daulton, T.L., and Thomopoulos, S. (2012). Mineral Distributions at the Developing Tendon Enthesis. *PLoS One* 7.

Schwartz, A.G., Long, F., and Thomopoulos, S. (2015). Enthesis fibrocartilage cells originate from a population of hedgehog responsive cells modulated by the loading environment. *Orthop. Res. Soc. Annu. Meet.* 196–206. Schweitzer, R., Chyung, J.H., Murtaugh, L.C., Brent, A.E., Rosen, V., Olson, E.N., Lassar, A., and Tabin, C.J. (2001). Analysis of the tendon cell fate using Scleraxis, a specific marker for tendons and ligaments. *Development* 3866, 3855–3866.

Schweitzer, R., Zelzer, E., and Volk, T. (2010). Connecting muscles to tendons: tendons and musculoskeletal development in flies and vertebrates. *Development* 137, 3347–3347.

Scott, A., Danielson, P., Abraham, T., Fong, G., Sampaio, A. V., and Underhill, T.M. (2011). Mechanical force modulates scleraxis expression in bioartificial tendons. *J. Musculoskelet. Neuronal Interact.* 11, 124–132. Screen, H.R.C., Birk, D.E., Kadler, K.E., Ramirez, F., and Young, M.F. (2015). Tendon Functional Extracellular Matrix. *J. Orthop. Res.* 17

Senol-cosar, O., Flach, R.J.R., Distefano, M., Chawla, A., Nicoloso, S., Straubhaar, J., Hardy, O.T., Noh, H.L., Kim, J.K., Wabitsch, M., et al. (2016). Tenomodulin promotes human adipocyte differentiation and beneficial visceral adipose tissue expansion. *Nat. Commun.* 6, 1–13.

Sharma, R.R., Pollock, K., Hubel, A., and Mckenna, D. (2014). Mesenchymal stem or stromal cells: a review of clinical applications and manufacturing practices. *Transfusion* 54, 1418–1437.

Shearn, J.T., Kinneberg, K.R.C., Dymant, N.A., Galloway, M.T., Kenter, K., Wylie, C., and Butler, D.L. (2011). Tendon tissue engineering: Progress, challenges, and translation to the clinic. *J. Musculoskelet. Neuronal Interact.* 11, 163–173.

Shellswell, B.G.B. (1977). The formation of discrete muscles from the chick wing dorsal and ventral muscle masses in the absence of nerves. *J. Embryol. Exp. Morph.* 41, 269–277.

Shen, H., Gelberman, R.H., Silva, M.J., Sakiyama-Elbert, S.E., and Thomopoulos, S.

(2013). BMP12 induces tenogenic differentiation of adipose-derived stromal cells. *PLoS One* 8, 1–14.

Shukunami, C., Oshima, Y., and Hiraki, Y. (2001). Molecular cloning of tenomodulin, a novel chondromodulin-I related gene. *Biochem. Biophys. Res. Commun.* 280, 1323–1327.

Shukunami, C., Takimoto, A., Oro, M., and Hiraki, Y. (2006). Scleraxis positively regulates the expression of tenomodulin, a differentiation marker of tenocytes. *Dev. Biol.* 298, 234–247.

Shukunami, C., Takimoto, A., Nishizaki, Y., Yoshimoto, Y., Tanaka, S., Miura, S., Watanabe, H., Sakuma, T., Yamamoto, T., Kondoh, G., et al. (2018). Scleraxis is a transcriptional activator that regulates the expression of Tenomodulin, a marker of mature tenocytes and ligamentocytes. *Sci. Rep.* 1–17.

Shwartz, Y., Farkas, Z., Stern, T., Aszódi, A., and Zelzer, E. (2012). Muscle contraction controls skeletal morphogenesis through regulation of chondrocyte convergent extension. *Dev. Biol.* 370, 154–163.

Shwartz, Y., Blitz, E., and Zelzer, E. (2013). One load to rule them all: mechanical control of the musculoskeletal system in development and aging. *Differentiation* 86, 104–111.

Smith, L.R., Cho, S., and Discher, D.E. (2018). Stem Cell Differentiation is Regulated by Extracellular Matrix Mechanics. *Physiology (Bethesda)*. 33, 16–25.

Smith, T.G., Sweetman, D., Patterson, M., Keyse, S.M., and Münsterberg, A. (2005). Feedback interactions between MKP3 and ERK MAP kinase control scleraxis expression and the specification of rib progenitors in the developing chick somite. *Development* 132, 1305–1314.

Speight, P., Kofler, M., Szászi, K., and Kapus, A. (2016). Context-dependent switch in chemo/mechanotransduction via multilevel crosstalk among cytoskeleton-regulated MRTF and TAZ and TGF β -regulated Smad3. *Nat. Commun.* 7, 11642.

Stavenschi, E., Labour, M.N., and Hoey, D.A. (2017). Oscillatory fluid flow induces the osteogenic lineage commitment of mesenchymal stem cells: The effect of shear stress magnitude, frequency, and duration. *J. Biomech.* 55, 99–106.

Stein, C., Bardet, A.F., Roma, G., Bergling, S., Clay, I., Ruchti, A., Agarinis, C., Schmelzle, T., Bouwmeester, T., Schübeler, D., et al. (2015). YAP1 Exerts Its Transcriptional Control via TEAD-Mediated Activation of Enhancers. *PLoS Genet.* 11, 1–28.

Subramanian, A., and Schilling, T.F. (2014). Thrombospondin-4 controls matrix assembly during development and repair of myotendinous junctions. *Elife* 2014, 1–21.

Subramanian, A., and Schilling, T.F. (2015). Tendon development and musculoskeletal assembly: emerging roles for the extracellular matrix. *Development* 142, 4191–4204.

Subramanian, A., Bunch, T., Wayburn, B., and Volk, T. (2007). Thrombospondin-mediated adhesion is essential for the formation of the myotendinous junction in. *Development* 1278, 1269–1278.

Sugimoto, Y., Takimoto, A., Akiyama, H., Kist, R., Scherer, G., Nakamura, T., Hiraki, Y., and Shukunami, C. (2013). Scx+/Sox9+ progenitors contribute to the establishment of the junction between cartilage and tendon/ligament. *Development* 140, 2280–2288.

Sun, Z., Guo, S.S., and Fässler, R. (2016). Integrin-mediated mechanotransduction. *J. Cell Biol.* 215. Suzuki, H., Ito, Y., Shinohara, M., Yamashita, S., Ichinose, S., Kishida, A., Oyaizu, T., Kayama, T., Nakamichi, R., Koda, N., et al. (2016). Gene targeting of the transcription factor Mohawk in rats causes heterotopic ossification of Achilles tendon via failed tenogenesis. *Proc. Natl. Acad. Sci. U. S. A.* 113, 7840–7845.

Szeto, S.G., Narimatsu, M., Lu, M., He, X., Sidiqi, A.M., Tolosa, M.F., Chan, L., De Freitas, K., Bialik, J.F., Majumder, S., et al. (2016). YAP/TAZ Are Mechanoregulators of TGF- β -Smad Signaling and Renal Fibrogenesis. *J. Am. Soc. Nephrol.* 27, 3117–3128.

Takarada, T., Hinoi, E., Nakazato, R., Ochi, H., Xu, C., Tsuchikane, A., Takeda, S., Karsenty, G., Abe, T., Kiyonari, H., et al. (2013). An analysis of skeletal development in osteoblast-specific and chondrocyte-specific runt-related transcription factor-2 (Runx2) knockout mice. *J. Bone Miner. Res.* 28, 2064–2069.

Takimoto, A., Oro, M., Hiraki, Y., and Shukunami, C. (2012). Direct conversion of tenocytes into chondrocytes by Sox9. *Exp. Cell Res.* 318, 1492–1507.

Tan, S.-L., Ahmad, R.E., Ahmad, T.S., Merican, A.M., Abbas, A.A., Ng, W.M., and Kamarul, T. (2012). Effect of Growth Differentiation Factor 5 on the Proliferation and Tenogenic Differentiation Potential of Human Mesenchymal Stem Cells in vitro. *Cells Tissues Organs* 196, 325–338.

Tempfer, H., Wagner, A., Gehwolf, R., Lehner, C., Tauber, M., Resch, H., and Bauer, H.C. (2009). Perivascular cells of the supraspinatus tendon express both tendon- and stem cell-related markers. *Histochem. Cell Biol.* 131, 733–741.

Thomopoulos, S., Williams, G.R., Gimbel, J. a., Favata, M., and Soslowsky, L.J. (2003). Variation of biomechanical, structural, and compositional properties along the tendon to bone insertion site. *J. Orthop. Res.* 21, 413–419.

Thomopoulos, S., Marquez, J.P., Weinberger, B., Birman, V., and Genin, G.M. (2006). Collagen fiber orientation at the tendon to bone insertion and its influence on stress concentrations. *J. Biomech.* 39, 1842–1851. Thorpe, C.T., Birch, H.L., Clegg, P.D., and Screen, H.R.C. (2013). The role of the non-collagenous matrix in tendon function. *Int. J. Exp. Pathol.* 94, 248–259.

Tidball, J.G., and Lin, C. (1989). Structural changes at the myogenic cell surface during the formation of myotendinous junctions. *Cell Tissue Res.* 257, 77–84.

Tozer, S., Bonnin, M., Relaix, F., Savino, S. Di, García-villalba, P., Coumailleau, P., and Duprez, D. (2007). Involvement of vessels and PDGFB in muscle splitting during chick limb development. *Development* 2591, 2579–2591.

Trainor, P.A., and Tam, P.P.L. (1995). Cranial paraxial mesoderm and neural crest cells of the mouse embryo: co-distribution in the craniofacial mesenchyme but distinct segregation in branchial arches. *Development* 2582, 2569–2582.

Trovato, F., Imbesi, R., Conway, N., and Castrogiovanni, P. (2016). Morphological and Functional Aspects of Human Skeletal Muscle. *J. Funct. Morphol. Kinesiol.* 1, 289–302.

Tsao, Y.T., Huang, Y.J., Wu, H.H., Liu, Y.A., Liu, Y.S., and Lee, O.K. (2017). Osteocalcin mediates biomineralization during osteogenic maturation in human mesenchymal

stromal cells. *Int. J. Mol. Sci.* 18.

Tsujii, M., Hirata, H., Yoshida, T., Imanaka-Yoshida, K., Morita, a., and Uchida, a. (2006). Involvement of tenascin-C and PG-M/versican in flexor tenosynovial pathology of idiopathic carpal tunnel syndrome. *Histol. Histopathol.* 21, 511–518.

Uemura, K., Hayashi, M., Itsubo, T., Oishi, A., Iwakawa, H., Komatsu, M., Uchiyama, S., and Kato, H. (2017). Myostatin promotes tenogenic differentiation of C2C12 myoblast cells through Smad3. *FEBS Open Bio* 7, 522–532.

Veyrac, A., Besnard, A., Caboche, J., Davis, S., and Laroche, S. (2014). The transcription factor Zif268/Egr1, brain plasticity, and memory (Elsevier Inc.).

Vogan, K.J., Epstein, D., Trasler, D.G., and Gros, P. (1993). The Splotch-Delayed (Spd) mouse mutant carries a point mutation within the Paired Box of the Pax-3 gene. *Genomics* 17, 364–369.

Volk, T., and VijayRaghavan, K. (1994). A central role for epidermal segment border cells in the induction of muscle patterning in the *Drosophila* embryo. *Development* 120, 59–70.

Volohonsky, G., Edenfeld, G., Klämbt, C., and Volk, T. (2007). Muscle-dependent maturation of tendon cells is induced by post-transcriptional regulation of stripeA. *Development* 134, 347–356.

Wachtler, F. (1981). On the determination of mesodermal tissues in the avian embryonic wing bud. *Anat. Embryol. (Berl.)* 170, 307–312.

Wackerhage, H., Re, D.P. Del, Judson, R.N., Sudol, M., and Sadoshima, J. (2014). The Hippo signal transduction network in skeletal and cardiac muscle | *Science Signaling* | Science/AAAS. *Stke.Sciencemag.Org.Mlprox.Csmc.Edu* 7, 1–13.

Wall, M.E., Dymont, N.A., Bodle, J., Volmer, J., Lobo, E., Cederlund, A., Fox, A.M., and Banes, A.J. (2016). Cell Signaling in Tenocytes: Response to Load and Ligands in Health and Disease. *Adv. Exp. Med. Biol.* 79–95. Wang, J.H.C. (2006). Mechanobiology of tendon. *J. Biomech.* 39, 1563–1582.

Wang, H., Noulet, F., Edom-Vovard, F., Le Grand, F., and Duprez, D. (2010). Bmp Signaling at the Tips of Skeletal Muscles Regulates the Number of Fetal Muscle Progenitors and Satellite Cells during Development. *Dev. Cell* 18, 643–654.

Wang, M., Vanhouten, J.N., Nasiri, A.R., Johnson, R.L., and Broadus, A.E. (2013). PTHrP regulates the modeling of cortical bone surfaces at fibrous insertion sites during growth. *J. Bone Miner. Res.* 28, 598–607.

Wang, T., Thien, C., Wang, C., Ni, M., Gao, J., Wang, A., Jiang, Q., Tuan, R.S., Zheng, Q., and Zheng, M.H. (2018a). 3D uniaxial mechanical stimulation induces tenogenic differentiation of tendon-derived stem cells through a PI3K/AKT signaling pathway. *FASEB J.* 32.

Wang, T., Chen, P., Zheng, M., Wang, A., Lloyd, D., Leys, T., Zheng, Q., and Zheng, M.H. (2018b). In vitro loading models for tendon mechanobiology. *J. Orthop. Res.* 36, 566–575.

Watanabe, B., Minami, S., Ishida, H., Yoshioka, R., Nakagawa, Y., Morita, T., and

Hayashi, K. (2015). Stereospecific inhibitory effects of CCG-1423 on the cellular events mediated by myocardin-related transcription factor A. *PLoS One* 10, 1–16.

Webster, M.T., Manor, U., Lippincott-Schwartz, J., and Fan, C.M. (2016). Intravital Imaging Reveals Ghost Fibers as Architectural Units Guiding Myogenic Progenitors during Regeneration. *Cell Stem Cell* 18, 243–252. Winding, B., JØrgensen, H., and Christiansen, C. (1999). Bone. Bone. Estrogens Antiestrogens II. *Handb. Exp. Pharmacol.* 135, 141–160.

Wolfman, N.M., Hattersley, G., Cox, K., Celeste, A.J., Nelson, R., Yamaji, N., Dube, J.L., DiBlasio-Smith, E., Nove, J., Song, J.J., et al. (1997). Ectopic induction of tendon and ligament in rats by growth and differentiation factors 5, 6, and 7, members of the TGF- β gene family. *J. Clin. Invest.* 100, 321.

Wu, X., Cheng, J., Li, P., Yang, M., Qiu, S., Liu, P., and Du, J. (2010). Mechano-sensitive transcriptional factor *egr-1* regulates insulin-like growth factor-1 receptor expression and contributes to neointima formation in vein grafts. *Arterioscler. Thromb. Vasc. Biol.* 30, 471–476.

Yamamoto-Shiraishi, Y.I., and Kuroiwa, A. (2013). Wnt and BMP signaling cooperate with Hox in the control of Six2 expression in limb tendon precursor. *Dev. Biol.* 377, 363–374.

Yan, Z., Yin, H., Nerlich, M., Pfeifer, C.G., and Docheva, D. (2018). Boosting tendon repair: interplay of cells, growth factors and scaffold-free and gel- based carriers. *J. Exp. Orthop.* 5, 1.

Yang, B., Sun, H., Song, F., Yu, M., Wu, Y., and Wang, J. (2017a). YAP1 negatively regulates chondrocyte differentiation partly by activating the β -catenin signaling pathway. *Int. J. Biochem. Cell Biol.* 87, 104–113.

Yang, G., Rothrauff, B.B., Lin, H., Yu, S., and Tuan, R.S. (2017b). Tendon-Derived Extracellular Matrix Enhances Transforming Growth Factor- β 3-Induced Tenogenic Differentiation of Human Adipose-Derived Stem Cells. *Tissue Eng. Part A* 23, 166–176.

Yang, Y., Beqaj, S., Kemp, P., Ariel, I., and Schuger, L. (2000). Stretch-induced alternative splicing of serum response factor promotes bronchial myogenesis and is defective in lung hypoplasia. *J. Clin. Invest.* 106, 1321–1330.

Yeung, C.-Y.C., Zeef, L. a. H., Lallyett, C., Lu, Y., Canty-Laird, E.G., and Kadler, K.E. (2015). Chick tendon fibroblast transcriptome and shape depend on whether the cell has made its own collagen matrix. *Sci. Rep.* 5, 13555.

Yi, L., Huang, X., Guo, F., Zhou, Z., Dou, Y., and Huan, J. (2016). Yes-associated protein (YAP) signaling regulates lipopolysaccharide-induced tissue factor expression in human endothelial cells. *Surg. (United States)* 159, 1436–1448.

Yin, H., Price, F., and Rudnicki, M. a (2013). Satellite cells and the muscle stem cell niche. *Physiol. Rev.* 93, 23–67.

Yin, Z., Guo, J., Wu, T.-Y., Chen, X., Xu, L.-L., Lin, S.-E., Sun, Y.-X., Chan, K.-M., Ouyang, H., and Li, G. (2016). Stepwise differentiation of mesenchymal stem cells augments tendon-like tissue formation and defect repair in vivo. *Stem Cells Transl. Med.* 5, 1106–1116.

Yonemura, S., Wada, Y., Watanabe, T., Nagafuchi, A., and Shibata, M. (2010). α -Catenin as a tension transducer that induces adherens junction development. *Nat. Cell Biol.*

12, 533–542. Yoon, J.H., and Halper, J. (2005). Tendon proteoglycans: biochemistry and function. *J. Musculoskelet. Neuronal Interact.* 5, 22–34.

Yoshimoto, Y., Takimoto, A., Watanabe, H., Hiraki, Y., Kondoh, G., and Shukunami, C. (2017). Scleraxis is required for maturation of tissue domains for proper integration of the musculoskeletal system. *Sci. Rep.* 7, 1–16.

Yu, F.-X., Zhao, B., Panupinthu, N., Jewell, J.L., Lian, I., Wang, L.H., Zhao, J., Yuan, H., Tumaneng, K., Li, H., et al. (2012). Regulation of the Hippo-YAP Pathway by G-Protein-Coupled Receptor Signaling. *Cell* 150, 780–791.

Zagurovskaya, M., Shareef, M.M., Das, A., Reeves, A., Gupta, S., Sudol, M., Bedford, M.T., Prichard, J., Mohiuddin, M., and Ahmed, M.M. (2009). EGR-1 forms a complex with YAP-1 and upregulates Bax expression in irradiated prostate carcinoma cells. *Oncogene* 28, 1121–1131.

Zanconato, F., Forcato, M., Battilana, G., Azzolin, L., Quaranta, E., Bodega, B., Rosato, A., Bicciato, S., Cordenonsi, M., and Piccolo, S. (2015). Genome-wide association between YAP/TAZ/TEAD and AP-1 at enhancers drives oncogenic growth. *Nat. Cell Biol.* 17, 1218–1227.

Zelzer, E., Blitz, E., Killian, M.L., and Thomopoulos, S. (2014). Tendon-to-bone attachment: from development to maturity. *Birth Defects Res. Part C* 102, 101–112.

Zhang, J., and Wang, J.H.-C. (2013). The effects of mechanical loading on tendons—an in vivo and in vitro model study. *PLoS One* 8, e71740.

Zhang, J., and Wang, J.H.C. (2015). Moderate exercise mitigates the detrimental effects of aging on tendon stem cells. *PLoS One* 10, 1–20.

Zhang, Y.-J., Chen, X., Li, G., Chan, K.-M., Heng, B.C., Yin, Z., and Ouyang, H.-W. (2018). Concise Review: Stem Cell Fate Guided By Bioactive Molecules for Tendon Regeneration. *Stem Cells Transl. Med.* 7, 404–414. Zhao, B., Tumaneng, K., and Guan, K. (2011). The Hippo pathway in organ size control, tissue regeneration and stem cell self-renewal. *Nat. Publ. Gr.* 13, 877–883.

Zhong, W., Li, Y., Li, L., Zhang, W., Wang, S., and Zheng, X. (2013). YAP-mediated regulation of the chondrogenic phenotype in response to matrix elasticity. *J. Mol. Histol.* 1–9.

Zhu, C., Li, L., and Zhao, B. (2014). The regulation and function of YAP transcription co-activator. *Acta Biochim. Biophys. Sin. (Shanghai)*. 47, 16–28.

X. Annexes

X.1 EGR1 Regulates Transcription Downstream of Mechanical Signals during Tendon Formation and Healing

RESEARCH ARTICLE

EGR1 Regulates Transcription Downstream of Mechanical Signals during Tendon Formation and Healing

Ludovic Gaut¹, Nicolas Robert¹, Antony Delalande², Marie-Ange Bonnin¹, Chantal Pichon², Delphine Duprez^{1*}

1 Sorbonne Universités, UPMC Univ Paris 06, CNRS UMR7622, Inserm U1156, IBPS-Developmental Biology Laboratory, F-75005 Paris, France, **2** CNRS UPR4301-CBM, 45071 rue Charles Sadron, Orléans CEDEX2, France

☯ These authors contributed equally to this work.

* delphine.duprez@upmc.fr



Abstract

Background

Tendon is a mechanical tissue that transmits forces generated by muscle to bone in order to allow body motion. The molecular pathways that sense mechanical forces during tendon formation, homeostasis and repair are not known. EGR1 is a mechanosensitive transcription factor involved in tendon formation, homeostasis and repair. We hypothesized that EGR1 senses mechanical signals to promote tendon gene expression.

Methodology/Principal findings

Using *in vitro* and *in vivo* models, we show that the expression of *Egr1* and tendon genes is downregulated in 3D-engineered tendons made of mesenchymal stem cells when tension is released as well as in tendon homeostasis and healing when mechanical signals are reduced. We further demonstrate that EGR1 overexpression prevents tendon gene downregulation in 3D-engineered tendons when tension is released. Lastly, ultrasound and microbubbles mediated EGR1 overexpression prevents the downregulation of tendon gene expression during tendon healing in reduced load conditions.

Conclusion/Significance

These results show that *Egr1* expression is sensitive to mechanical signals in tendon cells. Moreover, EGR1 overexpression prevents the downregulation of tendon gene expression in the absence of mechanical signals in 3D-engineered tendons and tendon healing. These results show that EGR1 induces a transcriptional response downstream of mechanical signals in tendon cells and open new avenues to use EGR1 to promote tendon healing in reduced load conditions.

OPEN ACCESS

Citation: Gaut L, Robert N, Delalande A, Bonnin M-A, Pichon C, Duprez D (2016) EGR1 Regulates Transcription Downstream of Mechanical Signals during Tendon Formation and Healing. PLoS ONE 11(11): e0166237. doi:10.1371/journal.pone.0166237

Editor: Chunfeng Zhao, Mayo Clinic Minnesota, UNITED STATES

Received: May 3, 2016

Accepted: October 25, 2016

Published: November 7, 2016

Copyright: © 2016 Gaut et al. This is an open access article distributed under the terms of the [Creative Commons Attribution License](https://creativecommons.org/licenses/by/4.0/), which permits unrestricted use, distribution, and reproduction in any medium, provided the original author and source are credited.

Data Availability Statement: All relevant data are within the paper.

Funding: This work was supported by the Fondation pour la Recherche Médicale (FRM DEQ20140329500). The funders had no role in study design, data collection and analysis, decision to publish, or preparation of the manuscript.

Competing Interests: The authors have declared that no competing interests exist.

Introduction

Tendon is a crucial component of the musculo-skeletal system, which transmits forces generated by skeletal muscle to bone to allow body motion. Mechanical signals are known to be involved in tendon development, homeostasis and repair [1–4]. However, the mechanotransduction pathways involved in tendon cell differentiation in normal or pathological situations are not fully understood.

The functional component of tendon is type I collagen, which displays a tendon-specific spatial organization that confers tendon mechanical properties [5]. Type I collagen is composed of a triple helix of collagen chains ($\alpha 1(2)$, $\alpha 2(1)$) coded by two different genes, *Col1a1* and *Col1a2*. Unfortunately, neither of the *Col1a* genes is specific to tendons. They are also expressed in many other connective tissues, making it difficult to assess tenogenesis using *Col1a* gene expression. The bHLH transcription factor Scleraxis (*Scx*) is specifically expressed in embryonic, fetal and postnatal tendons [6–8]. From the 4th postnatal month, *Scx* expression is restricted to the epitenon, but is reactivated in the tendon core by treadmill exercise [8]. Moreover, *Scx* expression is upregulated in tendons upon injury in animal models [9, 10]. The type II transmembrane glycoprotein tenomodulin (*Tnmd*) is also considered as a relevant marker of tendon cell differentiation in mouse, rat and human [11–13]. During development, *Scx* is required and sufficient for *Tnmd* expression in limb tendons [14, 15]. *Tnmd*^{-/-} mice show defective postnatal tendons [16] and reduced self-renewal of tendon stem cells in adult [17].

In addition to *Scx*, the Zinc finger transcription factor, Early Growth Response-1 (EGR1) has been identified as being involved in pre- and postnatal tendon formation [10, 18]. EGR1 is not specific to tendons, since it is expressed in many other tissues; however, EGR1 has the remarkable ability to be sufficient for promoting tendon gene expression, including *Scx* and *Col1a1*, during development [18], in mouse mesenchymal stem cells [10] and in rabbit tendon stem cells [19]. The DNA-binding protein EGR1 is known to be a mechanosensitive gene in various cellular systems. Mechanical stretch increases *Egr1* transcription in endothelial cells [20], vascular smooth muscle cells [21] or skeletal muscle cells [22]. Dynamic compression also activates *Egr1* transcription in 3-dimensional (3D) cultures of mouse primary chondrocytes [23]. EGR1 has been shown to be a mediator of mechanical input that contributes to vascular remodeling of vein grafts [24].

Since EGR1 is known to be a mechanosensitive gene and involved in tendon development, homeostasis and repair, we hypothesized that EGR1 transduces mechanical signals into transcriptional regulation to promote tendon cell differentiation during tendon formation, homeostasis and repair. We used *in vitro* 3-dimensional culture system and *in vivo* models to test this hypothesis.

Materials and Methods

Animals

The *Egr1*^{LacZ/+} mice bred in a C57BL/6j background carry an insertion of a LacZ-neo cassette that inactivates the *Egr1* gene [25] and allow the visualization of *Egr1* expression with LacZ activity in a heterozygous context [10]. C57BLj wild-type mice were purchased from Janvier (France). All animal experiments were conducted in accordance with the guidelines of the french national ethic comity for animal experimentation N°05. The animal experiments shown in this study have been approved by the french national ethic committee for animal experimentation N°05 and are registered under the number 01789.02.

Engineered tendons made of mesenchymal stem cells

Mouse mesenchymal stem cells, C3H10T1/2 [26] were used to establish fibrin-based 3D constructs. Tendon-like structures from mouse C3H10T1/2 cells or C3H10T1/2-EGR1 cells [10]

were performed as previously described [27]. For each construct, 400 μ l of cell suspension (7.5×10^5 cells) were mixed with 20 mg/ml fibrinogen (Sigma, St Louis, MO, USA) and 200 U/ml thrombin (Sigma, St Louis, MO, USA). The fibrin gels containing cells were seeded in already prepared SYLGARD-covered wells (Dow Chemical, Midland, MI, USA), in which two 8 mm-sutures (Ethicon, Sommerville, NJ, USA) were pinned 10 mm apart. Culture medium containing 200 μ M of L-ascorbic acid 2-phosphate was added to the wells and gels were scored every day for a proper contraction into a linear construct. After 7 days, the C3H10T1/2 and C3H10T1/2-EGR1 cells formed continuous tendon-like constructs between the 2 anchors. Tension release was obtained by cutting one end of the construct as previously described in [28]. Gene expression was analyzed 24 hours after tension release. Each tendon construct made of C3H10T1/2 or C3H10T1/2-EGR1 cells under tension or after tension release was considered as a biological sample. We analyzed 12 constructs made of C3H10T1/2 cells, 7 constructs made of C3H10T1/2-EGR1 cells, 7 de-tensioned-constructs made of C3H10T1/2 cells and 5 de-tensioned-constructs made of C3H10T1/2-EGR1 cells. The mRNA levels of each construct were analyzed by q-RT-PCR.

Botox injection in muscles and Achilles tendon injury in adult mice

For the analysis of mechanical signal involvement in tendon homeostasis, 6 UI/kg of Botox preparation (Allergan) [29] and physiological saline solution were injected into the Gastrocnemius muscles of right and left legs, respectively, of *Egr1^{LacZ/+}* (N = 6) and wild-type (N = 12) adult mice (two- to four-month-old). Botox injection reduces muscle contraction and movements and consequently mechanical signals to tendons [30]. Experimental animals did not display any obvious difficulty in moving, but limped on the Botox-injected legs. The Botox and physiological saline manipulated *Egr1^{LacZ/+}* animals were kept for one week (N = 6) and analyzed for LacZ staining. Tendons were fixed for 20 minutes in 4% paraformaldehyde and incubated in X-gal staining solution for 4 hours at 37°C. The Botox and physiological saline manipulated wild-type animals were kept for one (N = 8) or two (N = 11) weeks after injection (3 independent experiments) and then analyzed for gene expression.

For the analysis of mechanical signal involvement in tendon healing, Achilles tendon injury was performed on left legs of wild-type animals, as previously described in [10]. Briefly, adult mice were anesthetized by isoflurane inhalation. A 0.5-mm longitudinal full-thickness lesion parallel to the axis of the tendon was performed using a scalpel. In this type of injury, the tendon tension was maintained. After injury, the skin was sutured using 2-0 Mersilk, and the animals were kept for two weeks. The Botox or physiological saline was injected in the Gastrocnemius muscles of the manipulated left legs. The mouse group, which had undergone Achilles tendon injury and Botox injection, constitute the experimental group (N = 11) that was compared to the control group with Achilles tendon injury and physiological saline injection in muscles (N = 10). Experimental animals did not display any obvious difficulty in moving. However, the animals in the group that had Achilles tendon injury and Botox injection were limping compared to those in the group with Achilles tendon injury and physiological saline injection. Achilles tendons, in the above experimental conditions, were processed for RT-q-PCR analyzes.

Ultrasound and microbubbles-mediated EGR1 gene delivery in Achilles tendons followed by tendon injury and Botox injection into muscles

Ultrasound and microbubbles-mediated gene delivery is a technique also known as sonoporation, allowing for a high and sustained gene expression in mouse Achilles tendons [31]. 10 μ g of EGR1 encoding plasmid DNA [18, 32] and 3.75 μ l of MicroMarkerTM microbubbles

(Bracco) in a total volume of 10 µl were injected into the Achilles tendon. Injection was immediately followed by a 1-MHz ultrasound stimulation of 200 kPa (negative peak) during 10 minutes. Ultrasound was generated from a 0.5" diameter, IBMF-014 transducer with a frequency of 1 MHz (Sofranel, Sartrouville, France). A signal consisting of 40 cycles with a frequency of 1.0 MHz and a pulse repetition frequency of 10 kHz, a duty cycle of 40%, was generated by a 33220A arbitrary function generator (Agilent technologies, Les Ulis, France). The signal was amplified by a RF power amplifier (ADECE, Artannes, France) and used as the input for the transducer. The transducer was calibrated in a Perspex container using an HGL-200 PVDF bullet type hydrophone (Onda, Sunnyvale, CA). EGR1 sonoporation experiments were performed one day before tendon injury and Botox treatment because intratendinous injection requires the integrity of tendon sheath. Mice were euthanized 15 days after tendon injury and Botox injection and tendons were harvested in 500 µl of RNAlater solution (ThermoScientific) for RNA isolation and RT-q-PCR analyses. 10 mice displaying EGR1 overexpression, tendon injury and Botox injection and 6 mice displaying tendon injury and Botox injection were analyzed.

RNA isolation, reverse transcription and RT-q-PCR

Total RNAs were extracted from fibrin gel constructs made of C3H10T1/2 (N = 11) or C3H10T1/2-EGR1 cells (N = 7), tension-released fibrin gel constructs made of C3H10T1/2 cells (N = 7) or C3H10T1/2-EGR1 cells (N = 5). Total RNAs were extracted from adult mouse tendons under various experimental designs (following physiological saline or Botox injection in normal or injured conditions, after ultrasound-forced EGR1 expression followed by injury and Botox injection) according to the Qiagen RNeasy Minikit (QIAGEN, Germany). RNA (300 ng to 1 µg) was reverse transcribed using the High Capacity Retrotranscription Kit (Applied Biosystems). RT-q-PCR was performed using SYBR Green PCR Master Mix (Applied Biosystems). Relative mRNA levels were calculated using the $2^{-\Delta\Delta Ct}$ method [33]. In all our experimental designs, the Cts of two housekeeping genes *Gapdh* and *Hprt* did not show any variations in control versus experimental conditions. The ΔCt s were obtained from Cts normalized with *Gapdh* levels in each sample. RNA samples originating from 5 to 11 biological samples originating from 3 independent experiments were analyzed in duplicate. Primers used for RT-q-PCR are listed in Table 1.

Table 1. Primers used for quantitative RT-PCR.

Col1a1	Fwd 5' CCAGCGAAGAAGCTCATAACAGC
	Rev 5' GGACACCCCTTCTACGTTGT
Col1a2	Fwd 5' CCAGCGAAGAAGCTCATAACAGC
	Rev 5' GGACACCCCTTCTACGTTGT
Egr1	Fwd 5' -CAGCGCCTTCAATCCTCAAG
	Rev 5' -GCGATGTCAGAAAAGGACTCTGT
Gapdh	Fwd 5' TTGTGGAAGGGCTCATGACC
	Rev 5' TCTTCTGGGTGGCAGTGATG
Hprt	Fwd 5'AGGGCATATCCAACAACAACTT
	Rev 5'GTTAAGCAGTACAGCCCCAAA
Scx	Fwd 5' CCTTCTGCCTCAGCAACCAG
	Rev 5' GGTCCAAAGTGGGGCTCTCCGTGACT
Tgfb2	Fwd 5' GAATAAAAGCGAAGAGCTCGAGG
	Rev 5' GAGGTGCCATCAATACCTGCA
Tnmd	Fwd 5' AACACTTCTGGCCGAGGTAT
	Rev 5' AAGTGTGCTCCATGTCATAGGTTTT

doi:10.1371/journal.pone.0166237.t001

Statistical analysis

Sample sizes were based on historical experience of effect sizes for these types of experiments. Error bars in graphics represent the standard deviations or the standard errors of the mean, depending of the size of the samples. Statistics were calculated using non-parametric tests with the GraphPad Prism V6 software. The Mann-Whitney test was used for unpaired samples and the Wilcoxon test for paired samples.

Results

EGR1 overexpression prevents the decrease of tendon gene expression in 3D tendon constructs after tension release

Fibrin-based 3D cell cultures recapitulate tendon formation based on tenogenic marker expression and tendon-like collagen fibrillogenesis [27, 34–37]. This *in vitro* engineered tendon system involves tension [34, 35]. Forced expression of EGR1 in fibrin-based 3D C3H10T1/2 cell cultures increases *Scx*, *Colla1* and *Colla2* expression levels compared to control fibrin-based 3D C3H10T1/2 cell cultures [10]. We now show that the expression of the tendon differentiation marker *Tnmd* was also increased in the presence of EGR1 in 3D constructs (Fig 1A). The *Tgfb2* mRNA levels were also increased in EGR1-producing 3D constructs compared to 3D constructs (Fig 1A). The tension release of the 3D constructs induces the appearance of immature collagen fibrils with no preferred orientation in engineered chick tendons [27] and loss of *TNMD* expression in engineered human tendons [28]. The tension was released by cutting one edge of the engineered mouse tendons made of C3H10T1/2 cells (Fig 1B). Tension release led to a decrease in the expression of *Egr1* and tendon genes including *Scx*, *Tnmd*, *Colla1* and *Colla2* (Fig 1B). The expression of *Tgfb2* was also decreased in tension-released engineered tendons (Fig 1B). Tension release in *Egr1*-producing 3D-constructs did not trigger any significant changes in tendon gene expression compared to *Egr1*-producing 3D constructs under tension (Fig 1C). This shows that EGR1 overexpression is able to activate tendon gene expression independently of tension in engineered tendons. We conclude that *Egr1* expression is sensitive to tension in engineered mouse tendons and EGR1 forced expression prevents the downregulation of tendon gene expression in the absence of mechanical input.

The expression of tendon genes is downregulated in adult tendons when movements are reduced

In order to assess the importance of mechanical signals for tendon gene expression in homeostasis, we developed a reduced load model in adult mice based on botulinium toxin A (Botox) injection into the Gastrocnemius muscle of hindlimbs (Fig 2A). One week after injection of Botox or physiological saline solution in muscles of *Egr1^{LacZ/+}* mice, LacZ expression (reflecting *Egr1* expression) appeared to be decreased in Achilles tendons (Fig 2B and 2C). Consistently, the *Egr1* mRNA levels were decreased in Achilles tendons of Botox-injected legs compared to saline solution-injected legs, one and two weeks after injection in wild-type mice (Fig 2D). *Scx* expression was also decreased in tendons of Botox-injected legs compared to control legs, one and two weeks after Botox injection (Fig 2D), consistent with the decrease in *Scx* expression one week after Botox injection in *Scx*-GFP mice [30]. The tendon-associated collagen gene *Colla2* also displayed decreased expression levels one and two weeks after Botox injection (Fig 2D). The expression of the terminal differentiation tendon marker, *Tnmd* did not significantly change (Fig 2D). Interestingly, *Tgfb2* expression was also decreased in tendons, two weeks after Botox injection (Fig 2D). This showed that the expression of *Egr1*, *Tgfb2* and tendon genes (*Scx*

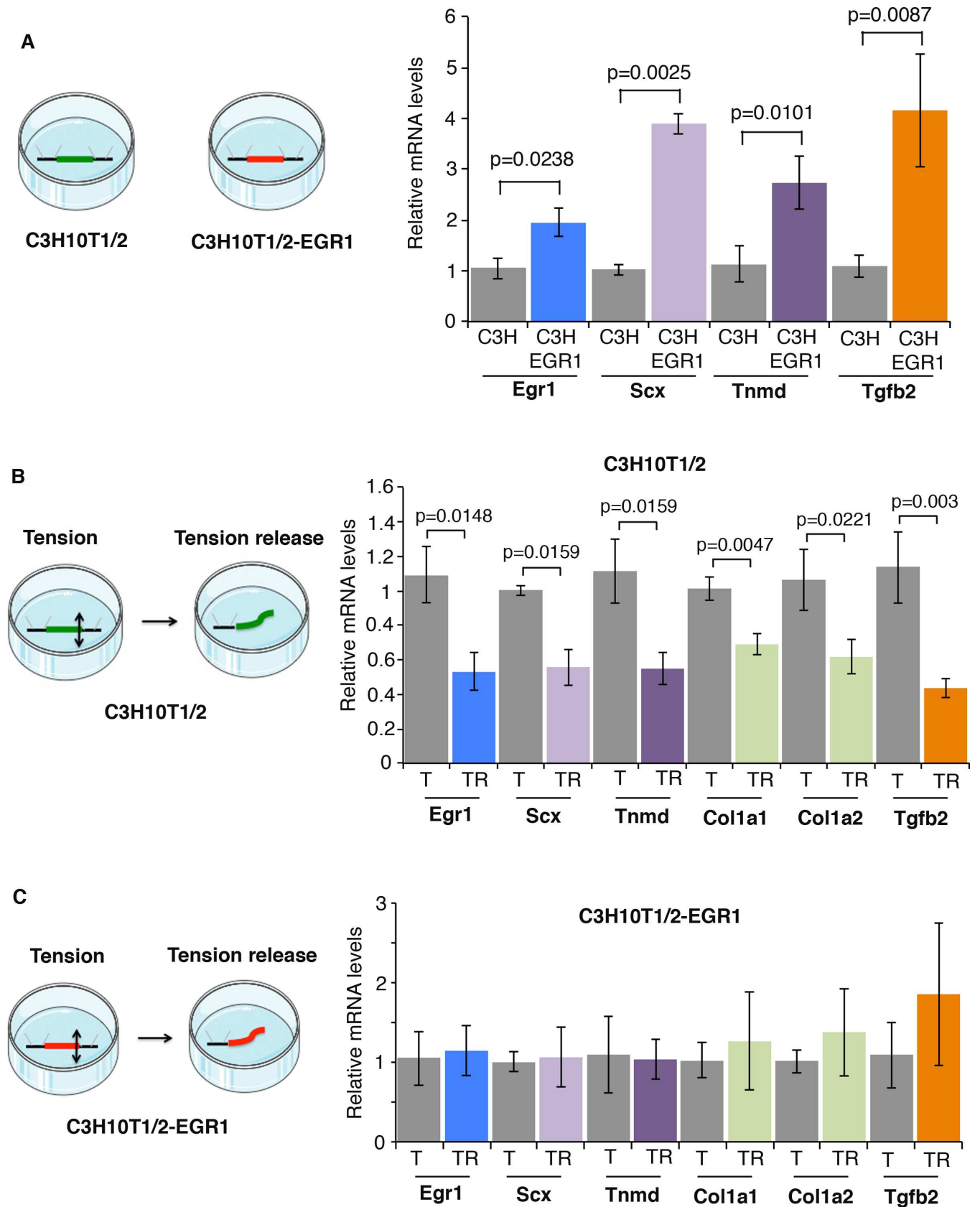


Fig 1. EGR1 overexpression prevents the downregulation of tendon-associated gene expression in tension released engineered tendons. (A) Two week-old fibrin gel constructs made of mouse C3H10T1/2 cells or C3H10T1/2-EGR1 cells were analyzed for tendon gene expression by RT-q-PCR analyses. The mRNA levels of C3H10T1/2 constructs were normalized to 1. Errors bars represent standard errors of the mean of 5 C3H10T1/2 constructs and 7 C3H10T1/2-EGR1 constructs. The *p* values were calculated using the Mann-Whitney test. The mRNA levels of *Egr1*, *Scx*, *Tnmd* and *Tgfb2* genes were increased in C3H10T1/2-EGR1 constructs compared to those of C3H10T1/2 constructs. (B) Tension was released in C3H10T1/2 constructs by sectioning one end of the construct. Transcript levels were analyzed by RT-q-PCR analyses in tension-released C3H10T1/2 constructs and compared to C3H10T1/2 constructs. The mRNA levels of C3H10T1/2 constructs were normalized to 1. Errors bars represent standard errors of the mean of 7 C3H10T1/2 constructs and 7 tension-released C3H10T1/2 constructs. The *p* values were calculated using the Mann-Whitney test. We observed a decrease in the transcript levels of *Egr1*, *Scx*, *Tnmd*, *Col1a1*, *Col1a2* and *Tgfb2* genes in tension-released C3H10T1/2 constructs (TR) compared to tensioned C3H10T1/2 constructs (T). (C) The mRNA levels of tendon genes were analyzed in tension-released C3H10T1/2-EGR1 constructs and compared with tensioned C3H10T1/2-EGR1 constructs by RT-q-PCR analyses. The mRNA levels of C3H10T1/2-EGR1 constructs were normalized to 1. Errors bars represent standard errors of the mean of 7 C3H10T1/2-EGR1 constructs and 5 tension-released C3H10T1/2-EGR1 constructs. The *p* values were calculated using the Mann-Whitney test. There was no significant change in tendon gene expression in tension-released C3H10T1/2-EGR1 constructs (TR) compared to tensioned C3H10T1/2-EGR1 constructs (T). T, Tension, TR, Tension release.

doi:10.1371/journal.pone.0166237.g001

and *Col1a2*) is sensitive to mechanical input in adult tendons. We conclude that mechanical signals are required for tendon gene expression in homeostasis.

Reduced mechanical signals decrease the transcriptional response during tendon healing after injury

In order to analyze the effect of mechanical signals during healing, we used an Achilles tendon injury model in adult wild-type mice as previously described [10]. In this tendon injury model, a longitudinal incision was performed along the axis of the Achilles tendon, in which the tension was maintained. One week after tendon injury, there is a dramatic increase in tendon gene expression, including *Scx*, *Tnmd*, *Col1a1* and *Col1a2* [10]. *Egr1* expression is also increased by fold-3.6 in tendons, after injury and *Egr1* is required for the normal tendon transcriptional response during the healing process [10]. In order to determine whether mechanical signals would influence the transcriptional response during tendon healing, we injected Botox or physiological saline solution in muscles in this mouse model of tendon injury (Fig 3A). We observed a significant decrease in the expression of *Egr1*, *Scx*, *Tnmd*, *Col1a1*, *Col1a2* and *Tgfb2* genes after Botox injection compared to physiological saline solution injections, in injury conditions (Fig 3B). The decrease of mRNA levels of tendon genes ranged from 40% to 60% (Fig 3). This shows that a diminution of mechanical signals modifies the transcriptional response during the tendon healing process following injury. We conclude that mechanical signals are required for the full transcriptional response during tendon healing.

EGR1 forced expression in tendons prevents the diminution of tendon gene response in reduced load conditions after injury

The expression of the mechanosensitive gene *Egr1* was decreased in reduced load conditions in tendon homeostasis (Fig 2) and healing (Fig 3). To assess whether EGR1 acts downstream of mechanical signals during tendon healing, we performed *in vivo* EGR1 rescue experiments in reduced load conditions and after tendon injury. We took advantage of an ultrasound-based gene delivery method, which has been found to be efficient in tendons [31]. Plasmid DNA encoding for the *Egr1* gene was delivered to the tendons with optimized parameters (1 MHz, 200 kPa, 10 min, 40% duty cycle and 10 kHz pulse repetition frequency). The following day, Botox was injected in muscle followed by tendon injury (Fig 4A). Two weeks after Botox injection in muscle and tendon injury, we compared the expression of tendon genes in tendons overexpressing EGR1 or not during tendon healing and in reduced load conditions. In this experiment, *Egr1* was increased by fold-2.6. EGR1 forced expression in tendons increased the expression of tendon-associated genes including *Scx*, *Tnmd*, *Col1a1*, *Col1a2* and *Tgfb2*, when

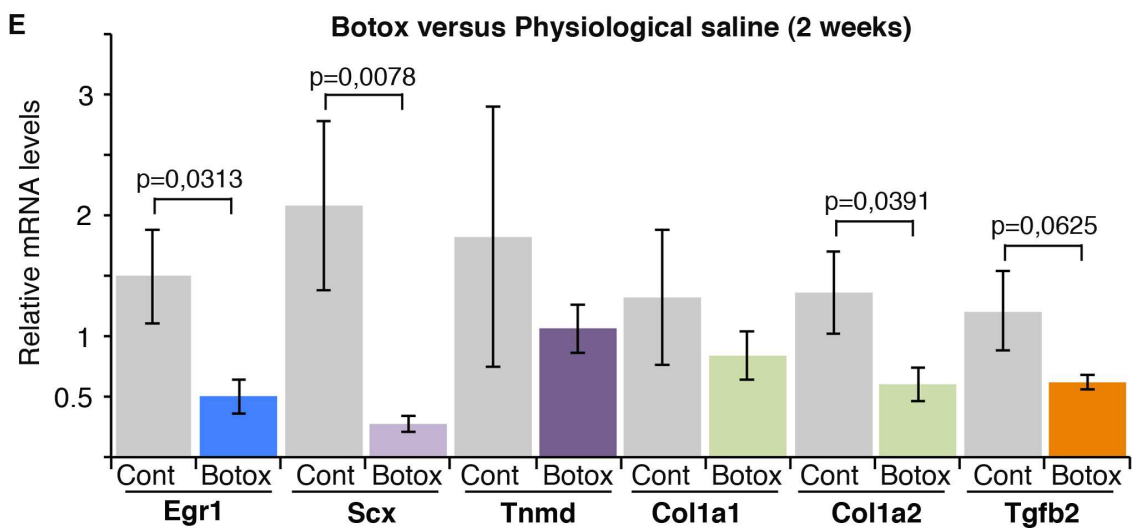
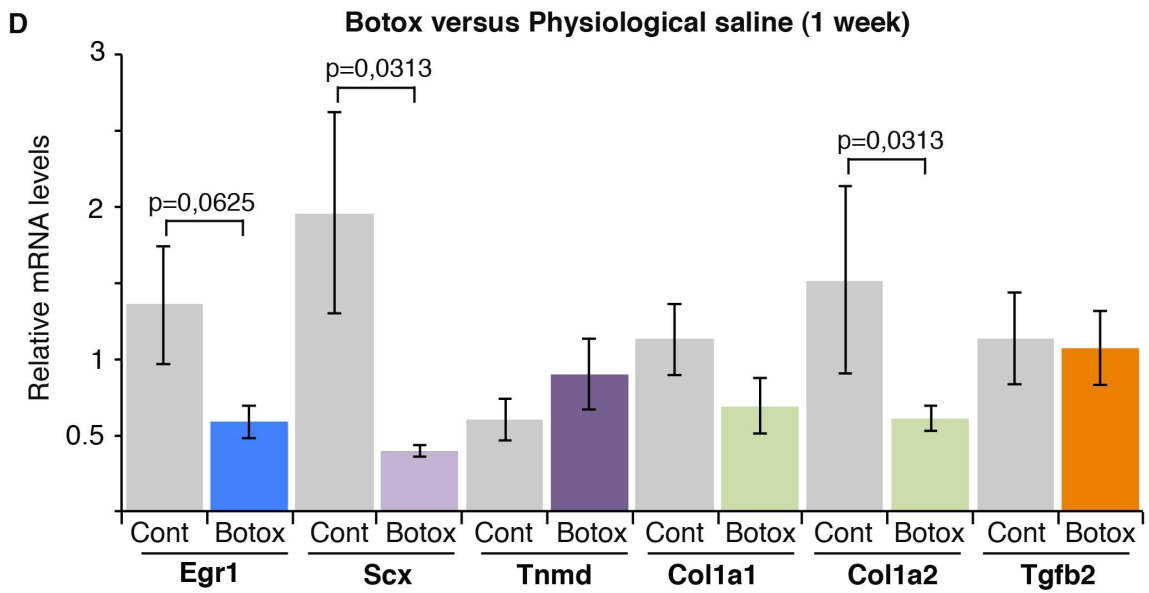
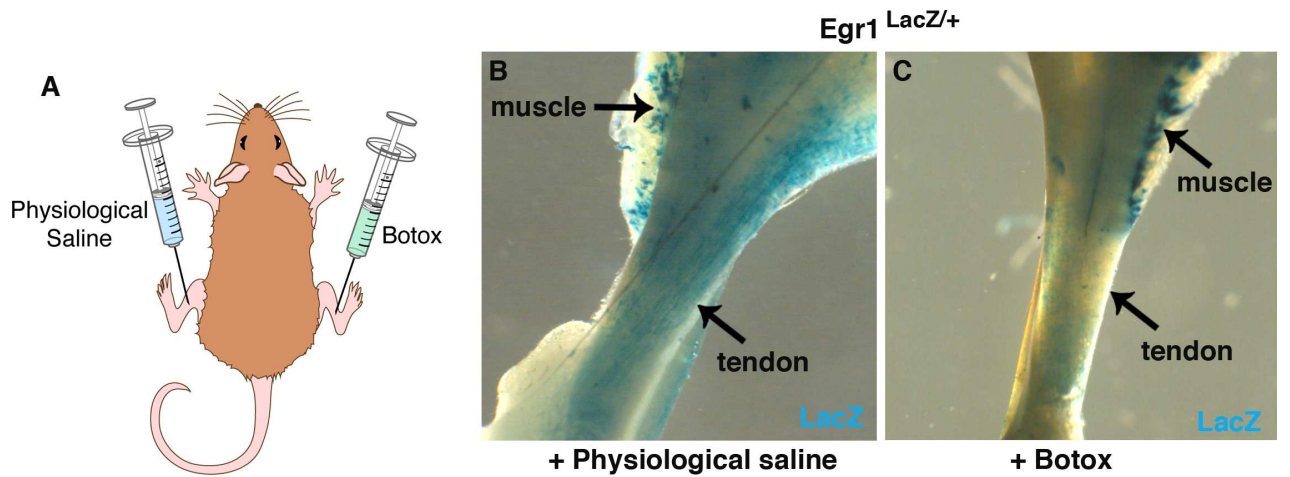


Fig 2. Reduced mechanical input induces a diminution of *Egr1* and *Scx* expression in adult tendons. (A) Botox or physiological saline injections in Gastrocnemius muscles of adult mice. (B,C) LacZ staining (reflecting *Egr1* expression) in tendons, 1 week following physiological saline or Botox injection in *Egr1*^{LacZ/+} adult mice. (D) RT-q-PCR analyses of tendons, one or two weeks after Botox or physiological saline injections in muscles in adult mice. The mRNA levels of tendons following Botox injection were compared to those of tendons with physiological saline injection. Errors bars represent the standard deviations of 5 (one week) and 7 (two weeks) biological samples. The mRNA levels of *Egr1*, *Scx*, *Col1a2*, *Tgfb2* genes were decreased one or two weeks after Botox injection compared to physiological saline injection. *Tnmd* mRNA levels were not significantly decreased after Botox injection. The *p* values were calculated using the Wilcoxon test.

doi:10.1371/journal.pone.0166237.g002

compared to control (Fig 4B). The levels of induction were similar to that of *Egr1* overexpression (Fig 4A). This shows that EGR1 is sufficient to prevent the diminution of tendon gene expression that is observed during healing in reduced load conditions.

Discussion

We show that reduced load conditions consistently lead to a decrease in expression of the transcription factor *Egr1* and tendon genes in tendon homeostasis, tendon healing and *in vitro* engineered tendons. We also demonstrate that EGR1 forced expression prevents the decrease of tendon gene expression in reduced load conditions during tendon healing and in engineered tendons.

Egr1 is a mechanosensitive gene, which has been shown to act downstream of mechanical signals in the vascular system [20, 21, 24]. Consistently, *Egr1* expression is systematically downregulated in reduced load conditions in the *in vivo* and *in vitro* models of tendon biology. The decrease of *Egr1* expression at the transcription level in reduced load conditions is consistent with the upregulation of *Egr1* expression in overload conditions in adult tendons [38, 39]. *Egr1* expression is induced as early as 15 minutes after a loading episode in rat Achilles tendons [40]. This indicates that *Egr1* expression reflects a rapid transcriptional response following loading changes in tendons. In addition to being sensitive to mechanical signals, *Egr1* appears to be sufficient to drive the tendon genetic program in the absence of mechanical signals. The presence of exogenous EGR1 abolishes the downregulation of *Scx*, *Col1a1* and *Tnmd* in engineered tendons subjected to tension release and EGR1 also prevents the decrease of *Scx*, *Col1a1* and *Tnmd* expression in Achilles tendons in reduced load conditions during tendon healing following injury. This shows that the Zinc-finger transcription factor *Egr1* senses mechanical signals in tendons and modulates tendon gene expression upon loading changes. Although EGR1 has the ability to induce the expression of tendon genes in normal [10] or reduced load (Figs 1 and 4) conditions, it remains unclear whether EGR1 directly regulates the transcription of tendon genes. Previous promoter and Chromatin Immuno-Precipitation (ChIP) analyses indicate that EGR1 trans-activates the tendon promoter of the mouse *Col1a1* gene [18, 32]. Moreover, EGR1 directly regulates *Tgfb2* transcription in adult mouse tendons [10]. *Tgfb2* expression is downregulated in reduced load conditions in tendon homeostasis or healing in adult mice (Figs 2 and 3) and in engineered tendons made of mouse mesenchymal stem cells (Fig 1). EGR1 rescue experiments in conditions of reduced mechanical signals induced *Tgfb2* expression in engineered tendons and during the tendon healing process (Figs 1 and 4). These results suggest that *Egr1* acts upstream of *Tgfb2* to activate tendon gene expression upon loading. It should be noted that TGF- β 1 supplementation was not sufficient to prevent the decrease of tendon gene expression in de-tensioned 3D engineered tendons derived from human tendon cells [28]. It is not clear whether TGF- β ligand is not sufficient to activate tendon gene expression in reduced load conditions or TGF- β 1 activity differs from TGF- β 2 activity. Antagonist effects between TGF- β 1 and TGF- β 2 ligands have been reported on *COL1A1* transcription in rat tendon fibroblasts [41]. TGF- β supplementation activates *Scx* expression in various cellular

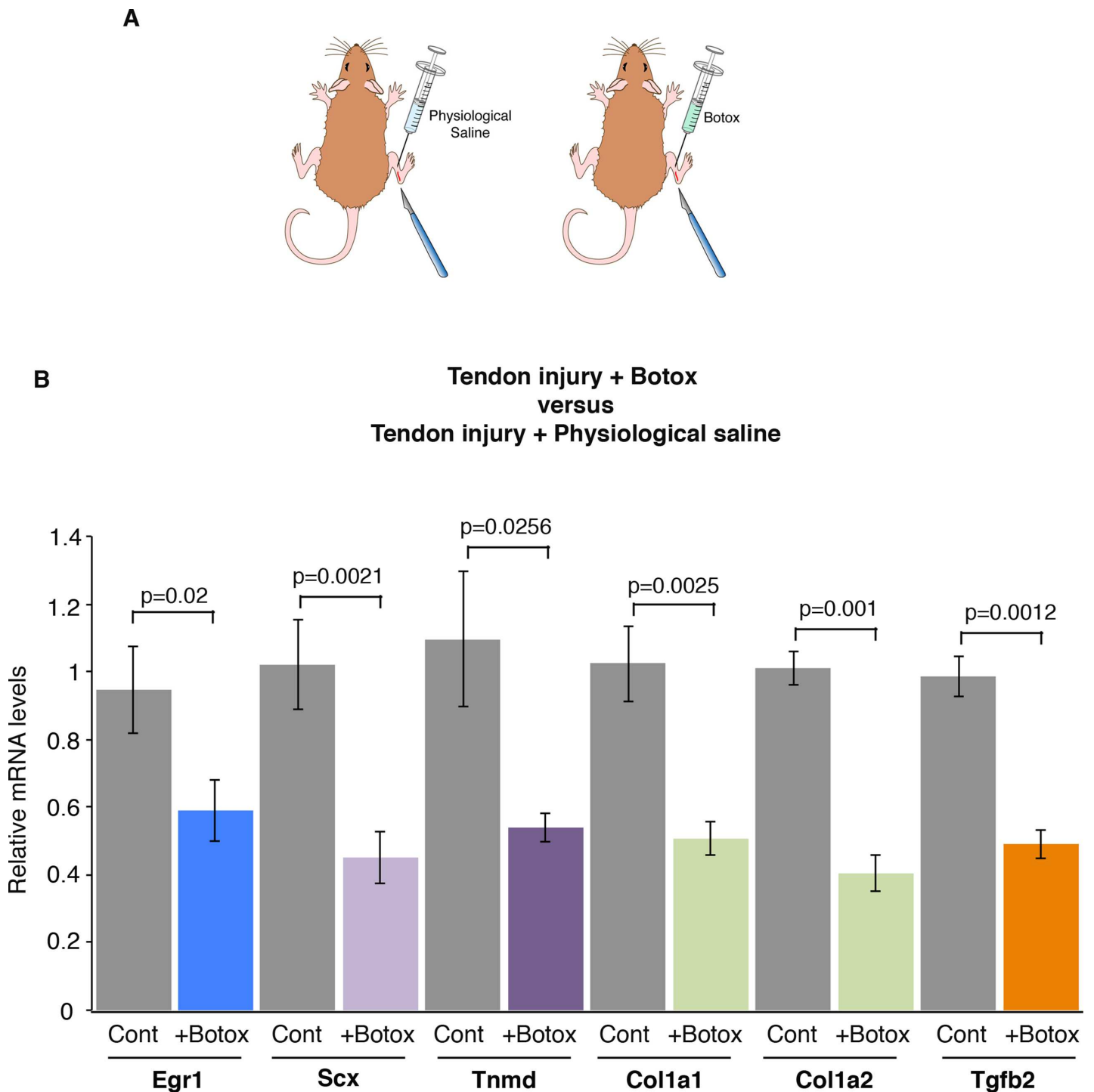


Fig 3. Mechanical signals are required for normal tendon gene response following tendon injury. (A) Botox or physiological saline injections in Gastrocnemius muscles and tendon injury in adult mice. (B) RT-q-PCR analyses of tendons, 2 weeks after tendon injury and Botox injection in muscles. The mRNA levels of tendons following injury and physiological saline injection in muscles were normalized to 1. The errors bars represent the standard error of the means of 10 and 11 biological samples of injured tendons after physiological saline or Botox injections, respectively. The *p* values were calculated using the Mann-Whitney test. The mRNA levels of the *Egr1*, *Scx*, *Tnmd*, *Col1a1*, *Col1a2* and *Tgfb2* genes were all significantly decreased in reduced movement conditions compared to controls during the healing process, following tendon injury.

doi:10.1371/journal.pone.0166237.g003

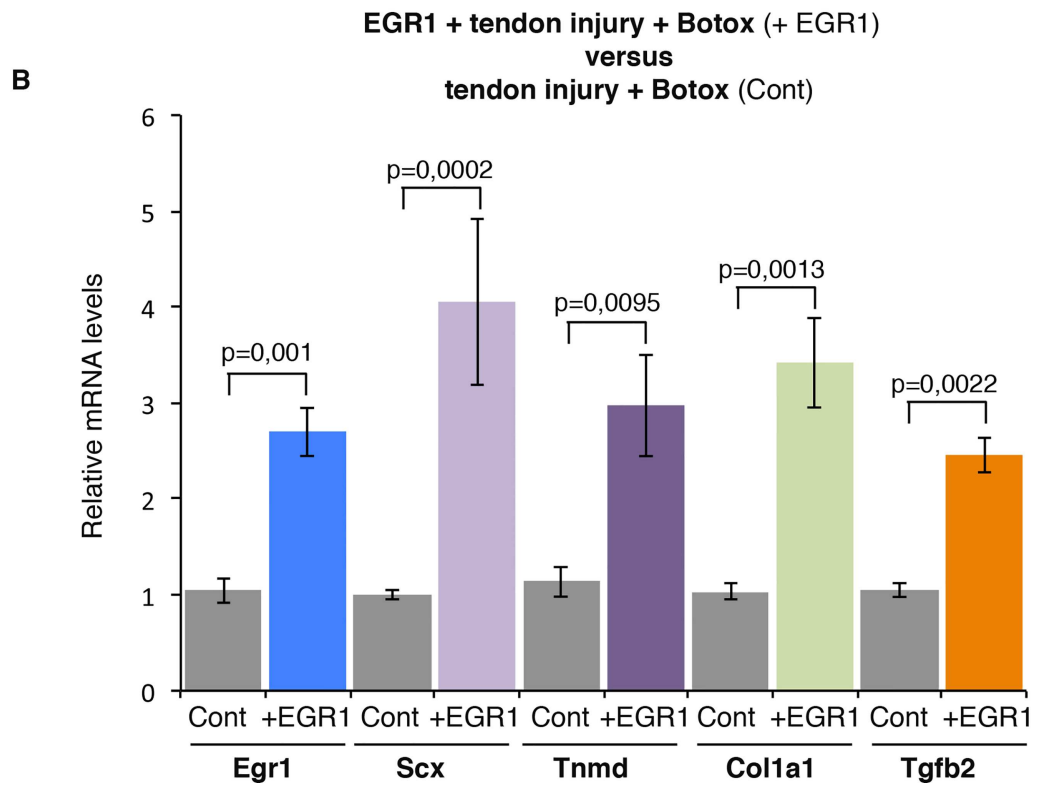
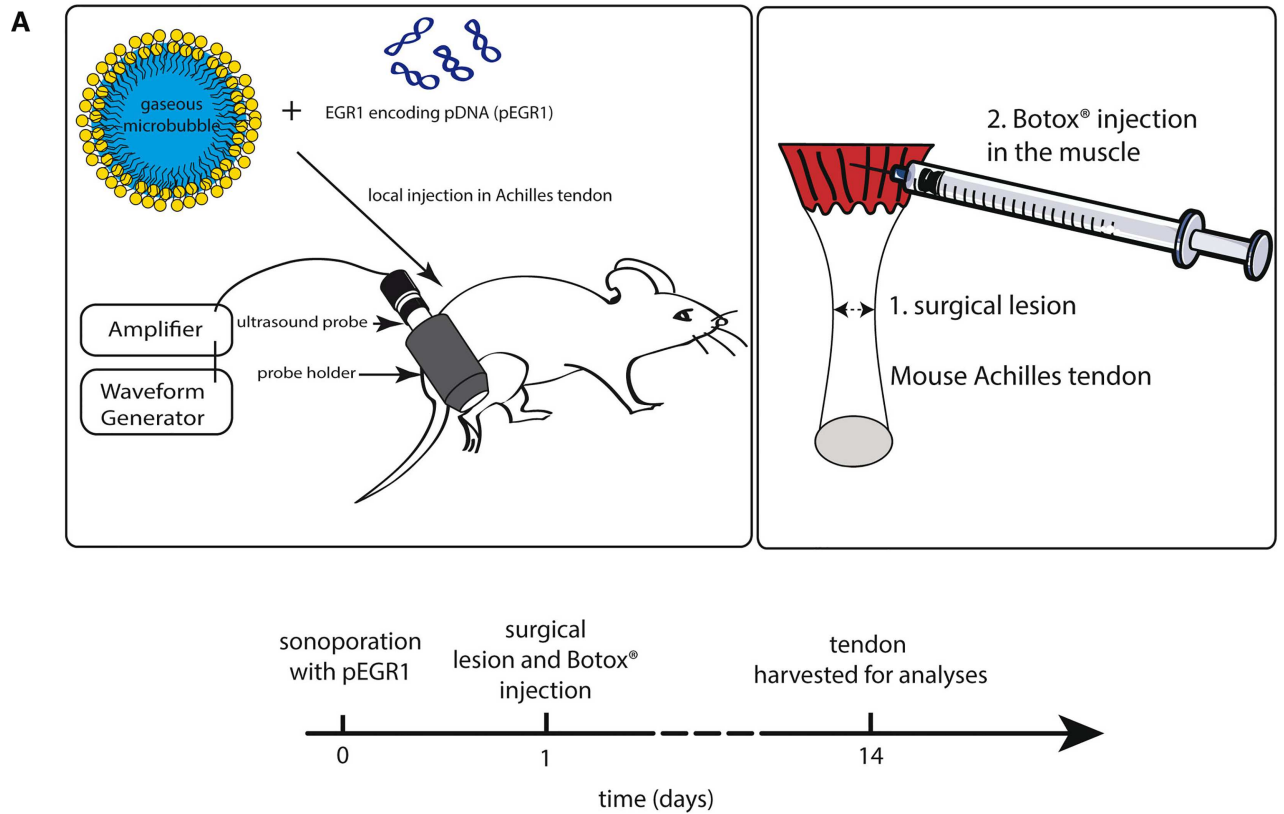


Fig 4. EGR1 forced expression in tendons prevents the diminution of tendon gene expression during tendon healing in reduced mechanical load. (A) Description of the experimental design for sonoporation. 10 µg of EGR1 encoding plasmid and 3.75 µl of MicroMarker microbubbles were injected in the Achilles tendon sheath. Tendons were then stimulated by ultrasound at 1 MHz during 10 minutes at 200 kPa, 40% duty cycle and 10 kHz pulse repeating frequency. The day after EGR1 sonoporation, a surgical lesion of the Achilles tendon was performed followed by a Botox or physiological saline solution injection in the muscle. Two weeks after treatment, tendons were harvested for analyses by RT-q-PCR. (B) RT-q-PCR analysis of tendon gene expression in EGR1-sonoporated tendons versus control-tendons, following tendon injury in immobilization conditions. The mRNA levels of control tendons following injury and Botox injection in muscles were normalized to 1. The error bars represent standard errors of the mean of 6 biological samples of injured tendons of Botox-injected legs in the absence of EGR1 and 10 biological samples of injured tendons of Botox-injected legs in presence of ectopic EGR1. The *p* values were calculated using the Mann-Whitney test. The mRNA levels of *Egr1*, *Scx*, *Tnmd*, *Col1a2* and *Tgfb2* were increased in *Egr1*-sonoporated tendons compared to control tendons, following tendon injury and Botox injection in muscles.

doi:10.1371/journal.pone.0166237.g004

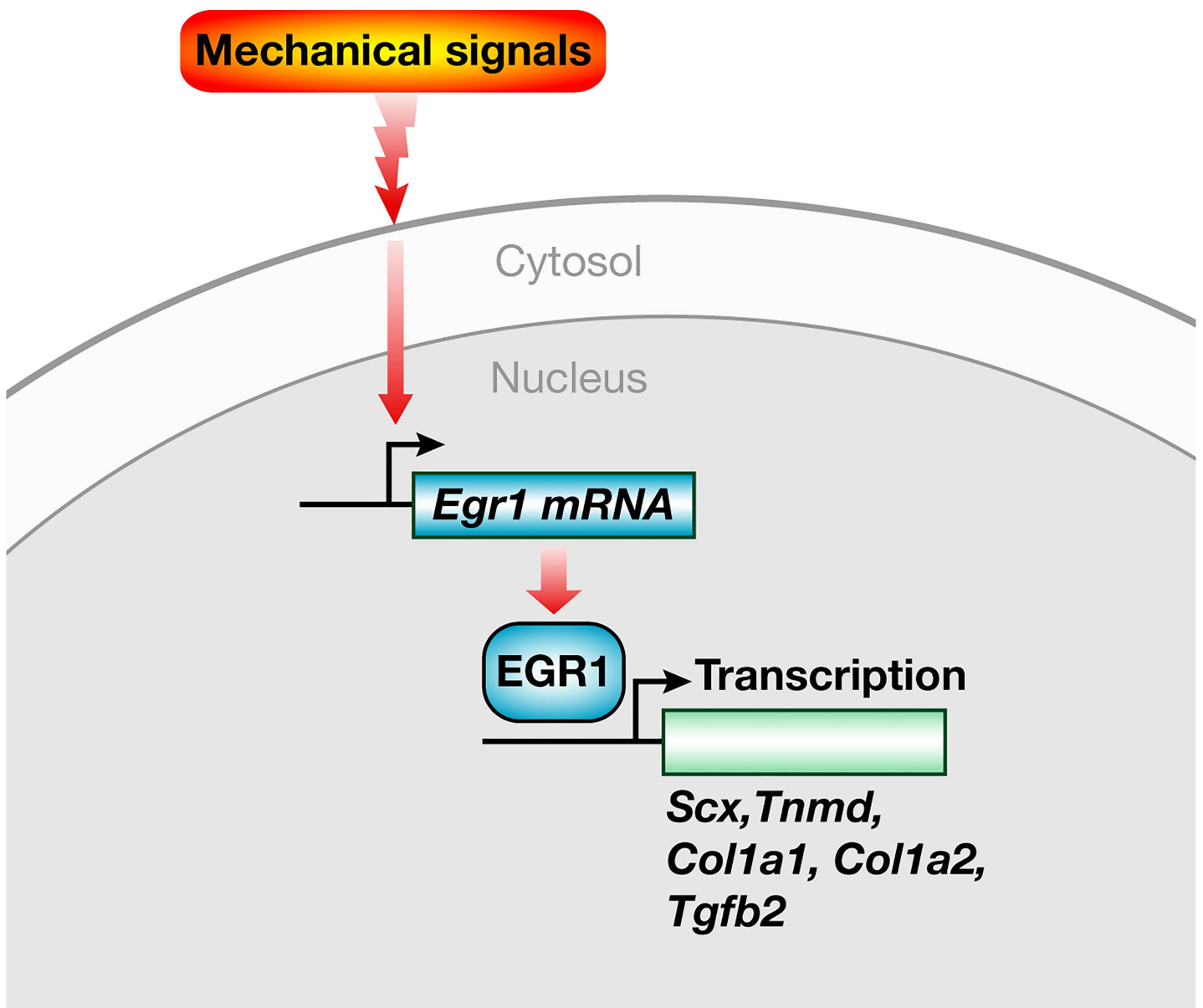


Fig 5. Schematic representation of EGR1 regulation and function downstream of mechanical signals. *Egr1* expression is regulated by mechanical signals in tendon cells. EGR1 positively regulates the transcription of tendon genes including *Scx*, *Tnmd*, *Col1a1* and *Col1a2*. The transcription of *Tgfb2* is also regulated by EGR1.

doi:10.1371/journal.pone.0166237.g005

models and loss of TGF- β leads to a decrease of *Scx* expression in developmental tendons [10, 42–44]. We failed to identify any EGR1 binding sites in mouse *Scx* promoter region and all our ChIP attempts to identify direct EGR1 recruitment to *Scx* promoter region were unsuccessful. Given the EGR1 direct binding to *Tgfb2* promoter [10], it is tempting to suggest that TGF- β 2 mediates the *Scx* induction by EGR1 in tendons. Consistently, SCX and SMAD3 (an intracellular component of the TGF- β pathway) physically interact in 10T1/2 cells [45] and SCX is required for Smad3-mediated gene transcription in cardiac fibroblasts [46]. Whether EGR1 activates *Tnmd* via TGF- β 2 is less clear, since TGF- β 2 has been shown to downregulate *Tnmd* expression in mouse stem cells cultured in 2D [10, 44, 47] and do not have any positive effect on *TNMD* expression in human 3D tissue cultures [28]. In contrast, SCX gain- and loss-of-function experiments lead to upregulation and downregulation of *Tnmd*, respectively, during development [14, 15]. This suggests that SCX could activate *Tnmd* expression during tendon differentiation.

In summary, we show that the expression of the zinc-finger transcription factor EGR1 is sensitive to mechanical signals and that EGR1 senses mechanical signals at the transcription level. Moreover, EGR1 is sufficient to promote tendon gene expression in the absence of mechanical forces during tendon formation and healing (Fig 5). This feature opens the possibility of exploiting EGR1 forced expression to accelerate tendon healing in reduced load conditions.

Acknowledgments

We thank laboratory members for comments on the manuscript and Sophie Gournet for illustrations.

Author Contributions

Conceptualization: DD CP.

Formal analysis: LG.

Funding acquisition: DD.

Investigation: LG NR AD MAB.

Methodology: LG NR AD MAB.

Writing – original draft: DD.

Writing – review & editing: DD LG AD CP.

References

1. Shwartz Y, Blitz E, Zelzer E. One load to rule them all: mechanical control of the musculoskeletal system in development and aging. *Differentiation; research in biological diversity*. 2013; 86(3):104–11. doi: [10.1016/j.diff.2013.07.003](https://doi.org/10.1016/j.diff.2013.07.003) PMID: [23953954](https://pubmed.ncbi.nlm.nih.gov/23953954/).
2. Wang JH, Guo Q, Li B. Tendon biomechanics and mechanobiology—a minireview of basic concepts and recent advancements. *Journal of hand therapy: official journal of the American Society of Hand Therapists*. 2012; 25(2):133–40; quiz 41. doi: [10.1016/j.jht.2011.07.004](https://doi.org/10.1016/j.jht.2011.07.004) PMID: [21925835](https://pubmed.ncbi.nlm.nih.gov/21925835/); PubMed Central PMCID: [PMC3244520](https://pubmed.ncbi.nlm.nih.gov/PMC3244520/).
3. Heinemeier KM, Kjaer M. In vivo investigation of tendon responses to mechanical loading. *Journal of musculoskeletal & neuronal interactions*. 2011; 11(2):115–23. PMID: [21625048](https://pubmed.ncbi.nlm.nih.gov/21625048/).
4. Lavagnino M, Wall ME, Little D, Banes AJ, Guilak F, Arnoczky SP. Tendon mechanobiology: Current knowledge and future research opportunities. *Journal of orthopaedic research: official publication of the Orthopaedic Research Society*. 2015; 33(6):813–22. doi: [10.1002/jor.22871](https://doi.org/10.1002/jor.22871) PMID: [25763779](https://pubmed.ncbi.nlm.nih.gov/25763779/); PubMed Central PMCID: [PMC4524513](https://pubmed.ncbi.nlm.nih.gov/PMC4524513/).

5. Nourissat G, Berenbaum F, Duprez D. Tendon injury: from biology to tendon repair. *Nature reviews Rheumatology*. 2015; 11(4):223–33. doi: [10.1038/nrrheum.2015.26](https://doi.org/10.1038/nrrheum.2015.26) PMID: [25734975](https://pubmed.ncbi.nlm.nih.gov/25734975/).
6. Schweitzer R, Chyung JH, Murtaugh LC, Brent AE, Rosen V, Olson EN, et al. Analysis of the tendon cell fate using Scleraxis, a specific marker for tendons and ligaments. *Development*. 2001; 128(19):3855–66. Epub 2001/10/05. PMID: [11585810](https://pubmed.ncbi.nlm.nih.gov/11585810/).
7. Pryce BA, Brent AE, Murchison ND, Tabin CJ, Schweitzer R. Generation of transgenic tendon reporters, ScxGFP and ScxAP, using regulatory elements of the scleraxis gene. *Developmental dynamics: an official publication of the American Association of Anatomists*. 2007; 236(6):1677–82. doi: [10.1002/dvdy.21179](https://doi.org/10.1002/dvdy.21179) PMID: [17497702](https://pubmed.ncbi.nlm.nih.gov/17497702/).
8. Mendias CL, Gumucio JP, Bakhurin KI, Lynch EB, Brooks SV. Physiological loading of tendons induces scleraxis expression in epitenon fibroblasts. *Journal of orthopaedic research: official publication of the Orthopaedic Research Society*. 2012; 30(4):606–12. doi: [10.1002/jor.21550](https://doi.org/10.1002/jor.21550) PMID: [21913219](https://pubmed.ncbi.nlm.nih.gov/21913219/); PubMed Central PMCID: PMC3245815.
9. Scott A, Sampaio A, Abraham T, Duronio C, Underhill TM. Scleraxis expression is coordinately regulated in a murine model of patellar tendon injury. *Journal of orthopaedic research: official publication of the Orthopaedic Research Society*. 2011; 29(2):289–96. doi: [10.1002/jor.21220](https://doi.org/10.1002/jor.21220) PMID: [20740671](https://pubmed.ncbi.nlm.nih.gov/20740671/); PubMed Central PMCID: PMC3951487.
10. Guerquin MJ, Charvet B, Nourissat G, Havis E, Ronsin O, Bonnin MA, et al. Transcription factor EGR1 directs tendon differentiation and promotes tendon repair. *The Journal of clinical investigation*. 2013; 123(8):3564–76. doi: [10.1172/JCI67521](https://doi.org/10.1172/JCI67521) PMID: [23863709](https://pubmed.ncbi.nlm.nih.gov/23863709/).
11. Jelinsky SA, Archambault J, Li L, Seeherman H. Tendon-selective genes identified from rat and human musculoskeletal tissues. *Journal of orthopaedic research: official publication of the Orthopaedic Research Society*. 2010; 28(3):289–97. doi: [10.1002/jor.20999](https://doi.org/10.1002/jor.20999) PMID: [19780194](https://pubmed.ncbi.nlm.nih.gov/19780194/).
12. Sugimoto Y, Takimoto A, Akiyama H, Kist R, Scherer G, Nakamura T, et al. Scx+/Sox9+ progenitors contribute to the establishment of the junction between cartilage and tendon/ligament. *Development*. 2013; 140(11):2280–8. doi: [10.1242/dev.096354](https://doi.org/10.1242/dev.096354) PMID: [23615282](https://pubmed.ncbi.nlm.nih.gov/23615282/).
13. Havis E, Bonnin MA, Olivera-Martinez I, Nazaret N, Ruggiu M, Weibel J, et al. Transcriptomic analysis of mouse limb tendon cells during development. *Development*. 2014; 141(19):3683–96. doi: [10.1242/dev.108654](https://doi.org/10.1242/dev.108654) PMID: [25249460](https://pubmed.ncbi.nlm.nih.gov/25249460/).
14. Shukunami C, Takimoto A, Oro M, Hiraki Y. Scleraxis positively regulates the expression of tenomodulin, a differentiation marker of tenocytes. *Developmental biology*. 2006; 298(1):234–47. doi: [10.1016/j.ydbio.2006.06.036](https://doi.org/10.1016/j.ydbio.2006.06.036) PMID: [16876153](https://pubmed.ncbi.nlm.nih.gov/16876153/).
15. Murchison ND, Price BA, Conner DA, Keene DR, Olson EN, Tabin CJ, et al. Regulation of tendon differentiation by scleraxis distinguishes force-transmitting tendons from muscle-anchoring tendons. *Development*. 2007; 134(14):2697–708. Epub 2007/06/15. dev.001933 [pii] doi: [10.1242/dev.001933](https://doi.org/10.1242/dev.001933) PMID: [17567668](https://pubmed.ncbi.nlm.nih.gov/17567668/).
16. Docheva D, Hunziker EB, Fassler R, Brandau O. Tenomodulin is necessary for tenocyte proliferation and tendon maturation. *Molecular and cellular biology*. 2005; 25(2):699–705. doi: [10.1128/MCB.25.2.699-705.2005](https://doi.org/10.1128/MCB.25.2.699-705.2005) PMID: [15632070](https://pubmed.ncbi.nlm.nih.gov/15632070/); PubMed Central PMCID: PMC543433.
17. Alberton P, Dex S, Popov C, Shukunami C, Schieker M, Docheva D. Loss of tenomodulin results in reduced self-renewal and augmented senescence of tendon stem/progenitor cells. *Stem cells and development*. 2015; 24(5):597–609. doi: [10.1089/scd.2014.0314](https://doi.org/10.1089/scd.2014.0314) PMID: [25351164](https://pubmed.ncbi.nlm.nih.gov/25351164/); PubMed Central PMCID: PMC4333258.
18. Lejard V, Blais F, Guerquin MJ, Bonnet A, Bonnin MA, Havis E, et al. EGR1 and EGR2 Involvement in Vertebrate Tendon Differentiation. *J Biol Chem*. 2011; 286(7):5855–67. Epub 2010/12/22. M110.153106 [pii] doi: [10.1074/jbc.M110.153106](https://doi.org/10.1074/jbc.M110.153106) PMID: [21173153](https://pubmed.ncbi.nlm.nih.gov/21173153/); PubMed Central PMCID: PMC3037698.
19. Tao X, Liu J, Chen L, Zhou Y, Tang K. EGR1 induces tenogenic differentiation of tendon stem cells and promotes rabbit rotator cuff repair. *Cellular physiology and biochemistry: international journal of experimental cellular physiology, biochemistry, and pharmacology*. 2015; 35(2):699–709. doi: [10.1159/000369730](https://doi.org/10.1159/000369730) PMID: [25592085](https://pubmed.ncbi.nlm.nih.gov/25592085/).
20. Stula M, Orzechowski HD, Gschwend S, Vetter R, von Harsdorf R, Dietz R, et al. Influence of sustained mechanical stress on Egr-1 mRNA expression in cultured human endothelial cells. *Molecular and cellular biochemistry*. 2000; 210(1–2):101–8. PMID: [10976763](https://pubmed.ncbi.nlm.nih.gov/10976763/).
21. Morawietz H, Ma YH, Vives F, Wilson E, Sukhatme VP, Holtz J, et al. Rapid induction and translocation of Egr-1 in response to mechanical strain in vascular smooth muscle cells. *Circulation research*. 1999; 84(6):678–87. PMID: [10189355](https://pubmed.ncbi.nlm.nih.gov/10189355/).
22. Pardo PS, Mohamed JS, Lopez MA, Boriek AM. Induction of Sirt1 by mechanical stretch of skeletal muscle through the early response factor EGR1 triggers an antioxidative response. *J Biol Chem*. 2011;



- 286(4):2559–66. doi: [10.1074/jbc.M110.149153](https://doi.org/10.1074/jbc.M110.149153) PMID: [20971845](https://pubmed.ncbi.nlm.nih.gov/20971845/); PubMed Central PMCID: PMC3024751.
23. Bougault C, Aubert-Foucher E, Paumier A, Perrier-Groult E, Huot L, Hot D, et al. Dynamic compression of chondrocyte-agarose constructs reveals new candidate mechanosensitive genes. *PloS one*. 2012; 7(5):e36964. doi: [10.1371/journal.pone.0036964](https://doi.org/10.1371/journal.pone.0036964) PMID: [22615857](https://pubmed.ncbi.nlm.nih.gov/22615857/); PubMed Central PMCID: PMC3355169.
 24. Wu X, Cheng J, Li P, Yang M, Qiu S, Liu P, et al. Mechano-sensitive transcriptional factor Egr-1 regulates insulin-like growth factor-1 receptor expression and contributes to neointima formation in vein grafts. *Arteriosclerosis, thrombosis, and vascular biology*. 2010; 30(3):471–6. doi: [10.1161/ATVBAHA.109.184259](https://doi.org/10.1161/ATVBAHA.109.184259) PMID: [19965784](https://pubmed.ncbi.nlm.nih.gov/19965784/).
 25. Topilko P, Schneider-Maunoury S, Levi G, Trembleau A, Gourdeji D, Driancourt MA, et al. Multiple pituitary and ovarian defects in Krox-24 (NGFI-A, Egr-1)-targeted mice. *Molecular endocrinology*. 1998; 12(1):107–22. doi: [10.1210/mend.12.1.0049](https://doi.org/10.1210/mend.12.1.0049) PMID: [9440815](https://pubmed.ncbi.nlm.nih.gov/9440815/).
 26. Reznikoff CA, Brankow DW, Heidelberger C. Establishment and characterization of a cloned line of C3H mouse embryo cells sensitive to postconfluence inhibition of division. *Cancer research*. 1973; 33(12):3231–8. PMID: [4357355](https://pubmed.ncbi.nlm.nih.gov/4357355/).
 27. Kapacee Z, Richardson SH, Lu Y, Starborg T, Holmes DF, Baar K, et al. Tension is required for fibroblast formation. *Matrix biology: journal of the International Society for Matrix Biology*. 2008; 27(4):371–5. doi: [10.1016/j.matbio.2007.11.006](https://doi.org/10.1016/j.matbio.2007.11.006) PMID: [18262777](https://pubmed.ncbi.nlm.nih.gov/18262777/).
 28. Bayer ML, Schjerling P, Herchenhan A, Zeltz C, Heinemeier KM, Christensen L, et al. Release of tensile strain on engineered human tendon tissue disturbs cell adhesions, changes matrix architecture, and induces an inflammatory phenotype. *PloS one*. 2014; 9(1):e86078. doi: [10.1371/journal.pone.0086078](https://doi.org/10.1371/journal.pone.0086078) PMID: [24465881](https://pubmed.ncbi.nlm.nih.gov/24465881/); PubMed Central PMCID: PMC3897642.
 29. Aoki KR. A comparison of the safety margins of botulinum neurotoxin serotypes A, B, and F in mice. *Toxicol: official journal of the International Society on Toxinology*. 2001; 39(12):1815–20. PMID: [11600142](https://pubmed.ncbi.nlm.nih.gov/11600142/).
 30. Maeda T, Sakabe T, Sunaga A, Sakai K, Rivera AL, Keene DR, et al. Conversion of mechanical force into TGF-beta-mediated biochemical signals. *Curr Biol*. 2011; 21(11):933–41. Epub 2011/05/24. S0960-9822(11)00423-4 [pii] doi: [10.1016/j.cub.2011.04.007](https://doi.org/10.1016/j.cub.2011.04.007) PMID: [21600772](https://pubmed.ncbi.nlm.nih.gov/21600772/); PubMed Central PMCID: PMC3118584.
 31. Delalande A, Bouakaz A, Renault G, Tabareau F, Kotopoulos S, Midoux P, et al. Ultrasound and micro-bubble-assisted gene delivery in Achilles tendons: long lasting gene expression and restoration of fibromodulin KO phenotype. *Journal of controlled release: official journal of the Controlled Release Society*. 2011; 156(2):223–30. doi: [10.1016/j.jconrel.2011.08.020](https://doi.org/10.1016/j.jconrel.2011.08.020) PMID: [21888933](https://pubmed.ncbi.nlm.nih.gov/21888933/).
 32. Lejard V, Brideau G, Blais F, Salingcarboriboon R, Wagner G, Roehrl MH, et al. Scleraxis and NFATc regulate the expression of the pro-alpha1(I) collagen gene in tendon fibroblasts. *J Biol Chem*. 2007; 282(24):17665–75. doi: [10.1074/jbc.M610113200](https://doi.org/10.1074/jbc.M610113200) PMID: [17430895](https://pubmed.ncbi.nlm.nih.gov/17430895/).
 33. Livak KJ, Schmittgen TD. Analysis of relative gene expression data using real-time quantitative PCR and the 2(-Delta Delta C(T)) Method. *Methods*. 2001; 25(4):402–8. doi: [10.1006/meth.2001.1262](https://doi.org/10.1006/meth.2001.1262) PMID: [11846609](https://pubmed.ncbi.nlm.nih.gov/11846609/).
 34. Kapacee Z, Yeung CY, Lu Y, Crabtree D, Holmes DF, Kadler KE. Synthesis of embryonic tendon-like tissue by human marrow stromal/mesenchymal stem cells requires a three-dimensional environment and transforming growth factor beta3. *Matrix biology: journal of the International Society for Matrix Biology*. 2010; 29(8):668–77. doi: [10.1016/j.matbio.2010.08.005](https://doi.org/10.1016/j.matbio.2010.08.005) PMID: [20736064](https://pubmed.ncbi.nlm.nih.gov/20736064/); PubMed Central PMCID: PMC3611595.
 35. Bayer ML, Yeung CY, Kadler KE, Qvortrup K, Baar K, Svensson RB, et al. The initiation of embryonic-like collagen fibrillogenesis by adult human tendon fibroblasts when cultured under tension. *Biomaterials*. 2010; 31(18):4889–97. doi: [10.1016/j.biomaterials.2010.02.062](https://doi.org/10.1016/j.biomaterials.2010.02.062) PMID: [20356622](https://pubmed.ncbi.nlm.nih.gov/20356622/); PubMed Central PMCID: PMC3485556.
 36. Breidenbach AP, Dyment NA, Lu Y, Rao M, Shearn JT, Rowe DW, et al. Fibrin gels exhibit improved biological, structural, and mechanical properties compared with collagen gels in cell-based tendon tissue-engineered constructs. *Tissue engineering Part A*. 2015; 21(3–4):438–50. doi: [10.1089/ten.TEA.2013.0768](https://doi.org/10.1089/ten.TEA.2013.0768) PMID: [25266738](https://pubmed.ncbi.nlm.nih.gov/25266738/); PubMed Central PMCID: PMC4333253.
 37. Yeung CY, Zeef LA, Lallyett C, Lu Y, Canty-Laird EG, Kadler KE. Chick tendon fibroblast transcriptome and shape depend on whether the cell has made its own collagen matrix. *Scientific reports*. 2015; 5:13555. doi: [10.1038/srep13555](https://doi.org/10.1038/srep13555) PMID: [26337655](https://pubmed.ncbi.nlm.nih.gov/26337655/); PubMed Central PMCID: PMC4559659.
 38. Eliasson P, Andersson T, Hammerman M, Aspenberg P. Primary gene response to mechanical loading in healing rat Achilles tendons. *Journal of applied physiology*. 2013; 114(11):1519–26. doi: [10.1152/jappphysiol.01500.2012](https://doi.org/10.1152/jappphysiol.01500.2012) PMID: [23519232](https://pubmed.ncbi.nlm.nih.gov/23519232/).

39. Hammerman M, Aspenberg P, Eliasson P. Microtrauma stimulates rat Achilles tendon healing via an early gene expression pattern similar to mechanical loading. *Journal of applied physiology*. 2014; 116(1):54–60. doi: [10.1152/jappphysiol.00741.2013](https://doi.org/10.1152/jappphysiol.00741.2013) PMID: [24177691](https://pubmed.ncbi.nlm.nih.gov/24177691/).
40. Eliasson P, Andersson T, Aspenberg P. Rat Achilles tendon healing: mechanical loading and gene expression. *Journal of applied physiology*. 2009; 107(2):399–407. doi: [10.1152/jappphysiol.91563.2008](https://doi.org/10.1152/jappphysiol.91563.2008) PMID: [19541731](https://pubmed.ncbi.nlm.nih.gov/19541731/).
41. Chan KM, Fu SC, Wong YP, Hui WC, Cheuk YC, Wong MW. Expression of transforming growth factor beta isoforms and their roles in tendon healing. *Wound repair and regeneration: official publication of the Wound Healing Society [and] the European Tissue Repair Society*. 2008; 16(3):399–407. doi: [10.1111/j.1524-475X.2008.00379.x](https://doi.org/10.1111/j.1524-475X.2008.00379.x) PMID: [18471258](https://pubmed.ncbi.nlm.nih.gov/18471258/).
42. Pryce BA, Watson SS, Murchison ND, Staverosky JA, Dunker N, Schweitzer R. Recruitment and maintenance of tendon progenitors by TGFbeta signaling are essential for tendon formation. *Development*. 2009; 136(8):1351–61. Epub 2009/03/24. 136/8/1351 [pii] doi: [10.1242/dev.027342](https://doi.org/10.1242/dev.027342) PMID: [19304887](https://pubmed.ncbi.nlm.nih.gov/19304887/); PubMed Central PMCID: [PMC2687466](https://pubmed.ncbi.nlm.nih.gov/PMC2687466/).
43. Brown JP, Finley VG, Kuo CK. Embryonic mechanical and soluble cues regulate tendon progenitor cell gene expression as a function of developmental stage and anatomical origin. *Journal of biomechanics*. 2014; 47(1):214–22. doi: [10.1016/j.jbiomech.2013.09.018](https://doi.org/10.1016/j.jbiomech.2013.09.018) PMID: [24231248](https://pubmed.ncbi.nlm.nih.gov/24231248/); PubMed Central PMCID: [PMC4157071](https://pubmed.ncbi.nlm.nih.gov/PMC4157071/).
44. Brown JP, Galassi TV, Stoppato M, Schiele NR, Kuo CK. Comparative analysis of mesenchymal stem cell and embryonic tendon progenitor cell response to embryonic tendon biochemical and mechanical factors. *Stem cell research & therapy*. 2015; 6:89. doi: [10.1186/s13287-015-0043-z](https://doi.org/10.1186/s13287-015-0043-z) PMID: [25956970](https://pubmed.ncbi.nlm.nih.gov/25956970/); PubMed Central PMCID: [PMC4425922](https://pubmed.ncbi.nlm.nih.gov/PMC4425922/).
45. Berthet E, Chen C, Butcher K, Schneider RA, Alliston T, Amirtharajah M. Smad3 binds Scleraxis and Mohawk and regulates tendon matrix organization. *Journal of orthopaedic research: official publication of the Orthopaedic Research Society*. 2013; 31(9):1475–83. doi: [10.1002/jor.22382](https://doi.org/10.1002/jor.22382) PMID: [23653374](https://pubmed.ncbi.nlm.nih.gov/23653374/); PubMed Central PMCID: [PMC3960924](https://pubmed.ncbi.nlm.nih.gov/PMC3960924/).
46. Bagchi RA, Roche P, Aroutiounova N, Espira L, Abrenica B, Schweitzer R, et al. The transcription factor scleraxis is a critical regulator of cardiac fibroblast phenotype. *BMC biology*. 2016; 14(1):21. doi: [10.1186/s12915-016-0243-8](https://doi.org/10.1186/s12915-016-0243-8) PMID: [26988708](https://pubmed.ncbi.nlm.nih.gov/26988708/); PubMed Central PMCID: [PMC4794909](https://pubmed.ncbi.nlm.nih.gov/PMC4794909/).
47. Liu H, Zhang C, Zhu S, Lu P, Zhu T, Gong X, et al. Mohawk promotes the tenogenesis of mesenchymal stem cells through activation of the TGFbeta signaling pathway. *Stem cells*. 2015; 33(2):443–55. doi: [10.1002/stem.1866](https://doi.org/10.1002/stem.1866) PMID: [25332192](https://pubmed.ncbi.nlm.nih.gov/25332192/).

X.2 The Osteogenic and Tenogenic Differentiation Potential of C3H10T1/2 (Mesenchymal Stem Cell Model) Cultured on PCL/PLA Electrospun Scaffolds in the Absence of Specific Differentiation Medium

Article

The Osteogenic and Tenogenic Differentiation Potential of C3H10T1/2 (Mesenchymal Stem Cell Model) Cultured on PCL/PLA Electrospun Scaffolds in the Absence of Specific Differentiation Medium

Timothée Baudequin ¹ , Ludovic Gaut ^{2,3}, Marc Mueller ⁴, Angela Huepkes ^{1,4}, Birgit Glasmacher ⁴, Delphine Duprez ^{2,3} , Fahmi Bedoui ⁵ and Cécile Legallais ^{1,*}

¹ CNRS, UMR 7338 Biomechanics and Bioengineering, Sorbonne Universités, Université de Technologie de Compiègne, 60200 Compiègne, France; timothee.baudequin@mail.mcgill.ca (T.B.); angela_huepkes@web.de (A.H.)

² CNRS UMR 7622 IBPS-Developmental Biology Laboratory, Sorbonne Universités, UPMC Univ Paris 06, F-75005 Paris, France; ludovic.gaut@upmc.fr (L.G.); delphine.duprez@upmc.fr (D.D.)

³ Inserm U1156, F-75005 Paris, France

⁴ Institute for Multiphase Processes, Leibniz Universität Hannover, D-30167 Hanover, Germany; mueller@imp.uni-hannover.de (M.M.); glasmacher@imp.uni-hannover.de (B.G.)

⁵ CNRS, UMR 7337 Roberval Laboratory for Mechanics, Sorbonne Universités, Université de Technologie de Compiègne, 60200 Compiègne, France; fahmi.bedoui@utc.fr

* Correspondence: cecile.legallais@utc.fr; Tel.: +33-344234423

Received: 3 November 2017; Accepted: 29 November 2017; Published: 4 December 2017

Abstract: The differentiation potential of mesenchymal stem cells (MSC) has been extensively tested on electrospun scaffolds. However, this potential is often assessed with lineage-specific medium, making it difficult to interpret the real contribution of the properties of the scaffold in the cell response. In this study, we analyzed the ability of different polycaprolactone/poly(lactic acid) PCL/PLA electrospun scaffolds (pure or blended compositions, random or aligned fibers, various fiber diameters) to drive MSC towards bone or tendon lineages in the absence of specific differentiation medium. C3H10T1/2 cells (a mesenchymal stem cell model) were cultured on scaffolds for 96 h without differentiation factors. We performed a cross-analysis of the cell–scaffold interactions (spreading, organization, and specific gene expression) with mechanical (elasticity), morphological (porosity, fibers diameter and orientation) and surface (wettability) characterizations of the electrospun fibers. We concluded that (1) osteogenic differentiation can be initiated on pure PCL-based electrospun scaffolds without specific culture conditions; (2) fiber alignment modified cell organization in the short term and (3) PLA added to PCL with an increased fiber diameter encouraged the stem cells towards the tendon lineage without additional tenogenic factors. In summary, the differentiation potential of stem cells on adapted electrospun fibers could be achieved in factor-free medium, making possible future applications in clinically relevant situations.

Keywords: scaffold; polymer; electrospinning; mesenchymal stem cell; cell differentiation; tissue engineering

1. Introduction

Electrospun fibers are promising scaffolds for tissue engineering and regenerative medicine with a growing interest over the last decade [1–4]. Compared to other fiber production processes (such as phase separation, extrusion or self-assembly [5]), electrospinning has several advantages for

both in vitro and in vivo studies. The electrospinning method is relevant at the laboratory scale for prospective studies (making possible custom-made devices) and for further mass production [5,6]. This method is highly versatile and tunable [4]. Depending on the choice of materials and procedures, electrospun scaffolds offer various degradation rates [5], as well as pore interconnectivity [6], high porosity [6], a high surface/volume ratio [4–6] and anisotropy at the molecular level in the case of fiber alignment [1,7,8]. These properties are well-known as ways of controlling cell adhesion and cell behavior [6,8,9]. Moreover, the submicrometric diameter of the electrospun fibers is similar to that of collagen fibers in natural extracellular matrix [1,10], establishing a biomimetic environment for cells. Electrospun scaffolds also show appropriate and adjustable mechanical properties, compared to other laboratory-made synthetic matrices [1,10], due to a stable structure with a smaller number of defects [5,6].

Many different electrospun polymer solutions have been studied as biomaterials to promote organ/tissue regeneration or repair, such as components of the musculoskeletal system, bone, tendon, ligament [11–15] or dental applications [16]. Polylactic acid (PLA), polycaprolactone (PCL) and polyglycolic acid (PGA) are frequently cited as the most commonly-used polymers and are approved by the Food and Drug Administration (FDA) [4,17]. PCL scaffolds have been extensively used for bone tissue engineering, in combination with the use of growth and differentiation factors or composite solutions [4,14,18]. In contrast, pure PLA has been shown to be the most relevant polymer for the development of tendon substitutes in comparison with PCL [19], PGA [20] or poly(lactic-co-glycolic) acid (PLGA) [20]. Moreover, the tunable morphological and mechanical properties of electrospun scaffolds are of primary interest as tendon regeneration is particularly dependent on these signals [11,13,21].

Mesenchymal stem cells (MSC) are multipotent stem cells that are able to differentiate into various lineages including muscle, bone, cartilage and tendons/ligaments with a specific differentiation medium [22–24]. The differentiation potential of MSCs has been extensively tested on different scaffolds. However, this potential is often assessed with lineage-specific differentiation media [25], making it difficult to interpret the real contribution of the properties of the scaffold in the differentiation process. Moreover, it can be important to remove additional chemical factors from the culture processes to avoid undesired effects in vivo after reaching the clinical stage [26,27]. The choice of biomaterial is effectively crucial for tendon, ligament or enthesis (tendon/ligament to bone interface) reconstruction [28,29]. We hypothesize that analyzing the properties of the biomaterials that drive cell lineage differentiation potential should be devoid on culture medium parameters. In this study, we analyzed the ability of different PCL/PLA electrospun scaffolds to drive MSCs towards bone or tendon lineages in the absence of specific differentiation media. C3H10T1/2 cells [30] are able to differentiate towards different cell lineages in controlled environments, including bone and tendon, and are frequently used as a model for studies at their early stage of development [25,31–33]. Cultures conducted on scaffolds were compared to cells maintained in regular culture conditions (flat culture substrate, proliferation medium without factors) to highlight specifically the intrinsic effects of the electrospun fibers' properties on the biological response.

2. Results

In order to test the ability of different biomaterials to drive MSC differentiation towards a specific lineage, we manufactured electrospun fibers based on PCL and PLA solutions with different compositions (pure or blended solutions) and structures (random or aligned fibers) and analyzed the bone/tendon differentiation of MSCs cultured on these biomaterials. The settings for different scaffolds are summarized in Table 1. Polymer solutions and fiber structures were chosen to analyze the respective effects of the production parameters and their combinations. To allow comparison and avoid variability, we applied the same mechanical characterization to all the scaffolds, in addition to using similar cell culture protocols (Figure 1).

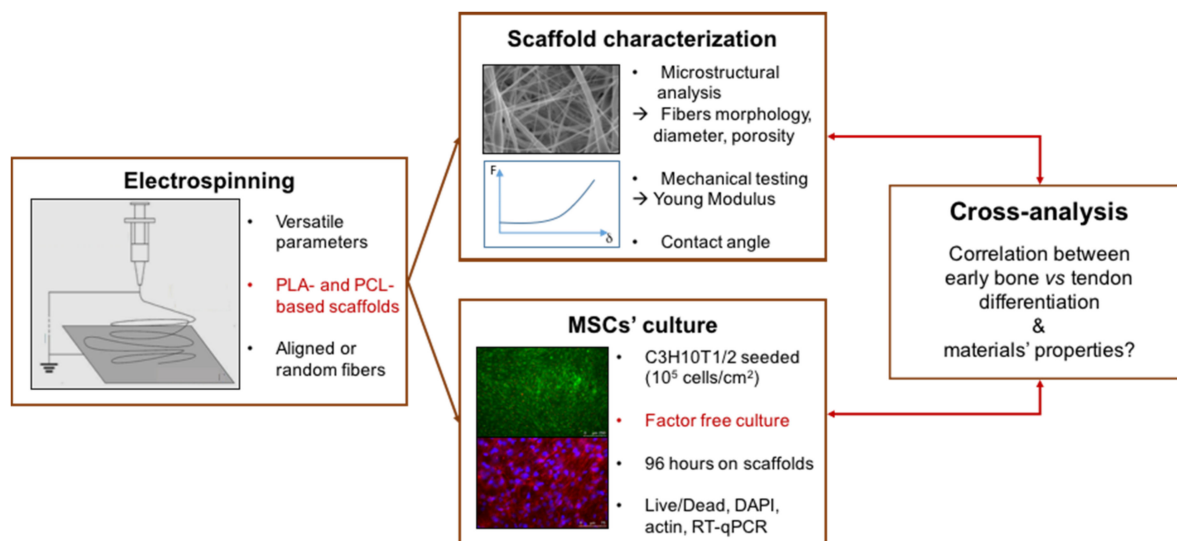


Figure 1. Design of the present study. The osteogenic and tenogenic potential of PCL- (polycaprolactone) and PLA-based (polylactic acid) electrospun scaffolds was investigated in the absence of specific differentiation media with a cross-analysis of biological, morphological and mechanical behaviors.

Table 1. Production parameters of the electrospun scaffolds studied.

Scaffold	Abbreviation	Polymer	Concentration	Solvent	Flow	Speed
					Rate	
Pure polycaprolactone	PCL600nm	PCL	15 wt/wt %	60 wt % DCM 40 wt % DMF	16,6 $\mu\text{L}/\text{min}$	/
Random PCL	PCL1000nm	PCL	100 mg/mL	TFE	50 $\mu\text{L}/\text{min}$ *	250 rpm
Pure polylactic acid	PLA	PLA	10 wt/wt %	70% DCM 30% acetone	67 $\mu\text{L}/\text{min}$	50 rpm
Aligned PCL	PCLaligned	PCL	100 mg/mL	TFE	50 $\mu\text{L}/\text{min}$ *	1000 rpm
PCL/PLA coaxial blend (PCL outside)	BlendPCLout	PCL (133 mg/mL) & PLA (66 mg/mL)		TFE	50 $\mu\text{L}/\text{min}$ *	250 rpm
PCL/PLA coaxial blend (PLA outside)	BlendPLAout					

*: 25 $\mu\text{L}/\text{min}$ for each solution. DCM: Dichloromethane, DMF: *N,N*-dimethylformamide. TFE: 2,2,2-trifluoroethanol.

2.1. Electrospun Fiber Morphology

Scanning electronic microscopy (SEM) observations highlighted that all the electrospun fibers were generally homogenous in size and devoid of bead formation for all the polymers used (Figure 2). The fibers were deposited randomly with a rotating speed of 50 rpm, while they were aligned when the speed reached 1000 rpm (PCL-aligned scaffold). The change in angle between the fibers and the direction of rotation was measured by using Axio Vision software (Carl Zeiss, Oberkochen, Germany), the lower the angle the higher the fiber alignment). Unaligned fibers showed a mean angle of $15.5^\circ \pm 3.1^\circ$ whereas aligned fibers showed a mean angle of $1.8^\circ \pm 1.8^\circ$. PLA scaffolds presented an upper layer of fibers less dense than the other scaffolds, which led to a macroscopic fluffy aspect with beads in some locations. This aspect didn't induce additional degradation in aqueous environment during culture. Moreover, the surface of the PLA fibers was itself rough, or even nanoporous, as seen with a higher SEM magnitude (inset on Figure 2). This specificity has already been observed in the literature and may be explained by the high volatility of dichloromethane [34,35]. However, no effect

on the cell behavior has been detected, possibly because the pore size is below the cellular detection threshold [36].

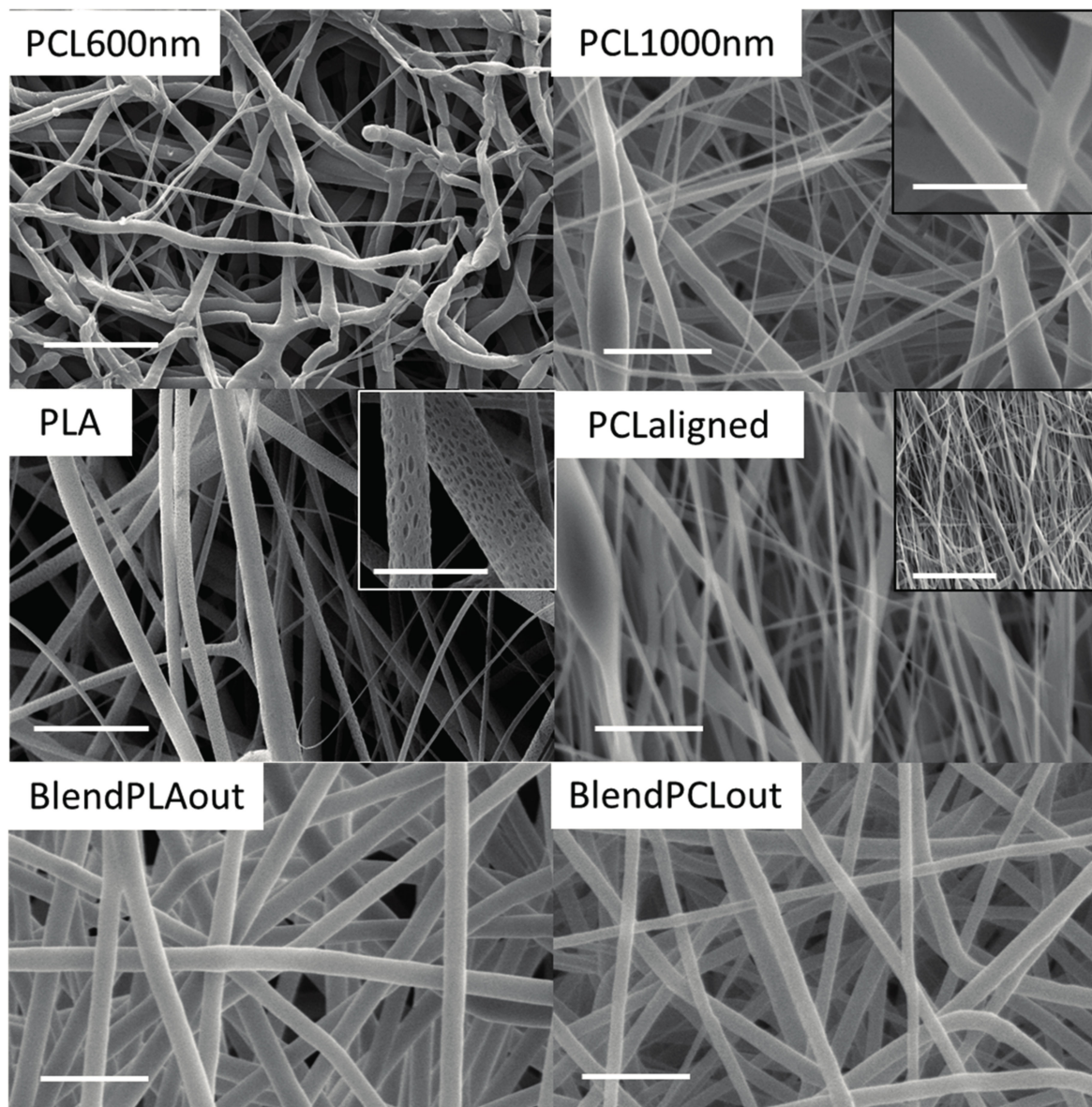


Figure 2. Scanning Electronic Microscopy (SEM) observations of the electrospun scaffolds. Insets in PLA, PCL1000nm and PCL-aligned panels: SEM observation of the PLA and PCL1000nm scaffolds to highlight porosity at the fiber scale, and of the PCL-aligned scaffold to highlight alignment. Main scale bars: 10 μm , PLA inset: 2 μm , PCL1000nm inset: 4 μm , PCL-aligned inset: 50 μm .

The fiber diameters of each scaffold were measured on SEM images. Based on the diameters of the fibers, the scaffolds were sorted into two groups. The fiber diameters of pure PCL and pure PLA scaffolds ranged from around 500 to 1000 nm (Figure 3A). Coaxial blends had diameters of 2000 nm or more, significantly different from the other scaffolds ($p < 0.001$), with a maximum of 2461 ± 353 nm for BlendPLAout (Figure 3A). Globally speaking, the diameters were in the same range as those obtained classically using the electrospinning technique [37–39].

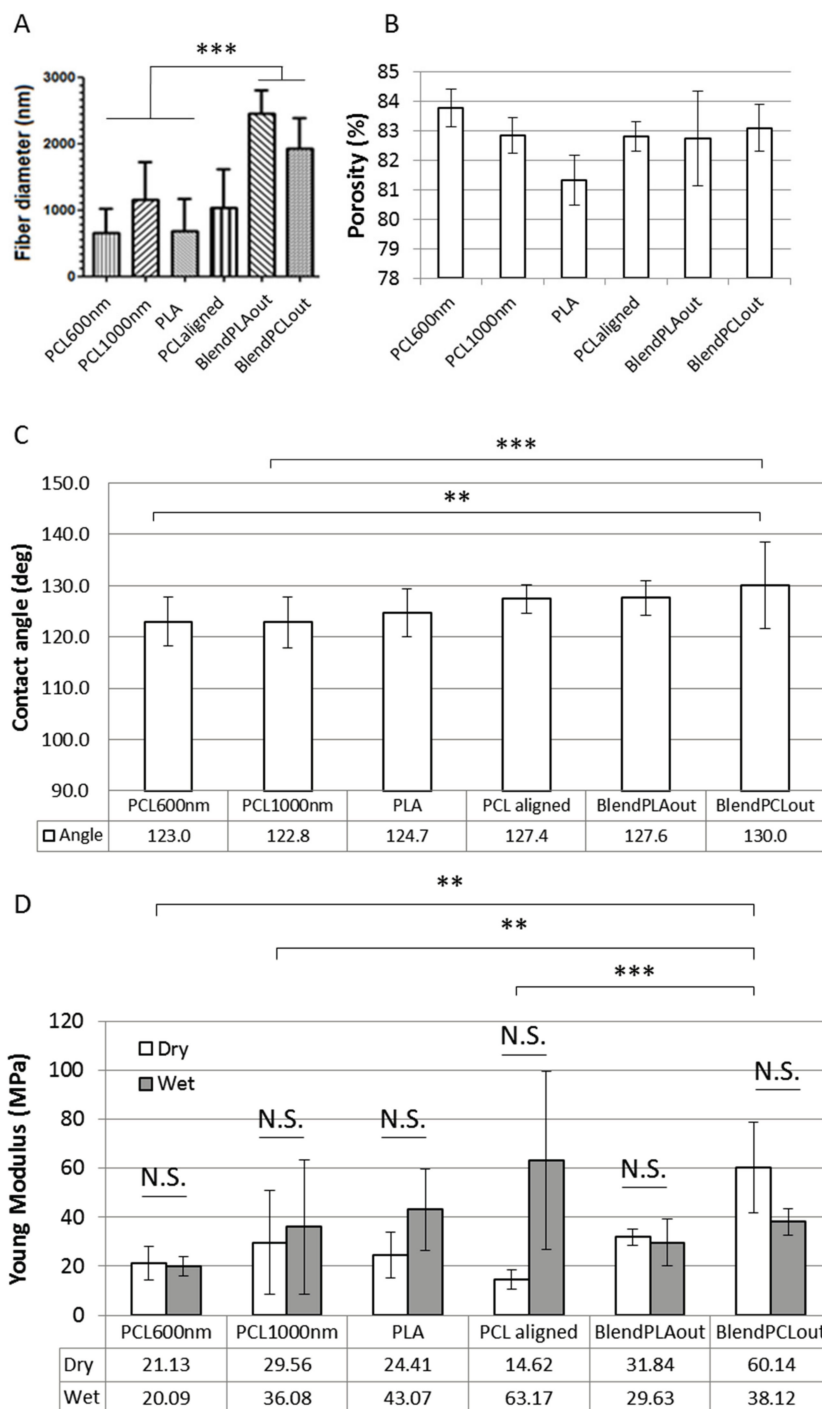


Figure 3. Morphological and mechanical characterization of the different scaffolds. **(A)** Fiber diameters of the electrospun scaffolds; **(B)** Estimation of scaffold porosity using image processing for the electrospun scaffolds. The $\mu + \delta$ threshold focuses on the porosity of the upper layers of fibers; **(C)** contact angle measured on each electrospun scaffold; **(D)** Young's moduli of each scaffold. Comparisons of Young's moduli were made between dry and wet samples, and between scaffolds based on dry samples. N.S., non-significant, $** p < 0.01$, $*** p < 0.001$.

2.2. Surface Characterization

The porosity assessments at the scaffold scale (pores induced by the space between the fibers) are reported in Figure 3B. The original SEM images were converted to black and white for various

binarization thresholds based on the mean (μ) and standard deviation (δ) of the image histogram [40,41]. The porosity was estimated from the black pixel (void)/white pixel (material) ratio. Three thresholds were studied ($\mu + \delta$; μ ; $\mu - \delta$), but the results presented here focus on the $\mu + \delta$ threshold, which only took into consideration the upper fiber layers after binarization. This threshold appears to be the most relevant for analyzing cell response because the cells are mostly in contact with the external fibers layers. These values can therefore be used to compare the morphology of the different scaffolds although only an estimation of the porosity of the whole scaffold could be derived [40–45]. The porosity varied from 80% to 84% among the different scaffolds (Figure 3B). The statistics information is not shown in the figure for readability reasons. Except for blended scaffolds, the differences between the scaffolds were found to be statistically significant ($p < 0.05$ to $p < 0.001$). Contact angle measurements were carried out on the surface of the dry electrospun fiber network. The results are summarized in Figure 3C. The scaffolds showed hydrophobic behavior with mean results from 122.7° (PLA) to 130.0° (BlendPCLout).

2.3. Mechanical Characterization of Electrospun Fibers

In order to characterize the mechanical properties of each scaffold, samples were submitted to tensile tests in dry or wet conditions. Wet conditions were defined as being after humidification in demineralized water. Young's moduli of each scaffold are reported in Figure 3D. Humidification of the scaffolds prior to measurement did not induce significant changes in Young's modulus values. Some samples showed a trend for a higher Young's modulus in wet conditions. Although such an increase can occur in polymeric samples [46], this behavior was not found to be significant here. It can be seen as a lack of overall effect of the humidification with an increase in data dispersion. It is particularly noticeable for PCLaligned samples, where the aligned layers of fibers could have more easily detached from each other after humidification and therefore increased the variability of the measurements. In dry conditions, blended scaffolds showed the highest stiffness with a maximum of 60.14 ± 18.52 MPa for BlendPCLout. This value was statistically different from all the other pure PCL scaffolds ($p < 0.001$ to $p < 0.01$), however PCL600nm, PCL1000nm and PCLaligned were not statistically different from each other. As the Young's Modulus has been shown to be linked to the fiber morphology [34,39,47], the differences in diameter from one PCL scaffold to the other could be here too slight to show differences in stiffness. There was no statistical difference between BlendPCLout and BlendPLAout (reverse coaxial structures). One can hypothesize that the overall stiffness of the blended fibers led to the same behavior regardless of the respective location of PCL and PLA in the core/shell studied structures. This mechanical characterization was meant to derive qualitative estimation of the stiffness of the scaffolds because fiber morphology, porosity and grip effects were not taken into consideration. Nevertheless, we estimate that this evaluation of mechanical properties was relevant for comparing scaffolds before cross-analyses of the biological response (Table 2).

Table 2. Summary of the main results of morphological, mechanical and biological characterization of the scaffolds seeded with C3H10T1/2 stem cells. Spreading was estimated from the SEM and fluorescence acquisitions as moderate (+), high (++) or very high (+++).

Scaffold	Contact Angle (°)	Young's Modulus (MPa)		Fiber Diameter (nm)	Porosity $\mu + \delta$ (%)	Cell Response	
		Dry	Wet			Spreading	Differentiation
PCL600nm	123	21	20	665	83.8	+++	Bone
PCL1000nm	123	30	36	1159	82.8	++	Bone
PLA	124.7	24	43	681	81.3	+	Unclear
PCLaligned	127	15	63	1032	82.8	++ Alignment	Bone
BlendPLAout	128	32	30	2461	82.7	++	Tendon
BlendPCLou	130	60	38	1928	83.1	++	Tendon

2.4. Cell—Scaffold Interactions

C3H10T1/2 stem cells were cultured for 96 h on the different electrospun scaffolds. C3H10T1/2 cells were plated at the same density on each scaffold and cultured in the same conditions with the same culture medium. A “Live/Dead” staining was used to observe living cells (Calcein AM, green) and dead cell nuclei (EthD-1, red) simultaneously (Figure 4A,B,E,F,I,J). The observations showed that all the scaffolds made possible the development of generally continuous and homogeneous tissue made from living cells covering the whole electrospun fiber network. The qualitative analysis of these images allowed us to conclude on excellent cell attachment and viability on all samples as a small number of dead cells was noticed. SEM observations further confirmed the development of a continuous cell layer. Cracks observed in several SEM images (Figure 4C,D,K,L) probably occurred during the preparation of the SEM samples as they were not seen in the fluorescence staining images of the cells. The fibers themselves appeared broken under the living tissue (Figure 4C). Cells cultured on pure PCL scaffolds showed the most continuous, dense and homogeneous tissue (Figure 4A,B,F). On the PLA scaffold, the floating upper electrospun fibers (Figure 2) led to the development of cells under these fibers, “inside” the scaffold (Figure 4G). Cell coverage thus appeared less dense on PLA-based than on pure PCL-based scaffolds, with some heterogeneous spots (Figure 4E). The observations for PCLaligned samples suggested an alignment of the cells (Figure 4F,H). Cell orientation was confirmed with the visualization of nuclei using DAPI simultaneously with actin filament staining (Figure 5A,B). The nuclei of C3H10T1/2 cells displayed an elliptic shape and were oriented parallel to the aligned actin filaments, in turn in the same orientation as the alignment of PCLaligned fibers (Figure 5B,D). In contrast, nuclei of cells cultured on PCL1000nm were round-shaped, consistent with an absence of any specific spatial organization (Figure 5A,C).

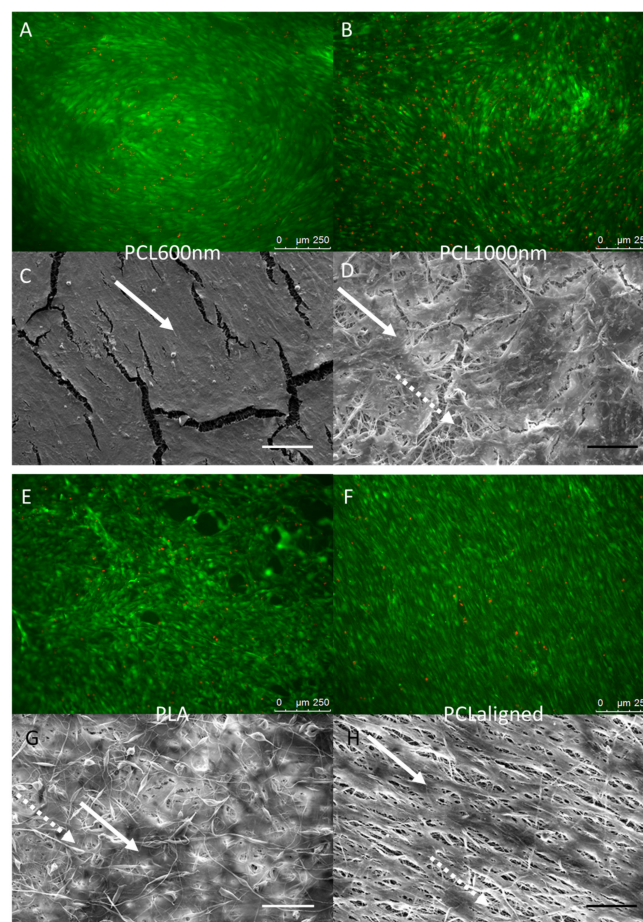


Figure 4. *Cont.*

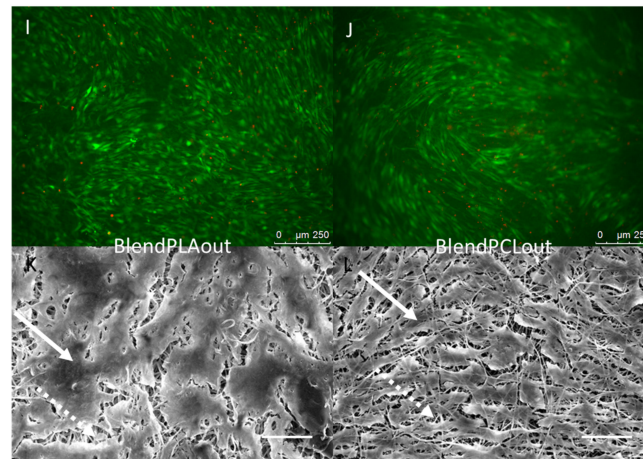


Figure 4. Fluorescence microscopy (A,B,E,F,I,J) and SEM observations (C,D,G,H,K,L) of C3H10T1/2 cells cultured for 96 h on PCL60nm (A,C), PCL1000nm (B,D), PLA (E,G), PCLaligned (F,H), BlendPLAout (I,K) and BlendPCLout (J,L) electrospun scaffolds. Fluorescence: Living cells (Calcein AM, green) and dead cell nuclei (EthD-1, red), scale bars 250 μm . SEM: scale bars 100 μm . Solid arrows: continuous cell tissue. Dashed arrows: fibers network visible due to cracks in the cell tissue or to a lower cell density.

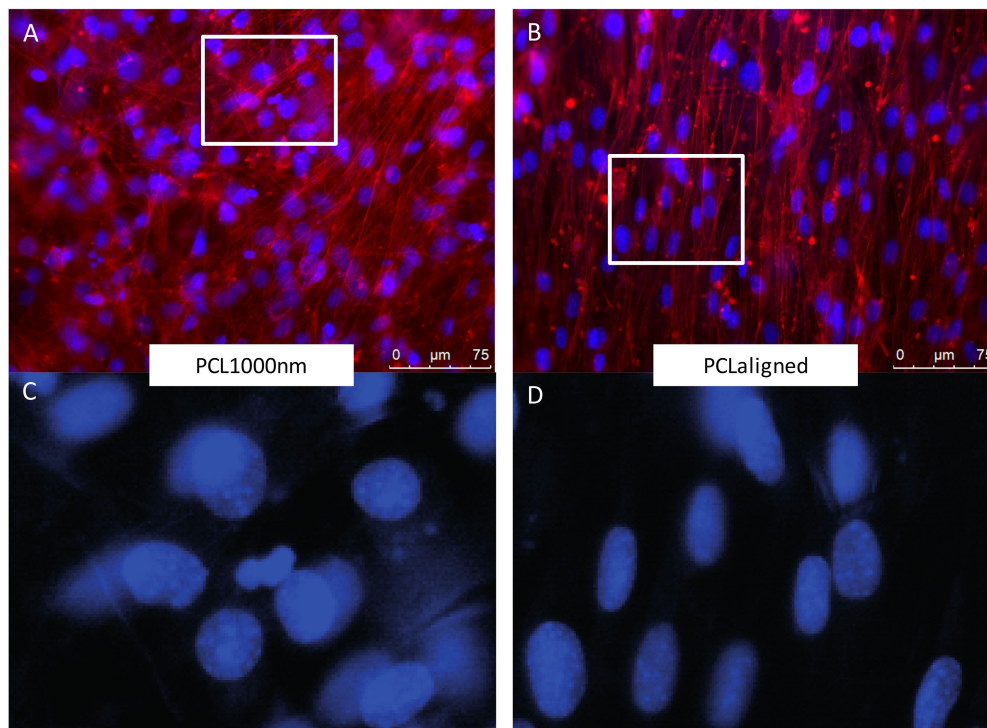


Figure 5. Fluorescence microscopy observations of C3H10T1/2 cells cultured for 96 h on PCL1000nm (A,B) and PCLaligned (C,D) scaffolds. (A,C) Actin filaments visualized with rhodamine-phalloidine (red) and nuclei visualized with DAPI (blue). (B,D) higher magnifications of nuclei (DAPI) of region of interest (white rectangles in A,C).

2.5. Cell Differentiation

The preferential differentiation outcomes of C3H10T1/2 cells cultured in the different electrospun scaffolds were evaluated with the expression of genes of interest by Reverse Transcription quantitative Polymerase Chain Reaction (RT-qPCR) at the end of 96 h of culture. Tendon- and bone-related markers

were simultaneously analyzed in cells cultured in each scaffold. *Dlx5*, a transcription factor regulating the activation of specific bone markers [48], Runx2, a specific bone transcription factor [49], and *Bglap* (also called Osteocalcin) a late marker involved in bone mineralization [49] were used as bone-related genes. To assess to what extent stem cells were committed to the tendon lineage, we used Scx (Scleraxis), a bHLH (basic helix-loop-helix) transcription factor expressed in tendon progenitors and differentiated cells [50,51], *Tnmd* (Tenomodulin) a late tendon-specific marker [50,51] and *Aqp1* (Aquaporin-1) a marker for tendon development [32]. The expression of the gene *Col1a1* was also analyzed, although we are aware that *Col1a1* is expressed in both bone and tendon tissues. The relative mRNA levels of bone and tendon genes in stem cells cultured with the different scaffolds are presented in Figure 6. Cells cultured in regular conditions (flat glass substrate, proliferation medium without any factors) were used as a control group to express increases and decreases caused specifically by the presence of the scaffolds in the other groups. PCL scaffolds (PCL600nm, PCL1000nm (significant) and PCLaligned (non-significant)) led to an increase in *Bglap* expression (up to four-fold increase, significance $p < 0.01$ to $p < 0.0001$), associated with decreased expression of the Scx tendon-related gene ($p < 0.01$) compared to the control plastic cultures, suggesting a shift toward bone differentiation (Figure 6A,G). Both PCL/PLA blended scaffolds induced stem cells towards tendon differentiation, as assessed by a significant increase in *Tnmd* expression (up to four-fold increase, $p < 0.01$, Figure 6B). Based on the decrease in Scx and *Col1a1* expression ($p < 0.01$), and the absence of bone marker modifications, we conclude that PLA was not favorable for tendon or bone differentiation (Figure 6A,D).

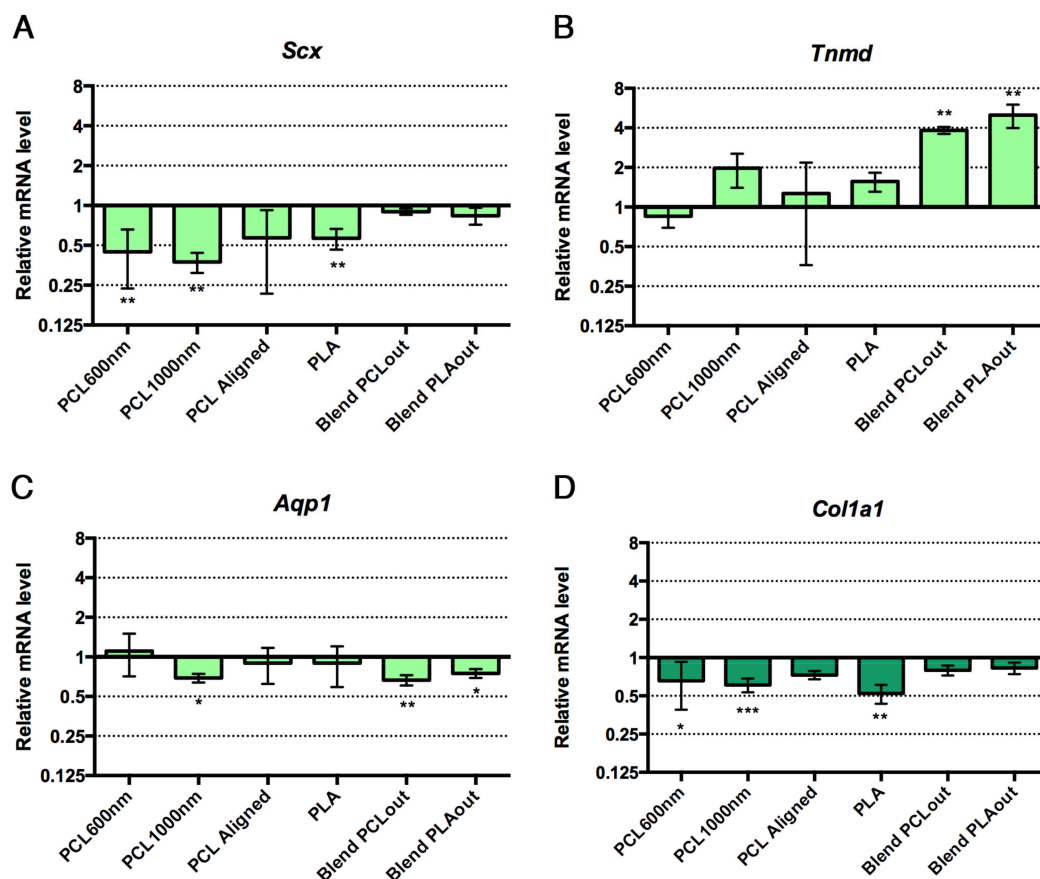


Figure 6. Cont.

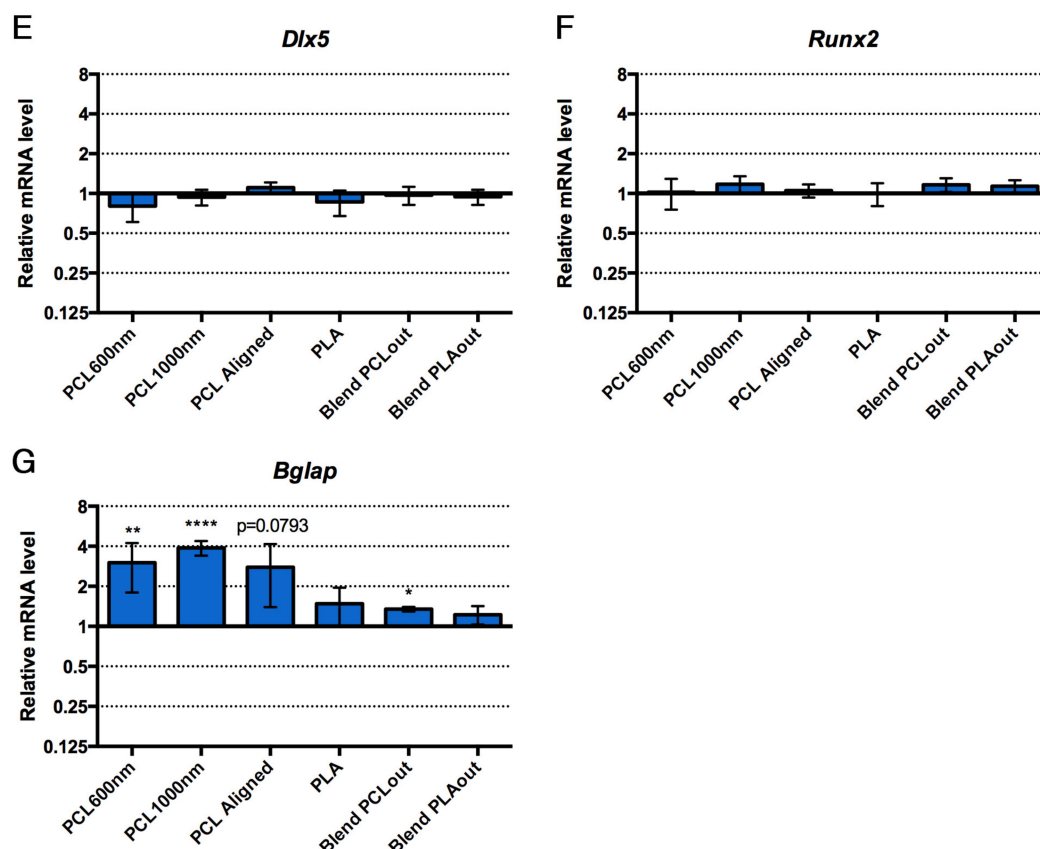


Figure 6. Relative expression of mRNA levels for tendon-related genes, *Scx* (A); *Tnmd* (B); *Aqp1* (C); (green bars) and bone-related genes, *Dlx5* (E); *Runx2* (F); *Bglap* (G); (blue bars) in C3H10T1/3 cells cultured on the different electrospun scaffolds compared to control conditions (cells without scaffold). *Col1a1*, a component of tendon and bone and is represented in dark green bars (D). Control conditions have been normalized to 1. Error bars represent s.d. * $p < 0.05$, ** $p < 0.01$, *** $p < 0.001$, **** $p < 0.0001$.

3. Discussion

In the present study, mouse C3H10T1/2 mesenchymal stem cells [30] were cultured on various PCL and PLA electrospun scaffolds in the absence of specific differentiation medium. The use of identical culture protocols (no addition of osteogenic or tenogenic differentiation factors) for C3H10T1/2 cells seeded on different materials over a short period (96 h) as well as undifferentiated control groups without scaffolds highlighted which biomaterials were preponderant in bone or tendon differentiation from a multipotential stem cell population. In particular, mechanical properties and fiber morphology were evaluated to perform a cross-analysis with biological behavior. The identification of scaffolds allowing mesenchymal stem cells to differentiate into bone and tendon lineages could lead to the development of new constructs for the regeneration of enthesis [52,53].

All the various settings made possible the formation of the electrospun fibers (Figure 2) with similar hydrophilic profiles (Figure 3). Data summarizing both biological and mechanical characterizations of the six scaffolds used in this study are shown in Table 2. Pure PCL-based scaffolds favor cell differentiation towards bone differentiation based on the increase in *Bglap* expression, a late bone marker involved in mineralization [48], while coaxial blend materials favor tendon differentiation based on an increase in *Tnmd* (Figure 6). *Bglap* upregulation reached a 4-fold increase compared to non-specific culture conditions with a strong significance ($p < 0.001$) on PCL1000nm samples. This initiation towards bone differentiation of stem cells cultured with PCL scaffolds is consistent with the literature data where it is described that PCL is widely-used for bone regeneration [14,18]. However, in most cases, bone differentiation was observed in the presence of osteogenic medium including

dexamethasone, ascorbic acid, or beta-glycerophosphate [14,49]. Therefore, the differentiation effect may not be attributed to the material itself. In the present study, random scaffolds (PCL600nm, PCL1000nm) and PCLaligned (to a lesser extent) pushed stem cells towards bone differentiation, while decreasing tendon differentiation. This finding is of major interest for the design of bone tissue engineering protocols that do not involve additional growth and differentiation factors, in order to avoid clinical complications (such as ectopic bone formation) and regulatory issues [26,27].

Scaffolds with aligned structures have been reported as pushing stem cells towards the tendon cell lineage [54]. On the PCLaligned scaffold, the nuclei and cytoskeleton of stem cells were found to be aligned along the same orientation of the electrospun fibers (Figure 5B,D). However, this orientated cell morphology did not lead to significant modification in tendon gene expression (Figure 6A–C,E). It has nevertheless been shown that the alignment of polymeric structures promotes the ligament lineage after a long culture time (7 to 14 days [50,55]); this suggests that the alignment of PCL fibers was not an efficient way of modifying stem cell differentiation towards the tendon lineage in short term cultures.

In contrast with cell behavior on pure PCL samples, the expression of the tendon-related gene *Tnmd* was upregulated in the presence of both PLA and PCL polymers (BlendPCLout and BlendPLAout scaffolds). The 4-fold increase in *Tnmd* expression compared to control was related to the same 4-fold upregulation obtained with Egr1-C3H10T1/2 cells compared to C3H10T1/2 cells in a previous study [25]. This similar range of increase of *Tnmd* expression upon Egr1 over-expression allowed us to conclude on a significant effect of the blended scaffolds on the stem cell fate towards tenogenic differentiation. Moreover, *Bglap* expression (assessing bone differentiation) was not significantly increased in these mixed PLA/PLC scaffolds, regardless of whether PLA or PCL was electrospun as the external layers (Figure 6). SEM observations of fiber networks did not reveal any morphological difference between either coaxial blend scaffolds (Figure 2). Moreover, PCL and PLA are not expected to mix during the fabrication process as seen in previous validation studies [56]. As the stem cells did not homogeneously cover the pure PLA scaffold (Figure 4E,G) and did not show any sign of either tendon or bone differentiation (Figure 6), we hypothesized that the presence of PCL provided high adhesion and proliferation potential while PLA enhanced the expression of the tendon-related genes after the state of confluence was reached. We concluded therefore that PCL and PLA acted together to initiate stem cell differentiation towards the tendon lineage: combining both polymers made it possible to reach optimal surface coverage followed by differentiation towards the tendon lineage in the absence of any specific factors. Triggering differentiation at short term (96 h), especially late markers such as *Tnmd* or osteocalcin, was an interesting result to obtain rapidly functional tissue engineering constructs in a clinical perspective. We hypothesized that this was achieved here by the combination of favorable chemical (polymer nature), biological (rapid proliferation and dense population) and mechanical (porosity, topography and alignment) environmental signals. We avoid completely the use of additional differentiation factors in this study to be relevant with clinical requirements [26,27]. As a comparison, literature suggests that pre-osteoblastic cells in differentiation culture conditions (without scaffold but with bone-promoting factors, from ascorbic acid only to 3-factor cocktail or novel chemicals) usually needs a longer culture time (10–12 days or more) to reach maturation [57–59].

It has to be mentioned that the nature of the polymer is probably not the only parameter that alters stem cell fate. The effect of adding PLA to PCL cannot be distinguished from the influence of fiber morphology, as the coaxial scaffolds led to the formation of the biggest fiber diameters in our samples (Table 2, Figure 3) with good homogeneity. According to our results, a linear correlation ($R^2 = 0.95$, MS Excel linear regression tool on *Tnmd* results) established a link between a high fiber diameter (around 2 μm) with the tenogenic differentiation potential of C3H10T1/2 cells. This trend is consistent with the findings of Cardwell et al. [60], who demonstrated that fiber diameter was a preponderant parameter for monitor stem cell differentiation towards tendon lineage. The non-monotonic response of bone cells to scaffold topography has already been noted, especially on PCL [36,61–63].

A strong proportionality relationship has been reported in the literature between fiber diameters and the Young moduli of scaffolds in the case of electrospun samples [34,39,47]. This proportionality can also be observed in our results but was not found to be significant, and a clear linear correlation didn't appear. We hypothesized that the differences in structure (alignment with multi-layers, coaxial composites) altered the proportionality relationships. However, the discussion on the effect of fiber diameter reported earlier could thus be conducted in terms of scaffold elasticity with the same conclusions. The elasticity values of electrospun materials showed considerable variability in the literature [18,38,64,65] which could be explained by changes in the polymer solution but also in technical procedures. We found here a Young's modulus from 15 MPa to 60 MPa for the dry materials, i.e., consistent with the medium-range values found in literature (Figure 3).

In summary, the nature of the polymer and the morphology of the electrospun scaffolds could act together to monitor the fate of stem cells grown on the surface without additional specific differentiation media. A bone lineage profile was observed on various pure PCL scaffolds, while the presence of both PCL and PLA, combined with a fiber diameter of more than 2000 nm, initiated tendon differentiation in C3H10T1/2 cells. Further investigations could focus on the eventual synergetic effects that may occur between the signals with the most influence. These results are of interest for the regeneration of the musculoskeletal system. This factor-free process could also help anticipate the behavior of a patient's own cells that would colonize the biomaterial implanted alone. There are still few tissue-engineered substitutes combining cells and scaffolds that have reached clinical trials. It should be noted that all the results analyzed here reflect the primary response of the C3H10T1/2 mesenchymal stem cells. These cells are frequently used as a MSC model to reveal the potential of various processes on the stem cell fate, including on electrospun scaffolds, for early-development studies [25,32,33]. Differentiation to one or other lineage needs to be assessed over longer culture periods and gene expression confirmed by proteomic studies to ensure that a mature state is reached before implantation. Following the screening of various electrospun fibers configurations reported in the present article using a MSC-like cell model, confirmation and further applications on the most promising scaffolds for each lineage will have to be performed with primary stem cells.

4. Materials and Methods

4.1. Materials

The PCL granules (Mw 70–90 kDa) were obtained from Sigma-Aldrich, St. Louis, MO, USA. The PLA powder (Mw 59–101 kDa, low viscosity) and granules (Mw 150 kDa) were obtained from Sigma-Aldrich, St. Louis, MO, USA (for the pure PLA scaffolds) and from Natureplast, Ifs, France (for the blends), respectively. Chloroform (CHCl₃, Sigma-Aldrich, St. Louis, MO, USA), dichloromethane (DCM, CH₂Cl₂, VWR International, West Chester, PA, USA), acetone (C₃H₆O, Labgros, France) and 2,2,2-trifluoroethanol (TFE, ABCR, Karlsruhe, Germany) were used as solvents.

4.2. Electrospinning Process

Two custom-made electrospinning devices were used at the Université de Technologie de Compiègne (UTC) and the Leibniz University of Hannover, with respectively a rotating drum collector (diameter 75 mm) from Nabond (Shenzhen, China) and a homemade drum (diameter 150 mm).

The technical parameter sets for each scaffold were tuned by adjusting polymer and solvent concentration, flow rate and voltage with a trial and error approach until optimal morphology of the fibers was obtained (i.e., homogeneous fiber diameter without beads). These final parameters, as well as the nomenclature, are summarized in Table 1.

Coaxial scaffolds were prepared with a homemade double-lumen needle. BlendPCLout scaffolds were prepared with pure PCL in the outer shell of the fiber and a blend of PCL/PLA in the core. In the case of BlendPLAout, the blend of PCL/PLA was in the outer shell and PCL in the core.

PCL was spun as aligned (PCL-aligned) or random fibers (PCL600nm, PCL1000nm). Random fibers were prepared with a rotating speed of 50–250 rpm and aligned fibers (PCL-aligned) with a rotating speed of 1000 rpm.

Pure PLA scaffolds were prepared at the UTC Compiègne; BlendPCLout, BlendPLAout, PCL-aligned and PCL1000nm scaffolds were prepared at the Institute for Multiphase Processes, Leibniz University of Hannover, Hanover, Germany. The PCL600nm scaffold samples were a gift from the University of Strasbourg, ICPEES, Strasbourg, France.

4.3. Morphological Characterization of the Scaffolds

Fiber morphology and mean diameter were evaluated with scanning electronic microscopy (SEM, Quanta FEG 250, FEI, Hillsboro, OR, USA). Samples were coated with gold before observations. Scaffold porosity was estimated using the method described by Ghasemi-Mobarakeh et al. [40]. Briefly, SEM images were converted into binary images with various thresholds, based on image histogram properties (mean and standard deviation of grey scale levels). The ratio between black pixels (pores) and the total number of pixels made it possible to evaluate the porosity of the electrospun scaffolds. Image processing was performed with the free software Scilab (5.4.1, Scilab Enterprises, Orsay, France).

4.4. Mechanical Characterization of the Scaffolds

Conventional tensile tests were carried out on the electrospun scaffolds using a Bose Electroforce 3200 device (Bose, Framingham, MA, USA) at the speed of 0.1 mm/s until plastic deformation was attained. Strips measuring 5 mm × 30 mm were cut out of large scaffold sheets and mounted on metallic clamps with gripping surfaces after the thickness has been measured with caliper (0.1 mm). The curve force versus displacement was recorded. The Young's Modulus was calculated from the linear elastic part of the stress-strain curves (Linear regression tool, MS Excel software, Microsoft, Redmond, WA, USA). Tests were conducted on dry and wet (humidification with demineralized water) samples. For the aligned fibers (PCLaligned), deformation was classically applied along the fiber alignment (this is also of interest as we expected the cell alignment in the same direction along the fibers). All the measurements were performed at room temperature.

4.5. Wettability

The wettability of the electrospun scaffolds was evaluated with water contact angle measurements using a Krüss DSA10 mk2 device and Drop Shape Analysis software (Krüss GmbH, Hamburg, Germany). Briefly, a droplet of demineralized water was placed on the fiber network with a syringe, and image acquisition was performed immediately. The angle between the horizontal surface and the bottom of the droplet was then estimated with the tangent-2 option of the software. Acute and obtuse angles indicate respectively hydrophilic and hydrophobic behaviors.

4.6. Cell Cultures on Electrospun Scaffolds

The same culture medium without lineage-specific additives was used for all the experiments. The murine mesenchymal stem cell line C3H10T1/2 [30] (ATCC CCL-26) initially proliferated in culture flasks at 37 °C, 5% CO₂, in 1 g/L glucose DMEM medium (Sigma-Aldrich, St. Louis, MO, USA) complemented with 10% of Fetal Bovine Serum (Gibco Invitrogen, Waltham, MA USA), 2% of penicillin-streptomycin (Gibco Invitrogen, Waltham, MA, USA) and 2% of 200 mM L-glutamine (Gibco Invitrogen, Waltham, MA, USA). They were harvested at 95% confluence.

Sodalime glass Petri dishes (40-mm diameter, 12-mm height, Duran, Wertheim, Germany) were precoated with Sigmacote (Sigma-Aldrich, St. Louis, MO, USA) to prevent cell adhesion and thus to promote cell growth specifically on the scaffolds and not on the Petri dishes. Tabs made from polydimethylsiloxane (PDMS) were placed on the dish caps to allow gas transfers with the environment.

The Petri dishes were sterilized by autoclaving (121 °C, 1 bar, 20 min). Scaffold samples (17 × 17 mm) placed in the dishes were immersed in 70% ethanol for 30 minutes and rinsed three times with Phosphate Buffered Saline (pH 7.4 PBS, Gibco Invitrogen, Waltham, MA, USA). 300,000 cells were then seeded on to each sample and cultured for 96 h in the culture medium described above without any additional bone or tenogenic differentiation factors. The medium was changed every 2 or 3 days. Cells were also cultured in dishes without coatings or scaffolds as a material-free control group.

4.7. Cell—Material Interactions

After 96 h of culture, some samples were immersed in Rembaum solution [66] for 1 h then rinsed three times with demineralized water. They were observed using SEM (Philips XL30 ESEM-FEG, Eindhoven, the Netherlands; quanta FEG 250, FEI, Hillsboro, OR, USA; Hitachi S-3400N, Tokyo, Japan) after gold coating.

Others were stained to observe the alignment of the actin filaments using fluorescence microscopy. Briefly, samples were fixed in paraformaldehyde (Agar Scientific, Stansted, UK), immersed for 45 min in a rhodamine/phalloidin solution (5 units/mL, Invitrogen, Waltham, MA, USA) then rinsed with PBS. The nuclei of the cells were also stained with DAPI (1 g/L, Invitrogen, Waltham, MA, USA). Samples were then observed (Leica Microsystems, Wetzlar, Germany) with excitation and emission wavelengths of 540/565 nm (rhodamine/phalloidin) and 358/461 nm (DAPI).

4.8. Cell Viability

Cell viability was estimated with a Live/Dead[®] kit (Invitrogen, Waltham, MA, USA) according to the manufacturer's protocol. Briefly, Calcein AM (1 mM) and Ethidium homodimer-1 (EthD-1, 1 mM) fluorescent dyes were used to stain viable and dead cells, respectively. The samples were observed using fluorescence microscopy (Leica microsystem, Wetzlar, Germany), allowing us to qualitatively determine cell viability and the morphology of the living cells.

4.9. Gene Expression Analysis

Gene expression was studied using RT-qPCR (reverse transcription quantitative polymerase chain reaction) after 96 h of culture on the scaffolds. Briefly, samples were lysed with 350 µL of RLT Buffer (Qiagen, Germany) and centrifuged to extract the RNA (ribonucleic acid) according to the manufacturer's protocol. RNA was transcribed to DNA (deoxyribonucleic acid) using a High Capacity cDNA Reverse Transcription kit (Applied Biosystems, Foster City, CA, USA) according to the manufacturer's protocol. RT-qPCR was performed using SYBR Green PCR Master Mix (Applied Biosystems). Relative mRNA levels were calculated using the $2^{-\Delta\Delta C_t}$ method [67]. The ΔC_t s were obtained from C_t normalized with the *Rn18S* or *Rplp0* gene levels in each sample. RNA samples originating from 3 to 8 independent experiments were analyzed in duplicate. The primers are listed in Table 3 and reactions were checked before experiments (efficiency > 80%, $R_2 > 0.99$). The final results were normalized with data from samples cultured without scaffolds, i.e., data were plotted as a ratio to a cell-only control group, highlighting the intrinsic effect of the scaffolds on the gene expression.

Table 3. Primer sequences used for the reverse transcription quantitative polymerase chain reaction (RT-qPCR) gene expression study on cultured electrospun scaffolds.

Gene Symbol	Gene Name	NCBI Reference Sequence	Primer Sequences
<i>Aqp1</i>	Aquaporin1	NM_007472.2	Fwd 5'-CAATTCACCTGGCCGCAATGACCT-3' Rev 5'-TACCAGCTGCAGAGTGCCAATGAT-3'
<i>Bglap</i>	Bone gamma carboxyglutamate protein/Osteocalcin	NM_007541.3	Fwd 5'-CAGCGGCCCTGAGTCTGA-3' Rev 5'-TTATTGCCCTCCTGCTTGGA-3'
<i>Col1a1</i>	Collagen 1 alpha 1	NM_007742.4	Fwd 5'-TGGAGAGAGCATGACCGATG-3' Rev 5'-GAGCCCTCGCTCCGTA-3'
<i>Dlx5</i>	Distal-less homeobox 5	NM_010056.3	Fwd 5'-CGTCTCAGGAATCGCCAACT-3' Rev5'-AGTCAGAATCGGTGGCCG-3'
<i>Rplp0</i>	Ribosomal protein, large, P0/36B4	NM_007475.5	Fwd 5'-ACCTCCTTCTCCAGGCTTT-3' Rev 5'-CTCCACCTTGCTCCAGTC-3'
<i>Runx2</i>	Runt related transcription factor 2	NM_001271627.1	Fwd 5'-GGTCCCCGGAACCAA-3' Rev 5'-GGCGATCAGAGAACAACACTAGGTTT-3'
<i>Scx</i>	Scleraxis	NM_198885.3	Fwd 5'-CCTTCTGCCTCAGCAACCAG-3' Rev 5'-GGTCCAAAGTGGGGCTCTCCGTGACT-3'
<i>Tnmd</i>	Tenomodulin	NM_022322.2	Fwd 5'-AACACTTCTGGCCGAGGTAT-3' Rev 5'-AAGTGTGCTCCATGTCATAGTTTT-3'
<i>Rn18s</i>	18S ribosomal RNA	NR_003278.3	Fwd 5'-GGCGACGACCCATTTCG-3' Rev 5'-ACCCGTGGTCACCATGGTA-3'

4.10. Statistic Tests

Six independent experiments were performed for each study. Means and standard deviations were calculated. Two-way analysis of variance with Tukey's test (mechanical and morphological characterization) and an unpaired *t*-test (gene expression) were used to define the significance of the results.

5. Conclusions

In this study, mesenchymal stem cells were cultured on various electrospun fibers under identical culture conditions to investigate the ability of these scaffolds to promote osteogenic or tenogenic cell differentiation. Pure PCL-based scaffolds with 600 or 1000 nm fiber diameters promoted the bone differentiation of stem cells, while blend/mixed materials were more prone to favor tendon differentiation. PLA added to PCL (coaxial blend) and fiber diameter (around 2 μ m) were shown to be additional parameters able to participate in a switch from bone to tendon differentiation in the same culture conditions. We conclude that the parameters of the commonly-used method of electrospinning can monitor the stem cell differentiation potential in the absence of specific differentiation factors. These findings are of interest for the development of clinically relevant tissue engineering processes for the regeneration of the musculoskeletal system, and should further be confirmed with long-term studies as well as the use of primary MSCs. With the intrinsic effect of the scaffolds fully analyzed, other microenvironmental signals can be applied to the cell culture to enhance further the stem cell differentiation in chemical factor-free conditions. In particular, mechanical solicitations are widely investigated for bone tissue engineering and can be easily applied to electrospun fiber mats in situ.

Acknowledgments: The authors would like to thank Guy Schlatter and Corinne Wittmer (ICPEES Strasbourg) for the pure PCL scaffolds and fruitful discussions. This research was supported by the Picardy region, the Equipex FIGURES, Convergence Sorbonne Universit es programme (MecaMusTen project) and the Fondation pour la Recherche M dicale (FRM; grant DEQ20140329500). This project was cofinanced by the European Union and the European Regional Development Fund. This work was carried out and funded in the framework of the Labex MS2T. It was supported by the French government, through the program "Investments for the Future" managed by the National Agency for Research (Reference ANR-11-IDEX-0004-02). Timoth e Baudequin acknowledges the financial support of the CNRS and the Collegium INSIS-UTC. Timoth e Baudequin and Marc Mueller

acknowledge the financial support of the yESAO exchange program. Angela Huepkes acknowledges the financial support of the Erasmus program.

Author Contributions: T.B. drafted the article (major contributor), designed the work (cell culture, biological and mechanical testing, material development and production), performed data analysis and interpretation. L.G. performed analysis regarding gene expression, and the differentiation/material properties cross-analysis. M.M. designed the blend and multilayer scaffolds, and performed analysis regarding materials' morphology and chemistry. A.H. designed the PLQ scaffolds and participated to cell culture and biological characterization. T.B., L.G., M.M. and A.H. performed data collection. B.G. conducted critical revision of the article based on her chemical and material expertise. D.D. performed data analysis and interpretation based on her expertise on tendon differentiation and biological development. F.B. performed data analysis and interpretation based on his expertise on material and mechanical characterization. C.L. performed data analysis and interpretation based on her tissue engineering expertise. F.B. and C.L. are co-PI of the study and conducted critical revision of the article. All authors approved the final version to be published.

Conflicts of Interest: The authors declare no conflicts of interest.

References

1. Szentivanyi, A.L.; Zernetsch, H.; Menzel, H.; Glasmacher, B. A review of developments in electrospinning technology: New opportunities for the design of artificial tissue structures. *Int. J. Artif. Organs* **2011**, *34*, 986–997. [[CrossRef](#)] [[PubMed](#)]
2. Katti, D.S.; Robinson, K.W.; Ko, F.K.; Laurencin, C.T. Bioresorbable nanofiber-based systems for wound healing and drug delivery: Optimization of fabrication parameters. *J. Biomed. Mater. Res. B Appl. Biomater.* **2004**, *70*, 286–296. [[CrossRef](#)] [[PubMed](#)]
3. Khorshidi, S.; Solouk, A.; Mirzadeh, H.; Mazinani, S.; Lagaron, J.M.; Sharifi, S.; Ramakrishna, S. A review of key challenges of electrospun scaffolds for tissue-engineering applications. *J. Tissue Eng. Regen. Med.* **2016**, *10*, 715–738. [[CrossRef](#)] [[PubMed](#)]
4. Zafar, M.; Najeeb, S.; Khurshid, Z.; Vazirzadeh, M.; Zohaib, S.; Najeeb, B.; Sefat, F. Potential of Electrospun Nanofibers for Biomedical and Dental Applications. *Materials* **2016**, *9*, 73. [[CrossRef](#)] [[PubMed](#)]
5. Saw, S.H.; Wang, K.; Yong, T.; Ramakrishna, S. Polymeric Nanofibers in Tissue Engineering. In *Nanotechnologies for the Life Sciences*; Wiley-VCH Verlag GmbH & Co. KGaA: Weinheim, Germany, 2007; ISBN 3527313893.
6. Li, W.; Shanti, R.M.; Tuan, R.S. Electrospinning Technology for Nanofibrous Scaffolds in Tissue Engineering. *Nanotechnol. Life Sci.* **2006**, *9*, 135–187. [[CrossRef](#)]
7. Sundararaghavan, H.G.; Saunders, R.L.; Hammer, D.A.; Burdick, J.A. Fiber alignment directs cell motility over chemotactic gradients. *Biotechnol. Bioeng.* **2013**, *110*, 1249–1254. [[CrossRef](#)] [[PubMed](#)]
8. Huang, C.; Hu, K.; Wei, Z. Comparison of cell behavior on pva / pva-gelatin electrospun nanofibers with random and aligned configuration. *Sci. Rep.* **2016**, *6*, 37960. [[CrossRef](#)] [[PubMed](#)]
9. Patlolla, A.; Arinzeh, T.L. Evaluating apatite formation and osteogenic activity of electrospun composites for bone tissue engineering. *Biotechnol. Bioeng.* **2014**, *111*, 1000–1017. [[CrossRef](#)] [[PubMed](#)]
10. Nair, L.S.; Bhattacharyya, S.; Laurencin, C.T. Nanotechnology and Tissue Engineering: The Scaffold Based Approach. In *Nanotechnologies for the Life Sciences*; Wiley-VCH Verlag GmbH & Co. KGaA: Weinheim, Germany, 2007; ISBN 3527313893.
11. Cardwell, R.D.; Kluge, J.A.; Thayer, P.A.; Guelcher, S.A.; Dahlgren, L.A.; Kaplan, D.L.; Goldstein, A.S. Static and Cyclic Mechanical Loading of Mesenchymal Stem Cells on Elastomeric, Electrospun Polyurethane Meshes. *J. Biomech. Eng.* **2015**, *137*, 71010. [[CrossRef](#)] [[PubMed](#)]
12. Full, S.M.; Delman, C.; Gluck, J.M.; Abdmaulen, R.; Shemin, R.J.; Heydarkhan-Hagvall, S. Effect of fiber orientation of collagen-based electrospun meshes on human fibroblasts for ligament tissue engineering applications. *J. Biomed. Mater. Res. B Appl. Biomater.* **2014**, 1–8. [[CrossRef](#)] [[PubMed](#)]
13. Chainani, A.; Hippensteel, K.J.; Kishan, A.; Garrigues, N.W.; Ruch, D.S.; Guilak, F.; Little, D. Multilayered electrospun scaffolds for tendon tissue engineering. *Tissue Eng. Part A* **2013**, *19*, 2594–2604. [[CrossRef](#)] [[PubMed](#)]
14. Yoshimoto, H.; Shin, Y.M.; Terai, H.; Vacanti, J.P. A biodegradable nanofiber scaffold by electrospinning and its potential for bone tissue engineering. *Biomaterials* **2003**, *24*, 2077–2082. [[CrossRef](#)]

15. Fu, Y.-C.; Nie, H.; Ho, M.-L.; Wang, C.-K.; Wang, C.-H. Optimized bone regeneration based on sustained release from three-dimensional fibrous PLGA/HAp composite scaffolds loaded with BMP-2. *Biotechnol. Bioeng.* **2008**, *99*, 996–1006. [[CrossRef](#)] [[PubMed](#)]
16. Qasim, S.B.; Najeeb, S.; Delaine-Smith, R.M.; Rawlinson, A.; Ur Rehman, I. Potential of electrospun chitosan fibers as a surface layer in functionally graded GTR membrane for periodontal regeneration. *Dent. Mater.* **2017**, *33*, 71–83. [[CrossRef](#)] [[PubMed](#)]
17. Hutmacher, D.W. Scaffolds in tissue engineering bone and cartilage. *Biomaterials* **2000**, *21*, 2529–2543. [[CrossRef](#)]
18. Bonani, W.; Maniglio, D.; Motta, A.; Tan, W.; Migliaresi, C. Biohybrid nanofiber constructs with anisotropic biomechanical properties. *J. Biomed. Mater. Res. B Appl. Biomater.* **2011**, *96*, 276–286. [[CrossRef](#)] [[PubMed](#)]
19. Song, Z.; Shi, B.; Ding, J.; Zhuang, X.; Zhang, X.; Fu, C.; Chen, X. A comparative study of preventing postoperative tendon adhesion using electrospun polyester membranes with different degradation kinetics. *Sci. China Chem.* **2015**, *58*, 1159–1168. [[CrossRef](#)]
20. Lu, H.H.; Cooper, J.A.; Manuel, S.; Freeman, J.W.; Attawia, M.A.; Ko, F.K.; Laurencin, C.T. Anterior cruciate ligament regeneration using braided biodegradable scaffolds: In vitro optimization studies. *Biomaterials* **2005**, *26*, 4805–4816. [[CrossRef](#)] [[PubMed](#)]
21. Ladd, M.R.; Lee, S.J.; Stitzel, J.D.; Atala, A.; Yoo, J.J. Co-electrospun dual scaffolding system with potential for muscle-tendon junction tissue engineering. *Biomaterials* **2011**, *32*, 1549–1559. [[CrossRef](#)] [[PubMed](#)]
22. Chamberlain, G.; Fox, J.; Ashton, B.; Middleton, J. Concise review: Mesenchymal stem cells: Their phenotype, differentiation capacity, immunological features, and potential for homing. *Stem Cells* **2007**, *25*, 2739–2749. [[CrossRef](#)] [[PubMed](#)]
23. Pittenger, M.F.; Mackay, A.M.; Beck, S.C.; Jaiswal, R.K.; Douglas, R.; Mosca, J.D.; Moorman, M.A.; Simonetti, D.W.; Craig, S.; Marshak, D.R. Multilineage potential of adult human mesenchymal stem cells. *Science* **1999**, *284*, 143–147. [[CrossRef](#)] [[PubMed](#)]
24. Caplan, A.I. Adult Mesenchymal Stem Cells for Tissue Engineering versus Regenerative Medicine. *J. Cell. Physiol.* **2007**, *341*–347. [[CrossRef](#)] [[PubMed](#)]
25. Guerquin, M.J.; Charvet, B.; Nourissat, G.; Havis, E.; Ronsin, O.; Bonnin, M.A.; Ruggiu, M.; Olivera-Martinez, I.; Robert, N.; Lu, Y.; et al. Transcription factor EGR1 directs tendon differentiation and promotes tendon repair. *J. Clin. Investig.* **2013**, *123*, 3564–3576. [[CrossRef](#)] [[PubMed](#)]
26. Woo, E.J. Adverse events after recombinant human BMP2 in nonspinal orthopaedic procedures. *Clin. Orthop. Relat. Res.* **2013**, *471*, 1707–1711. [[CrossRef](#)] [[PubMed](#)]
27. Lieberman, J.R.; Daluiski, A.; Einhorn, T.A. The Role of Growth Factors in the Repair of Bone. *J. Bone Jt. Surg.* **2006**, *84*, 1032–1044. [[CrossRef](#)]
28. Cooper, J.O.; Bumgardner, J.D.; Cole, J.A.; Smith, R.A.; Haggard, W.O. Co-cultured tissue-specific scaffolds for tendon/bone interface engineering. *J. Tissue Eng.* **2014**, *5*, 1–10. [[CrossRef](#)] [[PubMed](#)]
29. Benjamin, M.; Toumi, H.; Ralphy, J.R.; Bydder, G.; Best, T.M.; Milz, S. Where tendons and ligaments meet bone: Attachment sites (‘entheses’) in relation to exercise and/or mechanical load. *J. Anat.* **2006**, *208*, 471–490. [[CrossRef](#)] [[PubMed](#)]
30. Reznikoff, C.A.; Brankow, D.W.; Heidelberger, C. Establishment and Characterization of a Cloned Line of C3H Mouse Embryo Cells Sensitive to Postconfluence Inhibition of Division. *Cancer Res.* **1973**, *33*, 3231–3239. [[PubMed](#)]
31. Aubin, J.E. Bone stem cells. *J. Cell. Biochem. Suppl.* **1998**, *30*, 73–82. [[CrossRef](#)]
32. Havis, E.; Bonnin, M.-A.; Olivera-Martinez, I.; Nazaret, N.; Ruggiu, M.; Weibel, J.; Durand, C.; Guerquin, M.-J.; Bonod-Bidaud, C.; Ruggiero, F.; et al. Transcriptomic analysis of mouse limb tendon cells during development. *Development* **2014**, *141*, 3683–3696. [[CrossRef](#)] [[PubMed](#)]
33. Yin, Z.; Chen, X.; Song, H.; Hu, J.; Tang, Q.; Zhu, T.; Shen, W.; Chen, J.; Liu, H.; Heng, B.C.; et al. Electrospun scaffolds for multiple tissues regeneration in vivo through topography dependent induction of lineage specific differentiation. *Biomaterials* **2015**, *44*, 173–185. [[CrossRef](#)] [[PubMed](#)]
34. Keun Kwon, I.; Kidoaki, S.; Matsuda, T. Electrospun nano- to microfiber fabrics made of biodegradable copolyesters: Structural characteristics, mechanical properties and cell adhesion potential. *Biomaterials* **2005**, *26*, 3929–3939. [[CrossRef](#)] [[PubMed](#)]
35. Bognitzki, M.; Czado, W.; Frese, T.; Schaper, A.; Hellwig, M.; Steinhart, M.; Greiner, A.; Wendorff, J.H. Nanostructured Fibers via Electrospinning. *Adv. Mater.* **2001**, *13*, 70–72. [[CrossRef](#)]

36. Bigerelle, M.; Giljean, S.; Anselme, K. Existence of a typical threshold in the response of human mesenchymal stem cells to a peak and valley topography. *Acta Biomater.* **2011**, *7*, 3302–3311. [[CrossRef](#)] [[PubMed](#)]
37. Shin, M.; Yoshimoto, H.; Vacanti, J.P. In vivo bone tissue engineering using mesenchymal stem cells on a novel electrospun nanofibrous scaffold. *Tissue Eng.* **2004**, *10*, 33–41. [[CrossRef](#)] [[PubMed](#)]
38. Venugopal, J.R.; Low, S.; Choon, A.T.; Kumar, A.B.; Ramakrishna, S. Nanobioengineered electrospun composite nanofibers and osteoblasts for bone regeneration. *Artif. Organs* **2008**, *32*, 388–397. [[CrossRef](#)] [[PubMed](#)]
39. Lee, J.; Tae, G.; Kim, Y.H.; Park, I.S.; Kim, S.-H.; Kim, S.H. The effect of gelatin incorporation into electrospun poly(l-lactide-co- ϵ -caprolactone) fibers on mechanical properties and cytocompatibility. *Biomaterials* **2008**, *29*, 1872–1879. [[CrossRef](#)] [[PubMed](#)]
40. Ghasemi-Mobarakeh, L.; Semnani, D.; Morshed, M. A novel method for porosity measurement of various surface layers of nanofibers mat using image analysis for tissue engineering applications. *J. Appl. Polym. Sci.* **2007**, *106*, 2536–2542. [[CrossRef](#)]
41. Asran, A.S.; Razghandi, K.; Aggarwal, N.; Michler, G.H.; Groth, T. Nanofibers from Blends of Polyvinyl Alcohol and Polyhydroxy Butyrate as Potential Scaffold Material for Tissue Engineering of Skin. *Biomacromolecules* **2010**, *11*, 3413–3421. [[CrossRef](#)] [[PubMed](#)]
42. Mohammadzadehmoghadam, S.; Dong, Y.; Barbhuiya, S.; Guo, L.; Liu, D.; Umer, R.; Qi, X.; Tang, Y. Electrospinning: Current Status and Future Trends. In *Nano-Size Polymers*; Springer: Cham, Switzerland, 2016; pp. 89–154.
43. Elamparithi, A.; Punnoose, A.M.; Paul, S.F.D.; Kuruvilla, S. Gelatin electrospun nanofibrous matrices for cardiac tissue engineering applications. *Int. J. Polym. Mater. Polym. Biomater.* **2017**, *66*, 20–27. [[CrossRef](#)]
44. Lin, S.T.; Kimble, L.; Bhattacharyya, D. Polymer Blends and Composites for Biomedical Applications. In *Biomaterials for Implants and Scaffolds*; Springer: Berlin/Heidelberg, Germany, 2017; pp. 195–235.
45. Semnani, D.; Naghashzargar, E.; Hadjianfar, M.; Dehghan Manshadi, F.; Mohammadi, S.; Karbasi, S.; Effaty, F. Evaluation of PCL/chitosan electrospun nanofibers for liver tissue engineering. *Int. J. Polym. Mater. Polym. Biomater.* **2017**, *66*, 149–157. [[CrossRef](#)]
46. Bedoui, F.; Widjaja, L.K.; Luk, A.; Bolikal, D.; Murthy, N.S.; Kohn, J. Anomalous increase in modulus upon hydration in random copolymers with hydrophobic segments and hydrophilic blocks. *Soft Matter* **2012**, *8*, 2230. [[CrossRef](#)]
47. Wanasekara, N.; Chen, M.; Chalivendra, V.; Bhowmick, S. Investigation of the Young's Modulus of Fibers in an Electrospun PCL Scaffold Using AFM and its Correlation to cell Attachment. In *MEMS and Nanotechnology*; Springer: New York, NY, USA, 2011; ISBN 978-1-4419-8824-9.
48. Robledo, R.F.; Rajan, L.; Li, X.; Lufkin, T. The *Dlx5* and *Dlx6* homeobox genes are essential for craniofacial, axial, and appendicular skeletal development. *Genes Dev.* **2002**, *16*, 1089–1101. [[CrossRef](#)] [[PubMed](#)]
49. Szpalski, C.; Wetterau, M.; Barr, J.; Warren, S.M. Bone tissue engineering: Current strategies and techniques—Part I: Scaffolds. *Tissue Eng. Part B Rev.* **2012**, *18*, 246–257. [[CrossRef](#)] [[PubMed](#)]
50. Bashur, C.A.; Shaffer, R.D.; Dahlgren, L.A.; Guelcher, S.A.; Goldstein, A.S. Effect of fiber diameter and alignment of electrospun polyurethane meshes on mesenchymal progenitor cells. *Tissue Eng. Part A* **2009**, *15*, 2435–2445. [[CrossRef](#)] [[PubMed](#)]
51. Schweitzer, R.; Chyung, J.H.; Murtaugh, L.C.; Brent, A.E.; Rosen, V.; Olson, E.N.; Lassar, A.; Tabin, C.J. Analysis of the tendon cell fate using Scleraxis, a specific marker for tendons and ligaments. *Development* **2001**, *128*, 3855–3866. [[PubMed](#)]
52. Kim, B.S.; Kim, E.J.; Choi, J.S.; Jeong, J.H.; Jo, C.H.; Cho, Y.W. Human collagen-based multilayer scaffolds for tendon-to-bone interface tissue engineering. *J. Biomed. Mater. Res. Part A* **2014**, *102*, 4044–4054. [[CrossRef](#)] [[PubMed](#)]
53. Seidi, A.; Ramalingam, M.; Elloumi-Hannachi, I.; Ostrovidov, S.; Khademhosseini, A. Gradient biomaterials for soft-to-hard interface tissue engineering. *Acta Biomater.* **2011**, *7*, 1441–1451. [[CrossRef](#)] [[PubMed](#)]
54. Kishore, V.; Bullock, W.; Sun, X.; Van Dyke, W.S.; Akkus, O. Tenogenic differentiation of human MSCs induced by the topography of electrochemically aligned collagen threads. *Biomaterials* **2012**, *33*, 2137–2144. [[CrossRef](#)] [[PubMed](#)]
55. Shang, S.; Yang, F.; Cheng, X.; Frank Walboomers, X.; Jansen, J.A. The effect of electrospun fibre alignment on the behaviour of rat periodontal ligament cells. *Eur. Cells Mater.* **2010**, *19*, 180–192. [[CrossRef](#)]

56. Repanas, A.; Wolkers, W.F.; Gryshkov, O.; Kalozoumis, P.; Mueller, M.; Zernetsch, H.; Korossis, S.; Glasmacher, B. Coaxial Electrospinning as a Process to Engineer Biodegradable Polymeric Scaffolds as Drug Delivery Systems for Anti-Inflammatory and Anti-Thrombotic Pharmaceutical Agents. *Clin. Exp. Pharmacol.* **2015**, *5*, 192. [[CrossRef](#)]
57. Wang, D.; Christensen, K.; Chawla, K.; Xiao, G.; Krebsbach, P.H.; Franceschi, R.T. Isolation and characterization of MC3T3-E1 preosteoblast subclones with distinct in vitro and in vivo differentiation/mineralization potential. *J. Bone Miner. Res.* **1999**, *14*, 893–903. [[CrossRef](#)] [[PubMed](#)]
58. Yan, X.-Z.; Yang, W.; Yang, F.; Kersten-Niessen, M.; Jansen, J.A.; Both, S.K. Effects of Continuous Passaging on Mineralization of MC3T3-E1 Cells with Improved Osteogenic Culture Protocol. *Tissue Eng. Part C Methods* **2014**, *20*, 198–204. [[CrossRef](#)] [[PubMed](#)]
59. Chen, S.; Ye, X.; Yu, X.; Xu, Q.; Pan, K.; Lu, S.; Yang, P. Co-culture with periodontal ligament stem cells enhanced osteoblastic differentiation of MC3T3-E1 cells and osteoclastic differentiation of RAW264.7 cells. *Int. J. Clin. Exp. Pathol.* **2015**, *8*, 14596–14607. [[PubMed](#)]
60. Cardwell, R.D.; Dahlgren, L.A.; Goldstein, A.S. Electrospun fibre diameter, not alignment, affects mesenchymal stem cell differentiation into the tendon/ligament lineage. *J. Tissue Eng. Regen. Med.* **2014**, *8*, 937–945. [[CrossRef](#)] [[PubMed](#)]
61. Mashinchian, O.; Turner, A.; Matthew, J. Regulation of stem cell fate by nanomaterial substrates. *Nanomedicine* **2015**, *10*, 829–847. [[CrossRef](#)] [[PubMed](#)]
62. Szentivanyi, A.; Chakradeo, T.; Zernetsch, H.; Glasmacher, B. Electrospun cellular microenvironments: Understanding controlled release and scaffold structure. *Adv. Drug Deliv. Rev.* **2011**, *63*, 209–220. [[CrossRef](#)] [[PubMed](#)]
63. Faia-Torres, A.B.; Charnley, M.; Goren, T.; Guimond-Lischer, S.; Rottmar, M.; Maniura-Weber, K.; Spencer, N.D.; Reis, R.L.; Textor, M.; Neves, N.M. Osteogenic differentiation of human mesenchymal stem cells in the absence of osteogenic supplements: A surface-roughness gradient study. *Acta Biomater.* **2015**, *28*, 64–75. [[CrossRef](#)] [[PubMed](#)]
64. Carlisle, C.R.; Coulais, C.; Namboothiry, M.; Carroll, D.L.; Hantgan, R.R.; Guthold, M. The mechanical properties of individual, electrospun fibrinogen fibers. *Biomaterials* **2009**, *30*, 1205–1213. [[CrossRef](#)] [[PubMed](#)]
65. Huang, Z.-M.; Zhang, Y.Z.; Ramakrishna, S.; Lim, C.T. Electrospinning and mechanical characterization of gelatin nanofibers. *Polymer* **2004**, *45*, 5361–5368. [[CrossRef](#)]
66. Rajaraman, R.; Rounds, D.E.; Yen, S.P.S.; Rembaum, A. A scanning electron microscope study of cell adhesion and spreading in vitro. *Exp. Cell Res.* **1974**, *88*, 327–339. [[CrossRef](#)]
67. Livak, K.J.; Schmittgen, T.D. Analysis of relative gene expression data using real-time quantitative PCR and the 2⁻(Delta Delta C(T)) Method. *Methods* **2001**, *25*, 402–408. [[CrossRef](#)] [[PubMed](#)]



© 2017 by the authors. Licensee MDPI, Basel, Switzerland. This article is an open access article distributed under the terms and conditions of the Creative Commons Attribution (CC BY) license (<http://creativecommons.org/licenses/by/4.0/>).

X.3 Tendon development and diseases



Tendon development and diseases

Ludovic Gaut^{1,2,3} and Delphine Duprez^{1,2,3*}

Tendon is a uniaxial connective tissue component of the musculoskeletal system. Tendon is involved in force transmission between muscle and bone. Tendon injury is very common and debilitating but tendon repair remains a clinical challenge for orthopedic medicine. In vertebrates, tendon is mainly composed of type I collagen fibrils, displaying a parallel organization along the tendon axis. The tendon-specific spatial organization of type I collagen provides the mechanical properties for tendon function. In contrast to other components of the musculoskeletal system, tendon biology is poorly understood. An important goal in tendon biology is to understand the mechanisms involved in the production and assembly of type I collagen fibrils during development, postnatal formation, and healing processes in order to design new therapies for tendon repair. In this review we highlight the current understanding of the molecular and mechanical signals known to be involved in tenogenesis during development, and how development provides insights into tendon healing processes. © 2015 Wiley Periodicals, Inc.

How to cite this article:

WIREs Dev Biol 2015. doi: 10.1002/wdev.201

INTRODUCTION

The musculoskeletal system confers the ability to move. Muscle, tendon and bone are the main components of the musculoskeletal system. Muscle generates forces that are transmitted to bone to allow body motion. Tendon links muscle to bone and is the essential organ of the musculoskeletal system that transmits forces. Tendon is a specialized connective tissue displaying a specific spatial organization of type I collagen fibrils that are organized parallel to the tendon axis. The specific organization of collagen fibrils confers tendon mechanical properties. The molecular and mechanical factors driving collagen production and organization during tendon development, postnatal formation and repair are not fully understood.

Tendon collagen fibrillogenesis consists in the progressive assembly of collagen fibrils that form a functional and mature tendon. Successive and

overlapping phases of collagen fibril assembly and growth have been described in tendons.¹ Collagen fibril assembly occurs mostly during fetal stages, while collagen fibril growth and maturation occurs at postnatal stages.¹ The collagen fibril growth and maturation during postnatal stages are accompanied by a dramatic change of tendon mechanical properties. There is a 40,000-fold increase of the elastic modulus between adult tendons versus fetal tendons in chick.² Many components of the extracellular matrix (ECM) have been shown to be involved in collagen fibrillogenesis in tendons. Collagens, such as the fibrillar collagens III and V and the non fibrillar FACITs (fibril-associated collagens with interrupted triple helices) collagens XII and XIV, are important for collagen fibril formation, growth, and integrity in tendons (Table 1 and references therein). In addition to fibrillar and FACIT collagens, small leucine-rich proteoglycans (SLRPs) are also involved in type I collagen fibrillogenesis in tendons, mainly by regulating lateral collagen fibril growth.^{45,46} Mutations of one SLRP or combination of SLRPs systematically lead to a tendon phenotype in mice (Table 1 and references therein).

The main challenge to decipher the molecular mechanisms underlying tenogenesis is to understand the intrinsic and extrinsic regulators of type I collagen production (transcript and protein levels), collagen fibril assembly and maturation during development.

*Correspondence to: delphine.duprez@upmc.fr

¹CNRS UMR 7622, IBPS-Developmental Biology Laboratory, Paris, France

²Sorbonne Universités, UPMC Univ Paris 06, IBPS-Developmental Biology Laboratory, Paris, France

³Inserm U1156, Paris, France

Conflict of interest: The authors have declared no conflicts of interest for this article.

TABLE 1 | List of Molecules Involved in Tendon Development

Protein (gene)	Mouse	Chick	Zebrafish	Drosophila
Transcription factors				
Scleraxis (<i>Scx</i>)	<p><i>Scx</i>^{-/-}</p> <ul style="list-style-type: none"> -Severe tendon disruption⁴ -Tendon phenotype from E13.5⁴ -Loss of <i>Tnmd</i>, <i>Col14a1</i> expression in limb tendons from E16.5⁴ -Decrease of <i>Col1a1</i> expression in limb tendons from E16.5⁴ 	<p><i>Scx</i> overexpression in chick hindlimbs: Upregulation of <i>Tnmd</i> expression³</p>		
Mohawk (<i>Mkx</i>)	<p><i>Mkx</i>^{-/-}</p> <ul style="list-style-type: none"> -Postnatal hypoplastic tendons⁵⁻⁸ -Tendon phenotype from E16.5⁷ -Decrease of <i>Col1a1</i>, <i>Col1a2</i>, <i>Tnmd</i>, <i>Fmod</i>, <i>Dcn</i> expression in postnatal tendons⁵⁻⁸ 		<p><i>Mkx</i> Morphants:</p> <ul style="list-style-type: none"> -Neural crest and somitite defects and increase of <i>MyoD</i> expression⁹ 	
Early growth response 1 (<i>Egr1</i>)	<p><i>Egr1</i>^{-/-}</p> <ul style="list-style-type: none"> -Defects of collagen fibrils in tendons¹³ -Altered mechanical properties¹³ -Tendon phenotype from E18.5¹³ -Decrease of <i>Scx</i>, <i>Col1a1</i>, <i>Col1a2</i>, <i>Col3a1</i>, <i>Tnmd</i> expression in adult tendons¹³ 	<p><i>Egr1</i> overexpression in chick embryos: Upregulation of <i>Scx</i>, <i>Col1a1</i>, <i>Col3a1</i>, <i>Col5a1</i>, <i>Col12a1</i>, <i>Col14a1</i>, <i>Bmp4</i>, <i>Fgf8</i> expression¹⁰</p>		<p><i>stripe</i> mutant: Defect in tendon cell specification and differentiation^{11,12} <i>stripeA</i> gain-of-function experiments: Upregulation of <i>Tsp</i> and other tendon genes¹⁴</p>
Signaling pathways				
TGF-β2 (<i>Tgfb2</i>) TGF-β3 (<i>Tgfb3</i>)	<p><i>Tgfb2</i>^{-/-}; <i>Tgfb3</i>^{-/-}</p> <ul style="list-style-type: none"> -Loss of all tendons from E14.5¹⁶ -Loss of <i>Scx</i> and <i>Tnmd</i> expression¹⁶ <i>TGF-β2</i> bead implantation in mouse limbs: Upregulation of <i>Scx</i> expression¹⁶ 	<p>TGF-β1 gain-of-function experiments in E6 chick digits: Upregulation of <i>Scx</i> expression 1 Hour after bead application¹⁵</p>		
GDF-8/myostatin (<i>Mstn</i>)	<p><i>Mstn</i>^{-/-}</p> <ul style="list-style-type: none"> -Smaller and hypocellular postnatal tendons¹⁷ -Altered mechanical properties¹⁷ -Decrease of <i>Scx</i>, <i>Mkx</i>, <i>Col1a2</i>, <i>Tnmd</i> expression in postnatal tendons¹⁷ 			
Smad3 (<i>Smad3</i>)	<p><i>Smad3</i>^{-/-}</p> <ul style="list-style-type: none"> -Disruption of adult tendon architecture¹⁹ 		<p>Block of <i>Smad2/3</i> pathway using chemical inhibitors: Decrease in <i>Scx</i> expression¹⁸</p>	

TABLE 1 | Continued

	Mouse	Chick	Zebrafish	Drosophila
	-Decrease of type I Collagen ¹⁹ -Decrease in <i>Col1a1</i> , <i>Tnmd</i> expression ¹⁹ <i>Prx1-Cre</i> ; <i>Bmp4</i> ^{fl/fl} Defect in bone ridge formation ²¹ <i>FGF4</i> gain-of-function experiments in mouse somites: Upregulation of <i>Scx</i> expression ²²	<i>BMP</i> gain-of-function experiments in E4 chick limbs: Inhibition of <i>Scx</i> expression ²⁰ <i>FGF-4</i> or <i>FGF-8</i> gain-of-function experiments in somites and limbs: Upregulation of <i>Scx</i> , <i>Tnc</i> , <i>Pea3</i> , <i>Spry2</i> , <i>Mkp3</i> expression ^{23–26} <i>FGF</i> loss-of-function experiments in chick somites: Loss of <i>Scx</i> expression ^{23,26}		
BMP-4 (<i>Bmp4</i>)				
<i>FGF-4</i> (<i>Fgf4</i>)				
<i>FGF-8</i> (<i>Fgf8</i>)				
MAPK	<i>Block of MAPK pathways using chemical inhibitors in somites: Loss of Scx expression</i> ²² <i>Block of ERK MAPK pathway using chemical inhibitors in mouse limbs: Increase of Scx expression</i> ²⁷	<i>Block of ERK MAPK pathway using chemical inhibitors in somites: Loss of Scx, Pea3, Mkp3 expression</i> ²⁶		<i>Block of MAPK pathway using chemical inhibitors in embryos: Loss of Scx expression</i> ¹⁸
Transmembrane protein				
Tenomodulin (<i>Tnmd</i>)	<i>Tnmd</i> ^{-/-} -Defects in collagen fibrils in postnatal tendons ²⁸ -Defect in tendon stem cell proliferation ²⁹			
Extracellular matrix proteins				
Type I collagen (<i>Col1a1</i> , <i>Col1a2</i>)	<i>Col1a1</i> ^{-/-} Smaller diameters of collagen fibrils in adult tendons ³⁰			
Type III collagen (<i>Col3a1</i>)	<i>Col3a1</i> ^{-/-} Defects in type I collagen fibrillogenesis ³¹			
Type V collagen (<i>Col5a1</i>)	<i>Col5a1</i> ^{+/-} , <i>Col11a1</i> ^{+/-} Increased diameters and reduced collagen fibril number from E18 tendons ³²			
Type XII Collagen (<i>Col12a1</i>)	<i>Col12a1</i> ^{-/-} Skeletal abnormalities ³³			
FACIT collagen				
Type XIV Collagen (<i>Col14a1</i>)	<i>Col14a1</i> ^{-/-} Premature collagen fibril growth (increased diameters) in postnatal tendons ³⁴			

TABLE 1 | Continued

	Mouse	Chick	Zebrafish	Drosophila
FACIT collagen				
Type XXII Collagen (<i>Col22a1</i>)	-Expressed at muscle tips close to tendons ³⁵ -Binding to $\alpha 2\beta 1$ integrin ³⁵		<i>Col22a1</i> morphants: Destabilization of myotendinous junctions via the $\alpha 1\beta 1$ Integrin ³⁶	
FACIT collagen				<i>Tsp</i> mutants: Muscle cell failure to attach to tendon cells and reduced Integrin signaling ³⁸
Thrombospondin 4 (<i>Thbs4</i>)	<i>Thbs4</i> ^{-/-} -Larger collagen fibrils in adult tendons ³⁹ -Expression in fetal limb tendons ²⁷		<i>Tsp4b</i> morphants: Muscle detachment upon electric stimulation and reduced Integrin signaling ³⁷	
Fibromodulin (<i>Fmod</i>)	<i>Fmod</i> ^{-/-} Abnormal collagen fibrillogenesis (smaller diameters) in tendons ⁴⁰			
Lumican (<i>Lum</i>)	<i>Lum</i> ^{-/-} Abnormal collagen fibrillogenesis (larger diameters) in tendons ⁴⁰			
SLRP				
Decorin (<i>Dcn</i>)	<i>Dcn</i> ^{-/-} -Abnormal collagen fibrillogenesis (larger diameters) in tendons ^{41,42}			
SLRP				
Biglycan (<i>Bgn</i>)	<i>Bgn</i> ^{-/-} -Increase of <i>Bgn</i> expression ^{41,42}			
SLRP				
Lumican (<i>Lum</i>)	<i>Bgn</i> ^{-/-} -Abnormal collagen fibrillogenesis (smaller diameters) in tendons ^{42,43}			
Fibromodulin (<i>Fmod</i>)	<i>Lum</i> ^{-/-} ; <i>Fmod</i> ^{-/-} Abnormal collagen fibrillogenesis in tendons ⁴⁰			
Biglycan (<i>Bgn</i>)	<i>Bgn</i> ^{-/-} ; <i>Fmod</i> ^{-/-} -Disruption in collagen fibrillogenesis (smaller diameters) in tendons ⁴³			
Fibromodulin (<i>Fmod</i>)				
Biglycan (<i>Bgn</i>)				
Decorin (<i>Dcn</i>)	-Ectopic ossification ^{43,44} -Increase of tendon progenitor number ⁴⁴ -Increase of <i>Scx</i> expression ⁴⁴ <i>Bgn</i> ^{-/-} ; <i>Dcn</i> ^{-/-} Abnormal collagen fibrillogenesis ⁴²			

Tendon phenotypes reported in mice during development, postnatal, or adult stages. Studies reporting a tendon phenotype performed in chick, zebrafish, or *Drosophila* are also reported.

Developmental studies on the musculoskeletal system have focused mainly on muscle, cartilage, and bone. The master genes driving the skeletal muscle and cartilage lineages have been identified as the bHLH transcription factors *Myf5*, *MyoD*, and *Mrf4* (muscle) as well as the SOX transcription factor *Sox9* (cartilage). The absence of the three myogenic regulatory factors, *Myf5*, *MyoD*, and *Mrf4* leads to a loss of skeletal muscle in mice,⁴⁷ while the overexpression of each myogenic regulatory factor induces myoblast conversion *in vitro* or *in vivo*.^{48,49} A loss of *Sox9* activity results in a complete absence of cartilage,⁵⁰ while overexpression of *Sox9* converts cells to chondrocytes.⁵¹ The master regulator gene(s) of the tendon lineage has (have) not yet been identified. The task is made more difficult because of a lack of specific markers for tendon progenitors and differentiated cells (tenocytes). The main structural and functional component of tendon, type I collagen, is not specific to tendon and is expressed in many other tissues such as bone, skin, and cornea. None of the ECM components involved in type I collagen fibrillogenesis during tendon formation is specific to tendon; since they are also involved in collagen fibrillogenesis in other tissues.^{45,46} Tendons are characterized by the spatial and parallel organization of collagen fibrils. To date, the molecular and cellular mechanisms driving this tendon-specific spatial organization of type I collagen remain completely unknown. It has been shown that fibroblasts, responsible for type I collagen synthesis and organization, cell-autonomously spatially arrange themselves according to their *in vivo* origins.⁵² Fibroblasts isolated during fetal stages from tendon, cornea and skin and cultured in the same conditions, adopt a parallel, orthogonal or random organization, respectively.⁵² This experiment suggests that fetal tendon fibroblasts intrinsically contain tissue-specific information that drives the parallel organization of type I collagen fibrils. We believe that the identification of genes involved in the early steps of tenogenesis during development will benefit the understanding of the type I collagen fibrillogenesis in tendons, in normal and pathological conditions.

In this review, we describe the current knowledge of tendon development in vertebrates and refer to *Drosophila* tendon development when appropriate to establish parallels between invertebrates and vertebrates. We define the embryological origins of tendon versus the other components of the musculoskeletal system and highlight the intricate development of tendon with that of muscle and cartilage/bone tissues. We list the intrinsic and extrinsic molecular players known to be involved in tendon development and highlight the importance of mechanical forces in

tendon development. Finally, we emphasize the parallel between tendon development and tendon healing.

TENDON STRUCTURE IN VERTEBRATES

Tendon is a highly organized hypocellular connective tissue displaying a specific spatial organization of type I collagen fibers (Figure 1). The collagen molecules are

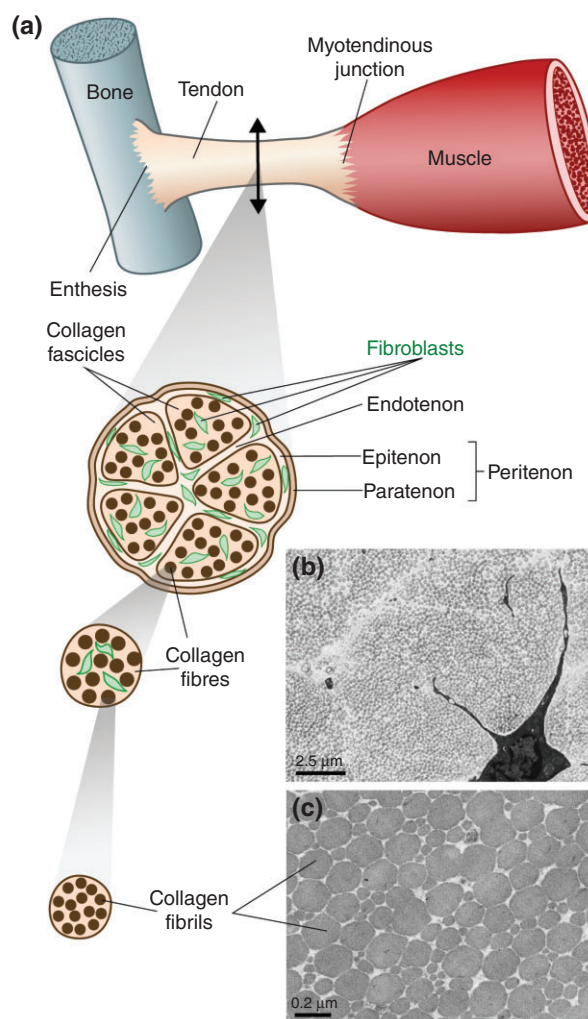


FIGURE 1 | Tendon organization. (a) Tendon links muscle to bone and is attached at one end to muscle by the myotendinous junction and at the other end to bone by the enthesis. Tendon is mainly composed of type collagen and of very few cells. Type I collagen displays a specific spatial organization parallel to the tendon axis. Tendon is formed of collagen fascicles, which are composed of collagen fibers, which are formed of collagen fibrils. The endotenon separates collagen fascicles. Tendon is surrounded by the tendon sheaths named the peritenon, which comprises paratenon and epitenon. (b and c) Collagen fibres and fibrils can be visualized at different scales with electron microscopy. Electron microscopy of transverse sections of a mouse Achilles tendon showing collagen fibrils (b,c).

synthesized by tendon fibroblasts or tenocytes, which display an elongated shape lying between the collagen fibers.⁵³ The cellular composition and collagen organization are not homogenous along the tendon axis and are different at both ends, close to the muscle (myotendinous junction) and the bone (enthesis) interfaces.

Tendon Proper/Tendon Midsubstance

Type I collagen is composed of a triple helix of two chains of $\alpha 1$ and one chain of $\alpha 2$ molecules, which are encoded by two different genes, *Col1a1* and *Col1a2*. In tendon, type I collagen displays a specific spatial organization that can be visualized at different scales (Figure 1). Collagen molecules assemble together successively forming collagen fibrils, collagen fibers, collagen bundles or fascicles and the tendon unit.⁵⁴ Parallel collagen fascicles are separated by the endotenon, a loose connective tissue that also contains fibroblasts as well as blood vessels and nerves.⁵³ The whole tendon is surrounded by the epitenon and then by a synovial sheath, the paratenon, composed of collagen fibers organized in a perpendicular direction to those of tendon.^{53,54} Tendon stem cells have been isolated from mouse, human, and rabbit tendons based on colony-forming unit assays.^{44,55} However, there is no available marker to allow the visualization of these stem cells *in vivo*.

Tendon and Muscle Interface (Myotendinous Junction)

Tendon is attached to muscle via the myotendinous junction. Structurally, the myotendinous junction has been well described. The interface between tendon and muscle consists of interdigitations of the plasma membranes of both tendon and muscle cells, named finger-like processes, which dramatically increase the interface between both cell types.⁵⁶ At a molecular level, collagen fibrils produced by tendon cells bind to laminin or integrins present at the level of sarcolemma and produced by muscle cells.⁵⁷ The developmental process of the myotendinous junction formation is not well characterized in vertebrates.⁵⁸ In contrast, myotendinous junction formation has been well studied in *Drosophila*.⁵⁹

Tendon to Bone Attachment (Enthesis)

The region where tendon attaches to bone is called the enthesis. Depending on the attachment sites, fibrous and fibrocartilaginous entheses have been described.⁶⁰ Histologically, the fibrocartilaginous enthesis is characterized by different cellular zones, proceeding from

tendon to bone: tenocytes, uncalcified fibrocartilage cells, calcified fibrocartilage cells and osteocytes. This cellular arrangement yields a direct connection between soft tissue (tendon) and hard tissue (bone). The part of the bone where the tendon will attach forms an eminence providing a stable anchoring. The development of the interface between tendon and bone has been recently addressed.⁶¹ The maturation of this interface occurs at postnatal stages, leading to mineralization of the enthesis.⁶²

The different cellular and collagen compositions of the myotendinous junction, tendon proper, and enthesis confer the different biomechanical properties of each part of the tendon. Consequently, tendon ruptures can be observed in the tendon midsubstance and at the enthesis but rarely at the myotendinous junction.

SCLERAXIS IS THE MAIN TENDON MARKER DURING VERTEBRATE DEVELOPMENT

The main structural and functional tendon component, type I collagen, is expressed in many tissues and organs (Figure 2). Consequently, tendon development cannot be studied just by following type I collagen expression. To date, the only early tendon marker in vertebrates is the bHLH transcription factor Scleraxis (*Scx*)^{20,63} (Figures 2 and 3). *Scx* has been shown to regulate positively *Col1a1* transcription in mouse tendons.^{4,64} However, *Scx* is not the unique transcription factor driving *Col1a1* transcription in tendons, since in *Scx*-deficient mice *Col1a1* transcription is diminished but not abolished in developing tendons.⁴ *Scx* is recognized to be a powerful marker for tendons during chick, mouse, and zebrafish development.^{18,20,23} *Scx* is also expressed in postnatal tendons⁶⁵ but is restricted to epitenon from 4 months postnatally⁶⁶ (Figure 3). At early stages, *Scx* is expressed in tendon presumptive regions at the level of branchial arches, somites and limbs.^{20,23,67} *Scx* labels tendon progenitor cells and the *Scx*-positive cell population gives rise to tendons.^{68,69} However, *Scx* is not the master regulatory gene of the tendon lineage as the myogenic regulatory factors are for the skeletal muscle lineage, since tendons retain their capacity to attach muscle to bone in *Scx* mutant mice.⁴ *Scx* mutant mice are viable and mobile.⁴ It is possible that *Scx* needs one or several partners to fulfill the function of master gene for tenogenesis. However, in the absence of *Scx* activity, force-transmitting tendons (limb and tail tendons) and intermuscular tendons are severely disrupted, while anchoring tendons (back tendons) are moderately affected.⁴ The first tendon defects are observed

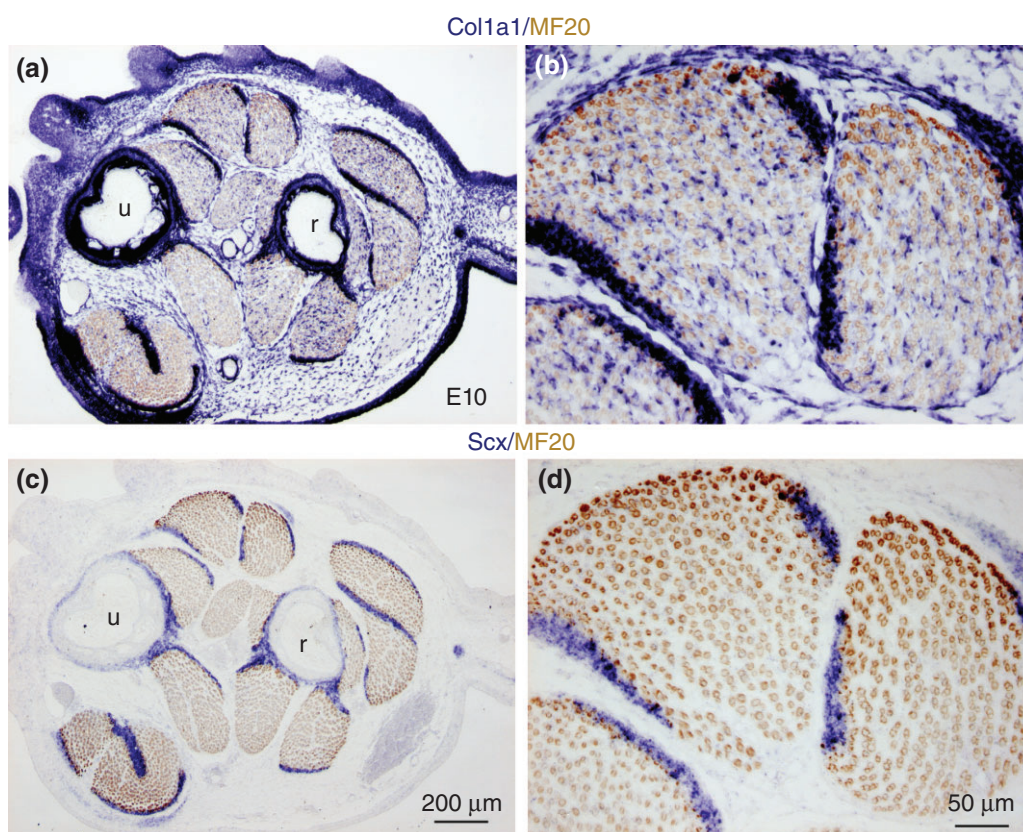


FIGURE 2 | Expression of *Col1a1* and *Scx* in chick limbs. (a–d) Adjacent and transverse forelimb sections of Embryonic Day 10 (E10) chick embryos were hybridized with *Col1a1* (a and b) and *Scx* (c and d) probes (blue) and then immunostained with the MF20 antibody, which recognizes myosins in skeletal muscles (brown). *Col1a1* is expressed in tendons but also around cartilage elements, in feather buds and connective tissues (a). *Scx* is expressed in tendons (c). (b and d) are higher magnifications of two dorsal muscles of forelimbs. *Col1a1* is expressed in tendons and muscle connective tissue (b), while *Scx* is expressed only in tendons (d). u, ulna; r, radius.

from E13.5 in mouse limbs, and *Col14a1* and *Tnmd* expression is completely lost in tendons from E16.5 in *Scx* mutant mice.⁴ *Tnmd* encodes a type II transmembrane glycoprotein and is considered a highly specific marker of differentiated tenocytes^{63,68,70} (Figure 3). *Tnmd* mutant mice display an altered structure of collagen fibrils (shift toward large diameters) in tendons at postnatal stages.²⁸ *Tnmd* deficient mice also display reduced self-renewal and increased senescence properties of tendon progenitors.²⁹ In addition to being required for *Tnmd* expression, *Scx* is also sufficient for *Tnmd* expression.³ In summary, *Tnmd* is a key marker for differentiated tenocytes and *Scx* is the unique early tendon marker that provides a powerful tool to study early stages of tendon development.

EMBRYOLOGICAL ORIGINS OF TENDONS

Tendons can be organized into three main groups according to their position in the body, head, trunk,

and limb tendons (Figure 4). Even if functionally similar, tendons of the different parts of the whole organism have distinct embryological origins, which have been studied mainly using the quail and chick chimera system.⁷¹ Using this technique, it has been shown that vertebrate tendons originate from mesoderm or mesectoderm (neural crest cells). The craniofacial tendons originate from neural crest cells, in mouse, chick, and zebrafish.^{18,67,72} Axial tendons derive from a somitic compartment, named the syndetome.²³ Limb tendons originate from limb lateral plate.⁷³

Whatever the tendon group, tendons share the same embryological origins with skeletal tissues such as cartilage and bone, and have origins distinct from those of skeletal muscles. In somites, the syndetome is a subregion of the sclerotome, which gives rise to the axial skeleton, while axial muscles originate from the dermomyotome.²³ In the head, neural crest cells give rise to facial skeleton and tendons, while skeletal muscles originate from head mesoderm.^{72,74}

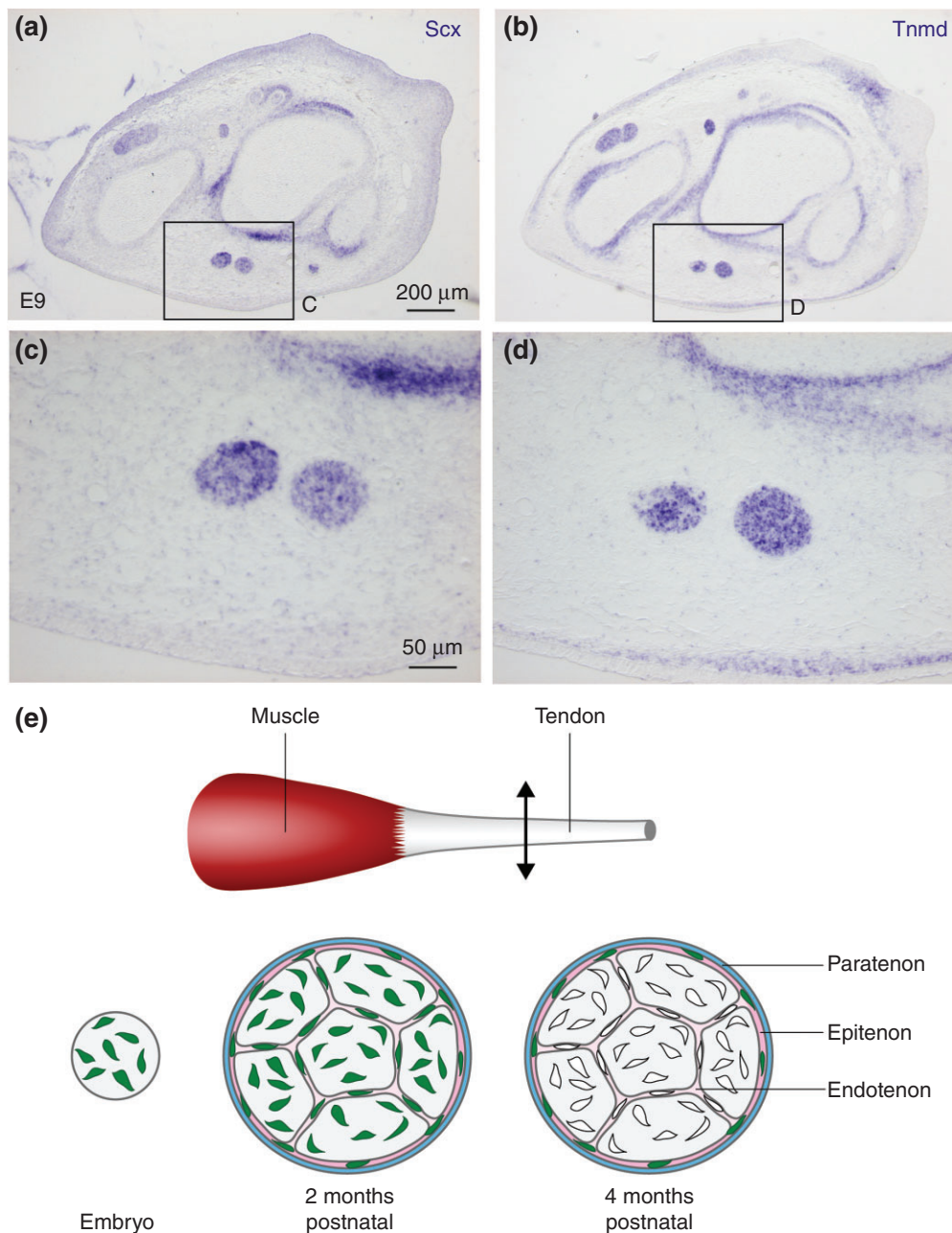


FIGURE 3 | Expression of *Scx* and *Tnmd* in chick limbs and schematic representation of *Scx* expression in developmental, postnatal, and adult tendons. (a–d) In situ hybridization to adjacent and transverse forelimb sections of Embryonic Day 9 (E9) chick embryos with *Scx* (a and c) and *Tnmd* (b and d) probes. *Scx* and *Tnmd* are expressed in tendons. (e) *Scx*-positive cells are schematized in green. During development, *Scx* expression is expressed in all tendon cells. During tendon maturation at postnatal stages, *Scx* is expressed in the tendon proper, endotenon, and external sheaths including epitenon and paratenon, but is restricted to the epitenon by the fourth postnatal month.

In limbs, both skeleton and tendons originate from limb lateral plate, while skeletal muscles derive from somites.^{75,76} It should be noted that in the head, tendon progenitors migrate into muscle-containing regions, whereas in limbs, muscle progenitors undergo a migration step toward the limb lateral-plate containing skeleton and tendon progenitors. In contrast

to the mesoderm or mesectoderm origins of vertebrate tendons, *Drosophila melanogaster* tendons originate from the ectoderm.^{77,78} However, like in vertebrates, drosophila tendons along with the exoskeleton share the same embryological ectoderm origin, which is distinct from that of skeletal muscles derived from mesoderm.⁷⁷

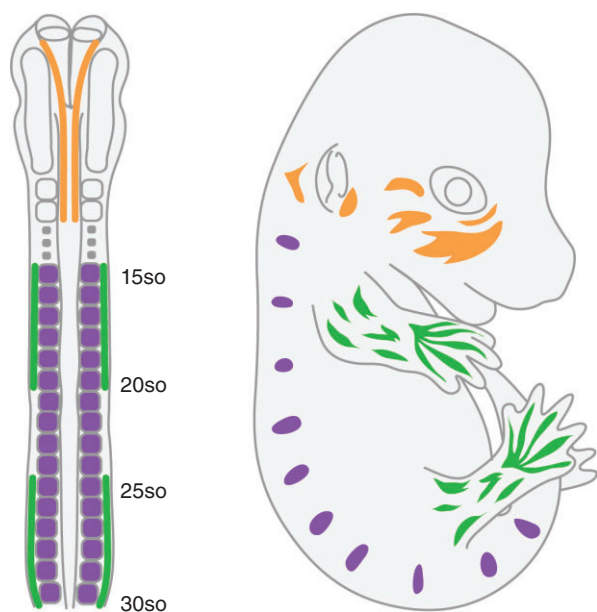


FIGURE 4 | Distinct embryological origins of vertebrate tendons. Tendons can be divided into head, axial, and limb tendons. Head tendons originate from neural crest cells (orange). Axial tendons originate from somites (purple). Limb tendons originate from limb lateral plate (green).

Thus in both vertebrates and invertebrates, tendons and skeleton have the same embryological origin, which is different from that of skeletal muscles.

TENDON INTERACTIONS WITH OTHER COMPONENTS OF THE MUSCULOSKELETAL SYSTEM

Tendon/Muscle Interactions

Despite the distinct embryological origins of the components of the musculoskeletal system, the development of muscle, tendon, and cartilage/bone occurs in close spatial and temporal association. Tendon development requires the presence of muscle, but the modalities of muscle requirement vary with the anatomic locations of tendons (Figure 5). Muscle is required for the initiation of tendon development at the axial level. *Scx* expression is not initiated in the absence of axial muscles. Surgical ablation of dermomyotomes prior to myotome formation leads to an absence of *Scx* expression in chick somites.²³ In E10.5 *Myf5*^{-/-}; *MyoD*^{-/-} double mutant embryos, *Scx* expression is absent in mouse somites.²² In *myod1-myf5*-deficient zebrafish embryos, *scxa* expression is never initiated in myosepta.¹⁸ In contrast, limb and head tendons initiate their development independently of muscle. In the absence of muscle, *Scx* expression is initiated normally in mouse and zebrafish

craniofacial tendons.^{18,67} *Scx* expression is also initiated and proceeds normally in muscleless limbs until E12 in *Pax3* mutant mice^{20,79} and until E6 in surgically manipulated chick embryos.²⁴ Similarly with observations in the chick and mouse, *Scxa* is expressed normally in fins of 53–58hpf *myod1-myf5*-deficient zebrafish embryos.¹⁸ The absence of muscle eventually prevents further tendon development and leads to a loss of *Scx* expression in head and limb tendons, in mouse, chick and zebrafish embryos.^{18,20,67,79} This demonstrates that muscles are not required for the initiation but are necessary for the maintenance of *Scx* expression in craniofacial and limb tendons (Figure 5).

Muscle is therefore important for the induction of *Scx* expression in axial tendons and for the maintenance of *Scx* expression in cranial and limb tendons, in mouse, chick, and zebrafish embryos. This pattern of muscle requirement has been conserved across these vertebrate species. Despite different embryological origins between vertebrates and invertebrates tendon cells (mesoderm versus ectoderm), two phases of tendon formation have been described in fruit fly. In *Drosophila*, the development of epidermal-derived tendon cells is initiated independently of muscles, but the final differentiation of tendon cells depends on specific interaction with muscles,^{11,77,80} indicating that *Drosophila* tendon development shares characteristics with that of head and limb vertebrate tendons.

Thus, muscle is required for full tendon formation in vertebrate and invertebrate tendons. We believe that the muscle requirement is related to a requirement for mechanical forces during tendon development.

Tendon/Bone Interaction

While the role of muscle in tendon development is well demonstrated, the role of cartilage in tendon development is more difficult to address, mainly because tendon and cartilage cells have the same embryological origins. *Sox9a-sox9b*-deficient zebrafish embryos display abnormal craniofacial tendons based on *scxa* and *tnmd* expression,¹⁸ suggesting that cartilage is necessary for the proper organization of tendon cells. However, it is difficult to dissociate tendon and cartilage defects. In somites, cartilage differentiation seems to repress tendon development. It has been observed that *Scx* is upregulated in *Sox5/Sox6* mouse mutant embryos (exhibiting cartilage defects),²² while overexpression of *Pax1* (known to promote cartilage formation) in sclerotome inhibits *Scx* expression in chick somites.²³ In limbs, cartilage and tendon cell fates also appear to be mutually exclusive. During limb development, the *Scx*+/*Sox9*+ progenitors repress *Sox9* (while sparing *Scx*) expression to form the tendon

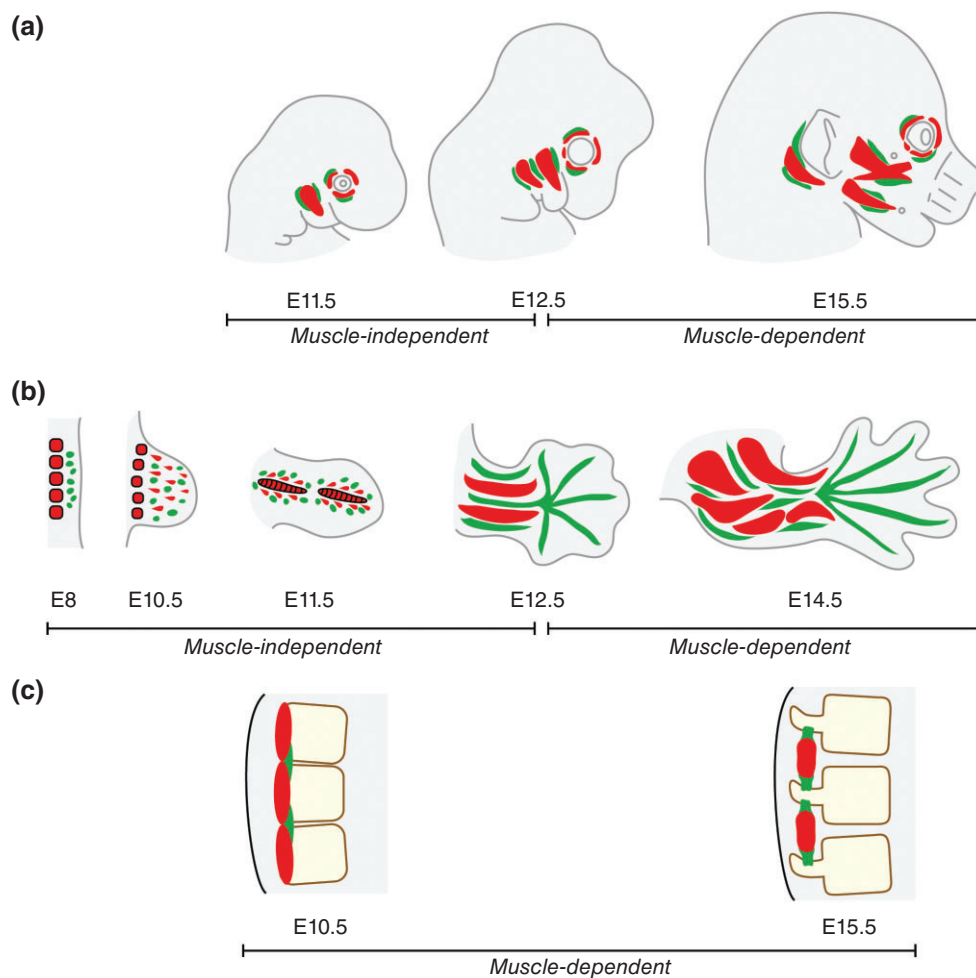


FIGURE 5 | Muscle-dependency for head, limb, and axial tendon development. Muscle and tendon are schematized in red and green, respectively. In the head (a) and limbs (b), tendons initiate their development independently of muscle, but further tendon development requires the presence of muscle. In contrast, the initiation of axial tendon development requires the presence of muscle (c).

side and downregulate *Scx* (and keep *Sox9*) expression to form the cartilaginous side of the tendon–bone interface.^{68,69} However, *Sox9* depletion in *Scx*+ cells does not affect tendon formation other than by altering the bone side of entesis formation,^{68,69} suggesting a relative independence of skeleton and tendon formation. However, at the digit levels, it has been reported that tendon blastema formation requires the presence of cartilage,⁸¹ indicating differences in tendon development according to proximodistal position in limbs.

INTRINSIC GENES INVOLVED IN TENDON DEVELOPMENT (OTHER THAN SCLERAXIS)

To date three transcription factors have been shown to be involved in vertebrate tendon development (Table 1): the bHLH transcription factor *Scx*,⁴ the

homeobox Mohawk (*Mkx*)^{5,7} and the Zinc finger transcription factor Early growth response 1 (*Egr1*).¹⁰ All of them have been shown to regulate *Coll1a* gene transcription and type I collagen fibril organization in developing tendons.^{4,5,7,10,64} Each of the three transcription factors *Scx*, *Mkx*, and *Egr1* is alone able to induce tenogenesis in stem cells, based on *Tnmd* expression.^{13,82–84} However, in contrast to *Scx*, *Mkx*, and *Egr1* are not specific to tendon, since they display numerous expression sites in addition to developing tendons.^{10,85,86}

Mohawk (*Mkx*)

Mkx^{-/-} mutant mice exhibit smaller tendons than wild-type mice and display defects in postnatal growth of tendon collagen fibrils.^{5–7} The first tendon defects in *Mkx*^{-/-} mice are observed at E16.5 fetal stages.⁵ In addition to the reduction of *Coll1a1* gene expression,

Mkx^{-/-} mice display significant reduction in *Tnmd*, *Fmod*, and *Dcn* gene expression in neonatal tendons.⁷ Notably, *Mkx* is expressed in early somites, in progenitor cell populations of skeletal muscle, tendon, cartilage, and bone, downstream of the somitic *paraxis* transcription factor.⁸⁵ *Mkx* has been shown to inhibit muscle differentiation in mouse cell culture and to impair muscle development in zebrafish embryos by directly repressing *MyoD* transcription.^{9,87,88} This would be consistent with a *Mkx* role in repressing the muscle lineage and promoting the tendon lineage. However, *Mkx* mutant mice do not display any obvious skeletal muscle defects.⁶ *Scx* and *Mkx* expression in developing tendons appears to be normal in *Mkx*^{-/-} and *Scx*^{-/-} mutant mice, respectively, suggesting that *Scx* and *Mkx* act in different genetic cascades during tendon development.^{6,7}

Early Growth Response 1 (Egr1)

During fetal development, *Egr1* is sufficient for the expression of *Scx*, *Tnmd* and tendon-associated collagens (*Col1a1*, *Col5a1*, *Col12a1*, and *Col14a1*) in chick embryos.¹⁰ *Egr1*^{-/-} mice display defects in collagen fibril organization in tendons at fetal and postnatal stages.^{10,13} *Egr1*-deficient tendons show a mechanical weakness and a deficiency in their capacity to heal following injury.¹³ In addition to the reduction of *Col1a1* and *Col1a2* gene expression, *Egr1*^{-/-} also displayed significant reductions in the expression of tendon-associated collagens (*Col3a1*, *Col5a1*, *Col12a1*, and *Col14a1*) and tendon-associated molecules *Tnmd*, *Fmod*, and *Dcn* in fetal limbs and adult tendons.^{10,13} *Scx* expression is downregulated, while *Mkx* is not modified in *Egr1*-deficient tendons.^{10,13}

Stripe (Drosophila)

In *Drosophila*, the transcription factor *stripe* is the key gene for tendon development.^{11,12,78} *Stripe* is the homolog of the vertebrate *Egr* gene family. The *stripe* gene produces two isoforms *stripeA* and *stripeB*. *StripeB* has been shown to be involved in tendon progenitor induction, while *stripeA* is involved at a later muscle-dependent stage of tendon differentiation.^{11,12,14}

Other transcription factors have been identified as being expressed in developing tendons, either by in situ hybridization experiments⁸⁹ or by global transcriptomic or RNA sequencing studies of mouse tendon cells during development.^{27,90} Among them, the sine oculis-related homeobox, *Six2* displays a specific expression in chick and mouse autopod tendons.^{89,90} However, there is currently no

functional data available relating these transcription factors to tendon development.

Although transcription factors have been identified as being involved in tendon development, the intrinsic program driving tenogenesis in vertebrates remains to be fully characterized.

SIGNALING PATHWAYS INVOLVED IN TENDON DEVELOPMENT

In addition to intrinsic regulators of tenogenesis, the TGF- β and FGF signaling pathways have been shown to be involved in tendon development in mouse and chick embryos.^{16,22–24,91} Bioinformatics analysis of a transcriptome of tendon cells also highlighted that these two were the main pathways displaying significant regulation during mouse limb development.²⁷

Tendon Cell Specification

TGF- β ligand is a potent inducer of *Scx* expression in embryonic mouse limbs, tendon progenitors, and mesenchymal stem cells. *Tgfb2* and *Tgfb3* are expressed in early chick and mouse limbs to fulfill a role in *Scx* induction.^{16,27,92} In mice, TGF- β 2 is sufficient to increase *Scx* expression in E10.5 limbs, tendon progenitors, and mesenchymal stem cells.^{16,27,93} Moreover, the canonical TGF- β intracellular pathway, SMAD2/3, has been shown to be required for *Scx* expression in E10.5 mouse limbs during the muscle-independent phase of limb tendon formation.²⁷ Blocking classical TGF- β intracellular pathway using chemical inhibitors also decreases *Scx* expression in zebrafish embryos.¹⁸ However, *Scx* expression appears to be normal in E11.5 limbs of *Tgfb2*^{-/-};*Tgfb3*^{-/-} double mutant mouse embryos,¹⁶ suggesting that other TGF- β ligands might be responsible for the initiation of *Scx* expression in mouse limbs. Another TGF- β ligand, myostatin (GDF-8), is a putative candidate to be involved in tendon development, since tendons are small, brittle, and hypocellular in *Mstn*^{-/-} mice.¹⁷ Moreover, myostatin treatment of primary culture of mouse tendon fibroblasts increases cell proliferation, in addition to increasing *Scx* and *Tnmd* expression.¹⁷

BMP ligands that signal via the intracellular Smad1/5/8 pathway have the opposite effect from TGF- β and restricts *Scx* expression, while inhibition of BMP signaling using the antagonist Noggin increases *Scx* expression in early chick limbs.²⁰ The antagonist roles of TGF- β and BMP signaling pathways in tendon cell specification is consistent with their antagonist role in the regulation of fetal muscle progenitors. Myostatin is a potent negative regulator

of muscle growth,⁹⁴ while BMP positively regulates muscle progenitors⁹⁵ during embryonic development.

FGF has been shown to be required and sufficient for the initiation of *Scx* expression in somites during axial tendon development. An ectopic source of FGF induces ectopic expression of *Scx* in chick and mouse somites and chick limbs,^{22–24} while inhibition of FGF signaling prevents *Scx* expression.^{22,23} *Pea3* (ERK MAPK effector) and *Sprouty2* (ERK MAPK modulator) are both expressed in tendon progenitor regions in chick syndetome and FGF has been shown to act on somitic tendon progenitors via the ERK MAPK intracellular pathway.^{26,91} In mouse limbs, the ERK MAPK signaling pathway appears to have a different effect, since a downregulation of ERK MAPK was sufficient to increase *Scx* expression in mouse limb explants and in mouse mesenchymal stem cells.²⁷ Consistent with this result, FGF inhibited *Scx* expression in mouse mesenchymal stem cells.²⁷

Tendon Cell Differentiation

In addition to being involved at early stages of tendon induction, the TGF- β and FGF extracellular signals have been shown to be involved in tendon differentiation during the muscle-dependent phase of limb tendon formation.^{16,24,27} In the absence of *Tgfb2* and *Tgfb3* function, there is a complete loss of *Scx* expression in head, axial, and limb tendons, and subsequently tendons are lost.¹⁶ TGF- β gain-of-function experiments in E12.5 mouse limbs lead to an upregulation of *Scx* and *Tnmd* expression.^{16,27} TGF- β gain-of-function experiments in a high-density cell culture system of HH25 chick hindlimbs (micromass) also lead to an up regulation of *Scx* and *Tnmd* expression via the SMAD2/3 intracellular pathway.¹⁵ TGF-interacting factor (*Tgif1*) has been shown to promote the fibrogenic effect of TGF- β SMAD2/3 intracellular pathway in chick micromass cultures.¹⁵ It has to be noted that the addition of TGF- β ligands in 2D cell culture systems activates *Scx*, but drastically inhibits *Tnmd* expression.^{13,84,96} This indicates that TGF- β ligands cannot induce complete tenogenesis in 2D stem cell cultures, in contrast to *ex vivo* experiments, where TGF- β activates *Tnmd* in addition to increasing *Scx* expression in mouse limb explants.²⁷

FGF has been shown to increase the number of *Scx*-positive cells at the expense of muscle cells in chick limbs during fetal development.^{24,97} The expression of the ERK effector *Pea3* and modulator *Spry2* is observed in both muscle and tendon and is increased at the muscle-tendon interface in chick and mouse limbs.²⁵ However, despite similar expression in fetal chick and mouse tendons of FGF signaling

components, FGF appears to have a distinct effect in mouse fetal tendon development compared to that in chick. FGF has been shown to downregulate *Scx* and *Tnmd* expression in mouse tendon cells isolated from E13 mouse embryos at the limb or axial levels.⁹⁶

To date, TGF- β /SMAD2/3, BMP/SMAD1/5/8 and FGF/ERK MAPK are the signaling pathways identified as being involved in the regulation of *Scx* expression in vertebrate embryos, although data are still missing to prove that all these pathways play similar roles in *Scx* induction or maintenance in mouse, chick, and zebrafish embryos. FGF appears to be crucial for *Scx* induction and maintenance in chick but not in mouse embryos. We also suspect that other signaling pathways are also involved in tendon cell specification or differentiation. The Wnt pathway is significantly regulated in mouse tendon cells during limb development, according to bioinformatics analysis of a tendon transcriptome.²⁷ Moreover, *Wnt3a* has been shown to positively regulate *Six2* expression in autopod tendons in developing chick limbs.⁸⁹

In *Drosophila*, signaling pathways have been shown to be involved in the muscle-dependent phase of tendon formation. The ligand *Vein* produced by muscle cells has been shown to activate the EGFR pathway in the tendon progenitors, leading to the expression of *stripeA*.^{77,98} The transmembrane protein *Kon-tiki* expressed by myotubes target tendon cell through its interaction with *Dgrip*.⁹⁹ All these events lead to a more durable interaction between myotubes and tendon cells through the integrins, notably via the heterodimers α PS1 β PS and α PS2 β PS integrins.⁵⁷ Integrin interactions at the muscle and tendon interface have been shown to maintain the expression of tendon-specific genes such as *stripeA* and β 1-*tubulin*.¹⁰⁰

MECHANICAL FORCES IN TENDON DEVELOPMENT

Mechanical forces are known to be involved in embryonic development by regulating organ formation.¹⁰¹ Because tendon is a mechanosensitive tissue, mechanical forces are crucial for tendon development. In humans, a diminution of embryo mobility leads to severe abnormalities, including musculoskeletal defects.¹⁰² Mechanical forces control the formation of all components of the musculoskeletal system during embryonic development.¹⁰³ Tendons are notably particularly sensitive to the absence of mechanical forces, since they do not form in the absence of muscles.^{20,79} The two main pathways known to be involved in tendon development, TGF- β /SMAD2/3 and FGF/ERK MAPK are also involved in mechanotransduction

processes.^{104,105} It has been shown that mechanical forces regulate *Scx* expression through activation of the TGF- β /SMAD2/3 pathway in adult tenocyte cultures.⁹³ During development, FGF4 is able to rescue the *Scx* expression in the absence of mechanical movements in chick muscleless limbs.²⁴ This leads to the hypothesis that TGF- β and FGF signaling pathways are downstream of mechanical forces to regulate tendon development. One possible mechanosensor molecule downstream of mechanical forces and upstream of TGF- β signaling is the transcription factor *Egr1*. *Egr1* is a mechanosensitive gene in the vascular system.¹⁰⁶ *Egr1* is involved in tendon development during the muscle-dependent phase in chick and mouse embryos¹⁰ and has been shown to activate *Tgfb2* transcription directly in adult mouse tendons.¹³ Another transcription factor, *Mkx*, involved in tendon development^{5,7} has also been reported to activate *Tgfb2* transcription directly in mouse stem cells.⁸⁴ Although there is no reported evidence that *Mkx* is a mechanosensitive gene, we speculate that transcription factors could sense mechanical forces and act upstream of TGF- β signaling during tendon development. Consistent with a mechanosensor role for *Egr1*, *Egr1* and *Egr2* expression have been reported to be increased within 15 minutes in response to loading in injured rat tendons.¹⁰⁷ The role of *Egr1* and *Mkx* transcription factors as mechanosensors upstream of TGF- β signaling remains to be demonstrated in the context of tendon development. In summary, mechanical forces are important parameters involved in tendon development but the mechanotransduction pathways downstream of forces remain to be characterized.

TENDON PATHOLOGIES

Tendon is a connective tissue displaying very little cell division.⁴⁴ Consequently, there is no cancer in tendon, consistent with the direct correlation between the number of stem cell divisions and variation in cancer risk.¹⁰⁸ Cancers are nevertheless observed in tendon sheaths with the giant-cell tumor of the tendon sheaths (GCTTS). GCTTS is a non malignant condition with an unknown etiology observed mostly but not exclusively in hands.¹⁰⁹ GCTTS is observed at the tendon surface but never arises from tenocytes of the tendon proper and may not arise systematically from tendon sheaths; as it has been suggested to arise from synovial cells.¹¹⁰ Genetic diseases affecting genes coding for proteins involved in type I collagen fibrillogenesis lead to tendon defects, but also to defects in all connective tissues.¹¹¹ Most tendon pathologies involve tendon injuries (Figure 6), which range from chronic to acute.

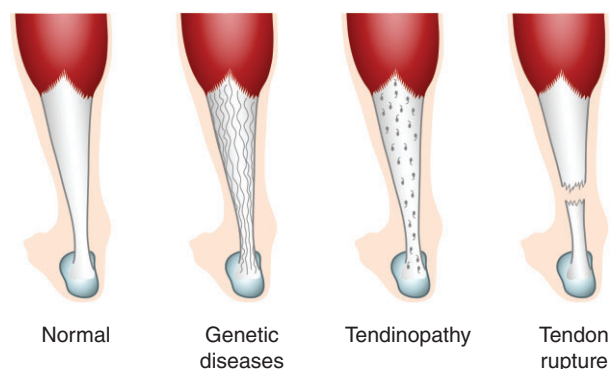


FIGURE 6 | Schematic representation of tendon pathologies. (a) Normal tendons. (b) Tendons in genetic diseases affecting collagen fibrillogenesis. (c) Chronic tendon injury or tendinopathy. (d) Acute tendon injury.

Chronic tendon injury or tendinopathy is characterized by pain and disability. The etiology and pathogenesis of tendinopathy are not well understood, although the main recognized cause of tendinopathy is abnormal mechanical loading.^{112,113} Acute tendon injury refers to partial or complete tears as a consequence of trauma.¹¹⁴ After acute tendon injury, tendons follow the typical wound healing process, including an early inflammatory phase, followed by cell migration, cell proliferation, and remodeling phases. However, the healing process is incomplete since healed tendons never regain their original biomechanical properties. The origin of the cells and the molecular mechanisms involved in tendon repair are not well established.

TENDON DEVELOPMENT AS TOOL FOR UNDERSTANDING TENDON HEALING

Natural tendon healing is thought to recapitulate tendon developmental processes. Both TGF- β and FGF signaling pathways, identified as being involved in tendon development, have been shown also to be important for tendon healing following injury.¹¹⁴ TGF- β and FGF ligands are released at the tendon injury sites in animal models.¹¹⁵ The loss of the canonical intracellular component of TGF- β pathway, *Smad3*, leads to reduced *Col1a1* transcription in healed tendons and to adhesion and scarring defects during tendon healing in *Smad3*^{-/-} mutant mice.¹¹⁶ Consequently, TGF- β ligands have been studied extensively as therapeutic candidates to promote tendon repair following tendon injury.¹¹⁵ FGF is also considered as a putative therapeutic target promoting tendon repair. However, the FGF effect on the tendon healing process is not always positive. Local FGF

application following tendon injury has been shown to promote cell proliferation in rat¹¹⁷ and to increase angiogenesis in a canine model,¹¹⁸ but FGF failed to improve mechanical or functional properties of the repaired tendons.^{117,118} Interestingly, in a chick tendon injury model, endogenous bFGF expression was downregulated during the early phase of tendon healing process.¹¹⁹ In addition, virally-mediated bFGF application enhanced *Scx* gene expression, and improved the biomechanical properties of repaired tendons in chick.^{120,121} The beneficial effect of FGF in the tendon healing process in the chick model is consistent with the FGF effect during chick tendon development.

The BMPs have been shown to accelerate tendon-bone junction healing in animal models.^{122,123} This effect is consistent with the BMP4 involvement

in tendon cells at their bone insertion during deltoid tuberosity development.²¹

CONCLUDING REMARKS

We believe that the understanding of tendon development will provide a basis for the identification of effective treatments of tendon injury. Transcription factors have been identified as promoting tenogenesis using developmental or stem cell models, and have been shown to promote tendon repair in animal models of tendon injury. In addition to transcription factors, signaling pathways have been shown to be involved in tendon development and healing. The relationship between intrinsic and extrinsic regulators of tenogenesis remains to be defined in the context of tendon development and healing and correlated with mechanical forces.

ACKNOWLEDGMENTS

We thank Sophie Gournet for illustrations. This work is supported by the FRM, ANR, AFM, INSERM, CNRS, and UPMC.

REFERENCES

1. Zhang G, Young BB, Ezura Y, Favata M, Soslowsky LJ, Chakravarti S, Birk DE. Development of tendon structure and function: regulation of collagen fibrillogenesis. *J Musculoskelet Neuronal Interact* 2005, 5:5–21.
2. Schiele NR, Marturano JE, Kuo CK. Mechanical factors in embryonic tendon development: potential cues for stem cell tenogenesis. *Curr Opin Biotechnol* 2013, 24:834–840.
3. Shukunami C, Takimoto A, Oro M, Hiraki Y. Scleraxis positively regulates the expression of tenomodulin, a differentiation marker of tenocytes. *Dev Biol* 2006, 298:234–247.
4. Murchison ND, Price BA, Conner DA, Keene DR, Olson EN, Tabin CJ, Schweitzer R. Regulation of tendon differentiation by scleraxis distinguishes force-transmitting tendons from muscle-anchoring tendons. *Development* 2007, 134:2697–2708.
5. Ito Y, Toriuchi N, Yoshitaka T, Ueno-Kudoh H, Sato T, Yokoyama S, Nishida K, Akimoto T, Takahashi M, Miyaki S, et al. The Mohawk homeobox gene is a critical regulator of tendon differentiation. *Proc Natl Acad Sci USA* 2010, 107:10538–10542.
6. Kimura W, Machii M, Xue X, Sultana N, Hikosaka K, Sharkar MT, Uezato T, Matsuda M, Koseki H, Miura N. *Irx11* mutant mice show reduced tendon differentiation and no patterning defects in musculoskeletal system development. *Genesis* 2011, 49:2–9.
7. Liu W, Watson SS, Lan Y, Keene DR, Ovitt CE, Liu H, Schweitzer R, Jiang R. The atypical homeodomain transcription factor Mohawk controls tendon morphogenesis. *Mol Cell Biol* 2010, 30:4797–4807.
8. Onizuka N, Ito Y, Inagawa M, Nakahara H, Takada S, Lotz M, Toyama Y, Asahara H. The Mohawk homeobox transcription factor regulates the differentiation of tendons and volar plates. *J Orthop Sci* 2014, 19:172–180.
9. Chuang H-N, Hsiao K-M, Chang H-Y, Wu C-C, Pan H. The homeobox transcription factor *Irx11* negatively regulates *MyoD* expression and myoblast differentiation. *FEBS J* 2014, 281:2990–3003.
10. Lejard V, Blais F, Guerquin MJ, Bonnet A, Bonnin MA, Havis E, Malbouyres M, Bidaud CB, Maro G, Gilardi-Hebenstreit P, et al. *EGR1* and *EGR2* involvement in vertebrate tendon differentiation. *J Biol Chem* 2011, 286:5855–5867.
11. Becker S, Pasca G, Strumpf D, Min L, Volk T. Reciprocal signaling between *Drosophila* epidermal muscle attachment cells and their corresponding muscles. *Development* 1997, 124:2615–2622.
12. Frommer G, Vorbrüggen G, Pasca G, Jäckle H, Volk T. Epidermal *egr*-like zinc finger protein of *Drosophila*

- participates in myotube guidance. *EMBO J* 1996, 15:1642–1649.
13. Guerquin MJ, Charvet B, Nourissat G, Havis E, Ronsin O, Bonnin MA, Ruggiu M, Olivera-Martinez I, Robert N, Lu Y, et al. Transcription factor EGR1 directs tendon differentiation and promotes tendon repair. *J Clin Invest* 2013, 123:3564–3576.
 14. Volohonsky G, Edenfeld G, Klämbt C, Volk T. Muscle-dependent maturation of tendon cells is induced by post-transcriptional regulation of stripeA. *Development* 2007, 134:347–356.
 15. Lorda-Diez CI, Montero JA, Martinez-Cue C, Garcia-Porrero JA, Hurlé JM. Transforming growth factors β coordinate cartilage and tendon differentiation in the developing limb mesenchyme. *J Biol Chem* 2009, 284:29988–29996.
 16. Pryce BA, Watson SS, Murchison ND, Staverosky JA, Dunker N, Schweitzer R. Recruitment and maintenance of tendon progenitors by TGF β signaling are essential for tendon formation. *Development* 2009, 136:1351–1361.
 17. Mendias CL, Bakhurin KI, Faulkner JA. Tendons of myostatin-deficient mice are small, brittle, and hypocellular. *Proc Natl Acad Sci USA* 2008, 105:388–393.
 18. Chen JW, Galloway JL. The development of zebrafish tendon and ligament progenitors. *Development* 2014, 141:2035–2045.
 19. Berthet E, Chen C, Butcher K, Schneider RA, Alliston T, Amirtharajah M. Smad3 binds Scleraxis and Mohawk and regulates tendon matrix organization. *J Orthop Res* 2013, 31:1475–1483.
 20. Schweitzer R, Chyung JH, Murtaugh LC, Brent AE, Rosen V, Olson EN, Lassar A, Tabin CJ. Analysis of the tendon cell fate using scleraxis, a specific marker for tendons and ligaments. *Development* 2001, 128:3855–3866.
 21. Blitz E, Viukov S, Sharir A, Shwartz Y, Galloway JL, Pryce BA, Johnson RL, Tabin CJ, Schweitzer R, Zelzer E. Bone ridge patterning during musculoskeletal assembly is mediated through SCX regulation of Bmp4 at the tendon-skeleton junction. *Dev Cell* 2009, 17:861–873.
 22. Brent AE, Braun T, Tabin CJ. Genetic analysis of interactions between the somitic muscle, cartilage and tendon cell lineages during mouse development. *Development* 2005, 132:515–528.
 23. Brent AE, Schweitzer R, Tabin CJ. A somitic compartment of tendon progenitors. *Cell* 2003, 113:235–248.
 24. Edom-Vovard F, Schuler B, Bonnin M-A, Teillet M-A, Duprez D. Fgf4 positively regulates scleraxis and tenascin expression in chick limb tendons. *Dev Biol* 2002, 247:351–366.
 25. Eloy-Trinquet S, Wang H, Edom-Vovard F, Duprez D. Fgf signaling components are associated with muscles and tendons during limb development. *Dev Dyn* 2009, 238:1195–1206.
 26. Smith TG, Sweetman D, Patterson M, Keyse SM, Münsterberg A. Feedback interactions between MKP3 and ERK MAP kinase control scleraxis expression and the specification of rib progenitors in the developing chick somite. *Development* 2005, 132:1305–1314.
 27. Havis E, Bonnin MA, Olivera-Martinez I, Nazaret N, Ruggiu M, Weibel J, Durand C, Guerquin MJ, Bonod-Bidaud C, Ruggiero F, et al. Transcriptomic analysis of mouse limb tendon cells during development. *Development* 2014, 141:3683–3696.
 28. Docheva D, Hunziker EB, Fa R, Brandau O. Tenomodulin is necessary for tenocyte proliferation and tendon maturation. *Mol Cell Biol* 2005, 25:699–705.
 29. Alberton P, Dex S, Popov C, Shukunami C, Schieker M, Docheva D. Loss of tenomodulin results in reduced self-renewal and augmented senescence of tendon stem/progenitor cells. *Stem Cells Dev* 2015, 24:597–609.
 30. Chen F, Guo R, Itoh S, Moreno L, Rosenthal E, Zappitelli T, Zirngibl RA, Flenniken A, Cole W, Grynopas M, et al. First mouse model for combined osteogenesis imperfecta and Ehlers-Danlos syndrome. *J Bone Miner Res* 2014, 29:1412–1423.
 31. Liu X, Wu H, Byrne M, Krane S, Jaenisch R. Type III collagen is crucial for collagen I fibrillogenesis and for normal cardiovascular development. *Proc Natl Acad Sci USA* 1997, 94:1852–1856.
 32. Wenstrup RJ, Smith SM, Florer JB, Zhang G, Beason DP, Seegmiller RE, Soslowsky LJ, Birk DE. Regulation of collagen fibril nucleation and initial fibril assembly involves coordinate interactions with collagens V and XI in developing tendon. *J Biol Chem* 2011, 286:20455–20465.
 33. Izu Y, Sun M, Zwolanek D, Veit G, Williams V, Cha B, Jepsen KJ, Koch M, Birk DE. Type XII collagen regulates osteoblast polarity and communication during bone formation. *J Cell Biol* 2011, 193:1115–1130.
 34. Ansoorge HL, Meng X, Zhang G, Veit G, Sun M, Klement JF, Beason DP, Soslowsky LJ, Koch M, Birk DE. Type IV collagen regulates fibrillogenesis: premature collagen fibril growth and tissue dysfunction in null mice. *J Biol Chem* 2009, 284:8427–8438.
 35. Zwolanek D, Veit G, Eble JA, Gullberg D, Ruggiero F, Heino J, Meier M, Stetefeld J, Koch M. Collagen XXII binds to collagen-binding integrins via the novel motifs GLQGER and GFKGER. *Biochem J* 2014, 459:217–227.
 36. Charvet B, Guiraud A, Malbouyres M, Zwolanek D, Guillon E, Bretaud S, Monnot C, Schulze J, Bader HL, Allard B, et al. Knockdown of col22a1 gene in zebrafish induces a muscular dystrophy by disruption of the myotendinous junction. *Development* 2013, 140:4602–4613.

37. Subramanian A, Schilling TF. Thrombospondin-4 controls matrix assembly during development and repair of myotendinous junctions. *Elife* 2014, 3:1–21.
38. Subramanian A, Wayburn B, Bunch T, Volk T. Thrombospondin-mediated adhesion is essential for the formation of the myotendinous junction in *Drosophila*. *Development* 2007, 134:1269–1278.
39. Frolova EG, Drazba J, Krukovets I, Kostenko V, Blech L, Harry C, Vasani A, Drumm C, Sul P, Jenniskens GJ, et al. Control of organization and function of muscle and tendon by thrombospondin-4. *Matrix Biol* 2014, 37:35–48.
40. Jepsen KJ, Wu F, Peragallo JH, Paul J, Roberts L, Ezura Y, Oldberg A, Birk DE, Chakravarti S. A syndrome of joint laxity and impaired tendon integrity in lumican- and fibromodulin-deficient mice. *J Biol Chem* 2002, 277:35532–35540.
41. Zhang G, Ezura Y, Chervoneva I, Robinson PS, Beason DP, Carine ET, Soslowsky LJ, Iozzo RV, Birk DE. Decorin regulates assembly of collagen fibrils and acquisition of biomechanical properties during tendon development. *J Cell Biochem* 2006, 98:1436–1449.
42. Corsi A, Xu T, Chen XD, Boyde A, Liang J, Mankani M, Sommer B, Iozzo RV, Eichstetter I, Robey PG, et al. Phenotypic effects of biglycan deficiency are linked to collagen fibril abnormalities, are synergized by decorin deficiency, and mimic Ehlers-Danlos-like changes in bone and other connective tissues. *J Bone Miner Res* 2002, 17:1180–1189.
43. Ameye L, Aria D, Jepsen K, Oldberg A, Xu T, Young MF. Abnormal collagen fibrils in tendons of biglycan/fibromodulin-deficient mice lead to gait impairment, ectopic ossification, and osteoarthritis. *FASEB J* 2002, 16:673–680.
44. Bi Y, Ehrchiou D, Kilts TM, Inkson CA, Embree MC, Sonoyama W, Li L, Leet AI, Seo BM, Zhang L, et al. Identification of tendon stem/progenitor cells and the role of the extracellular matrix in their niche. *Nat Med* 2007, 13:1219–1227.
45. Juneja SC, Veillette C. Defects in tendon, ligament, and enthesis in response to genetic alterations in key proteoglycans and glycoproteins: a review. *Arthritis* 2013, 2013:1–30, 154812.
46. Halper J. Advances in the use of growth factors for treatment of disorders of soft tissues. *Adv Exp Med Biol* 2014, 802:59–76.
47. Kassar-Duchossoy L, Gayraud-Morel B, Gomes D, Rocancourt D, Buckingham M, Shinin V, Tajbakhsh S. *Mrf4* determines skeletal muscle identity in *Myf5*: myod double-mutant mice. *Nature* 2004, 431:466–471.
48. Weintraub H. The *MyoD* family and myogenesis: redundancy, networks, and thresholds. *Cell* 1993, 75:1241–1244.
49. Delfini M-C, Duprez D. Ectopic *Myf5* or *MyoD* prevents the neuronal differentiation program in addition to inducing skeletal muscle differentiation, in the chick neural tube. *Development* 2004, 131:713–723.
50. Akiyama H, Chaboissier MC, Martin JF, Schedl A, De Crombrughe B. The transcription factor *Sox9* has essential roles in successive steps of the chondrocyte differentiation pathway and is required for expression of *Sox5* and *Sox6*. *Genes Dev* 2002, 16:2813–2828.
51. Takimoto A, Oro M, Hiraki Y, Shukunami C. Direct conversion of tenocytes into chondrocytes by *Sox9*. *Exp Cell Res* 2012, 318:1492–1507.
52. Doane J, Birk DE. Fibroblasts retain their tissue phenotype when grown in three-dimensional collagen gels. *Exp Cell Res* 1991, 442:432–442.
53. Benjamin M, Ralphs JR. The cell and developmental tendons and ligaments. *Int Rev Cytol* 2000, 196:85–130.
54. Screen HR, Berk DE, Kadler KE, Ramirez F, Young MF. Tendon functional extracellular matrix. *J Orthop Res* 2015, 33:793–799.
55. Zhang J, Wang JH-C. Mechanobiological response of tendon stem cells: implications of tendon homeostasis and pathogenesis of tendinopathy. *J Orthop Res* 2010, 28:639–643.
56. Tidball JG, Lin C. Structural changes at the myogenic cell surface during the formation of myotendinous junctions. *Cell Tissue Res* 1989, 257:77–84.
57. Bökel C, Brown NH. Integrins in development: moving on, responding to, and sticking to the extracellular matrix. *Dev Cell* 2002, 3:311–321.
58. Charvet B, Ruggiero F, Le Guellec D. The development of the myotendinous junction. A review. *Muscles Ligaments Tendons J* 2012, 2:53–63.
59. Schejter ED, Baylies MK. Born to run: creating the muscle fiber. *Curr Opin Cell Biol* 2010, 22:566–574.
60. Benjamin M, Kumai T, Milz S, Boszczyk BM, Boszczyk AA, Ralphs JR. The skeletal attachment of tendons — tendon ‘entheses’. *Comp Biochem Physiol A Mol Integr Physiol* 2002, 133:931–945.
61. Zelzer E, Blitz E, Killian ML, Thomopoulos S. Tendon-to-bone attachment: from development to maturity. *Birth Defects Res Part C* 2014, 102:101–112.
62. Schwartz AG, Pasteris JD, Genin GM, Daulton TL, Thomopoulos S. Mineral distributions at the developing tendon enthesis. *PLoS One* 2012, 7:1–11, e48630.
63. Huang AH, Lu HH, Schweitzer R. Molecular regulation of tendon cell fate during development. *J Orthop Res* 2015, 33:800–812.
64. Lejard V, Brideau G, Blais F, Salingcarnboriboon R, Wagner G, Roehrl MH, Noda M, Duprez D, Houillier P, Rossert J. Scleraxis and NFATc regulate the expression of the pro- $\alpha 1(I)$ collagen gene in tendon fibroblasts. *J Biol Chem* 2007, 282:17665–17675.
65. Pryce BA, Brent AE, Murchison ND, Tabin CJ, Schweitzer R. Generation of transgenic tendon

- reporters, ScxGFP and ScxAP, using regulatory elements of the scleraxis gene. *Dev Dyn* 2007, 236:1677–1682.
66. Mendias CL, Gumucio JP, Bakhurin KI, Lynch EB, Brooks SV. Physiological loading of tendons induces scleraxis expression in epitenon fibroblasts. *J Orthop Res* 2012, 30:606–612.
 67. Grenier J, Teillet M-A, Grifone R, Kelly RG, Duprez D. Relationship between neural crest cells and cranial mesoderm during head muscle development. *PLoS One* 2009, 4:e4381.
 68. Sugimoto Y, Takimoto A, Akiyama H, Kist R, Scherer G, Nakamura T, Hiraki Y, Shukunami C. Scx+/Sox9+ progenitors contribute to the establishment of the junction between cartilage and tendon/ligament. *Development* 2013, 140:2280–2288.
 69. Blitz E, Sharir A, Akiyama H, Zelzer E. Tendon-bone attachment unit is formed modularly by a distinct pool of Scx- and Sox9-positive progenitors. *Development* 2013, 140:2680–2690.
 70. Jelinsky SA, Archambault J, Li L, Seeherman H. Tendon-selective genes identified from rat and human musculoskeletal tissues. *J Orthop Res* 2010, 28:289–297.
 71. Dupin E, Le Douarin NM. The neural crest, a multifaceted structure of the vertebrates. *Birth Defects Res C Embryo Today* 2014, 102:187–209.
 72. Crane JF, Trainor PA. Neural crest stem and progenitor cells. *Annu Rev Cell Dev Biol* 2006, 22:267–286.
 73. Kieny M, Chevallier A. Autonomy of tendon development in the embryonic chick wing. *J Embryol Exp Morph* 1979, 49:153–165.
 74. Couly GF, Coltey PM, Le Douarin NM. The developmental fate of the cephalic mesoderm in quail-chick chimeras. *Development* 1992, 15:1–15.
 75. Chevallier BA, Kieny M, Mauger A. Limb-somite relationship : origin of the limb musculature. *J Embryol Exp Morph* 1977, 41:245–258.
 76. Christ B, Ordahl CP. Early stages of chick somite development. *Anat Embryol (Berl)* 1995, 191:381–396.
 77. Volk T. Singling out Drosophila tendon cells: a dialogue between two distinct cell types. *Trends Genet* 1999, 15:448–453.
 78. Volk T, VijayRaghavan K. A central role for epidermal segment border cells in the induction of muscle patterning in the Drosophila embryo. *Development* 1994, 120:59–70.
 79. Bonnin MA, Laclef C, Blaise R, Eloy-Trinquet S, Relaix F, Maire P, Duprez D, et al. Six1 is not involved in limb tendon development, but is expressed in limb connective tissue under Shh regulation. *Mech Dev* 2005, 122:573–585.
 80. Schweitzer R, Zelzer E, Volk T. Connecting muscles to tendons: tendons and musculoskeletal development in flies and vertebrates. *Development* 2010, 137:3347.
 81. Lorda-Diez CI, Montero JA, Garcia-porrero JA, Hurlle JM. Divergent differentiation of skeletal progenitors into cartilage and tendon: lessons from the embryonic limb. *ACS Chem Biol* 2014, 9:72–79.
 82. Alberton P, Popov C, Pragert M, Kohler J, Shukunami C, Schieker M, Docheva D. Conversion of human bone marrow-derived mesenchymal stem cells into tendon progenitor cells by ectopic expression of scleraxis. *Stem Cells Dev* 2012, 21:846–858.
 83. Otabe K, Nakahara H, Hasegawa A, Matsukawa T, Ayabe F, Onizuka N, Inui M, Takada S, Ito Y, Sekiya I, et al. Transcription factor mohawk controls tenogenic differentiation of bone marrow mesenchymal stem cells in vitro and in vivo. *J Orthop Res* 2015, 33:1–8. doi:10.1002/jor.22750.
 84. Liu, H, Zhang C, Zhu S, Lu P, Zhu T, Gong X, Zhang Z, Hu J, Yin Z, Heng BC, et al. Mohawk promotes the tenogenesis of mesenchymal stem cells through activation of the TGF β signaling pathway. *Stem Cells* 2015, 33:443–455.
 85. Anderson DM, Arredondo J, Hahn K, Valente G, Martin JF, Wilson-Rawls J, Rawls A. Mohawk is a novel homeobox gene expressed in the developing mouse embryo. *Dev Dyn* 2006, 235:792–801.
 86. Liu H, Liu W, Maltby KM, Lan Y, Jiang R. Identification and developmental expression analysis of a novel homeobox gene closely linked to the mouse Twirler mutation. *Gene Expr Patterns* 2006, 6:632–636.
 87. Anderson DM, Beres BJ, Wilson-Rawls J, Rawls A. The homeobox gene Mohawk represses transcription by recruiting the Sin3A/HDAC co-repressor complex. *Dev Dyn* 2009, 238:572–580.
 88. Anderson DM, George R, Noyes MB, Rowton M, Liu W, Jiang R, Wolfe SA, Wilson-Rawls J, Rawls A. Characterization of the DNA-binding properties of the Mohawk homeobox transcription factor. *J Biol Chem* 2012, 287:35351–35359.
 89. Yamamoto-Shiraishi YI, Kuroiwa A. Wnt and BMP signaling cooperate with Hox in the control of Six2 expression in limb tendon precursor. *Dev Biol* 2013, 377:363–374.
 90. Liu H, Xu J, Liu CF, Lan Y, Wylie C, Jiang R. Whole transcriptome expression profiling of mouse limb tendon development by using RNA-seq. *J Orthop Res* 2015, 33:840–848.
 91. Brent AE, Tabin CJ. FGF acts directly on the somitic tendon progenitors through the Ets transcription factors Pea3 and Erm to regulate scleraxis expression. *Development* 2004, 131:3885–3896.
 92. Lorda-Diez CI, Montero JA, Garcia-Porrero JA, Hurlle JM. Tgf β 2 and 3 are coexpressed with their extracellular regulator Ltbp1 in the early limb bud and modulate mesodermal outgrowth and BMP signaling in chicken embryos. *BMC Dev Biol* 2010, 10:69.
 93. Maeda T, Sakabe T, Sunaga A, Sakai K, Rivera AL, Keene DR, Sasaki T, Stavnezer E, Iannotti J,

- Schweitzer R, et al. Conversion of mechanical force into TGF- β -mediated biochemical signals. *Curr Biol* 2011, 21:933–941.
94. Manceau M, Gros J, Savage K, Thome V, McPherron A, Paterson B, Marcelle C. Myostatin promotes the terminal differentiation of embryonic muscle progenitors. *Genes Dev* 2008, 22:668–681.
95. Wang H, Noulet F, Edom-Vovard F, Le Grand F, Duprez D. Bmp signaling at the tips of skeletal muscles regulates the number of fetal muscle progenitors and satellite cells during development. *Dev Cell* 2010, 18:643–654.
96. Brown JP, Finley VG, Kuo CK. Embryonic mechanical and soluble cues regulate tendon progenitor cell gene expression as a function of developmental stage and anatomical origin. *J Biomech* 2014, 47:214–222.
97. Edom-Vovard F, Bonnin MA, Duprez D. Fgf8 transcripts are located in tendons during embryonic chick limb development. *Mech Dev* 2001, 108:203–206.
98. Yarnitzky T, Min L, Volk T. The Drosophila neuregulin homolog Vein mediates inductive interactions between myotubes and their epidermal attachment cells. *Genes Dev* 1997, 11:2691–2700.
99. Schnorrer F, Kalchauer I, Dickson BJ. The transmembrane protein kon-tiki couples to Dgrip to mediate myotube targeting in Drosophila. *Dev Cell* 2007, 12:751–766.
100. Martin-Bermudo MD. Integrins modulate the Egfr signaling pathway to regulate tendon cell differentiation in the Drosophila embryo. *Development* 2000, 127:2607–2615.
101. Mammoto T, Mammoto A, Ingber DE. Mechanobiology and developmental control. *Annu Rev Cell Dev Biol* 2013, 29:27–61.
102. Ward KA, Caulton JM, Adams JE, Mughal MZ. Perspective: cerebral palsy as a model of bone development in the absence of postnatal mechanical factors. *J Musculoskelet Neuronal Interact* 2006, 6:154–159.
103. Shwartz Y, Blitz E, Zelzer E. One load to rule them all: mechanical control of the musculoskeletal system in development and aging. *Differentiation* 2013, 86:104–111.
104. Kook S-H, Jang Y-S, Lee J-C. Involvement of JNK-AP-1 and ERK-NF-B signaling in tension-stimulated expression of Type I collagen and MMP-1 in human periodontal ligament fibroblasts. *J Appl Physiol* 2011, 111:1575–1583.
105. Nguyen J, Tang SY, Nguyen D, Alliston T. Load regulates bone formation and sclerostin expression through a TGF β -dependent mechanism. *PLoS One* 2013, 8:1–9, e53813.
106. Schwachtgen JL, Houston P, Campbell C, Sukhatme V, Braddock M. Fluid shear stress activation of egr-1 transcription in cultured human endothelial and epithelial cells is mediated via the extracellular signal-related kinase 1/2 mitogen-activated protein kinase pathway. *J Clin Invest* 1998, 101:2540–2549.
107. Eliasson P, Andersson T, Hammerman M, Aspenberg P. Primary gene response to mechanical loading in healing rat Achilles tendons. *J Appl Physiol* 2013, 114:1519–1526.
108. Tomasetti C, Vogelstein B. Variation in cancer risk among tissues can be explained by the number of stem cell divisions. *Science* 2015, 80:78–81.
109. Walsh EF, Mechrefe A, Akelman E, Schiller AL. Giant cell tumor of tendon sheath. *Am J Orthop (Belle Mead NJ)* 2005, 34:116–121.
110. Nakashima M, Uchida T, Tsukazaki T, Hamanaka Y, Fukuda E, Ito M, Sekine I. Expression of tyrosine kinase receptors Tie-1 and Tie-2 in giant cell tumor of the tendon sheath: a possible role in synovial proliferation. *Pathol Res Pract* 2001, 197:101–107.
111. Tozer S, Duprez D. Tendon and ligament: development, repair and disease. *Birth Defects Res C Embryo Today* 2005, 75:226–236.
112. Kaux JF, Forthomme B, le Goff C, Crielaard JM, Croisier JL. Current opinions on tendinopathy. *J Sport Sci Med* 2011, 10:238–253.
113. Magnusson SP, Langberg H, Kjaer M. The pathogenesis of tendinopathy: balancing the response to loading. *Nat Rev Rheumatol* 2010, 6:262–268.
114. Docheva D, Müller SA, Majewski M, Evans CH. Biologics for tendon repair. *Adv Drug Deliv Rev* 2014, 84:222–239.
115. Halper J. Advances in the use of growth factors for treatment of disorders of soft tissues. *Adv Exp Med Biol* 2014, 802:59–76.
116. Katzel EB, Wolenski M, Loiselle AE, Basile P, Flick LM, Langstein HN, Hilton MJ, Awad HA, Hammert WC, O’Keefe RJ. Impact of Smad3 loss of function on scarring and adhesion formation during tendon healing. *J Orthop Res* 2011, 29:684–693.
117. Chan BP, Fu S, Qin L, Lee K, Rolf CG, Chan K. Effects of basic fibroblast growth factor (bFGF) on early stages of tendon healing: a rat patellar tendon model. *Acta Orthop Scand* 2000, 71:513–518.
118. Thomopoulos S, Kim HM, Das R, Silva MJ, Sakiyama-Elbert S, Amiel D, Gelberman RH. The effects of exogenous basic fibroblast growth factor on intrasynovial flexor tendon healing in a canine model. *J Bone Joint Surg Am* 2010, 92:2285–2293.
119. Chen CH, Cao Y, Wu YF, Bais AJ, Gao JS, Tang JB. Tendon healing in vivo: gene expression and production of multiple growth factors in early tendon healing period. *J Hand Surg Am* 2008, 33:1834–1842.
120. Tang JB, Cao Y, Zhu B, Xin KQ, Wang XT, Liu PY. Adeno-associated virus-2-mediated bFGF gene transfer to digital flexor tendons significantly increases healing strength: an in vivo study. *J Bone Joint Surg Am* 2008, 90:1078–1089.

121. Tang JB, Chen CH, Zhou YL, McKeever C, Liu PY. Regulatory effects of introduction of an exogenous FGF2 gene on other growth factor genes in a healing tendon. *Wound Repair Regen* 2014, 22: 111–118.
122. Kim JG, Kim HJ, Kim SE, Bae JH, Ko YJ, Park JH. Enhancement of tendon-bone healing with the use of bone morphogenetic protein-2 inserted into the suture anchor hole in a rabbit patellar tendon model. *Cytotherapy* 2014, 16:857–867.
123. Chen CH, Chang CH, Wang KC, Su CI, Liu HT, Yu CM, Wong CB, Wang IC, Whu SW, Liu HW. Enhancement of rotator cuff tendon-bone healing with injectable periosteum progenitor cells-BMP-2 hydrogel in vivo. *Knee Surg Sport Traumatol Arthrosc* 2011, 19:1597–1607.

X.4 Signaux moléculaires et mécaniques intervenant dans la différenciation des cellules tendineuses

Signaux moléculaires et mécaniques intervenant dans la différenciation des cellules tendineuses

Ludovic Gaut, Marie-Ange Bonnin, Nicolas Robert, Mathias Mericskay, Delphine Duprez

Les tendons sont des formes uniques de tissu conjonctif du système musculo-squelettique. Ils sont formés par une matrice dense de fibres de collagène de type I qui sont orientées parallèlement à l'axe du tendon. Cette organisation spécifique leur donne la capacité de supporter les forces générées par le muscle pour les transmettre à l'os, permettant ainsi le mouvement. Le développement, l'homéostasie et la réparation du tendon reposent sur une combinaison spécifique de facteurs de transcription, de facteurs de croissance ainsi que de paramètres mécaniques régulant la production et l'assemblage des fibres de collagène [1, 2]. Les cascades moléculaires régissant la différenciation du tendon ne sont pas aussi bien décrites que celles des cellules musculaires. Toutefois, l'étude du tendon a été rendue possible grâce à la découverte de certains acteurs moléculaires tels que le facteur de transcription *Scx* [1-3], le plus spécifique et précoce dans le développement du tendon, ou encore le facteur de transcription mécanosensitif *Egr1* [1, 2, 4, 5]. Au cours des dernières années, de nombreuses études ont montré l'importance des forces mécaniques générées par les cellules ou les tissus au cours du développement ou des processus de différenciation cellulaire [6]. Notre objectif est de comprendre comment la cellule de tendon va intégrer les signaux mécaniques et d'identifier quelles voies de signalisation seront activées en aval de ces signaux pour déclencher la différenciation tendineuse.

La mécanobiologie du tendon a été étudiée *in vivo* au cours du développement. Une paralysie des embryons de poulet au stade E7.5 a été induite par traitement au bromure de décéméthonium (DMB), un agoniste du récepteur à l'acétylcholine bloquant la jonction neuromusculaire [7]. Le traitement au DMB va induire une paralysie musculaire et donc interrompre les mouvements rythmiques effectués par l'embryon (*Figure 1A*). Chez les embryons

paralysés, l'expression du marqueur de tendon SCX est diminuée dès 5h et à 48h de traitement (*Figure 1A*). Ce défaut a notamment été observé avant la diminution des marqueurs musculaires PAX7 et MYF5 (*Figure 1A*), indiquant que le changement observé est dû à une absence de contraction plutôt qu'à une perte d'un signal biochimique provenant du muscle adjacent.

La mécanobiologie a également été étudiée dans un système *in vitro* mimant la formation d'un tendon *in vitro*. Des cultures de cellules souches dans un système en trois dimensions (3D), consistant en un tube de gel de fibrine maintenu sous tension, miment la formation d'un tendon *in vitro* (*Figure 1B*) [8]. Des tendons *in vitro* ont ainsi été réalisés en utilisant une lignée murine de cellules souches mésenchymateuses (CSM), les C3H10T1/2. La comparaison de l'expression de différents gènes dans les CSM cultivées en 3D *versus* 2D met en évidence une augmentation des marqueurs de tendon *Scx*, et *Col1a1* ainsi que du facteur de transcription mécanosensitif *Egr1* (*Figure 1B*). La perte de tension de ces tendons *in vitro* (après section) conduit à la diminution de l'expression d'*Egr1* et des gènes de tendon, *Scx* et *Col1a1* (*Figure 1C*). L'expression forcée de *Egr1* dans les cellules C3H10T1/2 permet d'empêcher la diminution des marqueurs de tendons dans ces tendons *in vitro* sans tension (*Figure 1D*). Ces résultats démontrent l'importance des forces mécaniques dans le maintien de l'identité tendon des CSM. De plus, ils montrent l'implication du facteur de transcription *Egr1* en aval des forces mécaniques dans le maintien des marqueurs de tendons.

Ces résultats soulignent l'importance des signaux mécaniques pour le développement du tendon et la différenciation tendineuse à partir des cellules souches. Cependant, les liens existant entre les signaux mécaniques et moléculaires restent à être identifiés dans le contexte de la différenciation du tendon.

Ludovic Gaut
CNRS UMR 7622,
IBPS-Laboratoire
de Biologie
du Développement,
F-75005, Paris, France
Inserm U1156, F-75005
Paris, France
Sorbonne Universités,
UPMC Univ Paris 06,
IBPS, F-75005 Paris,
France
CNRS UMR 8256,
IBPS-Adaptation
Biologique et
Vieillesse, F-75005,
Paris, France
Inserm U1164, F-75005
Paris, France

Marie-Ange Bonnin
Nicolas Robert
Delphine Duprez
CNRS UMR 7622,
IBPS-Laboratoire
de Biologie
du Développement,
F-75005, Paris, France
Inserm U1156, F-75005
Paris, France
Sorbonne Universités,
UPMC Univ Paris 06,
IBPS, F-75005 Paris,
France

Mathias Mericskay
Sorbonne Universités,
UPMC Univ Paris 06,
IBPS, F-75005 Paris,
France
CNRS UMR 8256,
IBPS-Adaptation
Biologique
et Vieillesse,
F-75005, Paris, France
Inserm U1164, F-75005
Paris, France

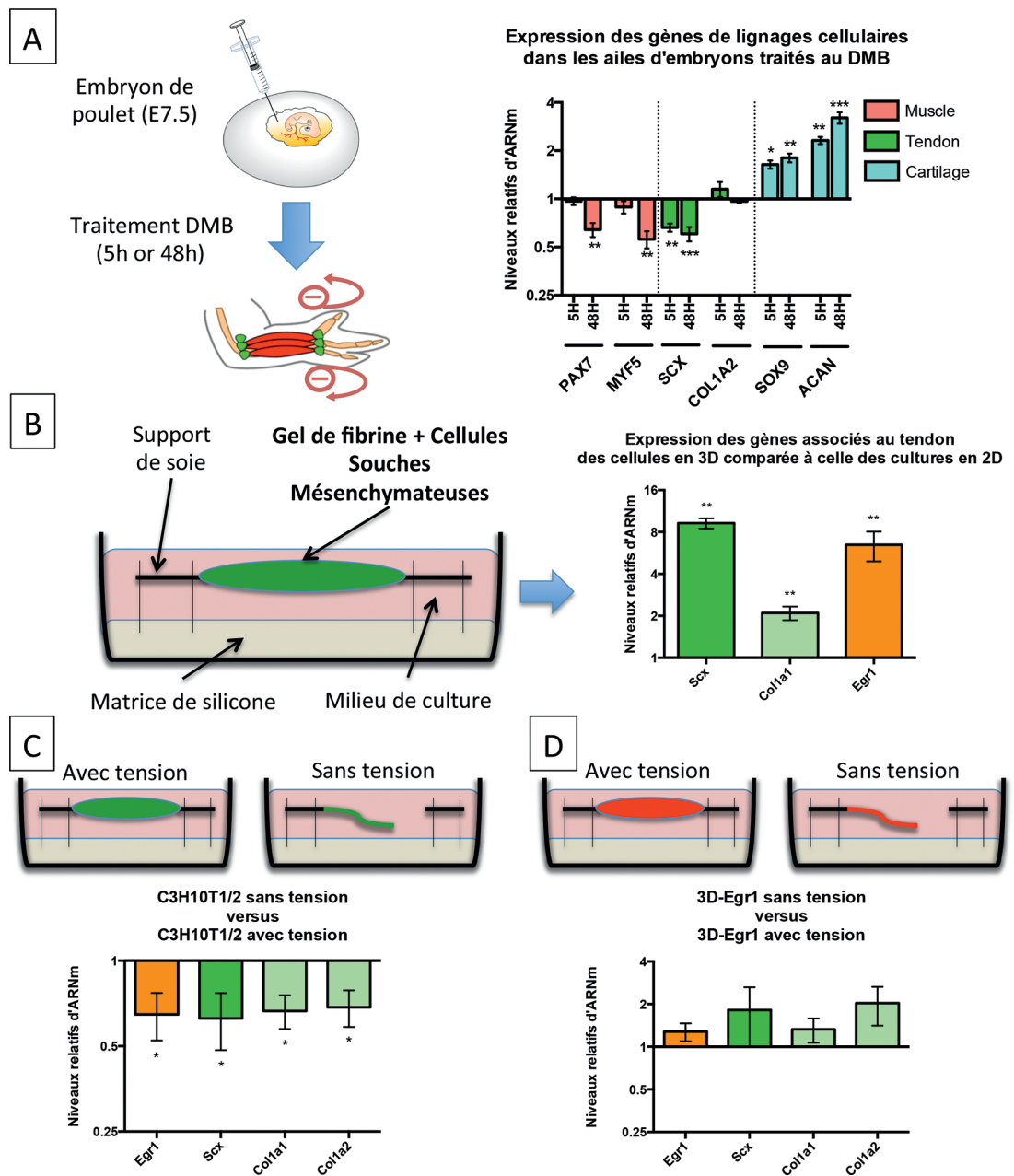


Figure 1

Signaux moléculaires et mécaniques intervenant dans la différenciation des cellules tendineuses.

(A) Procédure expérimentale du traitement au bromure de décaméthonium (DMB) induisant une inhibition des mouvements (flèches rouges) et expression des gènes associés aux différents lignages cellulaires. (B) Représentation d'une construction 3D de tendon *in vitro* et graphe d'expression des gènes dans des cultures cellulaires 3D comparée aux cultures 2D. (C) Représentation des constructions 3D avec tension (gauche) et sans tension (droit) et graphe d'expression des gènes associés aux tendons dans les 3D sans tension *vs* avec tension. (D) Représentation des constructions 3D surexprimant *Egr1* (3D-*Egr1*) avec tension (gauche) et sans tension (droit) et graphe d'expression des gènes associés aux tendons dans les 3D-*Egr1* avec tension *vs* sans tension. Tests statistiques utilisés sont les tests non-paramétriques de Mann-Whitney. * = p-value \leq 0,05 ; ** = p-value \leq 0,01 ; *** = p-value \leq 0,001.

Oral communications and Posters Awards 2015

Molecular and mechanical signals underlying tendon cell differentiation

LIENS D'INTÉRÊT

Les auteurs déclarent n'avoir aucun lien d'intérêt concernant les données publiées dans cet article.

RÉFÉRENCES

1. Gaut L, Duprez D. Tendon development and diseases. *Wiley Interdiscip Rev Dev Biol* 2016 ; 5 : 5-23.
2. Huang AH, Lu HH, Schweitzer R. Molecular regulation of tendon cell fate during development. *J Orthop Res* 2015 ; 33 : 800-12.
3. Schweitzer R, Chung JH, Murtaugh LC, *et al.* Analysis of the tendon cell fate using scleraxis, a specific marker for tendons and ligaments. *Development* 2001 ; 128 : 3855-66.
4. Lejard V, Blais F, Guerquin MJ, *et al.* EGR1 and EGR2 involvement in vertebrate tendon differentiation. *J Biol Chem* 2011 ; 286 : 5855-67.
5. Guerquin MJ, Charvet B, Nourissat G, *et al.* Transcription factor EGR1 directs tendon differentiation and promotes tendon repair. *J Clin Invest* 2013 ; 123 : 3564-76.
6. Mammoto T, Mammoto A, Ingber DE. Mechanobiology and developmental control. *Annu Rev Cell Dev Biol* 2013 ; 29 : 27-61.
7. Nowlan N, Sharpe J, Roddy K, *et al.* Mechanobiology of embryonic skeletal development: Insights from animal models. *Birth Defects Res C Embryo Today* 2010 ; 90 : 203-13.
8. Bayer M, Yeung C, Kadler K, *et al.* The initiation of embryonic-like collagen fibrillogenesis by adult human tendon fibroblasts when cultured under tension. *Biomaterials* 2010 ; 31 : 4889-97.

EMC
45TH EUROPEAN MUSCLE CONFERENCE

MONTPELLIER
2, 3, 4, 5, 6th of September
2016 - FRANCE

The Muscles

SESSIONS / SPEAKERS

- ▶ **Keynote lecture**
+ Andrew Marks (Columbia University, New York, USA)
- ▶ **Molecular motor and Contractile structure**
+ Anne Houdusse (France) & Lee Sweeney (USA)
- ▶ **Molecular motor and Contractile function (acto-myosin)**
+ Robin Candau (France) & Vincenzo Lombardi (Italy)
- ▶ **Muscle plasticity and Chronic disease**
+ Xavier Bigard (France) & Volker Adams (Germany)
- ▶ **Mechanotransduction (VIDD, Shear stress, Starling's law)**
+ Stefan Matecki (France) & Basil Petrof (Canada)
- ▶ **Muscle development and aging**
+ Robert Kelly (France) & Peter Zammit (UK)
- ▶ **Epigenetics of muscle regeneration**
+ Shohragim Tajbakhsh (France) & Esther Barreiro (Spain)
- ▶ **Excitation-contraction coupling in skeletal muscle**
+ Bruno Allard (France) & Hakan Westerblad (Sweden)
- ▶ **Excitation contraction coupling in cardiac muscle**
+ Alain Lacampagne (France) & Stephan Lehmann (Germany)
- ▶ **Metabolism... and bio-energetics**
+ Jeremy Fauconnier (France) & Martin Picard (USA)
- ▶ **Bio energetism... and Metabolism**
+ Philippe Dolez (France) & Fabio di Lisa (Italy)
- ▶ **Neuro-muscular disease and therapeutic approach**
+ Vincent Mouly (France) & Kevin Flanigan (USA)
- ▶ **Muscle cytoskeleton**
+ Olivier Cazorla (France) & Henk Granzier (USA)
- ▶ **Smooth muscle motility**
+ Vincent Sauzeau (France) & Katherine Morgan (USA)
- ▶ **Cardiomyopathy and Heart failure**
+ Bijan Ghaleh (France) & Michel Ovize (France)

WWW.
emc2016-montpellier.com

X.5 Curriculum Vitae

Ludovic Gaut

PhD candidate



04th of March,
1990



gaut.ludovic@gmail.com



46 Boulevard
Voltaire, 75011
Paris, France



+33 6 83 01 86 54



[www.linkedin.com/
in/ludovic-gaut](http://www.linkedin.com/in/ludovic-gaut)

FORMATION

2017 • D.U. Génie Biologique et Médical • UPMC - Paris 6

2017 • Formation Brevets et P.I. • URFIST

2014 • Diplôme du Cours Pasteur « Génétique cellulaire et moléculaire » • Institut Pasteur

2012 – 2014 • Master de Génétique – Magistère Européen de Génétique • Université Paris Diderot – Paris 7

2011 – 2012 • Licence de Génétique – Magistère Européen de Génétique • Université Paris Diderot – Paris 7

➤ **Secretary for student's association « Biologie et Génétique Appliquée »**

INFORMATIC SKILLS

Microsoft Office
GraphPad Prism
Photoshop & ImageJ

LANGUAGES

English: Fluent
German: Notions

PERSONAL

Scenario writing and Game Master for roleplaying games

MOOC Coursera: *Creative Writing* from Wesleyan University

Sports : Swimming, Aïkido

EXPERIENCE

2014 – 2018 • PhD candidate • IBPS - UPMC

Project: Mechanical and molecular signals underlying tendon cell differentiation.

PhD supervisors: Dr.Delphine Duprez & Dr.Mathias Mericskay

Prize for best oral communication – 13èmes journée de la Société Française de Myologie -Colloque Myogénèse-, Novembre 2015

Management of a Master 2 intern

2014 January-July • Master 2 intern • Institut Cochin, Paris, France

Développement musculaire génétique et physiopathologie, Dr.Pascal Maire & Dr.Philippe Daubas

Project: New molecular regulators of muscle regeneration in adult mice.

2013 April – August • Master 1 intern • St.Jude Children's Research Hospital, Memphis, Tennessee, USA

Experimental hematology department, Shannon McKinney-Freeman, PhD

Project: Identification and characterization of potential novel regulators of adult hematopoietic stem cell function.

2012 May – August • Summer intern • McGill University, Montréal, Québec, Canada

Meakins-Christie Laboratories, Pr.James G. Martin

Project : Effect of hypochloric acid-induced oxidative stress on the cysteinyl leukotrien biosynthetic pathway

PUBLICATIONS

Baudequin, T., **Gaut, L.**, Mueller, M., Huepkes, A., Glasmacher, B., Duprez, D., Bedoui, F., and Legallais, C. (2017). The Osteogenic and Tenogenic Differentiation Potential of C3H10T1/2 (Mesenchymal Stem Cell Model) Cultured on PCL / PLA Electrospun Scaffolds in the Absence of Specific Differentiation Medium. *Materials (Basel)*. 2, 1–19. doi: 10.3390/ma10121387

Gaut L., Robert N., Delalande A., Bonnin MA., Pichon C. and Duprez D., EGR1 regulates transcription downstream of mechanical signals during tendon formation and healing, *Plos One*, 2016. doi: 10.1371/journal.pone.0166237

Gaut et al., *Cahiers de la Myologie* (2016) doi:10.1051/myolog/201613019

Holmfeldt P., Ganuza M., Marathe H., He B., Hall T., Kang G., Moen J., Pardieck J., Saulsberry A., Cico A., **Gaut L.**, McGoldrick D., Finkelstein D., Tan K. and Mckinney-Freeman S., Functional screen identifies novel regulators of murine hematopoietic stem cell repopulation, *Journal of Experimental Medicine*, 2016. doi: 10.1084/jem.20150806

Gaut L. and Duprez D., Tendon development and diseases, *WIREs Dev Biol*, 2016. doi: 10.1002/wdev.201

LaTeX2e[1995/12/01] thcover[2017/11/21 v5.0 Build coverage 1 and 4 for french thesis
(J.Hare)] ifpdf graphicx geometry[2010/03/13] datetime etoolbox calc adjustbox xstring @p
skip@skip @skip=
bskip@bskip
thcover-psl
fpackageloadedhyperref

